

Design and Synthesis of Dual Kinase-Bromodomain Inhibitors Targeting ALK and BRD4

Ellen Watts

Medicinal Chemistry, Cancer Research UK Cancer Therapeutics Unit

The Institute of Cancer Research

University of London

This thesis is submitted in partial fulfilment of the requirements for the degree of Doctor of Philosophy

July 2019



Signed Declaration

I, Ellen Watts, confirm that the work presented in this thesis is my own. Where work has been performed by others, and where information has been derived from other sources, I confirm that this has been indicated in the thesis.

Ellen Watts

July 2019

Acknowledgements

Firstly, I would like to thank Swen and Ben for the opportunity to carry out my PhD at The Institute of Cancer Research and for all your guidance and support. I have learnt an incredible amount from the both of you.

A huge thank you to Lou and Lizzie from the Paediatric Solid Tumour Team for their expertise, help in understanding cellular biology and support with this exciting project. Thank you also to my collaborators Stefan and David for their insightful knowledge and experience in bromodomains and to Monika for the PLK-1 data.

I would like to thank everyone from the Med Chem 4 Team, both past and present: Hannah, Matt, Owen, Jack, Ana, Rosemary, Alfie, Alice, Charlie and Will. Thanks for being a great supportive team the past four years. A special thanks to Matt and Owen who witnessed nearly my whole PhD journey: thanks for your advice, daily chats and teaching me how to use hyphens - – —

Thank you to everyone else within Chemistry and Cancer Therapeutics who have helped me with one of the many new techniques I have learnt during my PhD. Thank you to Yvette and Harry for all your assay guidance, to Angela for DMPK help, to Mike for helping me become a docking pro, to Catherine for crystallography help and to Meirion, Amin, Maggie and Katia for help with structural chemistry.

Special thanks to the Quadvod Hype: Jonny, Josh, HT, HMac, Kate and Steve for the endless laughs, great nights at the bar and comradery in getting through our PhDs.

I would like to thank my parents for their continuous love and support throughout my PhD. And finally a huge thank you to my fave and FH (future husband), Tom. Thank you for being there every day and helping me see this through (especially at the end). I couldn't have done this without you.

Abstract

Neuroblastoma is a paediatric cancer of neural crest origin and is the most common extracranial solid tumour in childhood. In high-risk patients with poor clinical outcome, mutations within the kinase domain of anaplastic lymphoma kinase (ALK), such as ALK^{F1174L} , co-segregate with amplification of the *MYCN* gene. Transcription of *MYCN* is directly upregulated by ALK^{F1174L} , whilst BRD4, a member of the BET family of transcriptional co-regulators is essential for *MYCN* expression

The project hypothesis is that a dual ALK-BRD4 inhibitor is beneficial compared with single inhibitors of ALK and BRD4, avoiding the need for combinatorial trials and treatment. Thus the aim of the project is to generate dual ALK-BRD4 inhibitors that target both oncogenic mutations as an effective treatment for high-risk neuroblastoma patients.

BI-2536, a known dual PLK-1-BRD4 inhibitor with modest potency against ALK, was chosen as the starting point. Using structure based design, analogues of BI-2536 were prepared and tested with the aims of increasing ALK activity, decreasing PLK-1 activity and maintaining BRD4 activity. The testing of these compounds has provided SAR on how the potency can be modulated at ALK, BRD4 and PLK-1.

This work has led to a series of compounds with significantly improved dual ALK-BRD4 profiles, favourable kinase and bromodomain selectivity and on-target activity in cells. Furthermore this work highlights the challenges of designing and developing dual inhibitors; in particular balancing multiple potencies and the physicochemical properties whilst maintaining selectivity against other bromodomains and kinases.

Abbreviations

| | |
|--------------------|---|
| ALCL: | Anaplastic large cell lymphoma |
| ALK: | Anaplastic lymphoma kinase |
| AURKA: | Aurora kinase A |
| BET: | Bromodomain and extra-terminal (family) |
| BD1: | Bromodomain 1 |
| BD2: | Bromodomain 2 |
| BRD4: | Bromodomain-4 |
| CDK: | Cyclin dependent kinase |
| CHK1: | Checkpoint kinase 1 |
| CMBP: | Cyanomethylenetributylphosphorane |
| DCE: | 1,2-Dichloroethane |
| DEAD: | Diethyl azodicarboxylate |
| DMB: | 2,4-Dimethoxybenzyl |
| DMF: | Dimethylformamide |
| d.r: | Diastereomeric ratio |
| e.r: | Enantiomeric ratio |
| FDA: | Food and drug administration |
| GI ₅₀ : | Concentration for 50% of maximal inhibition of cell proliferation |
| HBTU: | N,N,N',N'-Tetramethyl-O-(1H-benzotriazol-1-yl)uronium hexafluorophosphate |
| HPLC: | High performance liquid chromatography |
| HRMS: | High-resolution mass spectrometry |
| IC ₅₀ : | Half maximal inhibitory concentration |
| INRG: | International neuroblastoma risk group |
| INRGSS: | International neuroblastoma risk group staging system |
| INSR: | Insulin receptor |
| KAc: | Acetylated lysine |
| K _d : | Dissociation constant |

| | |
|--------------------|---|
| KLIFS: | Kinase-ligand interaction fingerprints and structure database |
| LCMS: | Liquid-chromatography mass spectrometry |
| LLE: | Lipophilic ligand efficiency |
| MOE: | Molecular operating environment |
| MSD: | Meso-scale discovery |
| NSCLC: | Non-small-cell lung carcinoma |
| pALK: | Phosphorylated ALK |
| PAMPA: | Parallel artificial membrane permeability assay |
| PGP: | P-glycoprotein |
| pK _a : | negative log of the acid dissociation constant |
| pK _a H: | pK _a of the conjugated acid |
| PLK-1: | Polo-like kinase 1 |
| PLK-3: | Polo-like kinase 3 |
| p-loop: | Phosphate binding loop |
| PMB: | <i>Para</i> -methoxybenzyl |
| PROTAC: | Proteolysis targeting chimera |
| qRT-PCR: | Real-time quantitative polymerase chain reaction |
| SAR: | Structure activity relationships |
| S.D: | Standard deviation |
| S.E: | Standard error |
| SNAr: | Nucleophilic aromatic substitution |
| tALK: | total ALK |
| TFA: | Trifluoroacetic acid |
| Th: | Tyrosine Hydroxylase |
| T _m : | Thermal (shift) |
| TR-FRET: | Time-resolved-fluorescence energy transfer |
| WT: | Wildtype |

Contents

| | | |
|-----------|--|----|
| Chapter 1 | Introduction..... | 11 |
| 1.1 | Neuroblastoma | 11 |
| 1.1.1 | Neuroblastoma Risk Groups and Associated Treatments..... | 12 |
| 1.1.2 | Current Approaches to Targeting <i>MYCN</i> in Neuroblastoma..... | 13 |
| 1.2 | Anaplastic Lymphoma Kinase..... | 18 |
| 1.2.1 | Targeting ALK Mutations | 18 |
| 1.2.2 | ALK Point Mutations | 20 |
| 1.2.3 | First Generation Inhibitor Crizotinib..... | 23 |
| 1.2.4 | Second and Third Generation ALK Inhibitors..... | 24 |
| 1.3 | Bromodomain-4 | 25 |
| 1.3.1 | Bromodomain Function..... | 25 |
| 1.3.2 | Structure of BRD4 | 27 |
| 1.3.3 | Current BET Inhibitors | 28 |
| 1.4 | Polypharmacology | 33 |
| 1.5 | Dual Kinase-Bromodomain Inhibition..... | 34 |
| 1.5.1 | Identification of Dual Kinase-Bromodomain Inhibitors..... | 34 |
| 1.5.2 | Structural Analysis of Dual Kinase-Bromodomain Inhibitors | 36 |
| 1.5.3 | Current scope of Dual Kinase-Bromodomain Inhibitors..... | 38 |
| 1.6 | Project Aims | 40 |
| 1.6.1 | Project Hypothesis..... | 40 |
| 1.6.2 | ALK and BRD4 Synergy | 41 |
| 1.6.3 | Project Cascade | 41 |
| Chapter 2 | Design and Synthesis of First Generation Dual ALK-BRD4 Inhibitor.... | 44 |
| 2.1 | Introduction to BI-2536 | 44 |
| 2.1.1 | PLK-1 | 45 |
| 2.1.2 | Binding of BI-2536 to PLK-1 and BRD4..... | 46 |
| 2.1.3 | Literature Describing SAR of BI-2536..... | 47 |
| 2.2 | Design Rationale | 48 |

| | | |
|-----------|--|-----|
| 2.2.1 | Docking Experiments in ALK | 49 |
| 2.3 | Synthesis of BI-2536 Analogues | 50 |
| 2.4 | Biochemical Testing..... | 55 |
| 2.4.1 | Biochemical Assay Cascade..... | 55 |
| 2.4.2 | Caliper Mobility Shift Assay | 56 |
| 2.4.3 | LanthaScreen® Assay..... | 58 |
| 2.5 | SAR of Analogues | 59 |
| 2.5.1 | SAR of R ₃ – Methoxy Group | 59 |
| 2.5.2 | SAR of R ₄ – Solvent Channel Group | 62 |
| 2.5.3 | SAR of R ₁ – (<i>R</i>)-Ethyl Group | 64 |
| 2.5.4 | SAR of R ₂ – Cyclopentyl Group | 68 |
| 2.6 | Combining SAR Modifications | 71 |
| Chapter 3 | Exploring the R ₂ Region: Design and Synthesis of Second Generation Inhibitor | 73 |
| 3.1 | Design Hypothesis for Exploring the R ₂ Pocket | 73 |
| 3.2 | Synthetic Route Development | 74 |
| 3.2.1 | New Synthetic Route | 77 |
| 3.2.2 | Chiral Shift Experiments | 80 |
| 3.3 | SAR of R ₂ position | 81 |
| 3.3.1 | Benzyl Groups..... | 81 |
| 3.3.2 | Heterocycle Groups..... | 92 |
| 3.3.3 | Aliphatic Groups | 97 |
| 3.4 | Further SAR on Lead Compound 63 | 99 |
| 3.4.1 | Revisiting SAR of the Alkoxy Group (R ₃) | 99 |
| 3.4.2 | Revisiting SAR of the Solvent Channel Group (R ₄) | 101 |
| 3.5 | X-Ray Crystallography..... | 104 |
| 3.6 | Cellular Testing..... | 105 |
| 3.6.1 | ALK Phosphorylation | 105 |
| 3.6.2 | NanoBRET Cellular Potency..... | 107 |
| 3.7 | Selectivity | 108 |

| | | |
|-----------|--|-----|
| 3.7.1 | Bromodomain Selectivity | 108 |
| 3.7.2 | Kinase Selectivity | 110 |
| 3.7.3 | Cellular Selectivity between ALK and PLK-1..... | 112 |
| Chapter 4 | Improving the Selectivity and Physicochemical Properties..... | 115 |
| 4.1 | Synthesis of Single Diastereomers of Compound 105 | 115 |
| 4.1.1 | Mitsunobu Conditions | 115 |
| 4.1.2 | Separation and Characterisation of Diastereomers..... | 117 |
| 4.2 | Analysis of Diastereomer Inhibitors..... | 119 |
| 4.2.1 | Biochemical Data..... | 119 |
| 4.2.2 | Computational Modelling | 121 |
| 4.2.3 | Further SAR around (<i>R,S</i>)-Diastereomer Compound 135 | 124 |
| 4.3 | Further Cellular Testing | 128 |
| 4.3.1 | ALK Phosphorylation | 128 |
| 4.3.2 | BRD4 qRT-PCR | 129 |
| 4.3.3 | Growth Inhibition..... | 130 |
| 4.4 | Physicochemical Properties..... | 131 |
| 4.4.1 | Physicochemical Properties of Key Compounds 63 and 135 | 131 |
| 4.4.2 | Modifications to the Solvent Channel Region..... | 133 |
| 4.4.3 | Comparison of Methylated and Unmethylated Piperidine Analogues . | 136 |
| 4.4.4 | Cellular Testing of Unmethylated Piperidine Analogues..... | 139 |
| Chapter 5 | Epimerisation..... | 140 |
| 5.1 | Synthesis of Diastereomers | 140 |
| 5.1.1 | Differences in Synthetic Routes..... | 141 |
| 5.2 | Checking the Enantiopurity of Starting Material 8a | 143 |
| 5.3 | Checking Synthetic Steps by Chiral Shift NMR | 145 |
| 5.3.1 | Checking the S_NAr Step By Chiral Shift NMR | 145 |
| 5.3.2 | Checking the Methylation Step By Chiral Shift NMR | 146 |
| 5.3.3 | Checking the TFA Deprotection Step By Chiral Shift NMR | 147 |
| 5.4 | Optimisation of Methylation Step | 148 |
| 5.4.1 | HPLC Method | 148 |

| | | |
|-----------|---|-----|
| 5.4.2 | Optimisation of conditions..... | 149 |
| 5.5 | Checking Synthetic Steps by Chiral HPLC..... | 151 |
| 5.5.1 | Revisiting the Enantiopurity of Intermediates 6r and 90aj | 151 |
| 5.5.2 | Checking the Reductive Heterocyclisation Step By Chiral HPLC | 152 |
| 5.5.3 | Checking the TFA Deprotection Step By Chiral HPLC | 153 |
| 5.5.4 | Checking the Mitsunobu Step By Chiral HPLC | 153 |
| 5.6 | Conclusions and Solutions | 155 |
| Chapter 6 | Conclusions and Future Directions | 158 |
| Chapter 7 | Experimental | 162 |
| 7.1 | LanthaScreen® Binding Assay | 162 |
| 7.2 | ALK MSD Phosphorylation Assay ¹⁶⁷ | 162 |
| 7.3 | Kinetic Solubility by NMR..... | 163 |
| 7.4 | Docking with Glide..... | 163 |
| 7.5 | Conformational Analysis | 164 |
| 7.6 | General Synthetic Experimental | 164 |
| 7.7 | General Methods..... | 166 |
| 7.8 | Chemistry Experimental..... | 170 |
| Chapter 8 | Appendices..... | 308 |
| 8.1 | Appendix A: Kinome Screen Data for 63 | 308 |
| Chapter 9 | References..... | 310 |

Chapter 1 Introduction

1.1 Neuroblastoma

Neuroblastoma is an embryonal tumour derived from neural-crest cells in the sympathetic nervous system and is the most common extracranial solid tumour in childhood. Neuroblastoma accounts for 6% of the total number of childhood cancer diagnosis with just under 100 children in the UK diagnosed each year.¹ Neuroblastoma most frequently develops within one of the adrenal glands but can also develop within the spinal cord (Figure 1). The cancer can spread to other organs including bone marrow, bone and the liver. Cases of neuroblastoma are quite diverse, with a number of varying clinical and biological features.² The majority of cases are sporadic or non-familial with only 1 – 2% of cases running in families.³

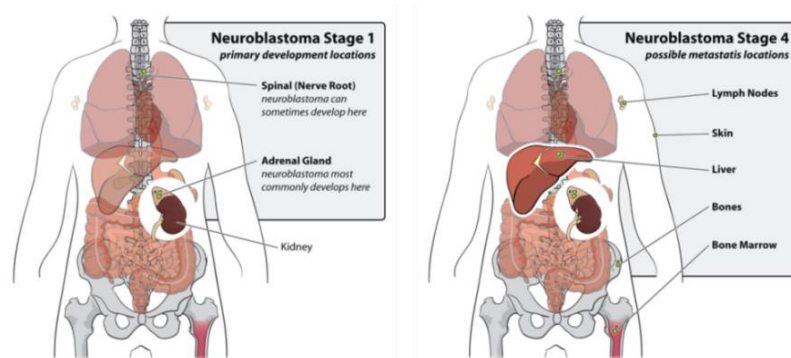


Figure 1. Locations of tumour development at primary and metastatic stages.⁴

After a patient is diagnosed with neuroblastoma, the neuroblastoma is classified by a stage. The International Neuroblastoma Risk Group Staging System (INRGSS) uses results from imaging tests, such as a computerised tomography (CT) or magnetic resonance imaging (MRI) scan, to help decide a stage before treatment has started.⁵ The assigned stage describes how much cancer is in the body ranging from the tumour being confined to one area (Stage L1) to tumours that have metastasised to another part of the body (Stage M or MS) (Table 1). To aid assessment the INRGSS uses image-defined risk factors, for example the tumour encasing important blood vessels or close proximity to vital organs.⁵

| Stage | Description |
|-----------|---|
| L1 | A tumour that is confined to one area. |
| L2 | A tumour that has not spread far from its primary location and has one image-defined risk factor. |
| M | A tumour that has metastasised to a distant part of the body. |
| MS | Metastatic disease in children < 18 months with cancer spread only to the skin, liver and/or bone marrow. |

Table 1. Neuroblastoma stage classification (INRGSS).⁵

1.1.1 Neuroblastoma Risk Groups and Associated Treatments

Patients are also assigned to a risk group based on their stage and several prognostic markers which help determine a child's prognosis. These include:

- Age – younger children under 12 – 18 months are more likely to be successfully treated.⁶
- Tumour histology – tumours that contain more abnormal cells are defined as having unfavourable histology and tend to have a poorer prognosis.⁷
- Grade of tumour differentiation – well-differentiated cancer cells appear more like normal cells and tend to grow and spread more slowly than poorly differentiated cancer cells.⁷
- *MYCN* Amplification – neuroblastoma cells with amplification of the *MYCN* oncogene is a well-established poor prognostic marker.⁸
- 11q aberration – tumour cells that are missing part of chromosome 11 have a less favourable prognosis.²
- DNA ploidy – diploid cells have the same amount of DNA as normal cells whilst hyperdiploid cells have more DNA than normal cells and are associated with better prognosis.⁹

Together, the prognostic markers and stage of cancer define a risk group for the patient, outlined in Table 2. The International Neuroblastoma Risk Group (INRG) classification system was based on data collected from 8,800 children diagnosed with neuroblastoma between 1990 and 2002, across North America, Australia, Europe and Japan.² The lower risk groups generally have favourable histology and do not have *MYCN* amplifications or 11q aberrations. Consequently the 5-year survival rate for very low and low risk patients is >95% with surgery being the primary method for

treatment.¹⁰ Intermediate risk patients usually require chemotherapy alongside surgery during treatment, with a 5-year survival rate of 90 – 95%.¹⁰ These patients can have unfavourable histology or 11q aberrations. High-risk patients have a poorer prognosis with a 5-year survival rate of 40 – 50% and require several intensive treatments including chemotherapy, surgery, radiation and immunotherapy.¹⁰ *MYCN* amplification is strongly associated with poor outcome and is present in 45% of high-risk cases.¹¹ Due to the poor clinical outcome in high-risk patients, novel treatment approaches are urgently required.

| INRG Stage | Age * | Histology | Tumour Differentiation | <i>MYCN</i> | 11q Aberration | Ploidy | Risk Group |
|------------|-------|--------------|--|----------------|----------------|-----------|-----------------------------|
| L1 | | Favourable | | NA Amp. | | | Very Low High |
| L2 | <18 | Favourable | | NA | No Yes | | Low Int. |
| | ≥18 | Unfavourable | Differentiating Poorly differentiated | NA Amp. | No Yes | | Low Int. Int. High |
| M | <18 | | | NA | | Hyperdip. | Low |
| | <18 | | | NA | | Diploid | Int. |
| | <18 | | | Amp. | | | High |
| | ≥18 | | | | | | High |
| MS | <18 | | | NA | No Yes | | Very Low |
| | | | | Amp. | | | High High |

Table 2. International Neuroblastoma Risk Group Classification Scheme.² *Age is in months. NA = not amplified, Amp. = amplified, Hyperdip. = hyperdiploid, Int. = intermediate.

1.1.2 Current Approaches to Targeting *MYCN* in Neuroblastoma

Amplification of *MYCN* is a defining feature of high-risk neuroblastoma and various strategies to therapeutically target the activity of *MYCN* have been pursued (Figure 2). MYC proteins are transcription factors, encoded by the *MYCN* gene, and due to the absence of stable and well defined pockets, are difficult structures to inhibit with a small molecule.^{12,13} Approaches to indirectly target MYC have been favoured including targeting *MYCN* transcription, *MYCN* protein stability and synthetic lethal interactions with MYCN.

One method that focuses on directly targeting MYC family members is blocking the interaction between MYC and its partner protein MAX.¹² *MYCN* requires MAX in order to function as a transcriptional activator as well as for proliferative and oncogenic functions.^{13,14} Therefore inhibition of this protein-protein interaction is an appealing

strategy. Two compounds, 10074-G5 and 10058-F4 have been shown to block the MYCN-MAX interaction and induce apoptosis in neuroblastoma cells (Figure 3). However the poor solubility and short half-life have limited the compounds development *in vivo*.^{15,16}

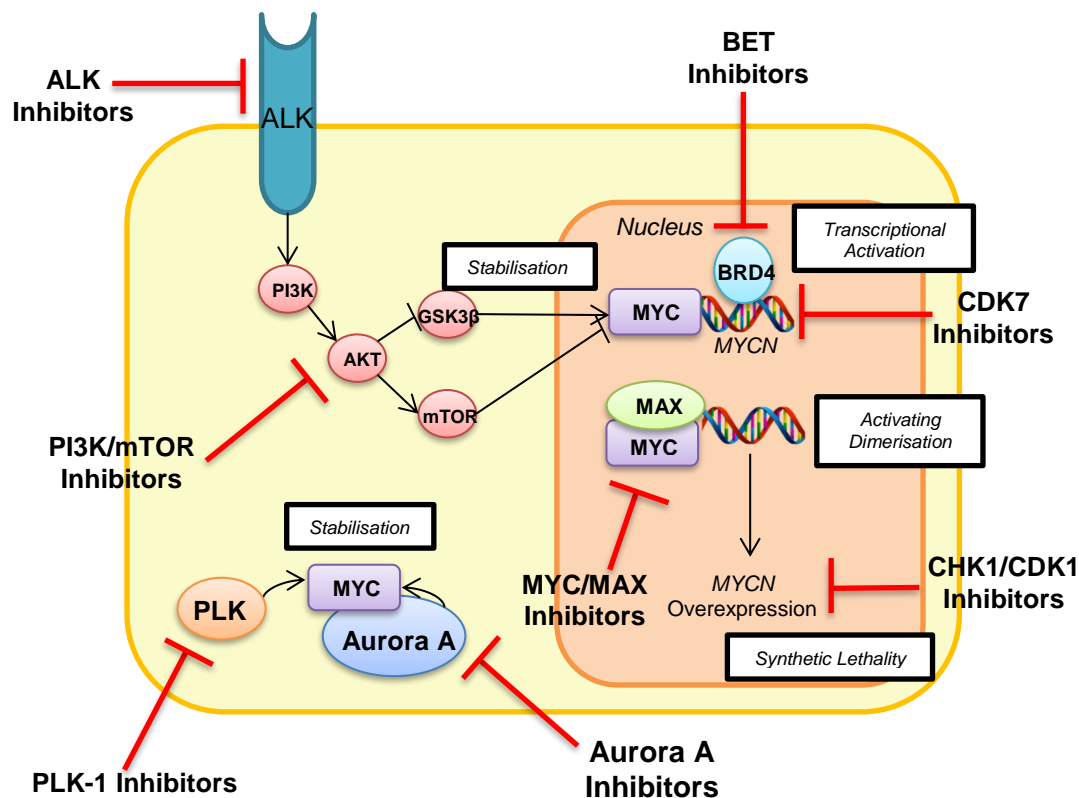


Figure 2. Current therapeutic approaches for *MYCN*-amplified neuroblastoma.

Inhibiting *MYCN* transcription has been a viable strategy through inhibition of cyclin-dependent kinase 7 (CDK7) or bromodomain-4 (BRD4) (see 1.1.2.1). In *MYCN*-amplified cells a super enhancer cluster of transcription factors and chromatin regulators occurs, including CDK7, which regulates and enhances *MYCN* transcription.¹⁷ THZ1, a covalent inhibitor of CDK7, is potent and selective for *MYCN*-amplified cells, suppressing *MYCN* transcription.¹⁸ The CDK7 inhibitor also showed significant tumour regression in a mouse model of high-risk neuroblastoma demonstrating the potential for a CDK7 inhibitor as a treatment for *MYCN*-driven cancers.¹⁸

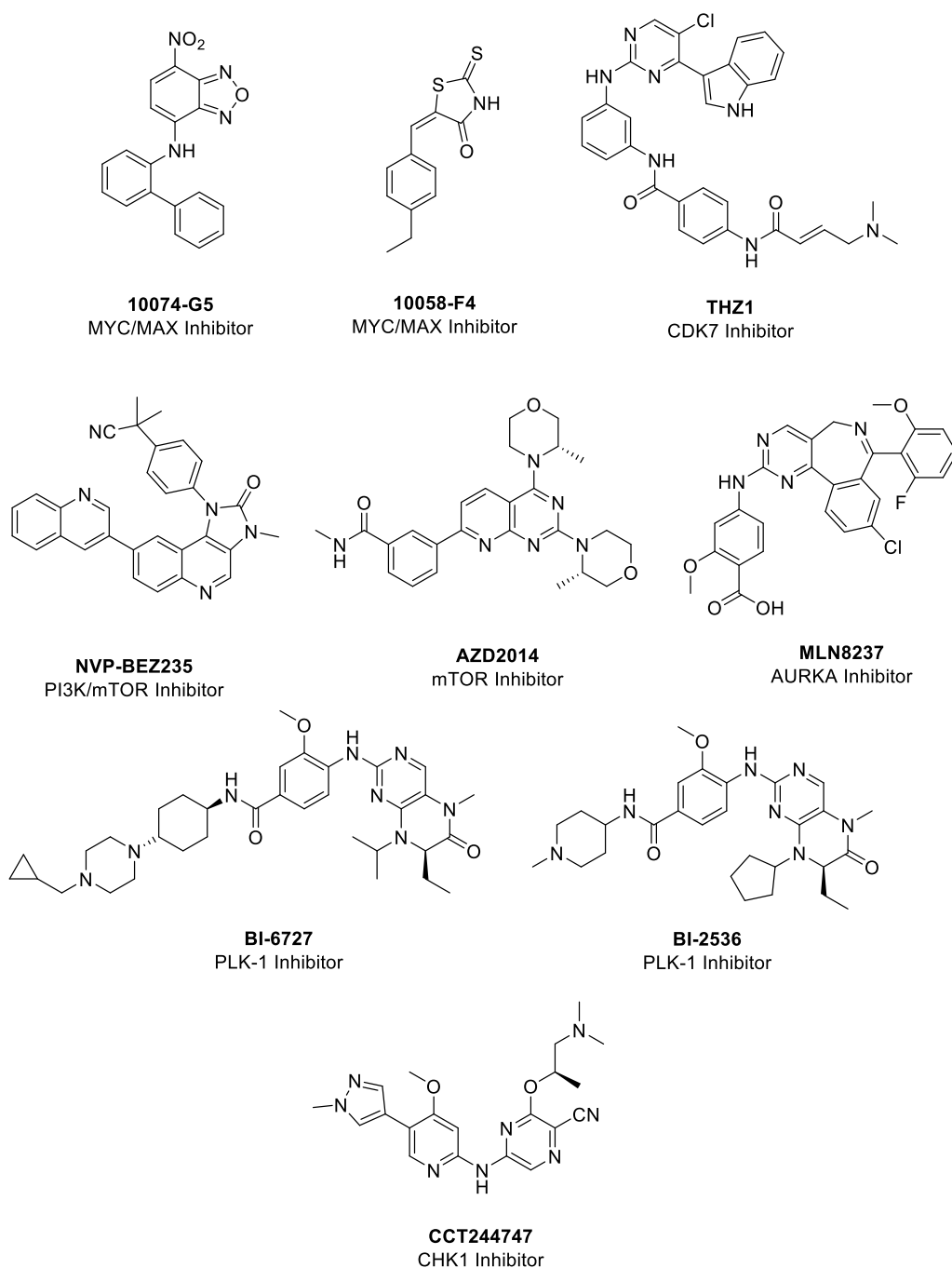


Figure 3. Structures of inhibitors for indirectly targeting MYCN.

Inhibiting proteins that stabilise MYCN has also been a promising strategy for indirectly targeting MYCN. Activation of the PI3K/AKT/mTOR pathway in neuroblastoma is associated with poor outcome and drives stabilisation of MYCN.^{12,19,20} MYCN is stabilised by the phosphorylation status of residues Thr58 and Ser62, allowing for increased oncogenic activity.²¹ Phosphorylation of Thr58 is regulated by GSK3 β , a downstream target of the PI3K/AKT pathway and phosphorylation of Ser62 is regulated by PP2A, a downstream target of mTOR (Figure 2). Targeting the PI3K/AKT/mTOR pathway is a suitable way to regulate

MYCN stability and stimulate degradation of MYCN. Combined PI3K/mTOR inhibitor NVP-BEZ235 has been shown to destabilise MYCN and cause tumour regression of *MYCN*-driven neuroblastoma *in vivo*.²¹ Inhibitors to reach neuroblastoma clinical trials include PI3K/mTOR inhibitor SF1126, although this trial was terminated due to too few patients recruited,²² and mTOR inhibitor AZD2014, for paediatric patients with molecular anomalies in relapsed or refractory tumours (NCT02813135).²³

An alternative approach is to disrupt the interactions between MYCN and Aurora A kinase (AURKA), which control the stability of MYCN and prevent proteasomal degradation.²⁴ Disruption of the association between MYCN and AURKA results in increased degradation of MYCN, as observed with AURKA inhibitor MLN8237.²⁵ However MLN8237 was not well tolerated in a phase I clinical trial (NCT0244484), leaving the development for improved AURKA inhibitors open.²⁶ Finally, polo-like kinase 1 (PLK-1) is also known to stabilise MYCN. Conversely MYCN directly activates PLK-1 transcription creating a positive activation loop which promotes tumour cell survival.¹⁷ Inhibitors of PLK-1, BI-6727 and BI-2536, have been shown to induce apoptosis in *MYCN*-amplified neuroblastoma cells.²⁷

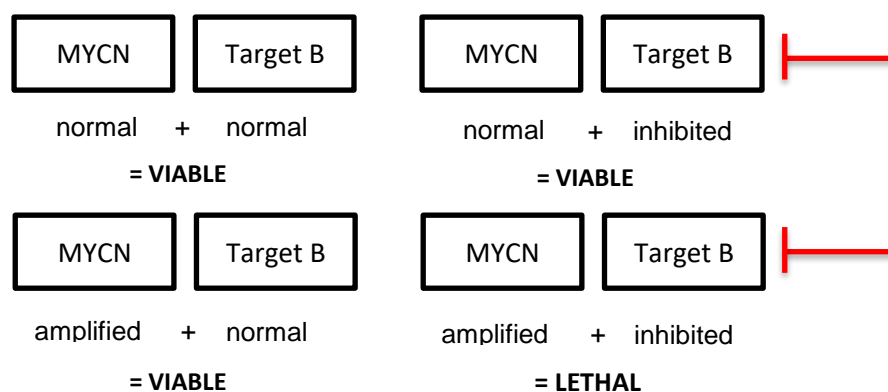


Figure 4. Synthetic lethal interactions between MYCN and target B (e.g. CHK1 and CDK1).

Inhibitors targeting synthetic lethal interactions with MYCN have also been explored. In the case of MYCN-mediated synthetic lethality, overexpression of MYCN and inhibition of a synthetic lethal gene to MYCN causes cell death, but just MYCN overexpression or inhibiting the gene does not (Figure 4).²⁸ Therefore targeting a gene synthetically lethal to MYCN should only cause cell death in cancer cells and not affect normal cells. Targets that are synthetically lethal towards MYCN have been identified through shRNA library screens, including checkpoint kinase 1 (CHK1) and cyclin-dependent kinase 1 (CDK1).^{29,30} Inhibiting CHK1 induces apoptosis in *MYCN*-amplified neuroblastoma cell lines, with CHK1 inhibitor sensitivity correlating with total

MYC levels.²⁹ Following from this, CHK1 inhibitor CCT244747 showed significant tumour reduction in a *MYCN*-driven transgenic model of neuroblastoma.³¹ Similarly, inhibiting CDK1 induces apoptosis in MYC-amplified cells and decreases tumour growth in MYC-dependent lymphoma and hepatoblastoma models.^{17,30} These results demonstrate the potential of targeting synthetic lethal interactions of MYCN in neuroblastoma and other MYC-driven cancers.

1.1.2.1 Targeting *MYCN* Transcription through BRD4 Inhibition

Targeting transcription of *MYCN* can be achieved through inhibition of BRD4. BET proteins, including BRD4, locate to MYC promoters and activate transcription of *MYCN*. In recent reports, BET inhibitors have shown therapeutic efficacy in targeting *MYCN* transcription. Puissant *et al.* reports the BET inhibitor JQ1 causes downregulation of *MYCN* transcription and inhibits the growth of neuroblastoma *in vitro* and *in vivo*.³² BRD4 binds acetyl lysine residues within the *MYCN* promoter region, recruiting additional proteins, including positive transcription elongation factor b (P-TEFb), that mediate chromatin density and allow for active *MYCN* transcription (Figure 5).³³⁻³⁵ The presence of JQ1 blocks binding of BRD4 to the *MYCN* promoter, downregulating *MYCN* and its target genes.³² This leads to cell cycle arrest, increased apoptosis and differentiation.

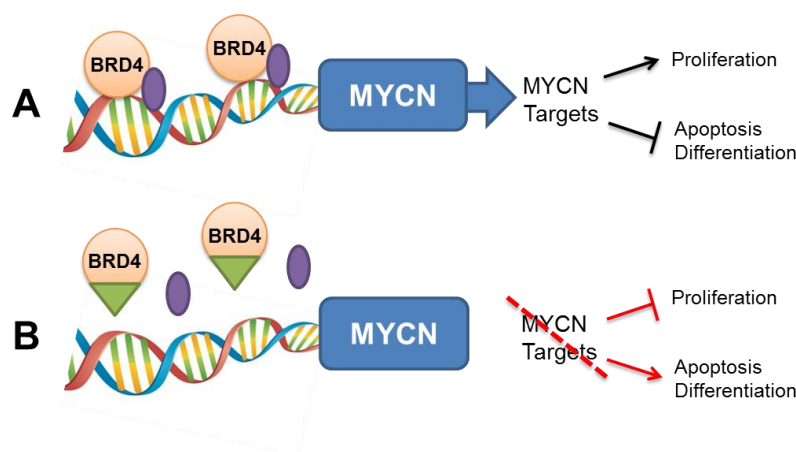


Figure 5 A) BRD4 binds to *MYCN* promoter region recruiting additional proteins (purple ovals) leading to active *MYCN* transcription. **B)** JQ1 (green triangles) inhibits BRD4 from binding thus inhibiting *MYCN* transcription.

Preclinical studies using *MYCN*-driven neuroblastoma models have been performed with BET inhibitor OTX015 (Figure 6). The compound demonstrated specific activity

against MYCN-target genes by disrupting transcription.³⁶ BET inhibitors have progressed to clinic for adult malignancies but there has been limited progress for paediatric trials.^{12,33} A Phase I study of BET inhibitor BMS-986158 is due to start June 2019 to evaluate the investigational drug in paediatric cancers including neuroblastoma.³⁷

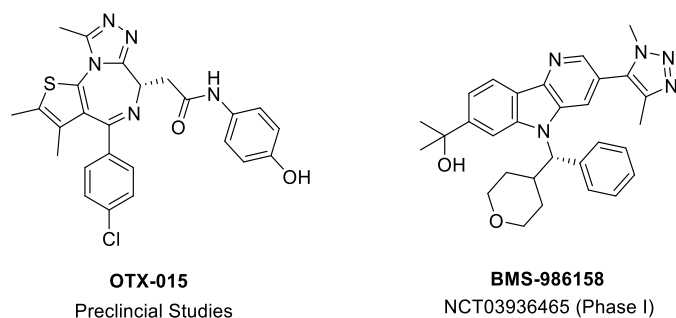


Figure 6. BET Inhibitors currently used in preclinical and clinical paediatric studies.

1.2 Anaplastic Lymphoma Kinase

1.2.1 Targeting ALK Mutations

Another common set of mutations in neuroblastoma is within the kinase domain of anaplastic lymphoma kinase (ALK), occurring in 10-15% of neuroblastoma cases.³ The most common point mutations in neuroblastoma are F1174L and R1275Q accounting for >80% of sporadic ALK mutations and result in ALK being constitutively activated.^{38,39} Gain-of-function mutations can also be found in familial cases of neuroblastoma, in particular R1275Q.³ Patients harbouring the F1174L mutations show a high rate of co-segregation with *MYCN* amplifications leading to the development of neuroblastomas with earlier onset, higher penetrance and enhanced lethality.⁴⁰ In addition, the activated ALK kinase further amplifies the oncogenic activity of MYCN via the PI3K/AKT/mTOR pathway which stabilises MYCN and activates transcription (Figure 2).⁴¹⁻⁴³ Berry *et al.* provided *in vivo* evidence of the synergistic relationship between ALK and MYCN and activation of the downstream signalling pathway, using an ALK^{F1174L}/MYCN transgenic model of high-risk neuroblastoma.⁴⁰ This ultra-high-risk subgroup exhibiting both amplification of MYCN and mutations of ALK have a survival of less than 15% in 3 years and represent an un-met clinical need.⁴⁴ Therapeutic approaches to target both *MYCN* and ALK are

desired, for example employing a combination of inhibitors from the strategies discussed (Figure 2).

In contrast to MYCN, ALK is an amenable therapeutic target with many small molecule inhibitors already known (Figure 7).⁴⁵⁻⁴⁸ However first-generation inhibitor crizotinib has shown limited efficacy in patients with ALK-driven neuroblastoma, in particular with the F1174L mutation.⁴⁹ This relates to the differential sensitivity of ALK mutants to crizotinib; crizotinib shows sustained tumour regression against R1275Q-mutant xenografts but is less effective against F1174L-driven tumours.³⁸ This may be due to insufficient blockage of the activating F1774L mutant kinase but also that MYCN amplification is maintained despite ALK being blocked. Second-generation inhibitor ceritinib shows greater potency compared to crizotinib and overcomes crizotinib-resistance mutations but is also only partially active against the F1174L mutant.^{50,51} Ceritinib is currently in phase I trials for neuroblastoma as a single treatment and in combination with CDK4/6 inhibitor ribociclib (Figure 7). The dual ALK and CDK4/6 combination previously showed complete tumour regression in neuroblastoma xenografts with the F1174L and F1245C mutations.⁵²

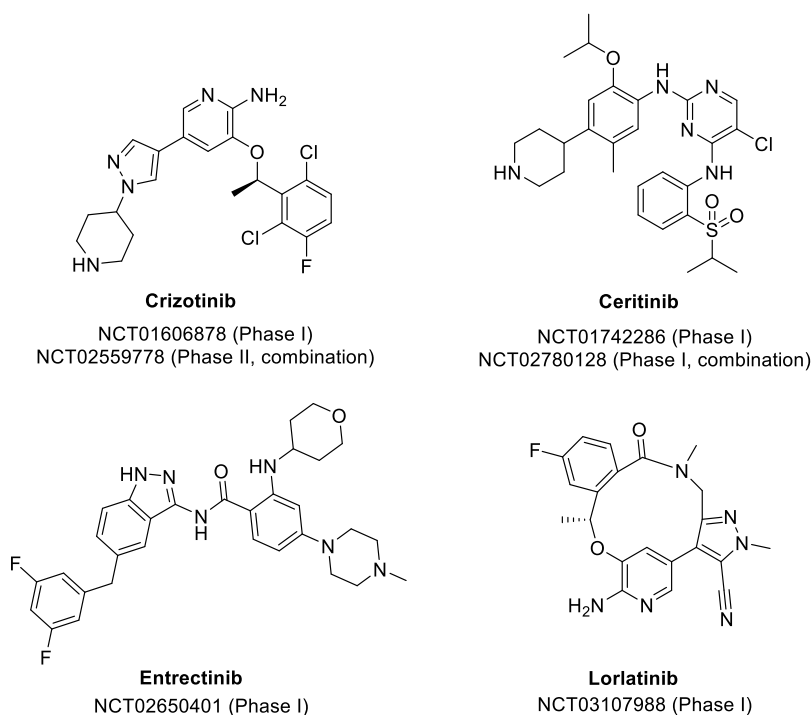


Figure 7. ALK inhibitors currently in clinical trials.

The third-generation ALK inhibitor lorlatinib has shown excellent efficacy in ALK-driven neuroblastoma models. Lorlatinib shows enhanced potency towards ALK mutants F1174L and F1245C compared to crizotinib and causes complete tumour

regression in crizotinib-resistant and sensitive xenografts as well as in xenografts with the F1174L and F1245C mutations.^{53,54} These promising preclinical results has allowed progression of Lorlatinib to clinical trials for patients with relapsed ALK-driven neuroblastoma (NCT03107988).⁵⁵

Anaplastic lymphoma kinase (ALK) is a receptor tyrosine kinase and part of the insulin receptor superfamily. ALK comprises of an extracellular ligand binding domain, a transmembrane region and intracellular region containing the kinase domain.⁵¹ ALK was first identified as a partner to nucleophosmin 1 (NPM1) in the NPM-ALK fusion protein which is activated in anaplastic large cell lymphoma (ALCL).⁵⁶ Translocation of ALK to form an ALK fusion protein, causes constitutive activation of ALK and subsequent activation of downstream signalling pathways. Since the identification of the NPM-ALK fusion protein, many other oncogenic ALK fusion proteins have been identified including NPM-ALK, EML4-ALK and TPM3-ALK and have been observed in in ALCL, non-small-cell lung cancer (NSCLC), diffuse large B cell lymphoma (DLBCL) and inflammatory myofibroblastic carcinoma (IMT).⁵⁷

Other mechanisms leading to aberrant ALK activity include gene amplifications, as observed in NSCLC, and point mutations, usually within the tyrosine kinase domain (Figure 8).^{38,39,58} Gain-of-function mutations are found mainly in neuroblastoma as well as thyroid cancer and NSCLC, whilst secondary resistance mutations following crizotinib treatment have been observed in NSCLC and IMT.⁵⁷

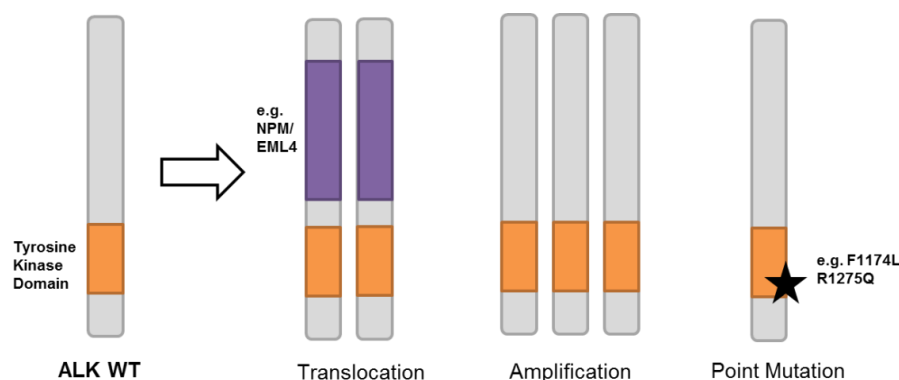


Figure 8. Possible abnormal forms of ALK expressed in cancer including gene amplification, gene fusion and point mutations.

1.2.2 ALK Point Mutations

Gain-of-function mutations of ALK are primarily observed in neuroblastoma, but have also been seen in thyroid and lung cancers.^{59,60} Most of the mutations are found

within the kinase domain, in particular around areas important for activation of ALK, the α -helix of the activation loop and the α C helix (Figure 9A).^{57,61} Mutations at R1275, F1174 and F1245, account for 85% of the ALK mutations found in patients with neuroblastoma, all constitutively activating the kinase.⁶²

In comparison to the gain-of-function mutations, secondary mutations arising from crizotinib resistance in NSCLC and IMT generally cluster around the inhibitor and ATP binding site (Figure 9B).⁵⁷

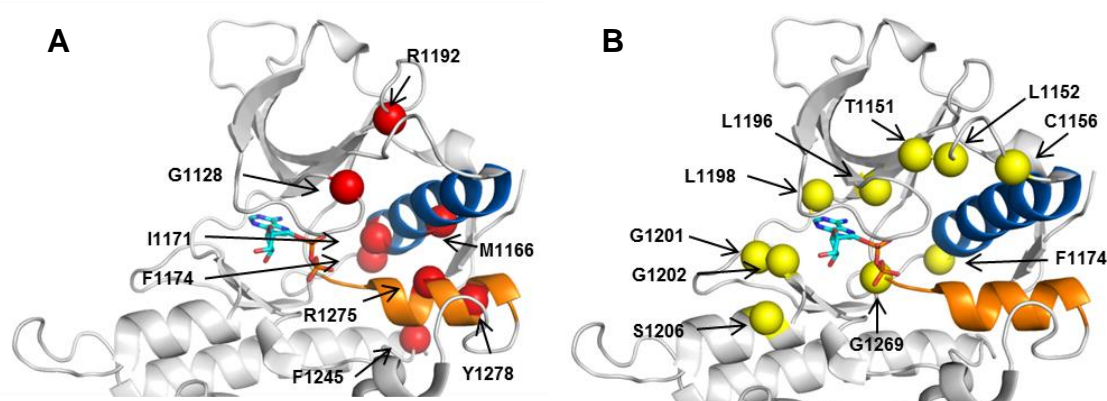


Figure 9. Comparison of **A)** gain-of-function and **B)** secondary resistant mutations found in ALK. Red spheres represent gain-of-function mutations; yellow spheres represent secondary resistant mutations. α C helix in blue, activation loop in orange.

1.2.2.1 ALK F1174L Mutation

The ALK^{F1174L} mutation is one of the most common neuroblastoma mutations, present in 41% of *MYCN*-amplified cases and 30% of cases overall.⁶² The F1174L mutation is an activating mutation and increases the catalytic turnover (k_{cat}) by approximately 40-fold, from $9.32 \pm 0.85 \text{ min}^{-1}$ to $365 \pm 61 \text{ min}^{-1}$.³⁸ This activation is achieved by a subtle change to the kinase conformation that triggers adoption of the active form. Phe1174 sits behind the ATP binding pocket and contributes to a hydrophobic phenyl core between the α C and activation loops (Figure 10A).⁶¹ Reducing the size of Phe1174 disrupts the packing, weakens interactions and allows the kinase domain to adopt an active conformation. Furthermore Phe1174 is in direct contact with Phe1271, part of the DFG motif. Asp1270, of the DFG loop, coordinates to a Mg^{2+} ion involved in ATP binding (Figure 10B). Reducing the size of Phe1174 to Leu1174 removes a structural constraint of the DFG loop and may allow Asp120 to adopt a more optimal coordination geometry, increasing binding affinity for ATP.³⁸

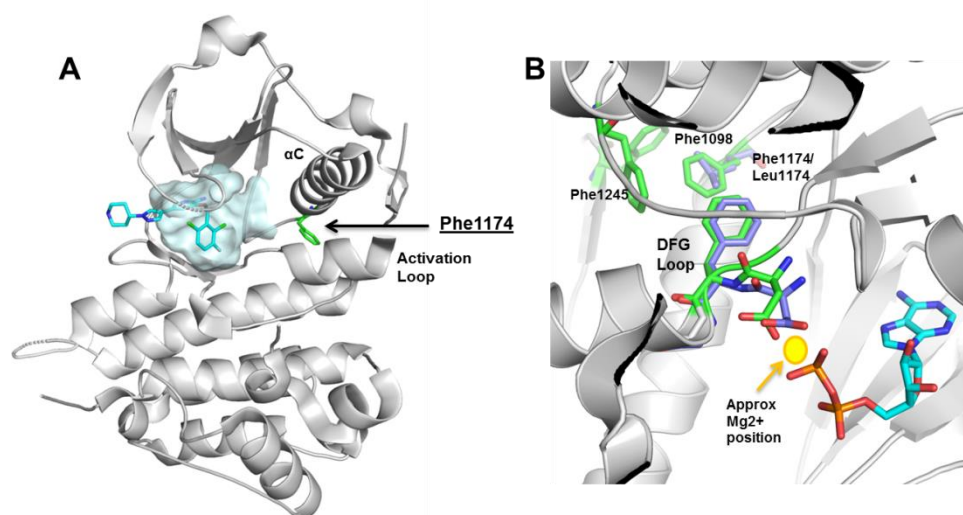


Figure 10. **A)** X-ray structure of crizotinib in ALK highlighting residue Phe1174 (2XP2). **B)** Overlay of ALK WT (green) and ALK^{F1174L} (purple) highlighting 'Phe' core, shift in DFG loop and ADP/Mg²⁺ coordination (2YJR and 3LCT).

1.2.2.2 ALK R1275Q Mutation

The ALK^{R1275Q} mutation is found in 45% of familial cases and 33% of sporadic cases of neuroblastoma.⁵¹ Arg1275 is positioned on a short α helix within the activation loop and provides stabilising hydrogen bond interactions with the α C helix (Figure 11A).⁶² These interactions contribute to stabilisation of the activation loop in its inactive conformation.

Mutation of this residue disrupts this stabilisation, and allows the activation loop to adopt a different, more extended conformation with the short α -helix no longer present (Figure 11B).⁶³ As a result, residue Tyr1278, a key driver of ALK activation, is now much more available for autophosphorylation compared to within the α -helix present in the wildtype structure.^{63,64} This provides a structural rationale for the activating R1275Q mutant which increases the k_{cat} 12-fold to $119 \pm 13 \text{ min}^{-1}$.³⁸

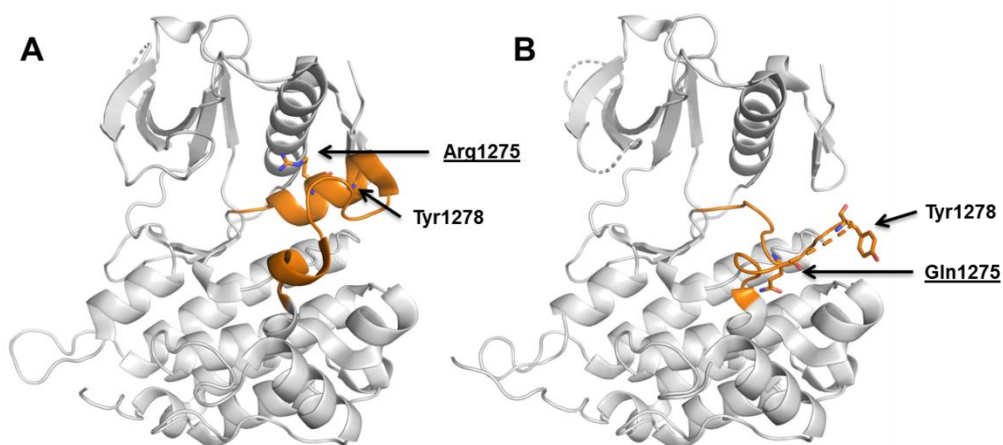


Figure 11. X-ray structure of **A)** apo ALK WT (3L9P) and **B)** apo ALK^{R1275Q} (4FNX) highlighting the mutant residue and shift in activation loop (orange).

1.2.3 First Generation Inhibitor Crizotinib

Crizotinib was the first ALK inhibitor to be approved by the FDA for treatment of ALK positive NSCLC (Figure 12). The compound was initially developed as a c-MET inhibitor by Pfizer with the ALK 'off-target' activity recognised later on in the project.⁶⁵ Crizotinib contains an 2-aminopyridine group which binds to the hinge residue Met1199 with the 3-benzyloxy group providing hydrophobic interactions within the ALK pocket.⁴⁵

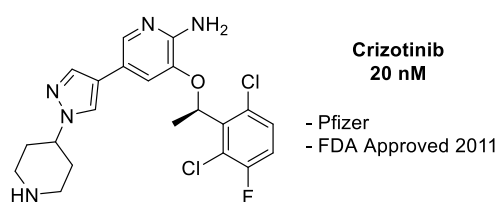


Figure 12. Structure of first-generation ALK inhibitor crizotinib.

However, the majority of patients develop resistance to crizotinib within 12 months due to various resistance mechanisms including amplification of the ALK fusion gene, by-pass signalling pathways and the development of secondary mutations.⁶⁶ Two secondary mutations were initially found in patients with the EML4-ALK fusion protein, gatekeeper residue L1196M and C1156Y, though many more mutations have been identified since around the ATP binding site (Figure 9B).⁶⁷⁻⁶⁹ The identification of

these mutations initiated the development of second-generation inhibitors to overcome these resistant mutations.

1.2.4 Second and Third Generation ALK Inhibitors

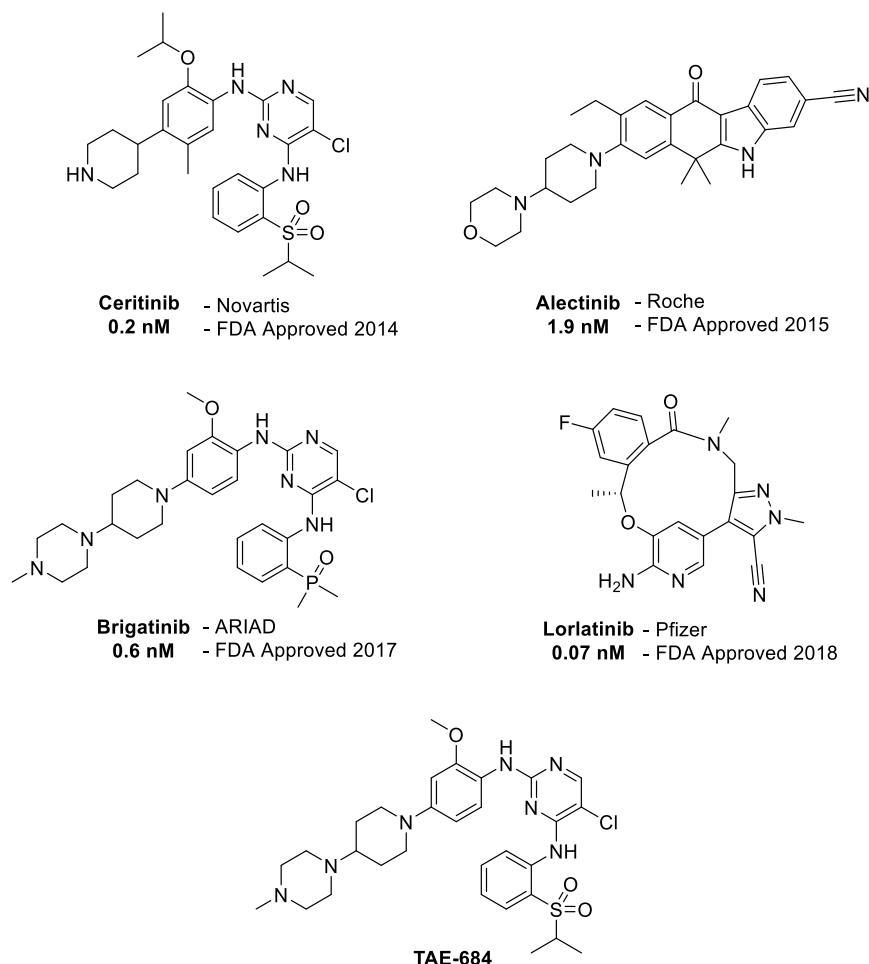


Figure 13. Structures of second- and third-generation ALK inhibitors.

Identification of secondary mutations quickly led to the development of novel second-generation inhibitors including ceritinib and alectinib (Figure 13). Ceritinib, developed by Novartis, received approval by the FDA in 2014, for NSCLC patients previously treated with crizotinib. Ceritinib is active against several crizotinib-resistant mutations including the gatekeeper mutations L1196M, G1269A, I1171T and S1206Y.⁵⁰ Ceritinib was developed from early ALK inhibitor TAE-684, improving the kinase selectivity by introducing the isopropoxy group and reducing metabolism on the electron rich aniline by reversing the piperidine attachment and inclusion of the methyl group *para* to the isopropoxy group.⁴⁶ The compound binds to the hinge region of ALK via a hydrogen bond donor and acceptor pair with the aminopyrimidine moiety.

The second ALK inhibitor approved by the FDA in 2014 was alectinib for patients with ALK positive NSCLC who have progressed or are intolerant to crizotinib treatment.⁷⁰ Alectinib is based upon a unique benzocarbazole core with the carbonyl interacting with hinge residue Met1199.⁷¹ Alectinib is sensitive to the L1196M gatekeeper mutation with a K_i of 1.6 nM as well as the C1156Y, F1174L and R1275Q mutations.^{65,72} The compound also has potent efficacy in other ALK-driven tumours including ALCL and neuroblastoma.⁷²

Brigatinib is a potent ALK, ROS1 and EGFR inhibitor and shows good selectivity over 9 crizotinib resistant mutations of the EML4-ALK fusion gene.⁷³ Brigatinib is similar in structure to ceritinib and TAE-684 but replaces the isopropyl sulfone group with a dimethyl phosphine oxide (DMPO). The DMPO aniline achieves similar potency to TAE-684 but improves selectivity over close family members insulin like growth factor 1 receptor (IGF1R) and insulin receptor (INSR).⁷⁴ In April 2017, the FDA approved brigatinib for the treatment of ALK positive NSCLC in patients with progressive disease with crizotinib treatment.⁷⁵

The third generation inhibitor lorlatinib was approved by the FDA in 2018, also for the treatment of ALK-driven NSCLC. Lorlatinib is a dual ALK-ROS1 inhibitor used to treat patients who have developed resistance to a crizotinib or second generation inhibitors ceritinib or alectinib. Lorlatinib was developed by Pfizer as a next generation inhibitor of crizotinib, with the aims of overcoming crizotinib resistant mutations and the ability to cross the blood brain barrier to target brain metastases.^{47,76} The compound has a novel macrocyclic scaffold containing the same aminopyridine hinge motif as crizotinib. Lorlatinib is brain penetrant, has high kinase selectivity and potently inhibits ALK resistance mutations from first or second generation inhibitor treatment including F1174L.^{47,73}

1.3 Bromodomain-4

1.3.1 Bromodomain Function

Acetylation of lysines on histone tails is a post-translational modification known to play an important role in chromatin modification and gene transcription.⁷⁷⁻⁷⁹ Dysfunctional levels of acetylation has been linked to the development of several diseases including cancer.^{80,81} The level of lysine acetylation is regulated by histoneacetyltransferases (HATs), which covalently modify the ϵ -amino group of

lysines, and histone deacetylases (HDACs) which remove the acetyl modification (Figure 14). In addition, post translational modifications such as acetylation are processed by ‘readers’. Bromodomains recognise and bind to acetylated histones, in turn recruiting other proteins to form transcriptional regulation and chromatin modelling complexes.^{82,83} The functional role and druggability of bromodomains has prompted the design of a rapidly increasing number of small-molecule bromodomain inhibitors to explore new phenotypes and to gain a better understanding on the function and role of bromodomains in different disease settings including cancer, inflammation and immunology.⁸⁴⁻⁸⁶

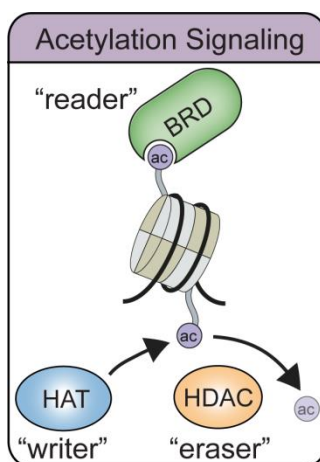


Figure 14. Acetylation signalling⁸⁷ – HATs add an acetyl moiety to the ϵ -amino lysine group and HDACs remove the acetyl moiety. Acetylated lysines on histones are recognised by bromodomains (BRD).

The human genome contains 61 bromodomains which are divided into eight subfamilies based on their sequence and structure (Figure 15).⁸⁸ Bromodomain-containing protein 4 is part of the bromo- and extra-terminal domain (BET) family and contains two sub bromodomain units, BRD4(1) and BRD4(2). Deregulation of BET proteins has been observed in cancer and inflammatory disease and consequently the BET family has been widely explored as a drug target with numerous chemical probes reported (see 1.3.3 for further discussion).^{84,89,90} Chemical probes and inhibitors targeting bromodomains other than the BET family have also been reported as reviewed by Moustakim *et al.*⁸³ Chemical probes have been developed for members of all the bromodomain subfamilies, aside from sub-family VI due to the challenge in finding hit compounds for their atypical binding residues, asparagine in MLL and threonine in TRIM28.⁸³

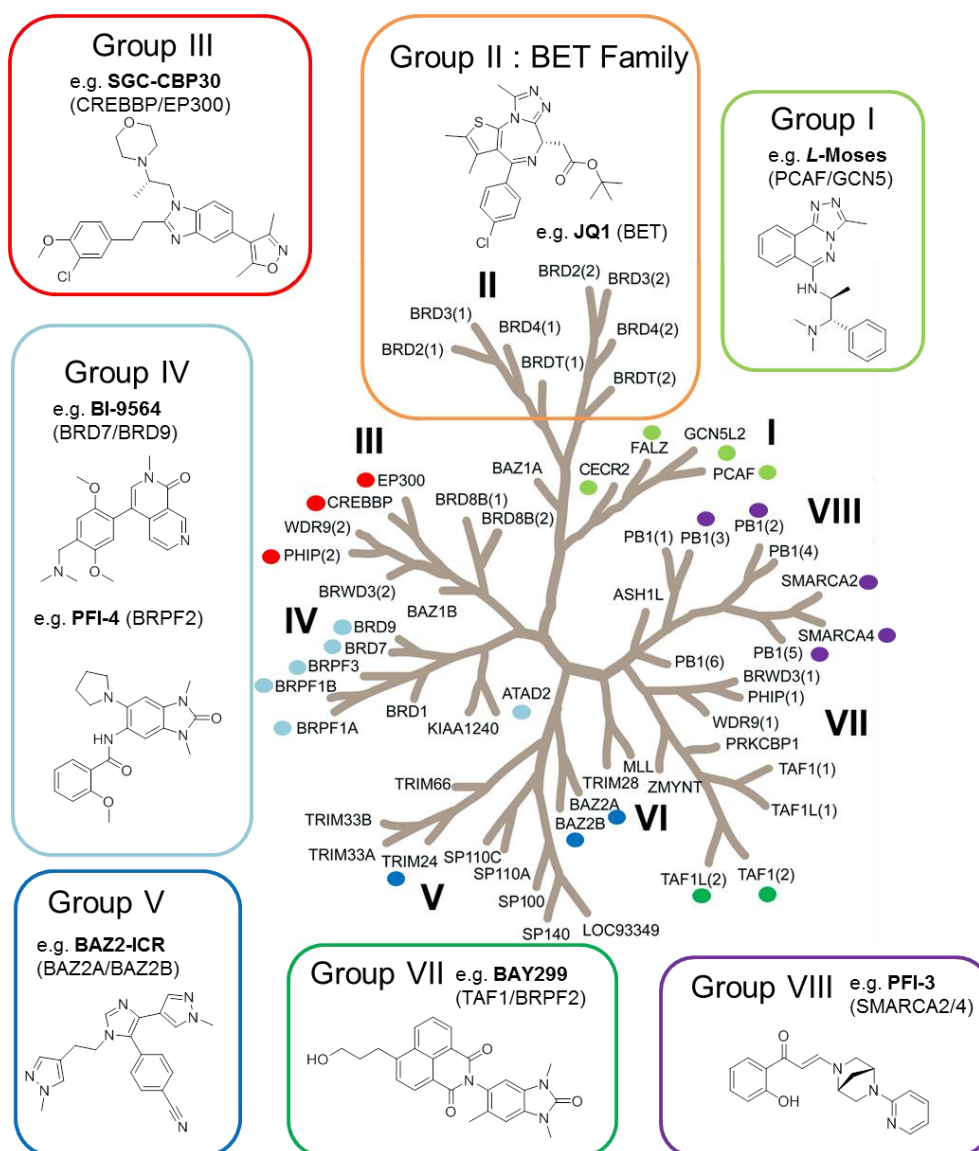


Figure 15. Bromodomain family tree consists of subfamilies I-VIII. Bromodomains marked with a circle have reported inhibitors. Example chemical probes/inhibitors for each subfamily are shown.

1.3.2 Structure of BRD4

The bromodomain structure consists of four α -helices linked by loop regions which surround the acetylated lysine binding pocket (Figure 16A).⁸⁵ The acetylated lysine forms a hydrogen bond with a conserved asparagine, in the case of BRD4(1) Asn140. Bromodomain inhibitors mimic this hydrogen bond interaction as demonstrated by the triazole of BET-inhibitor JQ1 (Figure 16B). In the BRD4 pocket is a network of conserved water molecules situated in the region known as the ZA channel which is

framed by the ZA loop.⁸⁴ Adjacent to the ZA channel is a region known as the 'WPF shelf' due to a conserved WPF motif in BET family members and a handful of other bromodomains such as PCAF and CECR2. Both the ZA channel and WPF shelf region provide further possibilities to enhance potency and selectivity over other bromodomain sub-families.⁸⁴ For example, bromodomain BAZ2B lacks the structure of the ZA channel and WPF shelf due to changes in pocket residues, BAZ2B inhibitor BAZ2-ICR adopts a π -stacking arrangement that cannot fit into the more enclosed BRD4 pocket hence achieving selectivity over the BET family.⁹¹ The final region used to achieve selectivity is the gatekeeper residue located at the entrance of the pocket. In BRD4 this residue is Ile146 but for bromodomains BRD9 and PCAF this residue is a tyrosine. This allows for inhibitors such as BI-9564 and *L*-Moses to form π - π stacking interactions and achieve selectivity over the BET family (Figure 15).^{92,93}

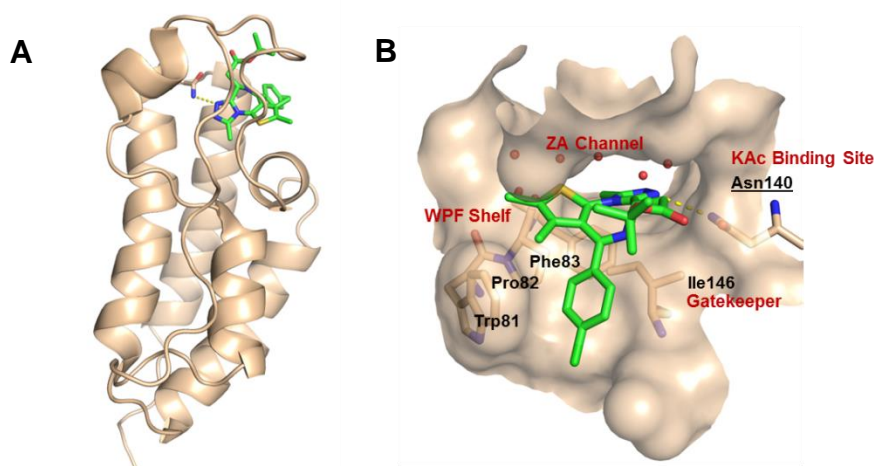


Figure 16. Overview of bromodomain binding site (3MXF). **A)** Structure of BRD4(1) and JQ1 complex showing 4 helix bundle and KAc binding site. **B)** Close up of KAc binding site with key amino acids and structural features highlighted.

1.3.3 Current BET Inhibitors

Many BET inhibitors have been identified and used as chemical probes to understand the molecular role of BET inhibition. BET proteins are considered to be very druggable targets and more inhibitors have been reported for the BET family than all of the other bromodomains combined.⁸⁴ The first potent and selective BET inhibitors disclosed were JQ1⁹⁴ and I-BET672⁹⁵, closely followed by I-BET151⁹⁶ and PFI-1⁹⁷ (Figure 17). These four compounds represent the three main types of KAc mimetic

observed in BET inhibitors: a triazole (JQ1 and I-BET762), a dimethyloxazole (I-BET151) and a pyridone-like moiety (PFI-1). All three motifs form a hydrogen bond interaction with Asn140 and a conserved water in the BRD4 pocket, which in turn interacts with Tyr97 (Figure 18). The majority of disclosed BET inhibitors contain one of these KAc mimetic motifs and several reviews discuss the vast variety of compounds since identified from those in Figure 17.^{80,84,86}

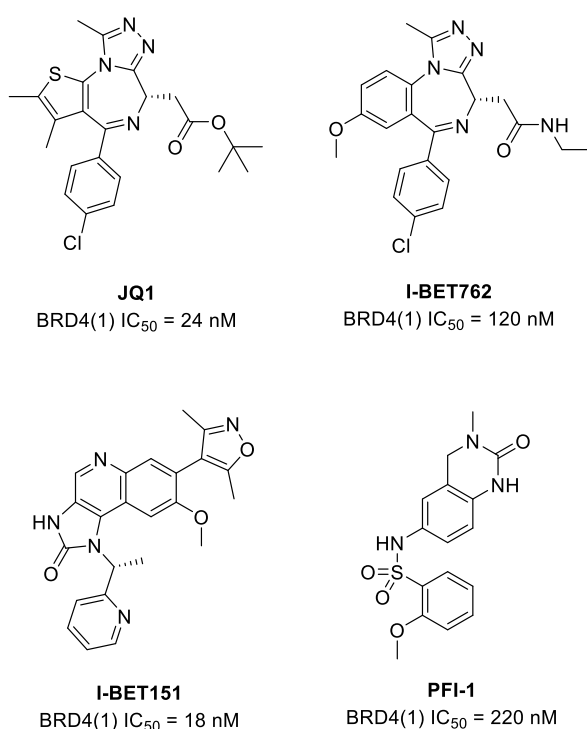


Figure 16. Structures of BET bromodomain inhibitors.

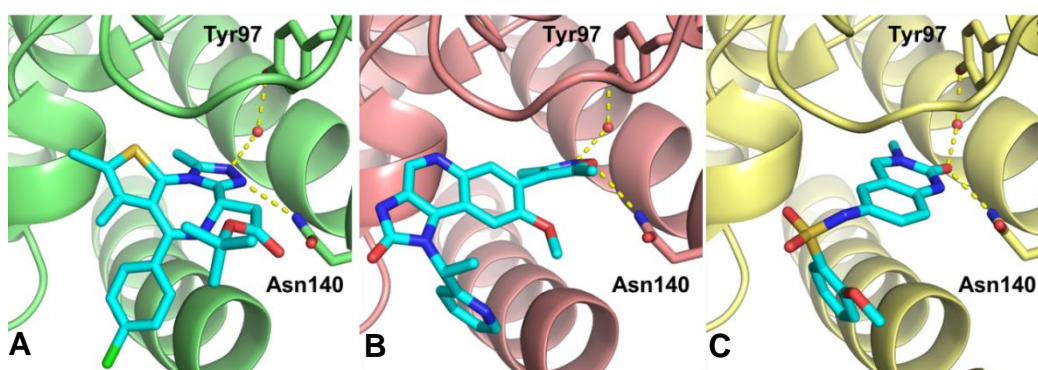


Figure 17. Key interactions for **A**) JQ1 (triazole, 3MXF), **B**) I-BET151 (dimethylisoxazole, 3ZYU) and **C**) PFI-1 (pyridone-like, 4E96).

Alternative approaches to BET inhibition have been reported, including bivalent inhibition and the use of protein targeting chimeras (PROTACs). The former approach

involves the simultaneous binding of the first and second bromodomains (BD1 and BD2) of BRD4, achieved by inhibitor BiBET (Figure 19).⁹⁸ The compound contains two triazole KAc mimetics, one at each end of the molecule, to allow bivalent binding to BD1 and BD2. BiBET demonstrates high cellular potency with an EC_{50} of 100 pM and enhanced cancer-cell growth inhibition compared to monovalent inhibitor I-BET762.⁹⁸

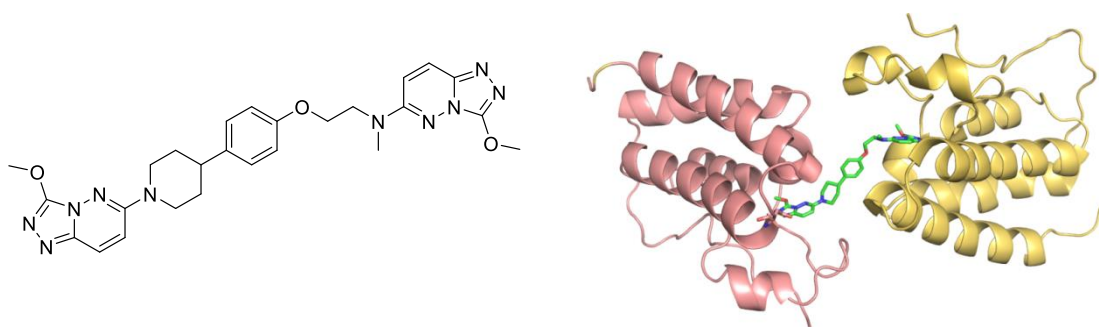


Figure 19. A) Structure of bivalent inhibitor BiBET. **B)** X-ray structure of BiBET with BRD4(1) dimer (5AD3).

The second alternative approach to target BRD4 is the use of the rapidly growing technique, targeted protein degradation. PROTACs are small molecules which bind to a target protein and recruit an E3 ubiquitin ligase to allow for ubiquitination of the target protein and subsequent degradation by the proteasome.⁹⁹ The molecule is comprised of three components: a small molecule inhibitor for the target protein, an E3 ligase binding ligand and a linker region (Figure 20). One example of a BRD4-targeted degrader is ARV825, which consists of OTX015 as the BRD4 binding ligand and pomalidomide to bind to the E3 ligase cereblon.¹⁰⁰ ARV825 induces effective degradation of the BET proteins as well as superior MYC suppression compared to JQ1 and OTX015.^{100,101} Similarly, compound MZ1 is able to effectively degrade BET bromodomains.¹⁰² MZ1 utilises a different E3 ligase, the von Hippel-Lindau E3 ligase, and JQ1 as the BRD4 binding ligand.

Interestingly MZ1 shows selective degradation for BRD4 over BRD2 and BRD3.¹⁰³ Achieving selectivity between the BET bromodomains is a challenge due to high homology between the family members; all BET bromodomains exhibit 95% sequence homology at the KAc binding site.¹⁰⁴ The majority of BET inhibitors are pan-BET inhibitors which poses an issue due to impacting numerous transcriptional pathways and the specific functions of BET members. Therefore MZ1 represents a

unique method to target BRD4 selectively rather than the use of a pan-BET inhibitor.¹⁰⁴

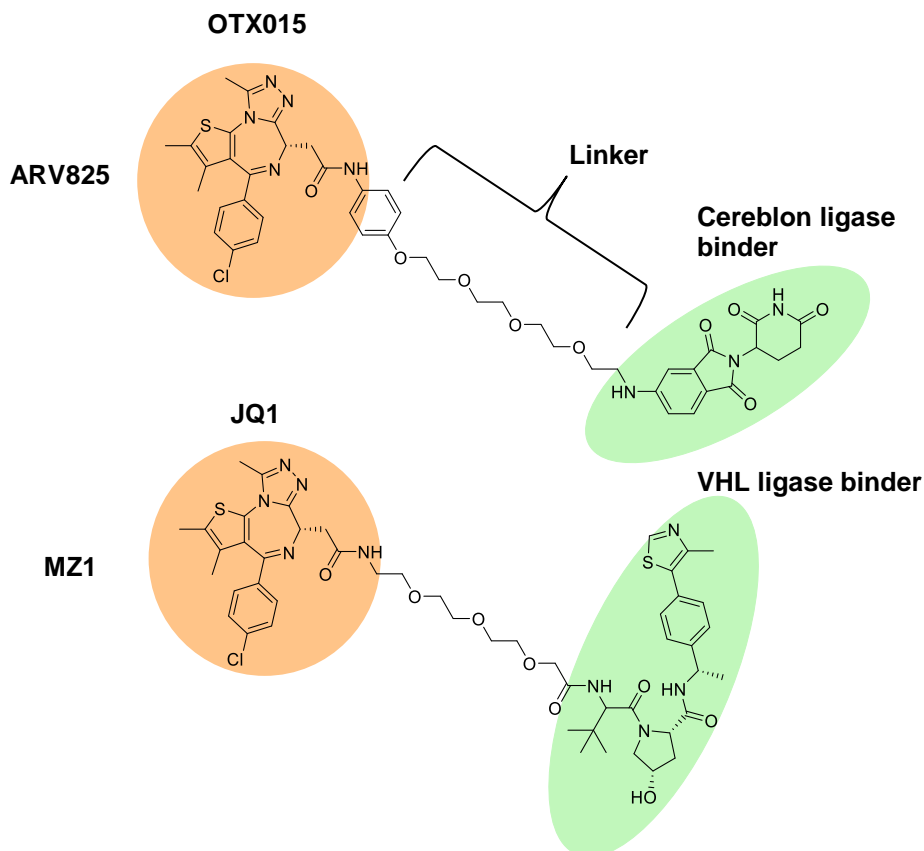


Figure 20. Structures of BRD4 PROTACs. PROTACs are made up of a small molecule inhibitor for the target protein (orange), a linker and a ligand for the E3 ubiquitin ligase (green).

Recently, small molecule inhibitors have been reported as being selective for BRD4 over other BET bromodomains. Raux *et al.* discovered a class of xanthine based inhibitors (**1**) with a greater than 10-fold selectivity towards BRD4-BD1 (Figure **21**).¹⁰⁵ This was attributed to the different dynamic behaviour of the ZA loop between the BET bromodomains whilst BD1 selectivity was achieved by interaction with a glutamine residue (a lysine in BD2). In 2015, Bayer disclosed compound BAY1238097 which shows selectivity for BRD4 (63 nM) over BRD3 (609 nM) and BRD2 (2430 nM).¹⁰⁶

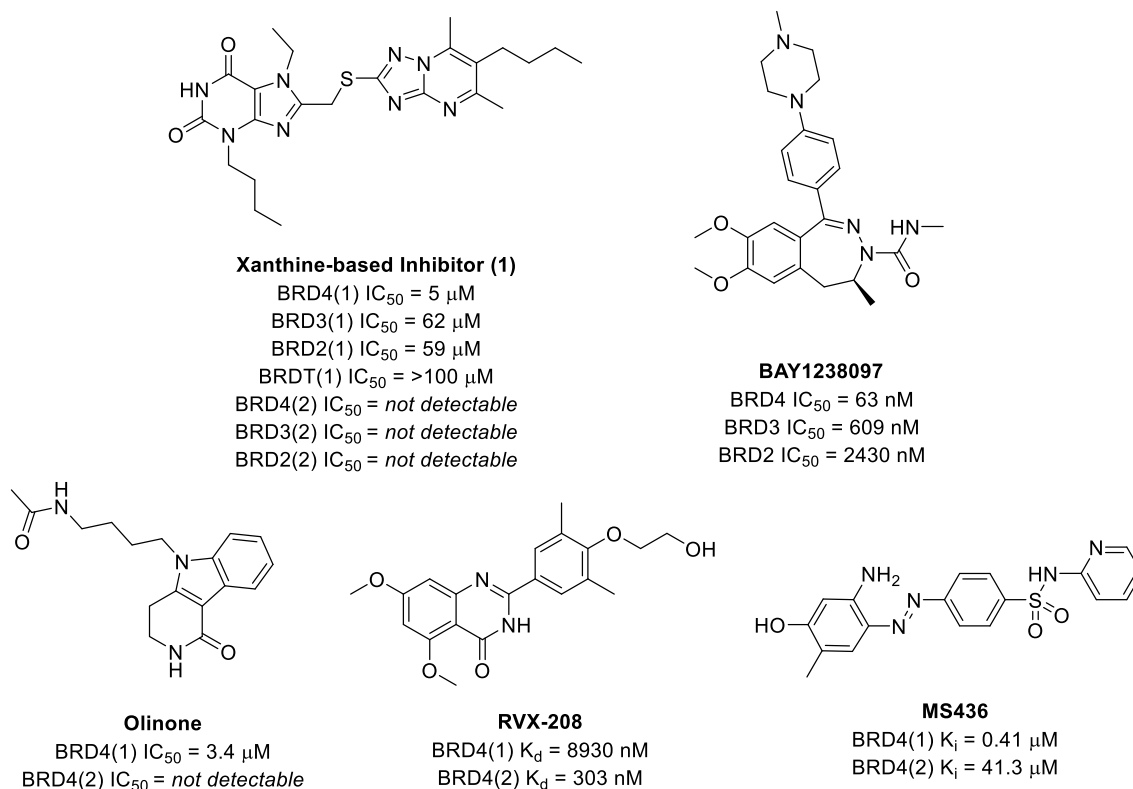


Figure 21. Scaffolds of inhibitors that achieve selectivity within the BET family or between BD1 and BD2.

Selective targeting of the first or second bromodomain of BRD4 also provides an opportunity to achieve selective transcriptional effects.¹⁰⁴ Discriminating between the first and second bromodomains of the BET family has shown more promise than achieving selectivity within the BET family due to exploitation of a few structural differences between the BD1 and BD2 pockets. Sequence comparison of BRD4(1) and BRD4(2) revealed three key differing residues: Gln85 in BD1 is Lys378 in BD2, Asp144 in BD1 is His437 in BD2 and Ile146 is Val439 in BD2 (Figure 22).

Preferential binding for BD1 has been observed with compound Olinone, exhibiting a greater than 100-fold selectivity over BD2 (Figure 21).¹⁰⁷ The tricyclic structure interacts with BD1 specific residue Asp144 but is predicted to clash with BD2 specific residue His437. Selectivity for BD1 has also been observed with a series of azobenzene BET inhibitors, with compound MS436 showing 10-fold selectivity towards BD1 over BD2.¹⁰⁸ In comparison, BD2 selectivity has been observed with compound RVX-208, showing a 30-fold selectivity for BD2 over BD1. Additional potency with the BD2 pocket is achieved by stacking of BD2 residue His437 against the phenyl ring.¹⁰⁹

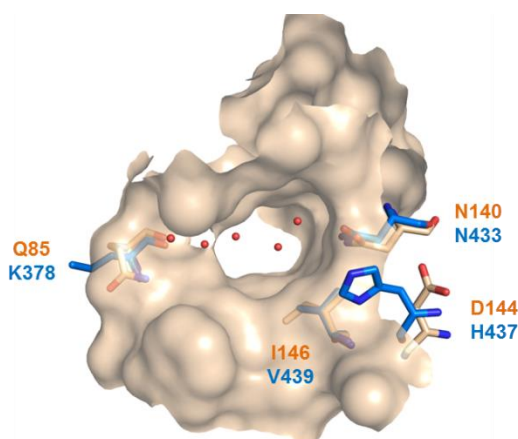


Figure 22. Residue differences between BRD4-BD1 (pale orange, 6Q3Z) and BRD4-BD2 (blue, 6FFD).

1.4 Polypharmacology

It is increasingly recognised that targeting multiple pathways that support cancer growth and survival is necessary to treat aggressive cancers and overcome resistance.^{110,111} Due to the molecular and genetic complexity of cancer, a single agent targeting a single oncogenic pathway might not be sufficient to provide a durable response.¹¹² Therefore focus is switching to drug discovery strategies which simultaneously target multiple pathways, either as a combination treatment or a polypharmacological drug. Over half of all combination trials are conducted in oncology highlighting the prevalence and interest in achieving effective combinations for cancer treatment.¹¹³

However, drug combinations can lead to undesired side effects, drug-drug interactions and pharmacokinetic complexity.¹¹⁴ In children, combination trials are much more complicated due to increased chance of toxicity when two agents are tested and an increased length of trials due to establishing a tolerable dose for each new agent in very small patient populations.

An alternative method for targeting multiple pathways is the use of a dual inhibitor. A single polypharmacological agent should have the same advantages as combinatorial treatments, such as improved therapeutic efficacy and prevent drug resistance, but should also minimise the liabilities.^{114,115} In addition to reducing the length and complexity of trials, the administration of a dual inhibitor would also decrease the

chance of drug-drug interactions, off-target toxicities and additive toxicities. A dual inhibitor would have a more predictable pharmacokinetic profile than multiple compounds administered in combination and also reduce costs in development and testing.¹¹⁶ Prominent examples of polypharmacological drugs are multi-kinase inhibitors, exploiting the secondary kinase activity to disrupt multiple pathways in cancer survival.¹¹⁷⁻¹¹⁹

The design and development of dual inhibitors that specifically inhibit two targets, particularly when they are structurally distinct and not from the same family, is challenging.¹¹⁰ It is difficult to balance multiple activities whilst also controlling the selectivity and physicochemical and pharmacokinetic properties of the compound.^{111,112} A further disadvantage is that with drug combinations the ratio of activities can be changed by modifying the dose of each compound but a single compound has a fixed ratio of activities. For biological investigation a selective target profile is desired; excessive promiscuity can lead to off-target toxicities.¹¹¹ Therefore managing the selectivity of two protein families within a small molecule scaffold, in this case kinases and bromodomains, is essential but challenging. Although multi-targeted kinase inhibitors have been used in oncology, the rational design and development of a dual kinase bromodomain inhibitor as a therapeutic has yet to be achieved.

1.5 Dual Kinase-Bromodomain Inhibition

1.5.1 Identification of Dual Kinase-Bromodomain Inhibitors

Co-targeting of kinases and bromodomains, which both play key roles in cancer and inflammatory disease is an attractive strategy to target multiple cancer pathways and overcome problems of resistance.^{115,120} Synergy between bromodomains and kinases has been identified in several settings, providing excellent rationale for the development of dual kinase-bromodomain inhibitors as potential therapeutics. For example, JAK kinase and BRD4 have key roles in multiple myeloma models^{101,121} and the FLT3 kinase and BRD4 are both drivers in acute myelogenous leukaemia (AML).¹²² In combination, the FLT3 inhibitor Ponatinib and JQ1 demonstrate a lethal effect in AML cell lines.¹²³ Synergistic effects have also been reported between Ibrutinib, a BTK inhibitor, and JQ1 against mantle cell lymphoma (MCL)¹²⁴ and between BET inhibitors and inhibitors targeting the PI3K pathway.^{125,126}

In 2014 Ciceri *et al.* discusses the possibility of rationally designing dual kinase-bromodomain inhibitors to improve current therapies.¹¹⁵ Cross-reactivity between 628 inhibitors and BRD4 was identified through AlphaScreen, with 12 compounds exhibiting strong inhibition of binding polyacetylated histone H4 peptide (Figure 23). At a similar time, Ember *et al.* established binding modes through BRD4 crystallisation studies of 194 kinase inhibitors, identifying a similar set of 14 kinase inhibitors with nanomolar or low micromolar bromodomain activity.¹²⁷

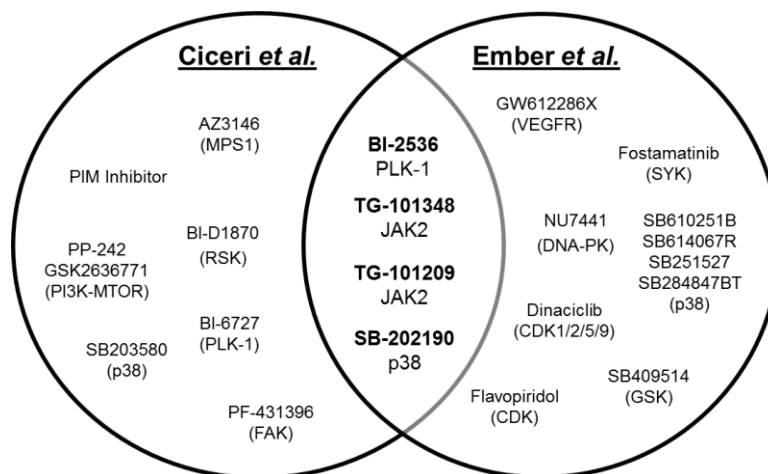


Figure 23. Kinase inhibitors identified by Ciceri *et al.* and Ember *et al.* showing BRD4 activity.

Two compounds that exhibit nanomolar potency for BRD4 and excellent selectivity for the BET family of bromodomains are the PLK-1 inhibitor BI-2536 and the JAK2 inhibitor TG-101348, with K_d values of 37 and 164 nM respectively (Figure 24A+B). Considering the kinase selectivity of the compounds, TG-101348 is a promiscuous kinase inhibitor and a good example of the difficulty in achieving selectivity with a cross-family dual inhibitor (Figure 24C). Conversely BI-2536 demonstrates relatively good kinase selectivity for PLK-1 with a handful of other targets below 200 nM potency, including CAMKK2, DAPK3 and ALK.¹²⁸ BI-2536 is an excellent example that demonstrates selective dual kinase-bromodomain inhibition can be achieved.

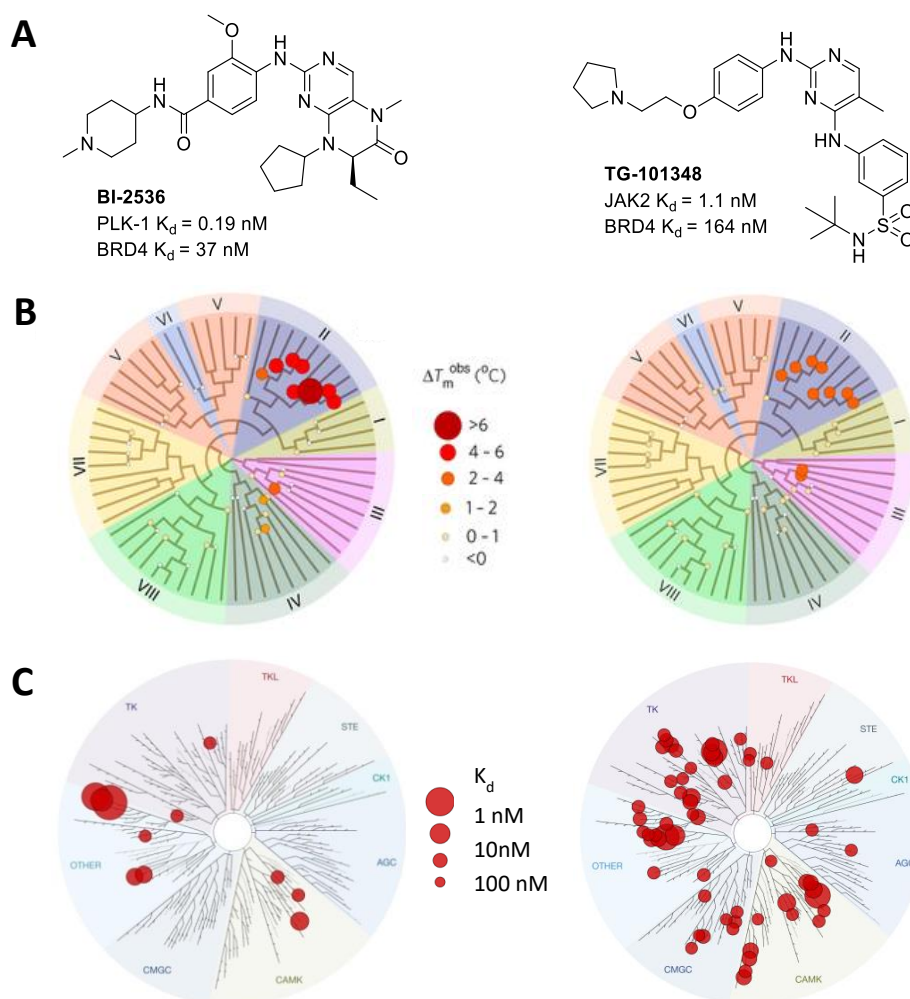


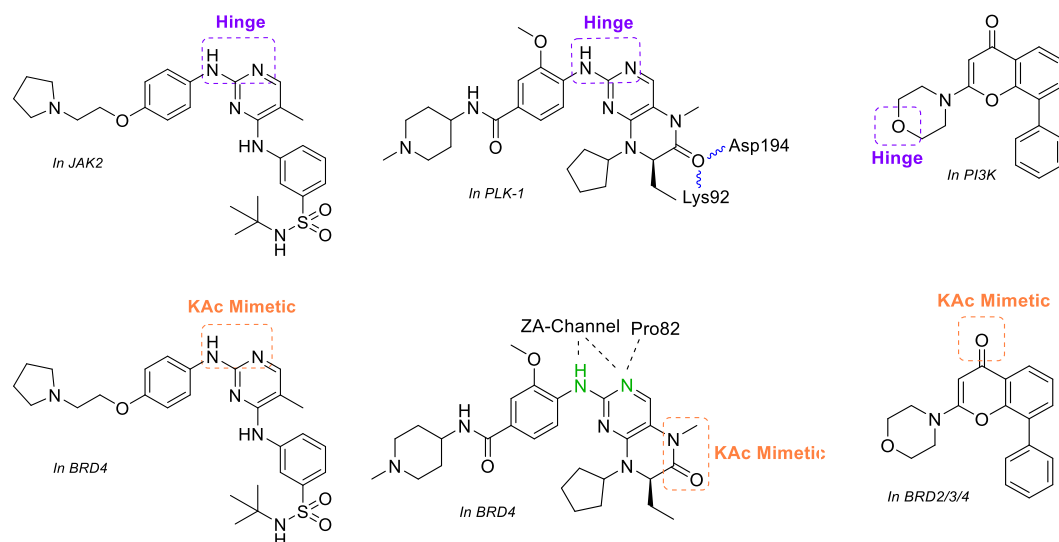
Figure 24. **A)** Structures and activities of dual inhibitors BI-2536 and TG-101348. **B)** Bromodomain interaction map of T_m shift data collected using a panel of 46 bromodomains.¹¹⁵ T_m shift represented by circle size and colour. **C)** Kinome interaction map showing interactions with K_d <250 nM.¹²⁸ Larger circles indicate higher affinity interactions.

1.5.2 Structural Analysis of Dual Kinase-Bromodomain Inhibitors

Structural analysis of the aforementioned inhibitors revealed different binding types for achieving dual kinase-bromodomain inhibition. Ember *et al.* classify the dual inhibitors into three different binding types: N Type, PZA/ZA Type and I Type (Table 3).¹²⁷

The first binding type is 'N-Type' which is when the kinase hinge binding motif also acts as the KAc mimetic, directly interacting with Asn140.¹²⁷ This is exemplified by TG-101209 and TG-101348 where the aminopyrimidine moiety binds to both the

hinge region and Asn140 via a hydrogen bond donor and acceptor. Designing novel dual inhibitors of this type may be challenging due to the overlapping binding regions. This binding region overlap makes it more difficult to extend and modify into two structurally different targets and may result in less potent inhibitors and also promiscuous inhibitors, like the kinase profile of TG-101348 (Figure **23C**).



| N-Type | PZA/ZA-Type | I-Type |
|---|--|---|
| Hinge binding region interacts with Asn140 | Hinge binding region interacts with Pro82 and/or ZA channel | Hinge binding region does not interact with bromodomain |
| KAc mimetic coincides with the hinge binding region | KAc mimetic forms polar interactions with conserved back pocket residues | KAc mimetic does not interact with kinase |
| e.g TG-101348 , TG-101209 | e.g BI-2536 , GW612286X | e.g. LY294002 , SB202190 |

Table 3. Summary of the binding modes of dual kinase-bromodomain inhibitors.

The second type of dual inhibitor is 'PZA- or ZA-Type' in which the hinge binding region interactions with Pro82 and/or the ZA channel of waters.¹²⁷ The KAc mimetic is elsewhere on the structure as observed with BI-2536; the KAc mimetic is spatially separated from the aminopyrimidine hinge motif on the dihydropteridinone core. Although the binding regions are still relatively close, this type of dual inhibitor potentially offers more room for modification to different targets compared to N-type dual inhibitors.

The final type is 'I-Type' in which the hinge region does not interact with the asparagine residue and the KAc mimetic does not interact with the hinge binding

region. An example of an I-type inhibitor is NU7441 where the morpholine interacts with the kinase and the carbonyl acts as the KAc mimetic.¹²⁷ This type of dual kinase-bromodomain inhibitor offers a lot of freedom for modification due to kinase and bromodomain binding regions being on separate parts of the molecule and not interacting with the other target.

1.5.3 Current scope of Dual Kinase-Bromodomain Inhibitors

The reports by Ciceri *et al.* and Ember *et al.* provide important precedence for dual kinase-bromodomain inhibition and structural insights. However the combination of bromodomain and kinase inhibited by these dual inhibitors was discovered serendipitously by screening selective kinase inhibitors against BRD4. To date, there are a few published reports of discovery efforts that aim to combine inhibition of a particular kinase with bromodomain inhibition into a single dual inhibitor to explore a specific disease hypothesis.

Several papers have expanded on the dual inhibitors identified by Ciceri *et al.* and Ember *et al.* Dual PLK-BRD4 inhibitors, BI-2536 and BI-6727, have showed efficacy as latency reversing agents for the treatment of HIV-1¹²⁹ whilst several papers discuss further modification of BI-2536 to modulate the kinase and bromodomain activity.^{130,131} This is exemplified by compound **2** which shows a balanced BRD4 and PLK-1 activity profile (Figure **25**).¹³²

Schonbrunns team have continued from their identification of TG-101209 to develop novel dual kinase-bromodomain agents based on the same di-aminopyrimidine scaffold.¹³³ Example compound **3** potently inhibits BRD4 ($IC_{50} = 34$ nM) and a series of tyrosine kinase inhibitors including JAK2, FLT3 and RET and ROS1 ($IC_{50}s = 0.9 - 1.1$ nM). Lead compounds including **3**, showed promising potential as novel cancer therapeutics with on target inhibition in several blood cancer cell lines.

Divakaran *et al.* expand on the 1,4,5-trisubstituted imidazole structure of SB284847BT, a p38 inhibitor.¹³⁴ For example compound **4** shows modest BRD4 potencies at 1.8 μ M but unexpectedly they achieve selectivity towards BD1 over BD2 due to steric hindrance of a histidine residue in BD2 (aspartic acid in BD1). With further development these compounds may reach potent and BD1 selective dual p38-BRD4 inhibitors.

Dual PI3K-BRD4 inhibitor SF2535, which has similar scaffold to previously identified LY294002 and NU7441, has been shown to disrupt function of MYC.¹³⁵ The dual inhibitor impairs PI3K and BRD4 signalling causing MYC downregulation and subsequent inhibition of cancer cell growth and metastasis. Importantly the dual inhibitor is compared to the two individual inhibitors combined and demonstrates improved efficacy and toxicity.

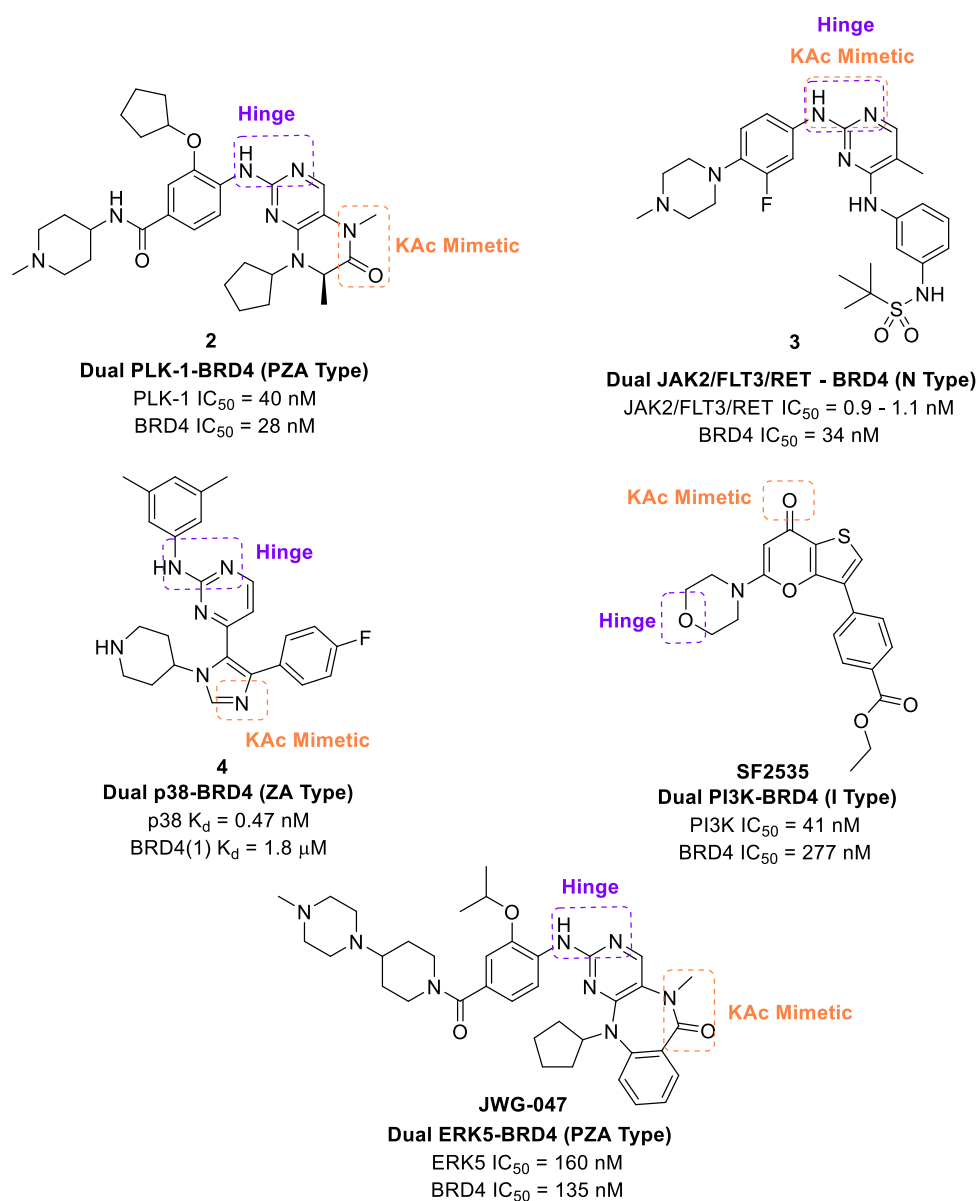


Figure 25. Recently identified dual kinase-bromodomain Inhibitors.

Finally a novel dual kinase-bromodomain combination was explored by Wang *et al.* with the development of JWG-047, an ERK5-BRD4 inhibitor.¹³⁶ This combination was proposed for potential cancer drug target combination although biological evidence for this combination is yet to be discussed.

Overall, there has been successful discovery of novel dual kinase-bromodomain inhibitors but these polypharmacological agents have yet to reach the clinic to demonstrate their therapeutic benefits.

1.6 Project Aims

1.6.1 Project Hypothesis

A possible effective but unavailable treatment for high-risk neuroblastoma patients is the concomitant inhibition of ALK and BRD4 in a single molecule to block both oncogenic drivers: the mutant ALK kinase and *MYCN*. Combining both ALK and BRD4 inhibition would serve two purposes. Firstly the dual inhibitor would target the two key oncogenic drivers of high-risk neuroblastoma and diminish *MYCN* expression, potentially resulting in strong antiproliferative or proapoptotic effects. In addition, blocking two targets at once lowers the risk of resistance, due to the probability of clonal adaptation to targeted therapy being lower for combination therapies.¹³⁷

No dual ALK-BRD4 inhibitor was identified in the kinase inhibitor screening performed by Ciceri *et al.* and Ember *et al.* and none has been described so far. Therefore the design strategies outlined in these papers would need to be applied to the new kinase-bromodomain combination to explore the specific disease hypothesis.

The overall hypothesis is that dual inhibition of ALK and BRD4 is beneficial to neuroblastoma patients when compared to single ALK and BRD4 inhibitors and that a dual ALK-BRD4 inhibitor can be rationally designed. The project aims are thus:

- Design and synthesise dual ALK-BRD4 inhibitors to validate the concept of dual inhibition in neuroblastoma cell lines.
- Compare effectiveness of dual inhibitors with stand-alone inhibition of ALK and BRD4 and combinations of ALK and BRD4 inhibitors.
- Contribute to the field of rationally designed dual kinase-bromodomain inhibition.

1.6.2 ALK and BRD4 Synergy

At the beginning of the project, it was important to investigate if the two targets, ALK and BRD4, displayed synergy rather than antagonism. The synergism between ALK and BRD4 was tested using the Chou-Taleley method, carried out by my collaborator Lizzie Tucker.¹³⁸ The GI_{50} of BRD4 inhibitor JQ1 and ALK inhibitor ceritinib were measured individually and also as a combination (Figure 26A). The GI_{50} of the combination of the two drugs is more potent used in combination at 0.6 μ M, compared to 3.1 μ M (JQ1) and 1.6 μ M (ceritinib). A combination index was then calculated for the two drugs at 50% surviving fraction giving a value of 0.25, which is within the synergistic region of the isobologram plot (Figure 26B). This provided good evidence that ALK and BRD4 are synergistic rather than antagonistic.

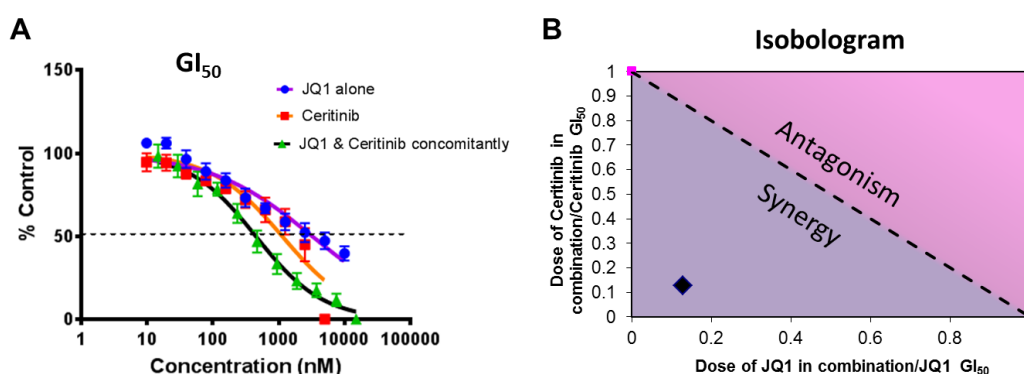
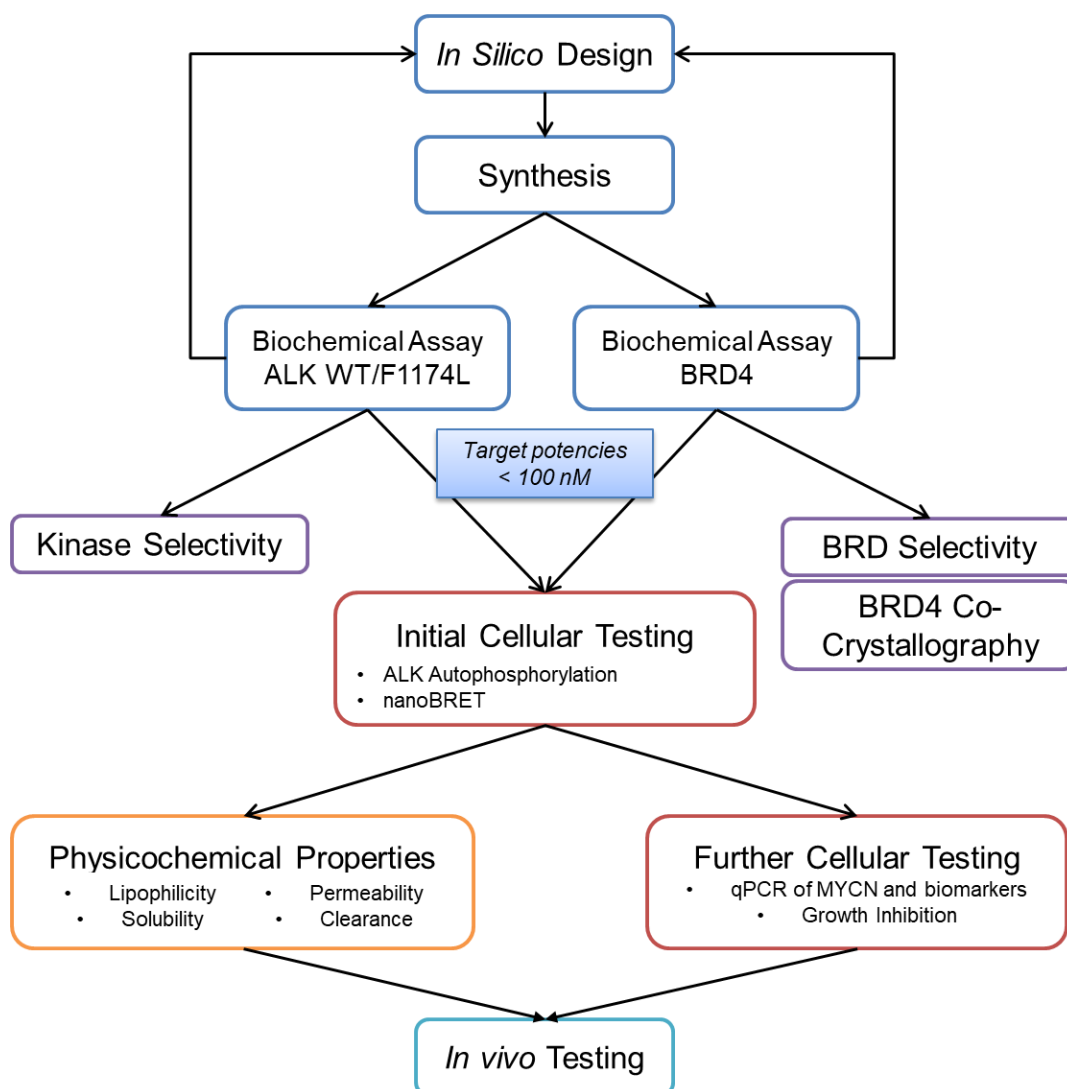


Figure 26. Chou Taleley experiment between JQ1 (BRD4 inhibitor) and ceritinib (ALK inhibitor) **A)** GI_{50} values of JQ1, ceritinib and as a combination **B)** Isobologram depicting the combination index between JQ1 and ceritinib. Performed by Lizzie Tucker.

1.6.3 Project Cascade

The project followed the cascade outlined in Scheme 1. The project started with the *in silico* design of the dual inhibitors, utilising docking methods and examining ALK and BRD4 structures and known inhibitors, to identify suitable modifications to benefit both targets. The dual inhibitors were synthesised and tested in biochemical assays against ALK (WT and F1174L mutant) and BRD4. This process was iterative until compounds with desired biochemical potencies of <100 nM at both targets were achieved.

Selected compounds were taken forward to look at the broader kinase and bromodomain selectivity. Co-crystal structures of selected compounds and BRD4 were solved, by my collaborators at the Goethe University of Frankfurt. Despite several attempts, ALK co-crystallography was not possible due to difficulties with protein production and purification and the modest activity of earlier analogues.



Scheme 1. Project cascade for the development of dual ALK-BRD4 inhibitors.

Potent compounds were also taken forward for initial cellular testing to confirm on-target engagement of the dual inhibitors in a cellular context. The first cellular experiments included measuring ALK autophosphorylation levels and nanoBRET target engagement assays. Further cellular experiments were available, in collaboration with the Paediatric Solid Tumour team at the ICR. This included measuring levels of BRD4-regulated transcripts MYCN and tyrosine hydroxylase (Th) using quantitative, reverse transcription, polymerase chain reaction (qRT-PCR), as

well as measuring growth inhibition in normal and resistant cell lines. Meanwhile the physicochemical properties of promising compounds were measured, including the solubility, permeability and clearance. Compounds with good biochemical and cellular potency as well as favourable physicochemical properties were suitable to put forward for *in vivo* experiments.

Chapter 2 Design and Synthesis of First Generation Dual ALK-BRD4 Inhibitor

Part of this chapter is published in E. Watts et al., *J. Med. Chem.*, 2019, 62, 2618-2637

2.1 Introduction to BI-2536

My aim at the start of the project was to discover starting points that showed significant activity against ALK and BRD4. Of particular interest was dual kinase-bromodomain inhibitor BI-2536 (Figure 27A). The compound was discovered and developed as a PLK-1 kinase inhibitor but was found to potently inhibit BRD4 by Knapp and Schönbrunn's labs.^{115,127,139}

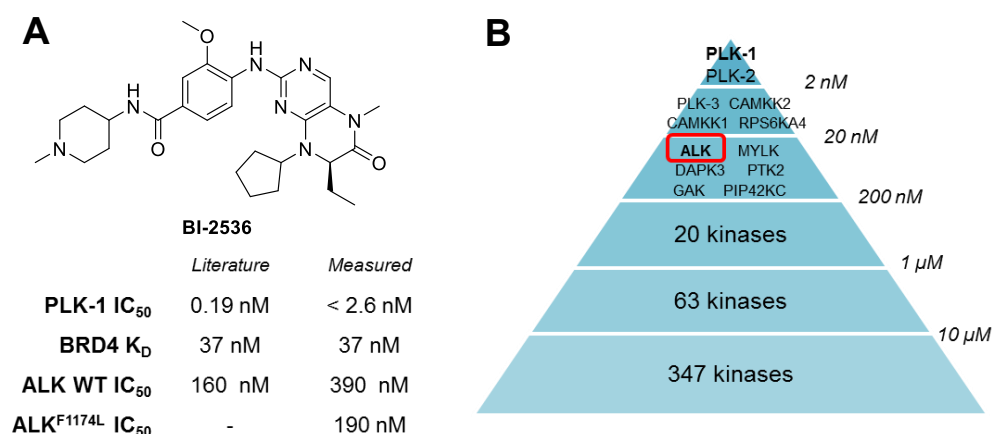


Figure 27. A) Biochemical activity data and **B)** kinase selectivity data for BI-2536.

A comprehensive screening of kinase inhibitors, including BI-2536, was performed by Davis *et al.* to understand kinase selectivity.¹²⁸ Among the results, BI-2526 exhibited modest activity against ALK at 160 nM and a binding preference for ALK over the majority of other kinases. (Figure 27B) The selectivity of BI-2536 is partially due to the presence of the methoxy substituent. Few kinases are able to accommodate this substituent due to a steric clash with a larger tyrosine or tryptophan residue in the hinge region. Amongst the exceptions are PLK-1 and importantly ALK due to the presence of a smaller leucine at this position.^{140,141}

Following from this finding, I tested BI-2536 tested against ALK WT and ALK^{F1174L} using a LanthaScreen® assay format showing comparable activities of 390 nM and

190 nM respectively. In addition, binding against BRD4 and PLK-1 were confirmed. The potency of BI-2536 against PLK-1 was beyond the dynamic range of the assay ($IC_{50} < 2.6\text{nM}$) consistent with a published K_d of 0.19 nM.¹²⁸

With BI-2536 established as a dual kinase-bromodomain inhibitor and demonstrating modest ALK activity and kinase selectivity, BI-2536 was a suitable starting point for the discovery of a dual ALK-BRD4 inhibitor.

2.1.1 PLK-1

Polo-like kinase 1 is a member of the PLK family of serine/threonine protein kinases and plays key roles during many stages of the cell cycle, in particular during mitosis. PLK-1 controls the G2/M checkpoint (mitotic entry) by activating the CDK1/cyclinB complex and regulates the spindle assembly checkpoint in preparation for metaphase (Figure 28).¹⁴² PLK-1 also plays roles in centrosome maturation, chromosome segregation by activation of the anaphase-promoting complex/cyclosome (APC/C) pathway and controls mitotic exit and cytokinesis.¹⁴³

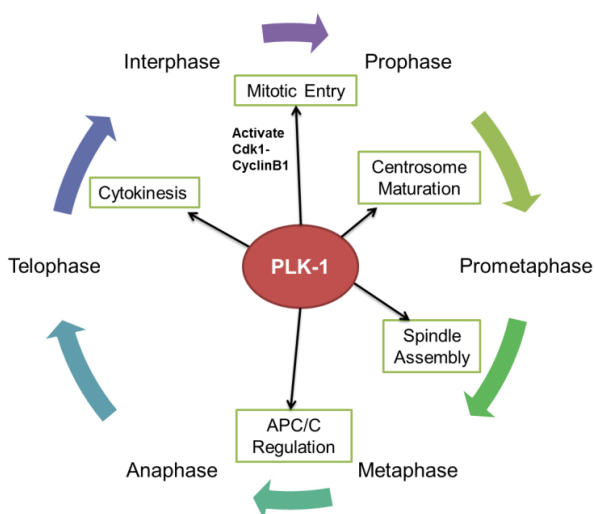


Figure 28. The involvement of PLK-1 during the cell cycle.

Due to the close involvement of PLK-1 in cell-cycle progression in normal proliferating tissues, PLK-1 has expectedly been found to be overexpressed in a variety of cancers.¹⁴⁴ Progression through mitosis is not possible if PLK-1 is inhibited,¹⁴⁵ thus inhibitors have been developed through targeting of the kinase domain as seen with BI-2536 and later analogue BI-6727, or the polo-box domain, which is unique to the PLK family.¹⁴⁶⁻¹⁴⁸

Due to its prevalence in cells and multiple functions in cell cycle, inhibition of PLK-1 has been shown to cause toxicity. As antimitotic compounds, PLK-1 inhibitors exhibit hematologic toxicity including neutropenia and thrombocytopenia.¹⁴⁹ Therefore, for designing a dual ALK-BRD4 inhibitor from BI-2536, it was important to remove the PLK-1 activity to improve the selectivity and toxicity profile.

2.1.2 Binding of BI-2536 to PLK-1 and BRD4

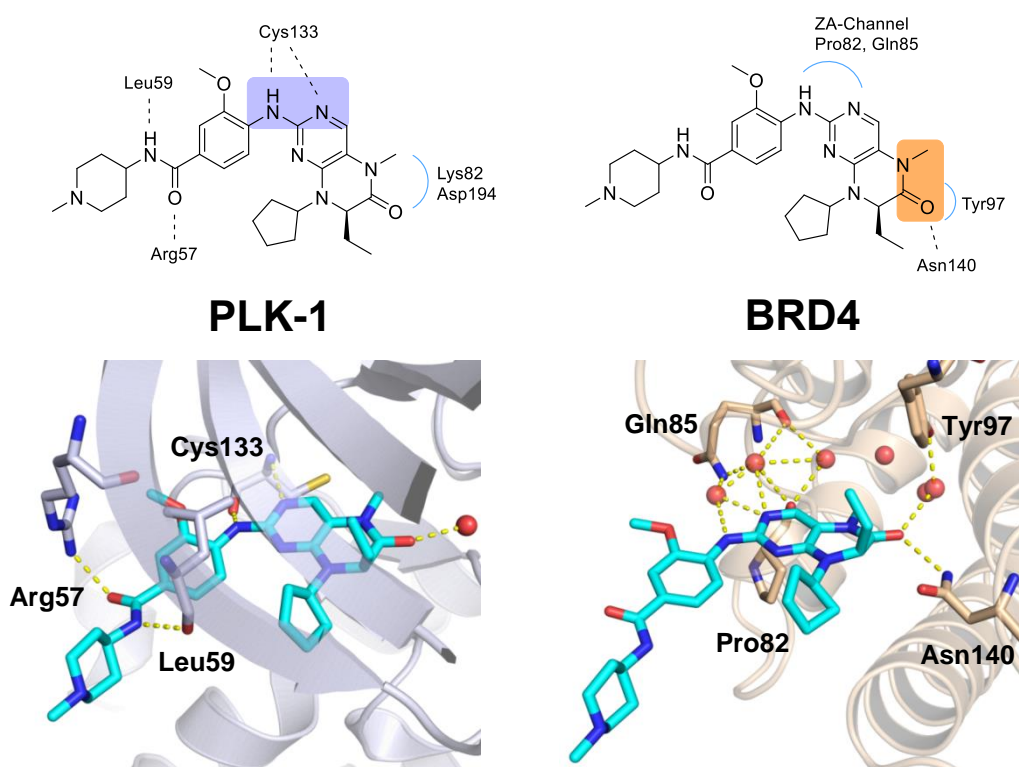


Figure 29. Binding mode of BI-2536 in PLK-1 and BRD4 showing hydrogen bonding interactions (yellow dotted lines) and water mediated interactions (blue curves).

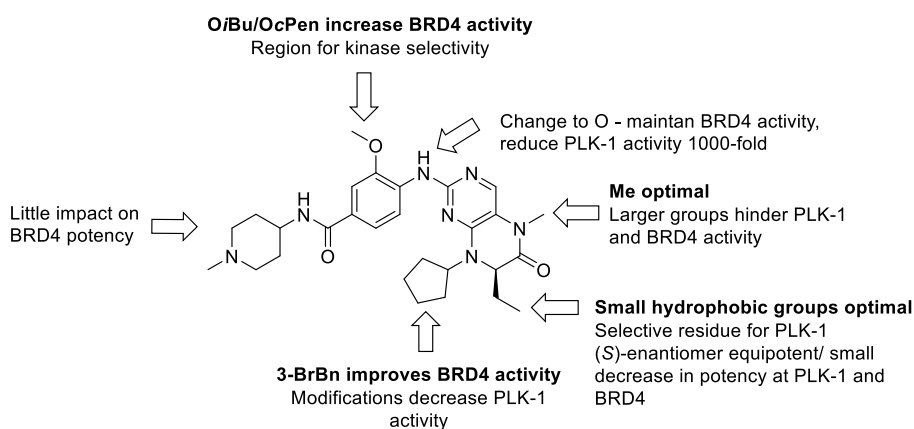
Co-crystal structures of BI-2536 in PLK-1 and BRD4 aided understanding of the dual kinase-bromodomain activity (Figure 29).¹¹⁵ The kinase hinge-region and bromodomain KAc mimetic are spatially separated from each other on the dihydropteridinone core. The aminopyrimidine of the dihydropteridinone core forms the key hinge-binding interaction with residue Cys133 in the PLK pocket whilst in BRD4, the diaminopyrimidine motif forms a network of hydrogen bond interactions with Pro82, Gln85 and waters in the ZA channel.

The dihydropteridinone carbonyl acts as the KAc mimetic, interacting with residue Asn140 in the BRD4 pocket. In PLK-1 the same carbonyl forms a hydrogen bond with a conserved water. Further hydrogen bond interactions occur in the PLK-1 pocket between the amide motif and residues Leu59 and Arg57 whilst the methoxy and ethyl substituents point into PLK-1 specific hydrophobic pockets, increasing PLK-1 selectivity.¹⁴⁰ Similarly the ethyl group points into a hydrophobic pocket within BRD4.

2.1.3 Literature Describing SAR of BI-2536

Recent papers discuss the SAR of BI-2536, as a PLK-1 inhibitor or more recently as a dual PLK-1-BRD4 inhibitor.^{131,132,140,150} The key points are highlighted in Scheme 2 establishing how the kinase and bromodomain activity can be manipulated.

Replacement of the methoxy group with a bulkier cyclopentoxy and isobutoxy improved BRD4 activity 2-fold however decreased PLK-1 activity.^{131,132} Removing the methoxy group does not affect BRD4 inhibition but caused more promiscuous inhibition against the kinase signifying the importance of the methoxy group in discriminating against kinases with a bulky residue at this position.¹⁴⁰



Scheme 2. Structure activity relationships of BI-2536 from published data.

Changing both the methyl and ethyl substituents to larger groups or removing the groups completely decreases potency at both targets revealing small hydrophobic groups were optimal.^{131,132} Importantly, the SAR of the methyl group confirmed the functional role of the methyl amide as a KAc mimetic in BRD4. Conflicting data has been published for the SAR of the ethyl group. Chen *et al.* reported that changing the stereochemistry of the ethyl group from *R*- to *S*- did not affect BRD4 potency and caused a 2-fold drop in potency against PLK-1. However Liu *et al.* showed changing

the chirality did have an effect on potency with BRD4 and PLK-1 potency decreasing 2-fold and 8-fold respectively.¹³²

Improvements in BRD4 potency were observed by changing the cyclopentyl to a 3-bromobenzyl moiety, increasing activity 7-fold.¹³¹ This group provided extra flexibility to reach the WPF shelf, a recurring area of interest in the development of potent bromodomain inhibitors.⁸⁴ For PLK-1, modifications to 3-bromobenzyl, isobutyl or isopropyl decreased activity, demonstrating the cyclopentyl group could be an important point of SAR to modulate the kinase and bromodomain activity.

Substitution of the pyrimidine NH with an O saw a greater than 1000-fold drop in potency yet only a 2-fold decrease in BRD4 potency. This result agrees with the importance of the NH as a hydrogen bond donor in the hinge interaction with Cys133. Finally Liu *et al.* demonstrate that changing the terminal piperidine to other alkyl and aromatic amines did not impact BRD4 potency.¹³²

2.2 Design Rationale

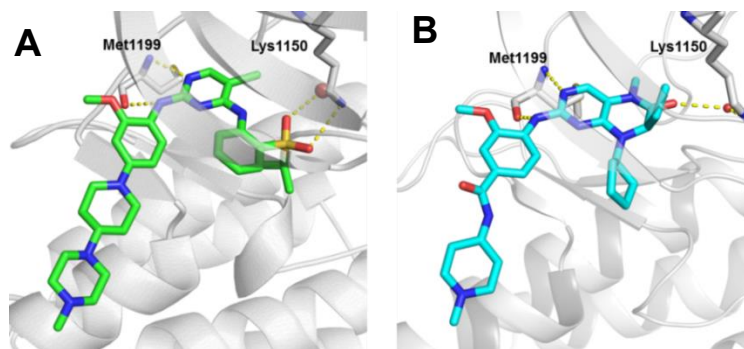


Figure 30 **A)** X-ray structure of TAE684 in ALK (2XB7). **B)** Docked structure of BI-2536 in ALK (2XB7) highlighting predicted interactions.

With no co-crystal structure of BI-2536 in ALK available, I performed docking studies with Glide of BI-2536 in ALK (2XB7) to support the initial hypothesis (Figure 30). This protein structure was chosen due to structural similarity between TAE684 and BI-2536 in particular the aminopyrimidine hinge binding motif and the *ortho*-methoxy phenyl group. For optimisation of the docking, see 2.2.1. Docking into ALK predicted the aminopyrimidine of BI-2536 to interact with the ALK hinge region including residue

Met1199 in a manner similar to PLK-1. The amide carbonyl was also predicted to interact with a conserved water in the back of the ALK pocket.

Considering the previous SAR work on BI-2536 and analysis of the ALK and BRD4 structures and known inhibitors, I established initial hypotheses on modifying BI-2536 to meet the aims of increasing ALK activity, decreasing PLK-1 activity whilst maintaining BRD4 activity. Based on the ALK docking and BRD4 X-ray structure, the key kinase and bromodomain binding motifs on the dihydropteridinone core were to be maintained. Structural analysis suggested several positions around the core structure offered significant scope for modification including the ethyl (R_1), cyclopentyl (R_2), methoxy (R_3) and the solvent channel (R_4) groups (Figure 31).

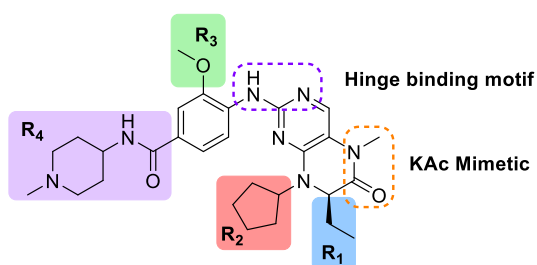


Figure 31. Highlighted regions for modification of BI-2536.

2.2.1 Docking Experiments in ALK

Initial docking experiments of BI-2536 in ALK (2XB7) did not produce suitable docking poses, with the dihydropteridinone shifted out of the pocket, forming no interaction with the hinge region (Figure 32A). I noticed that performing a restrained minimisation on the protein structure during protein preparation caused a shift in the conserved water in the ALK pocket. This minimisation refines the structure allowing hydrogen atoms to be freely minimised, while allowing for enough heavy-atom movement to relieve any strain.¹⁵¹ As seen in Figure 32B, before minimisation, the water is orientated to act as a hydrogen bond donor to the sulfone moiety in TAE684 and a hydrogen bond acceptor to Lys1150 (2XB7). This water is conserved in other ALK structures, including ceritinib and lorlatinib (4MKC and 4CLI).^{47,50} When the protein is minimised, this water rotates, maintaining its interaction with Lys1150 but losing its interaction with the sulfone (Fig 32C). The oxygen of the water is now facing into the pocket creating potential repulsion to other hydrogen bond acceptors, including the carbonyl of BI-2536.

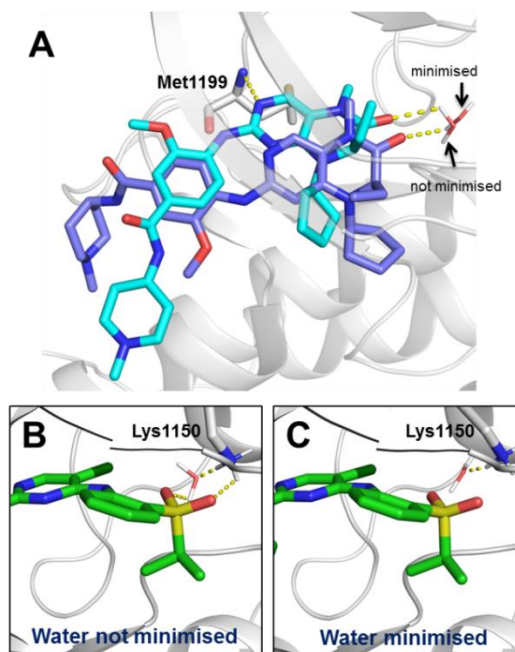


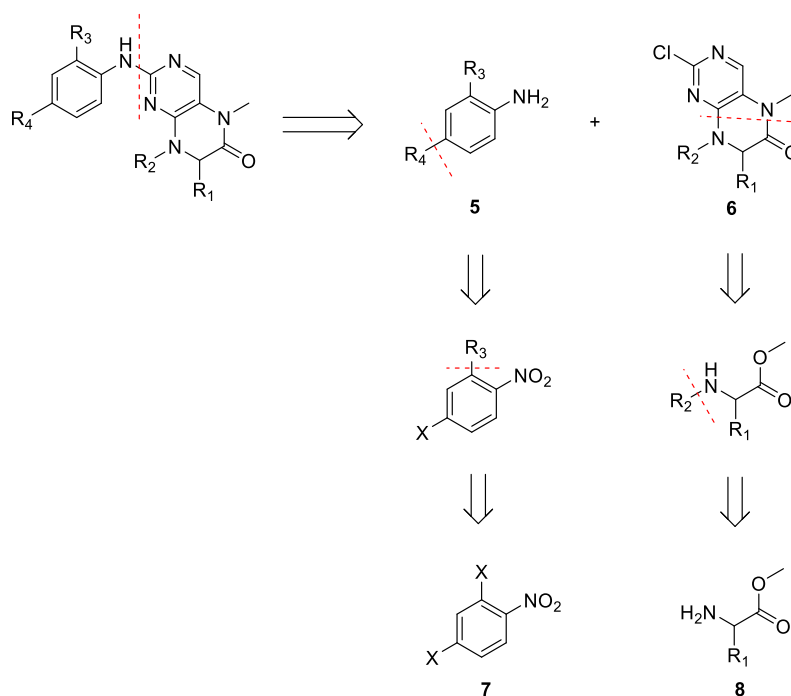
Figure 32 **A)** Comparison of docking poses of BI-2536 in ALK (2XB7) and orientation of the key conserved water following minimisation (purple) and no minimisation (blue). **B)** X-ray structure of TAE684 in ALK (2XB7) binding to conserved water and Lys1150. **C)** Structure of TAE684 in ALK after restrained minimisation.

I then docked BI2536 without the restrained minimisation to compare docking poses (Figure 32A). As a result, more suitable docking poses consistent with a hinge binding mode were predicted, with the aminopyrimidine motif interacting with the hinge-region and the carbonyl interacting with the conserved water. Going forward, all docking experiments were run in the same manner, following the Protein Preparation Wizard but without running the restrained minimisation.

2.3 Synthesis of BI-2536 Analogues

To address the different areas for modification, a convergent synthesis was established for analogues of BI-2536 (Scheme 3). The final analogues were synthesised via a coupling between intermediates **5** and **6**, the former containing the alkoxy (R_3) and solvent channel modifications (R_4), the latter containing the (*R*)-ethyl (R_1) and cyclopentyl (R_2) modifications. The converging intermediates could be taken back to a simple nitroaryl starting material **7** for installation of the R_3 and R_4 groups, and an amino acid building block **8** containing the R_1 substitution. Synthesis followed

procedures outlined in the literature for the synthesis of BI-2536, which were later optimised.^{131,152}

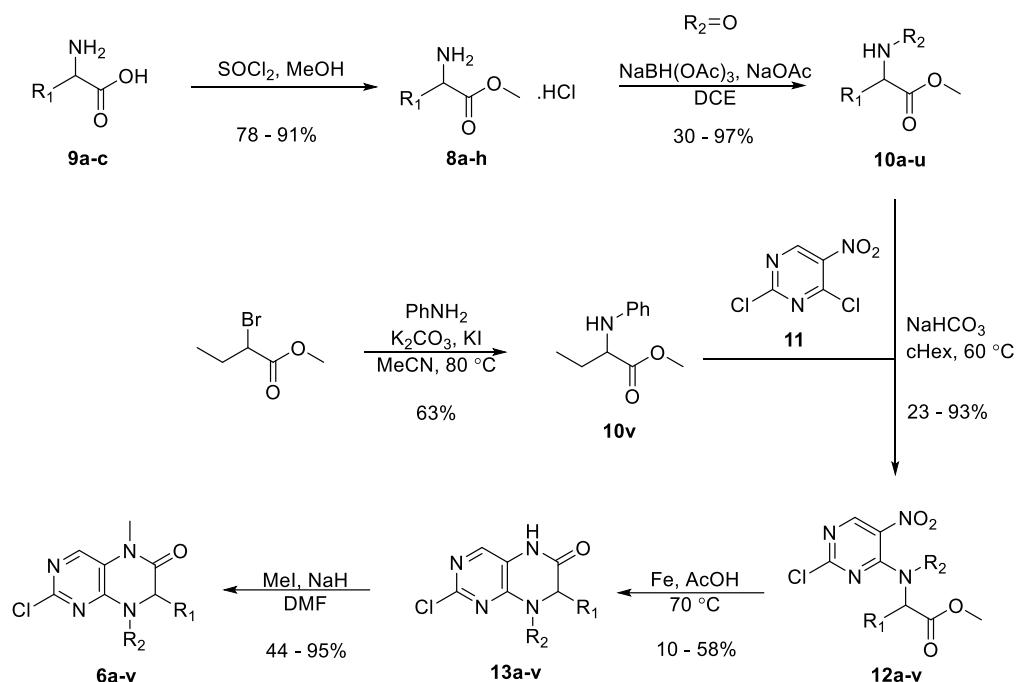


Scheme 3. Synthetic strategy for analogues of BI-2536.

For the synthesis of the dihydropteridinone pharmacophore, the starting material was enantiopure methyl ester amino acids **8a-h** (Scheme 4). In certain cases (when $R_1 = (R)\text{-Et}$, $(R)\text{-Me}$ and $(S)\text{-Et}$) I converted the free carboxylic acid **9a-c** to the methyl ester using thionyl chloride and methanol. Reductive amination with **8a-h** and the relevant aldehyde or ketone using sodium triacetoxyborohydride gave intermediates **10a-u**. Using 1,2-dichloroethane (DCE) as the solvent achieved higher yields compared to DCM and THF and faster reaction times.¹⁵³ I synthesised a phenyl analogue from methyl 2-bromobutanoate and aniline to give intermediate **10v**, taken forward as the racemic mixture.

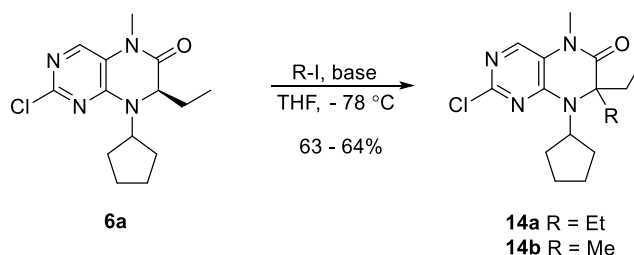
Regioselective S_NAr of **10a-v** with 2,5-dichloro-4-nitropyrimidine **11** was achieved to give intermediates **12a-v**. Initially, I used potassium carbonate and acetone for the S_NAr step as described in Chen *et al.* and Budin *et al.*^{131,152} However, substitution occurred at both the 2- and 4- position of the pyrimidine **11**. I tried alternative conditions using NaHCO_3 and cyclohexane, achieving sole substitution at the 4-position and thus higher yields.¹⁵⁴ The formation of the six-membered transition state between the nitroaryl substrate, nucleophile and alkali metal cation is highly stabilised in non-polar solvent, such as cyclohexane, compared to a more polar solvent,

achieving higher regioselectivity.¹⁵⁵ Next, iron reduction and cyclisation formed the dihydropteridinone scaffold **13a-v**, followed by methylation of the amide to give final intermediates **6a-v**.



Scheme 4. General procedure for the synthesis of dihydropteridinone intermediates **6a-v**.

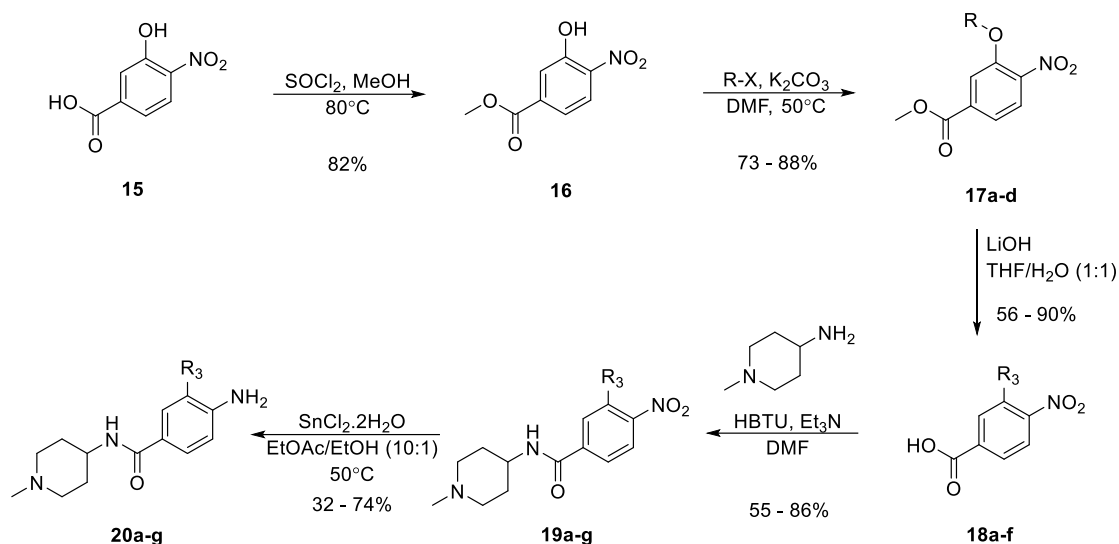
For the synthesis of analogues containing a dialkyl R_1 modification, I subjected intermediate **6a** to strong base to allow deprotonation of the *alpha*-carbonyl proton (Scheme 5). This was followed by addition of ethyl iodide or methyl iodide to give dialkyl R_1 intermediates **14a** and **14b**.



Scheme 5. General procedure for the synthesis of dialkyl R_1 intermediates **14a-b**.

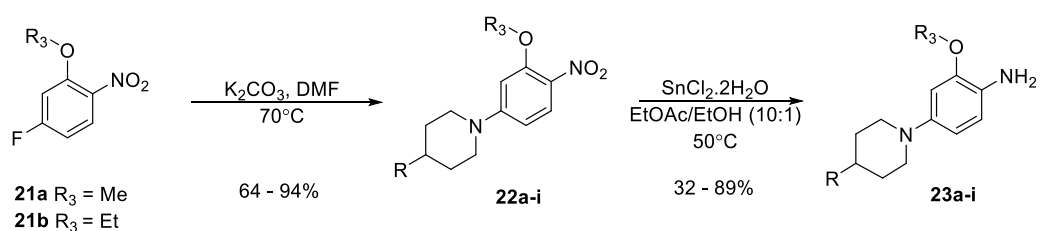
For the synthesis of the left-hand side aniline moieties containing the R_3 and R_4 modifications, I followed three synthetic procedures. For the amide-containing intermediates, I started with ester protection of 3-hydroxy-4-nitrobenzoic acid **15** (Scheme 6). Alkylation of **16** with various alkyl halides gave intermediates **17a-d**. The

ester was converted back to the carboxylic acid (**18a-d**), ready for amide coupling with 1-methylpiperidin-4-amine using coupling agent HBTU (1.6 eq.) and Et₃N (2.eq.). In the case of R₃ = H and OEt, intermediates **18e** and **18f** were commercially available for the amide coupling. Finally tin chloride nitro reduction of **19a-g** yielded the final amide intermediates **20a-g**.



Scheme 6. General procedure for the synthesis of left-hand side intermediates **20a-g**. R₃ = -H or -OR. Note. For intermediates **19g** and **20g**, *N*,1-dimethylpiperidin-4-amine was used.

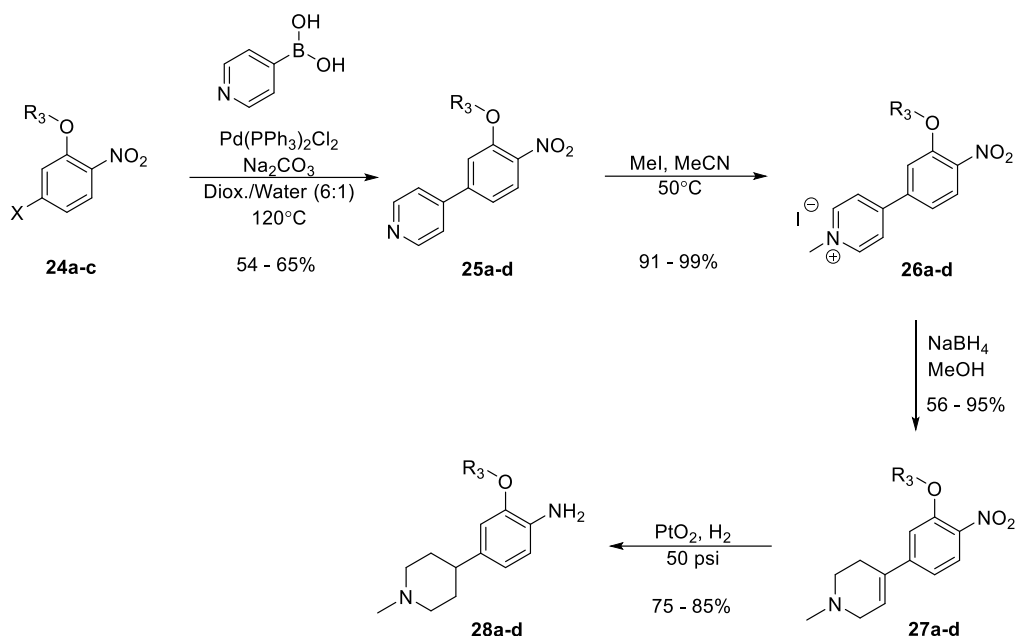
For left-hand side intermediates without the amide moiety, I coupled 4-fluoro-2-alkoxy-1-nitrobenzenes **21a-b** with a selection of piperidine-solubilising groups (Scheme 7).⁷⁴ The second and final step was tin chloride reduction of **22a-i** to give final intermediates **23a-i**.



Scheme 7. General procedure for the synthesis of left-hand side intermediates **23a-i**.

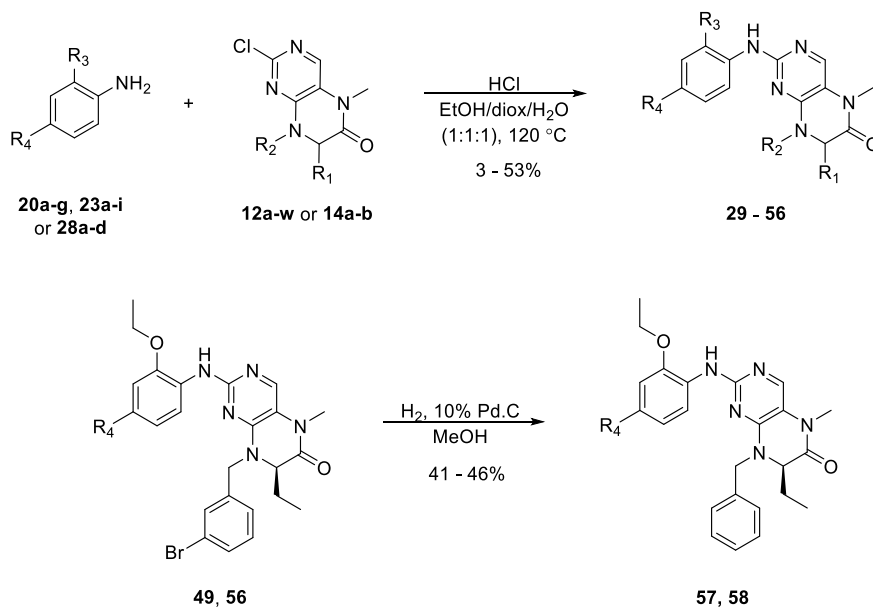
The final left-hand side intermediates had the amide functionality removed with the piperidine attached directly to the phenyl as seen similarly in ceritinib.⁴⁶ To introduce the 1-methyl-4-piperidine group, I started with a Suzuki coupling between an alkoxy-nitrobenzene **24a-c** and pyridine-4-ylboronic acid to give **25a-d** (Scheme 8). Methylation of the pyridine gave pyridinium iodides **26a-d** which were partially reduced to **27a-d** using sodium borohydride. Pressured hydrogenation (50 psi) using

PtO₂ reduced the nitro group and final double bond to give piperidine intermediates **28a-d**.



Scheme 8. General procedure for the synthesis of left-hand side intermediates **28-d**.

The final compounds were synthesised *via* acid promoted S_NAr between right-hand side intermediates **6a-w** and **14a-b** and either **20a-g**, **23a-i** and **28-d** (Scheme 9). The reaction proceeded typically between 24 – 48 hours achieving low to modest yields. Hydrogenation of compounds **49** and **56** to remove the aryl bromine yielded compounds **57** and **58**.

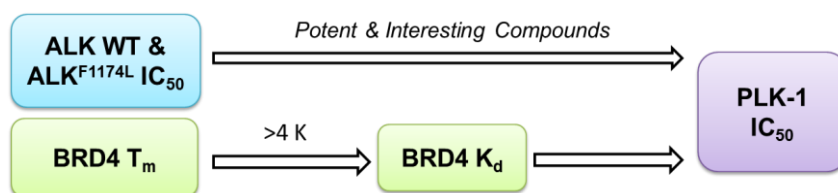


Scheme 9. General procedure for the synthesis of final compounds **29 - 56** and hydrogenation of final compounds **49** and **56** to give final compounds **57** and **58**.

2.4 Biochemical Testing

2.4.1 Biochemical Assay Cascade

At the start of the project I required biochemical assays against the two targets ALK and BRD4, as well as for the ALK^{F1174L} mutant in case of differing SAR to wildtype ALK (Scheme 10). For testing against ALK WT and the ALK^{F1174L} mutant, I initially ran a mobility shift assay but later replaced this assay format with a LanthaScreen® TR-FRET assay (see 2.4.2 & 2.4.3).



Scheme 10. Biochemical testing assay cascade. BRD4 T_m and K_d values measured by David Heidenreich, Goethe University of Frankfurt. PLK-1 IC_{50} values measured at ThermoFisher Select Screen Profiling Services.

The primary assay format for testing against BRD4 was a thermal shift assay, ran by my collaborator David Heidenreich. Compounds exhibiting modest to high degrees of thermal shift (>4 K) were then tested in an isothermal calorimetry assay to determine the K_d . There was no correlation observed between thermal shift measurements and K_d values (Figure 33), thus thermal shift was only used as an initial indicator that the compound was binding. As a key aim for the series was to decrease the PLK-1 activity of BI-2536, I also required a biochemical assay to measure PLK-1 activity. PLK-1 activity was measured using a Z'-Lyte™ Assay by ThermoFisher Select Screen Profiling Services.¹⁵⁶ Potent and interesting compounds against both ALK and BRD4, in particular the ALK^{F1174L} mutant, were tested against PLK-1 to determine any changes in kinase selectivity between ALK and PLK-1.

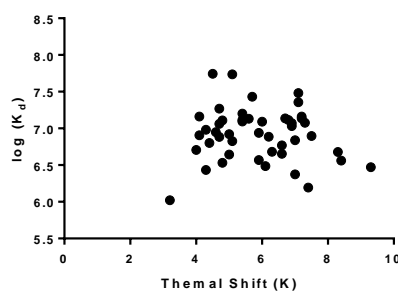


Figure 33. Correlation between T_m shift and K_d values measured for dual ALK-BRD4 series.

2.4.2 Caliper Mobility Shift Assay

Microfluidic mobility shift assays monitor the separation of a phosphorylated product from its substrate. The assay was performed using the Caliper LabChip EZ reader which holds a LabChip microfluidic multi-sipper chip that sips up aliquots from the incubated enzymatic reaction. The non-phosphorylated peptide substrate and phosphorylated product from the reaction migrate at different rates within the chip and are then detected via LED induced fluorescence (Figure 34). The relative heights of the substrate and product fluorescent peaks on the trace reveal the extent of the reaction and can be used to determine the % conversion. The addition of an inhibitor prevents phosphorylation of the substrate and consequently produces a dose dependent reduction in conversion which is used to calculate an IC_{50} .

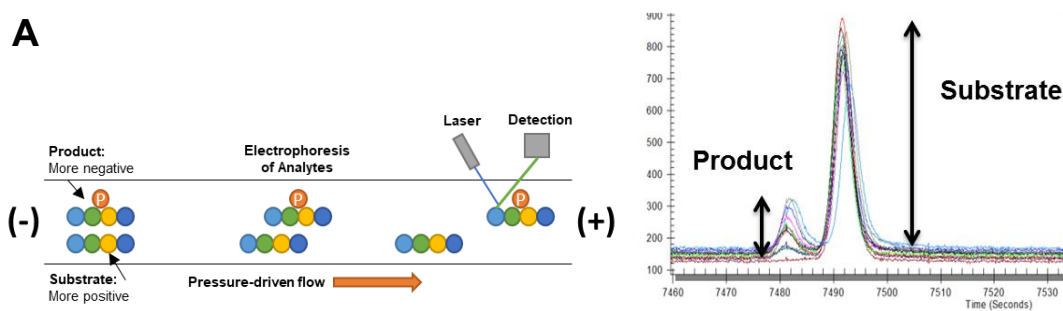


Figure 34 **A)** LabChip EZ reader technology – shift in mobility of non-phosphorylated substrate and phosphorylated product. **B)** Output from Caliper EZ reader demonstrating the shift in mobility between the substrate and product. Percent conversion from substrate to product can be determined using the peaks heights.

Several issues arose during development of the mobility shift assay with ALK WT and ALK^{F1174L}. Firstly during the enzyme titration experiments, the percent conversion was only reaching a maximum of 50% (Figure 35). I tried various conditions to improve the conversion and find out what was limiting the activity of the ALK protein, including different buffers, temperature, pH, enzyme and peptide suppliers and using protocols from previous work at the ICR and PerkinElmer. No improvement in percent conversion was made and thus the reason for low conversion is still not fully understood.

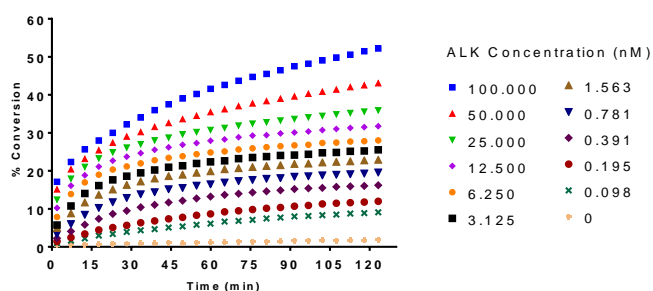
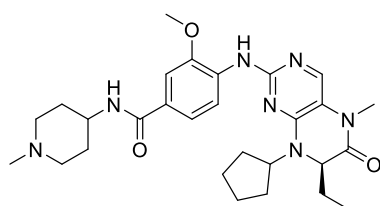


Figure 35. Example ALK enzyme titration experiment using Caliper mobility shift technology.

Despite the low conversion, I proceeded with the assay development by measuring the ATP K_m for ALK WT and ALK^{F1174L} and measuring the IC_{50} values of BI-2536 and synthesised analogues. The measured IC_{50} of BI-2536 against ALK was 290 nM and against ALK^{F1174L} was 620 nM. Though the ALK WT potency matched the literature and externally measured IC_{50} , the ALK^{F1174L} IC_{50} was 3-fold less active compared to the externally measured IC_{50} of 190 nM. This difference was factored to the results being measured in different assay formats.

A



BI-2536

| | ALK WT | ALK ^{F1174L} |
|---|--------|-----------------------|
| Literature | 160 nM | - |
| External IC_{50} | 390 nM | 190 nM |
| Caliper IC_{50} | 290 nM | 620 nM |
| LanthaScreen® IC_{50} | 410 nM | 260 nM |

B

| | Caliper pIC ₅₀ | S.Dev | Lantha pIC ₅₀ | S.Dev |
|----------------|------------------------------|-------|-----------------------------|-------|
| BI-2536 | 6.17 | 0.30 | 6.74 | 0.15 |
| 30 | 5.90 | 0.38 | 6.34 | 0.15 |
| 33 | 5.37 | 0.05 | 5.78 | 0.03 |
| 29 | 5.93 | 0.29 | 6.42 | 0.12 |
| 31 | 5.51 | 0.23 | 6.18 | 0.25 |
| 36 | 5.98 | 0.41 | 6.68 | 0.10 |
| 37 | 5.83 | 0.49 | 6.39 | 0.20 |
| 38 | 6.03 | 0.47 | 6.72 | 0.17 |
| 32 | 5.60 | 0.55 | 5.91 | 0.04 |

Figure 36. A) IC_{50} data for BI-2536 measured in different assay formats. **B)** Comparison of Caliper and Lantha pIC₅₀ values and standard deviations against ALK^{F1174L}.

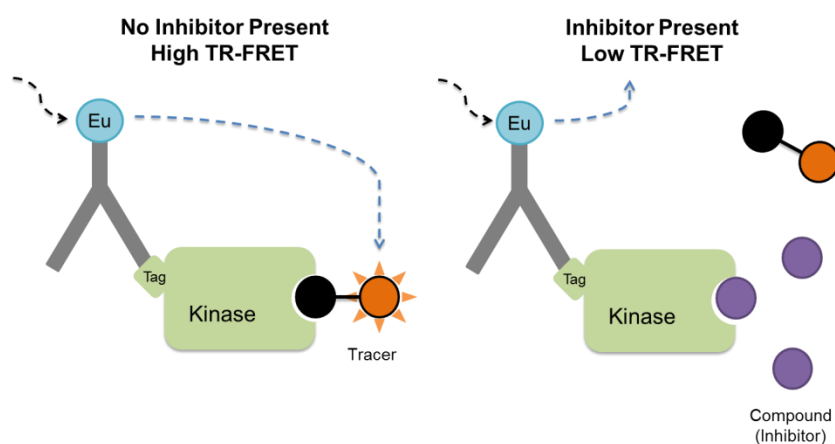
However, the standard deviations for the first set of synthesised analogues caused concern. As seen in in Figure 36B large deviations were observed for the pIC₅₀ of BI-2536 and compounds **29** – **33** and **36** – **38** against ALK^{F1174L}. For example compound **37** had a measured pIC₅₀ ranging between 5.25 – 6.38 (IC_{50} between 0.41 μ M – 5.6 μ M). An alternative assay format was pursued to verify the data collected in Caliper assay. Using the LanthaScreen® assay (see 2.4.3), IC_{50} values were measured for the same set of compounds and resulted in much smaller standard deviations. In

addition the Lantha data matched the external IC_{50} values, also measured by LanthaScreen®, for both ALK WT and ALK^{F1174L} (Figure 36A).

Due to the problems with low conversion and large standard deviations, as well as the Caliper LabChip EZ Reader requiring a more extensive set up compared to the simple mix and read LanthaScreen® assay, I changed the primary assay for testing ALK WT and ALK^{F1174L} mutant to LanthaScreen®.

2.4.3 LanthaScreen® Assay

The LanthaScreen® Eu Kinase Binding Assay is a time resolved-fluorescence resonance energy transfer (TR-FRET) assay based on the binding and displacement of a tracer, Alexa Fluor® 647, to the kinase of interest. Binding of the tracer to the kinase, in this case ALK WT or ALK^{F1174L}, was detected using a europium-labelled anti-GST antibody which binds to the GST-tagged kinase (Scheme 11). Simultaneous binding of the antibody and tracer results in a high degree of FRET between the close donor (Eu) and acceptor (tracer) fluorophores. Binding of an inhibitor to the kinase displaces the tracer causing a loss of FRET.



Scheme 11. Schematic of LanthaScreen® Eu Kinase Binding Assay. Binding of antibody and tracer to a kinase results in high degree of FRET whilst displacement of the tracer with an inhibitor results in a loss of FRET.

I first performed titrations of the tracer to find suitable concentrations of the Alexa Fluor® 647 tracer for the assay. K_d values of the tracer were measured as 13 nM and 30 nM for ALK WT and ALK^{F1174L} respectively. I then ran enzyme titrations to determine a concentration of ALK WT and ALK^{F1174L} with a suitable fluorescence window between the high TR-FRET and background signals. Though a low

concentration of enzyme would enable the testing of more compounds with a batch of protein, too low a concentration will have a small fluorescence window and it is hence difficult to generate an IC_{50} . The results from the enzyme titration showed concentrations of 5 nM for ALK WT and ALK^{F1174L} had a suitable window and hence used in the assays.

2.5 SAR of Analogues

2.5.1 SAR of R₃– Methoxy Group

Previous design of both ALK and PLK-1 inhibitors report the location of the alkoxy group as important for kinase selectivity. For PLK-1 inhibitor BI-2536, this is achieved with the methoxy group situated in a pocket next to the hinge region whilst for ALK inhibitor ceritinib a bulkier isopropoxy group is used at this position (Figure 37).^{46,140} In addition, larger alkoxy groups were known to improve interactions at BRD4.¹³¹ Consequently, the hypothesis was that changing the methoxy group to a larger alkoxy group, such as the isopropoxy in ceritinib, will promote ALK selectivity and BRD4 potency.

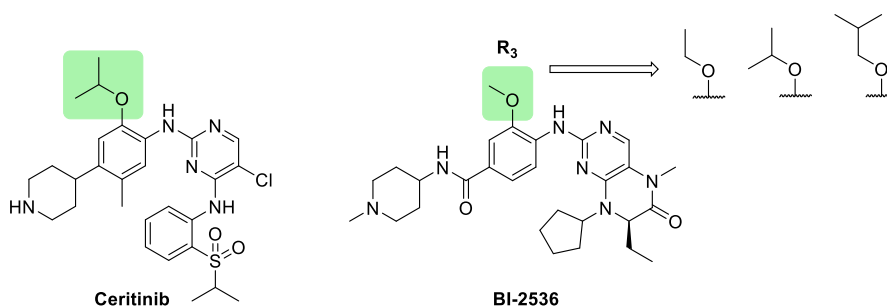


Figure 37. Alkoxy groups present on ceritinib and BI-2536 and proposed larger alkoxy groups for modification at the R₃ position.

I performed docking studies with analogues of BI-2536 modifying the alkoxy group to investigate if larger groups would be tolerated in the ALK and BRD4 pockets. Docking studies suggested that larger alkoxy groups such as an isobutoxy (Figure 38) could be tolerated in both targets, retaining the key hinge binding and KAc mimetic interactions. In ALK, the isobutoxy is predicted to further extend into the hydrophobic pocket formed by Arg1120, Glu1132 and the hinge region Leu1198 – Ala1200. Similarly in BRD4 the isobutoxy group fills a hydrophobic groove formed by Lys91 and Leu92.

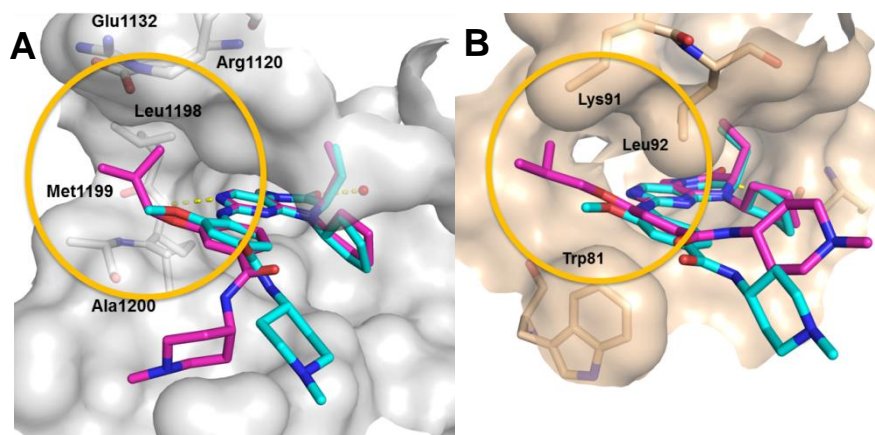
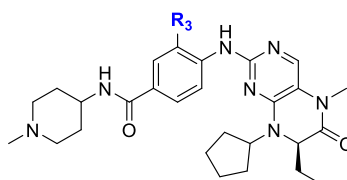


Figure 38. **A)** Docking of BI-2536 (blue) and isobutoxy analogue **33** (pink) into ALK (2XB7). **B)** Docking of isobutoxy analogue **33** (pink) overlaid with BI-2536 (blue) in BRD4 (4OGI). In both, the key pocket and residues are highlighted.

I synthesised six analogues of BI-2536 modifying the size of the methoxy group, following the general synthesis outlined in **2.3** using the relevant alkyl halide (Scheme **6**). The biochemical assay results for the methoxy group modification (R_3) are shown in Table **4**.

For ALK WT and ALK^{F1174L}, increasing the size of the alkoxy group caused a gradual decrease in activity, with the largest isobutoxy analogue **33** 11-fold (ALK WT) and 9-fold (ALK^{F1174L}) less potent than BI-2536. The IC_{50} values did not correlate with the docking studies which proposed larger groups were tolerated. When binding to ALK, the alkoxy group may be orientated slightly differently to the docking predication and instead clash with the pocket residues, lowering activity. Similarly in PLK-1, changing the methoxy to a larger alkoxy group causes a decrease in activity. This is exemplified by compounds **29**, **32** and **33** with a less than 50% percent inhibition at 10 nM, therefore indicating an IC_{50} of greater than 10 nM. This was confirmed with ethoxy analogue **29** with an IC_{50} of 12.6 nM, a 5-fold decrease in activity from BI-2536. The real effect on PLK-1 potency of this structural change is likely greater, however, as the potency of BI-2536 is below the dynamic range of our assay.

For BRD4, increasing the size of the alkoxy group gave an increase in thermal shift compared to **29** indicating that larger groups are stabilising the protein-compound complex. The measured K_d values confirmed that the majority of the alkoxy groups were tolerated with little change in binding affinities. Cyclopentoxy analogue **32** was the only analogue to give a large decrease in affinity, despite showing a high thermal shift. This reiterated the use of thermal shift only as an indicator of binding.



| | | ALK | | BRD4 | | PLK-1 | |
|----------------------|-------|-----------------------------|---------------------------------|---------------------|---------------------|--------------------------|-------------------------------|
| R₃ | | WT IC ₅₀ (nM) | F1174L IC ₅₀ (nM) | ΔT _m [K] | K _d (nM) | IC ₅₀ (nM) | % Inhibition (10 / 100 nM) |
| BI-2536 | OMe | 380 ± 70 | 180 ± 40 | 5.7 ± 0.3 | 37 | <2.6 | 80 / 98 |
| 29 | OEt | 970 ± 140 | 380 ± 60 | 6.0 ± 0.5 | 81 | 12.4 | 40 / 80 |
| 30 | OPr | 1600 ± 200 | 460 ± 100 | 7.2 ± 0.1 | 69 | - | 61 / 93 |
| 31 | | 2400 ± 630 | 670 ± 210 | 7.1 ± 0.1 | 33 | - | 54 / 96 |
| 32 | OcPen | 4400 ± 1600 | 1200 ± 70 | 7.4 ± 0.3 | 640 | - | 45 / 86 |
| 33 | OBu | 4400 ± 430 | 1700 ± 70 | 7.2 ± 0.2 | 73 | - | 43 / 82 |
| 34 | H | 5200 ± 1300 | 1100 ± 490 | 4.3 ± 0.2 | 104 | - | - |

Table 4. Biochemical assay data for SAR of the OMe group (R₃), - = not determined. ALK IC₅₀ values: mean ± S.E, n = 3. BRD4 ΔT_m: mean ± S.D, n = 2, compound concentration of 10 μM. BRD4 K_ds, n = 1. PLK-1 IC₅₀ values and % Inhibition: n = 1 (ATP = 10 μM)

I investigated the contribution of the alkoxy group to ALK and BRD4 potency with analogue **34**. Removing the methoxy group gave a large decrease in activity against ALK WT and ALK^{F1174L} indicating the methoxy group is desirable for potency. The removal of the methoxy group also reduced BRD4 activity 3-fold. From this series the most promising analogue was **29** with the ethoxy group at the R₃ position. Though **29** gave a small drop in potency (2-fold) against ALK^{F1174L}, the greater drop in PLK-1 activity and retained BRD4 activity provided the best balance of potencies and selectivity against PLK-1.

2.5.2 SAR of R₄ – Solvent Channel Group

The amide linker of BI-2536 facilitates a network of interactions between the N- and C-lobes of PLK-1 (Figure 39).¹⁴⁰ The carbonyl and NH directly interact with residues Arg57 and Leu59 through hydrogen bonds and interact with Arg136 via water-mediated hydrogen bonds and van der Waals contacts (Figure 39). The initial hypothesis was to remove the amide linker and the consequent hydrogen bond interactions to decrease PLK-1 activity (Figure 40).

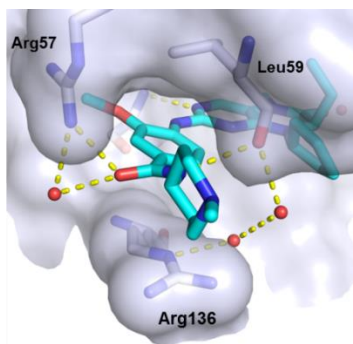


Figure 39. X-ray structure of BI-2536 in PLK-1 highlighting key residues and interactions with the amide moiety (2RKU).

Published SAR data for ALK inhibitors suggested a wide variety of groups are tolerated in this region including various saturated heterocycles, as seen in brigatinib and alectinib, aliphatic amines and fused rings. (Figure 40).^{74,157,158} The directly linked piperidine present in ceritinib is analogous to the proposed analogue of BI-2536 removing the amide moiety. As the proposed group should be tolerated in ALK, this supported the hypothesis of removing the amide to decrease PLK-1 activity.

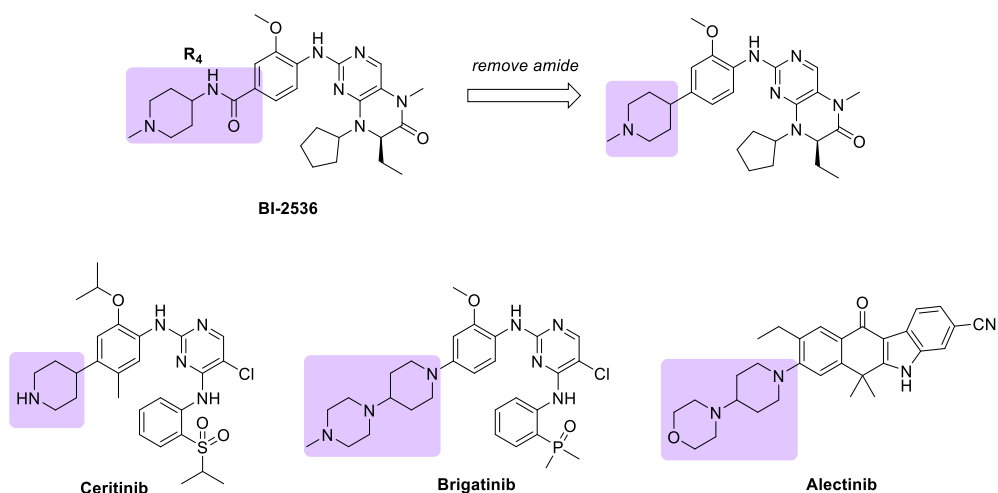


Figure 40. Solvent channel groups present on BI-2536, ALK inhibitors ceritinib, brigatinib and alectinib and proposed analogue of BI-2536 with amide removed.

I next docked the directly linked piperidine analogue **35** into ALK and BRD4 to support the modification would be tolerated in both targets and not affect the binding (Figure 41). In ALK, the docked structure was predicted to retain key interactions with the hinge and the R₄ modification pointing into solvent as with BI-2536. This further supported the hypothesis that removing the amide would not have much effect on ALK activity. In BRD4, the analogue **35** also retained its key interaction, with Asn140, and the R₄ modification pointing out of the pocket. This complemented previous SAR modifying the solvent channel region in which changing the group had little impact on BRD4 activity.¹³² Overall, the docking suggested modification to the R₄ solvent channel region would be tolerated in ALK and BRD4.

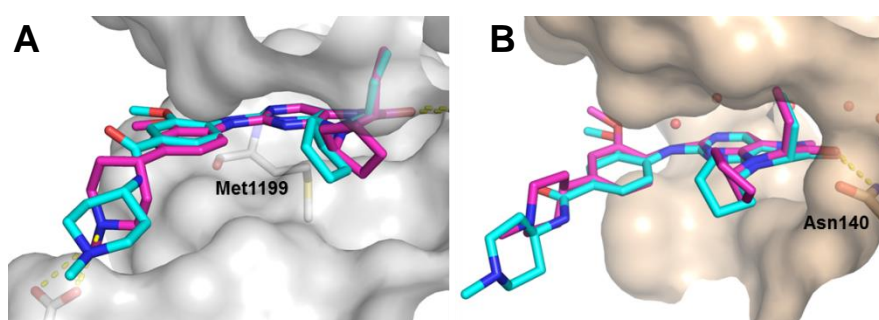
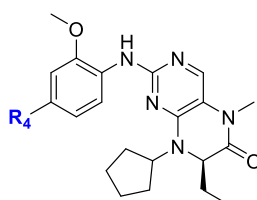


Figure 41. **A)** Docking of BI-2536 (blue) and **35** (pink) into ALK (2XB7). **B)** Docking of **35** (pink) overlaid with BI-2536 (blue) in BRD4 (4OGI). In both, key residues and predicted interactions highlighted.

Compounds modifying the solvent channel group were synthesised according to Scheme 4 using (*R*)-2-Aminobutyric acid **9a** and cyclopentanone. The solvent channel modifications followed Schemes 7 and 8 using a small selection of piperidine solubilising groups present in ALK inhibitors. The biochemical assay results for the four solvent channel modifications are shown in Table 5.

Removing the amide group (compound **35**) had little effect against ALK WT, ALK^{F1174L} and BRD4, supporting the hypothesis that the amide functionality is not crucial for activity at these targets. However, consistent with the hypothesis, removing the amide decreased PLK-1 activity, showing a greater than 4-fold reduction in potency compared to BI-2536. Alternative solubilising groups found in published ALK inhibitors were then considered. Compounds **36** – **38** also retained ALK WT and ALK^{F1174L} potency and gave similar decreases in PLK-1 potency to **35**. The solvent channel group has demonstrated to be a suitable modification to maintain ALK and BRD4 potency whilst decreasing PLK-1 potency.



| | | ALK | | BRD4 | | PLK-1 | |
|----------------|--|-----------------------------|---------------------------------|--------------|------------------------|--------------------------|-------------------------------|
| R ₄ | | WT IC ₅₀ (nM) | F1174L IC ₅₀ (nM) | ΔTm [K] | K _d (nM) | IC ₅₀ (nM) | % Inhibition (10 / 100 nM) |
| BI-2536 | | 380 ± 70 | 190 ± 40 | 5.7 ± 0.3 | 37.0 | <2.6 | 80 / 98 |
| 35 | | 310 ± 10 | 290 ± 70 | 5.4 ± 0.2 | 80.8 | 9.9 | 64 / 102 |
| 36 | | 500 ± 60 | 200 ± 30 | 4.7 ± 0.1 | 86.8 | - | 39 / 88 |
| 37 | | 620 ± 20 | 410 ± 100 | 4.7 ± 0.1 | 130.9 | - | 46 / 90 |
| 38 | | 350 ± 80 | 190 ± 50 | 4.6 ± 0.3 | 112.5 | 16 | 40 / 85 |

Table 5. Biochemical assay data for SAR of the solvent channel group (R₄), - = not determined. ALK IC₅₀ values: mean ± S.E, n = 3. BRD4 ΔTm: mean ± S.D, n = 2, compound concentration of 10 μM. BRD4 K_ds, n = 1. PLK-1 IC₅₀ values and % Inhibition: n = 1 (ATP = 10 μM).

2.5.3 SAR of R₁ – (*R*)-Ethyl Group

The (*R*)-ethyl group of BI-2536 conveys selectivity for PLK-1, poking into a small unique hydrophobic pocket at the top of the protein (Figure 42A). The cysteine residue at the top of this pocket is more commonly a valine in other kinases which interferes with the placement of the ethyl group.¹⁴⁰ The ethyl residue situates in a similar small hydrophobic pocket of BRD4 formed by Val87, Leu92, Leu94 and Tyr97. Chen *et al.*, report changing the ethyl to a larger benzyl group or a smaller proton decreases activity at both targets, concluding small hydrophobic groups are optimal.¹³¹ Conflicting activities were observed with the (*S*)-enantiomer by Chen *et al.* and Liu *et al.* The former states equipotent activity is observed between the enantiomers against BRD4 and a small drop in PLK-1 activity from 0.22 nM to 0.42

nM. Whereas the latter reports a 2-fold and 8-fold decrease in potency for BRD4 and PLK-1 respectively.¹³² From inspection of the co-crystal structures, it appears the (*S*)-enantiomer would clash with the bottom of the BRD4 and PLK-1 pockets (Figure 42B). It was important to confirm the difference in potencies between the (*R*)- and (*S*)-enantiomers.

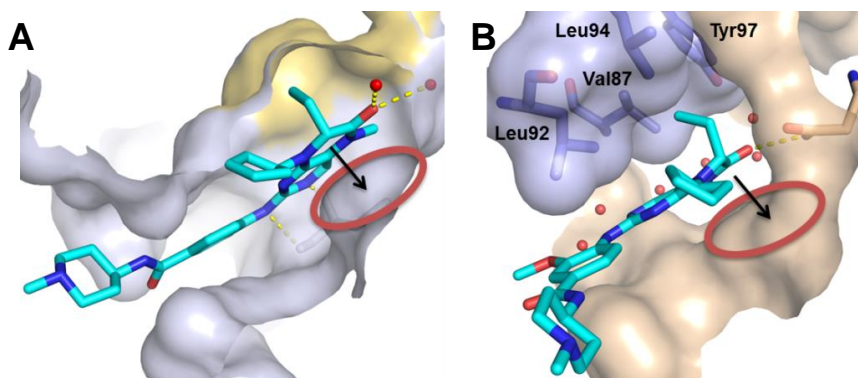


Figure 42. **A)** X-ray structure of BI-2536 in PLK-1 (2RKU) highlighting (*R*)-ethyl pocket (yellow). **B)** X-ray structure of BI-2536 in BRD4 (4OGI) highlighting (*R*)-ethyl pocket and residues (purple). Red circles highlight potential areas of clashing with (*S*)-enantiomer.

Previous docking of BI-2536 into ALK predicts the ethyl group to fit into a pocket formed by Ala1148, Val1130, Lys1150 and Leu1196 (Figure 43). The hypothesis was that a small hydrophobic group is required for ALK and BRD4 potency. As no crystal structure of BI-2536 in ALK was available, the aim was to change the size of the ethyl group to understand what size groups are tolerated and find a group that could distinguish between ALK and PLK-1. I also wanted to synthesise the (*S*)-enantiomer. If the (*S*)-enantiomer was indeed equipotent against BRD4 and also tolerated in ALK this could be a useful modification in developing a dual ALK-BRD4 inhibitor and removing PLK-1 activity.

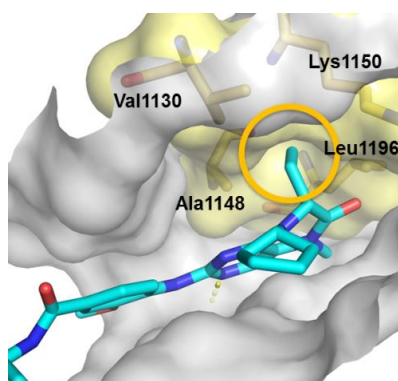
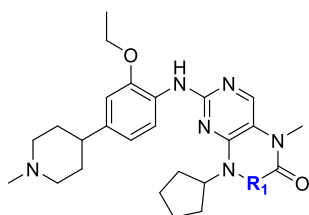


Figure 43. Docking of BI-2536 into ALK (2XB7) highlighting pocket residues and surface (yellow) where (*R*)-ethyl group is predicted to situate.

I synthesised a series of compounds modifying the size and orientation of the ethyl group according to Scheme 4 from the relevant amino acids **8a-h**. The biochemical assay results for the R₁ modifications are shown in Table 6.



| | | ALK | | BRD4 | | PLK-1 | |
|----------------|---------------------------|-----------------------------|---------------------------------|------------|------------------------|--------------------------|----------------------------------|
| R ₁ | | WT IC ₅₀ (nM) | F1174L IC ₅₀ (nM) | ΔTm [K] | K _d (nM) | IC ₅₀ (nM) | % Inhibition (10 nM / 100 nM) |
| 39 | (<i>R</i>)-Et | 220 ± 60 | 140 ± 20 | 6.3 ± 0.3 | 80 | 16 | 40 / 85 |
| 40 | (<i>S</i>)-Et | 1700 ± 150 | 860 ± 160 | 1.1 ± 0.1 | - | - | 18 / 18 |
| 41 | Et | 530 ± 40 | 300 ± 40 | 3.9 ± 0.4 | - | - | - |
| 42 | (<i>R</i>)- <i>i</i> Pr | 330 ± 50 | 70 ± 10 | 3.4 ± 0.3 | - | - | - |
| 43 | (<i>R</i>)-Me | 1300 ± 140 | 710 ± 30 | 7.5 ± 0.7 | 130 | - | 39 / 82 |
| 44 | (<i>S</i>)-Me | 3300 ± 280 | 970 ± 220 | 0.3 ± 0.3 | - | - | 17 / 37 |
| 45 | H | 1300 ± 120 | 850 ± 20 | 0.4 ± 0.1 | - | - | 12 / 29 |
| 46 | DiEt | 1400 ± 130 | 430 ± 30 | -0.5 ± 0.1 | - | - | - |
| 47 | Et, Me | 1800 ± 310 | 510 ± 120 | 0.2 ± 0.1 | - | - | - |
| 48 | Spiro-cPr | 660 ± 170 | 310 ± 50 | 3.5 ± 0.3 | 950 | 170 | 33 / 66 |

Table 6. Biochemical assay data for SAR of the (*R*)-ethyl group (R₁), - = not determined. ALK IC₅₀ values: mean ± S.E, n = 3. BRD4 ΔTm: mean ± S.D, n = 2, compound concentration of 10 μM. BRD4 K_ds, n = 1. PLK-1 IC₅₀ values and % Inhibition: n = 1 (ATP = 10 μM).

Importantly, the results show that the (*S*)-enantiomer (**40**) is detrimental to ALK, BRD4 and PLK-1 activity as expected from the X-ray but in contrast to the literature.¹³¹ The decrease in BRD4 T_m and PLK-1 inhibition is greater than both the literature reports on BI-2536 SAR. The contrasting results will be further discussed in Chapter 5. The racemic ethyl analogue **41** was also tested and was 2-fold less potent than (*R*)-ethyl analogue **39** against ALK and ALK^{F1174L}.

For ALK WT and ALK^{F1174L}, the (*R*)-methyl analogue **43** decreased potency but interestingly the (*R*)-*i*Pr analogue **42** was similar in potency to **39**. This indicates a larger alkyl group in the (*R*)-configuration is tolerated, filling a potential hydrophobic pocket in the ALK structure, as predicted in Figure **42**. However the BRD4 thermal shift was 3 K lower for **42** compared to **39** suggesting the larger group is less favourable in BRD4; a K_d measurement would be needed to confirm this.

I synthesised compound **45** to confirm the importance of the alkyl group in providing potency. In fact, removing the ethyl group decreased ALK, BRD4 and PLK-1 activity. This is consistent with the literature, with the ethyl group being important in providing potency against BRD4 and PLK-1.^{131,140} For ALK, the (*R*)- and (*S*)-methyl analogues **43** and **44** were equipotent to non-substituted **45**. This supports that a larger ethyl or isopropyl is important in providing additional potency against ALK.

Di-substitution at the R_1 position was also considered as an approach to distinguish between ALK and PLK-1. However the diethyl and ethyl-methyl analogues **46** and **47** showed a 3-fold decrease in ALK^{F1174L} activity compared to ethyl analogue **39** and completely diminished BRD4 activity. This drop in BRD4 activity, along with (*S*)-analogues **40** and **44** confirm that substitution is not tolerated on the opposite face in the BRD4 pocket. Finally spiro-cyclopropyl analogue **48** was moderately tolerated at ALK and showed a decrease in PLK-1 activity to 170 nM. BRD4 activity also decreased with a lower thermal shift value of 3.5 which translated to a significantly lower K_d of 950 nM.

Overall, the (*R*)-ethyl remained the most optimal group for ALK and BRD4 potency. Though reducing the size of the group and changing to the (*S*)-enantiomer reduced PLK-1 potency, ALK and BRD4 potency was also reduced and therefore not a constructive modification. Compound **42** with a (*R*)-isopropyl improved ALK^{F1174L} activity to 70 nM and would be an interesting analogue to follow up on by measuring the BRD4 K_d and PLK-1 IC_{50} .

2.5.4 SAR of R₂ – Cyclopentyl Group

Changing the cyclopentyl group (R₂) of the dihydropteridinone core was of particular interest due to previous SAR showing BRD4 and PLK-1 selectivity can be tuned.¹³¹ The presence of a 3-bromobenzyl group at this position increases BRD4 affinity 7-fold due to improved hydrophobic interactions with the WPF shelf but decreases PLK-1 activity (Figure 44A). This suggests that modifications in this region could be used to improve selectivity over PLK-1.

In ALK, the cyclopentyl of BI-2536 is predicted to situate in a similar region by docking to the isopropyl sulfonyl moiety found in ceritinib (Figure 44B). The sulfone forms hydrogen bond interactions with Lys1150 and a conserved water, whilst the isopropyl points towards a hydrophobic pocket on the bottom face. This hydrophobic pocket was considered an interesting area to explore, with the possibility of filling the pocket with suitable groups and/or forming polar interactions with pocket residues.

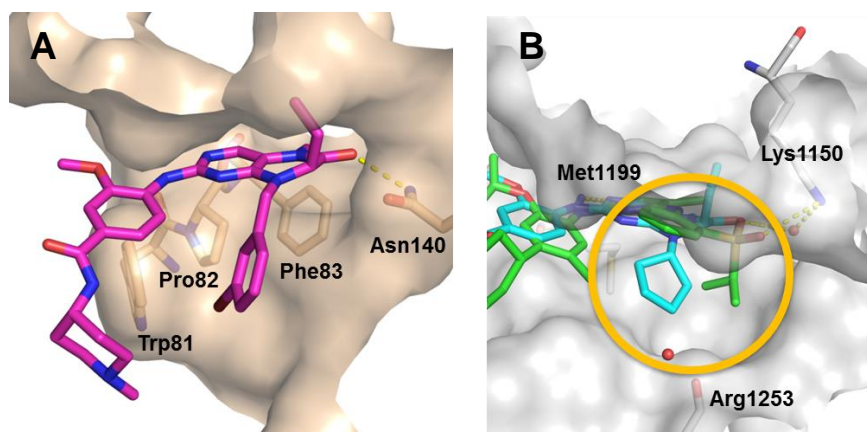
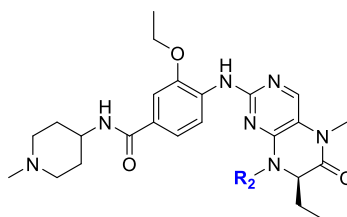


Figure 43. A) Docked structure of 3-BrBn analogue **50** with WPF residues highlighted. B) Docked structure of BI-2536 overlayed with ceritinib (4MKC) highlighting key residues and R₂ pocket. Polar interactions in yellow.

The hypothesis was further hydrophobic or polar interactions could be achieved in the ALK pocket by modifying the R₂ region. I synthesised a small set of analogues incorporating benzyl, heterocycle and aliphatic groups to gain an initial understanding of what type of groups were tolerated at the R₂ position. The majority of the R₂ groups were installed via reductive amination as described in Scheme 4, the exception being phenyl analogue **51**. The biochemical assay results for the cyclopentyl modification (R₂) are shown in Table 7.



| | | ALK | | BRD4 | | PLK-1 | |
|----------------|--|-----------------------------|---------------------------------|-----------|------------------------|--------------------------|----------------------------------|
| R ₂ | | WT IC ₅₀ (nM) | F1174L IC ₅₀ (nM) | ΔTm [K] | K _d (nM) | IC ₅₀ (nM) | % Inhibition (10 nM / 100 nM) |
| 29 | | 970 ± 140 | 380 ± 60 | 6.0 ± 0.5 | 81 | 12 | 40 / 80 |
| 57 | | 620 ± 70 | 440 ± 90 | 4.1 ± 0.1 | 69 | 84 | 13 / 57 |
| 49 | | 320 ± 40 | 490 ± 70 | 6.7 ± 0.3 | 73 | 114 ± 12 | 16 / 40 |
| 50 | | 500 ± 100 | 650 ± 140 | 4.0 ± 0.3 | 200 | - | 30 / 62 |
| 51* | | 1800 ± 90 | 1100 ± 350 | 1.5 ± 0.1 | - | - | - |
| 52 | | 290 ± 20 | 220 ± 10 | 6.8 ± 0.4 | 77 | - | - |
| 53 | | 2600 ± 300 | 4200 ± 1100 | 4.0 ± 0.1 | - | - | - |
| 54 | | 4600 ± 990 | 10000 ± 1900 | 1.5 ± 0.2 | - | - | - |
| 55 | | 2300 ± 560 | 2100 ± 300 | 1.6 ± 0.1 | - | - | - |

Table 7. Biochemical assay data for SAR of the cyclopentyl group (R₂), - = not determined.

*Racemate. ALK IC₅₀ values: mean ± S.E, n = 3. BRD4 ΔTm: mean ± S.D, n = 2, compound concentration of 10 μM. BRD4 K_ds, n = 1. PLK-1 IC₅₀ values and % Inhibition: mean ± S.D, n = 1/2, (ATP = 10 μM).

Compounds **57** and **49** with a benzyl and 3-bromobenzyl group respectively maintained BRD4 activity and led to a 30 – 40-fold decrease of the PLK-1 activity, as expected from previous reports.¹³¹ Compounds **49** and **57** were equipotent in ALK^{F1174L} activity, compared to **29** whilst for **49**, a 3-fold improvement in ALK WT activity was observed. Importantly, the divergent SAR between ALK and PLK-1 with **49** and **57** supported the hypothesis that the R₂ position could be used to optimise the

ALK/PLK-1 selectivity window. Moving the bromo to the *ortho*-position, compound **50**, observed comparable ALK potencies to *meta*-substituted **49** but gave a decrease in BRD4 activity. This suggests *meta*-substitution is more favourable, with improved reach into the hydrophobic WPF shelf region. Phenyl analogue **51** was 1.8 μM and 1.1 μM against ALK WT and ALK^{F1174L} respectively, therefore would expect the single (*R*)-enantiomer to be comparable to **29**, **49** and **57**.

Heterocycles were then considered, including thiophene **52**, pyrazole **53** and isoxazole **54**. Interestingly compound **52** improved ALK WT potency 3-fold and maintained modest ALK^{F1174L} activity compared to **29**. BRD4 activity was also maintained with thiophene analogue **52**. With the more polar heterocycle analogues **53** and **54**, a large drop in ALK activity was observed; in particular an 11-fold and 27-fold drop against ALK^{F1174L} for **53** and **54** respectively. This suggests that more polar substituents are not tolerated in this part of the ALK pocket. Additionally a large drop in thermal shift against BRD4 was observed; the polar heterocycles are less favoured in the hydrophobic WPF shelf region. As seen in Figure **45** the ALK pocket is quite hydrophobic in this region, on both the bottom face where the isopropyl of ceritinib is situated and the top face where the phenyl is positioned, forming a H- π interaction with Val1130. The main polar residue in this area is Lys1150 which interacts with ceritinib. The introduction of a polar group at the R₂ position would therefore require careful design, and if possible the use of X-ray crystallography, to guide suitable polar substituents that could interact with Lys1150 rather than situate in the predominant hydrophobic regions.

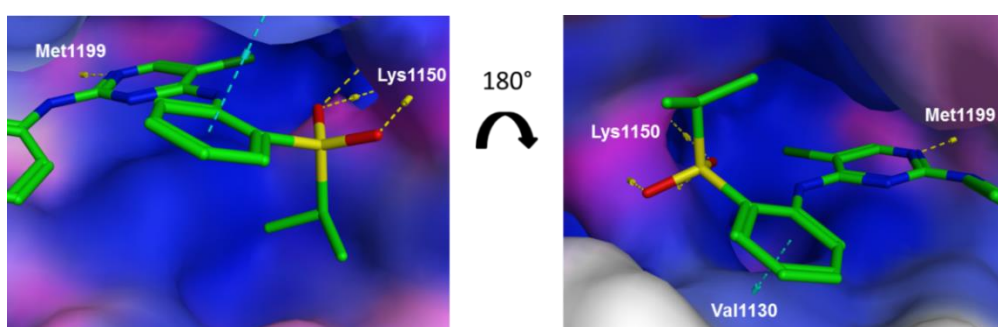


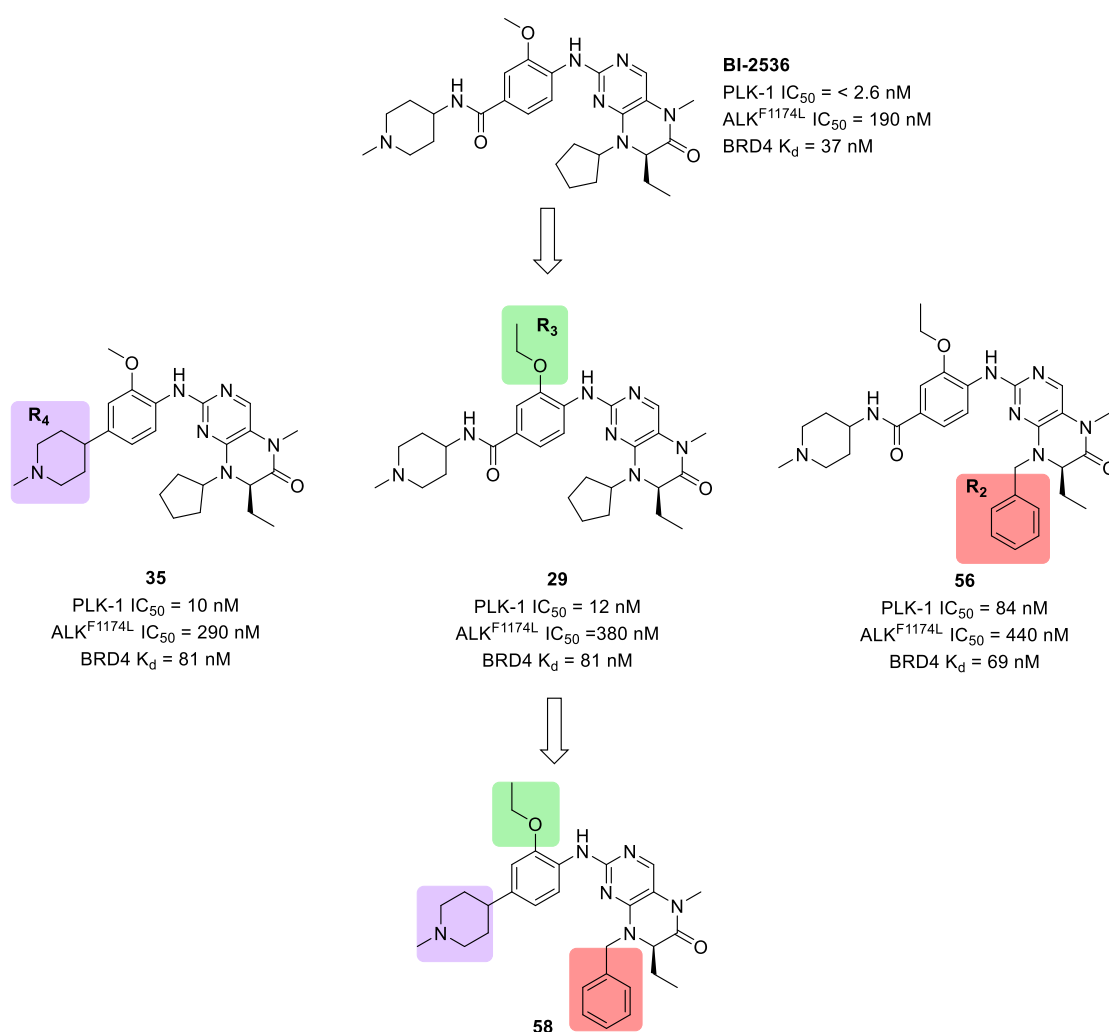
Figure 45. Protein surface of ALK showing hydrophobic regions (blue) and polar regions (pink). Key residue interactions with ceritinib are highlighted (yellow).

The final analogue **55** with an isobutyl group also decreased activity against ALK WT, ALK^{F1174L}, and BRD4. The larger benzyl and thiophene analogues **49**, **52** and **57** may

be filling the hydrophobic R₂ pocket more favourably whilst for BRD4 they are providing more favourable interactions with the WPF shelf region.

Initial modifications at the R₂ position resulted in **49** and **57** with maintained ALK and BRD4 potency and a significant 30 – 40-fold decrease in PLK-1 potency. This area for modification warranted further substrate scope to improve ALK activity and achieve selectivity over PLK-1.

2.6 Combining SAR Modifications

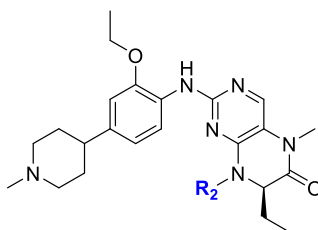


Scheme 12. Development of BI-2536 analogues modifying R₂, R₃ and R₄ positions.

Changes to the R₂, R₃ and R₄ groups had shown decreases in PLK-1 activity whilst maintaining ALK and BRD4 potency. This is exemplified by compounds **35**, **29** and **57**

which decreased PLK-1 potency 4, 5 and 32-fold respectively (Scheme 12). To conclude this initial SAR investigation, I combined these modifications to observe the overall effect on PLK-1 activity.

I synthesised compounds **56** and **58** with the combined modifications of a benzyl or 3-bromobenzyl group at R₂, ethoxy group at R₃ and removal of the amide at R₄. The biochemical assay results for the combined modifications are shown in Table 8.



| | | ALK | | BRD4 | | PLK-1 |
|----------------|--|-----------------------------|---------------------------------|-----------|------------------------|-----------------------|
| R ₂ | | WT IC ₅₀ (nM) | F1174L IC ₅₀ (nM) | ΔTm [K] | K _d (nM) | IC ₅₀ (nM) |
| 56 | | 120 ± 12 | 290 ± 17 | 5.0 ± 0.5 | 120 | 540 |
| 58 | | 120 ± 11 | 85 ± 19 | 4.7 ± 0.4 | 54 | 290 ± 45 |

Table 8. Biochemical assay data for the combined SAR of R₂, R₃ and R₄ groups. ALK IC₅₀ values: mean ± S.E, n = 3. BRD4 ΔTm: mean ± S.D, n = 2, compound concentration of 10 μM. BRD4 K_ds, n = 1. PLK-1 IC₅₀ values: mean ± S.D, n = 1/2, (ATP = 10 μM).

The combination of R₂, R₃ and R₄ modifications provided a greater decrease in PLK-1 activity for **56** and **58**, 210-fold and 115-fold respectively compared to BI-2536. With benzyl compound **58**, a 2-fold increase in ALK^{F1174L} potency was achieved compared to BI-2536 and also maintained potent BRD4 activity. This was the first analogue demonstrating greater potency at ALK^{F1174L} than at PLK-1 and hence a key milestone in the development of a dual ALK-BRD4 inhibitor by switching kinase selectivity.

Chapter 3 Exploring the R₂ Region: Design and Synthesis of Second Generation Inhibitor

Part of this chapter is published in E.Watts et al., J. Med. Chem, 2019, 62, 2618-2637

3.1 Design Hypothesis for Exploring the R₂ Pocket

So far, the greatest change in PLK-1 activity resulted from modifying the cyclopentyl to a benzyl or 3-bromobenzyl group (Table 7). Further inspection of this region in ALK and PLK-1 structures shows that PLK-1 has a larger phenylalanine residue (Phe183) at the bottom of this pocket compared with a smaller leucine residue (Leu1256) in ALK (Figure 46). Thus the hypothesis was that the more restricted PLK-1 pocket would be less tolerant to substitution at the R₂ position compared to the more open ALK structure.

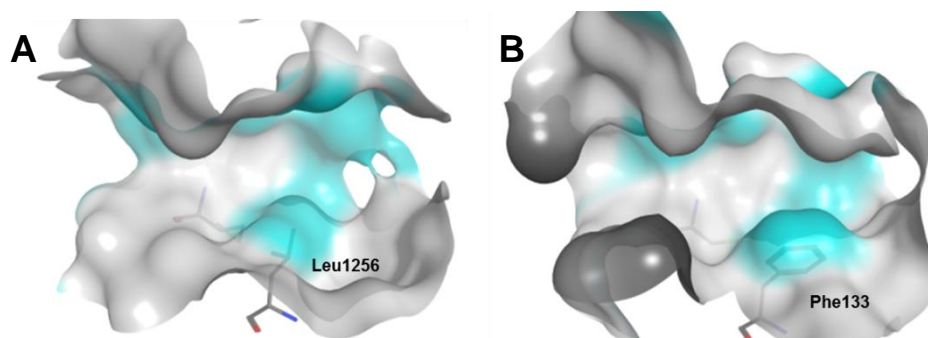


Figure 46. Surfaces of **A)** ALK (2XB7) and **B)** PLK-1 (2RKU) highlighting residues Leu1256 and Phe183.

To investigate this hypothesis further, I performed docking studies of 3-bromobenzyl analogue **56** in ALK and PLK-1 (Figure 47). The docking of **56** into ALK predicted the 3-bromobenzyl extending into the lower ALK pocket, when compared to the cyclopentyl of BI-2536. For PLK-1, the aminopyrimidine moiety was still predicted to bind to the hinge region including Cys133 but a shift in the core was observed. Additionally, the core of the molecule adopts a more strained, puckered conformation. Both differences in the predicted docking pose were likely caused by clashes of the bromobenzyl group with the side chain of Phe183 and were consistent with the

decrease in activity observed with benzyl analogues **56** and **58** and in the literature (Table 7).¹³¹

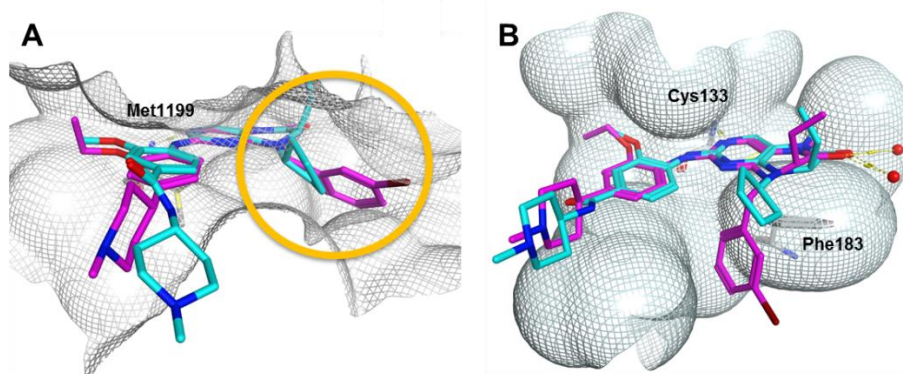
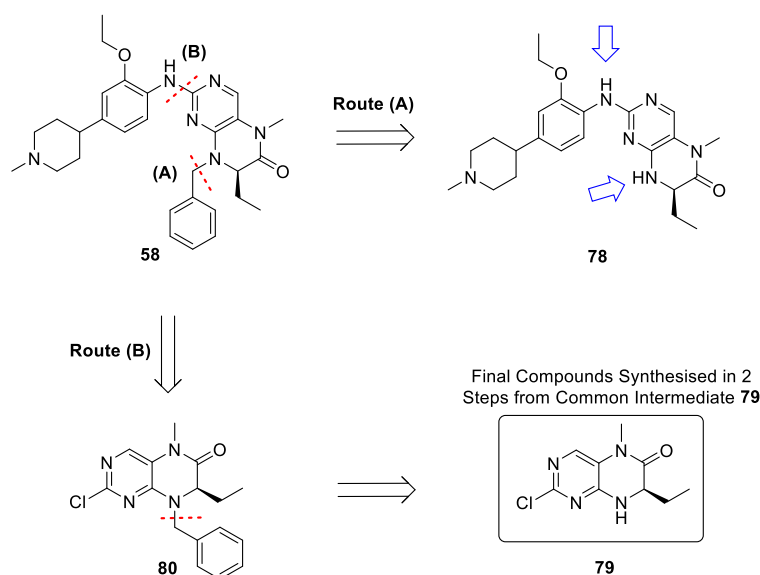


Figure 47. **A)** Docking of BI-2536 (blue) and 3-bromobenzyl analogue **56** (pink) into ALK (2XB7). **B)** Docking of 3-bromobenzyl analogue **56** (pink) overlaid with BI-2536 (blue) in PLK-1 (2RKU). Interaction surface is shown (MOE) with key residues and/or pocket highlighted.

3.2 Synthetic Route Development

Due to the lack of structural information for the dual ALK-BRD4 series in ALK and with no crystallography available, I continued to probe the ALK pocket through systematic synthesis and testing. A key issue in preparing a significant number of analogues varying the R_2 position was that this substituent was introduced early and preparation of each final compound required five steps (Scheme 4). There was no precedent in the literature for late stage variation at this position so to facilitate preparation of these derivatives, alternative approaches were attempted.

The optimum synthesis would install the R_2 group at the final step (Route A, Scheme 13). However retrosynthetically removing the R_2 group from final compound **58** gives intermediate **78** which has two free amines for potential reactivity. To avoid this regioselectivity issue, I proposed an alternative strategy which would take two steps to reach the final compounds from common intermediate **79** (Route B). For the forward synthesis, intermediate **79** could undergo an alkylation to give example intermediate **80**, followed by S_NAr to reach the final compound **58**.



Scheme 13. Design strategy for installing the R₂ group at a later stage in the synthesis.

To synthesise the common intermediate **79**, I attempted several synthetic routes, outlined in Table 9. I first attempted selective methylation of the amide on intermediate **81**. However after 1 hr, both the mono-methylated and dimethylated products were present. The products could not be separated from one another and so this method was not continued.

The second and third routes started with 2,4-dichloropyrimidin-5-amine which I methylated to give **82**. I attempted an S_NAr and a Buchwald coupling between **82** and methyl (*R*)-2-aminobutanoate **8a** but both were unsuccessful. The alternative method (3) focused on amide coupling between the methyl amine and acid of **84**. Amide coupling conditions using HBTU and T3P were attempted but these were also unsuccessful. In route 4, I tried a different formation of the core starting with an S_NAr between 5-bromo-2,4-dichloropyrimidine and 2-amino-*N*-methylbutanamide to give intermediate **84**. However intramolecular coupling between the bromine and amide was unsuccessful using both palladium and copper coupling conditions. This route would have made the desired intermediate **79** as the racemate so an alternative route was preferential.

The fifth and sixth approaches utilised a protecting group on the secondary amine. The protecting group needed to be stable during the synthesis and also the deprotection had to occur under reaction conditions that left the remainder of the compound intact. For example a Boc group could be labile during the acetic acid step and removal of Cbz or benzyl group by hydrogenation could remove the chloro atom.

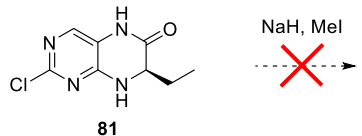
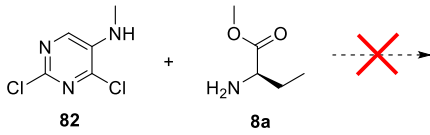
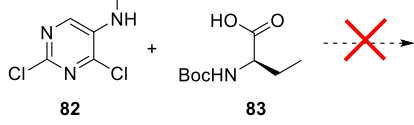
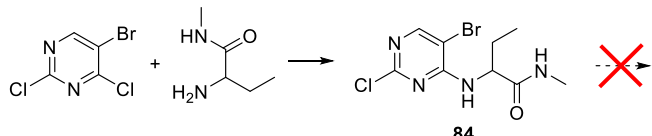
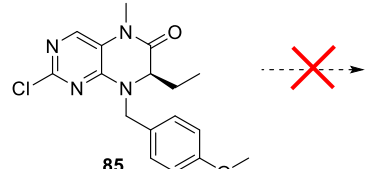
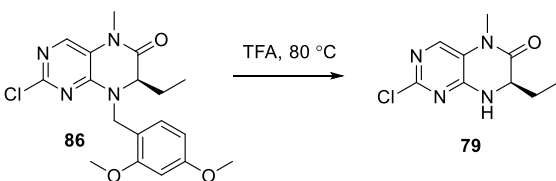
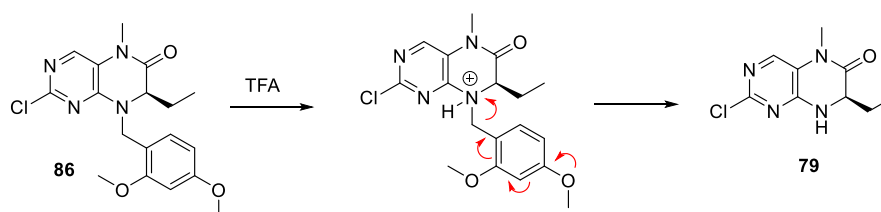
| | |
|--|--|
| Route 1. Selective Methylation  <p style="text-align: center;">81</p> | <p>Single and dimethylated products observed. Difficult to separate.</p> |
| Route 2. S_NAr/Buchwald  <p style="text-align: center;">82 8a</p> | <p>S_NAr conditions using K₂CO₃ unsuccessful. Buchwald coupling conditions using Pd(OAc)₂ and BINAP unsuccessful.</p> |
| Route 3. Amide Coupling  <p style="text-align: center;">82 83</p> | <p>Amide coupling conditions using HBTU or T3P unsuccessful.</p> |
| Route 4. Alternative Core Formation (Racemic)  <p style="text-align: center;">84</p> | <p>S_NAr to form 84 successful (65%) however coupling between amide and pyrimidine unsuccessful using Pd(OAc)₂ and CuI.</p> |
| Route 5. PMB Protection/Deprotection  <p style="text-align: center;">85</p> | <p>Attempted PMB removal using CAN (0%), DDQ (0%) and TFA (rt and 80 °C, 0%)</p> |
| Route 6. DMB Protection/Deprotection  <p style="text-align: center;">86 79</p> | <p>Attempted DMB removal using CAN (0%) and DDQ (0%) Removal using TFA was successful at 80 °C</p> |

Table 9. Attempted synthetic routes to form intermediate **79**.

A *para*-methoxybenzyl (PMB) group and dimethoxybenzyl (DMB) group were chosen as potentially suitable protecting groups (Routes 5 & 6, Table 9). The protecting groups were installed via a reductive amination using 4-methoxybenzaldehyde and 2,4-dimethoxybenzaldehyde, following the same synthetic route as previously discussed in Chapter 2 (Scheme 4) to get to intermediates **85** and **86**.

Various conditions can be used to remove PMB and DMB protecting groups including hydrogenation, oxidation and acidic cleavage, although the former was not pursued due to presence of the chloro atom. Deprotections using mild oxidising agents DDQ and CAN were attempted but did not remove the protecting group.^{159,160} PMB and DMB protecting groups can also be cleaved in the presence of strong acid (Scheme 14).¹⁵⁹ **85** and **86** were at first stirred in trifluoroacetic acid (TFA) at room temperature but no removal was observed. Heating both reactions to 80 °C saw removal of the DMB group after 4 hours, however the PMB group was not removed. The more electron donating DMB group is more labile in the presence of acid. The use of the DMB protecting group successfully made the desired intermediate **79** for accessible late stage functionalisation at the R₂ position.

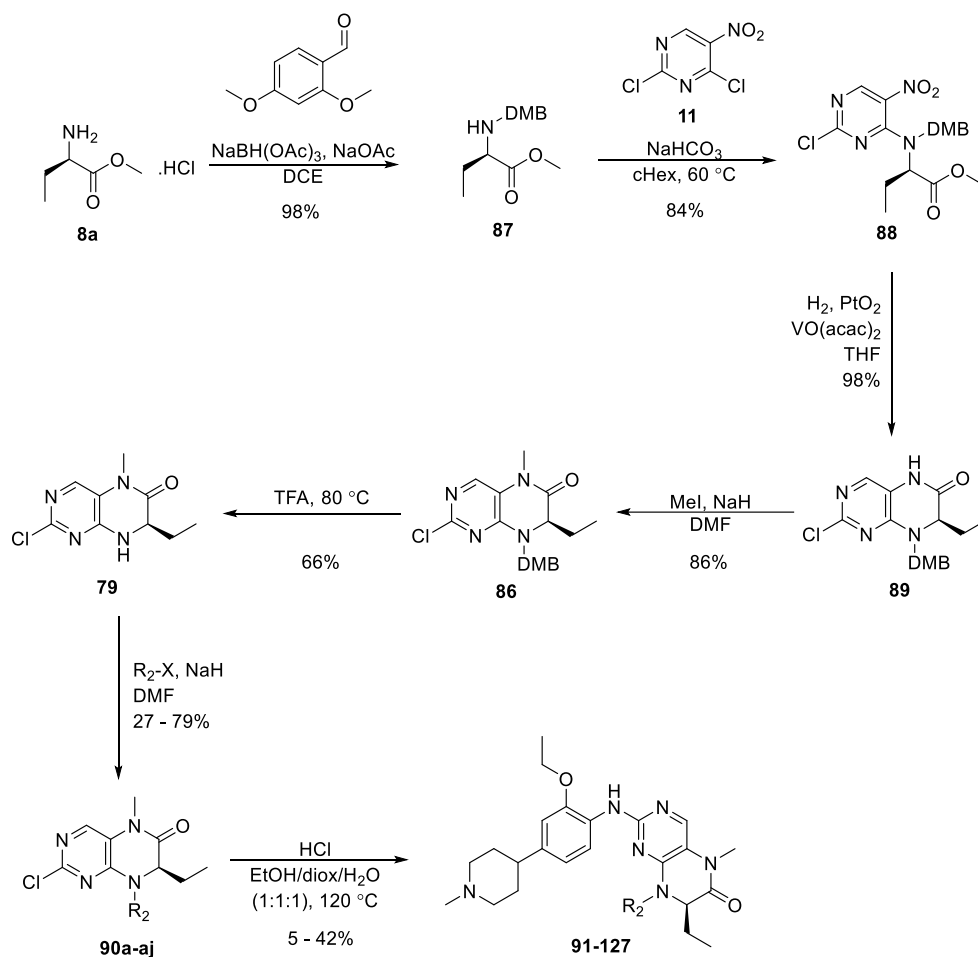


Scheme 14. Deprotection of the dimethoxybenzyl group using TFA to form **79**.

3.2.1 New Synthetic Route

Using the DMB protecting group, I synthesised final compounds according to Scheme 15 to introduce a wide range of groups at the R₂ position. This approach maintained many elements of the initial route (Scheme 4) including the reductive amination, S_NAr, reductive heterocyclisation and methylation steps to reach intermediate **86**. Deprotection of the DMB group gave common intermediate **79** from which different groups could be added via an S_N2 reaction, reaching intermediates **90a-aj**. The synthesis concluded with the same acid-catalysed S_NAr to reach final compounds **91 – 127**.

A key challenge in the synthesis was that the reductive cyclisation step on intermediate **88** using iron and acetic acid partially removed the DMB group, as well as being an overall low yielding step. I attempted using tin chloride as an alternative reduction to prevent removal of the protecting group but this led to poor yields (10%). The nitro group was reduced, as evident by LCMS, but no cyclised product was being formed.

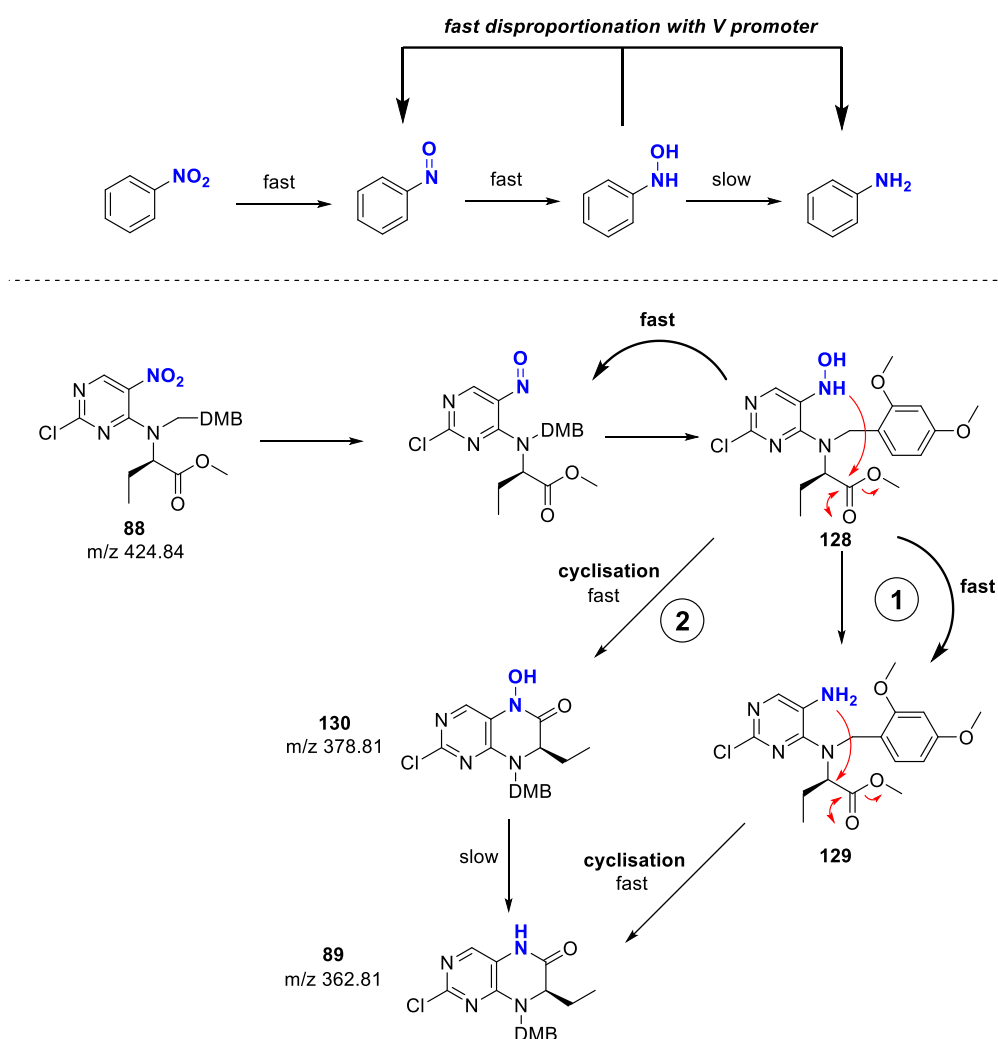


Scheme 15. Adapted synthetic route for R_2 variations.

It was hypothesised that hydrogenation conditions would pose problems due to removal of the DMB group and/or the chlorine atom. However, chemoselective hydrogenation of nitroarenes can be achieved using platinum oxide and vanadyl acetylacetonate.¹⁶¹ Vanadyl acetylacetonate is used to suppress the accumulation of the hydroxylamine intermediates which can be hazardous, thermally unstable and condense with the nitroso intermediate to form azo or azoxy products.¹⁶² The presence of the vanadium promoter bypasses the slow reduction step of the hydroxylamine amine by fast disproportionation to the nitroso and amine (Scheme 16).

For the synthesis of intermediate **89**, the reduction of nitropyrimidine **88** should undergo the same reductive steps to hydroxylamine **128**, with the vanadium promoter allowing fast disproportionation to reach amine intermediate **129** (Scheme 16 (1)). The free amine should then quickly cyclise with the ester to form the cyclised intermediate **89**. However, monitoring of the reaction by LCMS suggested an alternative mechanism, (2). During the course of the reaction, the starting material

and final compound masses, $[M+H]^+$ 425 and 363 were observed as well as unknown mass $[M+H]^+$ 379. The unknown mass was assigned to cyclised hydroxylamine intermediate **130**, indicating hydroxylamine **128** is also able to quickly cyclise. Over time, the cyclised hydroxylamine intermediate **130** slowly reduces to the final intermediate **89**. These conditions gave an excellent yield of 98% and importantly did not remove the DMB group or cause dehalogenation.



Scheme 16. General mechanism for vanadium promoted nitro reduction and proposed mechanism for reductive heterocyclisation of intermediate **88** to **89**.

Overall, the new synthetic route enabled preparation of key intermediate **79** on a multi-gram scale with a 46% overall yield. The synthesis allowed for a more efficient installation of a wide variety of groups to pragmatically explore the R_2 pocket in now only two steps from intermediate **79**.

3.2.2 Chiral Shift Experiments

The synthesis of dihydropteridinone intermediates **90a – aj** contained strong basic steps using sodium hydride and a strong acidic step using TFA. This caused concern for the ethyl chiral centre present on the molecule and its potential to epimerise. The original synthesis detailed in Chapter 2 also contained the same strong basic step. To confirm if the chiral centre had epimerised under either the strong basic and acidic conditions, I used chiral shift NMR on intermediates from both synthetic routes.

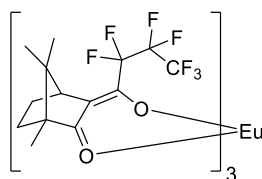


Figure 48. Structure of chiral shift NMR reagent $\text{Eu}(\text{hfc})_3$.

The chiral shift reagent used was $\text{Eu}(\text{hfc})_3$, a chiral camphor derivative complexed with a europium ion (Figure 48). The europium reagent coordinates with a Lewis base, resulting in a downfield chemical shift of protons nearby to the Lewis basic site. The chemical shift is induced by the weak paramagnetic character of the lanthanide from the unpaired electrons in its f shell.¹⁶³ This change in chemical shift can separate out the coordinated enantiomer complexes. A useful application of the lanthanide shift reagents is to determine the enantiomeric purity if sufficient separation between the enantiomers is obtained.¹⁶⁴

Intermediates **6r** and **90aj**, synthesised via Schemes 15 and 4 respectively were subjected to incremental additions of $\text{Eu}(\text{hfc})_3$, taking an NMR spectrum after each addition (Figure 49). The addition of $\text{Eu}(\text{hfc})_3$ to the racemates of **6r** and **90aj** caused splitting of its peaks, indicating the presence of both enantiomers. This is exemplified by the aromatic proton signal highlighted on **6r** and **90aj**. In contrast the addition of $\text{Eu}(\text{hfc})_3$ to the single enantiomer intermediates did not see splitting of its peaks. This confirmed that only one enantiomer was present and the strong basic and acidic conditions in the synthesis had not caused epimerisation.

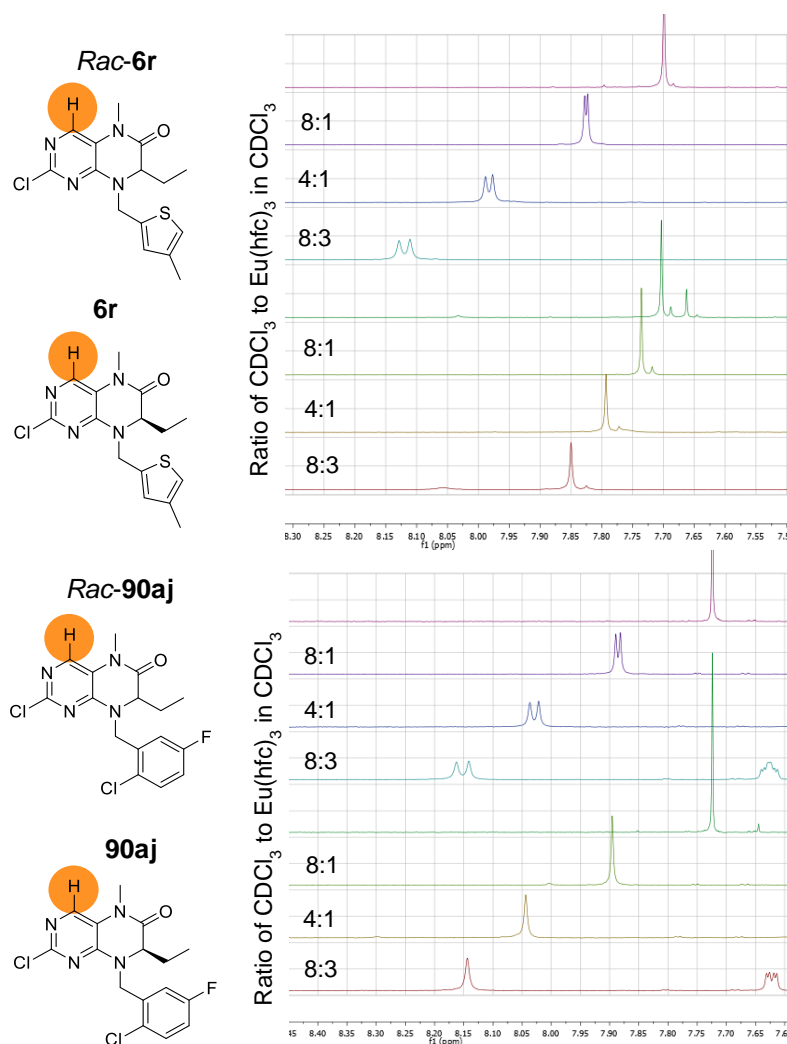


Figure 49. Chiral shift NMR experiments for **6r** and **90aj**, comparing the aromatic proton signal of the racemate and single enantiomer after increasing addition of $\text{Eu}(\text{hfc})_3$ (0.015 M).

3.3 SAR of R_2 position

3.3.1 Benzyl Groups

3.3.1.1 Exploring Substitution at the *meta*-Position

The first set of analogues I synthesised explored different substitutions at the *meta*-position on the benzyl group. I previously made *meta*-bromo analogue **56** which had modest potency against ALK and BRD4, and therefore decided to change the electronics and hydrophobicity of this group to build SAR.

Docking of bromo-analogue **56** predicts the benzyl to fill the R_2 pocket with the *meta*-bromo pointing towards solvent (Figure **50A**). In comparison docking of **59** with a

meta-fluoro positions the substituent either towards the top or bottom of the pocket. There may be some variance in the position of this *meta*-group, depending on the size and potential for further hydrophobic or polar interaction. The hypothesis was hydrophobic groups would be favoured in the predominantly hydrophobic pocket. In BRD4, the *meta*-substitution directs down into the WPF region, as observed in the literature with SAR on BI-2536 (Figure 50B).¹³¹ The conformation of the benzyl group differed between the ALK and BRD4 pockets but they were both predicted to be accessible low-energy conformations (Figure 50C). Previous SAR showed polar heterocycles being less tolerated in BRD4 so the hypothesis was that hydrophobic *meta*-substituents would also be preferred in this region.

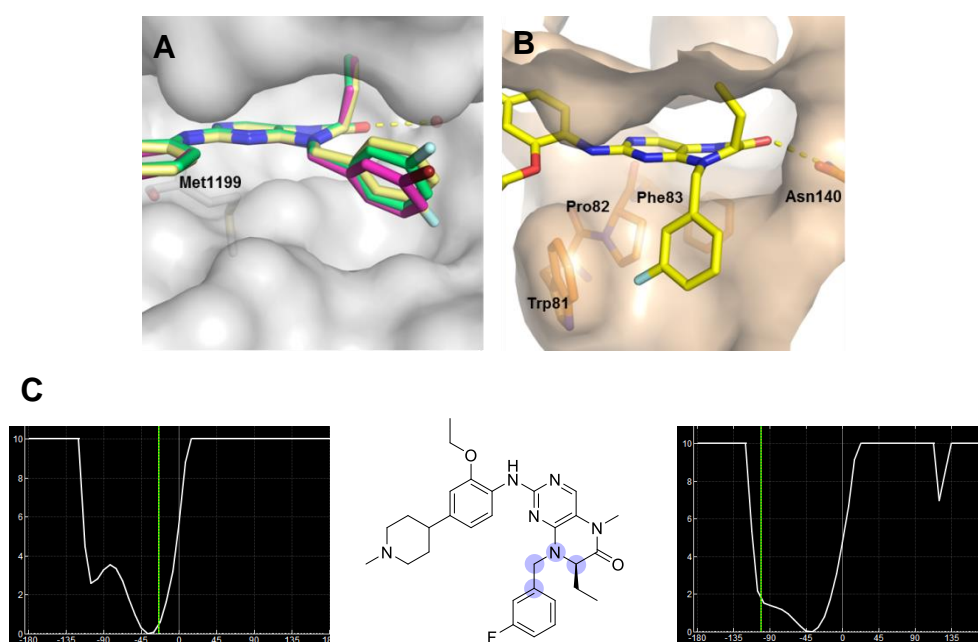
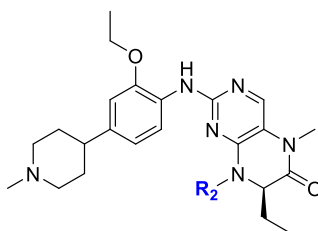


Figure 50. **A)** Docked structures of bromo-analogue **56** (pink) and fluoro-analogue **59** (green and yellow) in ALK (2XB7). **B)** Docked structure of **59** in BRD4 (4OGI). **C)** Torsion profile of **59** in ALK (left) and BRD4 (right), generated in the MOE Torsion Profile application. The four atoms used for generating the torsion profiles are highlighted in purple.

Compounds **59**, **60** and **91** – **98** were synthesised according to Scheme 4 or Scheme 15 and the biochemical results are shown in Table 10. I selected a series of different substituents based on the Craig's plot which compares two different substituents parameters, in this case the Hammett sigma constant versus hydrophobicity, to aid rational drug design.¹⁶⁵ The analogues I synthesised included polar and hydrophobic groups and ranged in electron donating and withdrawing character to understand which is preferred.



| | | ALK | | BRD4 | | PLK-1 |
|----------------|--|-----------------------------|---------------------------------|-----------|------------------------|-----------------------|
| R ₂ | | WT IC ₅₀ (nM) | F1174L IC ₅₀ (nM) | ΔTm [K] | K _d (nM) | IC ₅₀ (nM) |
| 58 | | 120 ± 11 | 85 ± 19 | 4.7 ± 0.5 | 54 | 290 ± 45 |
| 56 | | 120 ± 10 | 290 ± 20 | 5.0 ± 0.5 | 120 | 540 |
| 91 | | 80 ± 10 | 220 ± 40 | 6.2 ± 0.4 | 130 | 540 |
| 59* | | 140 ± 20 | 250 ± 60 | 6.4 ± 1.0 | - | - |
| 92 | | 480 ± 40 | 350 ± 30 | 5.1 ± 0.8 | - | - |
| 93 | | 140 ± 20 | 210 ± 60 | 6.3 ± 0.2 | - | - |
| 94 | | 190 ± 40 | 580 ± 90 | 5.3 ± 0.8 | - | - |
| 95 | | 100 ± 10 | 370 ± 20 | 4.8 ± 0.4 | 63 | 1800 |
| 96 | | 990 ± 350 | 1100 ± 130 | 3.5 ± 0.1 | - | - |
| 60* | | 5800 ± 500 | 3800 ± 940 | 0.7 ± 0.3 | - | - |
| 97 | | 1400 ± 120 | 940 ± 140 | 4.4 ± 0.3 | - | - |
| 98 | | 1800 ± 180 | 1700 ± 130 | 7.2 ± 0.2 | - | - |

Table 10. Biochemical assay data for benzyl groups (R₂), - = not determined. ALK IC₅₀ values: mean ± S.E, n = 3. BRD4 ΔTm: mean ± S.D, n = 2, compound concentration of 10 μM. BRD4 K_dS, n = 1. PLK-1 IC₅₀ values: mean ± S.D, n = 1/2 (ATP = 10 μM).

Overall, non-substituted benzyl **58** remained the most potent against ALK^{F1174L}. For ALK WT, both inductively withdrawing and donating groups were tolerated, including F, Cl, Br, Me, CN and CF₃, and were equipotent to non-substituted **58**. In general,

hydrophobic groups were well tolerated but polar groups decreased potency, matching the hypothesis. Polar analogues **60**, **96** and **97** gave a greater than 11-fold decrease in potency against ALK^{F1174L}. As previously observed with polar heterocycles, the hydrophobic R₂ pocket is less tolerating of polar groups.

The majority of analogues, both polar and hydrophobic, were tolerated in BRD4, with the benzyl likely to situate towards the WPF shelf. Although polar analogues **96** and **97** were tolerated, carboxylic acid analogue **60** gave a very small thermal shift indicating the acidic group is disfavoured in the BRD4 pocket. At this point I also tested compound **98** with a naphthalene group to see if larger bicyclic systems could be tolerated. Despite the BRD4 thermal shift being high, ALK WT and ALK^{F1174L} potency decreased 15- and 20-fold respectively suggesting the naphthalene group was too large.

I chose **91** and **95** to be tested against PLK-1 to see if improvements in PLK-1 selectivity were achieved. Chloro-analogue **91** had similar PLK-1 potency to **56** and **58** providing a similar 2 – 3-fold selectivity towards ALK^{F1174L}. Gratifyingly cyano compound **95** showed a greater decrease in PLK-1 potency to 1.8 μ M. This provided a 5-fold selectivity towards ALK^{F1174L} and was a >700-fold decrease in potency from BI-2536. Compound **95** demonstrated that PLK-1 activity can be substantially reduced by varying this position but I still needed to find a group that achieved this whilst maintaining or improving ALK^{F1174L} potency.

3.3.1.2 Alternative Substitution Positions

Following the exploration of substitution at the *meta*-position, the next strategy was to investigate substitution at alternative positions on the benzyl group (Figure 51). This included moving the substituent from the *meta*- to the *ortho*- and *para*-positions and also substituting at the benzylic position, to further probe the ALK pocket and test if further potency could be achieved.

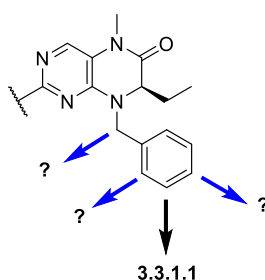


Figure 51. Alternative substitution positions on the benzyl group for exploration.

I first docked a series of analogues with an *ortho*-, *meta*- or *para*-chlorobenzyl at the R₂ position to understand what substitution patterns could be tolerated (Figure 52). In ALK, the benzyl of all three analogues was predicted to be situated in the R₂ pocket. The *ortho*-chloro (**100**) was predicted to situate towards the upper ALK surface whilst the *meta*- and *para*-chloro (**91** and **104**) were predicted to point out towards solvent. I also docked the series into BRD4, which predicted all the chlorobenzyls bending down into the WPF shelf region. The *meta*- and *para*-chloro further fill into this region compared to the *ortho*-analogue **100** which may result in improved potency. Overall, the docking suggested all three substitution positions could be tolerated in ALK, though for BRD4, *meta*- and *para*-substitution may be preferred.

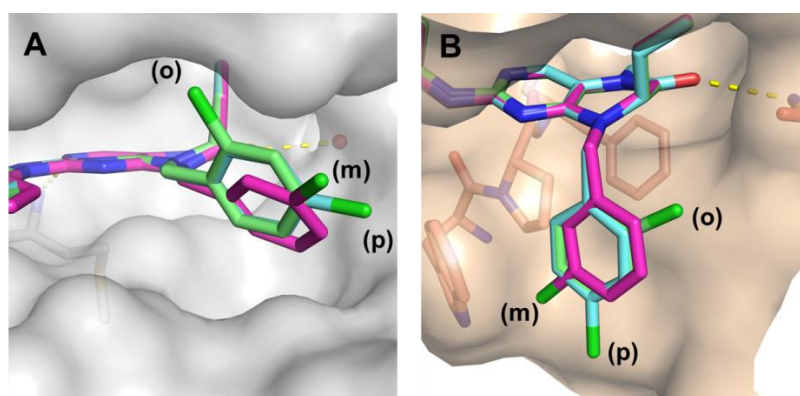
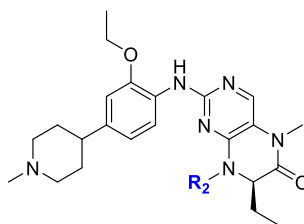


Figure 52. Docking of **100** (green), **91** (pink) and **104** (blue) with an *ortho*-, *meta*- and *para*-chlorobenzyl at R₂ respectively in **A**) ALK (2XB7) and **B**) BRD4 (4OGI).

Analogues with a chloro or bromo in the *ortho*- or *para*-position were synthesised according to Scheme 15 to compare with the already synthesised *meta*-analogues **56** and **91**. Due to the possibility of the *ortho*-substitution filling ALK pocket space, additional analogues with an *ortho*-fluoro or methyl were synthesised. The biochemical data for the *ortho*- and *para*-analogues are shown in Table 11.

Overall, changing the substitution from the *meta*- to the *ortho*- position saw no significant change in potency against ALK WT and ALK^{F1174L}, exemplified by the bromo pair **56** and **99** and the chloro pair **91** and **100**. The presence of a fluoro or methyl at the *ortho*-position (**101** and **102**) did not affect the potency either and were similarly equipotent to their *meta*-counterparts **59** and **93** (Table 10). Changing to the bromo and chloro *para*-substituted benzyl, **103** and **104**, resulted in a small decrease in potency compared to the *ortho*- and *meta*-position. This suggested substitution at the *para*-position is less tolerated within the ALK pocket or does not fill pocket space as well as the *ortho*- or *meta*- substituents.



| | | ALK | | BRD4 | | PLK-1 |
|----------------|--|-----------------------------|---------------------------------|-----------|---------------------|-----------------------|
| R ₂ | | WT IC ₅₀ (nM) | F1174L IC ₅₀ (nM) | ΔTm [K] | K _d (nM) | IC ₅₀ (nM) |
| 58 | | 120 ± 11 | 85 ± 19 | 4.7 ± 0.5 | 54 | 290 ± 45 |
| 56 | | 120 ± 10 | 290 ± 20 | 5.0 ± 0.5 | 120 | 540 |
| 91 | | 80 ± 10 | 220 ± 40 | 6.2 ± 0.4 | 130 | 540 |
| 99 | | 150 ± 10 | 150 ± 40 | 2.9 ± 0.8 | - | - |
| 100 | | 80 ± 30 | 180 ± 30 | 3.2 ± 0.2 | - | - |
| 101 | | 250 ± 30 | 130 ± 10 | 4.3 ± 0.1 | - | - |
| 102 | | 180 ± 10 | 220 ± 30 | 5.2 ± 0.2 | - | - |
| 103 | | 570 ± 20 | 680 ± 30 | 5.8 ± 0.9 | - | - |
| 104 | | 490 ± 80 | 330 ± 60 | 5.7 ± 0.4 | - | - |

Table 11. Biochemical assay data for benzyl groups (R₂), - = not determined. ALK IC₅₀ values: mean ± S.E, n = 3. BRD4 ΔTm: mean ± S.D, n = 2, compound concentration of 10 μM. BRD4 K_dS, n = 1. PLK-1 IC₅₀ values: mean ± S.D, n = 1/2 (ATP = 10 μM).

As seen in the previous SAR table, all of the substituted benzyls were less potent compared to the non-substituted analogue **58** against ALK^{F1174L}. However for ALK WT, **58** was equipotent to many of the *ortho*- and *meta*-substituted analogues. This suggested there is a slight difference in pocket shape resulting from the mutation. As previously discussed (1.2.2.1) the F1174L mutation causes a shift in the DFG loop which backs on to the R₂ pocket (Figure 53). Residue Asp1270 of the ALK mutant can be seen to extend further into the R₂ pocket. This may limit the pocket space hence why substitution on the benzyl is less tolerated compared to ALK WT.

For BRD4, the majority of analogues were tolerated as perceived from their moderate to high degrees of thermal shift. The slightly lower thermal shifts for the *ortho*-analogues **99** and **100** suggest the *meta*- or *para*-substituted analogues could be

more optimal in situating towards the hydrophobic WPF shelf region, as predicted in the docking experiments (Figure 52).

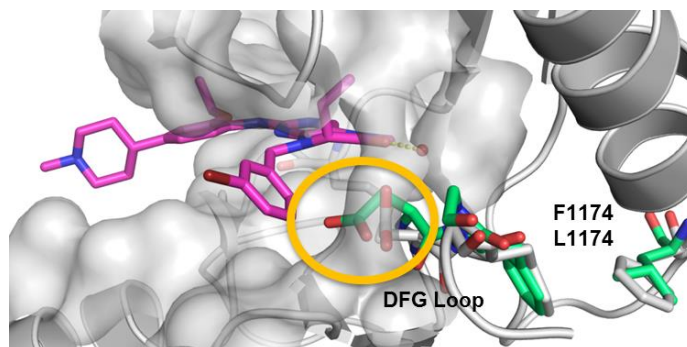


Figure 53. Overlay of ALK WT (grey, 2XB7) with docked analogue **56** and ALK^{F1174L} (green, 2YJR) structures highlighting the difference in DFG loop position.

Next I considered substitution at the benzylic position as a possible method to gain ALK potency. The hypothesis was that substituting at a different vector on the molecule may fill additional ALK pocket space and cause a change in the conformational preference of the molecule. The additional substitution and change in conformation may also lead to a further decrease in PLK-1 potency due to the more restricted R₂ pocket. As an initial test, analogues **105** and **106** with a methyl or ethyl group at the benzylic position were docked into ALK, comparing to non-substituted benzyl **58** (Figure 54). The docking experiments suggested the methyl and ethyl group situate towards a pocket on the upper surface with the phenyl remaining in the lower ALK R₂ pocket in a similar conformation to non-substituted **58**. This upper pocket is adjacent to the pocket predicted to be occupied by the R₁ (*R*)-ethyl group.

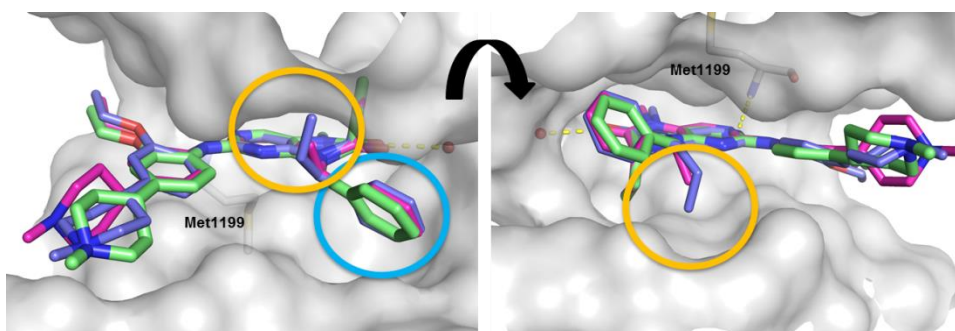
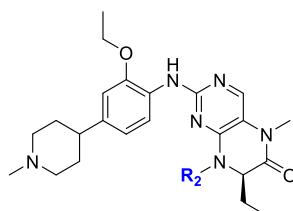


Figure 54. Docking of analogues **58**, (green) **105** (pink) and **106** (purple) into ALK (2XB7). Additional pocket filled by alkyl group highlighted in orange. R₂ ALK pocket highlighted in blue.

Both **105** and **106** were initially synthesised to test if filling additional pocket space from this unexplored vector provided additional potency. **105** and **106** were

synthesised according to Scheme **15** using racemic (1-bromoethyl)benzene and (1-bromopropyl)benzene. The biochemical assay results for substitution at the benzylic position are shown in Table **12**.

Pleasingly, the addition of the benzylic methyl group gave a 2-fold improvement in potency compared to **58** against the ALK^{F1174L} mutant to 31 nM, although equipotent compared to ALK WT. The slightly larger ethyl group decreased potency 10-fold against ALK^{F1174L} implying that groups larger than methyl are not tolerated. The ethyl group was also disfavoured in the BRD4 pocket with a low thermal shift measurement. Both **105** and **106** were made as a mixture of diastereomers and further investigation into the single diastereomer of **105** in particular is discussed in Chapter 4.



| | | ALK | | BRD4 | | PLK-1 |
|----------------|--|-----------------------------|---------------------------------|-----------|---------------------|-----------------------|
| R ₂ | | WT IC ₅₀ (nM) | F1174L IC ₅₀ (nM) | ΔTm [K] | K _d (nM) | IC ₅₀ (nM) |
| 58 | | 120 ± 11 | 85 ± 19 | 4.7 ± 0.5 | 54 | 290 ± 45 |
| 105 | | 180 ± 51 | 31 ± 5 | 3.6 ± 1.7 | - | - |
| 106 | | 630 ± 73 | 300 ± 49 | 1.3 ± 0.0 | - | - |

Table 12. Biochemical assay data for substitution at the benzylic position, - = not determined. ALK IC₅₀ values: mean ± S.E, n = 3. BRD4 ΔTm: mean ± S.D, n = 2, compound concentration of 10 μM. BRD4 K_ds, n = 1. PLK-1 IC₅₀ values: mean ± S.D, n = 2 (ATP = 10 μM).

Overall, exploring alternative substituent positions on the R₂ benzyl group did not result in a significant change to ALK or BRD4 potency. Regarding substitution on the benzyl ring, *ortho*- and *meta*- substituents were slightly preferred in ALK but the non-substituted benzyl **58** remained the most potent against ALK^{F1174L}. The only compound to improve ALK^{F1174L} potency was **105** with an additional methyl at the benzylic position.

3.3.1.3 Disubstituted Benzyl Groups

Due to the minimal change in ALK WT potency with the *ortho*- and *meta*-substituted benzyl analogues, I then decided to explore the possibility of disubstitution on the benzyl ring to see if potency could be enhanced. I further analysed the docked structures of *meta*- and *ortho*-substituted analogues **91** and **100** to establish suitable vectors for additional substitution (Figure 55). With the *meta*-substituted benzyl, it appeared *ortho*-substitution could be tolerated towards the bottom or top of the pocket, filling additional hydrophobic space. Complementary to this, a methyl could be tolerated in the *meta*-position of *ortho*-analogue **100**, filling into the lower ALK pocket. In addition, substitution at the 6-position on **100** could possibly be tolerated, also filling into the lower ALK pocket.

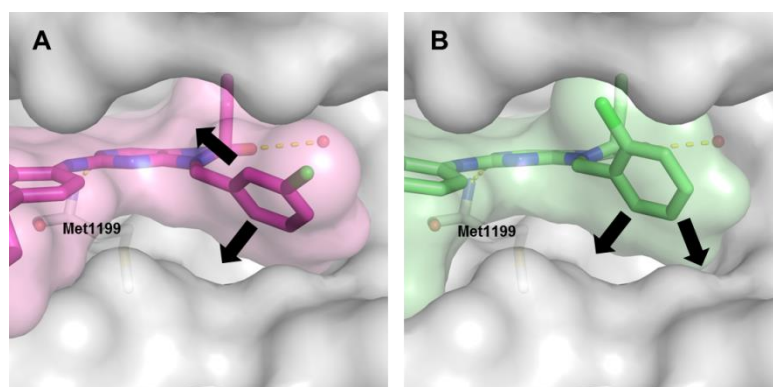


Figure 55. Docked structures of **A)** *meta*-chloro analogue **91** and **B)** *ortho*-chloro analogue **100**, highlighting possible vectors for substitution.

Therefore the strategy was to combine the *ortho*- and *meta*-substitutions to give the 2,3- and 2,5-substituted benzyl groups (Figure 56). As suggested from Figure 55B, the 2,6-substituted analogue would also be prepared to potentially fill ALK pocket space as well as the 2,4-analogue to complete the methyl scan around the ring.

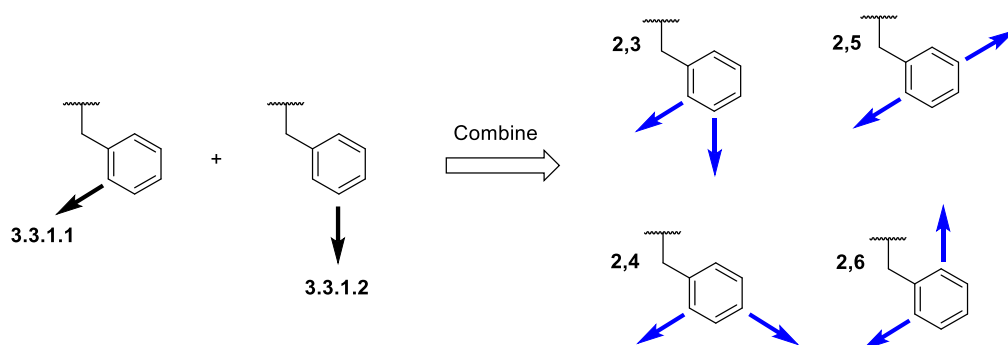


Figure 56. Design strategy for disubstituted benzyl analogues.

I docked the four dimethyl substituted combinations to further understand where the two groups could situate (Figure 57). Comparing the *ortho/meta* substituted rings, **107** and **109**, the 2,5-substitution appeared more favourable with the *ortho*-methyl situated towards the upper ALK pocket and the *meta*-methyl situated towards the lower ALK pocket. In comparison the aryl ring of **107** has twisted in the docked pose to accommodate the 2-and 3-methyl groups in the pocket and does not fill the pocket space as well. With the 2,6-analogue **110**, the methyl groups filled the upper and lower ALK pockets as predicted from Figure 54B. The 2,4-analogue **108** also predicted the *ortho*-methyl to situate towards to the upper pocket with the *para*-methyl situated towards solvent. In conclusion, the four disubstituted analogues were predicted to be tolerated in the ALK R₂ pocket but may vary in potency based on conformation and hydrophobic contacts.

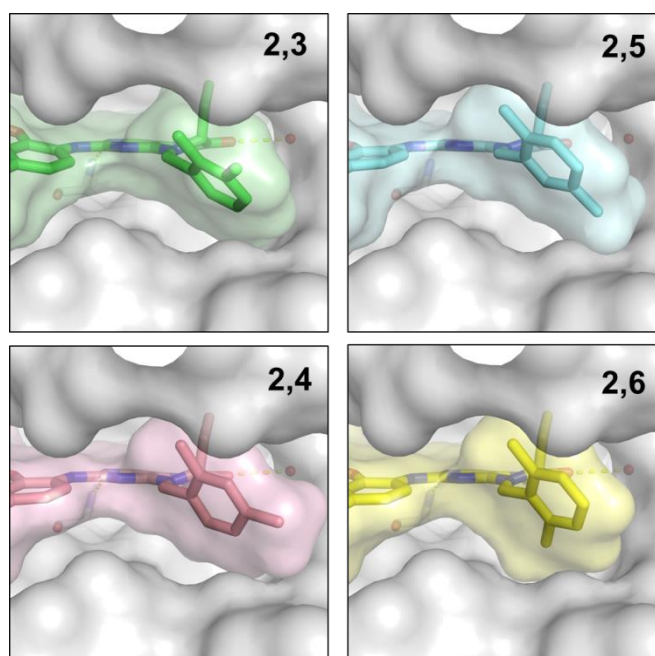
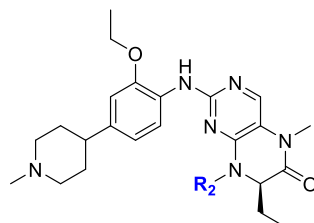


Figure 57. Docking of disubstituted analogues **107** (2,3), **108** (2,4), **109** (2,5) and **110** (2,6) in ALK (2XB7). Interaction surface of compounds shown.

The four disubstituted benzyl analogues **107** – **110** were prepared according to Scheme 15 with the biochemical assay results shown in Table 13.

For ALK WT, the 2,5-dimethyl substituted benzyl **109** showed the best potency at 55 nM. The additional methyl gained a 2 – 3-fold improvement in ALK potency compared to the mono-methyl substituted benzyls **93** and **102**. There was a clear preference for the 2,5 substitution pattern over the 2,3, 2,4 and 2,6, 3-fold, 6-fold and 14-fold respectively. Despite the docking predicting the methyls of 2,6 analogue **110** to

situate favourably towards the upper and lower ALK surface, this in fact was the least potent analogue. Yet again, there was a clear difference between ALK WT and ALK^{F1174L} SAR, with all the disubstituted analogues equipotent against ALK^{F1174L} and showing no improvement from the single methyl substituted benzyls **93** and **102**.



| | | ALK | | BRD4 | | PLK-1 |
|----------------|--|-----------------------------|---------------------------------|-----------|---------------------|-----------------------|
| R ₂ | | WT IC ₅₀ (nM) | F1174L IC ₅₀ (nM) | ΔTm [K] | K _d (nM) | IC ₅₀ (nM) |
| 102 | | 180 ± 13 | 220 ± 26 | 5.2 ± 0.2 | - | - |
| 93 | | 140 ± 15 | 210 ± 61 | 6.3 ± 0.2 | - | - |
| 91 | | 80 ± 7 | 220 ± 43 | 6.2 ± 0.4 | 130 | 540 |
| 56 | | 120 ± 12 | 290 ± 17 | 5.0 ± 0.5 | 120 | 540 |
| 107 | | 170 ± 38 | 200 ± 25 | 5.0 ± 0.7 | - | - |
| 108 | | 300 ± 93 | 360 ± 42 | 5.9 ± 1.2 | - | - |
| 109 | | 55 ± 19 | 200 ± 25 | 6.7 ± 1.3 | - | - |
| 110 | | 750 ± 69 | 230 ± 46 | 3.1 ± 0.3 | - | - |
| 61* | | 41 ± 6 | 140 ± 24 | 8.4 ± 0.7 | - | - |
| 111 | | 42 ± 5 | 250 ± 8 | 9.3 ± 0.1 | - | 280 |
| 112 | | 160 ± 23 | 660 ± 91 | 6.3 ± 0.4 | - | - |

Table 13. Biochemical assay data for disubstituted benzyl groups (R₂), - = not determined. ALK IC₅₀ values: mean ± S.E, n = 3. BRD4 ΔTm: mean ± S.D, n = 2, compound concentration of 10 μM. BRD4 K_ds, n = 1. PLK-1 IC₅₀ values: n = 1 (ATP = 10 μM).

Following from the improvement in ALK WT potency, disubstitution was applied to *meta*-chloro and bromo analogues **91** and **57** with the addition of a methyl in the 2-position. A similar 2 – 3-fold improvement in ALK WT potency with the additional methyl for **109** was observed with **61** and **111**. Introducing a fluoro to the 2-position however, as seen with 2-fluoro-5-bromo analogue **112**, lowered the potency against both ALK WT and ALK^{F1174L}.

I chose an example 2,5-disubstituted compound for testing against PLK-1 to see if the additional substitution would decrease PLK-1 potency further. However compound **111** did not show a change in PLK-1 potency from the *meta*-bromo analogue **56**. Overall, 2,5 disubstitution was preferred for ALK WT, resulting in a small improvement in potency compared to the mono-substituted benzyl. The disubstituted analogues were well tolerated against BRD4 but were still not as potent against ALK^{F1174L} as the non-substituted benzyl **58**.

3.3.2 Heterocycle Groups

3.3.2.1 Thiophene Analogues

From the initial set of analogues exploring the R₂ position, thiophene analogue **52** was one of the most interesting. The compound was the most potent R₂ analogue against ALK WT and ALK^{F1174L} (290 nM and 220 nM) and retained good BRD4 activity (77 nM). The first change I wanted to make with this compound was to remove the amide functionality. The hypothesis was that removing the amide would see a similar improvement in ALK potency and maintained BRD4 activity to **58** with a benzyl group at the R₂ position (Figure **58**). I also wanted to explore the thiophene group further, initially with a methyl scan around the ring and also removing the methyl to determine its impact on potency.

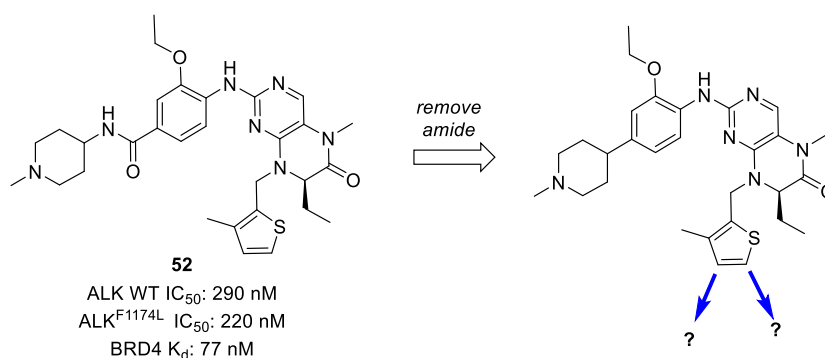


Figure 58. Design strategy for initial thiophene analogues.

I docked the three methyl-thiophene regioisomers **62** – **64** into ALK to understand how this heterocycle would fill the R₂ pocket (Figure 59). All three analogues were predicted to maintain the interaction with hinge residue Met1199 and place the thiophene in the R₂ pocket. The methyl groups of **62** and **63** were predicted to fill into the lower ALK pocket, matching to the ALK surface, possibly providing additional hydrophobic contacts. With 4-methyl thiophene **63**, it appears substitution at the 3-position could also be tolerated to further match the surface of the pocket. 5-Methyl thiophene **64** does not appear to fill the R₂ pocket as well as **62** and **63** suggesting this analogue could be less potent.

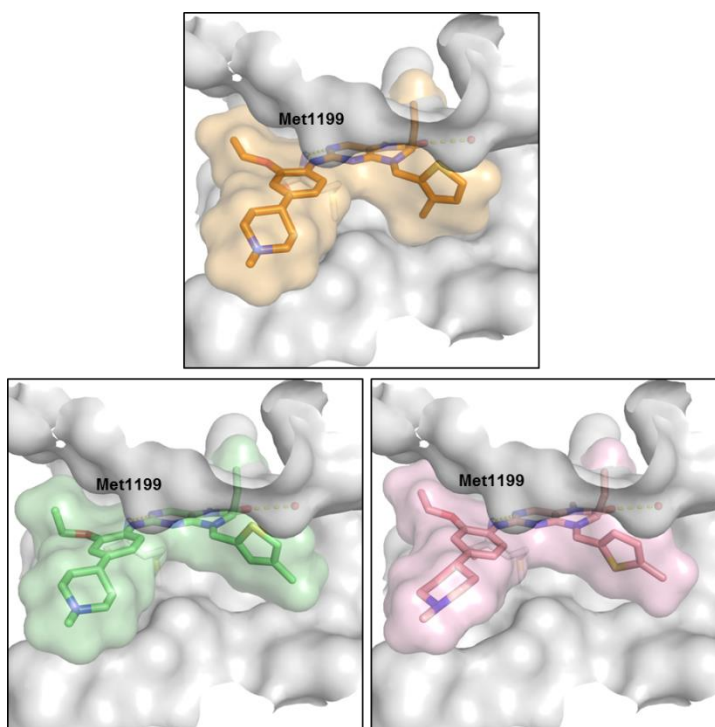
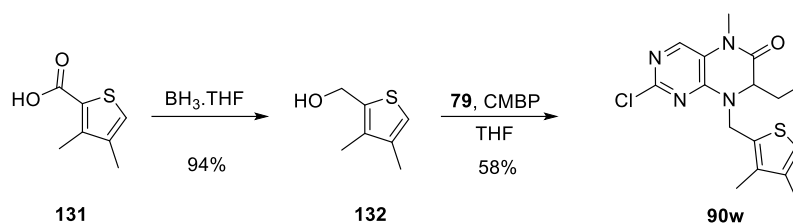


Figure 59. Docking of thiophene analogues **62** (orange), **63** (green) and **64** (pink) into ALK (2XB7) highlighting key interactions (yellow) and interaction surface of compound.

Compounds **62** – **64** were synthesised using Scheme 4 rather than the optimised R₂ synthesis, due to commercial availability of the aldehydes. As suggested from the docking, the 3,4-dimethylthiophene **114** was synthesised as well as the non-substituted thiophene **113**. For the dimethylthiophene analogue **114**, the halide or aldehyde wasn't available for alkylation via Scheme 15 or reductive amination via Scheme 4. However, the 3,4-dimethylthiophene-2-carboxylic acid **131** was commercially available which could be reduced to the alcohol using borane (Scheme 17). Alcohol **132** could then be added to intermediate **79** via a Mitsunobu reaction using cyanomethyltributylphosphorane (CMBP). Unfortunately racemisation occurred

during the synthesis of **90w**; details of this reaction and racemisation is further discussed in Chapters 4 and 5. The biochemical data for the thiophene analogues are shown in Table **14**.

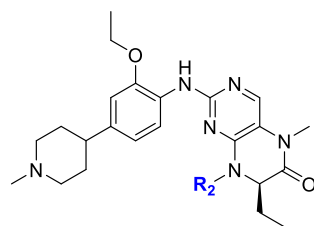


Scheme 17. Synthesis of 3,4-dimethyl intermediate **90w**.

As predicted, removing the amide functionality to give **62** improved ALK WT and ALK^{F1174L} potency 3-fold from compound **52**. The PLK-1 potency was equipotent to ALK^{F1174L} potency at 68 nM and BRD4 activity was maintained. Moving the methyl to the 4-position gave a further improvement in ALK^{F1174L} potency to 17 nM, whilst moving the methyl to the 5-position decreased activity 3 – 4-fold. Pleasingly compound **63** showed good BRD4 activity and a further small decrease in PLK-1 potency to 130 nM. This provided a 7-fold selectivity window towards ALK^{F1174L} over PLK-1 and was a small improvement from the 3-fold selectivity observed with benzyl analogue **58**.

For BRD4, compounds **62** and **63** showed potent activity and were equipotent to starting compound BI-2536. The combined change to the R₂, R₃ and R₄ groups had not disrupted the BRD4 binding and potent activity. **64** showed a large thermal shift for BRD4 but the K_d was 220 nM, 3 – 5-fold less potent compared to **62** and **63**. This reiterated the lack of correlation between thermal shift and potency and that thermal shift is only used as an initial guide for further testing.

Non-substituted thiophene **113** was 64 and 36 nM at ALK WT and ALK^{F1174L} respectively. This implies the 4-methyl (**63**) provides additional potency in the ALK pocket, as well as blocking the potential of frequently observed thiophene reactive metabolites.¹⁶⁶ However the methyl in the 3-position, despite being predicted to fill into the ALK pocket, does not aid potency. The racemic dimethylthiophene **114** was 120 nM against ALK^{F1174L} thus the single enantiomer is predicted to be around 60 nM. The additional methyl causes an approximate 4-fold decrease in potency from **63**, despite predicting to fill additional pocket space.



| | | ALK | | BRD4 | | PLK-1 | |
|----------------|--|-----------------------------|------------------------------------|------------|------------------------|--------------------------|-------------------------------------|
| R ₂ | | WT IC ₅₀ (nM) | F1174L IC ₅₀ (nM) | ΔTm [K] | K _d (nM) | IC ₅₀ (nM) | % Inhibition (10 nM / 100 nM) |
| 62* | | 89 ± 4 | 63 ± 10 | 5.4 ± 0.5 | 63 | 68 ± 0.6 | 25 / 60 |
| 63* | | 60 ± 12 | 17 ± 3.5 | 7.1 ± 0.1 | 44 | 130 ± 37 | 18 / 55 |
| 64* | | 550 ± 31 | 220 ± 71 | 8.3 ± 0.3 | 210 | - | - |
| 113 | | 140 ± 6 | 41 ± 7 | 4.4 ± 0.3 | - | - | 23 / 65 |
| 114** | | 190 ± 53 | 120 ± 33 | 4.3 ± 1.0 | - | - | - |
| 65* | | 64 ± 16 | 31 ± 5 | 6.9 ± 0.4 | 93 | 110 | 15 / 47 |
| 66* | | 150 ± 12 | 32 ± 13 | 7.3 ± 0.5 | 84 | - | 19 / 57 |
| 115 | | 63 ± 28 | 76 ± 11 | 3.0 ± 0.7 | - | - | - |
| 116 | | 230 ± 45 | 94 ± 11 | 4.8 ± 0.4 | - | - | - |

Table 14. Biochemical assay data for SAR of the benzyl group (R₂), - = not determined. ALK IC₅₀ values: mean ± S.E, n = 3. BRD4 ΔTm: mean ± S.D, n = 2, compound concentration of 10 μM. BRD4 K_ds, n = 1. PLK-1 IC₅₀ and % Inhibition values: mean ± S.D, n = 1/2 (ATP = 10 μM). *Synthesised by original scheme 4. **Racemate.

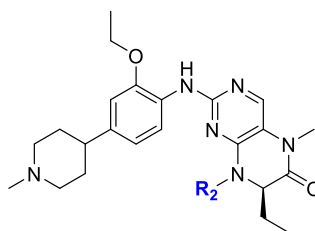
Following from the success of compound **63**, I changed the 4-methyl to a chloro and bromo group, both of which were tolerated in the benzyl analogue SAR. Compounds **65** and **66** were potent against the ALK mutant at 30 nM, although not quite as potent as methyl analogue **63**. I tested the PLK-1 potency to see if the chloro or large bromo affected the activity, but they were equipotent to methyl equivalent **63**. I also changed from the 2-thiophene to the 3-thiophene (**115** and **116**) but this reduced potency against ALK WT and ALK^{F1174L}.

Overall, changing from a benzyl to a thiophene at the R₂ position was a successful modification. Compounds with a 4-substituted thiophene, **63**, **65** and **66**, had the best potencies thus far against ALK^{F1174L} and retained potent BRD4 activity. 4-Methyl thiophene analogue **63** showed the best overall profile, with 17 nM ALK^{F1174L} activity and 7-fold selectivity over PLK-1.

3.3.2.2 Polar Heterocycles

Although the previous polar heterocycle examples from Chapter 2 decreased activity, I wanted to confirm the poor tolerance of polar heterocycles in the R₂ pocket. I decided to change the tolerated thiophene group to its more polar equivalent, a thiazole. I also wanted to synthesise a 6-membered heterocycle example – in particular a pyridine to compare to **58**. In general, the thiophene and benzyl analogues are quite lipophilic so if a heterocycle is tolerated this would aid the physicochemical properties of the series by reducing the lipophilicity. Five polar heterocycle analogues were synthesised according to Scheme **15** with the biochemical data shown in Table **15**.

Consistent with the previous data, polar heterocycles were less tolerated in the hydrophobic ALK pocket. The addition of a nitrogen to thiophene **113** decreases potency 4 - 6-fold against ALK^{F1174L} for **117** and **118**. Similarly for 3-methyl thiophene **62**, the addition of a nitrogen decreases ALK WT and ALK^{F1174L} activity approximately 5-fold (**119**). A greater decrease was observed with dimethylthiazole **120**, likely due to both the polarity of the heterocycle and disfavoured methyl groups. Pyridine **121** also decreased potency approximately 5-fold compared to its counterpart **58**. The majority of BRD4 thermal shifts were similar for the polar heterocycle analogues to **58** and **62**, implying the BRD4 pocket is much more accommodating to polar heterocycles in this solvent exposed region.



| | | ALK | | BRD4 | |
|----------------|--|-----------------------------|---------------------------------|-----------|------------------------|
| R ₂ | | WT IC ₅₀ (nM) | F1174L IC ₅₀ (nM) | ΔTm [K] | K _d (nM) |
| 113 | | 140 ± 6 | 41 ± 7 | 4.4 ± 0.3 | - |
| 62* | | 89 ± 4 | 63 ± 10 | 5.4 ± 0.5 | 63 |
| 117 | | 360 ± 14 | 170 ± 33 | 2.5 ± 0.1 | - |
| 118 | | 900 ± 150 | 250 ± 23 | 3.6 ± 0.1 | - |
| 119 | | 490 ± 87 | 370 ± 51 | 4.6 ± 1.4 | - |
| 120 | | 1200 ± 120 | 1700 ± 170 | 6.2 ± 2.9 | - |
| 58* | | 120 ± 11 | 85 ± 19 | 4.7 ± 0.5 | 54 |
| 121 | | 300 ± 74 | 460 ± 81 | 4.1 ± 0.1 | - |

Table 15. Biochemical assay data for SAR of the R₂ group with polar heterocycles, - = not determined. ALK IC₅₀ values: mean ± S.E, n = 3. BRD4 ΔTm: mean ± S.D, n = 2, compound concentration of 10 μM. BRD4 K_ds, n = 1.

3.3.3 Aliphatic Groups

The final functionality I chose to explore at the R₂ position was aliphatic groups. I wanted to explore aliphatic cycles to add sp³ character to the R₂ group, in particular a cyclohexyl (**122**) to directly compare to benzyl **58** (Figure **60**). Further analogues which reduced the size of the aliphatic cycle, added a heteroatom and opened the ring to form an aliphatic chain were also considered (**123** – **126**). I also planned to make the methyl analogue **127**, to confirm the importance of the benzyl or thiophene filling into the R₂ pocket.

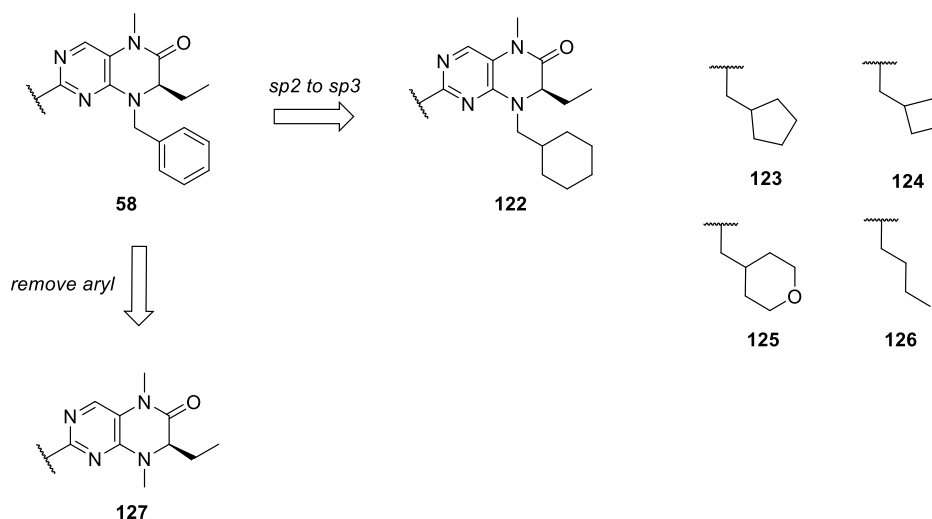


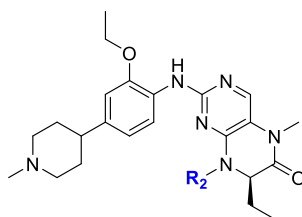
Figure 60. Design strategy for exploring aliphatic substituents at the R₂ position.

Compounds **122** – **127** were synthesised according to Scheme **15** with the biochemical assay data shown in Table **18**. Intermediate **133** for methyl analogue **127** was synthesised via double methylation of **81**, which was previously synthesised during synthetic route development, Table **9** (Scheme **18**).



Scheme 18. Synthesis of methyl intermediate **133**.

The majority of the aliphatic analogues did not provide additional potency. Comparing cyclohexyl **122** to benzyl **58**, a 3-fold decrease in ALK^{F1174L} potency was observed, though equipotent for ALK WT. Decreasing the size of the aliphatic cycle (**123** and **124**) decreased ALK WT potency further whilst the presence of an aliphatic heterocycle (**125**) hindered ALK WT and ALK^{F1174L} potency. Moderate thermal shift measurements were observed with the aliphatic analogues indicating both aliphatic and aromatic groups are suitable for extending to the WPF shelf region. Surprisingly the butyl chain analogue **126** improved ALK^{F1174L} potency to 60 nM, although hindered ALK WT activity. It is possible the flexibility of the alkyl chain allows the group to map the surface of the pocket, improving hydrophobic contacts. Clipping back to a methyl group at the R₂ position (**127**) saw a large decrease in potency at ALK WT and ALK^{F1174L}, as well as a lower thermal shift with BRD4. This confirmed the importance of the benzyl/thiophene group in providing potency to both targets.



| | | ALK | | BRD4 | |
|----------------|----|-----------------------------|---------------------------------|-----------|---------------------|
| R ₂ | | WT IC ₅₀ (nM) | F1174L IC ₅₀ (nM) | ΔTm [K] | K _d (nM) |
| 58 | | 120 ± 11 | 85 ± 19 | 4.7 ± 0.5 | 54 |
| 123 | | 200 ± 32 | 250 ± 12 | 5.3 ± 0.1 | - |
| 123 | | 550 ± 140 | 220 ± 28 | 4.0 ± 0.6 | - |
| 124 | | 580 ± 100 | 180 ± 39 | 4.7 ± 1.6 | - |
| 125 | | 2400 ± 61 | 430 ± 18 | 4.5 ± 0.3 | - |
| 126 | | 350 ± 42 | 60 ± 18 | 4.9 ± 0.1 | - |
| 127 | Me | 3600 ± 84 | 1700 ± 130 | 2.5 ± 0.2 | - |

Table 16. Biochemical assay data for SAR of the R₂ position with aliphatic groups, - = not determined. ALK IC₅₀ values: mean ± S.E, n = 3. BRD4 ΔTm: mean ± S.D, n = 2, compound concentration of 10 μM. BRD4 K_ds, n = 1.

3.4 Further SAR on Lead Compound 63

3.4.1 Revisiting SAR of the Alkoxy Group (R₃)

The work described in both Chapters 2 and 3 had yielded **63** as the most promising compound so far. With the 4-methyl thiophene installed at the R₂ position, it was important to reconsider other points of SAR (R₃ and R₄) to check that the best combinations of groups were in place.

I first returned to the R₃ substitution to establish if the ethoxy group was the most optimal. The docked structure of **63** shows the ethoxy occupies the selectivity region by residue Leu1198 (Figure 61A). Though there seems to be extra space to extend into, previous SAR had indicated larger groups lower ALK activity. I decided to reinstall a smaller and larger alkoxy group to confirm which size alkoxy group was best for achieving ALK potency. The methoxy and isopropoxy left hand side

intermediates **28a** and **28c** were synthesised according to Scheme 8 and coupled to intermediate **6r** (Figure 61B).

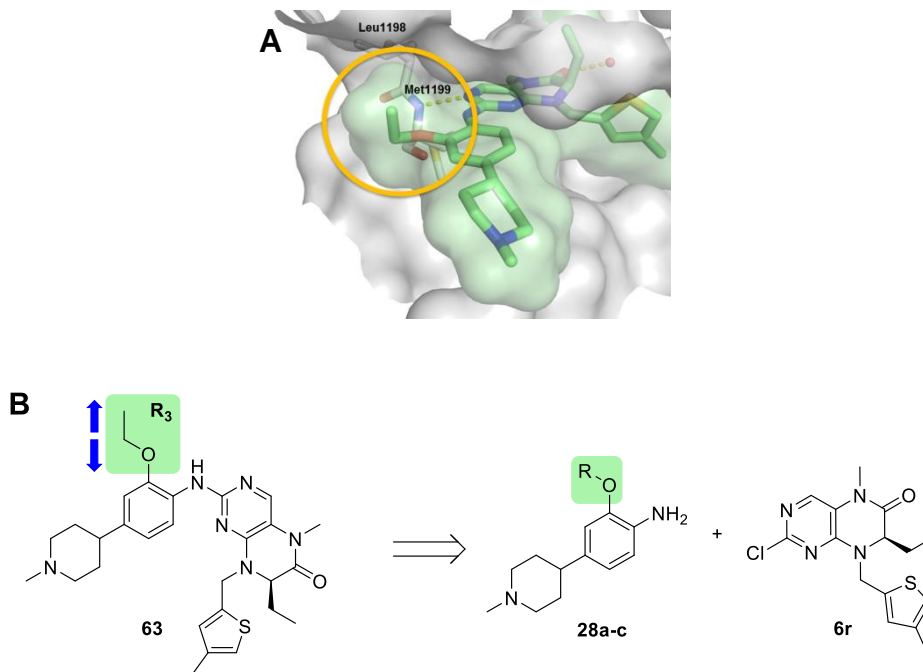
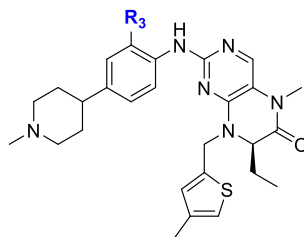


Figure 61. **A)** Docked structure of **63**, highlighting area for modification (R_3). **B)** Design strategy and synthesis for analogues varying the R_3 position on **63**.

In fact, the ethoxy group remained the most optimum in terms of its ALK WT and ALK^{F1174L} potency (Table 17). The smaller methoxy group (**67**) saw a small decrease in ALK^{F1174L} potency implying extension into the pocket slightly improves potency. However, increasing the size to the isopropoxy (**68**) also gave a similar small decrease in ALK^{F1174L} potency and a 4-fold decrease in ALK WT potency. This result complements the SAR discussed in Table 4. Therefore the ethoxy group was considered optimal at this stage and maintained in the synthesis of future analogues.



| | | ALK | | BRD4 | | PLK-1 |
|----------------|---------------|-----------------------------|---------------------------------|-----------|------------------------|-----------------------|
| R ₃ | | WT IC ₅₀ (nM) | F1174L IC ₅₀ (nM) | ΔTm [K] | K _d (nM) | IC ₅₀ (nM) |
| 63 | OEt | 60 ± 12 | 17 ± 4 | 7.1 ± 0.1 | 44 | 130 ± 37 |
| 67 | OMe | 63 ± 9 | 43 ± 12 | 5.6 ± 0.2 | - | - |
| 68 | O <i>i</i> Pr | 260 ± 38 | 48 ± 13 | 7.2 ± 0.4 | - | - |

Table 17. Biochemical assay data for SAR of the alkoxy group (R₃), - = not determined. ALK IC₅₀ values: mean ± S.E, n = 3. BRD4 ΔTm: mean ± S.D, n = 2, compound concentration of 10 μM. BRD4 K_ds, n = 1. PLK-1 IC₅₀ values: mean ± S.D, n = 2 (ATP = 10 μM).

3.4.2 Revisiting SAR of the Solvent Channel Group (R₄)

As discussed in Chapter 2, the solvent channel region proved to be a promising region for modification in that ALK and BRD4 activity could be maintained whilst PLK-1 activity decreased (Table 5). With the thiophene right hand side of the molecule optimised, I returned to modifying the R₄ group with previously attempted and new modifications to further decrease PLK-1 activity.

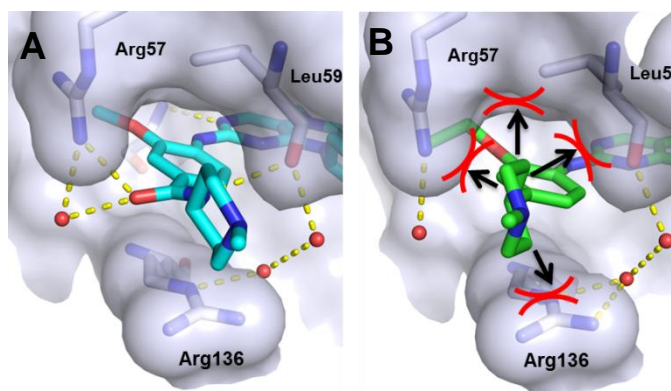


Figure 62. **A)** Co-crystal structure of BI-2536 in PLK-1 (2RKU) highlighting potential interactions to block within the solvent channel. **B)** Docking of **35** in PLK-1 (2RKU) highlighting areas for potential clash with the PLK-1 pocket.

The first strategy to lower PLK-1 activity involved the removal of hydrogen bond interactions with the amide functionality of BI-2536. (Figure **62A**). Previous design removed the amide to prevent hydrogen bond interactions with Arg57 and Leu59. As seen with the docking of analogue **35**, without the amide, no hydrogen bonds can be formed with the compound in the solvent channel region and consequently decreased PLK-1 potency >4-fold (Figure **62B**). Another plausible way to block one of the hydrogen bonds was methylation of the amide, as well as replacing with other solvent channel functionalities without hydrogen bond donors/acceptors (Figure **63**).

The second strategy to lower PLK-1 activity was considering the narrow channel in the PLK-1 pocket, formed by the flexible Arg57 and Arg136 chains, the latter not present in the ALK structure. The hypothesis was PLK-1 potency could be lowered if the solvent channel substituent clashes with the residues forming this solvent channel. Compound **35** with the amide removed, is predicted to situate the piperidine within the middle of the channel (Figure **62B**). Therefore substitution on a piperidine carbon could clash with the pocket and the molecule will have to rotate to accommodate this group (Figure **63**). This may lead to a disfavoured conformation of the molecule or cause a shift in the pocket residues which could lead to a decrease in potency.

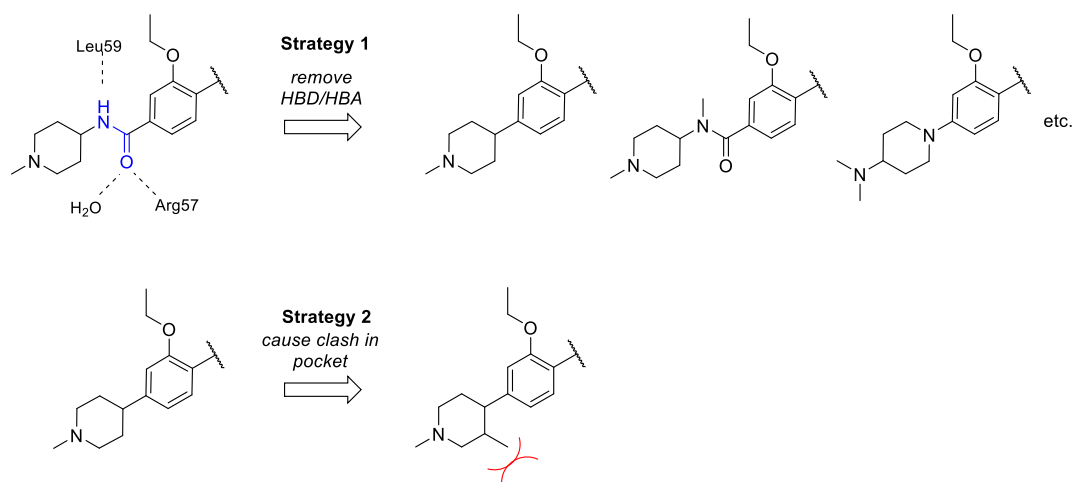
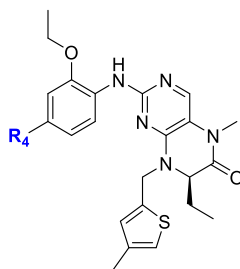


Figure 63. Design strategies for lowering PLK-1 activity, either removing hydrogen bond donors/acceptors or substitution on the piperidine to clash with the PLK-1 pocket.

Analogues with the methylated amide (**70**) and alternative solvent channel groups (**71-74**) were synthesised according to Schemes **6** and **7**. I also made the amide analogue **69** with the thiophene right hand side for direct comparison. For the second strategy, compound **75** with an additional methyl on the piperidine was synthesised

via Scheme 8 using (3-methylpyridin-4-yl)boronic acid. The biochemical data for all the solvent channel analogues is shown in Table 18.



| | | ALK | | BRD4 | | PLK-1 | |
|----------------|--|-----------------------------|---------------------------------|-----------|------------------------|--------------------------|-------------------------------------|
| R ₄ | | WT IC ₅₀ (nM) | F1174L IC ₅₀ (nM) | ΔTm [K] | K _d (nM) | IC ₅₀ (nM) | % Inhibition (10 / 100 nM) |
| 63 | | 60 ± 12 | 17 ± 4 | 7.1 ± 0.1 | 44 | 130 ± 37 | 18 / 55 |
| 69 | | 140 ± 18 | 98 ± 5 | 6.1 ± 0.2 | - | 22 | 40 / 82 |
| 70 | | 66 ± 11 | 90 ± 4 | 8.4 ± 0.0 | - | 73 | 18 / 60 |
| 71 | | 220 ± 32 | 120 ± 29 | 5.4 ± 0.6 | - | - | - |
| 72 | | 88 ± 15 | 36 ± 7 | 6.5 ± 0.3 | - | - | 19 / 48 |
| 73 | | 93 ± 12 | 55 ± 17 | 6.7 ± 0.9 | - | - | 10 / 43 |
| 74 | | 140 ± 22 | 66 ± 14 | 7.1 ± 0.8 | - | - | - |
| 75 | | 59 ± 5 | 26 ± 3 | 6.9 ± 0.1 | - | 150 | 15 / 45 |

Table 18. Biochemical assay data for SAR of the solvent channel group (R₄), - = not determined. ALK IC₅₀ values: mean ± S.E, n = 3. BRD4 ΔTm: mean ± S.D, n = 2, compound concentration of 10 μM. BRD4 K_ds, n = 1. PLK-1 IC₅₀ and % Inhibition values: mean ± S.D, n = 1/2 (ATP = 10 μM).

Control compound **69** confirmed the drop in PLK-1 potency achieved by removing the amide. PLK-1 potency decreased 5-fold whilst the ALK^{F1174L} potency improved 5-fold.

Methylation of the amide (**70**) also decreased PLK-1 potency, 3-fold, whilst maintaining ALK and BRD4 activity. From the alternative solvent channel groups, **72** and **73** showed good ALK WT and ALK^{F1174L} potency and also a similar decrease in PLK-1 activity to **63** and **70**. Overall, removing the hydrogen bond donors/acceptors of the R₄ group was a successful strategy in reducing PLK-1 activity.

Unfortunately the second strategy of adding a methyl to the piperidine did not cause a decrease in PLK-1 potency and remained equipotent to **75**. However compound **75** retained excellent potency against ALK^{F1174L} at 26 nM. Making the methyl substituent larger could have a greater effect on reducing PLK-1 potency but the synthesis of these analogues was challenging and therefore not pursued.

3.5 X-Ray Crystallography

Following SAR at the R₁ – R₄ regions of BI-2536, I now had promising compounds with good potencies against ALK and BRD4 (<100 nM) and small selectivity towards ALK^{F1174L} over PLK-1. With these promising compounds, **58**, **62** and **63**, I decided to profile them in depth using X-ray crystallography, cellular testing and selectivity screens.

I chose **58** and **63** as examples to co-crystallise with BRD4 to confirm the binding mode of the compounds in the BRD4 pocket. As previously mentioned, ALK crystallography proved difficult and was not possible to obtain, however BRD4 co-crystallography was well established with our collaborators at the Goethe University of Frankfurt. Due to structural similarity between the synthesised analogues and starting compound BI-2536 with the key acetyl-lysine binding motif being maintained, it was expected that the binding mode should be similar to that of BI-2536 (Figure **29**).

The co-crystal structures were solved by David Heidenreich and deposited into the protein databank as 6Q3Y and 6Q3Z for **58** and **63** respectively (Figure **64**). Both compounds bound into the acetyl-lysine binding site with the methyl amide moiety, retaining the key hydrogen bond interaction with Asp140. The methyl amide and pyrimidine moieties in both compounds retain interactions with conserved waters in the BRD4 pocket, whereas the thiophene and benzyl R₂ substituents are situated in the hydrophobic WPF shelf region.

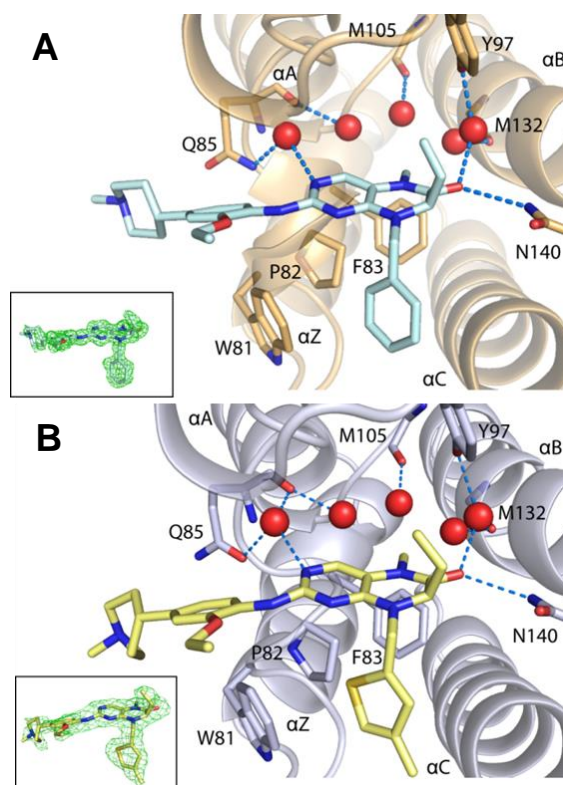


Figure 64 **A)** Co-crystal structures of **58** with BRD4 (6Q3Y) and associated $|2F_o| - |F_c|$ refined electron density map contoured at 1σ . **B)** Co-crystal structure of **63** with BRD4 (6Q3Z) and associated $|2F_o| - |F_c|$ refined electron density map contoured at 1σ . Both structures solved by David Heidenreich.

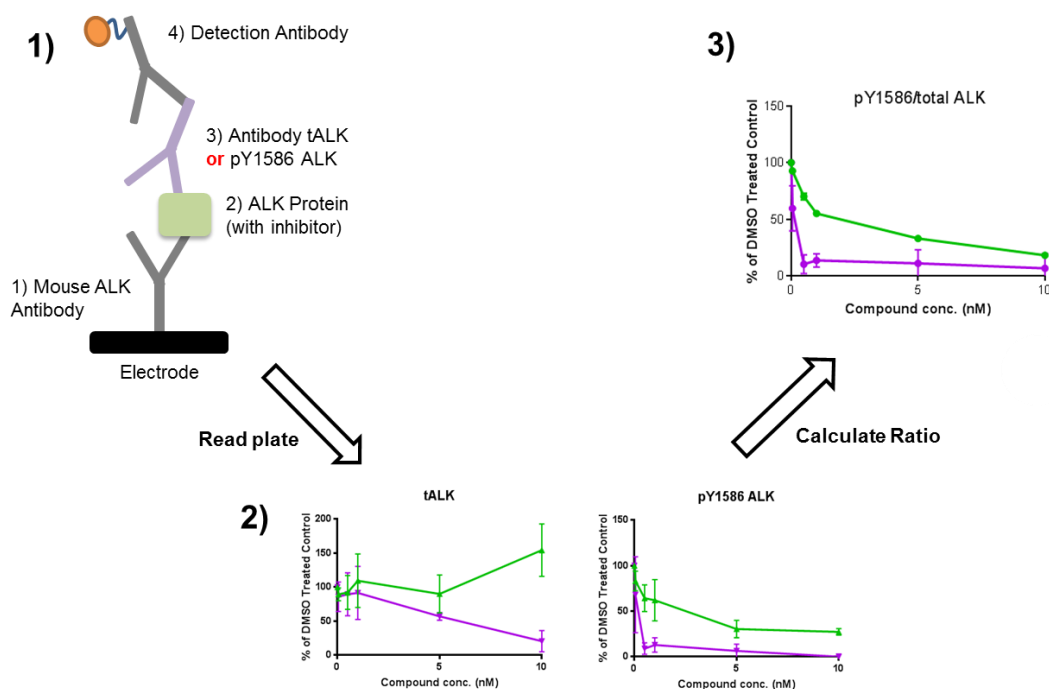
3.6 Cellular Testing

3.6.1 ALK Phosphorylation

With several compounds reaching initial target potencies of <100 nM at both ALK and BRD4, I next wanted to confirm that those compounds demonstrated on-target engagement of ALK and BRD4 in cells.

First, the effect of lead compounds on autophosphorylation of the ALK^{F1174L} mutant using a meso-scale discovery (MSD) assay was measured. The quantitative immunoassay was developed in-house by Lizzie Tucker to measure total ALK (tALK) and phosphorylated ALK (pALK) at biologically relevant phosphorylation sites, in this case pY1586.¹⁶⁷ The assay begins with the coating of an MSD plate, which has an electrode surface, with an ALK antibody (Scheme 19). This was followed by coating with cell lysates containing the target protein and selected inhibitor concentration, and then either an antibody specific for tALK or pY1586 ALK. Finally a detection antibody

is added, containing an electrochemiluminiscent label. The plate is then read, during which a voltage is applied to the plates electrodes causing the captured labels to emit light. The intensity of the emitted light is measured and provides a quantitative measurement for tALK and phosphorylated ALK (pY1586). If the inhibitor is bound to ALK, autophosphorylation is inhibited and levels of pALK are decreased. Therefore a decrease in the level of emitted light is observed. The ratio of tALK and pY1586 ALK is then calculated at the selected inhibitor concentrations and can be converted to an IC_{50} value for levels of phosphorylation.



Scheme 19. Schematic of in-house ALK MSD phosphorylation assay. Series of antibodies and target protein added in sequence to which a voltage is applied. The electrochemiluminiscent label allows a quantitative read out for tALK and pY1586 ALK. Green and purple lines represent example compound data.

ALK autophosphorylation levels were measured for key compounds **58**, **62** and **63** in two neuroblastoma cell lines, NBLW-R and Kelly, harbouring the F1174L mutation (Figure **65**). Ceritinib was tested as a positive control and also starting compound BI-2536 to see if the compounds had improved at inhibiting phosphorylation.

Compound **63** showed inhibition of ALK^{F1174L} phosphorylation at levels of 640 nM and 980 nM in the NBLW-R cell and Kelly lines respectively. **63** displayed a significant improvement in inhibiting autophosphorylation from starting compound BI-2536 in the Kelly cell line (10 μ M). **63** is also more potent compared to earlier analogues **58** and

62, which was in line with the biochemical IC₅₀ trends. Ceritinib was approximately 20-fold more potent at inhibiting ALK phosphorylation compared to **63**, corresponding with the 30-fold difference in biochemical potency between ceritinib (0.6 nM) and **63** (17 nM). Despite **63** not yet reaching the potencies of ceritinib, a significant improvement had been made from starting compound BI-2536 in its ALK activity *in vitro*.

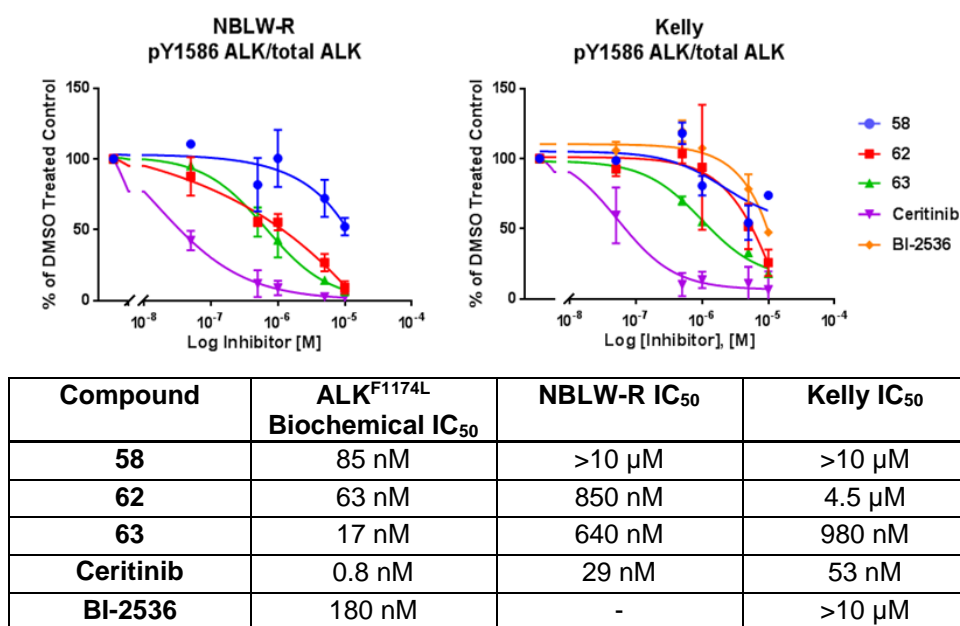


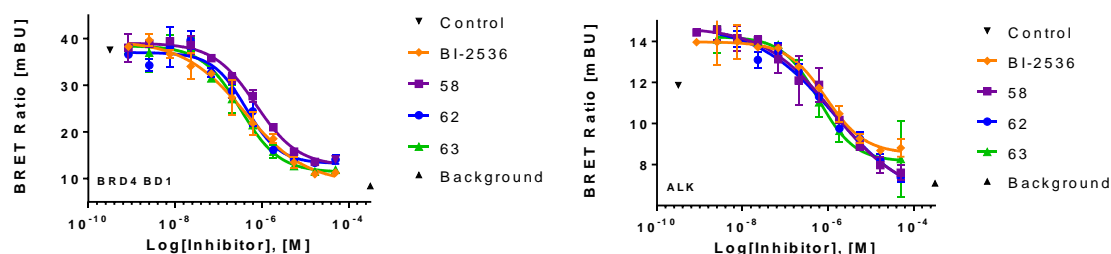
Figure 65. ALK MSD phosphorylation assays for key compounds **58**, **62** and **63** in the Kelly and NBLW-R cell lines. Performed by Lizzie Tucker. - = not determined.

3.6.2 NanoBRET Cellular Potency

The cellular potency of **58**, **62** and **63** were also tested against BRD4 and ALK WT using NanoBRET assays to confirm on-target engagement of both targets in cells (Figure 66). The BRD4 cellular potencies of **58**, **62** and **63** were comparable to starting compound BI-2536, consistent with the compounds minimal disruption with the BRD4 pocket. The cellular IC₅₀ of **63** was a 4-fold drop off from the biochemical IC₅₀ of 44 nM.

For ALK, **63** showed a cellular potency of 470 nM, an 8-fold drop off from its biochemical potency of 60 nM (ALK WT). Despite a 6-fold difference in biochemical potency between BI-2536 and **63** (390 nM and 60 nM), only a small improvement in cellular potency was observed in the nanoBRET experiment. However **63** was more

potent compared to earlier analogues **58** and **62**, complimentary to the improvement in biochemical potency. Overall, the nanoBRET experiments, along with the ALK MSD phosphorylation experiments, nicely demonstrate that **63** has on-target engagement with ALK and BRD4 in a cellular environment.



| Compound | BRD4 Biochemical IC ₅₀ (nM) | BRD4 IC ₅₀ (μM) | ALK WT Biochemical IC ₅₀ (nM) | ALK IC ₅₀ (nM) |
|-----------|--|-------------------------------|--|------------------------------|
| BI-2536 | 37 | 300 | 380 | 890 |
| 58 | 54 | 540 | 120 | 1640 |
| 62 | 63 | 310 | 89 | 1020 |
| 63 | 44 | 260 | 60 | 470 |

Figure 66. Cellular potency of lead analogues **58**, **62** and **63** against ALK and BRD4 using the NanoBRET assay format. Performed by David Heidenreich.

3.7 Selectivity

The broader kinase and bromodomain selectivity of **63** was next considered. A key challenge with developing a cross-family dual inhibitor is achieving selectivity across both protein families. Therefore it was important to assess if **63** maintained the kinase and bromodomain selectivity.

3.7.1 Bromodomain Selectivity

Compound **63** was tested against a panel of 27 BET and non-BET bromodomains (Figure 67). In this panel, **63** exhibited excellent BET family selectivity, in common with BI-2536 and other BET inhibitors including JQ1 and I-BET151.^{94,96} High thermal shifts were observed with BRD4(1+2), BRD3(1+2) and BRD2(2) followed by BRDT(1) and Group VIII member PB1(1). The remaining 20 bromodomains showed less than 1 °C shift or negative shift. Targeting the WPF shelf region, as achieved with compound **63** (Figure 64), is a known way to enhance BET selectivity.¹⁶⁸ The ‘WPF’ motif is

conserved within the whole BET family and a handful of other bromodomains such as PCAF and BAZ2B. Changes in size and/or hydrophobicity of this motif can allow for BET selectivity to be achieved.⁸⁴

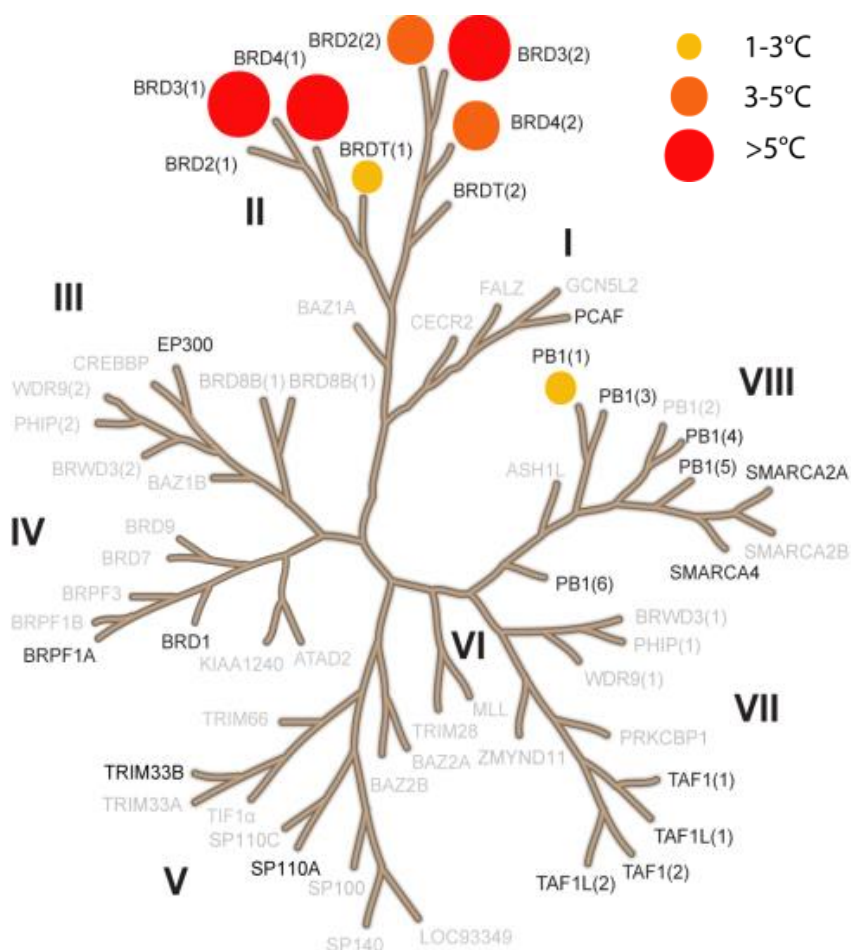


Figure 67. Screening of **63** against a panel of 27 bromodomains, showing ΔT_m as circles. Bromodomains in black text were tested with larger circles indicating greater ΔT_m .

No selectivity was observed between the first and second bromodomain of BRD4. Although the sequence homology is very high between the BET bromodomains there are a few differences between BD1 and BD2 that allow selectivity to be achieved (Figure 68).¹⁶⁹ These have been exploited in recent literature with the development of selective BD1 and BD2 inhibitors to help achieve selective transcriptional effects.^{105,107,169} Similar targeting of these residue differences could further improve the bromodomain selectivity of the dual ALK-BRD4 series. However this may be challenging as any change made to improve bromodomain selectivity could hinder the kinase potency. In particular, extending towards D144 and I146 via the thiophene may not be tolerated in the R₂ ALK pocket.

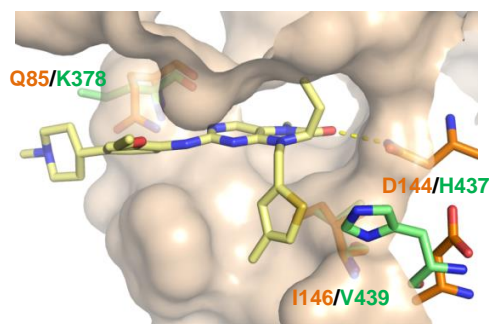
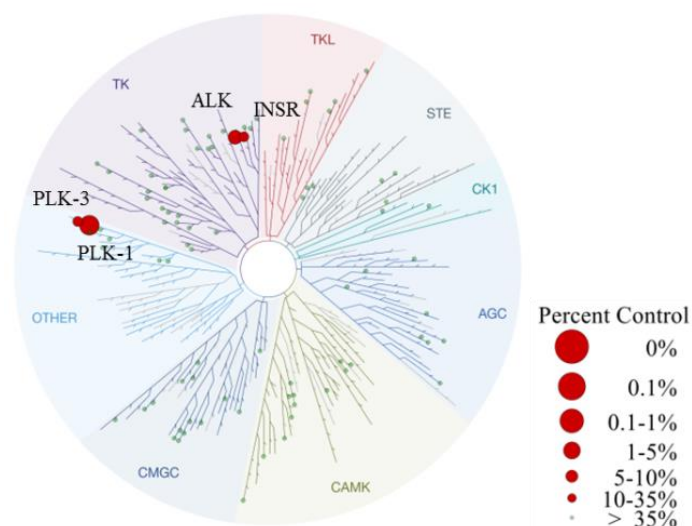


Figure 68. Comparison of BRD4 BD1 structure with **63** (orange, 6Q3Z) and BRD4 BD2 structure (green, 6FFD).

3.7.2 Kinase Selectivity

Compound **63** was tested against the DiscoverX scanEDGE panel of 97 kinases at a single point concentration of 1 μM . This panel was chosen as it included kinases across the different families, including ALK and PLK-1, and therefore would provide a good indication of the overall selectivity and whether the structural changes had made the compound more promiscuous compared to BI-2536.



| Kinase | Hits at 1 μM (% Control) | K_d (nM) |
|-----------------------|-------------------------------------|------------|
| ALK WT | 7.1 | 89 |
| INSR | 25 | 190 |
| PLK-1 | 1 | 11 |
| PLK-3 | 25 | 160 |
| ALK ^{F1174L} | - | 23 |

Figure 69. Screening of **63** against the Discover X scanEDGE panel of 97 kinases at single point concentration of 1 μM . K_d values for 'hits' (<35 % control) were then measured.

Pleasingly only four kinases were identified as hits from the 97 kinase panel, confirming that broad kinome selectivity had been maintained. The greatest inhibition was observed for ALK and PLK-1 followed by insulin receptor (INSR), a close family member to ALK, and PLK-3 (Figure 69 and Appendix A). Although close ALK family member INSR was observed as a hit with **63**, a further close family member IGF1R was not (77 % control). In addition kinases targeted by other ALK inhibitors such as MET (crizotinib⁴⁵), EGFR (brigatinib¹⁷⁰) and TRKA (entrectinib⁴⁸) were not potently inhibited by **63**.

Following the kinome screen, the K_d values for ALK, PLK-1, INSR and PLK-3, as well as for ALK^{F1174L}, were measured to understand how potent **63** is against the four hit kinases. **63** showed similar K_d values for PLK-1 and ALK^{F1174L} at 11 and 23 nM respectively, followed by 89 nM for ALK WT. The similar K_d values for PLK-1 and ALK^{F1174L} is discussed in 3.7.3. The next two active hits, PLK-3 and INSR showed similar K_d values of 160 nM and 190 nM.

The observed broad kinase selectivity of **63** was at least partially attributed to the ethoxy group. This group is positioned into a known vector to enhance kinase selectivity for ALK and PLK-1 inhibitors.^{76,140,171} The majority of the kinome has a larger residue at this position meaning the ethoxy group is likely to clash, as seen with TRKA (Figure 70). I analysed 295 kinases from the Kinase-Ligand Interaction Fingerprints and Structures (KLIFS) database and determined approximately 58% of kinases have a Tyr or Phe residue at this hinge position.¹⁷² Whilst 26% of the analysed kinases, including ALK, PLK-1, PLK-3 and INSR, have a smaller leucine residue and can therefore accommodate the ethoxy group of **63** (Figure 71). **63** showed selectivity over all the kinases within the kinase panel containing a Tyr or Phe residue.

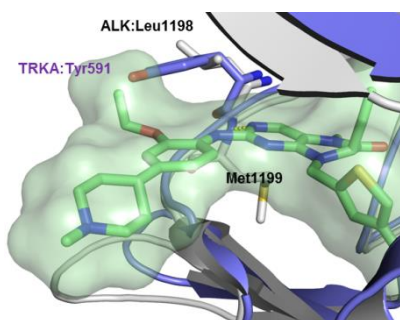


Figure 70. Overlay of docked **63** into ALK (2XB7) with TRKA (5H3Q) highlighting the selectivity determining residue.

| Amino Acid | Percentage |
|------------|------------|
| Tyr | 37.0 |
| Leu | 24.9 |
| Phe | 20.7 |
| Trp | 3.0 |
| Val | 2.3 |
| His | 2.3 |
| Cys | 2.0 |
| Met | 1.6 |
| Arg | 1.3 |
| Lys | 1.3 |
| Pro | 1.0 |
| Ile | 1.0 |
| Ala | 1.0 |
| Ser | 0.3 |
| Gln | 0.3 |

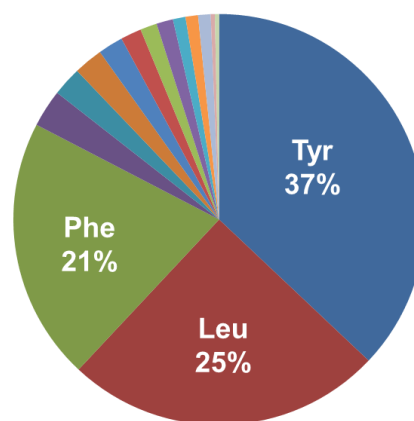


Figure 71. Analysis of the selectivity determining hinge residue for 295 kinases. Data compiled from the KLIFS database.¹⁷²

3.7.3 Cellular Selectivity between ALK and PLK-1

Despite very good overall selectivity in the DiscoverX scan, **63** showed similar K_d values for the ALK^{F1174L} mutant and PLK-1, at 23 nM and 11 nM respectively. (Figure 69). However, given **63** had translated efficiently into cellular assays with a relatively minor drop off, I considered that a larger drop-off for PLK-1 may lead to a better cellular selectivity window.

To investigate this hypothesis, I collaborated with Klaus Strebhardt's group to test **63** against PLK-1 in cells, investigating markers of PLK-1 inhibition and levels of mitotic arrest in the G2/M phase. In the literature, BI-2536 shows effects on markers PLK-1, cyclin B1 and phosphohistone H3 at concentration around 50nM, which is a 250-fold drop off from its K_d of 0.19 nM.¹⁷³ As **63** is structurally similar to BI-2536, I expected that a similar potency drop off in cells would be observed. In this case, the drop off would be to >2.5 μ M providing a small window of cellular selectivity towards ALK.

To assess the cellular selectivity, **63** and BI-2536 were assessed against the same markers, PLK-1, cyclin B1 and phosphohistone H3, in HeLa cells by our collaborators. Consistent with the literature, the potent PLK-1 inhibitor BI-2536 induced mitotic arrest and increased concentrations of PLK-1, cyclin B1, and phosphohistone H3 at a concentration as low as 50 nM (Figure 72).¹⁷³ In addition, an increase in PLK-1 phosphorylation at sites T210 and S137 was observed. In comparison, compound **63** did not cause an increase in levels of these mitotic markers and phosphorylation sites up to concentrations of 10 μ M. This is consistent with the improved selectivity achieved through the optimisation of BI-2536 to **63**.

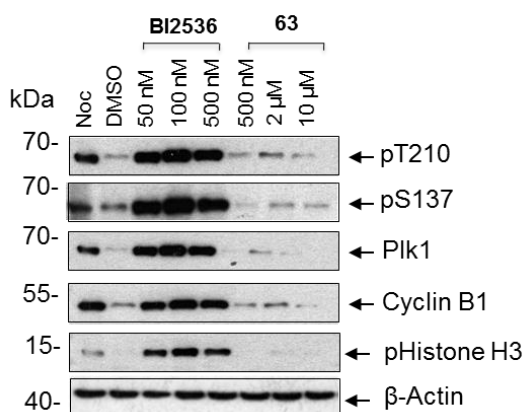


Figure 72. Induction of mitotic arrest by BI-2536 and **63** in HeLa cells. Changes in the fraction of cells arrested in mitosis were analyzed by Western Blots against phosphorylation sites pT210 and pS137 and mitotic markers PLK-1, Cyclin B1, and phospho-histone H3. Western blot run by Monika Raab.

Quantitative analysis of the cell cycle distribution by flow cytometry supported the data obtained by Western blot analysis (Figure 73). Increasing the concentration of BI-2536 considerably changed the cell cycle phase ratio, from 70% G0/G1 to 64% G2/M phase at 50 nM. The percentage of cells in G2/M phase increased further at 100 and 500 nM to 81%. This substantial change in cell cycle distribution corresponds to the mitotic arrest caused by BI-2536 and the subsequent accumulation of cells at the G2/M phase. In comparison **63** did not cause a significant change in the cell cycle distribution until 10 μ M where the G0/G1 phase decreased by 20% and the G2/M phase increased by 17%.

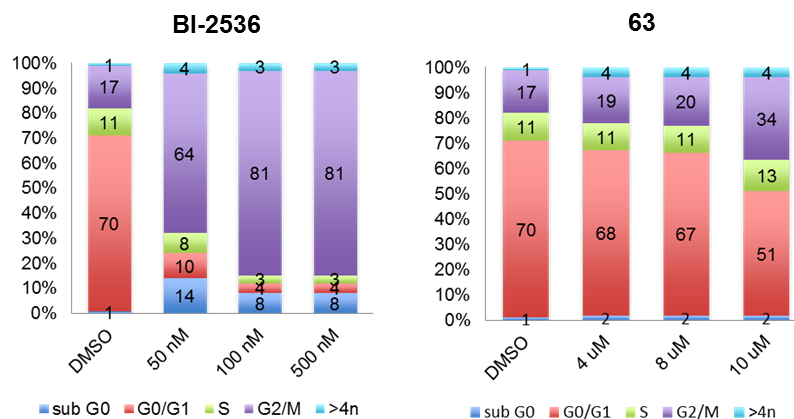


Figure 73. Cell cycle analysis of **63** compared to PLK-1 inhibitor BI-2536. Cell cycle analysis performed by Monika Raab.

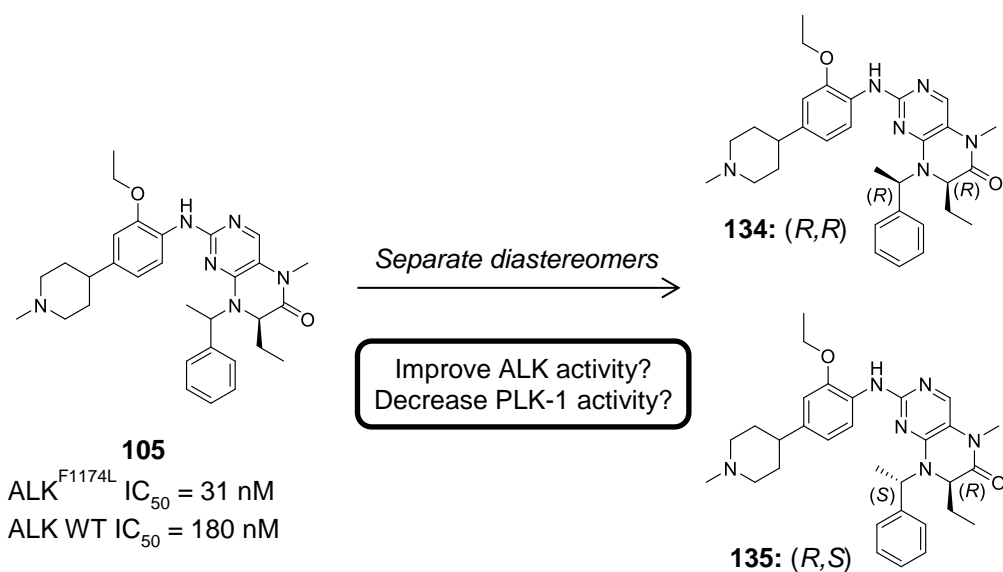
The cellular potency of **63** against PLK-1 (>10 μ M) was much greater than the concentration where ALK (470 nM NanoBRET, 640 – 980 nM, MSD) and BRD4 (260 nM NanoBRET) are inhibited in a cellular context (Figures **65** and **65**). The combination of the reduction in PLK-1 activity and the improvement in ALK^{F1174L} activity had resulted in a >10 – 20-fold selectivity window for ALK^{F1174L} over PLK-1 in cells.

In conclusion, profiling of compound **63** has shown the compound is broadly selective against kinases and bromodomains and has on-target engagement in cells. This compound represents a significant step from the initial goal of designing a potent and selective dual ALK-BRD4 inhibitor and is a suitable *in vitro* chemical probe for further experiments.

Chapter 4 Improving the Selectivity and Physicochemical Properties

4.1 Synthesis of Single Diastereomers of Compound 105

In Chapter 3, compound **105** was one of the most interesting compounds following modification at the R₂ position. The addition of the methyl at the benzylic position slightly improved potency from 85 nM to 31 nM against ALK^{F1174L}. Due to this promising result, I wanted to synthesise the single diastereomers **134** and **135**, to determine if one diastereomer was more potent than the other (Scheme 20). Furthermore, I speculated that addition of the methyl would not be tolerated in the more restricted PLK-1 pocket and hence would decrease PLK-1 potency further.

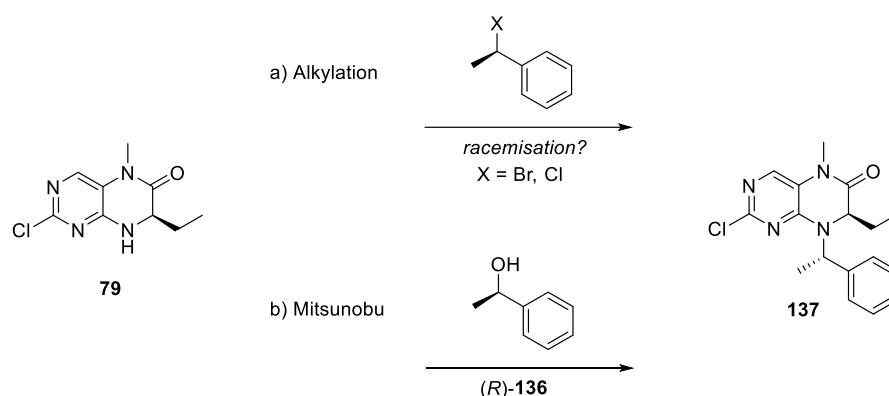


Scheme 20. Separation of diastereomers of **105**.

4.1.1 Mitsunobu Conditions

To synthesise the single diastereomers **134** and **135**, the original alkylation conditions were not used due to the potential for racemisation *via* an S_N1 mechanism rather than an S_N2 inversion (Scheme 21). An alternative method for installing the benzyl group enantioselectively was a Mitsunobu reaction between **79** and chiral benzyl alcohol

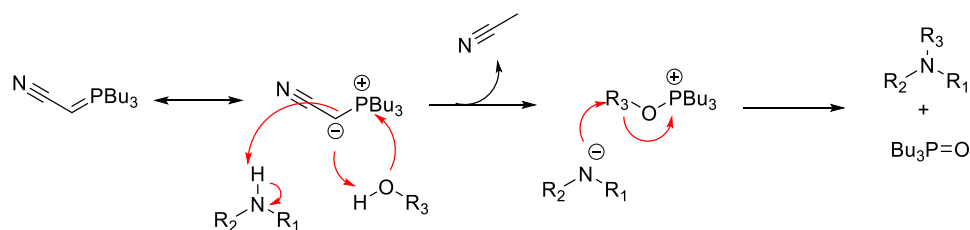
136 which generally proceeds with full inversion of the stereocentre.¹⁷⁴ The disadvantages of a traditional Mitsunobu reaction using triphenylphosphine and diethylazodicarboxylate (DEAD) include the potentially difficult removal of by-product triphenylphosphine oxide and the pK_a rule, in which the pK_a of the nucleophile needs to be less than 11 for a successful reaction.¹⁷⁵ This is due to the betaine formed by triphenylphosphine and DEAD having a pK_a of 13 which deprotonates the nucleophile, otherwise alkylation of DEAD will occur. The reaction between **79** and (*R*)-**136** did not proceed with the traditional Mitsunobu conditions using triphenylphosphine and DEAD, due to a higher pK_a of the amine.



Scheme 21. Proposed Mitsunobu reaction for the synthesis of single diastereomer **137**.

An alternative Mitsunobu reagent was used to overcome the pK_a restriction. Phosphorous ylide reagents cyanomethylenemethylphosphorane (CMMP) and cyanomethylenebutylphosphorane (CMBP) can replace the azo-compound and phosphine combination and overcome the pK_a restriction, facilitating reactions with nucleophiles in the pK_a range of 11 – 23.^{176,177} In addition, the side products of the Mitsunobu reaction, acetonitrile and tributylphosphine oxide or trimethylphosphine oxide, are easier to remove during work up than triphenylphosphine oxide.¹⁷⁸ A disadvantage of using CMMP and CMBP is that the reagents require anhydrous conditions as they are sensitive to air and moisture.

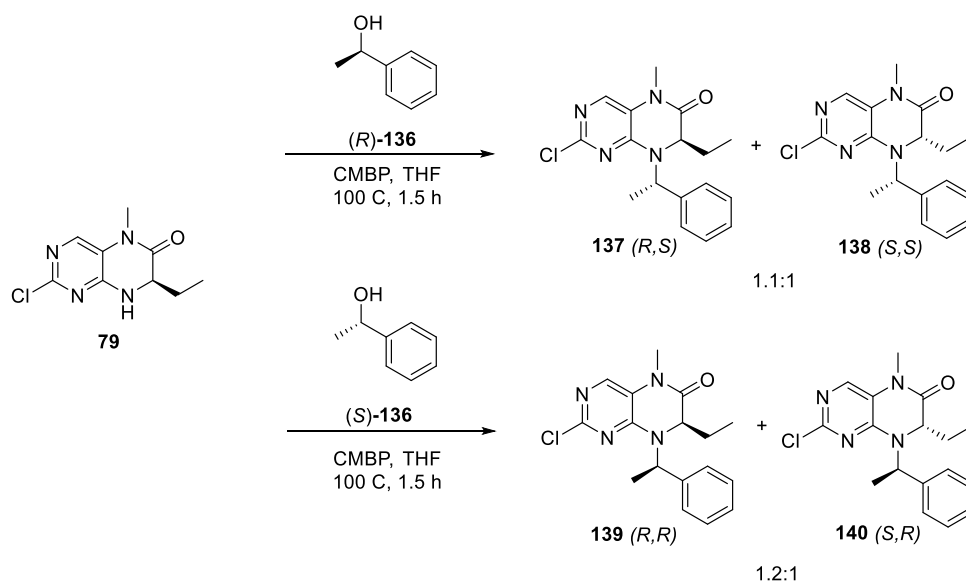
The Mitsunobu reaction using CMBP follows the mechanism outlined in Scheme **22**. The alcohol is deprotonated by the ylide and the resulting anion attacks the phosphonium group to give the alkoxy phosphonium. The cyanomethyl anion is protonated by the amine, yielding acetonitrile as a by-product. The resulting amine anion reacts with the alkoxy phosphonium to give the desired product and tributylphosphine oxide. Using CMBP, the Mitsunobu reaction between **79** and (*R*)-**136** was successful achieving 50% yield.



Scheme 22. Mechanism of Mitsunobu reaction using CMBP.¹⁷⁸

4.1.2 Separation and Characterisation of Diastereomers

When analysing the NMR of the product from the Mitsunobu reaction between **79** and (*R*)-**136**, two diastereomers were in fact present, **137** and **138** (Scheme 23). It was found the ethyl chiral centre had epimerised to give the (*R,S*) and (*S,S*) diastereomers; further discussion on distinguishing which diastereomers were formed and ways to prevent epimerisation can be found in Chapter 5.



Scheme 23. Synthesis of the four diastereomer intermediates **137** – **140**. Chiral centre nomenclature (ethyl, methyl).

The diastereomers were separated out by HPLC achieving diastereomeric ratios (d.r) of 20:1 and 18:1 for **137** and **138** respectively. The (*R,R*) and (*S,R*) diastereomers **139** and **140** were also synthesised as a 1:2:1 mixture using (*S*)-**136** and purified using the same HPLC method. It was assumed that the major diastereomer of the synthesised mixtures would have the ethyl in the (*R*)-configuration with the minor (*S*)-configuration as a result of epimerisation of the chiral centre. This was supported by

the elution time during HPLC purification and the NMR spectra of the major diastereomer from one Mitsunobu reaction (e.g. (*R,R*)) matching the minor diastereomer, its enantiomer, of the other Mitsunobu reaction (e.g. (*S,S*)).

I also conducted NOESY experiments on the four diastereomers to see which groups were close together in space and help determine which diastereomer was which. For diastereomer **137** (*R,S*), and its enantiomer **140**, a NOESY signal was observed between the proton at the α -position to the carbonyl and the benzylic methyl group, indicating these groups are close together in space (Figure **74A**). In comparison for diastereomer **139** (*R,R*), and its enantiomer **138**, no signal was observed between these groups and not close together in space (Figure **74B**). The observed NOESY for **137** did seem reasonable, considering both the α -proton and methyl are pointing down from the plane of the molecule in its lowest energy conformation generated in MOE (Figure **74C**).

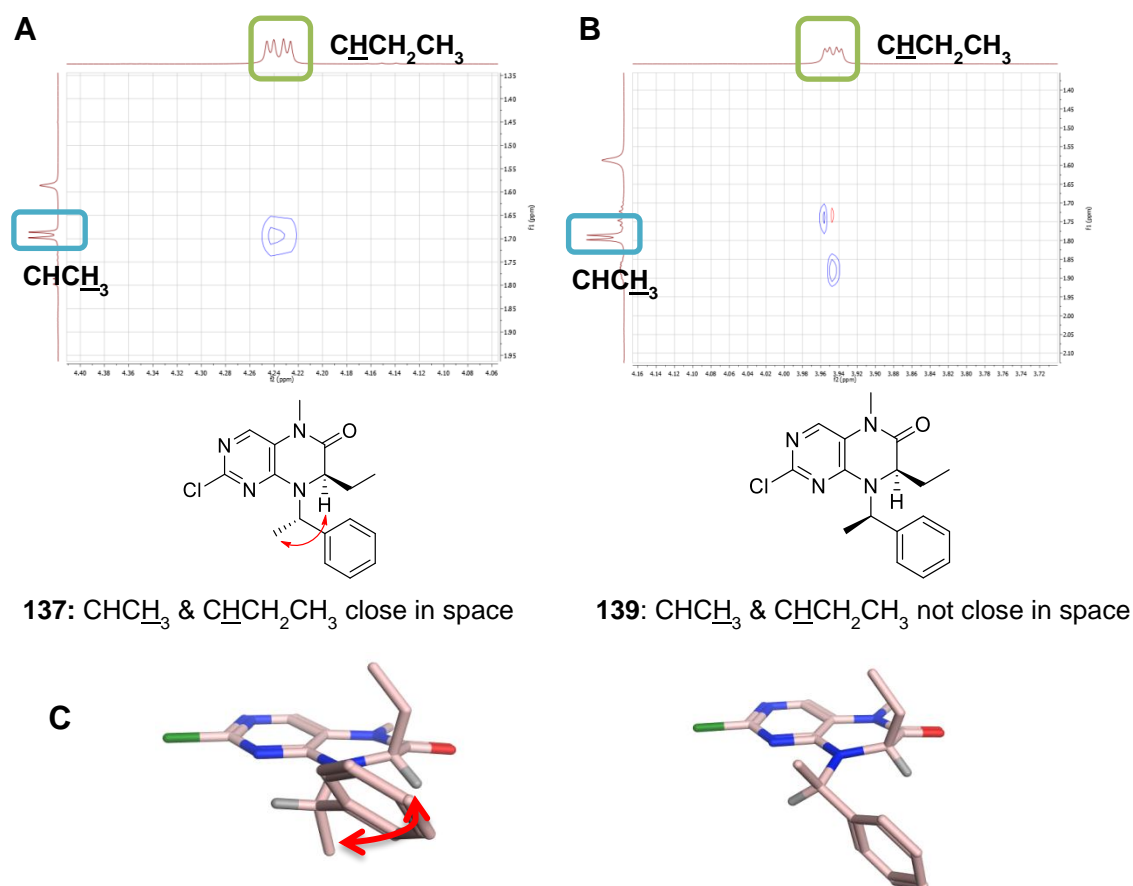
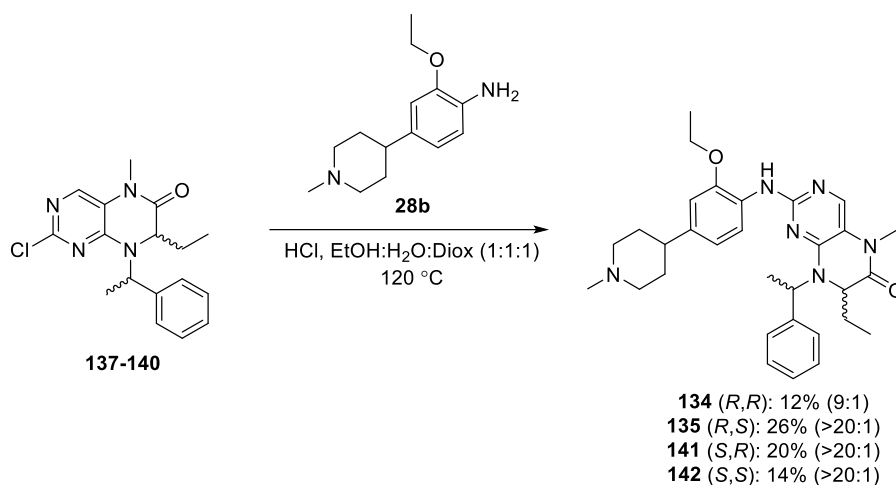


Figure 74. Comparison of NOESY signals between **137** and **139**. **A)** Observed NOE between the CHCH_3 and CHCH_2CH_3 signals of **137**. **B)** No NOE signal observed between the CHCH_3 and CHCH_2CH_3 of **139**. **C)** Lowest energy conformations of **137** (left) and **139** (right) generated by a stochastic conformation search in MOE.

The four intermediates **137** – **140** were coupled to the optimised left hand side intermediate **28b** and the resulting four diastereomeric final compounds **134**, **135**, **140** and **141** were taken forward for biochemical testing (Scheme 24, Table 19).



Scheme 24. Synthesis of diastereomeric final compounds **134**, **135**, **141** and **142**. Chiral centre nomenclature (ethyl, methyl).

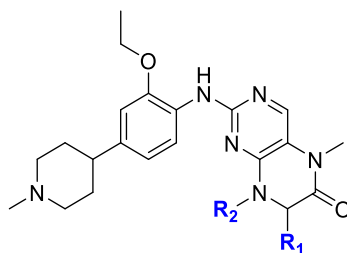
4.2 Analysis of Diastereomer Inhibitors

4.2.1 Biochemical Data

I first tested the four diastereomer final compounds against ALK WT and ALK^{F1174L} (Table 19). The (*R,S*) diastereomer **135** was significantly more potent than the other diastereomers at 22 nM, a 3-fold improvement in potency from **58** with no methyl present at the benzylic position. Comparing the (*R,S*) and (*S,S*) diastereomers **135** and **142**, the (*S*)-ethyl caused a greater than 10-fold decrease in potency, corresponding to the previous SAR data at the R₁ position which also saw a significant decrease with the (*S*)-ethyl (Table 6). Changing the methyl from the (*R*) to (*S*) configuration, **135** to **134**, saw a greater than 10-fold decrease in potency against ALK^{F1174L}. The (*R*)-methyl could be causing an unfavourable conformation or clashing with the ALK pocket, hence a lower potency.

In addition, the (*R,S*) diastereomer **135** showed the greatest thermal shift against BRD4. This corresponded to a K_d of 110 nM, a small decrease from **58**. The (*S*)-ethyl diastereomers **141** and **142** had very low thermal shifts of 1.0 and 1.3 K. This was

consistent with the drop in BRD4 potency previously observed with (*S*)-analogue **40** due to clashing with the opposite face of the BRD4 pocket (Figure **41**).



| | | | ALK | | BRD4 | | PLK-1 |
|-------------------------|-----------------|--|-----------------------------|---------------------------------|------------|------------------------|-----------------------|
| | | | WT IC ₅₀ (nM) | F1174L IC ₅₀ (nM) | ΔTm [K] | K _d (nM) | IC ₅₀ (nM) |
| 58 | (<i>R</i>)-Et | | 120 ± 11 | 85 ± 19 | 4.7 ± 0.5 | 54 | 290 ± 45 |
| 134 d.r 9:1 | (<i>R</i>)-Et | | 410 ± 12 | 330 ± 16 | 3.4 ± 0.1 | - | - |
| 141 d.r >20:1 | (<i>S</i>)-Et | | 870 ± 200 | 250 ± 85 | 1.0 ± 0.1 | - | - |
| 135 d.r >20:1 | (<i>R</i>)-Et | | 79 ± 12 | 22 ± 7 | 5.9 ± 0.3 | 110 | 3200 ± 110 |
| 142 d.r >20:1 | (<i>S</i>)-Et | | 1300 ± 200 | 290 ± 85 | 1.3 ± 0.1 | - | - |

Table 19. Biochemical assay data for SAR of the benzyl group (*R*₂), - = not determined. ALK IC₅₀ values: mean ± S.E, *n* = 3. BRD4 ΔTm: mean ± S.D, *n* = 2, compound concentration of 10 μM. BRD4 K_ds, *n* = 1. PLK-1 IC₅₀ values: mean ± S.D, *n* = 2 (ATP = 10 μM).

As **135** was the most potent diastereomer against ALK^{F1174L}, I had the PLK-1 activity measured to test the hypothesis of the additional methyl causing a decrease in PLK-1 potency. Pleasingly the PLK-1 potency of **135** was 3.2 μM, achieving an 11-fold drop off from **58** and an excellent (>)1200 fold drop off in potency from starting compound BI-2536. The (*R,S*) diastereomer showed a 150-fold selectivity towards ALK^{F1174L} over PLK-1, greatly improved from the 7-fold biochemical selectivity observed with 4-methyl thiophene analogue **63**. No docking poses of **135** into PLK-1 predicted an interaction with the hinge region suggesting that the additional methyl causes a conformation which is not tolerated in the more restricted PLK-1 pocket. In summary,

the addition of the methyl at the benzylic position was an excellent modification in meeting the aims of increasing ALK potency and decreasing PLK-1 potency.

4.2.2 Computational Modelling

Due to co-crystallography in ALK not being available, I used computational modelling to help understand how the α -methylbenzyl group fits into the ALK pocket, why the (*R,S*)-diastereomer was the most potent and to generate hypothesis for further modifications. Previous docking experiments of the α -methylbenzyl group (3.3.1.2) resulted in (*R,R*) diastereomer **134** having the best docking score, forming an interaction with hinge residue Met1199 and the benzyl sitting in the R_2 pocket. However **134** was not the most potent diastereomer.

One limitation of docking is insufficient conformer sampling,¹⁷⁹ thus I repeated docking experiments with the (*R,R*) and (*R,S*) analogues **134** and **135** using 176 and 183 conformations respectively generated using a stochastic conformation search in MOE. The lowest energy conformation of the (*R,R*)-diastereomer **134** matched the previous top scoring docking poses and again predicted to fit into the ALK pocket and interact with hinge residue Met1199 (Figure 75A). None of the generated docking poses for the (*R,S*)-diastereomer **135** predicted any interactions with the hinge region, with the compound situated out of the pocket to accommodate the (*S*)- α -methylbenzyl moiety (Figure 75B).

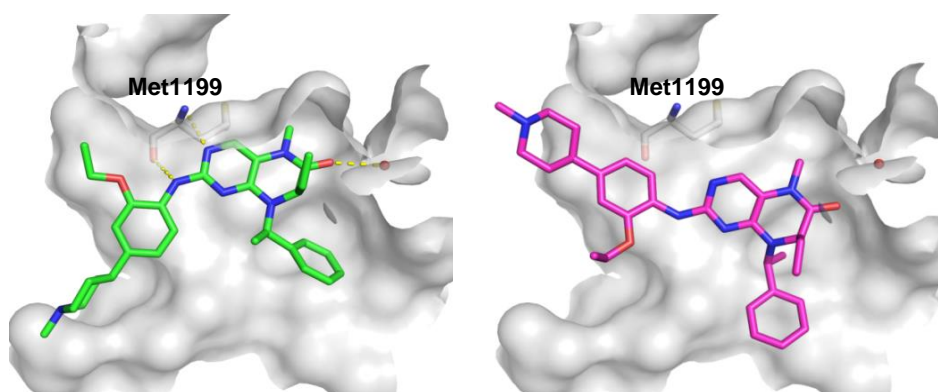


Figure 74. Docking of (*R,R*) analogue **134** and (*R,S*) analogue **135** into ALK (2XB7).

For further insight into the conformation of the diastereomers small molecule X-ray structures of intermediates **137** and **139** were solved (Figure 76). The X-ray structures of **137** and **139** confirmed the correct stereochemistry as (*R,S*) and (*R,R*) respectively, matching the NOESY experimental data in Figure 74. I superposed the

X-ray structures in MOE to previously docked analogue **58** to compare the conformation and position of the benzyl group. For the (*R,R*)-diastereomer **139**, the benzyl sits in a similar conformation to the docked structure of **134** with the benzyl in the lower portion of the R₂ pocket. The conformations generated by the docking for the (*R,R*) diastereomer were therefore considered to be reasonable. In comparison, the superposition of the (*R,S*) diastereomer **137** with **58** shows the benzyl would clash with the phosphate-binding loop (p-loop) of ALK. The benzyl is unable to be accommodated on the lower face, as the resulting conformation leads to a clash of the methyl with the pyrimidine (see Figure 78 (4.2.3)).

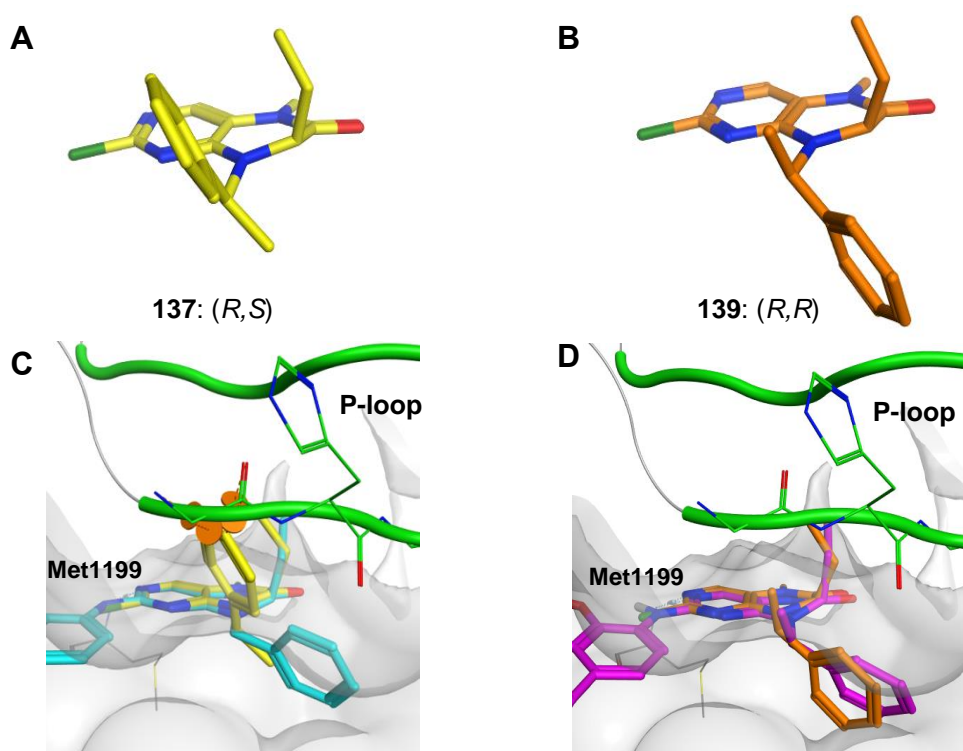


Figure 76. Small molecule X-ray structure of **A)** **137** (0.82 Å) and **B)** **139** (0.83 Å). Crystallographic data provided by the National Crystallographic Service at the University of Southampton and solved in house with the help of Catherine Fletcher. **C)** Superposed structure of **137** with docked **58** in ALK (2XB7) highlighting clashes with p-loop (orange discs) **D)** Superposed structure of **139** with docked **134** in ALK (2XB7).

The p-loop structure is a common motif in ATP- and GTP-binding proteins consisting of a glycine rich sequence and is known to be a highly flexible region in kinases.¹⁸⁰ I hypothesised that the p-loop could be moving to accommodate the (*S*)- α -methylbenzyl group. To analyse the flexibility of the p-loop in the ALK structure, I looked at the B-factors of the protein residues (Table 20). B-factors describe the displacement of atomic positions from the mean value, so the more flexible the atom,

the larger the displacement from the mean atom will be. The B-factors of the ALK structure 2XB7 indicate the p-loop is a flexible region with greater B-factors compared to the mean value. The flexibility of the p-loop may allow the (*R,S*)-diastereomer to fit into a conformation in the ALK pocket, which isn't captured in the docking and thus consistent with the hypothesis. The effectiveness of docking is limited in situations where a protein is flexible due to assumption of a rigid protein and this therefore provides an explanation for no favourable conformations of the (*R,S*)-diastereomer docking into ALK.¹⁷⁹

| Residue | H1124 | G1125 | A1126 | F1127 | G1128 | D1129 | M1199 | Mean |
|----------|-------|-------|-------|-------|-------|-------|-------|------|
| B-Factor | 53-67 | 53-55 | 56-57 | 55-63 | 50-53 | 46-62 | 21-28 | 34 |

Table 20. B-factors for p-loop residues and hinge M1199 in ALK (2XB7). B-factors 1 – 2 x greater than mean value indicate flexibility.

There are several examples of ALK structures highlighting the flexibility of the p-loop. For example a significant shift in the p-loop is observed in the co-crystal structure with entrectinib (Figure **77A**) with the alignment of residue Phe1127 in the p-loop with the difluorobenzyl group⁴⁸ whilst a more subtle shift in the p-loop is caused by the amide of lorlatinib (Figure **77B**).⁴⁷ There are also many examples of ALK structures where the p-loop is not fully resolved due to its flexibility, for example in the co-crystal structure of alectinib (Figure **77C**).⁷² I docked the (*R,S*)-diastereomer **135** into the ALK structures 3AOX and 4CLI with a shift in the p-loop and missing portion of the p-loop respectively but again no hinge binding interaction was predicted.

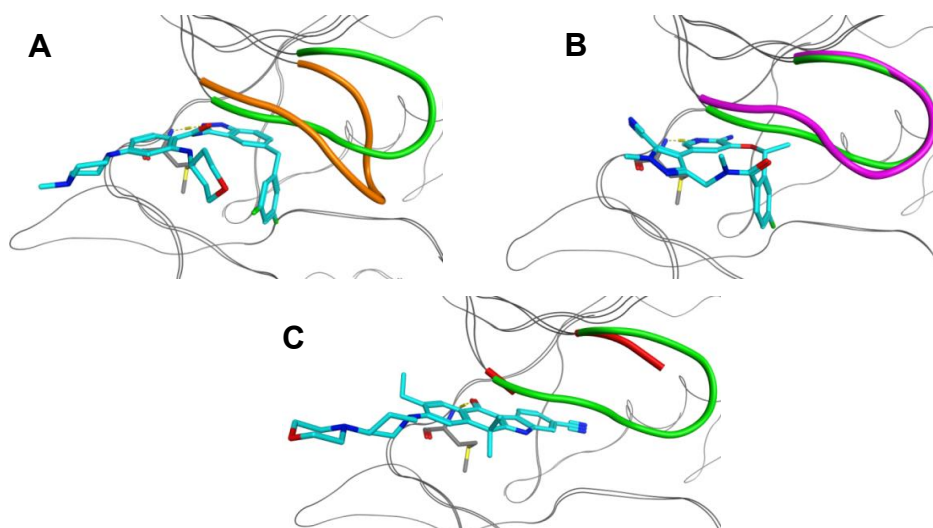


Figure 77. Comparison of p-loop structures. P-loop of 2XB7 shown in green **A**) p-loop structure with entrectinib (orange, 5FTO) **B**) p-loop structure with lorlatinib (pink, 4CLI) **C**) p-loop structure with alectinib (red, 3AOX).

In summary, attempts to predict the binding mode of the most potent diastereomer **135** using docking were not successful. The (*R,R*)-diastereomer **134** was favoured in terms of docking score and interacting with the hinge but is 10-fold less potent than **135**. Superposition of the small molecule X-ray structure of **137** suggested the benzyl would clash with the p-loop. The flexibility of the p-loop structure is not captured by docking using a rigid protein template and thus likely the reason for no docking poses consistent with hinge binding predicted for the (*R,S*) analogue in a favourable conformation. Co-crystallography of the compound in ALK would provide the answer of how the compound binds to ALK and whether the superior activity of the (*R,S*)-diastereomer **135** and poor docking predictions is related to a shift in the p-loop.

4.2.3 Further SAR around (*R,S*)-Diastereomer Compound **135**

With **135** as the most potent diastereomer, I decided to explore SAR around this compound further. Due to the different conformation of the benzyl group from the presence of the additional methyl, I predicted the SAR around **135** may be different to the non-substituted benzyls previously discussed in Chapter 3. The benzyl of **143** without the methyl is on the opposite face to the ethyl whilst (*R,S*)-diastereomer intermediate **137** with the methyl positions the benzyl on the same face as the ethyl (Figure 78). Rotation of the nitrogen-carbon bond of **137** to mimic the position of the benzyl in both the small X-ray structure and docked compound **58** shows the methyl would clash with the pyrimidine nitrogen. As the benzyl cannot accommodate the same conformation as **58**, different SAR was expected.

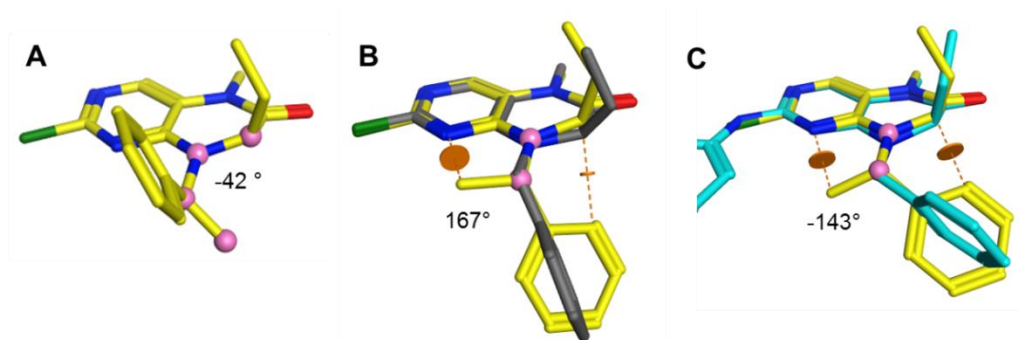


Figure 78 **A)** Small X-ray structure of **137** (yellow) highlighting dihedral angle of pink atoms. **B)** Rotation of nitrogen-carbon bond (pink atoms) to match benzyl position of **143** (grey, small molecule X-ray solved by Catherine Fletcher, 0.83 Å). **C)** Rotation of nitrogen-carbon bond (pink atoms) to match benzyl position of docked analogue **58** (blue). Atom clashes represented by orange discs.

For initial SAR I decided to explore changing the methyl substitution, adding substitution on the ring as well as changing the phenyl to a thiophene ring (Figure 79).

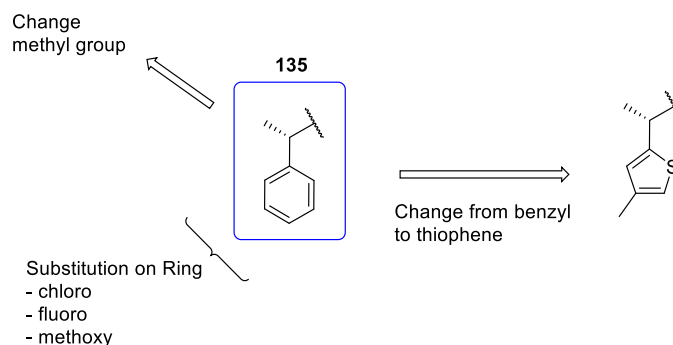
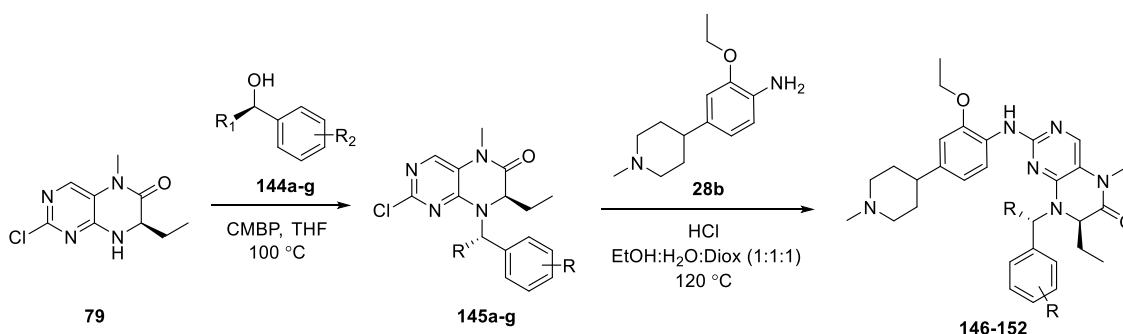


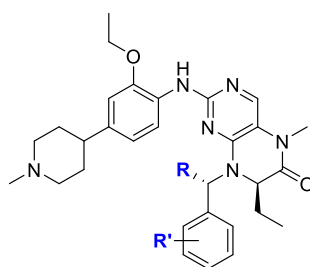
Figure 79. Initial SAR based on diastereomer compound **135**.

The first point of modification was the benzylic methyl group. I previously made the racemic ethyl (**106**) at this position which lowered ALK and BRD4 potency. For direct comparison to **135** I wanted to synthesise the single (*R,S*)- α -ethylbenzyl diastereomer. The single enantiomer (*R*)-1-phenylpropan-1-ol **144a** was commercially available and used in the Mitsunobu reaction with **79** (Scheme 25). A limited number of chiral alcohols were also commercially available for adding substitution onto the benzyl ring including the *ortho*-, *meta*- and *para*-chloro, fluoro and methoxy benzyls (**144b-g**). As mentioned in 4.1.2 and discussed further in Chapter 5, prior epimerisation of the ethyl chiral centre meant two diastereomers were formed following the Mitsunobu reactions between intermediate **79** and alcohols **144a-g**. The resulting diastereomers were separated using the same HPLC conditions used to separate the diastereomers **137** and **138**. Final compounds were then synthesised using the same acid-promoted S_NAr conditions between **145a-g** and left hand side intermediate **28b**.



Scheme 25. Synthetic route for (*R,S*)-diastereomer analogues **146 – 152**.

I initially synthesised and tested **146** with the ethyl at the benzylic position and **147** – **149** with an *ortho*-, *meta*- and *para*-chloro (Table 21). As observed with the racemate **106**, the presence of a larger group at the benzylic position (**146**) decreases potency against ALK^{F1174L} and BRD4, although equipotent against ALK WT. The methyl of **135** seems optimal for ALK^{F1174L} potency. Introducing a chloro in the *ortho*-position (**147**) gave a 5-fold decrease in potency compared to **135** and was less favoured compared to the *meta*- and *para*-positions. Both the *meta*- and *para*-chloro analogues **148** and **149** gave a small 2-fold drop off in ALK^{F1174L} potency and equipotent for ALK WT.



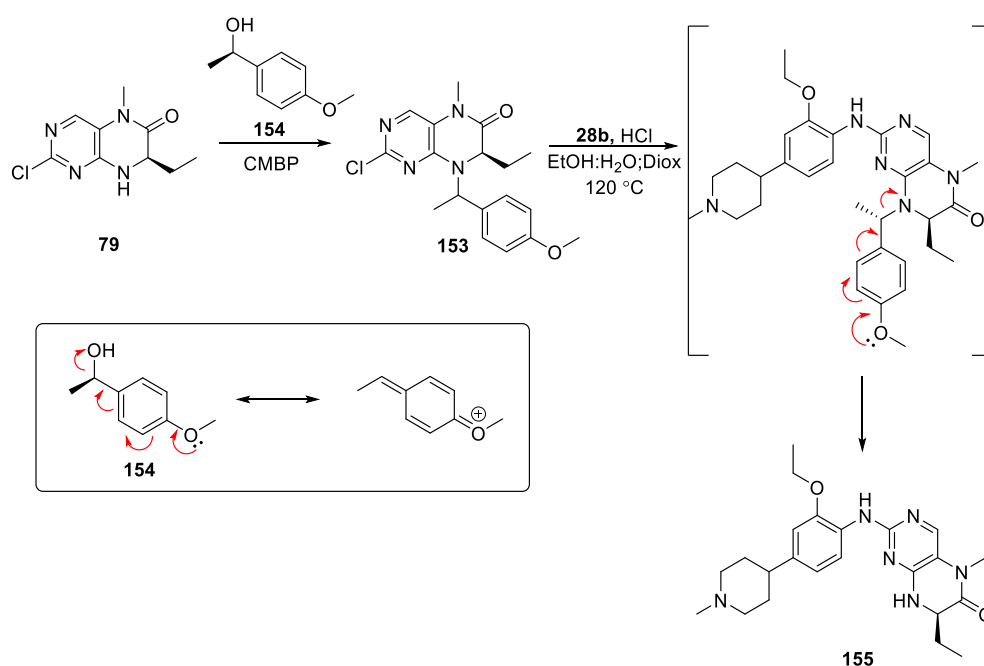
| | R | R' | ALK | | BRD4 | |
|------------|----|---------------|-----------------------------|---------------------------------|-----------|---------------------|
| | | | WT IC ₅₀ (nM) | F1174L IC ₅₀ (nM) | ΔTm [K] | K _d (nM) |
| 135 | Me | H | 79 ± 12 | 22 ± 7 | 5.9 ± 0.3 | 115 |
| 146 | Et | H | 65 ± 4 | 83 ± 5 | 1.3 ± 0.0 | - |
| 147 | Me | <i>o</i> -Cl | 100 ± 4 | 120 ± 17 | 4.3 ± 0.3 | - |
| 148 | Me | <i>m</i> -Cl | 45 ± 4 | 57 ± 9 | 7.6 ± 0.1 | - |
| 149 | Me | <i>p</i> -Cl | 140 ± 3 | 58 ± 8 | 7.6 ± 0.1 | - |
| 150 | Me | <i>m</i> -F | 78 ± 8 | 10 ± 1 | 5.6 ± 0.2 | 74 |
| 151 | Me | <i>p</i> -F | 100 ± 15 | 11 ± 2 | 5.1 ± 0.3 | 149 |
| 152 | Me | <i>m</i> -OMe | 91 ± 33 | 24 ± 3 | 6.4 ± 0.2 | - |

Table 21. Biochemical assay data for SAR of the benzyl group (R₂), - = not determined. ALK IC₅₀ values: mean ± S.E, n = 3. BRD4 ΔTm: mean ± S.D, n = 2, compound concentration of 10 μM. BRD4 K_ds, n = 1.

Due to preference for substitution in the *meta*- and *para*-position I changed the chloro to a fluoro or methoxy. The *meta*-fluoro **150**, *para*-fluoro **151** and *meta*-methoxy **152** analogues were all successfully synthesised according to Scheme 25. Compounds **150** and **151** with the *meta*- and *para*-fluoro respectively saw a small 2-fold improvement in ALK^{F1174L} potency to 10 and 11 nM whilst maintaining ALK WT and BRD4 activity (Table 21). The *meta*-methoxy analogue **152** also retained good potency, equipotent to **135**. This suggests substitution at the *meta*- and *para*-positions of the α-methylbenzyl is tolerated which differs from the SAR of the non-α-methyl

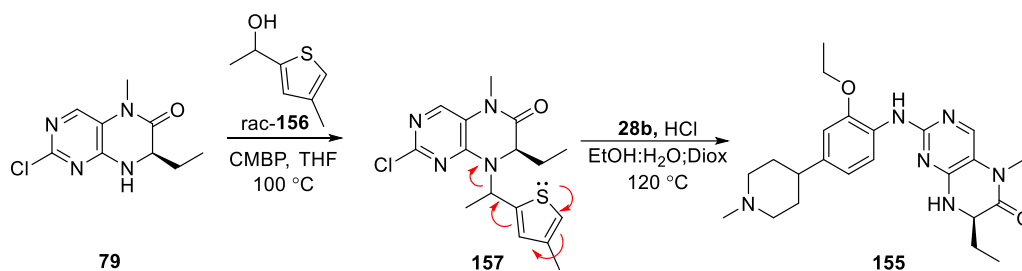
compounds (Table 11) in which *ortho*- and *meta*-substitution was preferred. Further SAR would confirm the limits of what is tolerated on the α -methyl benzyl ring.

I also wanted to prepare a *para*-methoxy analogue but during the synthesis a 1.8:1 ratio of diastereomers of **153** was formed (Scheme 26). As I had shown that epimerisation of the ethyl centre was not occurring during the Mitsunobu reaction (see 5.5.4), the epimerisation was likely due to rearrangement of the electron rich ring of **154**. I was unable to separate the diastereomers *via* HPLC so decided to take **153** forward as the mixture of diastereomers. Unfortunately during the final step, the *para*-methoxybenzyl was removed under the acidic conditions yielding compound **155**.



Scheme 26. Attempted synthesis of *para*-methoxy analogue **154**.

The final modification I wanted to achieve was changing the benzyl of **135** to a thiophene. The hypothesis was adding the equivalent of the benzylic methyl to potent thiophene analogue **63** may give a similar increase in potency. As the chiral alcohol of **156** wasn't commercially available I used *rac*-**156** with the aim of separating out the diastereomers after the Mitsunobu or final S_NAr step (Scheme 27). However the diastereomers of **157** could not be separated following the Mitsunobu step and during the final S_NAr step, the product formed was **155** without the thiophene group. The thiophene group is labile to acid in a similar manner to the *para*-methoxybenzyl group (Scheme 26). Alternative S_NAr conditions without an acid promoter should be attempted in the future for the synthesis of further analogues.



Scheme 27. Attempted synthesis of thiophene diastereomer.

Overall, substitution on the benzyl ring was tolerated, with the *meta*- and *para*- fluoro slightly improving ALK^{F1174L} potency to 10 and 11 nM and the *meta*-methoxy retaining potency at 23 nM. Changing the benzylic methyl to an ethyl decreased potency, indicating the small methyl is optimal at this position. Further exploration of (*R,S*)-diastereomer analogues is warranted to see if potency can be further optimised for ALK and BRD4, as well as determining the selectivity over PLK-1. The number of chiral commercially analogues with substitution on the ring is limited so further analogues could be prepared by chirally reducing the equivalent ketone *via* a CBS reduction.¹⁸¹

4.3 Further Cellular Testing

4.3.1 ALK Phosphorylation

Compound **135** was a further example of a potent and selective dual inhibitor that was suitable for progressing to cellular testing. To confirm the compound had on-target engagement in cells, **135** was first tested in the ALK MSD phosphorylation assay (3.6.1) and compared to thiophene analogues **62** and **63** and ALK inhibitor ceritinib in the Kelly cell line (Figure 80). **135** demonstrated on-target engagement in cells by effectively decreasing level of ALK phosphorylation with a comparable IC₅₀ to **63** of 880 nM.

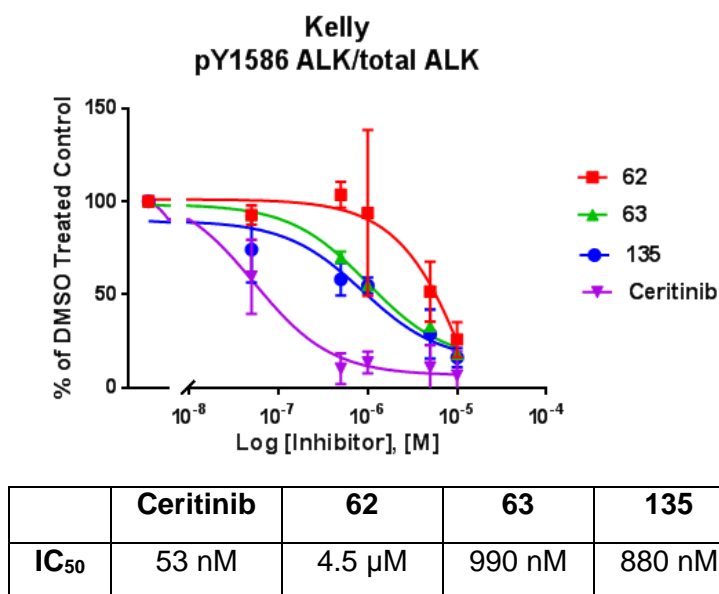


Figure 80. ALK MSD phosphorylation assay with compound **135** compared to **62**, **63** and ceritinib in the Kelly cell line. Performed by Lizzie Tucker.

4.3.2 BRD4 qRT-PCR

With **63** and **135** as suitable potent and selective *in vitro* probes, the compounds were taken forward to further cellular testing in collaboration with the Paediatric Solid Tumour Team at the ICR. The first experiment was to investigate the direct effect of the compounds on BRD4 and MYCN in cells using quantitative, reverse transcription, polymerase chain reaction (qRT-PCR) to monitor levels of MYCN and tyrosine hydroxylase (Th) mRNA transcripts, the expression of both being regulated by BRD4 (Figure **81**).³² The expression of Tyrosine hydroxylase, a specific BRD4 target, was effectively inhibited by **63** and **135**, comparable to BRD4 inhibitor JQ1. The compounds were also shown to decrease levels of MYCN with increasing concentration of **63** and **135** with the highest concentration (4 μ M) reaching MYCN levels similar to JQ1.

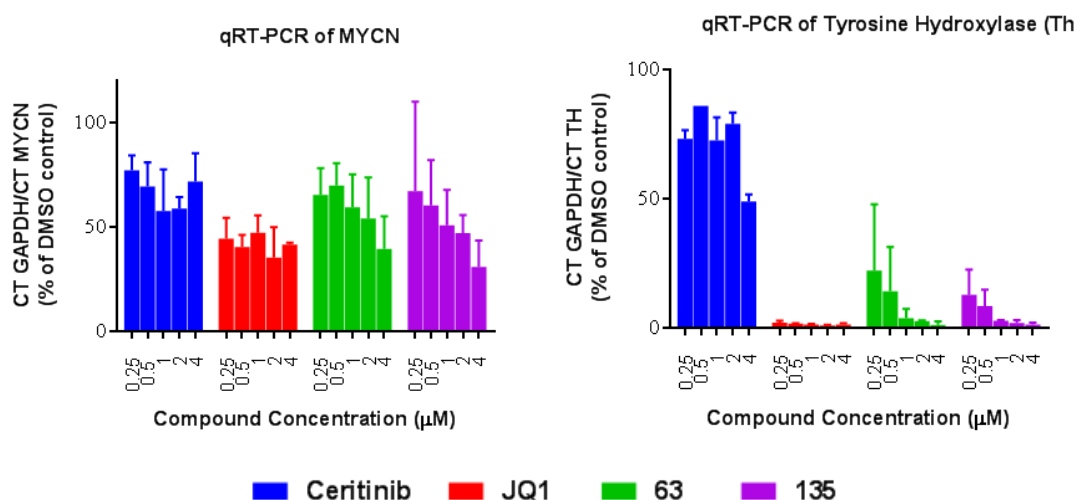


Figure 81. qRT-PCR of BRD4 markers MYCN and Th. Performed by Lizzie Tucker.

4.3.3 Growth Inhibition

GI₅₀ values for key compounds **58**, **62**, **63** and **135** were measured to test if the compounds had anti-proliferative effects. GI₅₀ values were initially measured in the NBLW-R neuroblastoma cell line with the ALK^{F1174L} mutation. (Table 22). The compounds were compared to ALK inhibitors lorlatinib, ceritinib and crizotinib and BRD4 inhibitor JQ1.

| | ALK ^{F1174L} IC ₅₀ (nM) | ALK MSD IC ₅₀ | | GI ₅₀ (NBLW-R) (μM) |
|-------------------|--|--------------------------|---------|-----------------------------------|
| | | (NBLW-R) | (Kelly) | |
| Lorlatinib | 0.2 | - | - | 0.08 |
| Ceritinib | 0.8 | 29 nM | 53 nM | 0.11 |
| Crizotinib | 1.2 | - | - | 0.18 |
| JQ1 | - | - | - | 0.52 |
| 58 | 85 | > 10 μM | > 10 μM | 3.50 |
| 62 | 63 | 850 nM | 4.5 μM | 0.65 |
| 63 | 17 | 640 nM | 980 nM | 0.38 |
| 135 | 22 | - | 880 nM | 0.29 |

Table 22. Biochemical IC₅₀, ALK MSD IC₅₀ and GI₅₀ values for key compounds and clinical ALK and BRD4 inhibitors. - = not determined. GI₅₀ analysis performed by Lizzie Tucker.

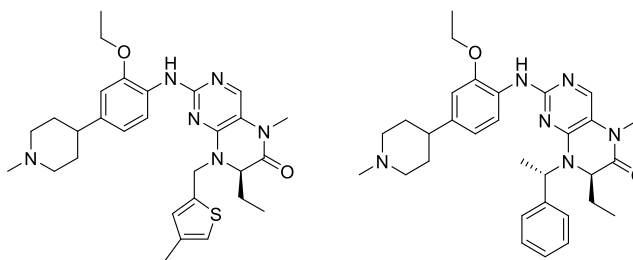
The GI₅₀ values demonstrated the compounds are permeating into cells and inhibit cell proliferation. In the NBLW-R cell line, the improvement in GI₅₀ from **58** to **63** and **135** is consistent with the increase in ALK^{F1174L} biochemical IC₅₀. The BRD4 biochemical potencies for the dual inhibitors are similar suggesting the increase in ALK potency increases inhibition of cell proliferation. Interestingly compound **135** had a similar GI₅₀ value to crizotinib despite being 20-fold less potent than crizotinib in the ALK^{F1174L} biochemical assay. A possible reason for the similar GI₅₀ values could be the BRD4 activity of **135** further driving the growth inhibition which would support the project hypothesis of an ALK and BRD4 combination being beneficial. A further experiment to test this hypothesis would be the design and testing of a compound in the dual inhibitor series with a comparable IC₅₀ to **63** and **135** but no BRD4 activity to see if BRD4 activity helps drive the anti-proliferative effects of 408 and 976. Similarly reaching compounds with similar potencies to the clinical ALK inhibitors would allow for a more direct comparison of potent ALK inhibitors with and without potent BRD4 activity. GI₅₀ analysis will be expanded to other ALK dependent cell lines to see if these initial trends are continued.

4.4 Physicochemical Properties

4.4.1 Physicochemical Properties of Key Compounds **63** and **135**

So far key compounds **63** and **135** showed good biochemical potencies, selectivity over PLK-1 and on-target engagement in cells with **63** also demonstrating good broad kinase and bromodomain selectivity. To progress the compounds as *in vitro* tools and to translate to *in vivo* work, it was important to consider the physicochemical properties of the compounds to improve the compounds' absorption, distribution metabolism and excretion (ADME) profile.¹⁸²

I chose to profile some of the physicochemical properties of key compounds **63** and **135** by measuring their solubility, permeability and microsomal clearance, as well as considering their structural properties, lipophilicity (clogP and clogD_{7.4}) and pK_aH (Table 23). I measured the kinetic aqueous solubility of the compounds using NMR¹⁸³ whilst permeability was measured by the DMPK team using the parallel artificial membrane permeability assay (PAMPA) and Caco-2 permeability assay.^{184,185} Both permeability assays measure the rate of permeation but in the Caco-2 assay the rate is effected by efflux as well as passive permeation. A microsomal stability assay to determine the *in vitro* intrinsic clearance of the compounds was also performed.¹⁸⁶



| | 63 | 135 |
|---|--------------------|--------------------|
| ALK^{F1174L} IC₅₀ | 17 nM | 22 nM |
| BRD4 K_d | 44 nM | 115 nM |
| clogP/clogD_{7.4} | 6.0 / 4.0 | 6.3 / 4.3 |
| pK_{aH} | 9.4 | 9.4 |
| Solubility (NMR) | 179 μ M | 162 μ M |
| PAMPA pH7.4 (x 10⁻⁶ cm/s) | 45.8 | 35.9 |
| Caco-2 A-B/B-A [efflux] (x 10⁻⁶ cm/s) | 1.5 / 4.8 [3.3] | 3.4 / 9.3 [2.7] |
| Clearance (h/m) (μL min⁻¹ mg⁻¹) | 137 / 33 | 537 / 60 |

Table 23. Physicochemical and *in vitro* DMPK properties of **63** and **135**. pK_a, logP and logD_{7.4} calculated using MOKA. pK_{aH} measurement is for the *N*-methyl piperidine. Kinetic aqueous solubility measured at pH7.4. Permeability and clearance measured by Angela Hayes. (h/m) = (human/mouse).

Compounds in the logP range 0 – 3 have a high likelihood of having a good balance of solubility and permeability.¹⁸⁷ Both **63** and **135** have a very high clogP at 6.0 and 6.3 respectively, thus the physicochemical properties were expected to be sub-optimal with poor solubility, high permeability and high potential for metabolism. The clogD values at pH_{7.4} were 4.0 and 4.3 for **63** and **135** due to protonation of the *N*-methyl piperidine at physiological pH. This protonation is likely to account for the surprisingly high solubility of **63** and **135**. As expected from the high lipophilicity, the compounds showed good permeability in the PAMPA assay though some efflux was observed in the Caco-2 permeability assay. The mouse clearance for **63** and **135** is moderate based on internal classification (low < 20, high > 60) but the human clearance, particularly for **135**, is high. Though the physicochemical properties of the compounds were satisfactory, I wanted to explore reducing the high lipophilicity of the compound.

4.4.2 Modifications to the Solvent Channel Region

To lower the lipophilicity of the dual ALK-BRD4 series, I needed to identify a suitable region of the molecule that could tolerate modification by introducing polarity or reducing hydrophobicity and retain potency. A high portion of the molecule was not suitable for modification, including the aminopyrimidine hinge binding region, the methyl amide KAc mimetic and the (*R*)-ethyl group (R_1), all of which provide key interactions and site closely alongside the pocket surface in ALK and BRD4 (Figure 82). The R_2 region offered potential for modification being part solvent exposed in ALK and BRD4 but so far polar heterocycles and groups which would help lower the logP were not tolerated in ALK. A more suitable region for modification was the solvent channel region (R_4). This portion of the molecule is solvent exposed in ALK and BRD4 so modifying this group will not disrupt key interactions within the pocket. Previously I had shown that modifying this region did not have a large impact on ALK and BRD4 potency (Chapter 2 & 3) and therefore I could install a wide range of groups to help lower the lipophilicity. This area has previously been used in other ALK inhibitor projects as a region for modifying physicochemical properties.^{46,74}

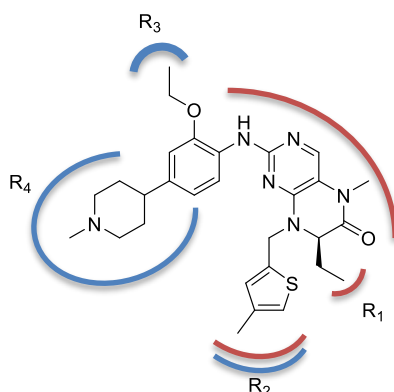


Figure 82. Structure of **63** highlighting the regions of the molecule which fit close to the pocket surface of ALK and BRD4 (red) or are solvent exposed (blue).

I first compared the clogP and clogD_{7.4} values of the solvent channel groups installed so far with the 4-methylthiophene scaffold (Figure 83). The morpholine, piperazine and *N,N*-dimethylpiperidin-4-amine analogues **71** – **73** have a higher clogP and/or clogD_{7.4} compared to **63**. The presence of the amide in **69** reduced the clogP and clogD_{7.4} though the compound was not as potent as the more lipophilic compounds **63** and **72** against ALK^{F1174L}. In general, ALK contains quite a lipophilic pocket and so the more lipophilic compounds are likely to be favoured for potency.¹⁸⁸

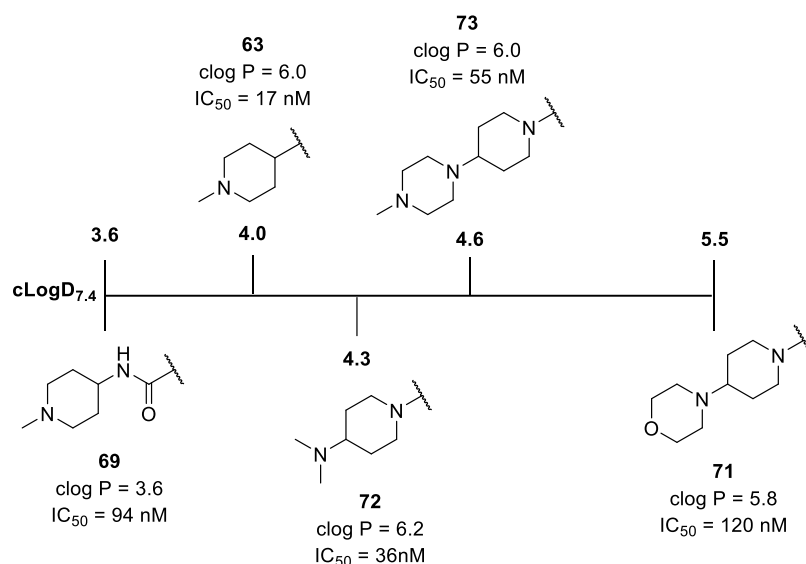


Figure 83. Comparison of clogD_{7.4}, clogP and ALK^{F1174L} IC₅₀ values for previous solvent channel modifications. All the groups are linked on to the 4-methylthiophene scaffold of **63**. clogP and clogD_{7.4} values generated using MOKA.

To expand the current set of solvent channel groups, I focused on groups that would reduce the logP and/or the logD_{7.4} values. I considered several ways that are known to lower the lipophilicity of a drug (Figure 84).¹⁸² The first is to remove lipophilic groups; a suitable modification in the solvent channel region for **63** is to remove the methyl on the piperidine to give the free amine. Removing the methyl increases the basicity of the amine from a calculated pK_aH of 9.4 to 10.4 for **158** and also significantly lowers the clogP and clogD_{7.4} by 1.5. The second method I considered to reduce lipophilicity was adding ionisable groups. With compound **159**, there are two ionisable centres present in the solvent channel group, the piperidine and piperazine. Both groups will be protonated at physiological pH hence a lower clogD_{7.4} value of 3.5. The disadvantage of this compound is the clogP is still predicted high at 6.0, equal to **63**, but the lower logD_{7.4}, relevant for physiological conditions, may be advantageous. Finally I considered adding polar atoms to the solvent channel group to lower lipophilicity. The addition of a nitrogen to **63** to form the piperazine (**160**) lowers the clogP from 6.0 to 5.3 whilst adding an carbonyl lowers the clogP further to 4.4 (**161**). A further example I considered to lower the lipophilicity was **162** containing a thiomorpholine 1,1-dioxide group, which lowered to clogP and clogD_{7.4} to 3.5. Analogues **161** and **162** were not synthesised initially due to their lack of basicity which could hinder solubility.

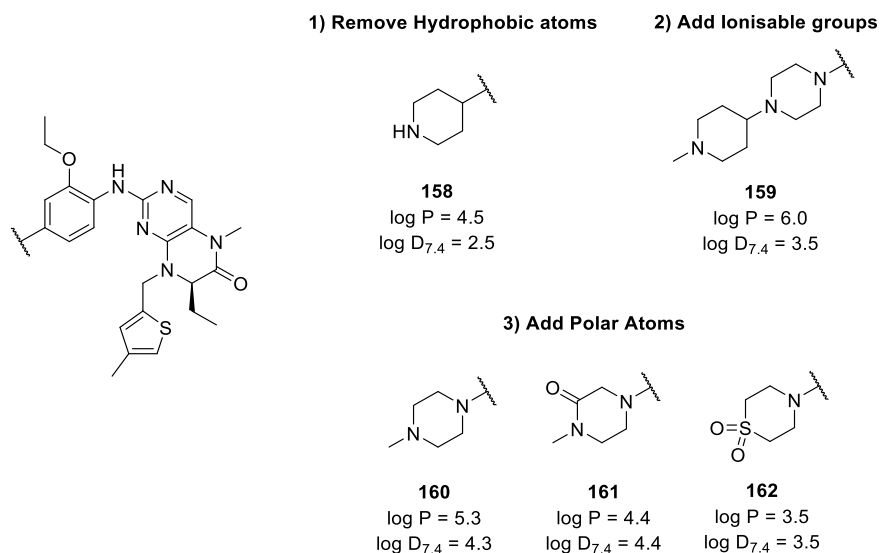
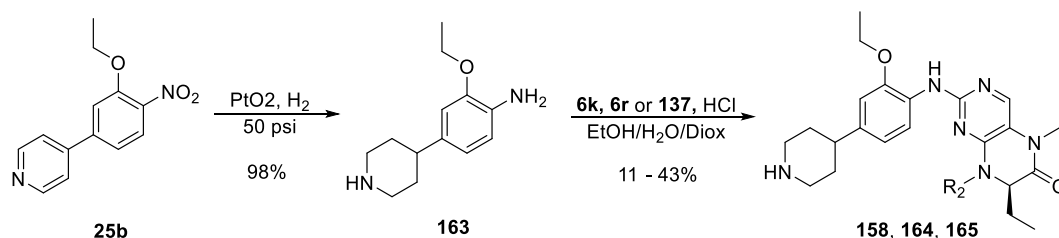


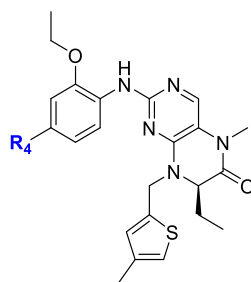
Figure 84. Modifications to the solvent channel region to reduce lipophilicity.

The left-hand side intermediates of analogues **159** and **160** were synthesised according to previous Schemes 7. For **158**, intermediate **25b** was subjected to high pressure hydrogenation conditions to reduce the nitro and pyridine groups to give **163** (Scheme 28). **163** was then coupled to **6r** to give final compound **158**. The biochemical data for the new solvent channel analogues are shown in Table 24, along with their kinetic solubility.



Scheme 28. Synthesis of unmethylated piperidine analogues.

Compounds **158**, **159** and **160** were all potent against ALK^{F1174L}, in particular **158** with the unmethylated piperidine at 7.9 nM (Table 24). Compound **62** slightly improved the lipophilic ligand efficacy to 1.91, similar to previous analogue **69**. Compound **158** significantly improved the LLE to 3.60 due to the 2-fold improvement in potency and reduced clogP. The majority of analogues had high aqueous solubility, especially considering the clogP values are within the range of 4.5 – 6. Compounds **71** and **73** with the highest clogD_{7.4} values had poor solubility as well as **159** despite having an extra ionisable centre. Overall **158** was the most promising modification to the solvent channel region (R₄) for improving the physicochemical properties of the series.



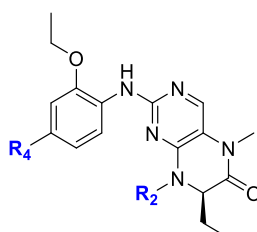
| R₄ | | ALK^{F1174L} IC₅₀ (nM) | clogP | clogD_{7.4} | LLE | NMR Solubility (μM) |
|----------------------|--|--|--------------|----------------------------|------------|--------------------------------|
| 71 | | 120 ± 29 | 5.8 | 5.5 | 1.11 | 19 |
| 73 | | 55 ± 17 | 6.0 | 4.6 | 1.26 | 0 |
| 72 | | 36 ± 7.1 | 6.2 | 4.3 | 1.24 | 250 |
| 63 | | 17 ± 3.5 | 6.0 | 4.0 | 1.67 | 180 |
| 69 | | 94 ± 5.4 | 5.1 | 3.6 | 1.93 | 100 |
| 160 | | 62 ± 14 | 5.3 | 4.3 | 1.91 | 100 |
| 159 | | 38 ± 3.3 | 6.0 | 3.5 | 1.42 | 11 |
| 158 | | 7.9 ± 1.1 | 4.5 | 2.5 | 3.60 | 120 |

Table 24. Biochemical assay, clogP, clogD_{7.4}, LLE and NMR solubility data for SAR of the solvent channel group (R₄). ALK IC₅₀ values: mean ± S.E, n = 3. clogPs and clogDs generated using MOKA.²² Kinetic aqueous solubility measured at pH7.4.

4.4.3 Comparison of Methylated and Unmethylated Piperidine Analogues

Due to the unmethylated piperidine analogue **158** showing an improvement in potency and lowering the lipophilicity, I applied this group to other lead compounds **62** and **135** to give **164** and **165** (Table 25). Both compounds were synthesised according to Scheme 28 between **163** and **6k** or **137**. I first measured ALK^{F1174L} IC₅₀ values for **164** and **165** which showed a similar 2-fold improvement in potency from their methylated equivalents **62** and **135** as observed with **158** and **63**. Alongside fluoro-substituted benzyls **150** and **151**, **158** and **165** were the most potent analogues

against ALK^{F1174L} in the dual ALK-BRD4 series. For BRD4 removing the methyl decreased the K_d values for analogous **158** and **164** 4-fold and 10-fold though remained equipotent for **165**. Whilst **62** and **63** have similar activities for ALK and BRD4, **158** and **165** exhibit an increased activity at ALK relative to BRD4. The differing ratios of kinase and bromodomain activities may be useful in future experiments to understand the ideal efficacious ratio of ALK and BRD4 activity.



| R ₂ | | | | | | |
|--|---------------|---------------|---------------|---------------|---------------|--------------|
| R ₄ | | | | | | |
| Compound | 62 | 164 | 63 | 158 | 135 | 165 |
| ALK ^{F1174L} IC ₅₀ (nM) | 63 ± 10 | 25 ± 9.4 | 17 ± 3.5 | 7.9 ± 1.1 | 22 ± 7 | 8.8 ± 1.1 |
| BRD4 K _d (nM) | 63 | 270 | 44 | 449 | 115 | 145 |
| PLK-1 IC ₅₀ (nM) | 68 ± 0.6 | 160 | 130 ± 37 | 230 | 3200 ± 110 | 3500 |
| clogP/clogD _{7.4} | 5.8/3.7 | 5.2/2.3 | 6.0/4.0 | 5.5/2.6 | 6.3/4.3 | 5.8/2.9 |
| LLE (ALK ^{F1174L}) | 1.52 | 2.02 | 1.67 | 3.60 | 1.36 | 2.20 |
| Solubility NMR (μM) | 202 | 180 | 179 | 115 | 162 | 180 |
| PAMPA pH7.4 (x 10 ⁻⁶ cm/s) | 25.9 | 11.8 | 45.8 | 17.8 | 35.9 | 13.1 |
| Caco-2 A-B/B-A [efflux] (x 10 ⁻⁶ cm/s) | 2.1/8.3 (3.9) | 1.3/18 (14.0) | 1.5/4.8 (3.3) | 1.6/17 (10.3) | 3.4/9.3 (2.7) | 2.5/20 (7.8) |
| Clearance h/m (μL min ⁻¹ mg ⁻¹) | 181/49 | 137/33 | 140/54 | 54/19 | 537/60 | 298/46 |

Table 25. Biochemical assay, physicochemical and *in vitro* DMPK data for key compounds. ALK IC₅₀ values: mean ± S.E, n = 3. BRD4 K_ds, n = 1. PLK-1 IC₅₀ values: mean ± S.D, n = 1/2 (ATP = 10 μM). clogPs and clogDs generated using MOKA.²² Kinetic aqueous solubility measured at pH7.4. Permeability and clearance measured by Angela Hayes. (h/m) = (human/mouse).

For PLK-1, the IC₅₀ values were similar between the methylated and unmethylated piperidines. With the improvement in ALK activity and maintained PLK-1 activity, **165** demonstrated the greatest kinase selectivity thus far of 380-fold towards ALK^{F1174L} over PLK-1.

As expected, removing the methyl lowered the clogP and clogD_{7.4} values with the logD_{7.4} values reaching the ideal range (1 – 3) for good a balance of solubility and permeability.¹⁸² Due to the improvement in potency and reduced lipophilicity, the LLE for **158**, **164** and **165** improved greatly, in particular for **158**.

I next compared the physicochemical properties of the methylated and unmethylated analogues. All the analogues displayed good solubility and no significant difference was observed by removing the methyl group and lowering the logP. Removing the methyl on the piperidine lowered the passive permeability of **158**, **164** and **165** in the PAMPA assay and significantly more efflux in the Caco-2 assay. This is an unsurprising result as lowering the lipophilicity of the compound and a greater number of hydrogen bond donors are associated with poorer lipid bilayer permeability. The Caco-2 assay was also performed in the presence of an inhibitor of the P-glycoprotein (PGP) transporter, a major efflux transporter that facilitates the export of compounds from cells.¹⁸² With the PGP inhibitor present, the efflux of **158**, **164** and **165** was lowered, indicating the compounds are substrates for PGP (Table 26). A small level of efflux remains for **158**, **164** and **165** as well as for **62**, **63** and **135** so another unknown transporter allows efflux of these compounds. Finally removing the methyl group lowered the clearance in human and mouse for **158**, **164** and **165**. This data strongly supported the methyl group as a key site of metabolism, likely *N*-dealkylation of the piperidine or that the lower clogP reduces the binding of the compound to metabolic enzymes.

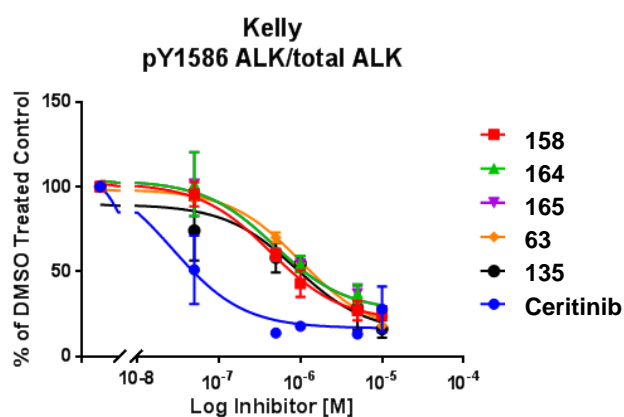
| | Efflux Ratio (B>A)/(A>B) | Efflux Ratio with PGP Inhibitor (B>A)/(A>B) |
|------------|-----------------------------|--|
| 62 | 3.9 | 3.7 |
| 163 | 14.0 | 3.2 |
| 63 | 3.3 | 3.3 |
| 157 | 10.3 | 1.8 |
| 135 | 2.7 | 1.6 |
| 164 | 7.8 | 2.0 |

Table 26. Efflux ratios in Caco-2 assay with or without PGP inhibitor present. Performed by Angela Hayes.

Though removing the methyl group improved the ALK^{F1174L} biochemical potency against ALK, improved selectivity over PLK-1 and lowered the clogP and clogD7.4. **158**, **164** and **165** were substrates of the PGP transporter causing an increase in efflux and for **158** and **164** the BRD4 potency was lowered. Overall the methylated analogues **62**, **63** and **135** showed the best overall profiles with **63** favoured from its lower clearance compared to **135** and improved permeability and potency from **62**. This work highlighted the importance in considering the physicochemical properties and not solely focusing on the potencies which may result in compounds with unfavourable profiles for translating to *in vivo* work.

4.4.4 Cellular Testing of Unmethylated Piperidine Analogues

As the unmethylated piperidine analogues were among the most potent analogues against ALK^{F1174L}, I tested the analogues in the ALK MSD phosphorylation assay to engage how potent the compounds were in cells. I compared **158**, **164** and **165** against **63** and **135** with ceritinib as a control compound (Figure 85). The cellular IC₅₀ values for **158**, **164** and **165** were of similar potencies, 430 – 480 nM, and a small improvement from the methylated piperidine compounds **63** and **135**, complementary to the improvement in biochemical potencies. Though **158**, **164** and **165** demonstrated high efflux, the compounds were still efficacious in cells and may be useful as comparative *in vitro* tools with a kinase-biased potency ratio.



| | Ceritinib | 63 | 135 | 158 | 164 | 165 |
|-----------------------|-----------|-----|-----|-----|-----|-----|
| IC ₅₀ (nM) | 27 | 990 | 880 | 430 | 480 | 480 |

Figure 85. ALK MSD phosphorylation assay for compounds **158**, **164** and **165** compared to **63**, **135** and ceritinib in the Kelly cell line.

Chapter 5 Epimerisation

5.1 Synthesis of Diastereomers

As discussed in Chapter 4, synthesis of diastereomer **137** was achieved by a Mitsunobu reaction between chiral alcohol **136** and **79** (Figure **86**). However, NMR revealed that two diastereomers were present in a 1:1 ratio following the Mitsunobu reaction meaning one of the chiral centres had racemised (Figure **86B**). The two diastereomers could either be the ethyl in the (*R*) or (*S*) configuration, the methyl in the (*R*) or (*S*) configuration, or a combination of all four. Racemisation was also observed when installing the (*S*)-enantiomer of **136** to **79**.

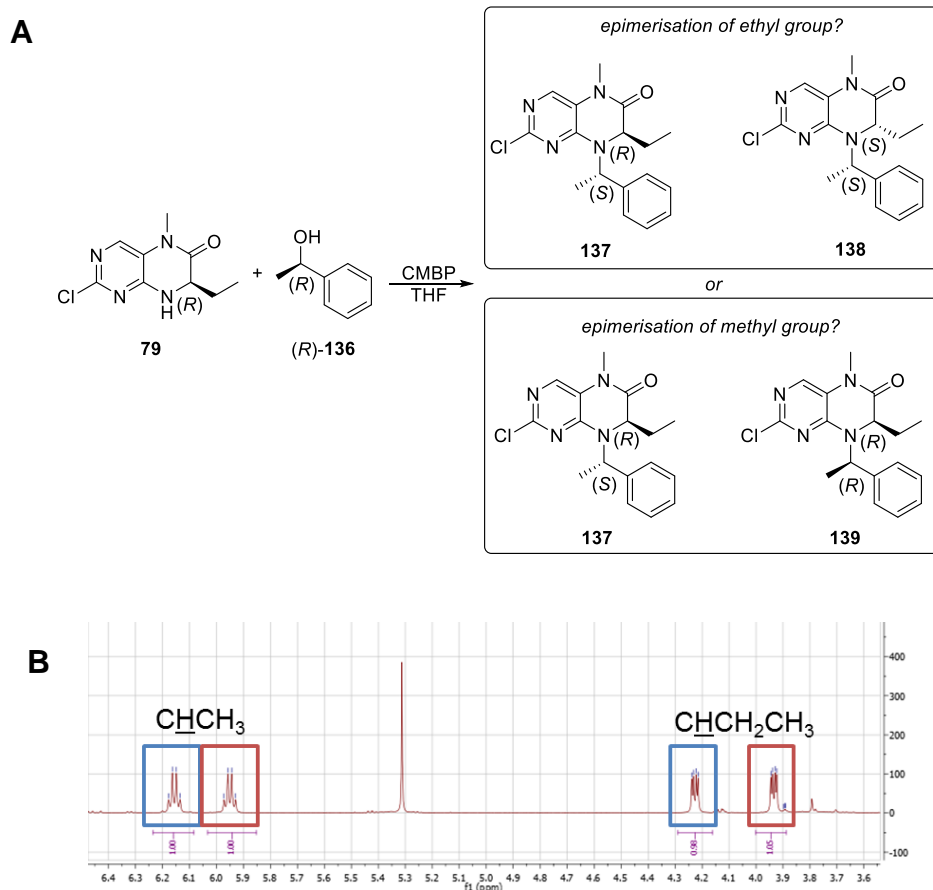


Figure 86 A) Possible diastereomer combinations resulting from the Mitsunobu reaction with **79** and (*R*)-**136** with either the ethyl or methyl group epimerising. **B)** ^1H -NMR of **137** indicating the presence of two diastereomers in the mixture (blue and red)

First, I decided to confirm if the starting materials were enantiopure. I checked the optical rotation of alcohol (*R*)-**136**, measured as +43.1 (*c* = 1.0, MeOH) and its enantiomer (*S*)-**136**, measuring at -42.1 (*c* = 1.0, MeOH) which closely matched the literature.¹⁹⁰ Therefore poor enantiomeric purity of alcohols (*R*)-**136** and (*S*)-**136** was not the problem. Next I checked the batch of starting material **79** using chiral shift NMR to determine if the ethyl chiral centre had already epimerised (Figure 87). Indeed, **79** saw splitting of its peaks upon addition of Eu(hfc)₃ in a roughly 2:1 ratio. This indicated two enantiomers were present in the mixture and that the ethyl centre had already partially epimerised prior to the Mitsunobu step. Although this did not confirm whether the methyl or ethyl group had further epimerised during the Mitsunobu reaction, I first set to resolve the issue of the ethyl group epimerising prior to this step.

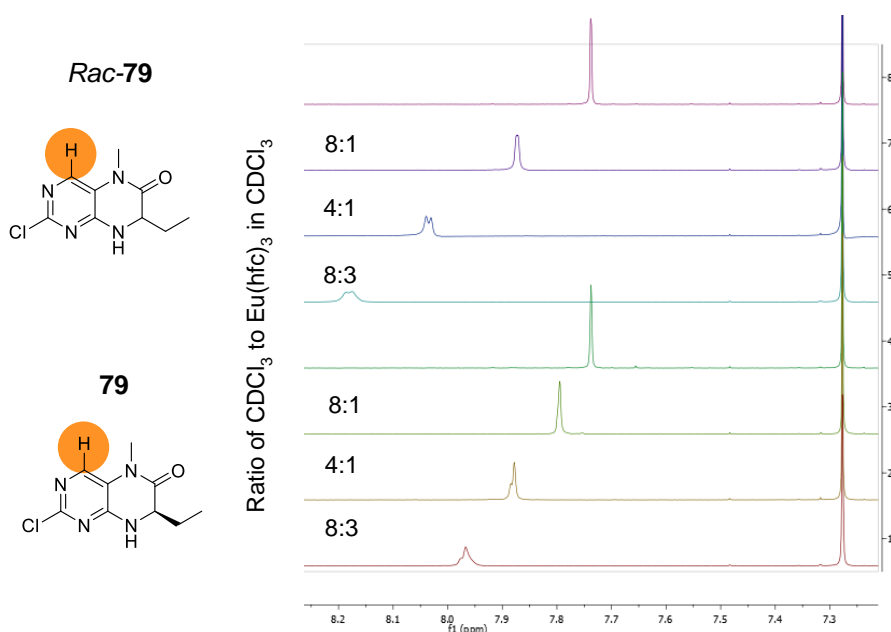
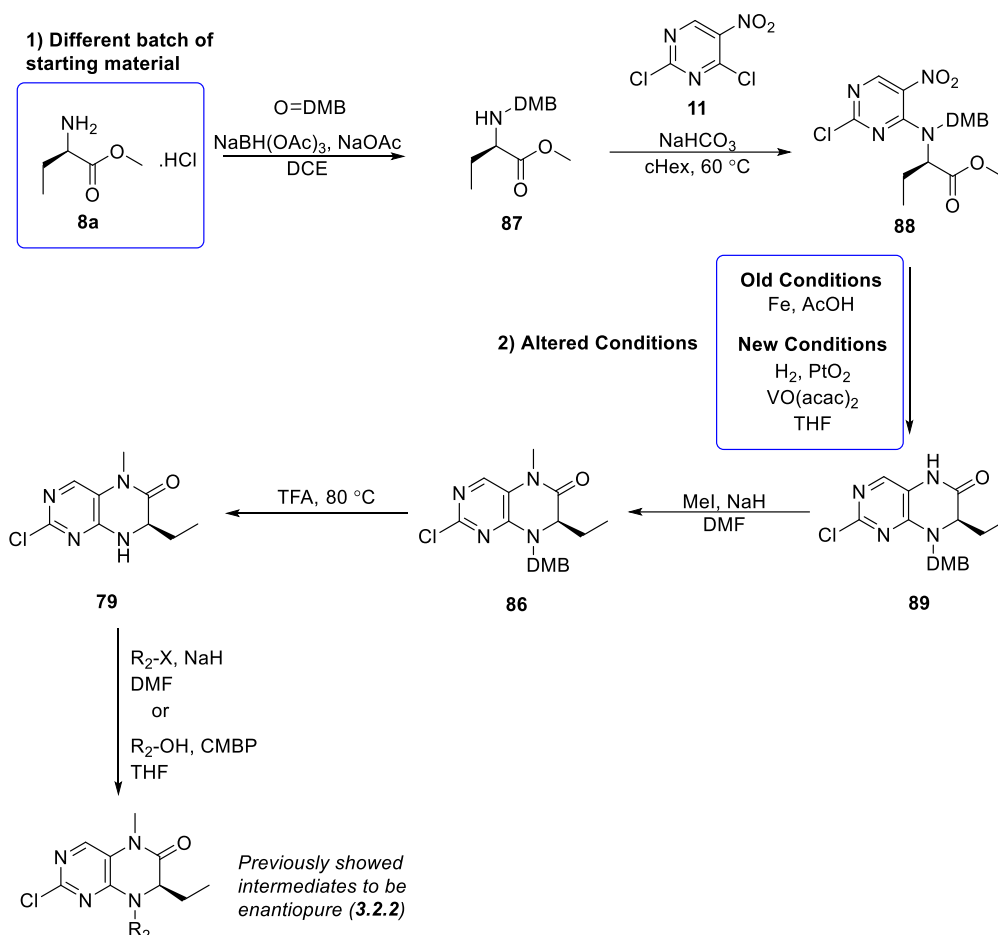


Figure 87. Chiral shift NMR of **79**, comparing the racemate and presumed single enantiomer intermediates after increasing addition of Eu(hfc)₃ (0.015 M). Zoomed in to look at the singlet aromatic proton peak (7.3 – 8.2 ppm).

5.1.1 Differences in Synthetic Routes

The formation of diastereomers was unexpected, especially as previous chiral shift NMR experiments showed that no epimerisation was observed during the original and adapted synthesis for R₂ variations (see 3.2.2). These experiments showed that despite the strong basic and acidic steps, the single enantiomer was synthesised.



Scheme 29. Synthetic route for R₂ variations highlighting the differences in synthesis between intermediates discussed in Chapter 3 and diastereomers in Chapter 4.

The synthesis of diastereomers **137** and **138** followed the same adapted synthetic route for R₂ analogues, starting with installation of the DMB protecting group (Scheme **29**). The only variations in the synthetic route for diastereomers **137** and **138** were the batch of starting amino acid **8a** and the reductive heterocyclisation conditions. Though the PtO₂/VO(acac)₂ conditions had been previously used for the synthesis of intermediates, including **6r** which was concluded to be a single enantiomer, I wanted to confirm whether the conditions had the potential to epimerise the chiral centre. I used chiral shift NMR on the racemic and presumed single enantiomer of **89** following the PtO₂/VO(acac)₂ step (Figure **88**). The addition of Eu(hfc)₃ to the *rac*-**89** caused the two enantiomer peaks to split, as observed with the amide proton. In comparison addition of Eu(hfc)₃ to the presumed (*R*)-enantiomer, did not see splitting of its peaks and hence verified as the single enantiomer. Due to no splitting in the chiral shift NMR and the rest of the synthetic route the same, it was assumed the starting amino acid **8a** was not enantiopure and the cause of the poor enantiomeric ratio.

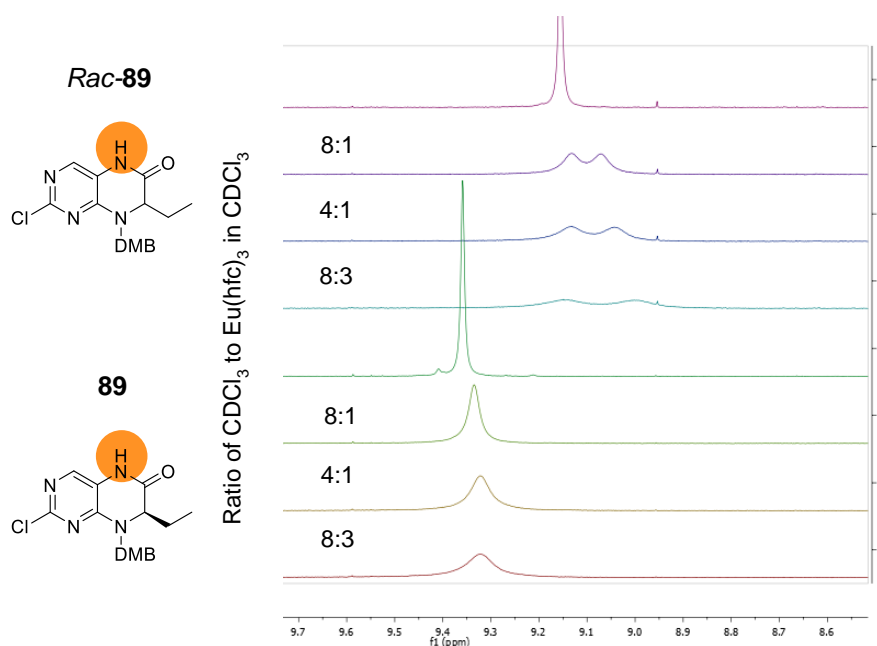


Figure 88. Chiral shift NMR of **89**, comparing the racemate and presumed single enantiomer intermediates after increasing addition of $\text{Eu}(\text{hfc})_3$ (0.015 M). Zoomed in to look at the singlet amide proton peak (9.7 – 8.6 ppm).

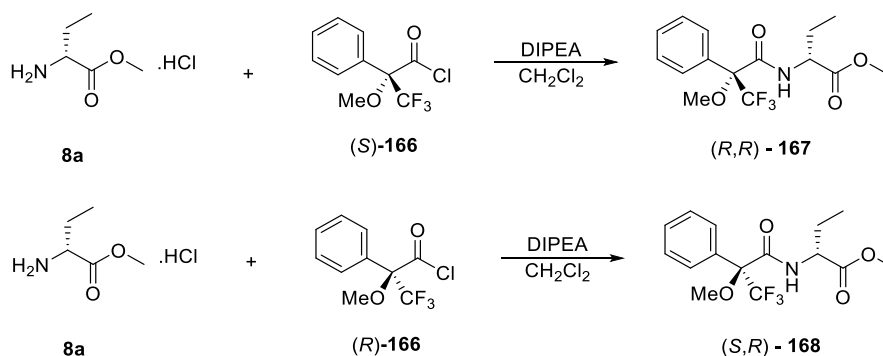
5.2 Checking the Enantiopurity of Starting Material **8a**

With a new batch of starting amino acid **8a**, I proceeded to repeat the synthesis of key intermediate **79**. However repeating the Mitsunobu reaction with alcohol (*R*)-**136** still gave two diastereomers in a 1.5:1 ratio. I subsequently checked the enantiopurity of the batches of starting material **8a** via optical rotation and the use of a chiral derivatising agent.

Fluorochem, the supplier of starting material **8a**, provided a reference optical rotation value of -15.99 . I measured the optical rotation of two separate batches of **8a** and got similar values of -17.3 and -17.5 . I also measured the optical rotation of the (*S*)-enantiomer **8b** as $+17.8$ which closely matched the literature value of $+17$.¹⁹¹ Though the measured optical rotations were similar to previously reported measurements, this did not confirm the enantiopurity of the compound and at worst the material was mostly one enantiomer.

As chiral shift NMR was not successful with *rac*-**8a**, I decided to use Mosher's acid chloride as a chiral derivatising agent.¹⁹² A chiral derivatising agent acts as a chiral

auxiliary to convert a mixture of enantiomers into diastereomers which may be distinguishable by NMR or HPLC.¹⁹³ I formed diastereomer intermediates **166** and **167** via an amide formation between **8a** and the (*R*)- and (*S*)-Mosher's acid chloride **165** (Scheme 30). Chromatography purification was not performed in case of selective enrichment of one diastereomer.¹⁹³



Scheme 30. Synthesis of diastereomers **167** and **168** using the Mosher's acid chiral derivatising agent.

Different NMR spectra were observed for **167** and **168** as seen with the ethyl proton peaks in Figure **89A**. A closer inspection of the CH_2 protons reveals no presence of the opposite diastereomer within each spectra (Figure **89B**). This confirmed the starting material was indeed the single enantiomer (> 98%) and the epimerisation of the ethyl centre must be occurring during the synthesis.

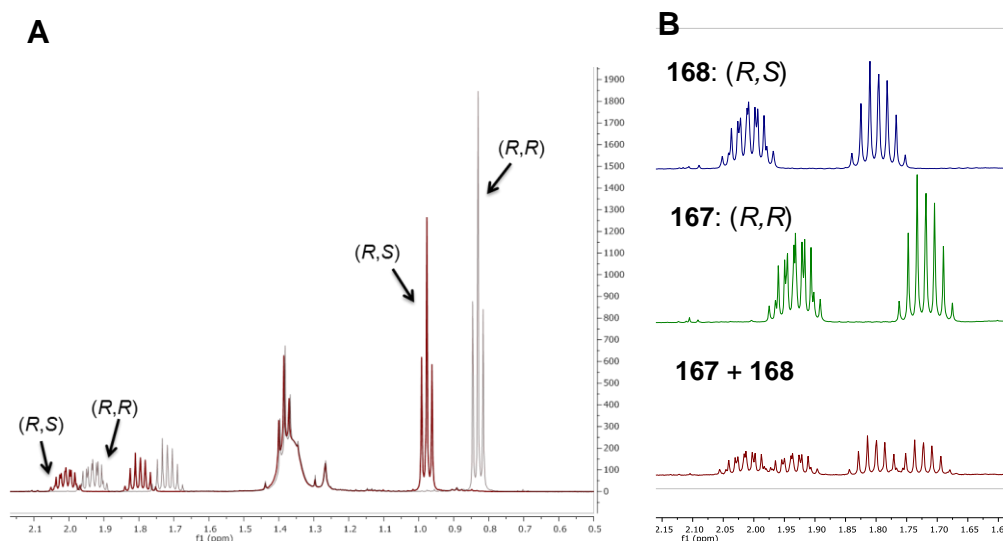
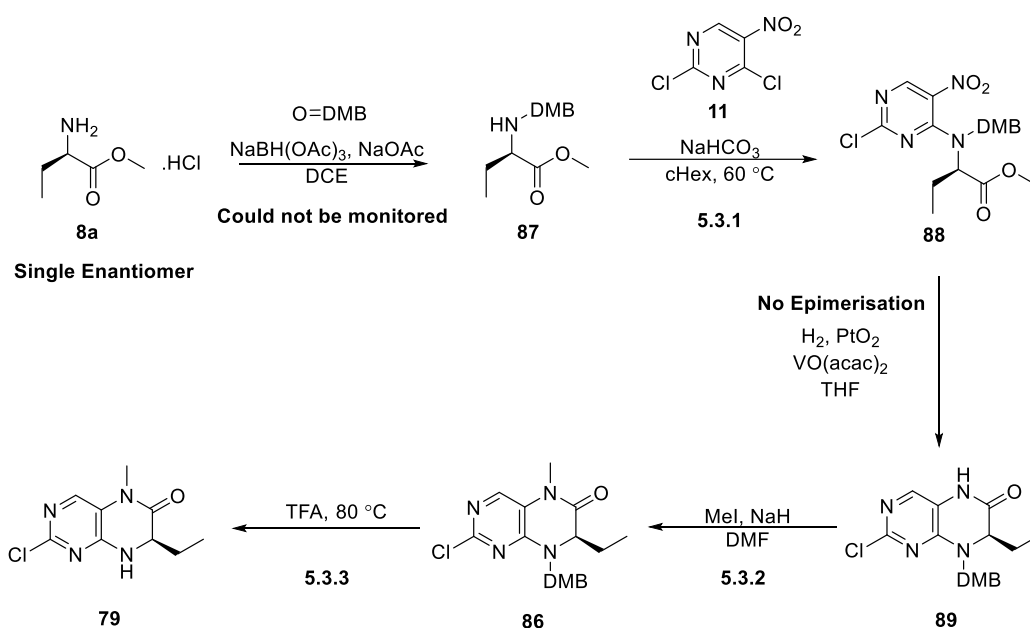


Figure 89. A) Overlay of **167** (*R,R*) and **168** (*R,S*) ^1H -NMR spectra. **B)** Zoomed in spectra showing the CHCH_2CH_3 peaks of **167** and **168** and as a combination (2.15 – 1.60 ppm).

5.3 Checking Synthetic Steps by Chiral Shift NMR

As the starting amino acid **8a** was confirmed as the single enantiomer, I proceeded to check all the synthetic steps individually using chiral shift NMR to understand where epimerisation was occurring (Scheme 31). The first reductive amination could not be monitored by chiral shift NMR due to the enantiomer peaks of *racemic*-**87** not splitting in the presence of $\text{Eu}(\text{hfc})_3$. I also attempted to use a chiral derivatising agent to monitor this step but no reaction took place between Mosher's acid chloride **166** and **87**. As the reductive heterocyclisation step had already been checked by chiral shift NMR (5.2) this left the $\text{S}_{\text{N}}\text{Ar}$, methylation and deprotection steps to be analysed.



Scheme 31. Checking of epimerisation using chiral shift NMR during the synthesis of intermediate **79**.

5.3.1 Checking the $\text{S}_{\text{N}}\text{Ar}$ Step By Chiral Shift NMR

The $\text{S}_{\text{N}}\text{Ar}$ step between **11** and **87** used a weak base, NaHCO_3 , so was reasoned less likely for this step to cause epimerisation. The racemic intermediate of **88** was compared to the presumed (*R*)-enantiomer of **88** using chiral shift NMR (Figure 90). The addition of $\text{Eu}(\text{hfc})_3$ caused splitting of the racemic intermediate **88** peaks as observed by the aromatic proton, however the (*R*)-enantiomer did not see splitting. Therefore the $\text{S}_{\text{N}}\text{Ar}$ and also the previous reductive amination step had not caused epimerisation at the α -position to the carbonyl.

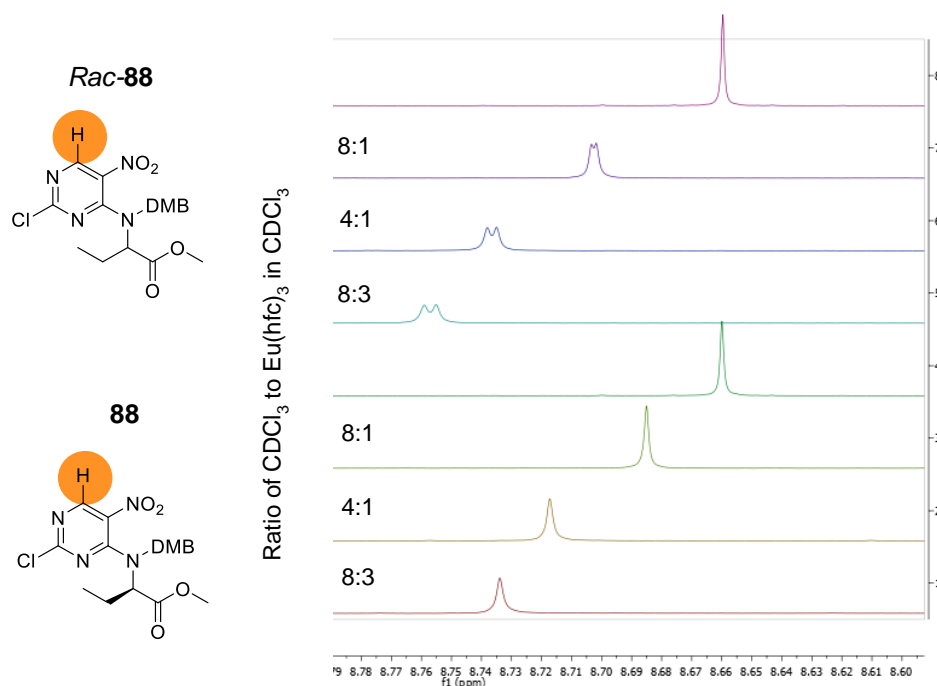


Figure 90. Chiral shift NMR of **88**, comparing the racemate and presumed single enantiomer intermediates after increasing addition of $\text{Eu}(\text{hfc})_3$ (0.015 M). Zoomed in to look at the singlet aromatic proton peak (8.8 – 8.6 ppm).

5.3.2 Checking the Methylation Step By Chiral Shift NMR

The methylation step was a previous cause of concern when the synthesis was previously checked for epimerisation (**3.2.2**). Sodium hydride is a strong base and is likely able to deprotonate the α -carbon causing epimerisation. Deprotonation of the α -carbon was previously achieved with strong bases *n*-BuLi and LiHMDS for the synthesis of analogues **14a** and **14b** with disubstitution at this position (Scheme 5). Chiral shift NMR revealed the presumed (*R*)-enantiomer **86** had epimerised with the single aromatic peak splitting into the two enantiomers, despite using the same reaction conditions in the previous synthesis which did not epimerise (Figure 91). A plausible reason for epimerisation not occurring during the previous synthesis of **86** could be due to the quality of the sodium hydride being poor, with partial quenching to sodium hydroxide. As a weaker base compared to sodium hydride, sodium hydroxide may not cause epimerisation and hence a higher enantiomeric ratio was achieved. Following this result, I conducted optimisation of the methylation step (see **5.4.2**).

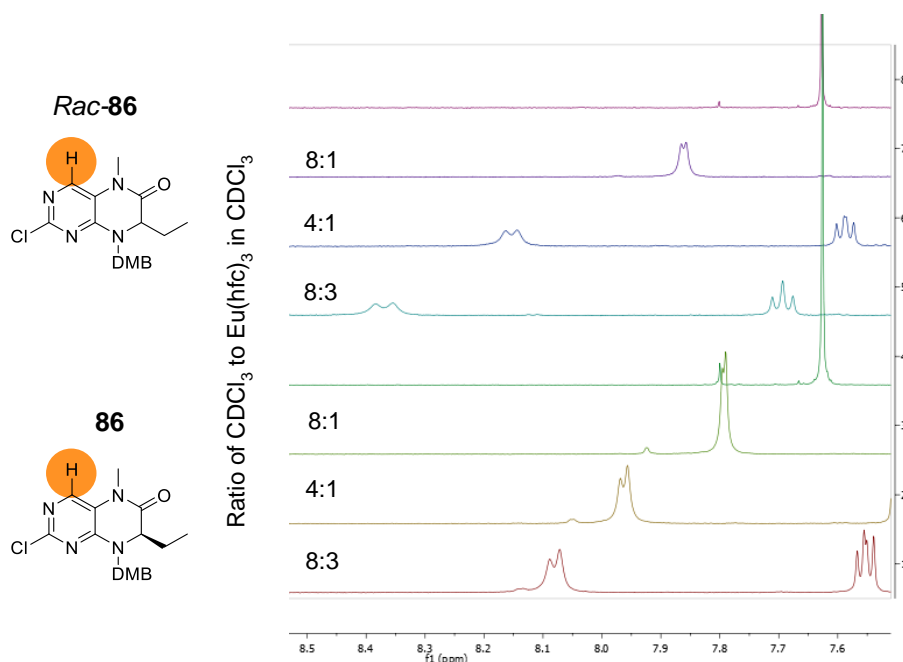


Figure 91. Chiral shift NMR of **86**, comparing the racemate and presumed single enantiomer intermediates after increasing addition of $\text{Eu}(\text{hfc})_3$ (0.015 M). Zoomed in to look at the singlet aromatic proton peak (8.5 – 7.6 ppm).

5.3.3 Checking the TFA Deprotection Step By Chiral Shift NMR

Strong acid is also known to cause epimerisation of chiral centres thus it was important to check the deprotection step using TFA. As the batch of **86** synthesised in Figure 91 had epimerised, I used a previous enantiopure batch of **86** for deprotection, in particular the batch used for synthesis of enantiopure **90aj**. Comparing the racemate of **79** and the presumed (*R*)-enantiomer, addition of $\text{Eu}(\text{hfc})_3$ caused splitting of the racemate as observed by the aromatic proton (Figure 92). However addition of $\text{Eu}(\text{hfc})_3$ to the (*R*)-enantiomer did not cause splitting and so the deprotection of the DMB group using TFA had not caused epimerisation.

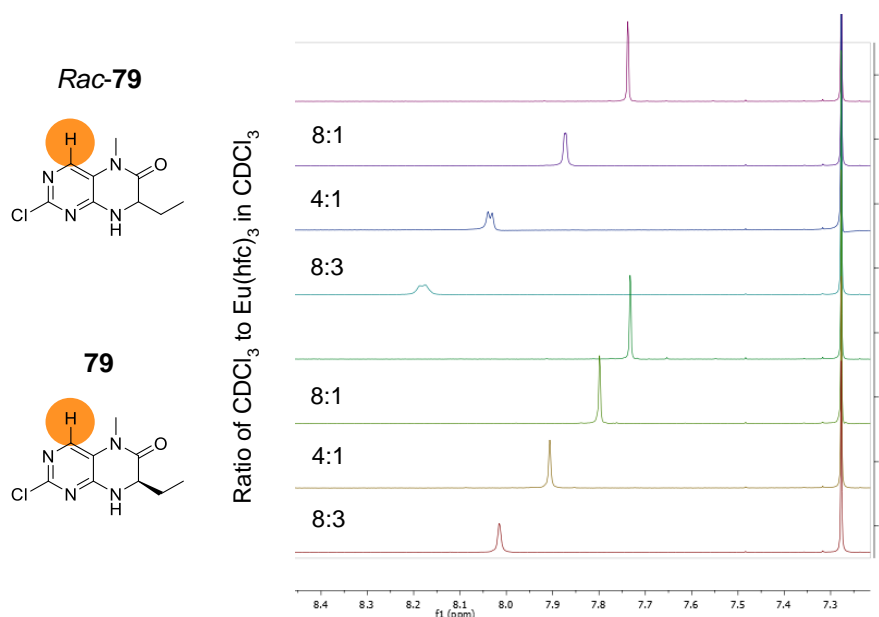


Figure 92. Chiral shift NMR of **79**, comparing the racemate and presumed single enantiomer intermediates after increasing addition of $\text{Eu}(\text{hfc})_3$ (0.015 M). Zoomed in to look at the singlet aromatic proton peak (8.5 – 7.6 ppm).

5.4 Optimisation of Methylation Step

5.4.1 HPLC Method

With the methylation step identified as the cause for epimerisation during the synthesis, I sought to optimise this step to prevent epimerisation. At this point I decided to check if a HPLC method could be developed to measure the enantiomeric ratio of intermediate **86**. Although chiral shift NMR had been previously used, determining an enantiomeric ratio using chiral shift NMR requires the enantiomeric peaks to split completely. This can be difficult to achieve due to broadening of the signals by the europium reagent and limited sensitivity by NMR. Therefore I wanted a more robust method that offered quantitative measurement for the level of epimerisation.

A HPLC method was developed by Reach Separations using a Lux i-Cellulose-5 column with a MeOH eluent (Figure 93). An equivalent column available in-house (CHIRALPAK IC®) also using MeOH as the eluent showed a similar 2 minute separation between the enantiomers of **86** and was subsequently used to monitor the methylation step.¹⁹⁴

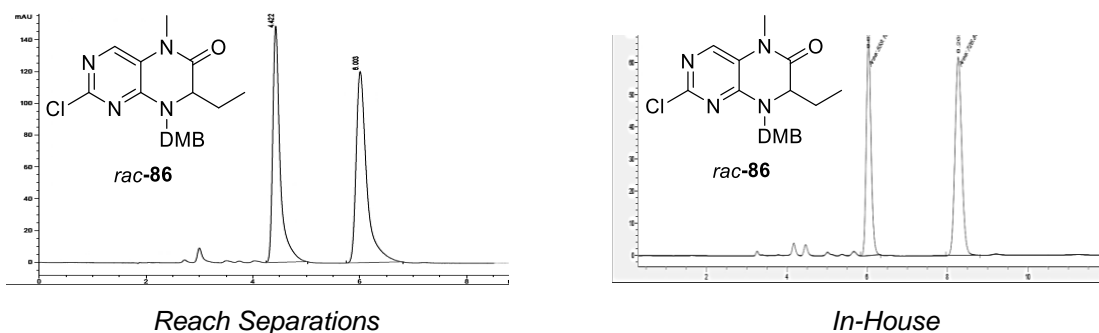


Figure 93. Chiral HPLC trace for *racemic-86* developed by Reach Separations and run in-house.

5.4.2 Optimisation of conditions

To prevent epimerisation during the methylation step, I made several modifications to the synthesis including changing the base, changing the equivalents and switching the order of addition. The products were monitored by the developed chiral HPLC method to determine the enantiomeric ratio (Table 27).

The original conditions for the methylation step used 1.2 equiv. of sodium hydride added at -10°C , after the addition of methyl iodide. I first lowered the equivalents of sodium hydride to lower the chance of additional base deprotonating the α -position of the carbonyl. However using 1 equiv. or 0.9 equiv. also caused complete racemisation.

Next I decided to change the order of addition of the base and electrophile. Adding a slight excess of electrophile first, followed by the base means the deprotonated nucleophile is quickly quenched by the electrophile, whilst adding the base first allows full deprotonation of the nucleophile before the electrophile is added. Switching to the latter approach saw a significant improvement in the enantiomeric ratio to 9:1. Lowering the equivalents of sodium hydride with this swapped order of addition did not see further improvement in the enantiomeric ratio.

I also considered using a weaker base than sodium hydride for the methylation step, in particular potassium carbonate and sodium hydroxide. I chose sodium hydroxide in particular as an older batch of sodium hydride could be partially quenched to sodium hydroxide, so I wanted to confirm what effect this base had. Both potassium carbonate and sodium hydroxide reduced the level of epimerisation to 9:1, the same

ratio observed with changing the order of addition. This implies potassium carbonate and sodium hydroxide are capable of deprotonating the amide, but not the α -position to the carbonyl which has a higher pK_a . No product formation was observed when DIPEA and triethylamine were used.

| | Change | Enantiomeric Ratio |
|--------------------------|--|--------------------|
| Original Conditions | <ul style="list-style-type: none"> 1.2 equiv. NaH 1.2 equiv. MeI added first | 1:1 |
| Change Equivalents | <ul style="list-style-type: none"> 1 equiv. NaH | 1:1 |
| | <ul style="list-style-type: none"> 0.9 equiv NaH | 1:1 |
| Change Order of Addition | <ul style="list-style-type: none"> Add NaH first (1 equiv.) | 9:1 |
| | <ul style="list-style-type: none"> Add NaH first (0.9 equiv.) | 9:1 |
| Change Base | <ul style="list-style-type: none"> K_2CO_3 (1 equiv.) | 9:1 |
| | <ul style="list-style-type: none"> NaOH (1 equiv.) | 9:1 |
| | <ul style="list-style-type: none"> DIPEA (1 equiv.) | No reaction |
| | <ul style="list-style-type: none"> NEt_3 (1 equiv.) | No reaction |

Table 27. Modified conditions to the methylation step with their associated enantiomeric ratio, measured by chiral HPLC (CHIRALPAK IC®, MeOH eluent).

Though several conditions had improved the level of epimerisation, I was intrigued by the fact a weaker base such as potassium carbonate still showed an enantiomeric ratio of 9:1. I decided to check if the HPLC method could be used on the racemate of starting material **89** and hence confirm its enantiopurity prior to the methylation step. The racemic starting material **89** was successfully separated into its enantiomers using the same HPLC method as previously described (Figure 94). Subsequently the batch of starting material **89** used for the optimisation in Table 29 was analysed using chiral HPLC and revealed the compound was in fact a 9:1 mixture of enantiomers. Therefore the compound was already partially epimerised at the start of the methylation step. As the starting amino acid **8a** was conclusively shown to be the single enantiomer, epimerisation was also occurring earlier in the synthesis. Despite using chiral shift NMR to analyse the previous S_NAr and reductive heterocyclisation steps, the chiral shift experiments did not allow for quantitative measurement of the enantiomeric ratio and so the 10% of the (S)-enantiomer could have been missed. Using sodium hydride caused complete racemisation of the compound but using potassium carbonate, sodium hydroxide or changing the order of addition successfully prevented further epimerisation and maintained the 9:1 ratio.

Following this result, I wanted to check what effect the base had on the starting material **89** and product **86** with no electrophile present. Adding excess sodium hydride to the unmethylated starting material **89** resulted in no change to the enantiomeric ratio of 9:1 (Table **28**). However adding excess sodium hydride to the methylated product **86** with a 9:1 e.r. saw full racemisation. This indicates that deprotonation of the α -position to the carbonyl only occurs after the compound is methylated when the α -proton is more acidic.

Table 28. Enantiomeric ratios of **89** and **86** following the sole addition of sodium hydride.

5.5.1 Revisiting the Enantiopurity of Intermediates 6r and 90aj

151

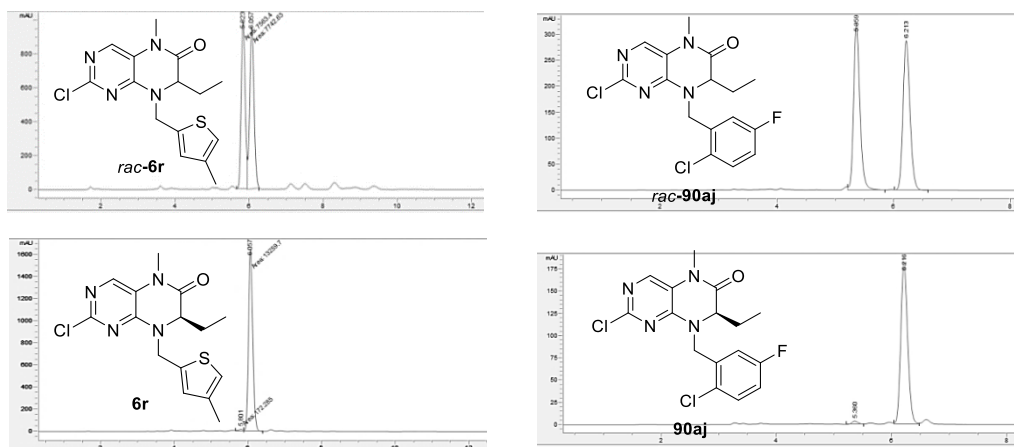


Figure 95. HPLC Traces of **6r** and **90aj** as the racemate and single (*R*)-enantiomer.

5.5.2 Checking the Reductive Heterocyclisation Step By Chiral HPLC

Intermediates **87** and **88** following the reductive amination and S_NAr steps could not be separated using the developed chiral HPLC method. Therefore the only step before the methylation that could be partially checked by chiral HPLC was the reductive heterocyclisation step giving intermediate **89**. This synthetic step usually takes between 24 – 48 hours so this variation in time and exposure to the catalysts may lead to epimerisation. I stirred intermediate **89** with either excess PtO_2 , $VO(acac)_2$ or a combination of the two to see if the 9:1 ratio changed. The results in Figure **96** show the 9:1 ratio was maintained and the catalysts do not cause epimerisation to intermediate **89**.

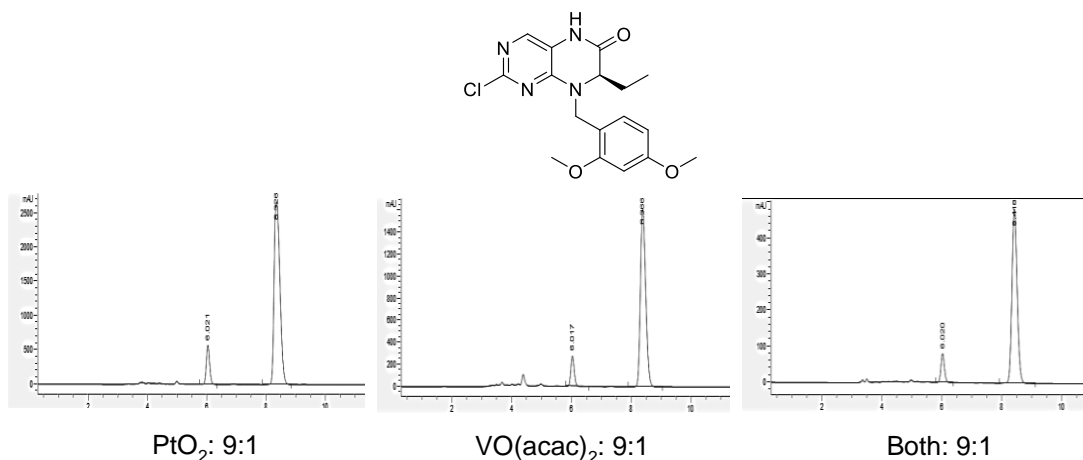


Figure 96. HPLC Traces of **89** following exposure to excess PtO_2 , $VO(acac)_2$ or as a combination.

5.5.3 Checking the TFA Deprotection Step By Chiral HPLC

Next I used chiral HPLC to check the TFA deprotection step. I analysed the starting material **86** and product **79** from the deprotection step to monitor any difference in enantiomeric ratio (Figure 97). As suggested from the chiral shift NMR on the same batch of **79** (5.3.3), the presence of strong acid TFA had not caused epimerisation. The enantiomeric ratio of **79** was 96:4 and resulted in the formation **90aj** in a 98:2 enantiomeric ratio.

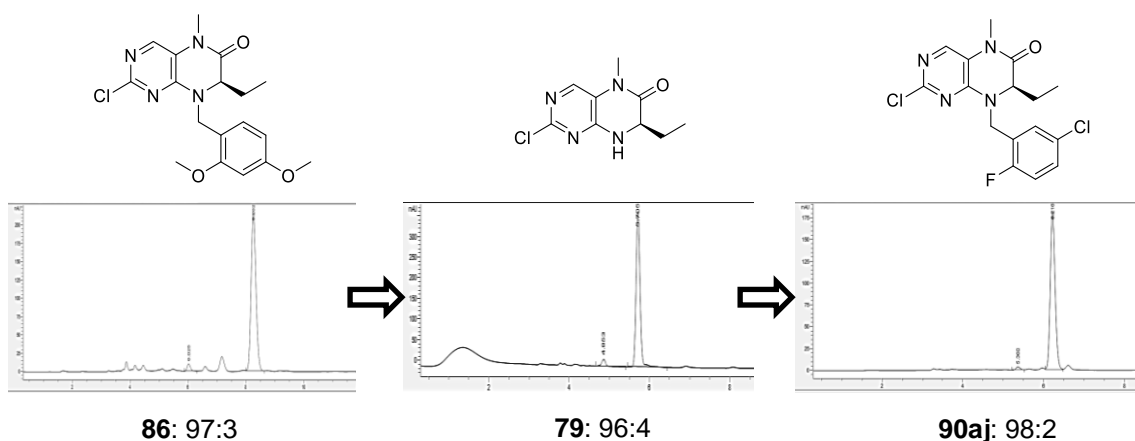
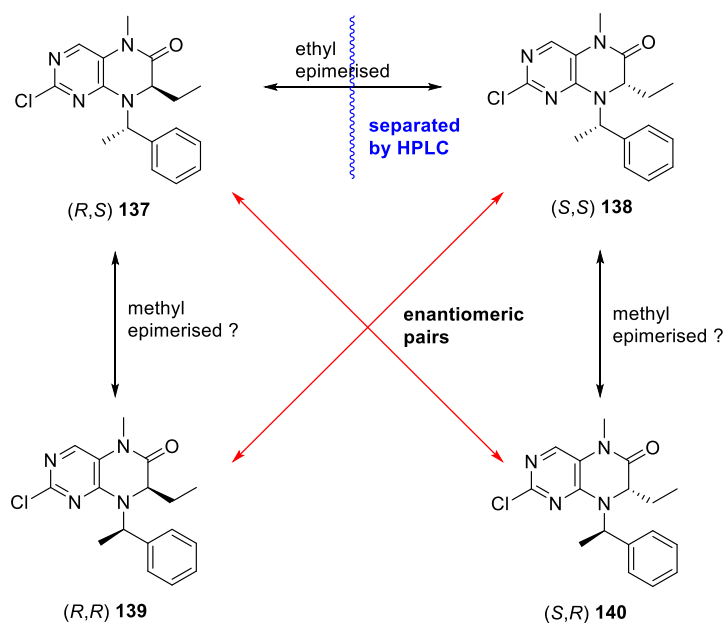


Figure 97. Monitoring the synthesis of **90aj** using chiral HPLC.

5.5.4 Checking the Mitsunobu Step By Chiral HPLC

With a HPLC method developed, I also returned to monitor the Mitsunobu step for epimerisation. As previously discussed using chiral alcohol **136**, two diastereomers **137** and **138** were formed with the epimerised ethyl group (*R*) or (*S*). I wanted to check that the methyl group had not also epimerised in fact forming the four possible diastereomers (Scheme 32). If the methyl group had epimerised, the enantiomer pairs would be present, **137** and **140** and **138** and **139**, following the HPLC separation of diastereomers.



Scheme 32. Four potential diastereomers of **137** resulting from the Mitsunobu reaction.

I used chiral HPLC on the enantiomeric pair (R,S) **137** and (S,R) **140** to confirm if the opposite enantiomer was indeed present following the HPLC separations. A scalemic mixture of **137** and **140** was separated successfully using the previously developed HPLC method (Figure 98) whilst chiral HPLC of **138** and **140** individually showed the intermediates had a high enantiomeric ratio of 99:1 and 98:2. Therefore the methyl group was not epimerising during the Mitsunobu reaction and the product was the single diastereomer and enantiomer.

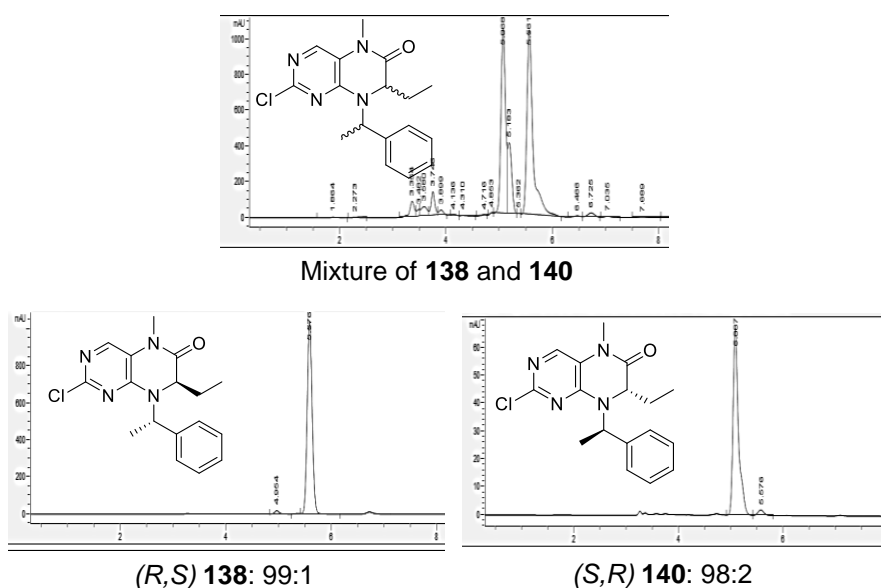
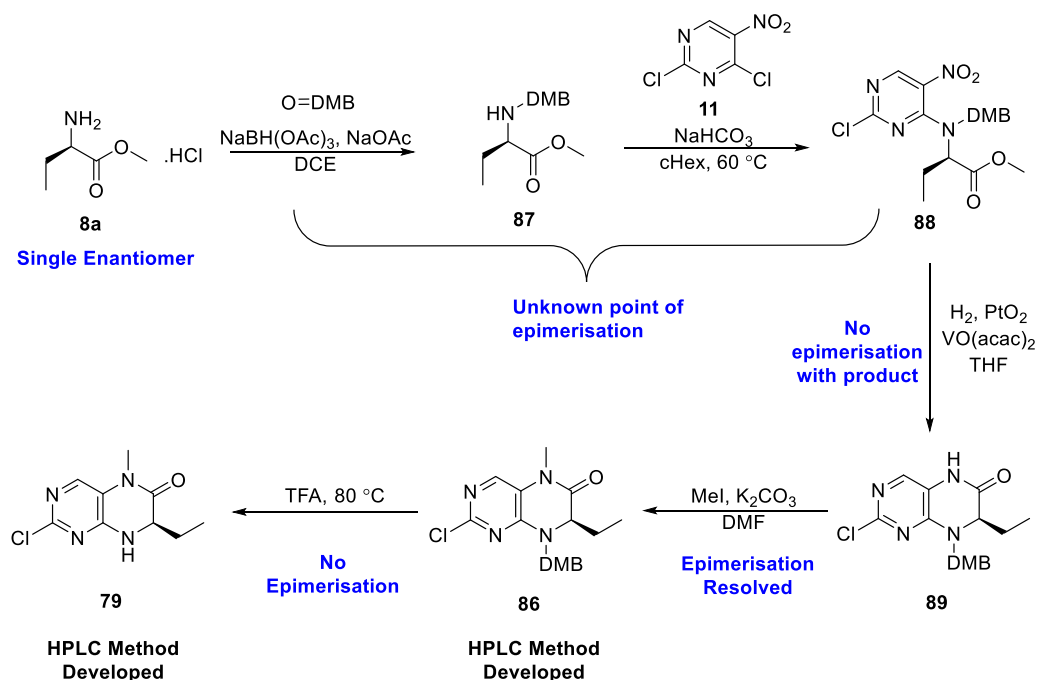


Figure 98. HPLC Traces of **138** and **140** and as a scalemic mixture.

5.6 Conclusions and Solutions

Overall, the α -carbon chiral centre present on the dual ALK-BRD4 series is very susceptible to deprotonation and the chirality of this scaffold needs to be carefully monitored for the development of future analogues in this work and others. I have concluded my findings from the chiral shift NMR and chiral experiments in Scheme 33.

The use of chiral shift NMR and chiral HPLC revealed the methylation and deprotection steps can cause epimerisation of the chiral centre, although not always, due to the presence of strong acid or base. While a solution for epimerisation had been achieved for the methylation step, there was still an unknown factor causing epimerisation before this point. This problem could be resolved by developing chiral HPLC methods for **87** and **88** so every step in the synthesis could then be measured quantitatively for epimerisation. Chiral shift NMR suggested the S_NAr and reductive heterocyclisation steps did not cause epimerisation but a quantitative method, such as chiral HPLC, would conclude this. Although reaction conditions were kept consistent throughout the synthesis of this dual inhibitor series, a slight difference in reaction time or equivalents may make that much of a difference to this susceptible chiral centre.

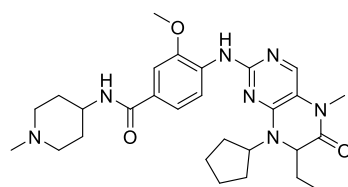


Scheme 33. Conclusions from monitoring the chirality during the synthesis of **79**.

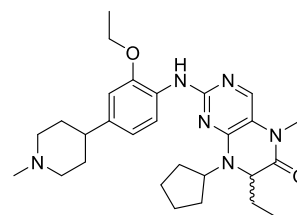
The first solution detailed for preventing epimerisation was changing the base for the methylation step from sodium hydride to potassium carbonate or sodium hydroxide. As a strong base, sodium hydride is able to deprotonate both the amide and α -position to the carbonyl but a weaker base is unable to deprotonate the α -position hence preventing epimerisation. However there was clear evidence that no epimerisation was occurring using sodium hydride in the synthesis of **6r** and **90aj** with enantiomeric ratios of 99:1 and 98:2. This could be due to the quality of the sodium hydride batch being poorer, with partial quenching of the sodium hydride to sodium hydroxide. The reaction can still proceed with sodium hydroxide (Table **27**) and not cause epimerisation so this may explain why certain batches made with sodium hydride see less epimerisation. In addition, sodium hydride is usually dispersed in mineral oil and thus the equivalents added could in fact be less depending on the ratio of sodium hydride to oil. Using a base like potassium carbonate or sodium hydroxide also resolves this problem as they can be weighed out more easily as a powder.

A definitive, but expensive solution to the epimerisation problem is chiral separation of the intermediates. Intermediate **79**, **86** and **89** could all be easily separated using the developed chiral HPLC method. To allow the synthesis of further enantiopure final compounds, I had intermediate **79** chirally separated on 1 g scale by Reach Separations using supercritical fluid chromatography (LuxC4 column, 50:50 MeOH;CO₂ (0.2% v/v NH₃)). Though this did not resolve the problem of where epimerisation is occurring, this did allow for the synthesis and testing of enantiopure final compounds to continue. Importantly all the tested compounds, unless indicated, were chirally pure.

The observed epimerisation of the chiral centre helped explain the differences previously discussed between the reported potencies of the (*R*)- and (*S*)-enantiomers of BI-2536 (see **2.5.3**). Within the dual ALK-BRD4 series, a significant difference in the BRD4 thermal shifts and PLK-1 activity was observed between the (*R*) and (*S*)-enantiomer of BI-2536 as well as for similar analogues **39** and **40** (Table **29**). In comparison, one report in the literature observes equipotent activity between the (*R*)- and (*S*)-enantiomers of BI-2536.¹³¹ This could be due to epimerisation occurring during the synthesis of these molecules hence equipotent potencies. Epimerisation of the chiral centre is not mentioned in these papers with no chiral separations or measurements reported to confirm the enantiopurity of the compounds. This work provides solutions to help prevent and resolve epimerisation in future work with the BI-2536 scaffold.



BI-2536



39/40

| | | (R)-BI-2536 | (S)-BI-2536 | (R)-39 | (S)-40 |
|-----------------------------------|----------------------------------|---------------------|-------------|--------------------|---------|
| Chen <i>et al.</i> ¹³¹ | BRD4 | 56 nM | 54 nM | - | - |
| | PLK-1 | 0.22 nM | 0.42 nM | - | - |
| Liu <i>et al.</i> ¹³² | BRD4 | 205 nM | 489 nM | - | - |
| | PLK-1 | 4 nM | 32.5 nM | - | - |
| Own work | BRD4 T _m Shift [K] | 5.7 | -0.2 | 6.3 | 1.1 |
| | PLK-1* | 80 / 98 (2.6 nM) | 19 / 54 | 40 / 85 (16 nM) | 18 / 18 |

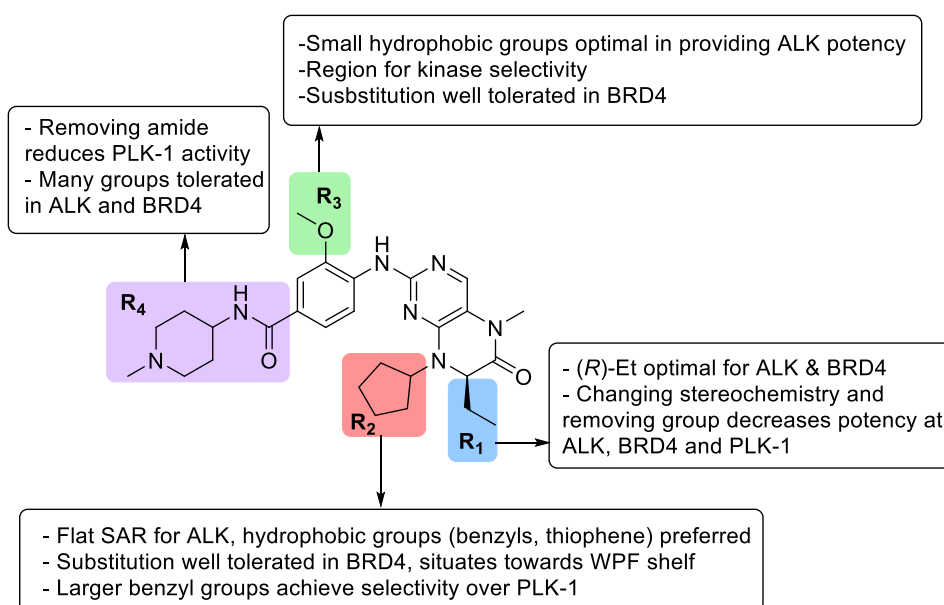
Table 29. Comparing activities of the (R)- and (S)-enantiomers of BI-2536 and **39** and **40**.

*PLK-1 % inhibition at 10 nM and 100 nM

Chapter 6 Conclusions and Future Directions

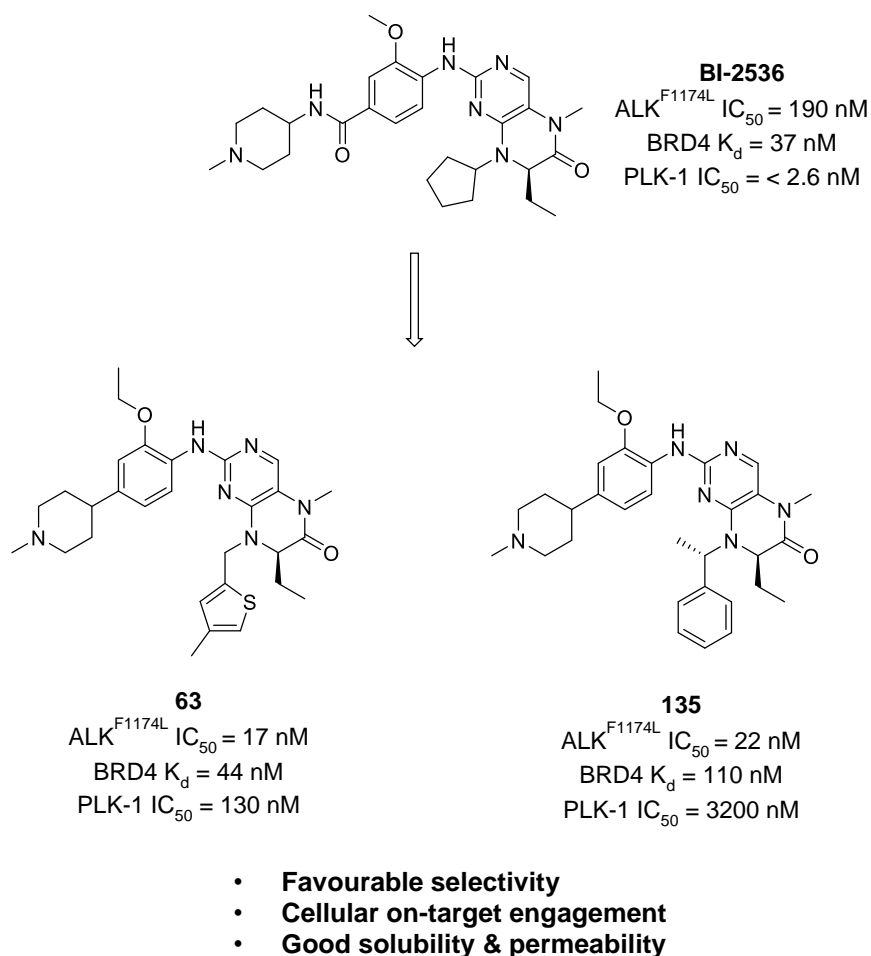
The aim of the project was to design a dual ALK-BRD4 inhibitor to target key oncogenes, ALK and MYCN, in patients with high-risk neuroblastoma. The starting point of the project was dual PLK-1-BRD4 inhibitor BI-2536 which showed moderate activity and selectivity towards ALK compared to the majority of the kinome. Using structure based design I redesigned the series towards compounds with a dual ALK-BRD4 profile by improving ALK activity, greatly reducing PLK-1 activity whilst maintaining BRD4 potency and overall kinome selectivity. A summary of the four areas chosen for modification is shown in Scheme 34.

The R₁ region did not tolerate much change with the (*R*)-ethyl optimal for achieving ALK and BRD4 potency whilst the R₃ region was limited to small hydrophobic groups in providing ALK potency. The presence of the alkoxy group was important in achieving kinase selectivity as demonstrated by the favourable kinase selectivity of **63** (Figure 69). For the R₄ region, the initial hypothesis was to remove the amide to remove polar interactions with the PLK-1 pocket. This was achieved with compound **35** whilst maintaining ALK and BRD4 potency. Different solvent channel groups were well tolerated in ALK and BRD4 which prompted for this region to be chosen for improving the physicochemical properties of the series.



Scheme 34. SAR of BI-2536 for modifying ALK, BRD4 and PLK-1 activity.

The main area for modification I focused on was the R₂ region due to the hypothesis that the more restricted PLK-1 pocket would be less tolerant to substitution compared to the more open ALK structure. Due to ALK crystallography not being available a systematic design and testing approach was taken and I developed a new synthetic route (Scheme 15) to allow for a more efficient installation of groups at the R₂ position. Epimerisation of the ethyl chiral centre during the methylation step of the synthesis was prevented by switching to a weaker base and chiral separation conditions were identified to ensure the compounds synthesised were enantiopure. Overall ALK SAR was quite flat at this position and proved difficult to achieve gains in potency, especially without structural information of the series in ALK. However an approximately 10-fold improvement in ALK^{F1174L} activity from BI-2536 was achieved with **6r** and **135** showing improvements in potency can be made in this region with the right substitution (Scheme 35). Compound **135** also showed 150-fold selectivity towards ALK^{F1174L} over PLK-1 as a result of PLK-1 being less tolerant to substitution at the R₂ position.



Scheme 35. Development of dual ALK-BRD4 inhibitors **63** and **135** from BI-2536.

A major drawback for the project was the lack of structural information on how the series would bind in ALK and being unable to do iterative X-ray driven structure based design. Attempts for co-crystallography in ALK were unsuccessful due to difficulties with protein production and purification and the modest activity of earlier analogues. Without a co-crystal of the dual ALK-BRD4 series in ALK, the binding pose was not confirmed and so the position of substituents in the binding pocket was unknown. This made it difficult to know what groups would cause a gain in potency and rationalise the SAR. Despite the lack of X-ray, a 10 – 15-fold improvement in ALK activity was achieved with a series of analogues modifying the R₂ region including lead compounds **63** and **135**, as well as **150** and **151**. The improvement in ALK activity was achieved whilst importantly maintaining BRD4 activity and lowering PLK-1 activity.

Docking was used to predict the binding mode of the series in ALK and decide which groups were suitable for SAR exploration. However in general, docking did not match the observed SAR. For example, larger alkoxy groups were predicted to be tolerated at the R₃ position but in fact decreased potency and the docking predicted no suitable docking poses for the most potent benzyl diastereomer **135**. Future work for the project would be to focus on establishing ALK crystallography to post rationalise changes made and rationalise future changes to improve ALK potency. Compounds with a further 10-fold improvement in ALK potency, and maintained BRD4 potency, would allow for a more direct comparison to current ALK inhibitors and test the potential benefits of dual ALK and BRD4 inhibition.

One key challenge of designing and developing a dual inhibitor is managing the multiple target potencies, especially in this case for two structurally different protein families. Modifications to certain areas which may have led to an improvement in kinase potency, such as the methyl substituent and (*R*)-ethyl group, had to remain untouched due to loss of BRD4 activity. In addition for this project, I had to monitor not only ALK and BRD4 potency but also the remaining PLK-1 activity. BI-2536 is a very potent PLK-1 inhibitor and excellent progress was made in reducing PLK-1 activity, >1200-fold with **135**, whilst controlling the ALK and BRD4 activity. The R₂ position proved to be a useful modification for achieving kinase selectivity towards ALK over PLK-1, without losing BRD4 activity. Importantly compound **63** showed selectivity over PLK-1 in cells underlining the design effort to change the kinase selectivity from PLK-1 to ALK.

Related to this challenge is not only ensuring potent inhibition of ALK and BRD4 but also selectivity within both protein families, kinase and bromodomains. Pleasingly the kinome and bromodomain screens for **63** showed the compound was relatively selective across both protein-families, addressing a key issue with cross-family dual inhibitors. Important to this progress was maintaining the alkoxy group that is not tolerated in the majority of kinases. For future work, it would be interesting to see the broader kinase selectivity of **135** which was more selective towards ALK over PLK-1 compared to **63**, as well as a full kinome scan of **63** to identify any further kinase hits.

With the dual ALK-BRD4 series I was aware of the high lipophilicity of key compounds **62**, **63** and **135**. Initial efforts were taken to reduce the clogP by modifying the solvent channel region. With compounds **158**, **164** and **165**, removing the methyl on the piperidine lowered the clogP and improved ALK^{F1174L} potency however the compounds showed high efflux by PGP. Due to its potent ALK and BRD4 activity, cellular on-target engagement and best overall physicochemical properties, compound **63** has been chosen for initial PK studies. Though the compounds are surprisingly soluble for highly lipophilic compounds, the high lipophilicity may have a greater effect on its PK properties such as low bioavailability resulting from high clearance. Many other solubilising groups could be tried at the solvent channel region as well as modifying other lipophilic groups on the scaffold such as the R₂ and R₃ positions.

Overall, the project met the first hypothesis of designing a dual ALK-BRD4 inhibitor and has resulted in a series of suitable *in vitro* tool compounds. I successfully tuned the kinase activity of BI-2536 to a kinase-bromodomain combination for a specific disease hypothesis: targeting the two key drivers of neuroblastoma, ALK and MYCN. Key compound **63** demonstrated on-target engagement of ALK and BRD4 in cellular assays and favourable kinase and bromodomain selectivity, as well as good solubility and permeability (Scheme **35**). The dual ALK-BRD4 inhibitors will be used in further *in vitro* experiments to test the second part of the hypothesis of the dual inhibitor being beneficial compared to single agents and combination treatments.

Chapter 7 Experimental

7.1 LanthaScreen® Binding Assay

ALK, ALK^{F1174L} and ALK^{R1275Q} activity were measured in a LanthaScreen® Eu kinase binding assay. The assay was performed in 384-well plates containing either ALK, ALK^{F1174L} or ALK^{R1275Q} enzyme (5 nM, Carna Biosciences), Kinase Tracer 236 (30 nM, Thermo Fisher Scientific), LanthaScreen® Eu-anti-GST antibody (2 nM, Thermo Fisher Scientific), either 1% (v/v) DMSO or the test compound (in the range from 0.5 nM to 100 µM in 1% (v/v) DMSO), and assay buffer (50 mM HEPES pH 7.5, 10 mM MgCl₂, 1 mM EGTA and 0.01% (w/v) Brij-35, 1 mM DTT). The reaction was incubated for 60 mins at room temperature. The plate was read on an EnVision multilabel plate reader (Perkin Elmer, UK) calculating an emission ratio between the acceptor/tracer emission (665 nM) and the antibody/donor emission (615 nM). IC₅₀ values were determined using a non-linear regression fit of the log(inhibitor concentration) versus emission ratio with variable slope equation.

7.2 ALK MSD Phosphorylation Assay¹⁶⁷

Protein Samples: The human neuroblastoma Kelly or NBLW-R cell line was maintained in RPMI media with 10% FCS. For dose-response experiments, cells were seeded into 10 cm dishes and following attachment, treated with the indicated compound concentration in fresh media. After 3 hrs, the plates were transferred onto ice, the media taken off and the cells washed once with ice-cold PBS, before adding 5% CHAPS lysis buffer. After 20 mins in lysis buffer, cells were scraped, transferred into eppendorfs and spun at 4 °C for 12 mins at 12,000 rpm. The supernatant was transferred to a fresh tube and the protein content was quantified using the Direct Detect system (Millipore). *Performed by Lizzie Tucker.*

ALK immunoassay analysis: Multiarray 96-well plates (Meso Scale Discovery) were coated overnight at 4 °C with 25 µL of mouse total ALK antibody (Clone 31F12; Cell Signaling Technology Inc.) diluted in PBS buffer (11 µL in 3 mL of buffer). Plates were washed X 3 in wash buffer (0.1% Tween 20 in Tris-buffered saline) and incubated for 1 hr with blocking buffer (5% BSA in wash buffer). After washing, 15 µg of protein

samples in CHAPS Buffer (total volume 25 – 30 μL per well) were added in duplicate and incubated overnight at 4 °C. After washing, the plates were incubated for 1 hr with either 0.4 $\mu\text{g.mL}^{-1}$ total ALK D5F3 or pY1586 ALK 3B4, washed and incubated for a further 1 hr with 0.5 $\mu\text{g.mL}^{-1}$ anti-rabbit SULFO-tag antibody. The plates were washed, 2 X Read Buffer (Meso Scale Discovery) were added to wells, and electrochemiluminescence counts were made using a MSD SECTOR Imager 6000. IC_{50} values were determined using a non-linear regression fit of the log(inhibitor concentration) versus % DMSO treated control. *Performed by Lizzie Tucker or myself.*

7.3 Kinetic Solubility by NMR

Solubility samples were prepared by adding 171 μL of PBS buffer (pH 7.4) to 9 μL of 10 mM DMSO stock of compound in a 384-deep well plate, giving a final concentration of 500 μM with 5% DMSO. The plate is centrifuged for 1 min at 1000 rpm and incubated for 20 hours. The plate is again centrifuged for 1 min at 1000 rpm and the solubility samples transferred from the plate to 3 mm NMR tubes using the Gilson-GX281 liquid handler.

All data was acquired and processed using Bruker Topspin 4.0. The quantitative ^1H -NMR spectrum (@qHNMR3_bua) were acquired using an in-house 1D pulse sequence lc1pngppsf2 with 32 scans. The sweep width was 6.2 ppm, and the FID contained 16k time-domain data points. Relaxation delay was set to 20 sec. The ^1H spectrum of the samples were referenced to the internal deuterated solvent and acquired at a temperature of 298 K. The NMR data was processed using MestReNova.

7.4 Docking with Glide

Docking studies were performed using Glide, Schrödinger, LLC, New York, NY, 2018. Preparation of protein structures ALK using PDB code 2XB7, BRD4 using PDB code 4OGI and PLK-1 using PDB code 2RKU were performed using Schrödinger Suite 2018-3 Protein Preparation Wizard; Epik, Schrödinger, LLC, New York, NY, 2018 and preparation of ligands were performed using LigPrep, Schrödinger, LLC, New York, NY, 2018.

Crystal structures and docking images were prepared using The PyMOL Molecular Graphics System, Version 2.0 Schrödinger, LLC.

7.5 Conformational Analysis

Conformational searches were performed using a stochastic search and an Energy window of 7 kcal/mol in Molecular Operating Environment (MOE), Version MOE 2019.0101, Chemical Computing Group ULC, 2019. Conformations were analysed using the dihedral profiles generated in MOE, using the Torsion Profile application, and Mogul Analysis, Version 1.8.2, Cambridge Crystallographic Data Centre, Cambridge, UK, 2019.

7.6 General Synthetic Experimental

All anhydrous solvents and reagents were obtained from commercial suppliers (Acros, Alfa Aesar, Apollo, Fisher Scientific, Fluorochem, Sigma Aldrich, Thermo Scientific and VWR) and used without further purification. All reactions were carried out under a positive pressure of N₂ and moisture sensitive reagents transferred via syringe. All compounds reported at >95% purity unless stated.

Analytical thin layer chromatography (TLC) was performed on pre-coated aluminium sheets (60 F₂₄₅ nm, Merck) and visualised by short-wave UV light. Semi-automated flash column chromatography was carried out using a Biotage SP4 purification system, using Biotage SNAP KP-Si cartridges. Semi-preparative separations were carried out using a 1200 Series Preparative HPLC over a 15 minute gradient elution (Grad15min20mls.m) from 90:10 to 0:100 water:methanol (both modified with 0.1% formic acid) at a flow rate of 20 mL/min. For diastereomer separations a 15-minute gradient elution from 60:40 to 75:25 water:methanol (both modified with 0.1% formic acid). For chiral HPLC, separations were carried out using an Agilent 1260 Series UHPLC over a 12 minute gradient elution with 100% methanol and the CHIRALPAK IC® column.

All microwave reactions were performed using Biotage Initiator Microwave Synthesizer. Melting points were determined on a Stanford Research EZ-melt apparatus and are uncorrected. IR analyses were carried out on a Bruker Alpha-P FT-IR spectrometer and absorptions are specified in wavenumbers (cm⁻¹). Optical

rotations were recorded on a Bellingham & Stanley Ltd. ADP440 Polarimeter with a path length of 0.1 dm, using a light emitting diode with interference filter (298 nm). Concentrations (*c*) are quoted in g/100mL.

¹H NMR spectra were recorded on a Bruker AMX 500 (500 MHz) spectrometer using an internal deuterium lock. Chemical shifts were measured in parts per million (ppm) relative to tetramethylsilane ($\delta = 0$) using the follow residual solvent signals: CDCl₃ (δ_{H} 7.26) and CD₃OD (δ_{H} 3.32). Data are presented in the following format: chemical shift (integration, multiplicity, coupling constants (*J*) in Hz, assignment). Coupling constants, *J*, are measured to the nearest 0.1 Hz, Atom numbering is arbitrary and does not refer to IUPAC nomenclature.

¹³C NMR spectra were recorded at 126 MHz on a Bruker AMX 500 (500 MHz) spectrometer using an internal deuterium lock. Chemical shifts were measured in parts per million (ppm) relative to tetramethylsilane ($\delta = 0$) using the following residual solvent signals: CDCl₃ (δ_{C} 77.2) and CD₃OD (δ_{C} 49.0). Data are presented in the following format: chemical shift (assignment) and for selected signals, multiplicities were assigned. Chemical shifts are quoted to 0.1 ppm. Atom numbering is arbitrary and does not refer to IUPAC nomenclature.

¹⁹F NMR were recorded at 471 MHz on a Bruker AMX 500 (500 MHz) spectrometer using an internal deuterium lock. Chemical shifts were measured in parts per million (ppm) relative to tetramethylsilane ($\delta = 0$). Data are presented in the following format: chemical shift (multiplicity, coupling constants (*J*) in Hz). Coupling constants *J* are measured to the nearest 1 Hz.

LCMS and HRMS analyses were performed on an Agilent 1200 series HPLC and diode array detector coupled to a 6120 time of flight mass spectrometer with dual multimode APCI/ESI source. Samples were supplied at approximately 1 mg/mL solutions in MeOH with 0.5-10 μ L injected on a partial loop fill. For standard LCMS, analytical separation was carried out at 40 °C on a Merck Chromolith Flash column (RP-18e, 25 x 2 mm) using a flow rate of 1.5 mL/min in a 2 minute gradient elution with detection at 254 nm. The mobile phase was a mixture of methanol (solvent A) and water containing formic acid at 0.1% (solvent B). Gradient elution was as follows: 5:95 (A/B) to 100:0 (A/B) over 1.25 min, 100:0 (A/B) for 0.5 min, and then reversion back to 5:95 (A/B) over 0.05 min, finally 5:95 (A/B) for 0.2 min. For HRMS and extended LCMS, Analytical separation was carried out at 30 °C on a Merck Chromolith Flash column (RP-18e, 25 x 2 mm) using a flow rate of 0.75 mL/min in a 4 minute gradient elution with detection at 254 nm. The mobile phase was a mixture of methanol (solvent A) and water containing formic acid at 0.1% (solvent B). Gradient

elution was as follows: 5:95 (A/B) to 100:0 (A/B) over 2.5 min, 100:0 (A/B) for 1 min, and then reversion back to 5:95 (A/B) over 0.1 min, finally 5:95 (A/B) for 0.4 min. HRMS references: caffeine $[M+H]^+$ 195.08765; hexakis (2,2-difluoroethoxy)phosphazene $[M+H]^+$ 622.02896; and hexakis(1H,1H,3H-tetrafluoropnetoxy)phosphazene $[M+H]^+$ 922.00980.

7.7 General Methods

General Method 1 – Methyl ester formation

A carboxylic acid (1 equiv.) was suspended in MeOH (0.1 M) and SOCl_2 (2 equiv.) was added dropwise at 0 °C. The reaction was heated at reflux for 4 – 5 h during which time LCMS analysis revealed the progress of the reaction. Upon its completion the volatiles were removed *in vacuo* and the residue was triturated with diethyl ether. The resulting solid was filtered and dried *in vacuo* to afford the title compound.

General Method 2 – Reductive amination

Methyl 2-aminobutanoate (1 equiv.) and the relevant aldehyde or ketone (0.8 – 1 equiv.) were dissolved in DCE (0.1 M). The reaction was cooled to 0 °C and NaOAc (1 equiv.) and $\text{NaBH}(\text{OAc})_3$ (1.6 equiv.) were added. The reaction was stirred at rt for 16 – 20 h during which time LCMS analysis revealed the progress of the reaction. Upon completion, sat. aq. NaHCO_3 was added and the aqueous phase extracted with CH_2Cl_2 (X2). The combined organic phases were washed with water, dried over MgSO_4 , filtered and concentrated *in vacuo* to afford the title compound.

General Method 3 – $\text{S}_\text{N}\text{Ar}$

An amine (1 equiv.) and sodium bicarbonate (4 equiv.) were dissolved in cyclohexane (0.1 M) and stirred for 30 mins. 2,4-Dichloro-5-nitropyrimidine **11** (1.1 equiv.) was added and the reaction stirred at 60 °C for 16 – 20 h during which time LCMS analysis revealed the progress of the reaction. Upon completion, the reaction mixture was filtered, washed with CH_2Cl_2 and concentrated *in vacuo*. The residue was purified by column chromatography (cHex/EtOAc 0 – 20%) to afford the title compound.

General Method 4 – Iron reduction and cyclisation

A nitro compound (1 equiv.) was dissolved in glacial acetic acid (0.4 M) and the mixture heated to 70 °C. Iron powder (1.2 equiv.) was added portionwise over 5 mins and the reaction stirred for 6 h during which time LCMS analysis revealed the progress of the reaction. Upon completion, the mixture was filtered through Celite,

washing through with MeOH and concentrated *in vacuo*. The residue was purified by column chromatography (cHex/EtOAc 0 – 30%) to afford the title compound.

General Method 5 – Methylation

A pteridinone (1 equiv.) was dissolved in DMF (0.1 M), methyl iodide (1 - 1.3 equiv.) added and the mixture cooled to –10 °C. Sodium hydride (1.2 equiv.) was added and the reaction stirred at rt for 16 – 20 h during which time LCMS analysis revealed the progress of the reaction. Upon completion, ice was added and the aqueous phase extracted with EtOAc (X3). The combined organic phases were washed with water (X2), dried over MgSO₄, filtered and concentrated *in vacuo*. The residue was purified by flash column chromatography (cHex:EtOAc 0 – 20%) to afford the title compound.

General Method 6 – Alkylation

Methyl 3-hydroxy-4-nitrobenzoate, HCl (1 equiv.) was dissolved in DMF (0.1 M). Potassium carbonate (5 equiv.) and an alkyl halide (1.4 equiv.) were added and the reaction stirred at 50 °C for 16 – 20 h during which time LCMS analysis revealed the progress of the reaction. Upon completion, EtOAc was added and the mixture washed with water (X2) and brine (X1), dried over MgSO₄, filtered and solvent removed *in vacuo*. The residue was purified by column chromatography (cHex/EtOAc 0-20%) to afford the title compound.

General Method 7 – Hydroxylation

An alkoxy-nitrobenzoate (1 equiv.) was dissolved in a solvent mixture of THF:H₂O, (1:1, 0.1 M). LiOH (10 equiv.) was added and the reaction stirred at rt for 16 – 20 h during which time LCMS analysis revealed the progress of the reaction. Upon completion, the aqueous layer was acidified to pH 1 with 1 M HCl and extracted with EtOAc (X3). The combined organic phases were dried over MgSO₄, filtered and concentrated *in vacuo* to afford the title compound.

General Method 8 – Amide formation

An alkoxy-nitrobenzoic acid (1 equiv.) was dissolved in DMF (0.1 M). HBTU (1.6 equiv.), triethylamine (2 equiv.) and 1-methylpiperidin-4-amine (1 equiv.) were added sequentially and the reaction stirred at rt for 16 – 20 h during which time LCMS analysis revealed the progress of the reaction. Upon completion, the reaction mixture was partitioned between EtOAc and water and the aqueous layer extracted with EtOAc (X2). The organic phases were combined, dried over MgSO₄, filtered and solvent removed *in vacuo*. The residue was purified by column chromatography (CH₂Cl₂/MeOH 0-15%) to afford the title compound.

General Method 9 – Tin mediated nitro reduction

A nitro compound (1 equiv.) was dissolved in a solvent mixture of EtOAc:EtOH, (10:3, 0.1 M). Tin(II) chloride dihydrate (5 equiv.) was added and the reaction stirred at 50 °C for 16 – 20 h during which time LCMS analysis revealed the progress of the reaction. Upon completion, sat. aq. NaHCO₃ was added and the reaction mixture partitioned between NaHCO₃ and EtOAc. The aqueous layer was extracted with further EtOAc (X2) and the combined organic phases dried over MgSO₄, filtered and concentrated *in vacuo* to afford the title compound.

General Method 10 – Alkylation

Amine (1 equiv.) was dissolved in DMF (0.1 M). Potassium carbonate (1.2 equiv.) and 4-fluoro-2-methoxy-1-nitrobenzene (1 equiv.) were added and the reaction stirred at 70 °C for 16 – 20 h during which time LCMS analysis revealed the progress of the reaction. Upon completion, the reaction was cooled and concentrated *in vacuo* and the residue partitioned between EtOAc and brine. The aqueous phase was extracted with EtOAc (X3) and the combined organic phases were dried over MgSO₄, filtered and concentrated *in vacuo*. The residue was purified by column chromatography (CH₂Cl₂/MeOH 0 – 10%) to afford the title compound.

General Method 11 – Transfer Hydrogenation

To a microwave vial with a nitro compound (1 equiv.) in MeOH (0.15 M) was added 10% Pd.C (0.1 equiv.) and ammonium formate (6 equiv.) The reaction vial was flushed with N₂ and stirred for 16 – 20 h at rt during which time LCMS analysis revealed the progress of the reaction. Upon completion the catalyst was filtered through celite and the filtrate concentrated *in vacuo*. The residue was purified by Biotage column chromatography (CH₂Cl₂:MeOH 0 – 20%) to afford the title compound.

General Method 12 – Suzuki Cross-Coupling

An alkoxy-nitrobenzene (1 eq), pyridine-4-ylboronic acid (1 equiv.) Na₂CO₃ (1.6 equiv.) and Pd(PPh₃)₂Cl₂ (0.03 eq.) were dissolved in a solvent mixture of 1,4-dioxane:water. (6:1, 0.38 M) and heated at 120 °C for 30 mins under microwave irradiation. Upon completion the mixture was diluted with EtOAc and water and the aqueous phase extracted with EtOAc (X3). The organic phases were combined, dried over MgSO₄, filtered and concentrated *in vacuo*. The residue was purified by Biotage column chromatography (CH₂Cl₂/MeOH, 0 – 10%) to afford the title compound.

General Method 13 – Pyridine Methylation

A nitrophenyl pyridine (1.equiv.) and methyl iodide (3.5 equiv.) were dissolved in acetonitrile (0.1 M) and the reaction heated for 4 h at 50 °C during which time LCMS analysis revealed the progress of the reaction. Upon completion the mixture was concentrated *in vacuo* to afford the title compound.

General Method 14 – NaBH₄ reduction

A pyridinium iodide (1 equiv.) was dissolved in MeOH (0.05 M) and cooled to 0 °C. NaBH₄ (10 equiv.) was added portionwise. The reaction was allowed to warm to rt and stirred for 2 h during which time LCMS analysis revealed the progress of the reaction. The reaction was quenched with 1 M HCl and MeOH partially removed *in vacuo*. The residue was partitioned between EtOAc and 1 M NaOH until pH 12 was reached. The EtOAc layer was washed with 1 M NaOH, dried over MgSO₄, filtered and concentrated *in vacuo* to give the title compound.

General Method 15 – Pt/H Reduction

Tetrahydropyridine (1 equiv.) and PtO₂ (0.3 equiv.) were dissolved in acetic acid (0.03 M) and the mixture purged with N₂. The mixture was placed under 50 psi of H₂ gas at rt for 16 h. The mixture was filtered through celite, washed with MeOH and concentrated *in vacuo*. The residue was purified by Biotage column chromatography (CH₂Cl₂/MeOH, 0 – 10%) to afford the title compound.

General Method 16 – HCl assisted S_NAr

Dihydropteridinone (1 equiv.) and an amine (0.9 – 1 equiv.) were dissolved in solvent mixture dioxane/EtOH/water, (1:1:1, 0.1 M). Concentrated HCl (2.1 equiv.) was added and the reaction mixture refluxed for 24 – 72 h during which time LCMS analysis revealed the progress of the reaction. Upon completion, the reaction mixture was partitioned between EtOAc and NaOH (1 M) and the aqueous layer extracted with further EtOAc (X2). The organic phases were combined, dried over MgSO₄ and concentrated *in vacuo*. The residue was purified by Biotage column chromatography (CH₂Cl₂:20% methanoic ammonia in CH₂Cl₂ 0 – 40%) and reverse phase column chromatography (Water:MeOH 0 – 100%) to afford the title compound.

General Method 17 - Hydrogenation

Aryl bromine (1 equiv.) and 10% Palladium on carbon (0.3 equiv.) in MeOH (0.01 M) was stirred at rt under a hydrogen atmosphere (1 atm.) for 30 mins during which time LCMS analysis revealed the progress of the reaction. The mixture was filtered through celite and washed with MeOH. The solvent was removed *in vacuo* and the

residue purified by reverse phase column chromatography (Water:MeOH 0 – 100%) to afford the title compound.

General Method 18 – Pt/V Reductive Heterocyclisation

To a nitro compound (1 equiv.) in THF (0.3 M) was added 10% Pt.C (0.1 equiv.) and VO(acac)₂ (0.08 equiv.). The mixture was stirred at rt under a hydrogen atmosphere for 48 h during which time LCMS analysis revealed the progress of the reaction. Upon completion the mixture was filtered through celite and solvent removed *in vacuo* to afford the title compound.

General Method 19 – Alkylation of R₂ Group

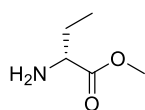
Dihydropteridinone **79** (1 equiv.) was dissolved in DMF (0.1 M) and an alkyl halide (1.2 equiv.) was added. The mixture was cooled to –10 °C to which NaH (60% dispersion in mineral oil, 1.2 equiv.) was added/. The reaction was stirred at rt for 16 – 20 h during which time LCMS analysis revealed the progress of the reaction. Upon completion, ice was added and the aqueous phase extracted with EtOAc (X3). The combined organic phases were washed with water (X2), dried over MgSO₄, filtered and concentrated *in vacuo*. The residue was purified by flash column chromatography (cHex:EtOAc 0 – 30%) to afford the title compound.

General Method 20 – Mitsunobu

To dihydropteridinone **79** (1 equiv.) in THF (0.1 M) was added alcohol (1.3 – 1.6 equiv.) and (cyanomethylene)tributylphosphorane (2.8 equiv., 33% solution in THF) under a nitrogen atmosphere. The mixture was heated at 100 °C for 1 – 2 h under microwave irradiation. Upon completion, water was added and the THF removed *in vacuo*. The residue was purified by Biotage column chromatography (cHex:EtOAc 0 – 40%) to afford the title compound. Co-eluting diastereomers were further purified using semi-preparative HPLC (Water:MeOH 40 – 60%).

7.8 Chemistry Experimental

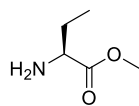
(*R*)-Methyl 2-aminobutanoate, **8a**



(*R*)-2-Aminobutyric acid **9a** (1 g, 9.70 mmol) was subjected to general method **1** to afford the title compound **8a** (HCl salt) as a white solid (1.36 g, 91%). LCMS purity >95%, ret. time 0.12 mins; HRMS (ESI +ve): found [M+H]⁺ 118.0859, [C₅H₁₂NO₂]⁺ requires 118.0863; [α]_D^{21.9}: –13.5° (c 1.0, MeOH); δ_H

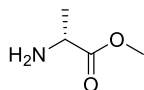
(CDCl₃, 500 MHz): 8.81 (2H, s, NH₂), 4.15 – 4.09 (1H, m, CHCH₂CH₃), 3.83 (3H, s, CO₂CH₃), 2.21 – 2.09 (2H, m, CHCH₂CH₃), 1.13 (3H, t, *J* = 7.4 Hz, CHCH₂CH₃); δ_C (CDCl₃, 126 MHz): 169.7 (C=O₂CH₃), 54.4 (CHCH₂CH₃), 53.1 (CO₂CH₃), 23.9 (CHCH₂CH₃), 9.6 (CHCH₂CH₃)

(S)-Methyl 2-aminobutanoate, 8b



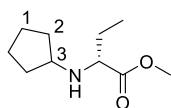
(S)-2-Aminobutyric acid **9b** (1 g, 9.70 mmol) was subjected to general method **1** to afford the title compound **8b** (HCl salt) as a white solid (1.36 g, 91%). LCMS purity >95%, ret. time 0.11 mins; HRMS (ESI +ve): found [M+H]⁺ 118.0859, [C₅H₁₂NO₂]⁺ requires 118.0863; [α]_D^{21.8}: +12.8° (c 1.0, MeOH); δ_H (CDCl₃, 500 MHz): 8.79 (2H, s, NH₂), 4.20 – 4.11 (1H, m, CHCH₂CH₃), 3.83 (3H, s, OCH₃), 2.21 – 2.09 (2H, m, CHCH₂CH₃), 1.12 (3H, t, *J* = 7.4 Hz, CHCH₂CH₃); δ_C (CDCl₃, 126 MHz): 169.7 (C=O₂CH₃), 54.4 (CHCH₂CH₃), 53.1 (CO₂CH₃), 23.8 (CHCH₂CH₃), 9.7 (CHCH₂CH₃)

(R)-Methyl 2-aminopropanoate, 8c

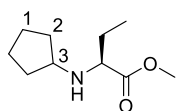


(R)-2-Aminopropanoic acid **9c** (1.5 g, 16.8 mmol) was subjected to general method **1** to afford the title compound **8c** (HCl salt) as a white solid (1.85 g, 78%). LCMS purity >95%, ret. time 0.12 mins; HRMS (ESI +ve): found [M+H]⁺ 104.0708, [C₄H₁₀NO₂]⁺ requires 104.0712; [α]_D^{22.1}: -23.5° (c 1.0, MeOH); δ_H (CDCl₃, 500 MHz): 8.42 (2H, s, NH₂), 4.06 – 3.97 (1H, m, CHCH₃), 3.69 (3H, s, CO₂CH₃), 1.42 (3H, d, *J* = 6.9 Hz, CHCH₃); δ_C (CDCl₃, 126 MHz): 171.5 (C=O₂CH₃), 54.0 (CO₂CH₃), 50.0 (CHCH₃), 16.4 (CHCH₃)

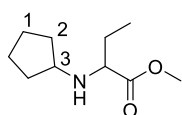
(R)-Methyl 2-(cyclopentylamino)butanoate, 10a



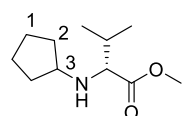
(R)-Methyl 2-aminobutanoate, **8a** (HCl salt, 1.5 g, 9.77 mmol), was reacted with cyclopentanone (0.87 mL, 9.77 mmol) using general method **2** to the title compound **10a** as a yellow oil (1.45 g, 80%). LCMS purity >95%, ret. time 0.18 mins; HRMS (ESI +ve): found [M+H]⁺ 186.1498, [C₁₀H₂₀NO₂]⁺ requires 186.1494; [α]_D^{21.8}: -12.0° (c 1.0, MeOH); δ_H (CDCl₃, 500 MHz): 3.73 (3H, s, CO₂CH₃), 3.22 (1H, t, *J* = 6.6 Hz, CHCH₂CH₃), 2.97 (1H, quin., *J* = 6.7 Hz, H3), 1.83 – 1.60 (6H, m, cPeH & CHCH₂CH₃), 1.55 – 1.47 (2H, m, H1), 1.35 – 1.27 (2H, m, H2), 0.92 (3H, t, *J* = 7.6 Hz, CHCH₂CH₃); δ_C (CDCl₃, 126 MHz): 176.5 (C=O₂CH₃), 61.6 (CHCH₂CH₃), 58.1 (C3), 51.5 (CO₂CH₃), 33.7 (C2), 32.7 (C2'), 27.0 (CHCH₂CH₃), 23.9 (C1), 23.8 (C1'), 10.2 (CHCH₂CH₃)

(S)-Methyl 2-(cyclopentylamino)butanoate, 10b

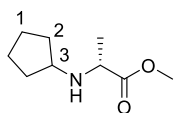
(S)-Methyl 2-aminobutanoate **8b** (HCl salt, 1.34 g, 8.72 mmol), was reacted with cyclopentanone (0.78 mL, 8.72 mmol) using general method **2** to afford the title compound **10b** as a brown oil (1.42 g, 88%). LCMS purity >95%, ret. time 0.18 mins; HRMS (ESI +ve): found $[M+H]^+$ 186.1498, $[C_{10}H_{20}NO_2]^+$ requires 186.1494; $[\alpha]_D^{22.0}$: +11.8° (*c* 1.0, MeOH); δ_H (CDCl₃, 500 MHz): 3.71 (3H, s, CO₂CH₃), 3.20 (1H, t, *J* = 6.6 Hz, CHCH₂CH₃), 2.96 (1H, p, *J* = 6.7 Hz, H₃), 1.83 – 1.58 (6H, m, cPeH & CHCH₂CH₃), 1.55 – 1.47 (2H, m, H₁), 1.35 – 1.27 (2H, m, H₂), 0.91 (3H, t, *J* = 7.6 Hz, CHCH₂CH₃); δ_C (CDCl₃, 126 MHz): 176.5 (CO₂CH₃), 61.6 (CHCH₂CH₃), 58.1 (C₃), 51.5 (CO₂CH₃), 33.7 (C₂), 32.7 (C₂'), 27.0 (CHCH₂CH₃), 23.9 (C₁), 23.8 (C₁'), 10.2 (CHCH₂CH₃)

Methyl 2-(cyclopentylamino)butanoate, 10c

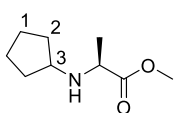
Methyl 2-aminobutanoate, **8d** (HCl salt, 800 mg, 5.21 mmol), was reacted with cyclopentanone (0.46 mL, 5.21 mmol) using general method **2** to the title compound **10c** as a yellow oil (728 mg, 75%). LCMS purity >95%, ret. time 0.18 mins; HRMS (ESI +ve): found $[M+H]^+$ 186.1487, $[C_{10}H_{20}NO_2]^+$ requires 186.1494; δ_H (CDCl₃, 500 MHz): 3.73 (3H, s, CO₂CH₃), 3.22 (1H, t, *J* = 6.6 Hz, CHCH₂CH₃), 2.97 (1H, quin., *J* = 6.7 Hz, H₃), 1.83 – 1.60 (6H, m, cPeH & CHCH₂CH₃), 1.55 – 1.47 (2H, m, H₁), 1.35 – 1.27 (2H, m, H₂), 0.92 (3H, t, *J* = 7.6 Hz, CHCH₂CH₃); δ_C (CDCl₃, 126 MHz): 176.5 (CO₂CH₃), 61.6 (CHCH₂CH₃), 58.1 (C₃), 51.5 (CO₂CH₃), 33.7 (C₂), 32.7 (C₂'), 27.0 (CHCH₂CH₃), 23.9 (C₁), 23.8 (C₁'), 10.2 (CHCH₂CH₃)

Methyl cyclopentyl-D-valinate, 10e

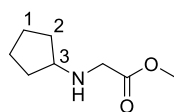
Methyl *D*-valinate **8e** (HCl salt, 1.80 g, 10.7 mmol), was reacted with cyclopentanone (0.27 mL, 9.66 mmol) using general method **2** to afford the title compound **10e** as a colourless oil (1.26 g, 59%). LCMS purity >95%, ret. time 0.26 mins; HRMS (ESI +ve): found $[M+H]^+$ 200.1651, $[C_{11}H_{21}NO_2]^+$ requires 200.1645; $[\alpha]_D^{22.9}$: -10.4° (*c* 1.0, MeOH); δ_H (CDCl₃, 500 MHz): 3.73 (3H, s, CO₂CH₃), 3.01 (1H, d, *J* = 6.3 Hz, CHCH(CH₃)₂), 2.93 (1H, quin, *J* = 6.3 Hz, H₃), 1.90 – 1.76 (2H, m, CHCH(CH₃)₂ & C₂), 1.75 – 1.65 (3H, cPeH), 1.55 – 1.47 (3H, m, cPeH), 1.34 – 1.26 (2H, m, H₂), 0.94 (3H, d, *J* = 6.9 Hz, CH(CH₃)(C'H₃)), 0.92 (3H, d, *J* = 6.9 Hz, CH(CH₃)(C'H₃)); δ_C (CDCl₃, 126 MHz): 176.4 (CO₂CH₃), 66.1 (CHCH(CH₃)₂), 58.4 (C₃), 51.4 (OCH₃), 33.8 (C₂), 32.6 (C₂'), 31.8 (CH(CH₃)₂), 23.9 (C₁), 23.8 (C₁'), 19.1 (CH(CH₃)(C'H₃)), 18.8 (CH(CH₃)(C'H₃))

(R)-Methyl 2-(cyclopentylamino)propanoate, 10e

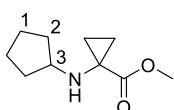
(*R*)-Methyl 2-aminopropanoate **8c** (HCl salt, 400 mg, 3.88 mmol), was reacted with cyclopentanone (0.34 mL, 3.88 mmol) using general method **2** to afford the title compound **10e** as a colourless oil (200 mg, 30%). LCMS purity >95%, ret. time 0.20 mins; HRMS (ESI +ve): found $[M+H]^+$ 172.1340, $[C_9H_{18}NO_2]^+$ requires 172.1337; $[\alpha]_D^{22.3}$: -10.2° (*c* 1.0, MeOH); δ_H (CDCl₃, 500 MHz): 3.72 (3H, s, CO₂CH₃), 3.39 (1H, q, *J* = 6.9 Hz, CHCH₃), 2.99 (1H, quin, *J* = 6.9 Hz, H₃), 1.85 – 1.76 (2H, m, H₂), 1.73 – 1.64 (2H, m, H₁), 1.56 – 1.46 (2H, m, H₁), 1.35 – 1.26 (2H, m, H₂), 1.28 (3H, d, *J* = 7.1 Hz, CHCH₃); δ_C (CDCl₃, 126 MHz): 176.8 (CO₂CH₃), 58.0 (C₃), 55.4 (CHCH₃), 51.8 (CO₂CH₃), 33.6 (C₂), 32.8 (C_{2'}), 24.0 (C₁), 23.9 (C_{1'}), 19.6 (CHCH₃)

(S)-Methyl 2-(cyclopentylamino)propanoate, 10f

(*S*)-Methyl 2-aminopropanoate **8f** (HCl salt, 1.30 g, 12.6 mmol), was reacted with cyclopentanone (1.11 mL, 12.6 mmol) using general method **2** to afford the title compound **10f** as a colourless oil (2.10 g, 97%). LCMS purity >95%, ret. time 0.11 mins; HRMS (ESI +ve): found $[M+H]^+$ 171.1332, $[C_9H_{18}NO_2]^+$ requires 172.1337; $[\alpha]_D^{23.6}$: $+11.8^\circ$ (*c* 1.0, MeOH); δ_H (CDCl₃, 500 MHz): 3.70 (3H, s, CO₂CH₃), 3.37 (1H, q, *J* = 6.9 Hz, CHCH₃), 2.98 (1H, quin., *J* = 6.9 Hz, H₃), 1.85 – 1.76 (2H, m, H₂), 1.73 – 1.64 (2H, m, H₁), 1.56 – 1.46 (2H, m, H₁), 1.35 – 1.26 (2H, m, H₂), 1.28 (3H, d, *J* = 7.3 Hz, CHCH₃); δ_C (CDCl₃, 126 MHz): 176.8 (CO₂CH₃), 58.0 (C₃), 55.3 (CHCH₃), 51.7 (OCH₃), 33.6 (C₂), 32.8 (C_{2'}), 24.0 (C₁), 23.9 (C_{1'}), 19.6 (CHCH₃)

Methyl cyclopentylglycinate, 10g

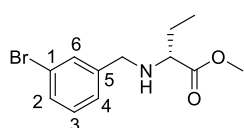
Glycine methyl ester **8g** (HCl salt, 1.10 g, 8.77 mmol) was reacted with cyclopentanone (0.62 mL, 7.01 mmol) using general method **2** to afford the title compound **10g** as a colourless oil (535 mg, 38%). LCMS purity >95%, ret. time 0.19 min HRMS (ESI +ve): found $[M+H]^+$ 158.1176, $[C_8H_{16}NO_2]^+$ requires 158.1176; δ_H (500 MHz, CDCl₃): 3.73 (3H, s, CO₂CH₃), 3.42 (1H, s, NHCH₂), 3.07 (1H, quin, *J* = 6.5 Hz, H₃), 1.85 – 1.77 (2H, m, H₂), 1.75 – 1.66 (2H, m, H₁), 1.60 – 1.50 (2H, m, H₁), 1.40 – 1.32 (2H, m, H₂); δ_C (CDCl₃, 126 MHz): 173.1 (CO₂CH₃), 59.3 (C₃), 51.8 (NHCH₂), 49.6 (CO₂CH₃), 33.0 (C₂), 24.0 (C₁)

Methyl 1-(cyclopentylamino)cyclopropanecarboxylate, 10h

Methyl 1-aminocyclopropanecarboxylate **8h** (735 mg, 6.4 mmol), was reacted with cyclopentanone (0.56 mL, 6.4 mmol) using general

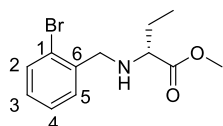
method **2** to afford the title compound **10h** as a colourless oil (667 mg, 57%). LCMS purity >95%, ret. time 0.24 mins; HRMS (ESI +ve): found $[M+H]^+$ 184.1330, $[C_{10}H_{18}NO_2]^+$ requires 184.1337; δ_H (CDCl₃, 500 MHz): 3.69 (3H, s, OCH₃), 3.25 (1H, quin, $J = 7.3$ Hz, H₃), 1.87 – 1.80 (2H, m, H₂), 1.70 – 1.62 (2H, m, H₁), 1.55 – 1.46 (2H, m, H₁) 1.33 – 1.26 (2H, m, H₂), 1.24 (2H, dd, $J = 7.3, 4.1$ Hz, C(CH₂)(CH₂'), 1.00 (2H, dd, $J = 7.3, 4.1$ Hz, C(CH₂)(CH₂')); δ_C (CDCl₃, 126 MHz): 176.1 (C=O₂CH₃), 59.0 (C₃), 51.9 (CO₂CH₃), 40.3 (C(CH₂)₂), 33.6 (C₂), 23.4 (C₁), 17.1 (C(CH₂)₂)

(R)-Methyl 2-((3-bromobenzyl)amino)butanoate, 10i

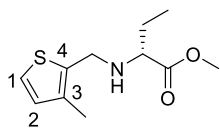


(*R*)-Methyl 2-aminobutanoate **8a** (HCl salt, 800 mg, 5.21 mmol), was reacted with 3-bromobenzaldehyde (0.61 mL, 5.21 mmol) using general method **2** to afford the title compound **10i** as a yellow oil (1.37 g, 92%). LCMS purity >95%, ret. time 0.92 mins; HRMS (ESI +ve): found $[M+H]^+$ 286.0431, $[C_{12}H_{17}BrNO_2]^+$ requires 286.0437; $[\alpha]_D^{21.9}$: +22.9° (c 1.0, MeOH); δ_H (CDCl₃, 500 MHz): 7.52 (1H, t, $J = 1.6$ Hz, H₂), 7.38 (1H, dt, $J = 7.9, 1.6$ Hz, H₆), 7.28 – 7.25 (1H, m, H₄), 7.20 – 7.17 (1H, m, H₃), 3.80 (1H, d, $J = 13.2$ Hz, ArCHH), 3.74 (3H, s, OCH₃), 3.60 (1H, d, $J = 13.2$ Hz, ArCHH), 3.20 (1H, t, $J = 6.6$ Hz, CHCH₂CH₃), 1.76 – 1.62 (2H, m, CHCH₂CH₃), 0.96 (3H, t, $J = 7.6$ Hz, CHCH₂CH₃); δ_C (CDCl₃, 126 MHz): 175.8 (C=O₂CH₃), 142.3 (C₅), 131.2 (C₂), 130.1 (C₆), 129.9 (C₃), 126.7 (C₄), 122.5 (C₁), 61.9 (CHCH₂CH₃), 51.7 (CO₂CH₃), 51.5 (ArCH₂), 26.6 (CHCH₂CH₃), 10.2 (CHCH₂CH₃)

(R)-Methyl 2-((2-bromobenzyl)amino)butanoate, 10j

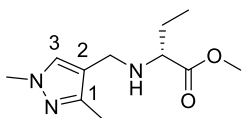


(*R*)-Methyl 2-aminobutanoate **8a** (HCl salt, 700 mg, 4.56 mmol), was reacted with 2-bromobenzaldehyde (0.53 mL, 4.56 mmol) using general method **2** to afford the title compound **10j** as a colourless oil (1.11 g, 85%). LCMS purity >95%, ret. time 0.86 mins; HRMS (ESI +ve): found $[M+H]^+$ 286.0437, $[C_{12}H_{17}BrNO_2]^+$ requires 286.0443; $[\alpha]_D^{21.8}$: +13.9° (c 1.0, MeOH); δ_H (CDCl₃, 500 MHz): 7.54 (1H, dd, $J = 7.8, 1.4$ Hz, H₂), 7.43 (1H, dd, $J = 7.8, 1.6$ Hz, H₅), 7.31 – 7.27 (1H, m, H₄), 7.12 (1H, td, $J = 7.8, 1.6$ Hz, H₃), 3.90 (1H, d, $J = 14.2$ Hz, ArCHH), 3.77 (1H, d, $J = 14.2$ Hz, ArCHH), 3.71 (3H, s, CO₂CH₃), 3.24 (1H, t, $J = 6.6$ Hz, CHCH₂CH₃), 1.78 – 1.65 (2H, m, CHCH₂CH₃), 0.96 (3H, t, $J = 7.4$ Hz, CHCH₂CH₃); δ_C (CDCl₃, 126 MHz): 175.6 (C=O₂CH₃), 138.9 (C₆), 132.8 (C₂), 130.2 (C₅), 128.6 (C₃), 127.4 (C₄), 124.1 (C₁), 62.2 (CHCH₂CH₃), 52.0 (ArCH₂), 51.7 (CO₂CH₃), 26.6 (CHCH₂CH₃), 10.3 (CHCH₂CH₃)

Methyl (*R*)-2-(((3-methylthiophen-2-yl)methyl)amino)butanoate, 10k

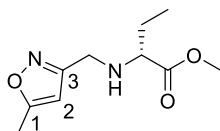
(*R*)-Methyl 2-aminobutanoate **8a** (HCl salt, 500 mg, 4.26 mmol), was reacted with 3-methylthiophene-2-carbaldehyde (0.46 mL, 4.26 mmol) using general method **2** to afford the title compound

10k as a yellow oil (720 mg, 74%). LCMS purity >95%, ret. time 0.43 mins; HRMS (ESI +ve): found $[M+H]^+$ 228.1061, $[C_{11}H_{18}NO_2S]^+$ requires 228.1053; $[\alpha]_D^{22.6}$: +23.6° (c 1.0, MeOH); δ_H (CDCl₃, 500 MHz): 7.10 (1H, d, J = 5.2 Hz, H1), 6.78 (1H, d, J = 5.2, H2), 3.93 (1H, d, J = 13.9 Hz, ArCHH), 3.76 – 3.73 (4H, m, ArCHH & CO₂CH₃), 3.27 (1H, t, J = 6.6 Hz, CHCH₂CH₃), 2.17 (3H, s, CH₃), 1.74 – 1.62 (2H, m, CHCH₂CH₃), 0.95 (3H, t, J = 6.9 Hz, CHCH₂CH₃); δ_C (CDCl₃, 126 MHz): 175.8 (CO₂CH₃), 136.6 (C3), 133.8 (C4), 130.0 (C2), 122.8 (C1), 61.7 (CHCH₂CH₃), 51.6 (CO₂CH₃), 44.7 (C5), 26.6 (CHCH₂CH₃), 13.4 (CH₃), 10.2 (CHCH₂CH₃)

Methyl (*R*)-2-(((1,3-dimethyl-1H-pyrazol-4-yl)methyl)amino)butanoate, 10l

(*R*)-Methyl 2-aminobutanoate **8a** (HCl salt, 500 mg, 4.26 mmol), was reacted with 1,3-dimethylpyrazole-4-carbaldehyde (477 mg, 3.84 mmol) using general method **2** to afford the title compound

10l as a colourless oil (720 mg, 74%). LCMS purity >95%, ret. time 0.18 mins; HRMS (ESI +ve): found $[M+H]^+$ 226.1559, $[C_{11}H_{20}N_3O_2]^+$ requires 226.1550; $[\alpha]_D^{22.6}$: +13.2° (c 1.0, MeOH); δ_H (CDCl₃, 500 MHz): 7.22 (1H, s, H3), 3.79 (3H, s, NCH₃), 3.73 (3H, s, CO₂CH₃), 3.59 (1H, d, J = 12.9 Hz, ArHH), 3.45 (1H, d, J = 12.9 Hz, ArHH), 3.21 (1H, t, J = 6.9 Hz, CHCH₂CH₃), 2.22 (3H, s, ArCH₃), 1.72 – 1.59 (2H, m, CHCH₂CH₃), 0.92 (3H, t, J = 7.6 Hz, CHCH₂CH₃); δ_C (CDCl₃, 126 MHz): 175.9 (CO₂CH₃), 147.1 (C1), 129.9 (C3), 117.2 (C2), 61.9 (CHCH₂CH₃), 51.6 (CO₂CH₃), 41.6 (C4), 38.5 (NCH₃), 26.6 (CHCH₂CH₃), 11.6 (ArCH₃), 10.2 (CHCH₂CH₃)

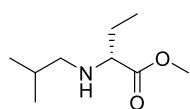
Methyl (*R*)-2-(((5-methylisoxazol-3-yl)methyl)amino)butanoate, 10m

(*R*)-Methyl 2-aminobutanoate **8a** (HCl salt, 500 mg, 4.26 mmol), was reacted with 5-methylisoxazole-3-carbaldehyde (474 mg, 4.26 mmol) using general method **2** to afford the title compound **10m**

as a colourless oil (520 mg, 57%). LCMS purity >95%, ret. time 0.22 mins; HRMS (ESI +ve): found $[M+H]^+$ 172.1340, $[C_{10}H_{17}N_2O_3]^+$ requires 172.1337; $[\alpha]_D^{22.4}$: +16.6° (c 1.0, MeOH); δ_H (CDCl₃, 500 MHz): 5.99 (1H, d, J = 1.0 Hz, H2), 3.85 (1H, d, J = 14.2 Hz, ArHH), 3.73 (3H, s, CO₂CH₃), 3.69 (1H, d, J = 14.2 Hz, ArHH), 3.23 (1H, t, J = 6.5 Hz, CHCH₂CH₃), 2.40 (1H, d, J = 1.0 Hz, ArCH₃), 1.88 (1H, s, NH), 1.75 – 1.63 (2H, m, CHCH₂CH₃), 0.93 (3H, t, J = 7.4 Hz, CHCH₂CH₃); δ_C (CDCl₃, 126 MHz): 175.4

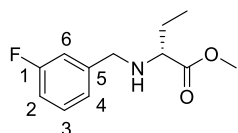
(CO_2CH_3), 169.4 (C1), 162.9 (C3), 101.0 (C1), 61.8 (CHCH_2CH_3), 51.8 (CO_2CH_3), 43.3 (C4), 26.4 (CHCH_2CH_3), 12.3 (ArCH_3), 19.6 (CHCH_2CH_3)

Methyl (*R*)-2-(isobutylamino)butanoate, 10n



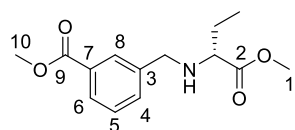
(*R*)-Methyl 2-aminobutanoate **8a** (HCl salt, 600 mg, 5.12 mmol), was reacted with 2-methylpropanal (0.37 mL, 4.10 mmol) using general method **2** to afford the title compound **10n** as a colourless oil (283 mg, 31%). LCMS purity >95%, ret. time 0.17 mins; HRMS (ESI +ve): found $[\text{M}+\text{H}]^+$ 174.1487, $[\text{C}_9\text{H}_{18}\text{NO}_2]^+$ requires 174.1489; $[\alpha]_D^{22.3}$: -16.6° (*c* 1.0, MeOH); δ_{H} (CDCl_3 , 500 MHz): 3.74 (3H, s, CO_2CH_3), 3.23 (1H, t, $J = 6.6$ Hz, CHCH_2CH_3), 2.35 (2H, d, $J = 6.6$ Hz, NHCH_2), 2.02 (1H, s, NH), 1.78 – 1.67 (3H, m, $\text{CH}(\text{CH}_3)_2$ & CHCH_2CH_3), 0.94 – 0.89 (9H, m, $\text{CH}(\text{CH}_3)_2$ & CHCH_2CH_3); δ_{C} (CDCl_3 , 126 MHz): 175.6 (CO_2CH_3), 62.8 (CHCH_2CH_3), 55.9 (NHCH_2), 51.7 (CO_2CH_3), 28.3 ($\text{CH}(\text{CH}_3)_2$), 26.2 (CHCH_2CH_3), 2.07 ($\text{CH}(\text{CH}_3)_2$), 10.1 (CHCH_2CH_3)

Methyl (*R*)-2-((3-fluorobenzyl)aminol)butanoate, 10o



(*R*)-Methyl 2-aminobutanoate **8a** (HCl salt, 500 mg, 3.26 mmol), was reacted with 3-fluorobenzaldehyde (297 μL , 2.80 mmol) using general method **2** to afford the title compound **10o** as a colourless oil (690 mg, 94%). LCMS purity >95%, ret. time 0.36 mins; HRMS (ESI +ve): found $[\text{M}+\text{H}]^+$ 226.1240, $[\text{C}_{12}\text{H}_{16}\text{FNO}_2]^+$ requires 226.1238; $[\alpha]_D^{22.4}$: $+20.1^\circ$ (*c* 1.0, MeOH); δ_{H} (CDCl_3 , 500 MHz): 7.31 – 7.26 (1H, m, H3), 7.12 – 7.08 (2H, m, H4 & H6), 6.97 – 6.93 (1H, m, H2), 3.84 (1H, d, $J = 13.6$ Hz, ArCHH), 3.75 (3H, s, CO_2CH_3), 3.63 (1H, d, $J = 13.6$ Hz, ArCHH), 3.22 (1H, t, $J = 6.6$ Hz, CHCH_2CH_3), 1.80 (1H, s, NH), 1.75 – 1.63 (2H, m, CHCH_2CH_3), 0.96 (3H, t, $J = 7.6$ Hz, CHCH_2CH_3); δ_{C} (CDCl_3 , 126 MHz): 175.8 (CO_2CH_3), 163.0 (d, $J_{\text{C-F}} = 245$ Hz, C1) 142.7 (d, $J_{\text{C-F}} = 7.3$ Hz, C5), 129.8 (d, $J_{\text{C-F}} = 8.3$ Hz, C3), 123.7 (d, $J_{\text{C-F}} = 2.8$ Hz, C4), 114.9 (d, $J_{\text{C-F}} = 21.1$ Hz, C6), 113.9 (d, $J_{\text{C-F}} = 21.1$ Hz, C2), 61.9 (CHCH_2CH_3), 51.7 (CO_2CH_3), 51.5 (ArCH_2), 26.7 (CHCH_2CH_3), 10.2 (CHCH_2CH_3); $\delta_{\text{F}\{\text{H}\}}$ (CDCl_3 , 471 MHz): -113.3

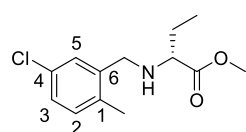
Methyl (*R*)-3-(((1-methoxy-1-oxobutan-2-yl)amino)methyl)benzoate, 10p



(*R*)-Methyl 2-aminobutanoate **8a** (HCl salt, 700 mg, 5.98 mmol), was reacted with methyl 3-formylbenzoate (981 mg, 5.98 mmol) using general method **2** to afford the title compound **10p** as a colourless oil (1.30 g, 82%). LCMS purity >95%, ret. time 0.85 mins; HRMS (ESI +ve): found $[\text{M}+\text{H}]^+$ 266.1388, $[\text{C}_{14}\text{H}_{20}\text{NO}_4]^+$ requires 266.1387; $[\alpha]_D^{22.1}$: $+26.3^\circ$ (*c* 1.0, MeOH); δ_{H} (CDCl_3 , 500 MHz): 8.01 (1H, s, H8), 7.93 (1H, d, $J =$

7.7 Hz, H6), 7.56 (1H, d, $J = 7.7$ Hz, H4), 7.40 (1H, t, $J = 7.7$ Hz, H5), 3.92 (3H, s, H10), 3.87 (1H, d, $J = 13.2$ Hz, ArCHH), 3.74 (3H, s, H1), 3.68 (1H, d, $J = 13.2$ Hz, ArCHH), 3.21 (1H, t, $J = 6.6$ Hz, CHCH₂CH₃), 1.84 (1H, s, NH), 1.74 – 1.62 (2H, m, CHCH₂CH₃), 0.95 (3H, t, $J = 7.4$ Hz, CHCH₂CH₃); δ_c (CDCl₃, 126 MHz): 175.8 (C2), 167.1 (C9), 140.4 (C3), 132.8 (C5), 130.3 (C8), 129.3 (C9), 128.5 (C6), 128.3 (C7), 62.0 (CHCH₂CH₃), 52.1 (C11), 51.7 (C1), 43.4 (C4), 26.6 (CHCH₂CH₃), 10.2 (CHCH₂CH₃)

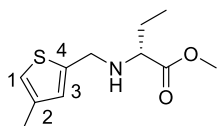
Methyl (*R*)-2-((5-chloro-2-methylbenzyl)aminol)butanoate, **10q**



(*R*)-Methyl 2-aminobutanoate **8a** (HCl salt, 800 mg, 5.21 mmol), was reacted with 5-chloro-2-methyl-benzaldehyde (723 mg, 4.69 mmol) using general method **2** to afford the title compound **10q**

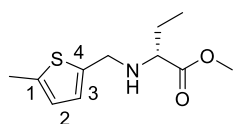
as a colourless oil (1.19 g, 89%). LCMS purity >95%, ret. time 0.99 mins; HRMS (ESI +ve): found $[M+H]^+$ 256.1099, $[C_{13}H_{18}ClNO_2]^+$ requires 256.1099; $[\alpha]_D^{22.3}$: +6.9° (c 1.0, MeOH); δ_H (CDCl₃, 500 MHz): 7.33 (2H, d, $J = 2.2$ Hz, H5), 7.13 (1H, dd, $J = 8.0, 2.2$ Hz, H3), 7.07 (1H, d, $J = 8.0$ Hz, H2), 3.76 – 3.74 (4H, m, CO₂CH₃ & ArCHH), 3.56 (1H, d, $J = 13.2$ Hz, ArCHH), 3.22 (1H, t, $J = 6.5$ Hz, CHCH₂CH₃), 2.30 (1H, s, ArCH₃), 1.77 – 1.62 (3H, m, NH & CHCH₂CH₃), 0.97 (3H, t, $J = 7.5$ Hz, CHCH₂CH₃); δ_c (CDCl₃, 126 MHz): 175.9 (CO₂CH₃), 139.7 (C6), 134.9 (C1), 131.4 (C2 & C4), 128.4 (C5), 126.9 (C3), 62.4 (CHCH₂CH₃), 51.7 (CO₂CH₃), 49.6 (ArCH₂), 26.7 (CHCH₂CH₃), 18.4 (ArCH₃), 10.3 (CHCH₂CH₃)

Methyl (*R*)-2-(((4-methylthiophen-2-yl)methyl)amino)butanoate, **10r**



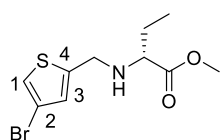
(*R*)-Methyl 2-aminobutanoate **8a** (HCl salt, 3.0 g, 19.5 mmol), was reacted with 4-methylthiophene-2-carbaldehyde (0.46 mL, 4.26 mmol) using general method **2** to afford the title compound **10r**

as a brown oil (4.36 mg, 98%). LCMS purity >95%, ret. time 0.70 mins; HRMS (ESI +ve): found $[M+H]^+$ 228.1062, $[C_{11}H_{18}NO_2S]^+$ requires 228.1053; $[\alpha]_D^{22.5}$: +28.4° (c 1.0, MeOH); δ_H (CDCl₃, 500 MHz): 6.78 (1H, t, $J = 1.2$ Hz, H1), 6.73 (1H, s, H3), 3.98 (1H, dd, $J = 13.9, 1.0$ Hz, ArCHH), 3.78 (1H, dd, $J = 13.9, 1.0$ Hz, ArCHH), 3.74 (3H, s, CO₂CH₃), 3.29 (1H, t, $J = 6.6$ Hz, CHCH₂CH₃), 2.22 (3H, d, $J = 1.2$ Hz, ArCH₃), 1.81 (1H, s, NH), 1.74 – 1.62 (2H, m, CHCH₂CH₃), 0.95 (3H, t, $J = 7.4$ Hz, CHCH₂CH₃); δ_c (CDCl₃, 126 MHz): 175.7 (CO₂CH₃), 143.5 (C4), 137.2 (C2), 127.5 (C3), 119.7 (C1), 61.5 (CHCH₂CH₃), 51.7 (CO₂CH₃), 46.9 (ArCH₂), 26.7 (CHCH₂CH₃), 15.7 (CH₃), 10.2 (CHCH₂CH₃)

Methyl (*R*)-2-(((5-methylthiophen-2-yl)methyl)amino)butanoate, 10s

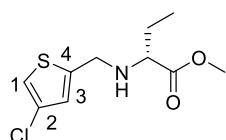
(*R*)-Methyl 2-aminobutanoate **8a** (HCl salt, 600 mg, 5.12 mmol), was reacted with 5-methylthiophene-2-carbaldehyde (0.44 mL, 4.10 mmol) using general method **2** to afford the title compound

10s as a brown oil (892 mg, 77%). LCMS purity >95%, ret. time 0.41 mins; HRMS (ESI +ve): found $[M+H]^+$ 228.1049, $[C_{11}H_{18}NO_2S]^+$ requires 228.1053; $[\alpha]_D^{22.2}$: +25.6° (c 1.0, MeOH); δ_H (CDCl₃, 500 MHz): 6.68 (1H, d, J = 3.2 Hz, H3), 6.58 – 6.55 (1H, m, H2), 3.95 (1H, d, J = 13.9 Hz, ArCH_H), 3.75 (1H, d, J = 13.9 Hz, ArCH_H), 3.73 (3H, s, CO₂CH₃), 3.28 (1H, t, J = 6.6 Hz, CHCH₂CH₃), 2.45 (3H, s, ArCH₃), 1.89 (1H, s, NH), 1.74 – 1.61 (2H, m, CHCH₂CH₃), 0.94 (3H, t, J = 6.9 Hz, CHCH₂CH₃); δ_C (CDCl₃, 126 MHz): 175.7 (CO₂CH₃), 141.2 (C4), 139.1 (C1), 125.0 (C3), 124.5 (C2), 61.3 (CHCH₂CH₃), 51.6 (CO₂CH₃), 47.0 (ArCH₂), 26.6 (CHCH₂CH₃), 15.4 (ArCH₃), 10.2 (CHCH₂CH₃)

Methyl (*R*)-2-(((4-bromothiophen-2-yl)methyl)amino)butanoate, 10t

(*R*)-Methyl 2-aminobutanoate **8a** (HCl salt, 852 mg, 5.55 mmol), was reacted with 4-bromothiophene-2-carbaldehyde (1.06 g, 5.55 mmol) using general method **2** to afford the title compound **10t** as

a brown oil (1.60 g, 99%). *Used in next step without further purification* LCMS purity >65%, ret. time 0.73 mins; HRMS (ESI +ve): found $[M+H]^+$ 291.9999, $[C_{10}H_{15}BrNO_2S]^+$ requires 292.0001; $[\alpha]_D^{22.5}$: +26.3° (c 1.0, MeOH); δ_H (CDCl₃, 500 MHz): 7.11 (1H, d, J = 1.6 Hz, H1), 6.84 – 6.83 (1H, m, H3), 4.02 (1H, dd, J = 14.4, 1.0 Hz, ArCH_H), 3.78 (1H, dd, J = 14.4, 1.0 Hz, ArCH_H), 3.74 (3H, s, CO₂CH₃), 3.27 – 3.23 (1H, m, CHCH₂CH₃), 1.82 (1H, s, NH), 1.74 – 1.60 (2H, m, CHCH₂CH₃), 0.96 (3H, t, J = 7.4 Hz, CHCH₂CH₃); δ_C (CDCl₃, 126 MHz): 175.6 (CO₂CH₃), 145.6 (C4), 127.3 (C3), 121.8 (C1), 108.9 (C2), 61.5 (CHCH₂CH₃), 51.8 (CO₂CH₃), 46.6 (ArCH₂), 26.6 (CHCH₂CH₃), 10.2 (CHCH₂CH₃)

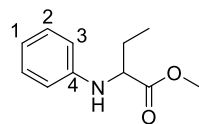
Methyl (*R*)-2-(((4-chlorothiophen-2-yl)methyl)amino)butanoate, 10u

(*R*)-Methyl 2-aminobutanoate **8a** (HCl salt, 900 mg, 5.86 mmol), was reacted with 4-chlorothiophene-2-carbaldehyde (859 mg, 5.86 mmol) using general method **2** to afford the title compound **10u** as

a colourless oil (1.33 g, 92%). LCMS purity >95%, ret. time 0.68 mins; HRMS (ESI +ve): found $[M+H]^+$ 248.0514, $[C_{10}H_{15}ClNO_2S]^+$ requires 248.0507; $[\alpha]_D^{22.4}$: +29.1° (c 1.0, MeOH); δ_H (CDCl₃, 500 MHz): 6.99 (1H, d, J = 1.6 Hz, H1), 6.79 – 6.78 (1H, m, H3), 3.99 (1H, dd, J = 14.2, 1.0 Hz, ArCH_H), 3.77 – 3.74 (4H, m, ArCH_H & CO₂CH₃), 3.25 (1H, t, J = 6.6 Hz, CHCH₂CH₃), 1.85 (1H, s, NH), 1.76 – 1.62 (2H, m, CHCH₂CH₃)

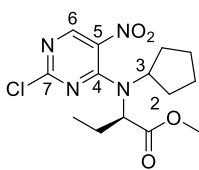
m, CHCH₂CH₃), 0.96 (3H, t, J = 7.6 Hz, CHCH₂CH₃); δ_c (CDCl₃, 126 MHz): 175.6 (CO₂CH₃), 145.0 (C4), 125.0 (C2), 124.2 (C3), 119.0 (C1), 61.5 (CHCH₂CH₃), 51.8 (CO₂CH₃), 46.8 (ArCH₂), 26.6 (CHCH₂CH₃), 10.2 (CHCH₂CH₃)

Methyl 2-(phenylamino)butanoate, 10v

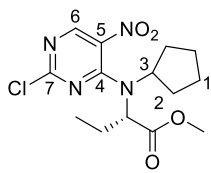


Methyl 2-bromobutanoate (0.64 mL, 5.52 mmol) and aniline (0.50 mL, 5.52 mmol) were dissolved in acetonitrile (0.1 M). Potassium carbonate (1.53 g, 11.1 mmol) and potassium iodide (0.92 g, 5.52 mmol) were added and the reaction stirred at reflux for 16 h during which time LCMS analysis revealed the progress of the reaction. Upon completion the reaction mixture was diluted with EtOAc, washed with sat. aq. NaHCO₃ and the organic phase dried over MgSO₄, filtered and concentrated *in vacuo*. The residue was purified by Biotage column chromatography (cHex/EtOAc, 9:1) to afford the title compound **10v** as a colourless oil (667 mg, 63%). LCMS purity >95%, ret. time 1.35 mins; HRMS (ESI +ve): found $[M+H]^+$ 194.1166, $[C_{11}H_{16}NO_2]^+$ requires 194.1176; δ_H (CDCl₃, 500 MHz): 7.21 – 7.16 (2H, m, H2), 6.75 (1H, tt, J = 7.6, 1.0 Hz, H1), 6.65 – 6.61 (2H, m, H3), 4.17 – 4.12 (1H, d, J = 7.6 Hz, NH), 4.08 – 4.02 (1H, m, CHCH₂CH₃), 3.74 (3H, s, CO₂CH₃), 1.96 – 1.87 (1H, m, CHCH₂CH₃), 1.87 – 1.77 (1H, m, CHCH₂CH₃), 1.01 (3H, t, J = 7.6 Hz, CHCH₂CH₃); δ_c (CDCl₃, 126 MHz): 174.5 (CO₂CH₃), 146.8 (C4), 129.3 (C2), 118.2 (C1), 113.4 (C3), 57.7 (CHCH₂CH₃), 52.0 (CO₂CH₃), 26.0 (CHCH₂CH₃), 9.9 (CHCH₂CH₃)

Methyl (R)-2-((2-chloro-5-nitropyrimidin-4-yl)(cyclopentyl)amino)butanoate, 12a

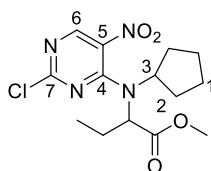


Aminobutanoate **10a** (700 mg, 3.78 mmol) was reacted with pyrimidine **11** (806 mg, 4.16 mmol) using general method **3** to afford the title compound **12a** as a yellow solid (1.03 g, 79%). LCMS purity >95%, ret. time 1.59 mins; HRMS (ESI +ve): found $[M+H]^+$ 343.1165, $[C_{15}H_{22}ClN_4O_4]^+$ requires 343.1173; $[\alpha]_D^{21.8}$: +228.5° (c 1.0, MeOH); δ_H (CDCl₃, 500 MHz): 8.67 (1H, s, H6), 3.78 – 3.72 (1H, m, CHCH₂CH₃), 3.76 (3H, s, CO₂CH₃), 3.60 – 3.52 (1H, m, H3), 2.47 – 2.36 (1H, m, CHCH₂CH₃), 2.26 – 2.17 (1H, m, H2), 2.09 – 1.98 (1H, m, CHCH₂CH₃), 1.98 – 1.91 (1H, m, H2), 1.84 – 1.56 (6H, m, cPeH), 1.05 (3H, t, J = 7.6 Hz, CHCH₂CH₃); δ_c (CDCl₃, 126 MHz): 170.9 (CO₂CH₃), 159.4 (C7), 156.5 (C6), 154.2 (C4), 131.1 (C5), 64.0 (C3), 60.2 (CHCH₂CH₃), 52.5 (CO₂CH₃), 30.3 (C2), 27.4 (C2'), 23.1 (C1), 23.0 (C1'), 22.9 (CHCH₂CH₃), 11.6 (CHCH₂CH₃)

Methyl (S)-2-((2-chloro-5-nitropyrimidin-4-yl)(cyclopentyl)amino)butanoate, 12b

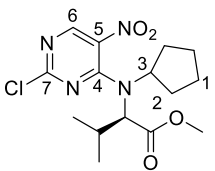
Aminobutanoate **10b** (1.40 g, 7.56 mmol) was reacted with pyrimidine **11** (1.61 g, 8.31 mmol) using general method **3** to afford the title compound **12b** as a yellow solid (830 mg, 32%). LCMS purity >95%, ret. time 1.59 mins; HRMS (ESI +ve): found $[M+H]^+$

343.1171, $[C_{14}H_{20}ClN_4O_4]^+$ requires 343.1173; $[\alpha]_D^{22.0}$: -229.9° (c 1.0, MeOH); δ_H (CDCl₃, 500 MHz): 8.67 (1H, s, H6), 3.78 – 3.72 (1H, m, CHCH₂CH₃), 3.76 (3H, s, CO₂CH₃), 3.60 – 3.51 (1H, m, H3), 2.46 – 2.36 (1H, m, CHCH₂CH₃), 2.25 – 2.17 (1H, m, H2), 2.09 – 2.01 (1H, m, CHCH₂CH₃), 1.99 – 1.90 (1H, m, H2), 1.84 – 1.47 (6H, m, cPeH), 1.05 (3H, t, $J = 7.6$ Hz, CHCH₂CH₃); δ_C (CDCl₃, 126 MHz): 170.9 (CO₂CH₃), 159.3 (C7), 156.6 (C6), 154.2 (C4), 131.1 (C5), 64.0 (C3), 60.2 (CHCH₂CH₃), 52.5 (CO₂CH₃), 30.3 (C2), 27.3 (C2'), 23.0 (C1), 22.9 (C1'), 22.9 (CHCH₂CH₃), 11.6 (CHCH₂CH₃)

Methyl 2-((2-chloro-5-nitropyrimidin-4-yl)(cyclopentyl)amino)butanoate, 12c

Aminobutanoate **10c** (728 mg, 3.93 mmol) was reacted with pyrimidine **11** (838 mg, 4.32 mmol) using general method **3** to afford the title compound **12c** as a yellow solid (554 mg, 41%). LCMS purity >95%, ret. time 1.59 mins; HRMS (ESI +ve): found

$[M+H]^+$ 343.1166, $[C_{14}H_{20}ClN_4O_4]^+$ requires 343.1173; δ_H (CDCl₃, 500 MHz): 8.67 (1H, s, H6), 3.78 – 3.72 (1H, m, CHCH₂CH₃), 3.76 (3H, s, OCH₃), 3.60 – 3.51 (1H, m, H3), 2.46 – 2.36 (1H, m, CHCH₂CH₃), 2.25 – 2.17 (1H, m, H2), 2.09 – 2.01 (1H, m, CHCH₂CH₃), 1.99 – 1.90 (1H, m, H2), 1.84 – 1.47 (6H, m, cPeH), 1.05 (3H, t, $J = 7.6$ Hz, CHCH₂CH₃); δ_C (CDCl₃, 126 MHz): 170.9 (CO₂CH₃), 159.3 (C7), 156.6 (C6), 154.2 (C4), 131.1 (C5), 64.0 (C3), 60.2 (CHCH₂CH₃), 52.5 (CO₂CH₃), 30.3 (C2), 27.3 (C2'), 23.0 (C1), 22.9 (C1'), 22.9 (CHCH₂CH₃), 11.6 (CHCH₂CH₃)

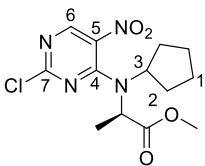
Methyl N-(2-Chloro-5-nitropyrimidin-4-yl)-N-cyclopentyl-D-valinate, 12d

Aminobutanoate **10d** (1.26 g, 6.32 mmol) was reacted with pyrimidine **15** (1.35 g, 6.95 mmol) using general method **3** to afford the title compound **12d** as a brown oil (1.06 g, 47%). LCMS purity >95%, ret. time 1.63 mins; HRMS (ESI +ve): found $[M+H]^+$

357.1312, $[C_{15}H_{22}ClN_4O_4]^+$ requires 357.1324; $[\alpha]_D^{22.7}$: $+118.4^\circ$ (c 1.0, MeOH); δ_H (CDCl₃, 500 MHz): 8.67 (1H, s, H6), 3.74 (3H, s, CO₂CH₃), 3.62 – 3.56 (1H, m, H3), 3.45 (1H, d, $J = 8.8$ Hz, CHCH(CH₃)₂), 2.86 – 2.76 (1H, m, CHCH(CH₃)₂), 1.93 – 1.47 (8H, m, cPeH), 1.23 (3H, d, $J = 7.6$ Hz, CH(CH₃)(C'H₃)), 0.90 (3H, d, $J = 7.6$ Hz, CH(CH₃)(C'H₃)); δ_C (CDCl₃, 126 MHz): 170.9 (CO₂CH₃), 159.4 (C7), 156.6 (C6),

154.3 (C4), 130.7 (C5), 64.3 ($\underline{\text{CHCH}}(\text{CH}_3)_2$), 64.0 (C3), 53.4 ($\text{CO}_2\underline{\text{CH}}_3$), 30.5 (C2), 27.7 ($\text{CH}\underline{\text{CH}}(\text{CH}_3)_2$), 22.6 (C1), 22.4 (C1'), 22.3 ($\text{CH}(\underline{\text{CH}}_3)(\text{C}'\text{H}_3)$), 19.9 ($\text{CH}(\text{CH}_3)(\underline{\text{C}}'\text{H}_3)$)

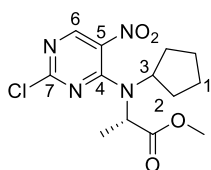
Methyl(*R*)-2-((2-chloro-5-nitropyrimidin-4-yl)(cyclopentyl)amino)propanoate, 12e



Aminobutanoate **10e** (200 mg, 1.17 mmol) was reacted with pyrimidine **11** (249 mg, 1.28 mmol) using general method **3** to afford the title compound **12e** as a brown solid (90 mg, 23%). LCMS purity >95%, ret. time 1.53 mins; HRMS (ESI +ve): found $[\text{M}+\text{H}]^+$

329.1026, $[\text{C}_{13}\text{H}_{18}\text{ClN}_4\text{O}_4]^+$ requires 329.1011; $[\alpha]_D^{22.0}$: +240.3° (c 1.0, MeOH); δ_{H} (CDCl_3 , 500 MHz): 8.64 (1H, s, H6), 4.00 (1H, q, $J = 6.7$ Hz, $\underline{\text{CHCH}}_3$), 3.77 (3H, s, $\text{CO}_2\underline{\text{CH}}_3$), 3.60 (1H, quin., $J = 8.1$, H3), 2.29 – 2.20 (1H, m, H2), 2.01 – 1.94 (1H, m, H2), 1.91 – 1.84 (1H, m, H2), 1.80 – 1.71 (2H, m, H1), 1.68 (3H, d, $J = 6.7$ Hz, CHCH_3), 1.65 – 1.53 (3H, m, cPeH); δ_{C} (CDCl_3 , 126 MHz): 171.0 ($\underline{\text{CO}}_2\underline{\text{CH}}_3$), 159.4 (C7), 156.5 (C6), 153.6 (C4), 130.9 (C5), 63.4 (C3), 54.3 ($\underline{\text{CHCH}}_3$), 52.7 ($\text{CO}_2\underline{\text{CH}}_3$), 29.9 (C2), 27.3 (C2'), 23.9 (C1), 23.8 (C1'), 16.0 ($\text{CH}\underline{\text{CH}}_3$)

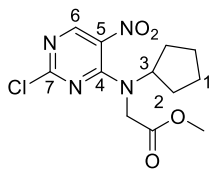
Methyl(*S*)-2-((2-chloro-5-nitropyrimidin-4-yl)(cyclopentyl)amino)propanoate, 12f



Aminobutanoate **10f** (1.15 g, 6.71 mmol) was reacted with pyrimidine **11** (1.43 g, 7.39 mmol) using general method **3** to afford the title compound **12f** as a yellow solid (1.29 g, 58%).

LCMS purity >95%, ret. time 1.50 mins; HRMS (ESI +ve): found $[\text{M}+\text{H}]^+$ 343.1171, $[\text{C}_{13}\text{H}_{18}\text{ClN}_4\text{O}_4]^+$ requires 343.1173; $[\alpha]_D^{23.4}$: -164.2° (c 1.0, MeOH); δ_{H} (CDCl_3 , 500 MHz): 8.64 (1H, s, H6), 4.00 (1H, q, $J = 6.7$ Hz, $\underline{\text{CHCH}}_3$), 3.77 (3H, s, $\text{CO}_2\underline{\text{CH}}_3$), 3.60 (1H, quin., $J = 8.2$ Hz, H3), 2.29 – 2.20 (1H, m, H2), 2.01 – 1.94 (1H, m, H2), 1.91 – 1.84 (1H, m, H2), 1.80 – 1.71 (2H, m, H1), 1.69 (3H, d, $J = 6.7$ Hz, CHCH_3), 1.65 – 1.55 (3H, m, cPeH); δ_{C} (CDCl_3 , 126 MHz): 171.0 ($\underline{\text{CO}}_2\underline{\text{CH}}_3$), 159.4 (C7), 156.5 (C6), 153.6 (C4), 130.9 (C5), 63.5 (C3), 54.3 ($\underline{\text{CHCH}}_3$), 52.6 ($\text{CO}_2\underline{\text{CH}}_3$), 29.9 (C2), 27.3 (C2'), 23.9 (C1), 23.8 (C1'), 16.0 ($\text{CH}\underline{\text{CH}}_3$)

Methyl 2-((2-chloro-5-nitropyrimidin-4-yl)-cyclopentyl-amino)acetate, 12g

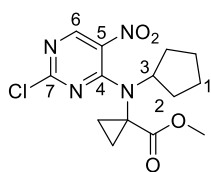


Aminoacetate **10g** (766 mg, 3.95 mmol) was reacted with pyrimidine **11** (431 mg, 7.19 mmol) using general method **3** to afford the title compound **12g** as a yellow solid (577 mg, 51%).

LCMS purity >95%, ret. time 1.45 mins; HRMS (ESI +ve): found $[\text{M}+\text{H}]^+$ 315.0850, $[\text{C}_{12}\text{H}_{16}\text{ClN}_4\text{O}_4]^+$ requires 315.0860; δ_{H} (CDCl_3 , 500 MHz): 8.65 (1H, s, H6), 4.17 (1H, s, NCH_2), 3.98 – 3.88 (1H, m, H3), 3.79 (3H, s, $\text{CO}_2\underline{\text{CH}}_3$), 2.16 – 2.07 (2H, m, H2), 1.78 – 1.70 (2H, m, H1), 1.64 – 1.53 (4H, m, cPeH); δ_{C} (CDCl_3 , 126

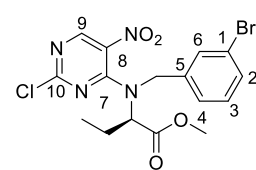
MHz): 168.8 (CO_2CH_3), 160.2 (C7), 156.3 (C6), 154.9 (C4), 131.1 (C5), 63.5 (C5), 62.3 (C3), 52.7 (CO_2CH_3), 46.8 (NCH_2), 29.0 (C2), 23.9 (C1)

Methyl 1-((2-chloro-5-nitropyrimidin-4-yl)-cyclopentyl-amino)cyclopropanecarboxylate, 12h



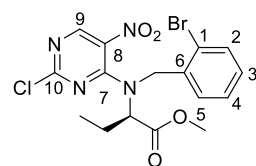
Carboxylate **10h** (667 mg, 3.64 mmol) was reacted with pyrimidine **11** (777 mg, 4.00 mmol) using general method **3** to afford the title compound **12h** as a yellow oil (1.10 g, 89%). LCMS purity >95%, ret. time 1.56 mins; HRMS (ESI +ve): found $[\text{M}+\text{H}]^+$ 341.1005, $[\text{C}_{14}\text{H}_{18}\text{ClN}_4\text{O}_4]^+$ requires 341.1011; δ_{H} (CDCl_3 , 500 MHz): 8.65 (1H, s, H6), 4.23 (1H, quin., $J = 8.8$ Hz, H3), 3.84 (3H, s, CO_2CH_3), 2.27 – 2.10 (2H, m, H2), 2.08 – 1.93 (4H, m, cPeH), 1.66 – 1.54 (4H m, 2 x H1 & $\text{C}(\text{CH}_2)_2$), 1.35 – 1.30 (1H, m, $\text{C}(\text{CH}_2)_2$), 1.14 – 1.09 (1H, m, $\text{C}(\text{CH}_2)_2$); δ_{C} (CDCl_3 , 126 MHz): 171.4 (CO_2CH_3), 159.7 (C7), 156.1 ($\text{C}(\text{CH}_2)_2$ & C6), 15.42 (C4), 132.7 (C5), 67.2 (C3), 52.9 (CO_2CH_3), 30.3 (C2), 29.8 (C2'), 25.3 (C1), 20.7 ($\text{C}(\text{CH}_2)(\text{C}'\text{H}_2)$), 18.5 ($\text{C}(\text{CH}_2)(\text{C}'\text{H}_2)$)

Methyl (R)-2-((3-bromobenzyl)(2-chloro-5-nitropyrimidin-4-yl)amino)butanoate, 12i



Aminobutanoate **10i** (1.30 g, 4.54 mmol) was reacted with pyrimidine **11** (0.97 g, 5.00 mmol) using general method **3** to afford the title compound **12i** as a yellow oil (1.81 g, 90%). LCMS purity >95%, ret. time 1.64 mins; HRMS (ESI +ve): found $[\text{M}+\text{H}]^+$ 443.0118, $[\text{C}_{16}\text{H}_{17}\text{BrClN}_4\text{O}_4]^+$ requires 443.0122; $[\alpha]_{\text{D}}^{22.0}$: +12.0° (c 1.0, MeOH); δ_{H} (CDCl_3 , 500 MHz): 8.64 (1H, s, H9), 7.45 (1H, s, H6), 7.41 (1H, d, $J = 8.2$ Hz, H2), 7.23 (1H, d, $J = 7.6$ Hz, H4), 7.17 – 7.13 (1H, m, H3), 4.75 (1H, d, $J = 15.8$ Hz, ArCHH), 4.73 – 4.68 (1H, m, CHCH_2CH_3), 4.59 (1H, d, $J = 15.8$ Hz, ArCHH), 3.82 (3H, s, CO_2CH_3), 2.32 – 2.23 (1H, m, CHCHHCH_3), 2.10 – 2.00 (1H, m, CHCHHCH_3), 1.07 (3H, t, $J = 7.4$ Hz, CHCH_2CH_3); δ_{C} (CDCl_3 , 126 MHz): 170.7 (CO_2CH_3), 160.6 (C10), 156.8 (C9), 155.3 (C7), 135.7 (C5), 131.8 (C6), 131.6 (C8), 131.4 (C2), 130.3 (C3), 127.3 (C4), 122.7 (C1), 64.9 (CHCH_2CH_3), 52.8 (ArCH_2), 52.6 (CO_2CH_3), 23.5 (CHCH_2CH_3), 11.2 (CHCH_2CH_3)

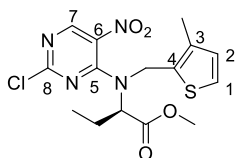
Methyl (R)-2-((2-bromobenzyl)(2-chloro-5-nitropyrimidin-4-yl)amino)butanoate, 12j



Aminobutanoate **10j** (1.00 g, 3.49 mmol) was reacted with pyrimidine **11** (0.75 g, 3.84 mmol) using general method **3** to afford the title compound **12j** as a yellow oil (1.28 g, 83%).

LCMS purity >95%, ret. time 0.99 mins; HRMS (ESI +ve): found $[M+H]^+$ 445.0102, $[C_{16}H_{17}BrClN_4O_4]^+$ requires 445.0121; $[\alpha]_D^{22.2}$: +27.0° (c 1.0, MeOH); δ_H (CDCl₃, 500 MHz): 8.71 (1H, s, H9), 7.58 (1H, dd, J = 8.0, 1.1 Hz, H2), 7.37 – 7.34 (1H, m, H5), 7.30 – 7.25 (1H, m, H4), 7.21 – 7.17 (1H, m, H3), 4.69 (1H, d, J = 16.5 Hz, ArCHH), 4.63 (1H, d, J = 16.5 Hz, ArCHH), 4.39 – 4.34 (1H, m, CHCH₂CH₃), 3.71 (3H, s, CO₂CH₃), 2.34 – 2.25 (1H, m, CHCHHCH₃), 2.10 – 2.00 (1H, m, CHCHHCH₃), 1.07 (3H, t, J = 7.6 Hz, CHCH₂CH₃); δ_C (CDCl₃, 126 MHz): 170.3 (CO₂CH₃), 157.2 (C10), 156.6 (C9), 155.3 (C7), 133.2 (C2), 132.6 (C6), 131.7 (C8), 129.8 (C3 & C5), 127.5 (C4), 124.4 (C1), 64.3 (CHCH₂CH₃), 52.8 (ArCH₂), 52.4 (CO₂CH₃), 23.5 (CHCH₂CH₃), 11.4 (CHCH₂CH₃)

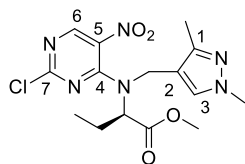
Methyl (*R*)-2-((2-chloro-5-nitropyrimidin-4-yl)((3-methylthiophen-2-yl)methyl)amino)butanoate, 12k



Aminobutanoate **10k** (0.77 g, 3.39 mmol) was reacted with pyrimidine **11** (0.72 g, 3.72 mmol) using general method **3** to afford the title compound **12k** as a yellow solid (1.18 g, 91%).

LCMS purity >95%, ret. time 1.67 mins; HRMS (ESI +ve): found $[M+H]^+$ 385.0732, $[C_{15}H_{18}ClN_4O_4S]^+$ requires 386.0732; $[\alpha]_D^{22.1}$: +4.9° (c 1.0, MeOH); δ_H (CDCl₃, 500 MHz): 8.65 (1H, s, H7), 7.15 (1H, d, J = 5.2 Hz, H1), 6.70 (1H, d, J = 5.2 Hz, H2), 4.92 (1H, dd, J = 5.4, 4.1 Hz, CHCH₂CH₃), 4.75 (2H, s, ArCH₂), 3.80 (3H, s, CO₂CH₃), 2.30 – 2.20 (1H, m, CHCHHCH₃), 2.16 (3H, s, ArCH₃), 2.07 – 2.00 (1H, m, CHCHHCH₃), 1.09 (3H, t, J = 7.4 Hz, CHCH₂CH₃); δ_C (CDCl₃, 126 MHz): 170.8 (CO₂CH₃), 160.5 (C8), 156.4 (C7), 155.3 (C5), 138.4 (C4), 133.1 (C6), 131.6 (C3), 129.9 (C2), 126.1 (C1), 64.1 (CHCH₂CH₃), 52.5 (CO₂CH₃), 46.7 (NCH₂), 23.1 (CHCH₂CH₃), 13.8 (ArCH₃), 11.1 (CHCH₂CH₃)

Methyl (*R*)-2-((2-chloro-5-nitropyrimidin-4-yl)((1,3-dimethylpyrazol-4-yl)methyl)amino)butanoate, 12l

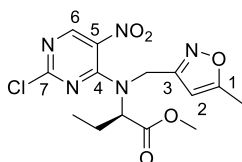


Aminobutanoate **10l** (0.72 g, 3.20 mmol) was reacted with pyrimidine **11** (0.68 g, 3.52 mmol) using general method **3** to afford the title compound **12l** as a yellow solid (299 mg, 24%).

LCMS purity >95%, ret. time 1.48 mins; HRMS (ESI +ve): found $[M+H]^+$ 383.1264, $[C_{15}H_{20}ClN_6O_4]^+$ requires 383.1234; $[\alpha]_D^{22.1}$: +2.1° (c 1.0, MeOH); δ_H (CDCl₃, 500 MHz): 8.66 (1H, s, H6), 7.19 (1H, s, H3), 4.75 (1H, dd, J = 10.1, 4.7 Hz, CHCH₂CH₃), 4.41 (2H, d, J = 4.4 Hz, ArCH₂), 3.78 (3H, s, CO₂CH₃), 3.75 (3H, s, NCH₃), 2.29 – 2.19 (1H, m, CHCHHCH₃), 2.14 (3H, s, ArCH₃), 2.10 – 2.01 (1H, m, CHCHHCH₃), 1.04 (3H, t, J = 7.4 Hz, CHCH₂CH₃); δ_C (CDCl₃, 126 MHz): 171.0

(CO₂CH₃), 160.4 (C7), 156.3 (C6), 154.8 (C4), 147.7 (C1), 131.7 (C5), 131.6 (C3), 110.4 (C2), 64.0 (CHCH₂CH₃). 52.5 (CO₂CH₃), 44.5 (C4), 38.9 (NCH₃), 23.0 (CHCH₂CH₃), 11.4 (ArCH₃), 11.1 (CHCH₂CH₃)

Methyl (*R*)-2-((2-chloro-5-nitropyrimidin-4-yl)((5-methylisoxazol-3-yl)methyl)amino)butanoate, 12m

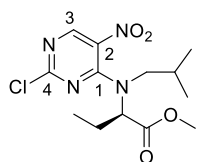


Aminobutanoate **10m** (0.50 g, 2.34 mmol) was reacted with pyrimidine **11** (0.50 g, 2.59 mmol) using general method **3** to afford the title compound **12m** as a yellow solid (820 mg, 94%).

LCMS purity >95%, ret. time 1.67 mins; HRMS (ESI +ve): found

[M+H]⁺ 370.0896, [C₁₄H₁₆ClN₅O₅]⁺ requires 370.0913; [α]_D^{22.6}: +26.3° (c 1.0, MeOH); δ_H (CDCl₃, 500 MHz): 8.75 (1H, s, H6), 6.09 (1H, d, *J* = 1.0 Hz, H2), 4.75 (1H, d, *J* = 16.1 Hz, ArHH), 4.68 (1H, d, *J* = 16.1 Hz, ArHH), 4.64 – 4.58 (1H, m, CHCH₂CH₃), 3.79 (3H, s, CO₂CH₃), 2.39 (3H, d, *J* = 1.0 Hz, ArCH₃), 2.27 – 2.19 (1H, m, CHCH₂CH₃), 2.10 – 2.01 (1H, m, CHCH₂CH₃), 0.99 (3H, t, *J* = 7.4 Hz, CHCH₂CH₃); δ_C (CDCl₃, 126 MHz): 170.7 (CO₂CH₃), 170.4 (C1), 160.6 (C7), 158.4 (C3), 157.0 (C6), 155.4 (C4), 131.6 (C5), 101.6 (C2), 64.3 (CHCH₂CH₃), 52.6 (CO₂CH₃), 45.1 (ArCH₂), 23.1 (CHCH₂CH₃), 12.3 (ArCH₃), 11.1 (CHCH₂CH₃)

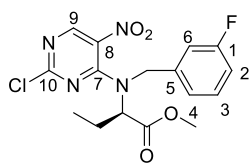
Methyl (*R*)-2-((2-chloro-5-nitropyrimidin-4-yl)-isobutyl-amino)butanoate, 12n



Aminobutanoate **10n** (0.30 g, 1.73 mmol) was reacted with pyrimidine (0.37 g, 1.90 mmol) using general method **3** to afford the title compound **12n** as a yellow oil (490 mg, 86%). LCMS purity >95%, ret. time 1.48 mins; HRMS (ESI +ve): found [M+H]⁺ 331.1162,

[C₁₃H₂₀ClN₄O₄]⁺ requires 331.1168; [α]_D^{22.3}: +182° (c 1.0, MeOH); δ_H (CDCl₃, 500 MHz): 8.68 (1H, s, H3), 4.25 – 4.17 (1H, m, CHCH₂CH₃), 3.74 (3H, s, CO₂CH₃), 3.22 (1H, dd, *J* = 13.9, 8.8 Hz, NCHH), 3.07 (1H, dd, *J* = 14.8, 6.3 Hz, NCHH), 2.21 – 2.13 (1H, m, CHCH₂CH₃), 2.07 – 1.98 (1H, m, CHCH₂CH₃), 1.96 – 1.88 (1H, m, CH(CH₃)₂), 1.02 (3H, t, *J* = 7.4 Hz, CHCH₂CH₃), 0.87 (3H, d, *J* = 6.6 Hz, CH(CH₃)(C'H₃)), 0.80 (3H, d, *J* = 6.6 Hz, CH(CH₃)(C'H₃)); δ_C (CDCl₃, 126 MHz): 170.2 (CO₂CH₃), 160.2 (C4), 156.6 (C3), 156.5 (C1), 131.7 (C2), 66.1 (CHCH₂CH₃), 58.2 (NCH₂), 52.4 (CO₂CH₃), 26.4 (CH(CH₃)₂), 22.7 (CHCH₂CH₃), 20.3 (CH(CH₃)(C'H₃)), 19.9 (CH(CH₃)(C'H₃)), 10.9 (CHCH₂CH₃)

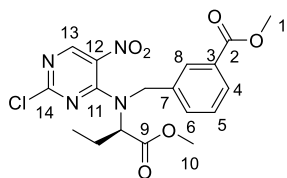
Methyl (R)-2-((2-chloro-5-nitropyrimidin-4-yl)(3-fluorobenzyl)amino)butanoate, 12o



Aminobutanoate **10o** (690 mg, 3.06 mmol) was reacted with pyrimidine **11** (654 mg, 3.37 mmol) using general method **3** to afford the title compound **12o** as a yellow gum (910 mg, 78%).

LCMS purity >95%, ret. time 1.57 mins; HRMS (ESI +ve): found $[M+H]^+$ 383.0907, $[C_{16}H_{17}ClFN_4O_4]^+$ requires 383.0917; $[\alpha]_D^{22.6}$: +12.5° (c 1.0, MeOH); δ_H (CDCl₃, 500 MHz): 8.62 (1H, s, H7), 7.26 – 7.23 (1H, m, H3), 7.06 – 7.00 (2H, m, H4 & H6), 6.97 (1H, td, J = 8.4, 2.5 Hz, H2), 4.93 (1H, dd, J = 9.8, 5.0 Hz, CHCH₂CH₃), 4.80 (1H, d, J = 15.8 Hz, ArCHH), 4.53 (1H, d, J = 15.8 Hz, ArCHH), 3.82 (3H, s, CO₂CH₃), 2.32 – 2.23 (1H, m, CHCH₂CH₃), 2.12 – 2.01 (1H, m, CHCH₂CH₃), 1.08 (3H, t, J = 7.4 Hz, CHCH₂CH₃); δ_C (CDCl₃, 126 MHz): 170.8 (CO₂CH₃), 162.8 (d, J_{C-F} = 247 Hz, C1), 160.7 (C10), 156.7 (C9), 155.4 (C7), 135.9 (C6), 131.7 (C8), 130.4 (d, J_{C-F} = 8.2 Hz, C3), 124.4 (d, J_{C-F} = 2.8 Hz, C4), 115.6 (d, J_{C-F} = 22.9 Hz, C6), 115.4 (d, J_{C-F} = 21.1 Hz, C2), 65.0 (CHCH₂CH₃), 52.8 (ArCH₂), 52.6 (OCH₃), 23.5 (CHCH₂CH₃), 11.2 (CHCH₂CH₃); $\delta_{F(H)}$ (CDCl₃, 471 MHz): -111.7

Methyl (R)-2-((2-chloro-5-nitropyrimidin-4-yl)(1-methoxy-1-oxobutan-2-yl)amino)methyl)benzoate, 12p

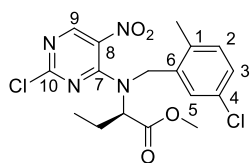


Aminobutanoate **10p** (1.30 g, 4.90 mmol) was reacted with pyrimidine **11** (1.05 g, 5.39 mmol) using general method **3** to afford the title compound **12p** as a yellow oil (1.80 g, 87%).

LCMS purity >95%, ret. time 1.55 mins; HRMS (ESI +ve): found $[M+H]^+$ 423.1071, $[C_{18}H_{20}ClN_4O_6]^+$ requires 423.1066; $[\alpha]_D^{22.6}$: +20.8° (c 1.0, MeOH); δ_H (CDCl₃, 500 MHz): 8.55 (1H, s, H14), 7.94 – 7.89 (2H, m, H4 & H8), 7.47 (1H, d, J = 7.9 Hz, H6), 7.37 – 7.30 (1H, m, H5), 4.79 (1H, d, J = 15.8 Hz, ArCHH), 4.72 – 4.66 (1H, m, CHCH₂CH₃), 4.64 (1H, d, J = 15.8 Hz, ArCHH), 3.87 (3H, s, H1), 3.78 (3H, s, H10), 2.30 – 2.20 (1H, m, CHCH₂CH₃), 2.08 – 2.01 (1H, m, CHCH₂CH₃), 1.04 (3H, t, J = 7.4 Hz, CHCH₂CH₃); δ_C (CDCl₃, 126 MHz): 170.5 (C9), 166.2 (C1), 160.4 (C14), 156.6 (C13), 155.1 (C11), 133.8 (C7), 132.9 (C6), 131.5 (C12), 130.6 (C3), 129.8 (C4), 129.3 (C8), 128.7 (C5), 64.9 (CHCH₂CH₃), 53.1 (ArCH₂), 52.4 (C10), 52.1 (C1), 23.3 (CHCH₂CH₃), 11.0 (CHCH₂CH₃)

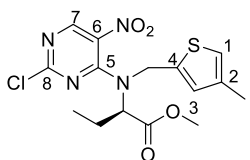
Methyl (R)-2-((5-chloro-2-methylbenzyl)(2-chloro-5-nitropyrimidin-4-yl)amino)butanoate, 12q

Aminobutanoate **10q** (1.17 g, 4.58 mmol) was reacted with pyrimidine **11** (976 mg, 5.03 mmol) using general method **3** to afford the title compound **12q** as a yellow oil



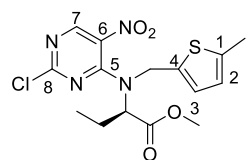
(1.06 g, 56%). LCMS purity >95%, ret. time 1.63 mins; HRMS (ESI +ve): found $[M+H]^+$ 413.0772, $[C_{17}H_{19}Cl_2N_4O_4]^+$ requires 413.0778; $[\alpha]_D^{22.4}$: +28.4° (c 1.0, MeOH); δ_H (CDCl₃, 500 MHz): 8.67 (1H, s, H9), 7.22 (1J, d, J = 2.0 Hz, H5), 7.17 (1H, dd, J = 8.1, 2.0 Hz, H3), 7.09 (1H, d, J = 8.0 Hz, H2), 4.55 – 4.50 (3H, m, ArCH₂ & CHCH₂CH₃), 3.75 (CO₂CH₃), 2.34 – 2.26 (1H, m, CHCH₂CH₃), 2.25 (3H, s, ArCH₃), 2.10 – 2.01 (1H, m, CHCH₂CH₃), 1.08 (3H, t, J = 7.4 Hz, CHCH₂CH₃); δ_C (CDCl₃, 126 MHz): 170.3 (CO₂CH₃), 160.5 (C10), 156.6 (C9), 155.1 (C7), 135.1 (C1), 133.2 (C6), 132.1 (C2), 131.9 (C4), 131.7 (C8), 128.2 (C3), 127.8 (C5), 64.4 (CHCH₂CH₃), 52.5 (CO₂CH₃), 50.6 (ArCH₂), 23.4 (CHCH₂CH₃), 18.8 (ArCH₃), 11.3 (CHCH₂CH₃)

Methyl (R)-2-((2-chloro-5-nitropyrimidin-4-yl)((4-methylthiophen-2-yl)methyl)amino)butanoate, 12r



Aminobutanoate **10r** (1.26 g, 4.85 mmol) was reacted with pyrimidine **11** (1.04 g, 5.34 mmol) using general method **3** to afford the title compound **12r** as a yellow oil (1.46 g, 72%). LCMS purity >95%, ret. time 1.60 mins; HRMS (ESI +ve): found $[M+H]^+$ 385.0738, $[C_{15}H_{18}ClN_4O_4S]^+$ requires 385.0732; $[\alpha]_D^{22.5}$: +5.6° (c 1.0, MeOH); δ_H (CDCl₃, 500 MHz): 8.70 (1H, s, H7), 6.82 – 6.81 (1H, m, H1), 6.71 (1H, s, H3), 4.95 – 4.80 (3H, m, CHCH₂CH₃ & ArCH₂), 3.82 (3H, s, CO₂CH₃), 2.31 – 2.21 (1H, m, CHCH₂CH₃), 2.18 (3H, s, ArCH₃), 2.09 – 1.99 (1H, m, CHCH₂CH₃), 1.06 (3H, t, J = 7.4 Hz, CHCH₂CH₃); δ_C (CDCl₃, 126 MHz): 170.9 (CO₂CH₃), 160.5 (C8), 156.7 (C7), 155.3 (C5), 137.2 (C2), 135.1 (C4), 133.1 (C3), 131.4 (C7), 122.9 (C1), 64.4 (CHCH₂CH₃), 52.6 (CO₂CH₃), 48.6 (ArCH₂), 23.3 (CHCH₂CH₃), 15.5 (ArCH₃), 11.1 (CHCH₂CH₃)

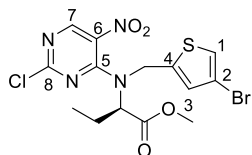
Methyl (R)-2-((2-chloro-5-nitropyrimidin-4-yl)((5-methylthiophen-2-yl)methyl)amino)butanoate, 12s



Aminobutanoate **10s** (892 mg, 3.92 mmol) was reacted with pyrimidine **11** (837 mg, 4.32 mmol) using general method **3** to afford the title compound **12s** as a yellow gum (1.30 g, 86%). LCMS purity >95%, ret. time 1.60 mins; HRMS (ESI +ve): found $[M+H]^+$ 385.0729, $[C_{15}H_{17}ClN_4O_4S]^+$ requires 385.0732; $[\alpha]_D^{22.4}$: -2.8° (c 1.0, MeOH); δ_H (CDCl₃, 500 MHz): 8.70 (1H, s, H7), 6.67 (1H, d, J = 3.5 Hz, H3), 6.53 – 6.51 (1H, m, H2), 4.98 – 4.93 (1H, m, CHCH₂CH₃), 4.84 (1H, d, J = 15.9 Hz, ArCH₂), 4.81 (1H, d, J = 15.9 Hz, ArCH₂), 3.82 (3H, s, CO₂CH₃), 2.39 (3H, s, ArCH₃), 2.31 – 2.21 (1H, m, CHCH₂CH₃), 2.08 – 2.00 (1H, m, CHCH₂CH₃), 1.07 (3H, t, J = 7.4 Hz,

CHCH₂CH₃); δ_{C} (CDCl₃, 126 MHz): 171.0 (CO₂CH₃), 160.5 (C8), 156.8 (C7), 155.3 (C5), 142.8 (C1), 132.7 (C4), 131.4 (C6), 131.0 (C3), 124.5 (C2), 64.3 (CHCH₂CH₃), 52.6 (CO₂CH₃), 48.7 (ArCH₂), 23.3 (CHCH₂CH₃), 15.5 (ArCH₃), 11.1 (CHCH₂CH₃)

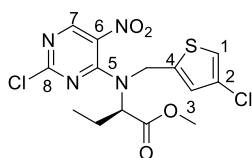
Methyl (R)-2-((2-chloro-5-nitropyrimidin-4-yl)((4-bromothiophen-2-yl)methyl)amino)butanoate, 12t



Aminobutanoate **10t** (1.40 g, 4.79 mmol) was reacted with pyrimidine **11** (1.02 g, 5.27 mmol) using general method **3** to afford the title compound **12t** as a brown solid (1.62 g, 75%).

LCMS purity >95%, ret. time 1.62 mins; HRMS (ESI +ve): found $[M+H]^+$ 450.9644, $[C_{14}H_{15}BrClN_4O_4S]^+$ requires 450.9658; $[\alpha]_D^{22.5}$: +7.6° (c 1.0, MeOH); δ_{H} (CDCl₃, 500 MHz): 8.75 (1H, s, H7), 7.17 (1H, d, J = 1.2 Hz, H1), 6.91 – 6.89 (1H, m, H3), 4.88 (2H, dd, J = 7.3, 1.0 Hz, ArCH₂), 4.71 – 4.63 (1H, m, CHCH₂CH₃), 3.81 (3H, s, CO₂CH₃), 2.30 – 2.22 (1H, m, CHCH₂CH₃), 2.07 – 1.95 (1H, m, CHCH₂CH₃), 1.02 (3H, t, J = 7.5 Hz, CHCH₂CH₃); δ_{C} (CDCl₃, 126 MHz): 170.8 (CO₂CH₃), 160.9 (C8), 157.1 (C7), 155.5 (C5), 137.6 (C4), 132.6 (C3), 131.4 (C6), 124.8 (C1), 109.0 (C2), 64.7 (CHCH₂CH₃), 52.7 (CO₂CH₃), 47.6 (ArCH₂), 23.6 (CHCH₂CH₃), 11.1 (CHCH₂CH₃)

Methyl (R)-2-((2-chloro-5-nitropyrimidin-4-yl)((4-chlorothiophen-2-yl)methyl)amino)butanoate, 12u

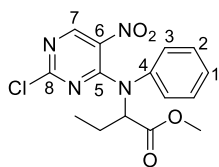


Aminobutanoate **10u** (1.33 g, 5.37 mmol) was reacted with pyrimidine **11** (1.15 g, 5.91 mmol) using general method **3** to afford the title compound **12u** as a brown solid (1.26 g, 58%).

LCMS purity >95%, ret. time 1.61 mins; HRMS (ESI +ve): found $[M+H]^+$ 405.0178, $[C_{14}H_{15}Cl_2N_4O_4S]^+$ requires 405.0186; $[\alpha]_D^{22.5}$: +7.6° (c 1.0, MeOH); δ_{H} (CDCl₃, 500 MHz): 8.76 (1H, s, H7), 7.05 (1H, d, J = 1.6 Hz, H1), 6.87 – 6.85 (1H, m, H3), 4.87 (2H, dd, J = 7.9, 1.0 Hz, ArCH₂), 4.73 – 4.64 (1H, m, CHCH₂CH₃), 3.82 (3H, s, CO₂CH₃), 2.31 – 2.22 (1H, m, CHCH₂CH₃), 2.14 – 1.95 (1H, m, CHCH₂CH₃), 1.03 (3H, t, J = 7.5 Hz, CHCH₂CH₃); δ_{C} (CDCl₃, 126 MHz): 170.9 (CO₂CH₃), 157.1 (C8), 155.5 (C5), 136.9 (C4), 130.6 (C6), 130.3 (C3), 12.5 (C2), 121.9 (C1), 64.7 (CHCH₂CH₃), 52.7 (CO₂CH₃), 47.8 (ArCH₂), 23.6 (CHCH₂CH₃), 11.1 (CHCH₂CH₃)

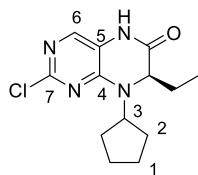
Methyl 2-((2-chloro-5-nitropyrimidin-4-yl)(phenyl)amino)butanoate, 12v

Aminobutanoate **10v** (660 mg, 3.42 mmol) was reacted with pyrimidine **11** (730 mg, 3.76 mmol) using general method **3** to afford the title compound **12v** as a yellow solid (900 mg, 75%). LCMS purity >95%, ret. time 1.51 mins; HRMS (ESI +ve): found



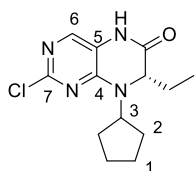
$[M+H]^+$ 351.0843, $[C_{15}H_{16}ClN_4O_4]^+$ requires 351.0855; δ_H ($CDCl_3$, 500 MHz): 8.57 (1H, s, H7), 7.43 – 7.35 (2H, m, H2), 7.33 (1H, tt, $J = 7.3, 1.0$ Hz, H1), 7.23 – 7.15 (2H, m, H3), 4.68 (1H, dd, $J = 9.5, 5.7$ Hz, $CHCH_2CH_3$), 3.77 (3H, s, CO_2CH_3), 2.34 – 2.16 (2H, m, $CHCH_2CH_3$), 1.16 (3H, t, $J = 7.4$ Hz, $CHCH_2CH_3$); δ_C ($CDCl_3$, 126 MHz): 170.5 (CO_2CH_3), 160.3 (C8), 155.8 (C7), 154.2 (C5), 142.7 (C4), 132.6 (C6), 130.1 (C2), 128.4 (C1), 125.2 (C3), 67.8 ($CHCH_2CH_3$), 52.5 (CO_2CH_3), 22.0 ($CHCH_2CH_3$), 11.6 ($CHCH_2CH_3$)

(R)-2-chloro-8-cyclopentyl-7-ethyl-7,8-dihydropteridin-6(5H)-one, 13a



Aminobutanoate **12a** (1.00 g, 2.92 mmol) was subjected to general method **4** to afford the title compound **13a** as a yellow solid (345 mg, 42%). LCMS purity >95%, ret. time 1.51 mins; HRMS (ESI +ve): found $[M+H]^+$ 281.1163, $[C_{13}H_{18}ClN_4O]^+$ requires 281.1169; $[\alpha]_D^{22.1}$: -96.2° (c 1.0, MeOH); δ_H ($CDCl_3$, 500 MHz): 9.39 (1H, s, NH), 7.68 (1H, s, H6), 4.37 – 4.29 (1H, m, H3), 4.21 (1H, dd, $J = 7.4, 3.6$ Hz, $CHCH_2CH_3$), 2.11 – 2.05 (1H, m, H2), 2.00 – 1.74 (7H, m, cPeH & $CHCH_2CH_3$), 1.70 – 1.61 (2H, m, H1), 0.96 (3H, t, $J = 7.6$ Hz, $CHCH_2CH_3$); δ_C ($CDCl_3$, 126 MHz): 165.7 (CONH), 154.2 (C7), 151.8 (C4), 138.9 (C6), 118.0 (C5), 60.9 ($CHCH_2CH_3$), 59.6 (C3), 29.4 (C2), 29.2 (C2'), 26.9 ($CHCH_2CH_3$), 23.9 (C1), 23.8 (C1'), 8.8 ($CHCH_2CH_3$)

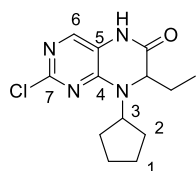
(S)-2-chloro-8-cyclopentyl-7-ethyl-7,8-dihydropteridin-6(5H)-one, 13b



Aminobutanoate **12b** (815 mg, 2.38 mmol) was subjected to general method **4** to afford the title compound **13b** as a yellow solid 186 mg, 28%). LCMS purity >95%, ret. time 1.51 mins; HRMS (ESI +ve): found $[M+H]^+$ 281.1163, $[C_{13}H_{18}ClN_4O]^+$ requires 281.1169; $[\alpha]_D^{22.1}$: $+96.2^\circ$ (c 1.0, MeOH); δ_H ($CDCl_3$, 500 MHz): 9.67 (1H, s, NH), 7.70 (1H, s, H6), 4.32 (1H, quin, $J = 8.4$ Hz, H3), 4.21 (1H, dd, $J = 7.3, 3.5$ Hz, $CHCH_2CH_3$), 2.12 – 2.04 (1H, m, H2), 2.00 – 1.73 (7H, m, cPeH & $CHCH_2CH_3$), 1.70 – 1.60 (2H, m, H1), 0.94 (3H, t, $J = 7.6$ Hz, $CHCH_2CH_3$); δ_C ($CDCl_3$, 126 MHz): 165.9 (CONH), 154.2 (C7), 151.8 (C4), 138.9 (C6), 118.1 (C5), 60.9 ($CHCH_2CH_3$), 59.3 (C3), 29.4 (C2), 29.2 (C2'), 27.2 ($CHCH_2CH_3$), 22.9 (C1), 22.8 (C1'), 8.8 ($CHCH_2CH_3$)

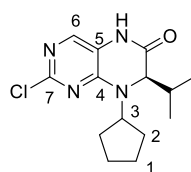
2-Chloro-8-cyclopentyl-7-ethyl-7,8-dihydropteridin-6(5H)-one, 13c

Aminobutanoate **12c** (554 mg, 1.62 mmol) was subjected to general method **4** to afford the title compound **13c** as a yellow solid (126 mg, 28%). LCMS purity >95%, ret. time 1.51 mins; HRMS (ESI +ve): found $[M+H]^+$ 281.1163, $[C_{13}H_{18}ClN_4O]^+$



requires 281.1169; δ_{H} (CDCl_3 , 500 MHz): 9.67 (1H, s, NH), 7.70 (1H, s, H6), 4.32 (1H, quin., $J = 8.4$ Hz, H3), 4.21 (1H, dd, $J = 7.3, 3.5$ Hz, CHCH_2CH_3), 2.12 – 2.04 (1H, m, H2), 2.00 – 1.73 (7H, m, cPeH & CHCH_2CH_3), 1.70 – 1.60 (2H, m, H1), 0.94 (3H, t, $J = 7.6$ Hz, CHCH_2CH_3); δ_{C} (CDCl_3 , 126 MHz): 165.9 (CONH), 154.2 (C7), 151.8 (C4), 138.9 (C6), 118.1 (C5), 60.9 (CHCH_2CH_3), 59.3 (C3), 29.4 (C2), 29.2 (C2'), 27.2 (CHCH_2CH_3), 22.9 (C1), 22.8 (C1'), 8.8 (CHCH_2CH_3)

(R)-2-Chloro-8-cyclopentyl-7-isopropyl-7,8-dihydropteridin-6(5H)-one, 13d

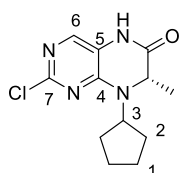


Aminobutanoate **12d** (1.05 g, 2.94 mmol) was subjected to general method **4** to afford the title compound **13e** as a yellow solid (567 mg, 65%). LCMS purity >95%, ret. time 1.57 mins; HRMS (ESI +ve): found $[\text{M}+\text{H}]^+$ 295.1325, $[\text{C}_{14}\text{H}_{20}\text{ClN}_4\text{O}]^+$ requires 295.1320; $[\alpha]_D^{22.6}$: -46.4° (c 1.0, MeOH); δ_{H} (CDCl_3 , 500 MHz): 8.67 (1H, s NH), 7.61 (1H, s, H6), 4.22 (1H, quin., $J = 8.4$ Hz, H3), 4.08 (1H, d, $J = 4.1$ Hz, $\text{CHCH}(\text{CH}_3)_2$), 2.20 – 2.04 (2H, m, $\text{CHCH}(\text{CH}_3)_2$ & C2), 2.03 – 1.77 (5H, m, cPeH), 1.70 – 1.58 (2H, m, cPeH), 1.13 (3H, d, $J = 6.9$ Hz, $\text{CH}(\text{CH}_3)(\text{C}'\text{H}_3)$), 0.88 (3H, d, $J = 6.9$ Hz, $\text{CH}(\text{CH}_3)(\text{C}'\text{H}_3)$); δ_{C} (CDCl_3 , 126 MHz): 163.6 (CONH), 154.1 (C7), 151.9 (C4), 138.5 (C6), 118.4 (C5), 70.0 ($\text{CHCH}(\text{CH}_3)_2$), 60.9 (C3), 35.4 ($\text{CHCH}(\text{CH}_3)_2$), 29.6 (C2), 29.5 (C2'), 24.1 (C1), 23.9 (C1'), 20.2 ($\text{CH}(\text{CH}_3)(\text{C}'\text{H}_3)$), 16.6 ($\text{CH}(\text{CH}_3)(\text{C}'\text{H}_3)$)

(R)-2-Chloro-8-cyclopentyl-7-methyl-7,8-dihydropteridin-6(5H)-one, 13e

Aminobutanoate **12e** (85 mg, 0.26 mmol) was subjected to general method **4** to afford the title compound **13e** as a white solid (40 mg, 58%). LCMS purity >95%, ret. time 1.47 mins; HRMS (ESI +ve): found $[\text{M}+\text{H}]^+$ 267.1022, $[\text{C}_{12}\text{H}_{16}\text{ClN}_4\text{O}]^+$ requires 267.1013; $[\alpha]_D^{21.1}$: -26.3° (c 1.0, MeOH); δ_{H} (CDCl_3 , 500 MHz): 9.45 (1H, s, CONH), 7.73 (1H, s, H6), 4.45 (1H, quin., $J = 8.4$ Hz, H3), 4.28 (1H, q, $J = 6.8$ Hz, CHCH_3), 2.14 – 2.06 (1H, m, H2), 2.03 – 1.96 (1H, m, H2), 1.91 – 1.62 (6H, m, cPeH), 1.44 (3H, d, $J = 6.8$ Hz, CHCH_3); δ_{C} (CDCl_3 , 126 MHz): 167.0 (CONH), 154.5 (C7), 151.3 (C4), 139.3 (C6), 118.0 (C5), 58.7 (C3), 55.2 (CHCH_3), 29.7 (C2), 29.4 (C2'), 23.9 (C1), 23.6 (C1'), 19.7 (CHCH_3)

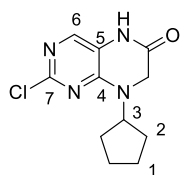
(S)-2-Chloro-8-cyclopentyl-7-methyl-7,8-dihydropteridin-6(5H)-one, 13f



Aminobutanoate **12f** (2.10 g, 12.2 mmol) was subjected to general method **4** to afford the title compound **13f** as a white solid (1.70 g, 42%). LCMS purity >95%, ret. time 1.47 mins; HRMS (ESI +ve): found $[\text{M}+\text{H}]^+$ 267.1003, $[\text{C}_{12}\text{H}_{16}\text{ClN}_4\text{O}]^+$ requires 267.1007; $[\alpha]_D^{23.5}$:

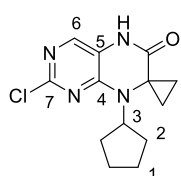
–17.3° (*c* 1.0, MeOH); δ_{H} (CDCl₃, 500 MHz): 8.65 (1H, s, NH), 7.68 (1H, s, H₆), 4.36 (1H, quin, *J* = 8.4 Hz, H₃), 4.28 (1H, q, *J* = 6.8 Hz, CHCH₃), 2.14 – 2.07 (1H, m, H₂), 2.03 – 1.96 (1H, m, H₂), 1.91 – 1.64 (6H, m, cPeH), 1.44 (3H, d, *J* = 6.9 Hz, CHCH₃); δ_{C} (CDCl₃, 126 MHz): 166.5 (CONH), 154.5 (C₇), 151.3 (C₄), 139.2 (C₆), 117.9 (C₅), 58.7 (C₃), 55.2 (CHCH₃), 29.7 (C₂), 29.4 (C_{2'}), 23.9 (C₁), 23.6 (C_{1'}), 19.7 (CHCH₃)

2-Chloro-8-cyclopentyl-7-ethyl-7,8-dihydropteridin-6(5H)-one, **13g**



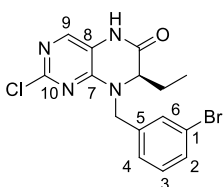
Aminobutanoate **12g** (410 mg, 1.30 mmol) was subjected to general method **4** to afford the title compound **13g** as a yellow solid 101 mg, 31%). LCMS purity >95%, ret. time 1.19 mins; HRMS (ESI +ve): found [M+H]⁺ 253.0854, [C₁₁H₁₄ClN₄O]⁺ requires 254.0851; δ_{H} (CDCl₃, 500 MHz): 7.98 (1H, s, NH), 7.60 (1H, s, H₇), 6.15 (1H, quin, *J* = 8.4 Hz, H₃), 4.11 (2H, s, COCH₂), 1.98 – 1.89 (2H, m, H₂), 1.80 – 1.57 (6H, m, cPeH); δ_{C} (CDCl₃, 126 MHz): 162.7 (CONH), 155.9 (C₈), 151.5 (C₅), 138.8 (C₇), 117.5 (C₆), 55.2 (C₃), 45.0 (COCH₂), 27.1 (C₂), 24.1 (C₁)

2-Chloro-8-cyclopentyl-5,8-dihydro-6H-spiro(cyclopropane-1,7-pteridin)-6-one, **13h**



Aminobutanoate **12h** (1.10 g, 3.23 mmol) was subjected to general method **4** to afford the title compound **13h** as a yellow solid 90 mg, 10%). LCMS purity >95%, ret. time 1.53 mins; HRMS (ESI +ve): found [M+H]⁺ 279.0996, [C₁₃H₁₆ClN₄O]⁺ requires 279.1007; δ_{H} (CDCl₃, 500 MHz): 3.59 (1H, quin, *J* = 8.8 Hz, H₃), 2.20 – 2.12 (2H, m, H₂), 2.08 – 2.00 (2H, m, H₂), 1.75 – 1.66 (2H, m, H₁), 1.60 – 1.53 (4H, m, H₁ & C(CH₂)(CH₂)), 1.34 – 1.27 (2H, m, C(CH₂)(CH₂)); δ_{C} (CDCl₃, 126 MHz): 166.7 (CONH), 153.5 (C_{4/7}), 1527 (C_{4/7}), 138.5 (C₆), 118.8 (C₅), 57.4 (C₃), 43.9 (C(CH₂)₂), 28.8 (C₂), 25.6 (C₁), 13.5 (C(CH₂)₂)

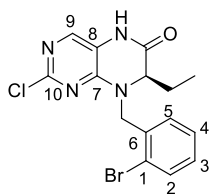
(R)-2-chloro-8-(3-bromobenzyl)-7-ethyl-7,8-dihydropteridin-6(5H)-one, **13i**



Aminobutanoate **12i**, (1.80 g, 4.06 mmol) was subjected to general method **4** to afford the title compound **13i** as an orange solid (280 mg, 18%). LCMS purity >95%, ret. time 1.56 mins; HRMS (ESI +ve): found [M+H]⁺ 383.0078, [C₁₅H₁₅BrClN₄O]⁺ requires 383.0091; $[\alpha]_{\text{D}}^{22.0}$: –18.0° (*c* 1.0, MeOH); δ_{H} (CDCl₃, 500 MHz): 9.33 (1H, s, CONH), 7.71 (1H, s, H₉), 7.48 – 7.45 (1H, m, H₄), 7.45 (1H, s, H₆), 7.26 – 7.23 (2H, m, H₂ & H₃), 5.62 (1H, d, *J* = 15.1, ArCHH), 4.16 – 4.12 (1H, m, CHCH₂CH₃), 4.08 (1H, d, *J* = 15.1, ArCHH), 2.05 – 1.97 (1H, m, CHCH₂CH₃), 1.96 – 1.86 (1H, m, CHCH₂CH₃), 0.91

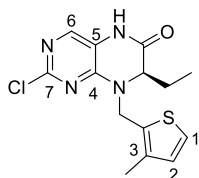
(3H, t, $J = 7.4$ Hz, CHCH_2CH_3); δ_{C} (CDCl_3 , 126 MHz): 165.2 (CONH), 154.4 (C10), 151.8 (C7), 139.4 (C9), 137.3 (C5), 131.5 (C2), 131.3 (C6), 130.6 (C3), 126.9 (C4), 123.1 (C1), 117.3 (C8), 60.3 (CHCH_2CH_3), 47.0 (ArCH_2), 24.3 (CHCH_2CH_3), 8.4 (CHCH_2CH_3)

(*R*)-2-chloro-8-(2-bromobenzyl)-7-ethyl-7,8-dihydropteridin-6(5*H*)-one, 13j



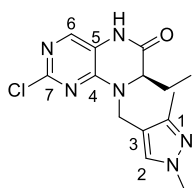
Aminobutanoate **12j**, (1.20 g, 2.70 mmol) was subjected to general method **4** to afford the title compound **13j** as an orange solid (350 mg, 34%). LCMS purity >95%, ret. time 1.60 mins; HRMS (ESI +ve): found $[\text{M}+\text{H}]^+$ 383.0085, $[\text{C}_{15}\text{H}_{15}\text{BrClN}_4\text{O}]^+$ requires 383.0118; $[\alpha]_D^{21.8}$: -24.2° (c 1.0, MeOH); δ_{H} (CDCl_3 , 500 MHz): 9.64 (1H, s, CONH), 7.72 (1H, s, H9), 7.59 (1H, dd, $J = 7.9, 1.2$ Hz, H2), 7.35 (1H, dd, $J = 7.6, 1.9$ Hz, H5), 7.31 (1H, *app.* td, $J = 7.6, 1.2$ Hz, H4), 7.20 (1H, *app.* td, $J = 7.9, 1.9$ Hz, H3), 5.64 (1H, d, $J = 15.5$, ArCHH), 4.34 (1H, d, $J = 15.5$, ArCHH), 4.15 (1H, dd, $J = 6.2, 3.6$ Hz, CHCH_2CH_3), 2.05 – 1.90 (2H, m, CHCH_2CH_3), 0.95 (3H, t, $J = 7.4$ Hz, CHCH_2CH_3); δ_{C} (CDCl_3 , 126 MHz): 165.7 (CONH), 154.4 (C10), 152.0 (C7), 139.3 (C9), 134.1 (C6), 131.5 (C2), 130.6 (C5), 129.9 (C3), 127.9 (C4), 124.1 (C1), 117.5 (C8), 60.5 (CHCH_2CH_3), 47.7 (ArCH_2), 24.8 (CHCH_2CH_3), 8.6 (CHCH_2CH_3)

(*R*)-2-chloro-7-ethyl-8-((3-methylthiophen-2-yl)methyl)-7,8-dihydropteridin-6(5*H*)-one, 13k



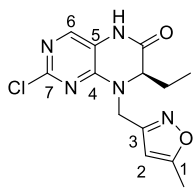
Aminobutanoate **12k**, (960 mg, 2.49 mmol) was subjected to general method **4** to afford the title compound **13k** as an orange solid (380 mg, 47%). LCMS purity >95%, ret. time 1.54 mins; HRMS (ESI +ve): found $[\text{M}+\text{H}]^+$ 323.0727, $[\text{C}_{14}\text{H}_{16}\text{ClN}_4\text{OS}]^+$ requires 323.0728; $[\alpha]_D^{22.2}$: -11.1° (c 1.0, MeOH); δ_{H} (CDCl_3 , 500 MHz): 9.20 (1H, s, NH), 7.69 (1H, s, H7), 7.18 (1H, d, $J = 5.2$ Hz, H1), 6.83 (1H, d, $J = 5.2$ Hz, H2), 5.64 (1H, d, $J = 15.5$ Hz, ArCHH), 4.29 (1H, d, $J = 15.5$ Hz, ArCHH), 4.24 (1H, dd, $J = 6.3, 3.5$ Hz, CHCH_2CH_3), 2.26 (3H, s, ArCH_3), 2.05 – 1.99 (1H, m, CHCH_2CH_3), 1.98 – 1.87 (1H, m, CHCH_2CH_3), 0.92 (3H, t, $J = 7.6$, CHCH_2CH_3); δ_{C} (CDCl_3 , 126 MHz): 165.4 (CONH), 154.4 (C8), 151.4 (C5), 139.1 (C7), 136.8 (C4), 130.3 (C2), 130.2 (C3), 124.6 (C1), 117.4 (C6), 59.9 (CHCH_2CH_3), 40.5 (C4), 24.6 (CHCH_2CH_3), 14.0 (ArCH_3), 8.5 (CHCH_2CH_3)

(R)-2-chloro-8-((1,3-dimethyl-1H-pyrazol-4-yl)methyl)-7-ethyl-7,8-dihydropteridin-6(5H)-one, 13l



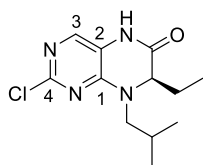
Aminobutanoate **12l**, (849 mg, 2.21 mmol) was subjected to general method **4** to afford the title compound **13l** as colourless oil (130 mg, 18%). LCMS purity >95%, ret. time 1.31 mins; HRMS (ESI +ve): found $[M+H]^+$ 321.1228, $[C_{14}H_{18}ClN_6O]^+$ requires 321.1225; $[\alpha]_D^{22.1}$: -2.4° (c 1.0, MeOH); δ_H (CDCl₃, 500 MHz): 9.64 (1H, s, NH), 7.67 (1H, s, H6), 7.35 (1H, s, H3), 5.32 (1H, d, $J = 15.5$ Hz, ArCHH), 4.19 (1H, dd, $J = 6.3, 3.2$ Hz, CHCH₂CH₃), 3.99 (1H, d, $J = 15.5$ Hz, ArCHH), 3.82 (3H, s, NCH₃), 2.21 (ArCH₃), 2.03 – 1.96 (1H, m, CHCH₂HCH₃), 1.92 – 1.84 (1H, m, CHCH₂HCH₃), 0.91 (3H, t, $J = 7.7$, CHCH₂CH₃); δ_C (CDCl₃, 126 MHz): 171.3 (CONH), 154.5 (C7), 151.6 (C4), 147.5 (C1), 138.9 (C6), 131.2 (C3), 117.5 (C5), 112.3 (C3), 59.8 (CHCH₂CH₃), 38.8 (NCH₃), 37.9 (ArCH₂), 24.5 (CHCH₂CH₃), 11.9 (ArCH₃), 8.4 (CHCH₂CH₃)

(R)-2-chloro-7-ethyl-8-((5-methylisoxazol-3-yl)methyl)-7,8-dihydropteridin-6(5H)-one, 13m



Aminobutanoate **12m**, (820 mg, 2.21 mmol) was subjected to general method **4** to afford the title compound **13m** as yellow oil (100 mg, 15%). LCMS purity >95%, ret. time 1.33 mins; HRMS (ESI +ve): found $[M+H]^+$ 308.0914, $[C_{13}H_{15}ClN_5O_2]^+$ requires 308.0909; $[\alpha]_D^{22.0}$: -12.5° (c 1.0, MeOH); δ_H (CDCl₃, 500 MHz): 8.97 (1H, s, NH), 7.69 (1H, s, H6), 6.07 (1H, d, $J = 1.0$ Hz, H2), 5.31 (1H, d, $J = 15.5$ Hz, ArCHH), 4.41 (1H, d, $J = 15.5$ Hz, ArCHH), 4.32 (1H, dd, $J = 6.0, 3.2$ Hz, CHCH₂CH₃), 2.43 (3H, s, ArCH₃), 2.09 – 1.94 (1H, m, CHCH₂CH₃), 0.87 (3H, t, $J = 7.4$ Hz, CHCH₂CH₃); δ_C (CDCl₃, 126 MHz): 170.7 (C1), 165.0 (CONH), 159.0 (C3), 154.3 (C7), 151.5 (C4), 139.2 (C6), 101.6 (C5), 61.3 (CHCH₂CH₃), 40.0 (ArCH₂), 24.4 (CHCH₂CH₃), 12.4 (ArCH₃), 8.2 (CHCH₂CH₃)

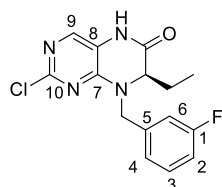
(R)-2-chloro-7-ethyl-8-isobutyl-5,7-dihydropteridin-6(5H)-one, 13n



Aminobutanoate **12n**, (480 mg, 1.45 mmol) was subjected to general method **4** to afford the title compound **13n** as an orange solid (120 mg, 30%). LCMS purity >95%, ret. time 1.45 mins; HRMS (ESI +ve): found $[M+H]^+$ 269.1156, $[C_{12}H_{18}ClN_4O]^+$ requires 269.1164; $[\alpha]_D^{22.2}$: -56.1° (c 1.0, MeOH); δ_H (CDCl₃, 500 MHz): 9.51 (1H, s, NH), 7.67 (1H, s, H6), 4.20 – 4.15 (2H, m, NCHH & CHCH₂CH₃), 2.71 (1H, dd, $J = 13.7, 7.1$ Hz, NCHH), 2.15 – 2.07 (CH(CH₃)₂), 2.00 – 1.91 (1H, m, CHCH₂HCH₃), 1.90 – 1.82 (1H, m, CHCH₂HCH₃), 0.99 (3H, d, $J = 6.6$, CH(CH₃)(C'H₃)), 0.93 – 0.90 (6H,

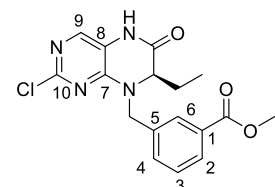
m, CH(CH₃)(C'H₃) & CHCH₂CH₃); δ_{C} (CDCl₃, 126 MHz): 162.7 (CONH), 154.5 (C4), 152.2 (C1), 138.9 (C3), 117.5 (C2), 62.0 (CHCH₂CH₃), 52.0 (NCH₂), 26.1 (CH(CH₃)₂), 25.0 (CHCH₂CH₃), 19.9 (CH(CH₃)₂), 8.8 (CHCH₂CH₃)

(R)-2-Chloro-7-ethyl-8-(3-fluorobenzyl)-7,8-dihydropteridin-6(5H)-one, 13o



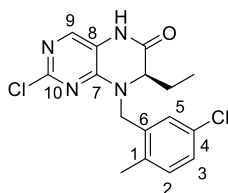
Aminobutanoate **12o**, (910 mg, 2.38 mmol) was subjected to general method **4** to afford the title compound **13o** as an orange solid (252 mg, 33%). LCMS purity >95%, ret. time 1.48 mins; HRMS (ESI +ve): found $[M+H]^+$ 321.0908, $[C_{15}H_{15}ClFN_4O]^+$ requires 321.0913; $[\alpha]_D^{22.4}$: -18.0° (c 1.0, MeOH); δ_{H} (CDCl₃, 500 MHz): 8.79 (1H, s, NH), 7.68 (1H, s, H9), 7.36 – 7.32 (1H, m, H3), 7.09 (1H, d, $J = 7.9$ Hz, H4), 7.06 – 7.00 (2H, m, H2 & H6), 5.63 (1H, d, $J = 15.1$ Hz, ArCHH), 4.16 – 4.11 (2H, m, CHCH₂CH₃ & ArCHH), 2.05 – 1.97 (1H, m, CHCHHCH₃), 1.95 – 1.86 (1H, m, CHCHHCH₃), 0.91 (3H, d, $J = 7.4$ Hz, CHCH₂CH₃); δ_{C} (CDCl₃, 126 MHz): 165.0 (CONH), 163.1 (d, $J_{\text{C-F}} = 247$ Hz, C1), 154.6 (C10), 151.8 (C7), 139.3 (C9), 137.5 (d, $J_{\text{C-F}} = 6.4$ Hz, C5), 130.6 (d, $J_{\text{C-F}} = 8.3$ Hz, C3), 123.9 (d, $J_{\text{C-F}} = 2.8$ Hz, C4), 117.2 (C8), 115.4 (d, $J_{\text{C-F}} = 21.1$ Hz, C6), 115.2 (d, $J_{\text{C-F}} = 22.9$ Hz, C2), 60.4 (CHCH₂CH₃), 47.1 (ArCH₂), 24.4 (CHCH₂CH₃), 8.4 (CHCH₂CH₃); $\delta_{\text{F}\{\text{H}\}}$ (CDCl₃, 471 MHz): -111.8

Methyl (R)-3-((2-chloro-7-ethyl-6-oxo-6,7-dihydropteridin-8(5H)-yl)methyl)benzoate, 13p



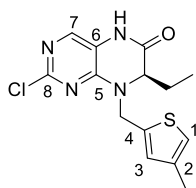
Aminobutanoate **12p**, (1.80 g, 4.26 mmol) was subjected to general method **4** to afford the title compound **13p** as a white solid (307 mg, 20%). LCMS purity >95%, ret. time 1.56 mins; HRMS (ESI +ve): found $[M+H]^+$ 361.1054, $[C_{17}H_{18}ClN_4O_3]^+$ requires 361.1062; $[\alpha]_D^{22.7}$: -19.2° (c 1.0, MeOH); δ_{H} (CDCl₃, 500 MHz): 8.65 (1H, s, NH), 8.01 (1H, d, $J = 7.6$ Hz, H2), 7.97 (1H, s, H6), 7.67 (1H, s, H9), 7.53 (1H, d, $J = 7.3$ Hz, H4), 7.46 (1H, m, H3), 5.68 (1H, d, $J = 15.2$ Hz, ArCHH), 4.18 (1H, d, $J = 15.2$ Hz, ArCHH), 4.12 (1H, t, $J = 4.7$ Hz, CHCH₂CH₃), 3.94 (3H, s, CO₂CH₃), 2.04 – 1.97 (1H, m, CHCHHCH₃), 1.96 – 1.87 (1H, m, CHCHHCH₃), 0.91 (3H, t, $J = 7.4$ Hz, CHCH₂CH₃); δ_{C} (CDCl₃, 126 MHz): 166.6 (CO₂CH₃), 164.8 (CONH), 154.5 (C10), 151.9 (C7), 139.2 (C9), 135.5 (C5), 132.8 (C4), 130.9 (C1), 129.6 (C2), 129.4 (C6), 129.2 (C3), 117.3 (C8), 60.3 (CHCH₂CH₃), 52.4 (CO₂CH₃), 47.3 (ArCH₂), 24.4 (CHCH₂CH₃), 8.4 (CHCH₂CH₃)

(*R*)-2-Chloro-8-(5-chloro-2-methylbenzyl)-7-ethyl-7,8-dihydropteridin-6(5*H*)-one, 13q



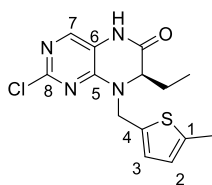
Aminobutanoate **12q**, (1.04 g, 2.52 mmol) was subjected to general method **4** to afford the title compound **13q** as an orange solid (247 mg, 28%). LCMS purity >95%, ret. time 1.58 mins; HRMS (ESI +ve): found $[M+H]^+$ 351.0768, $[C_{16}H_{17}Cl_2N_4O]^+$ requires 351.0774; $[\alpha]_D^{22.2}$: -4.2° (*c* 1.0, MeOH); δ_H (CDCl₃, 500 MHz): 10.0 (1H, s, NH), 7.77 (1H, s, H₉), 7.21 (1H, dd, *J* = 7.9, 2.2 Hz, H₃), 7.16 (1H, d, *J* = 2.2 Hz, H₅), 7.13 (1H, d, *J* = 7.9 Hz, H₂), 5.65 (1H, d, *J* = 15.5 ArCHH), 4.05 – 4.01 (2H, m, ArCHH & CHCH₂CH₃), 2.24 (3H, s, CH₃), 2.00 – 1.86 (2H, m, CHCH₂CH₃), 0.93 (3H, t, *J* = 8.2 Hz, CHCH₂CH₃); δ_C (CDCl₃, 126 MHz): 166.0 (CONH), 154.4 (C10), 151.8 (C7), 139.5 (C9), 135.4 (C1), 134.2 (C6), 132.3 (C2), 132.0 (C4), 128.7 (C5), 128.4 (C3), 117.3 (C8), 59.7 (CHCH₂CH₃), 45.2 (ArCH₂), 24.4 (CHCH₂CH₃), 18.9 (CH₃), 8.5 (CHCH₂CH₃)

(*R*)-2-Chloro-7-ethyl-8-((4-methylthiophen-2-yl)methyl)-7,8-dihydropteridin-6(5*H*)-one, 13r



Aminobutanoate **12r**, (6.70 g, 17.4 mmol) was subjected to general method **18** to afford the title compound **13r** as an orange solid (5.38 g, 96%). LCMS purity >95%, ret. time 1.50 mins; HRMS (ESI +ve): found $[M+H]^+$ 323.0728, $[C_{14}H_{16}ClN_4OS]^+$ requires 323.0728; $[\alpha]_D^{22.8}$: -18.0° (*c* 1.0, MeOH); δ_H (CDCl₃, 500 MHz): 7.73 (1H, s, H₇), 6.86 (1H, s, H₃), 6.83 (1H, s, H₁), 5.58 (1H, d, *J* = 15.5 Hz, ArCHH), 4.32 – 4.28 (2H, m, ArCHH & CHCH₂CH₃), 2.23 (3H, s, ArCH₃), 2.07 – 1.99 (1H, m, CHCH₂CH₃), 1.97 – 1.86 (1H, m, CHCH₂CH₃), 0.89 (3H, t, *J* = 7.4 Hz, CHCH₂CH₃); δ_C (CDCl₃, 126 MHz): 165.7 (CONH), 154.3 (C8), 151.4 (C5), 139.2 (C7), 137.6 (C2), 136.7 (C4), 130.3 (C3), 121.6 (C1), 117.5 (C6), 60.0 (CHCH₂CH₃), 42.6 (ArCH₂), 24.4 (CHCH₂CH₃), 15.6 (ArCH₃), 8.3 (CHCH₂CH₃)

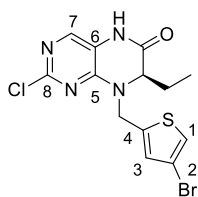
(*R*)-2-Chloro-7-ethyl-8-((5-methylthiophen-2-yl)methyl)-7,8-dihydropteridin-6(5*H*)-one, 13s



Aminobutanoate **12s**, (1.30 g, 3.38 mmol) was subjected to general method **4** to afford the title compound **13s** as an orange solid (200 mg, 18%). LCMS purity >95%, ret. time 1.51 mins; HRMS (ESI +ve): found $[M+H]^+$ 323.0724, $[C_{14}H_{16}ClN_4OS]^+$ requires 323.0728; $[\alpha]_D^{22.5}$: -18.7° (*c* 1.0, MeOH); δ_H (CDCl₃, 500 MHz): 8.70 (1H, s, NH), 7.65 (1H, s, H₇), 6.86 (1H, d, *J* = 3.3 Hz, H₃), 6.63 – 6.61 (1H, m, H₂), 5.55 (1H, d, *J* = 15.5 Hz,

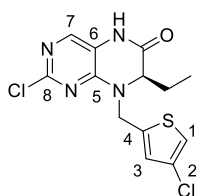
ArCHH), 4.33 – 4.28 (2H, m, CHCH₂CH₃ & ArCHH) 2.46 (3H, s, ArCH₃), 2.07 – 1.88 (2H, m, CHCH₂CH₃), 0.90 (3H, d, *J* = 7.4 Hz, CHCH₂CH₃); δ_c (CDCl₃, 126 MHz): 165.2 (CONH), 154.4 (C8), 151.4 (C5), 141.4 (C1), 138.9 (C7), 134.3 (C4), 128.1 (C3), 124.9 (C2), 117.3 (C6), 60.0 (CHCH₂CH₃), 42.9 (ArCH₂), 24.5 (CHCH₂CH₃), 15.4 (ArCH₃), 8.4 (CHCH₂CH₃)

(*R*)-8-((4-Bromothiophen-2-yl)methyl)-2-chloro-7-ethyl-7,8-dihydropteridin-6(5*H*)-one, 13t



Aminobutanoate **12t**, (1.97 g, 4.37 mmol) was subjected to general method **4** to afford the title compound **13t** as a yellow solid (395 mg, 23%). LCMS purity >95%, ret. time 1.54 mins; HRMS (ESI +ve): found $[M+H]^+$ 323.0724, $[C_{13}H_{13}BrClN_4OS]^+$ requires 323.0728; $[\alpha]_D^{22.4}$: -12.5° (c 1.0, MeOH); δ_H (CDCl₃, 500 MHz): 7.67 (2H, m, NH & H7), 7.19 (1H, d, *J* = 1.3 Hz, H1), 7.00 – 6.99 (1H, m, H3), 5.50 (1H, dd, *J* = 15.7, 0.8 Hz, ArCHH), 4.41 (1H, d, *J* = 15.7 Hz, ArCHH), 4.29 (1H, dd, *J* = 6.2, 3.3 Hz, CHCH₂CH₃), 2.10 – 2.02 (1H, m, CHCH₂CH₃), 1.96 – 1.88 (CHCH₂CH₃), 0.89 (3H, t, *J* = 7.6 Hz, CHCH₂CH₃); δ_c (CDCl₃, 126 MHz): 164.6 (CONH), 154.4 (C8), 151.2 (C5), 139.4 (C7), 138.9 (C4), 130.3 (C3), 123.8 (C1), 117.3 (C6), 109.5 (C2), 60.8 (CHCH₂CH₃), 42.8 (ArCH₂), 24.6 (CHCH₂CH₃), 8.3 (CHCH₂CH₃)

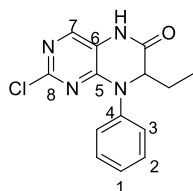
(*R*)-8-((4-Chlorothiophen-2-yl)methyl)-2-chloro-7-ethyl-7,8-dihydropteridin-6(5*H*)-one, 13u



Aminobutanoate **12u**, (1.25 g, 3.08 mmol) was subjected to general method **4** to afford the title compound **13u** as an orange solid (127 mg, 12%). LCMS purity >95%, ret. time 1.53 mins; HRMS (ESI +ve): found $[M+H]^+$ 343.0174, $[C_{13}H_{13}Cl_2N_4OS]^+$ requires 343.0182; $[\alpha]_D^{22.4}$: -29.8° (c 1.0, MeOH); δ_H (CDCl₃, 500 MHz): 8.79 (1H, s, NH), 7.68 (1H, s, H7), 7.07 (1H, d, *J* = 1.6 Hz, H1), 6.96 – 6.95 (1H, m, H3), 5.47 (1H, dd, *J* = 15.5, 0.8 Hz, ArCHH), 4.39 (1H, d, *J* = 15.5 Hz, ArCHH), 4.29 (1H, dd, *J* = 6.2, 3.3 Hz, CHCH₂CH₃), 2.09 – 2.04 (1H, m, CHCH₂CH₃), 1.96 – 1.88 (1H, m, CHCH₂CH₃), 0.89 (3H, t, *J* = 7.4 Hz, CHCH₂CH₃); δ_c (CDCl₃, 126 MHz): 164.8 (CONH), 154.4 (C8), 151.3 (C5), 139.2 (C7), 138.2 (C4), 128.0 (C3), 124.9 (C2), 120.9 (C1), 117.3 (C6), 60.8 (CHCH₂CH₃), 43.0 (ArCH₂), 24.6 (CHCH₂CH₃), 8.3 (CHCH₂CH₃)

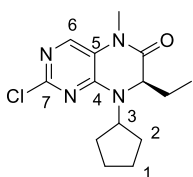
2-Chloro-7-ethyl-8-phenyl-7,8-dihydropteridin-6(5*H*)-one 13v

Aminobutanoate **12v** (890 mg, 2.54 mmol) was subjected to general method **4** to afford the title compound **13v** as a yellow solid (195 mg, 27%). LCMS purity >95%,



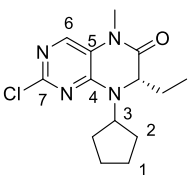
ret. time 1.38 mins; HRMS (ESI +ve): found $[M+H]^+$ 289.0867, $[C_{14}H_{14}ClN_4O]^+$ requires 289.0856; δ_H ($CDCl_3$, 500 MHz): 7.67 (1H, s, H7), 7.54 – 7.48 (3H, m, H1 & H2), 7.43 – 7.40 (2H, m, H3), 4.72 (1H, dd, $J = 5.7, 3.2$ Hz, $CHCH_2CH_3$), 2.05 – 1.95 (1H, m, $CHCH_2CH_3$), 1.73 – 1.64 (1H, m, $CHCH_2CH_3$), 0.96 (3H, t, $J = 7.4$ Hz, $CHCH_2CH_3$); δ_C ($CDCl_3$, 126 MHz): 163.0 (\underline{CONH}), 156.2 (C8), 151.7 (C5), 139.1 (C4), 138.4 (C7), 129.2 (C2), 127.7 (C1), 127.3 (C3), 119.8 (C6), 64.4 ($\underline{CHCH_2CH_3}$), 24.4 ($\underline{CHCH_2CH_3}$), 6.9 ($\underline{CHCH_2CH_3}$)

(R)-2-chloro-8-cyclopentyl-7-ethyl-5-methyl-7,8-dihydropteridin-6(5H)-one, 6a



Dihydropteridinone **13a** (345 mg, 1.22 mmol) was reacted with methyl iodide (100 μ L, 1.60 mmol) using general method **5** to afford the title compound **6a** as a white solid (308 mg, 85%). LCMS purity >95%, ret. time 1.53 mins; HRMS (ESI +ve): found $[M+H]^+$ 295.1321, $[C_{14}H_{20}ClN_4O]^+$ requires 295.1326; $[\alpha]_D^{21.4}$: +88.3° (c 1.0, MeOH); δ_H ($CDCl_3$, 500 MHz): 7.62 (1H, s, H6), 4.41 – 4.29 (1H, m, H3), 4.25 (1H, dd, $J = 7.6, 3.5$ Hz, $CHCH_2CH_3$), 3.33 (3H, s, NCH_3), 2.12 – 2.04 (1H, m, H2), 2.02 – 1.58 (9H, m, cPeH & $CHCH_2CH_3$), 0.86 (3H, t, $J = 7.4$ Hz, $CHCH_2CH_3$); δ_C ($CDCl_3$, 126 MHz): 163.7 ($\underline{CONCH_3}$), 154.0 (C7), 152.3 (C4), 137.9 (C6), 121.2 (C5), 60.7 ($\underline{CHCH_2CH_3}$), 59.4 (C3), 29.4 (C2), 29.2 (C2'), 28.2 (NCH_3), 27.4 ($\underline{CHCH_2CH_3}$), 23.9 (C1), 23.7 (C1'), 8.9 ($\underline{CHCH_2CH_3}$)

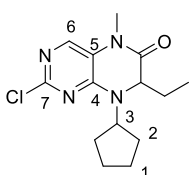
(S)-2-chloro-8-cyclopentyl-7-ethyl-5-methyl-7,8-dihydropteridin-6(5H)-one, 6b



Dihydropteridinone **13b** (180 mg, 0.64 mmol) was reacted with methyl iodide (52 μ L, 0.83 mmol) using general method **5** to afford the title compound **6b** as a white solid (180 mg, 95%). LCMS purity >95%, ret. time 1.54 mins; HRMS (ESI +ve): found $[M+H]^+$ 295.1321, $[C_{14}H_{20}ClN_4O]^+$ requires 295.1326; $[\alpha]_D^{21.5}$: +93.5° (c 1.0, MeOH); δ_H ($CDCl_3$, 500 MHz): 7.65 (1H, s, H6), 4.37 – 4.28 (1H, m, H3), 4.23 (1H, dd, $J = 7.6, 3.8$ Hz, $CHCH_2CH_3$), 3.31 (3H, s, NCH_3), 2.10 – 2.02 (1H, m, H2), 2.00 – 1.58 (9H, m, cPeH & $CHCH_2CH_3$), 0.85 (3H, t, $J = 7.6$ Hz, $CHCH_2CH_3$); δ_C ($CDCl_3$, 126 MHz): 163.7 ($\underline{CONCH_3}$), 153.9 (C7), 152.2 (C4), 137.9 (C6), 121.1 (C5), 60.7 ($\underline{CHCH_2CH_3}$), 59.4 (C3), 29.3 (C2), 29.2 (C2'), 28.2 (NCH_3), 27.3 ($\underline{CHCH_2CH_3}$), 23.9 (C1), 23.7 (C1'), 8.9 ($\underline{CHCH_2CH_3}$)

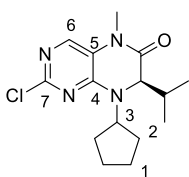
2-Chloro-8-cyclopentyl-7-ethyl-5-methyl-7,8-dihydropteridin-6(5H)-one, 6c

Dihydropteridinone **13c** (126 mg, 0.45 mmol) was reacted with methyl iodide (36.5 μ L, 0.58 mmol) using general method **5** to afford the title compound **6c** as a yellow solid



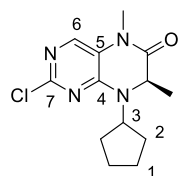
(70 mg, 53%). LCMS purity >95%, ret. time 1.53 mins; HRMS (ESI +ve): found $[M+H]^+$ 295.1324, $[C_{14}H_{20}ClN_4O]^+$ requires 295.1326; δ_H ($CDCl_3$, 500 MHz): 7.62 (1H, s, H6), 4.41 – 4.29 (1H, m, H3), 4.25 (1H, dd, $J = 7.6, 3.5$ Hz, $CHCH_2CH_3$), 3.33 (3H, s, $CONCH_3$), 2.12 – 2.04 (1H, m, H2), 2.02 – 1.58 (9H, m, cPeH & $CHCH_2CH_3$), 0.86 (3H, t, $J = 7.4$ Hz, $CHCH_2CH_3$); δ_C ($CDCl_3$, 126 MHz): 163.7 ($CONCH_3$), 154.0 (C7), 152.3 (C4), 137.9 (C6), 121.2 (C5), 60.7 ($CHCH_2CH_3$), 59.4 (C3), 29.4 (C2), 29.2 (C2'), 28.2 ($CONCH_3$), 27.4 ($CHCH_2CH_3$), 23.9 (C1), 23.7 (C1'), 8.9 ($CHCH_2CH_3$)

(R)-2-chloro-8-cyclopentyl-7-isopropyl-5-methyl-7,8-dihydropteridin-6(5H)-one, 6d

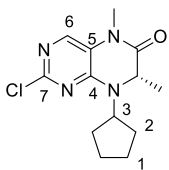


Dihydropteridinone **13d** (567 mg, 1.92 mmol) was reacted with methyl iodide (144 μ L, 2.31 mmol) using general method **5** to afford the title compound **6d** as a white solid (250 mg, 42%). LCMS purity >95%, ret. time 1.57 mins; HRMS (ESI +ve): found $[M+H]^+$ 309.1480, $[C_{15}H_{21}ClN_4O]^+$ requires 309.1477; $[\alpha]_D^{22.6}$: -42.9° (c 1.0, MeOH); δ_H ($CDCl_3$, 500 MHz): 7.63 (1H, s, H6), 4.27 – 4.21 (1H, m, H3), 4.13 (1H, d, $J = 3.8$ Hz, $CHCH(CH_3)_2$), 3.32 (3H, s, $CONCH_3$), 2.14 – 2.01 (3H, m, $CHCH(CH_3)_2$ & C2), 2.00 – 1.78 (4H, m, cPeH), 1.78 – 1.61 (2H, m, C1), 1.09 (3H, d, $J = 6.9$ Hz, $CH(CH_3)(C'H_3)$), 0.77 (3H, d, $J = 6.6$ Hz, $CH(CH_3)(C'H_3)$); δ_C ($CDCl_3$, 126 MHz): 162.1 ($CONCH_3$), 153.8 (C7), 152.3 (C4), 137.6 (C6), 120.9 (C5), 65.6 ($CHCH(CH_3)_2$), 60.7 (C3), 34.6 ($CHCH(CH_3)_2$), 29.6 (C2), 28.0 ($CONCH_3$), 24.1 (C1), 23.9 (C1'), 20.2 ($CH(CH_3)(C'H_3)$), 16.8 ($CH(CH_3)(C'H_3)$)

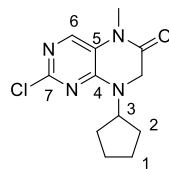
(R)-2-Chloro-8-cyclopentyl-7-methyl-5-methyl-7,8-dihydropteridin-6(5H)-one, 6e



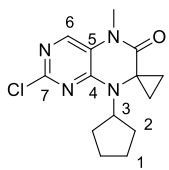
Dihydropteridinone **13e** (35.0 mg, 0.13 mmol) was reacted with methyl iodide (8.20 μ L, 0.13 mmol) using general method **5** to afford the title dihydropteridinone **6e** as a white solid (18 mg, 49%). LCMS purity >95%, ret. time 1.48 mins; HRMS (ESI +ve): found $[M+H]^+$ 281.1173, $[C_{13}H_{18}ClN_4O]^+$ requires 281.1169; $[\alpha]_D^{23.5}$: -36.7° (c 1.0, MeOH); δ_H ($CDCl_3$, 500 MHz): 7.71 (1H, s, H6), 4.49 – 4.41 (1H, m, H3), 4.34 (1H, q, $J = 6.8$ Hz, $CHCH_3$), 3.32 (3H, s, NCH_3), 2.12 – 2.05 (1H, m, H2), 2.04 – 1.96 (1H, m, H2), 1.90 – 1.62 (6H, m, cPeH), 1.36 (3H, t, $J = 6.9$ Hz, $CHCH_3$); δ_C ($CDCl_3$, 126 MHz): 65.0 ($CONCH_3$), 154.2 (C7), 151.9 (C4), 121.2 (C5), 58.6 (C3), 55.1 ($CHCH_3$), 29.7 (C2), 29.4 (C2'), 28.4 (NCH_3), 23.9 (C1), 23.6 (C1'), 19.6 ($CHCH_2CH_3$)

(S)-2-chloro-8-cyclopentyl-5,7-dimethyl-7,8-dihydropteridin-6(5H)-one, 6f

Dihydropteridinone **13f** (255 mg, 0.96 mmol) was reacted with methyl iodide (78 μ L, 1.24 mmol) using general method **5** to afford the title compound **6f** as a white solid (167 mg, 62%). LCMS purity >95%, ret. time 1.47 mins; HRMS (ESI +ve): found $[M+H]^+$ 281.1159, $[C_{13}H_{18}ClN_4O]^+$ requires 281.1164; $[\alpha]_D^{20.8}$: +31.9° (c 1.0, MeOH); δ_H (CDCl₃, 500 MHz): 7.71 (1H, s, H6), 4.45 (1H, quin, J = 8.4 Hz, H3), 4.34 (1H, q, J = 6.6 Hz, CHCH₃), 3.32 (3H, s, NCH₃), 2.12 – 2.05 (1H, m, H2), 2.01 – 1.96 (1H, m, H2), 1.89 – 1.82 (1H, m, H1), 1.80 – 1.63 (4H, m, cPeH), 1.36 (3H, d, J = 6.6 Hz, CHCH₃); δ_C (CDCl₃, 126 MHz): 164.5 (CONCH₃), 154.2 (C7), 151.9 (C4), 138.3 (C6), 121.2 (C4), 56.6 (C3), 55.1 (CHCH₃), 29.7 (C2), 29.4 (C2'), 28.4 (NCH₃), 23.9 (C1), 23.6 (C1'), 19.5 (CHCH₃)

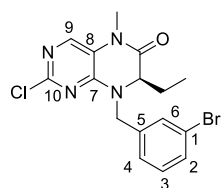
2-Chloro-8-cyclopentyl-5-methyl-7,8-dihydropteridin-6(5H)-one, 6g

Dihydropteridinone **13g** (85 mg, 0.37 mmol) was reacted with methyl iodide (27 μ L, 0.44 mmol) using general method **5** to afford the title compound **6g** as a white solid (53 mg, 59%). LCMS purity >95%, ret. time 1.40 mins; HRMS (ESI +ve): found $[M+H]^+$ 267.1010, $[C_{12}H_{16}ClN_4O]^+$ requires 267.1013; δ_H (CDCl₃, 500 MHz): 7.67 (1H, s, H7), 5.14 (1H, quin, J = 8.4 Hz, H3), 4.13 (2H, s, COCH₂), 3.33 (3H, s, NCH₃), 1.97 – 1.91 (2H, m, H2), 1.81 – 1.65 (4H, m, H1), 1.64 – 1.56 (2H, m, H2); δ_C (CDCl₃, 126 MHz): 161.6 (CONCH₃), 154.2 (C8), 152.6 (C5), 138.0 (C7), 120.9 (C6), 55.2 (C3), 45.0 (COCH₂), 28.0 (NCH₃), 27.1 (C2), 24.1 (C1)

2-Chloro-8-cyclopentyl-5-methyl-5,8-dihydro-6H-spiro(cyclopropane-1,7-pteridin)-6-one, 6h

Dihydropteridinone **13h** (90 mg, 0.32 mmol) was reacted with methyl iodide (26 μ L, 0.42 mmol) using general method **5** to afford the title compound **6h** as a white solid (49 mg, 52%). LCMS purity >95%, ret. time 1.55 mins; HRMS (ESI +ve): found $[M+H]^+$ 293.1172, $[C_{14}H_{18}ClN_4O]^+$ requires 293.1164; δ_H (CDCl₃, 500 MHz): 7.66 (1H, s, H6), 3.64 (1H, quin, J = 8.8 Hz, H3), 3.28 (3H, s, CH₃), 2.16 – 2.08 (2H, m, H2), 2.05 – 1.97 (2H, m, H1), 1.73 – 1.66 (2H, m, H2), 1.58 – 1.50 (4H, m, 2 x H1 & C(CH₂)(C'H₂)), 1.27 – 1.22 (2H, m, C(CH₂)(C'H₂)); δ_C (CDCl₃, 126 MHz): 165.6 (CONCH₃), 155.3 (C4), 153.1 (C7), 137.9 (C6), 122.1 (C5), 57.5 (C3), 43.7 (C(CH₂)₂), 28.8 (NCH₃ & C2), 25.5 (C1), 13.4 (C(CH₂)₂)

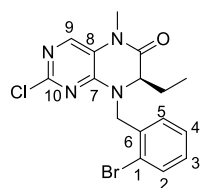
(*R*)-8-(3-Bromobenzyl)-2-chloro-7-ethyl-5-methyl-7,8-dihydropteridin-6(5*H*)-one, **6i**



Dihydropteridinone **13i** (270 mg, 0.71 mmol) was reacted with methyl iodide (58 μ L, 0.92 mmol) using general method **5** to afford the title compound **6i** as a yellow solid (200 mg, 71%). LCMS purity >95%, ret. time 1.61 mins; HRMS (ESI +ve): found $[M+H]^+$

395.0269, $[C_{16}H_{17}BrClN_4O]^+$ requires 395.0274; $[\alpha]_D^{22.1}$: +5.2° (c 1.0, MeOH); δ_H (CDCl₃, 500 MHz): 7.73 (1H, s, H₉), 7.48 – 7.44 (2H, m, H₂ & H₆), 7.25 – 7.22 (2H, m, H₃ & H₄), 5.62 (1H, d, J = 15.1 Hz, ArCH_H), 4.17 (1H, dd, J = 6.3, 3.5 Hz, CHCH₂CH₃), 4.09 (1H, d, J = 15.1 Hz, ArCH_H), 3.35 (3H, s, NCH₃), 2.02 – 1.93 (1H, m, CHCH₂CH₃), 1.90 – 1.80 (1H, m, CHCH₂CH₃), 0.84 (3H, t, J = 7.4 Hz, CHCH₂CH₃); δ_C (CDCl₃, 126 MHz): 163.4 (CONH), 154.2 (C₁₀), 152.2 (C₇), 138.3 (C₉), 137.4 (C₅), 131.4 (C₆), 131.3 (C₂), 130.5 (C₃), 126.7 (C₄), 123.0 (C₁), 120.4 (C₈), 60.2 (CHCH₂CH₃), 47.1 (ArCH₂), 28.3 (NCH₃), 24.8 (CHCH₂CH₃), 8.5 (CHCH₂CH₃)

(*R*)-8-(2-Bromobenzyl)-2-chloro-7-ethyl-5-methyl-7,8-dihydropteridin-6(5*H*)-one, **16j**

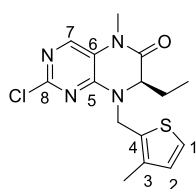


Dihydropteridinone **13j** (330 mg, 0.87 mmol) was reacted with methyl iodide (70 μ L, 1.12 mmol) using general method **5** to afford the title compound **16j** as a yellow solid (300 mg, 88%). LCMS purity >95%, ret. time 1.41 mins; HRMS (ESI +ve): found $[M+H]^+$

397.0250, $[C_{16}H_{17}BrClN_4O]^+$ requires 397.0274; $[\alpha]_D^{21.5}$: +20.1° (c 1.0, MeOH); δ_H (CDCl₃, 500 MHz): 7.72 (1H, s, H₉), 7.59 (1H, dd, J = 7.9, 1.1 Hz, H₂), 7.36 (1H, dd, J = 7.9, 1.8 Hz, H₅), 7.30 (1H, *app.* td, J = 7.7, 1.1 Hz, H₄), 7.20 (1H, *app.* td, J = 7.7, 1.8 Hz, H₃), 5.64 (1H, d, J = 15.1 Hz, ArCH_H), 4.33 (1H, d, J = 15.1 Hz, ArCH_H), 4.19 (1H, dd, J = 6.5, 3.6 Hz, CHCH₂CH₃), 3.35 (3H, s, NCH₃), 2.02 – 1.84 (1H, m, CHCH₂CH₃), 0.87 (3H, t, J = 7.4 Hz, CHCH₂CH₃); δ_C (CDCl₃, 126 MHz): 163.6 (CONCH₃), 154.1 (C₁₀), 152.4 (C₇), 138.1 (C₉), 134.2 (C₆), 133.3 (C₂), 130.7 (C₅), 129.8 (C₃), 127.8 (C₄), 124.1 (C₁), 120.6 (C₈), 60.6 (CHCH₂CH₃), 47.9 (ArCH₂), 28.2 (NCH₃), 25.2 (CHCH₂CH₃), 8.8 (CHCH₂CH₃)

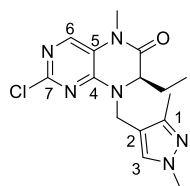
(*R*)-2-chloro-7-ethyl-5-methyl-8-((3-methylthiophen-2-yl)methyl)-7,8-dihydropteridin-6(5*H*)-one, **6k**

Dihydropteridinone **13k** (370 mg, 1.15 mmol) was reacted with methyl iodide (72 μ L, 1.15 mmol) using general method **5** to afford the title compound **6k** as a yellow solid (186 mg, 48%). LCMS purity >95%, ret. time 1.53 mins; HRMS (ESI +ve): found



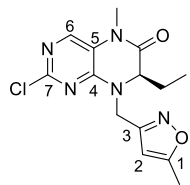
[M+H]⁺ 337.0901, [C₁₅H₁₈ClN₄OS]⁺ requires 337.0884; [α]_D^{23.3}: +6.9° (c 1.0, MeOH); δ_H (CDCl₃, 500 MHz): 7.69 (1H, s, H7), 7.17 (1H, d, *J* = 5.4 Hz, H1), 6.83 (1H, d, *J* = 5.4 Hz, H2), 5.61 (1H, d, *J* = 15.4 Hz, ArCH_H), 4.29 (1H, d, *J* = 15.4 Hz, ArCH_H), 4.27 (1H, dd, *J* = 6.6, 3.5 Hz, CHCH₂CH₃), 3.32 (3H, s, NCH₃), 2.25 (3H, s, ArCH₃), 2.03 – 1.93 (1H, m, CHCH₂CH₃), 1.91 – 1.81 (1H, m, CHCH₂CH₃), 0.84 (3H, t, *J* = 7.6 Hz, CHCH₂CH₃); δ_C (CDCl₃, 126 MHz): δ 163.6 (CONCH₃), 154.2 (C8), 151.9 (C5), 138.1 (C7), 136.8 (C4), 130.3 (C3), 130.2 (C2), 124.6 (C1), 120.5 (C6), 59.9 (CHCH₂CH₃), 40.6 (ArCH₂), 28.2 (NCH₃), 25.0 (CHCH₂CH₃), 14.0 (ArCH₃), 8.7 (CHCH₂CH₃)

(R)-2-chloro-8-((1,3-dimethyl-1H-pyrazol-4-yl)methyl)-7-ethyl-5-methyl-7,8-dihydropteridin-6(5H)-one, 6l



Dihydropteridinone **13l** (110 mg, 0.34 mmol) was reacted with methyl iodide (21 μ L, 0.34 mmol) using general method **5** to afford the title compound **6l** as a yellow solid (50 mg, 44%). LCMS purity >95%, ret. time 1.33 mins; HRMS (ESI +ve): found [M+H]⁺ 335.1377, [C₁₅H₂₀ClN₆O]⁺ requires 335.1382; [α]_D^{23.5}: +20.8° (c 1.0, MeOH); δ_H (CDCl₃, 500 MHz): 7.67 (1H, s, H6), 7.35 (1H, s, H3), 5.31 (1H, d, *J* = 15.2 Hz, ArCH_H), 4.23 (1H, dd, *J* = 6.6, 3.5 Hz, CHCH₂CH₃), 4.00 (1H, d, *J* = 15.2 Hz, ArCH_H), 3.82 (3H, s, NCH₃), 3.32 (3H, s, CONCH₃), 2.22 (3H, s, ArCH₃), 2.00 – 1.94 (1H, m, CHCH₂CH₃), 1.92 – 1.80 (1H, m, CHCH₂CH₃), 0.83 (3H, t, *J* = 7.4 Hz, CHCH₂CH₃); δ_C (CDCl₃, 126 MHz): 163.6 (CONCH₃), 154.2 (C7), 152.0 (C4), 147.5 (C1), 137.9 (C6), 131.2 (C3), 120.5 (C5), 112.4 (C2), 59.9 (CHCH₂CH₃), 38.8 (NCH₃), 38.1 (ArCH₂), 28.2 (CONCH₃), 25.0 (CHCH₂CH₃), 11.9 (ArCH₃), 8.6 (CHCH₂CH₃)

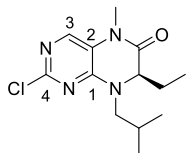
(R)-2-chloro-7-ethyl-5-methyl-8-((5-methylisoxazol-3-yl)methyl)-7,8-dihydropteridin-6(5H)-one, 6m



Dihydropteridinone **13m** (60 mg, 0.20 mmol) was reacted with methyl iodide (12 μ L, 0.20 mmol) using general method **5** to afford the title compound **6m** as an orange oil (30 mg, 24%). *used in next step without further purification.* LCMS purity >75%, ret. time 1.32 mins; HRMS (ESI +ve): found [M+H]⁺ 322.1063, [C₁₄H₁₇ClN₅O₂]⁺ requires 322.1071; δ_H (CDCl₃, 500 MHz): 7.71 (1H, s, H6), 6.05 (1H, d, *J* = 1.0 Hz, H2), 5.33 (1H, d, *J* = 15.1 Hz, ArCH_H), 4.39 (1H, d, *J* = 15.1 Hz, ArCH_H), 4.31 (1H, dd, *J* = 6.6, 3.5 Hz, CHCH₂CH₃), 3.32 (3H, s, NCH₃), 2.40 (3H, d, *J* = 1.0 Hz, ArCH₃), 2.04 – 1.98 (1H, m, CHCH₂CH₃), 1.94 – 1.87 (1H, m, CHCH₂CH₃), 0.77 (3H, t, *J* = 7.6 Hz, CHCH₂CH₃); δ_C (CDCl₃, 126 MHz): 170.6 (C1), 163.3 (CONCH₃), 159.0 (C3), 153.9 (C7), 152.0

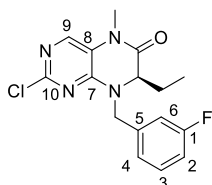
(C4), 138.1 (C6), 120.6 (C5), 101.6 (C2), 61.2 ($\underline{\text{CHCH}_2\text{CH}_3}$), 40.1 (ArCH_2), 28.2 (NCH_3), 24.9 ($\text{CH}\underline{\text{CH}_2\text{CH}_3}$), 12.3 ($\text{Ar}\underline{\text{CH}_3}$), 8.3 ($\text{CHCH}_2\underline{\text{CH}_3}$)

(R)-2-chloro-8-7-ethyl-8-isobutyl-5-methyl-7,8-dihydropteridin-6(5H)-one, 6n



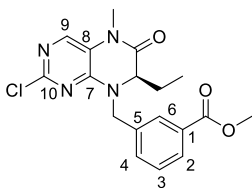
Dihydropteridinone **13n** (90 mg, 0.33 mmol) was reacted with methyl iodide (21 μL , 0.33 mmol) using general method **5** to afford the title compound **6n** as a yellow solid (42 mg, 44%). LCMS purity >95%, ret. time 1.47 mins; HRMS (ESI +ve): found $[\text{M}+\text{H}]^+$ 283.1308, $[\text{C}_{13}\text{H}_{20}\text{ClN}_4\text{O}]^+$ requires 283.1320; $[\alpha]_D^{22.1}$: -33.9° (c 1.0, MeOH); δ_{H} (CDCl_3 , 500 MHz): 7.65 (1H, s, H3), 4.21 – 4.16 (2H, m, NCH_2H & CHCH_2CH_3), 3.34 (3H, s, NCH_3), 2.68 (1H, dd, $J = 13.9, 7.3$ Hz, NCH_2H), 2.14 – 2.05 (1H, m, $\text{CH}(\text{CH}_3)_2$), 1.96 – 1.88 (1H, m, CHCH_2CH_3), 1.85 – 1.76 (1H, m, CHCH_2CH_3), 0.97 (3H, d, $J = 6.6$ Hz, $\text{CH}(\text{CH}_3)(\text{C}'\text{H}_3)$), 0.91 (3H, d, $J = 6.6$ Hz, $\text{CH}(\text{CH}_3)(\text{C}'\text{H}_3)$), 0.85 (3H, t, $J = 7.6$ Hz, CHCH_2CH_3); δ_{C} (CDCl_3 , 126 MHz): 163.7 ($\underline{\text{CONCH}_3}$), 154.3 (C4), 152.7 (C1), 138.2 (C9), 137.9 (C3), 120.6 (C2), 62.1 ($\underline{\text{CHCH}_2\text{CH}_3}$), 52.2 (NCH_2), 28.2 (NCH_3), 26.1 ($\text{CH}(\text{CH}_3)_2$), 25.3 ($\text{CH}\underline{\text{CH}_2\text{CH}_3}$), 20.2 ($\text{CH}(\underline{\text{CH}_3})(\text{C}'\text{H}_3)$), 19.9 ($\text{CH}(\text{CH}_3)(\underline{\text{C}'\text{H}_3})$), 9.0 ($\text{CHCH}_2\underline{\text{CH}_3}$)

(R)-2-Chloro-7-ethyl-8-(3-fluorobenzyl)-5-methyl-7,8-dihydropteridin-6(5H)-one, 6o



Dihydropteridinone **13o** (250 mg, 0.78 mmol) was reacted with methyl iodide (49 μL , 0.78 mmol) using general method **5** to afford the title compound **6o** as a white solid (96 mg, 37%). LCMS purity >95%, ret. time 1.50 mins; HRMS (ESI +ve): found $[\text{M}+\text{H}]^+$ 335.1051, $[\text{C}_{16}\text{H}_{17}\text{ClFN}_4\text{O}]^+$ requires 335.1069; $[\alpha]_D^{23.4}$: -6.2° (c 1.0, MeOH); δ_{H} (CDCl_3 , 500 MHz): 7.72 (1H, s, H9), 7.24 – 7.29 (1H, m, H3), 7.07 (1H, d, $J = 7.9$ Hz, H4), 7.03 – 7.00 (2H, m, H2 & H6), 5.61 (1H, d, $J = 15.1$ Hz, ArCH_2H), 4.16 (1H, dd, $J = 6.3, 3.5$ Hz, CHCH_2CH_3), 4.12 (1H, d, $J = 15.1$ Hz, ArCH_2H), 3.35 (3H, s, CONCH_3), 2.01 – 1.92 (1H, m, CHCH_2CH_3), 1.88 – 1.79 (1H, m, CHCH_2CH_3), 0.83 (3H, t, $J = 7.4$ Hz, CHCH_2CH_3); δ_{C} (CDCl_3 , 126 MHz): 163.4 ($\underline{\text{CONCH}_3}$), 163.1 (d, $J_{\text{C-F}} = 247.4$ Hz, C1), 154.2 (C10), 152.3 (C7), 138.3 (C9), 137.6 (d, $J_{\text{C-F}} = 6.4$ Hz, C5 (C8)), 130.6 (d, $J_{\text{C-F}} = 8.3$ Hz, C3), 123.9 (d, $J_{\text{C-F}} = 2.8$ Hz, C4), 115.3 (dd, $J_{\text{C-F}} = 21.1, 5.5$ Hz, C2 & C6), 60.3 ($\underline{\text{CHCH}_2\text{CH}_3}$), 42.3 (ArCH_2), 28.3 ($\underline{\text{CONCH}_3}$), 24.8 ($\text{CH}\underline{\text{CH}_2\text{CH}_3}$), 8.6 ($\text{CHCH}_2\underline{\text{CH}_3}$); $\delta_{\text{F}\{\text{H}\}}$ (CDCl_3 , 471 MHz): -112.0

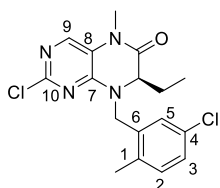
Methyl (*R*)-3-((2-chloro-7-ethyl-5-methyl-6-oxo-6,7-dihydropteridin-8(5*H*)-yl)methyl)benzoate, 6p



Dihydropteridinone **13n** (300 mg, 0.83 mmol) was reacted with methyl iodide (52 μ L, 0.83 mmol) using general method **5** to afford the title compound **6p** as a yellow solid (108 mg, 35%).

LCMS purity >95%, ret. time 1.47 mins; HRMS (ESI +ve): found $[M+H]^+$ 375.1214, $[C_{18}H_{20}ClN_4O_3]^+$ requires 375.1218; $[\alpha]_D^{23.4}$: -2.8° (c 1.0, MeOH); δ_H (CDCl₃, 500 MHz): 7.99 – 7.94 (2H, m, H2 & H6), 7.70 (1H, s, H9), 7.50 (1H, d, J = 7.6 Hz, H4), 7.44 – 7.41 (1H, m, H3), 5.64 (1H, d, J = 15.1 Hz, ArCHH), 4.16 (1H, d, J = 15.1 Hz, ArCHH), 4.14 – 4.08 (1H, m, CHCH₂CH₃), 3.90 (3H, s, CO₂CH₃), 3.32 (3H, s, CONCH₃), 1.99 – 1.92 (1H, m, CHCH₂CH₃), 1.89 – 1.80 (1H, m, CHCH₂CH₃), 0.81 (3H, t, J = 7.3 Hz, CHCH₂CH₃); δ_C (CDCl₃, 126 MHz): 166.6 (CO₂CH₃), 163.4 (CONCH₃), 154.2 (C10), 152.3 (C7), 138.3 (C9), 135.6 (C5), 132.9 (C4), 130.9 (C1), 129.5 (C2 & C6), 129.2 (C3), 120.5 (C8), 60.3 (CHCH₂CH₃), 52.3 (CO₂CH₃), 47.4 (ArCH₂), 28.2 (CONCH₃), 24.8 (CHCH₂CH₃), 8.5 (CHCH₂CH₃)

(*R*)-2-Chloro-8-(5-chloro-2-methylbenzyl)-7-ethyl-5-methyl-7,8-dihydropteridin-6(5*H*)-one, 6q

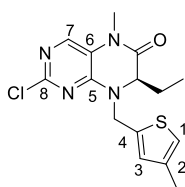


Dihydropteridinone **13q** (240 mg, 0.68 mmol) was reacted with methyl iodide (56 μ L, 0.88 mmol) using general method **5** to afford the title compound **6q** as a yellow solid (175 mg, 70%). LCMS purity >95%, ret. time 1.46 mins; HRMS (ESI +ve): found $[M+H]^+$

365.0921, $[C_{17}H_{19}Cl_2N_4O]^+$ requires 365.0930; $[\alpha]_D^{22.2}$: $+6.9^\circ$ (c 1.0, MeOH); δ_H (CDCl₃, 500 MHz): 7.73 (1H, s, H9), 7.23 – 7.20 (1H, m, H3), 7.16 (1H, d, J = 1.9 Hz, H5), 7.12 (1H, d, J = 8.2 Hz, H2), 5.64 (1H, d, J = 15.3 Hz, ArCHH), 4.05 (1H, dd, J = 6.5, 3.6 Hz, CHCH₂CH₃), 4.02 (1H, d, J = 15.3 Hz, ArCHH), 3.35 (3H, s, CONCH₃), 2.24 (3H, s, CH₃), 2.00 – 1.92 (1H, m, CHCH₂CH₃), 1.89 – 1.80 (1H, m, CHCH₂CH₃), 0.85 (3H, t, J = 7.6 Hz, CHCH₂CH₃); δ_C (CDCl₃, 126 MHz): 163.5 (CONCH₃), 154.2 (C10), 152.3 (C7), 138.3 (C9), 135.4 (C1), 134.4 (C6), 132.3 (C2), 131.9 (C4), 128.9 (C5), 128.4 (C3), 120.6 (C8), 59.7 (CHCH₂CH₃), 45.4 (ArCH₂), 28.3 (CONCH₃), 24.8 (CHCH₂CH₃), 18.9 (ArCH₃), 8.7 (CHCH₂CH₃)

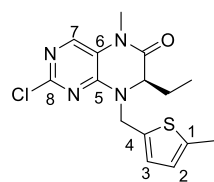
(*R*)-2-Chloro-7-ethyl-5-methyl-8-((4-methylthiophen-2-yl)methyl)-7,8-dihydropteridin-6(5*H*)-one, 6r

Dihydropteridinone **13r** (5.40 g, 16.7 mmol) was reacted with methyl iodide (1.36 mL, 21.7 mmol) using general method **5** to afford the title compound **6r** as a brown solid (4.22 g, 75%). LCMS purity >95%, ret. time 1.52 mins; HRMS (ESI +ve): found



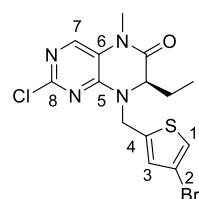
[M+H]⁺ 337.0881, [C₁₅H₁₈ClN₄OS]⁺ requires 337.0890; [α]_D^{23.3}: +4.9° (c 1.0, MeOH); δ _H (CDCl₃, 500 MHz): 7.69 (1H, s, H7), 6.86 (1H, s, H3), 6.82 (1H, s, H1), 5.56 (1H, d, *J* = 15.5 Hz, ArCHH), 4.33 – 4.29 (2H, m, ArCHH & CHCH₂CH₃), 3.31 (3H, s, CONCH₃), 2.22 (3H, s, ArCH₃), 2.03 – 1.95 (1H, m, CHCHHCH₃), 1.91 – 1.84 (1H, m, CHCHHCH₃), 0.81 (3H, t, *J* = 7.4 Hz, CHCH₂CH₃); δ _C (CDCl₃, 126 MHz): 163.5 (CONCH₃), 154.1 (C8), 151.8 (C5), 138.0 (C7), 137.5 (C2), 136.7 (C4), 130.3 (C3), 121.6 (C1), 120.5 (C6), 60.0 (CHCH₂CH₃), 42.8 (ArCH₂), 28.2 (CONCH₃), 24.9 (CHCH₂CH₃), 15.6 (ArCH₃), 8.5 (CHCH₂CH₃)

(*R*)-2-Chloro-7-ethyl-5-methyl-8-((5-methylthiophen-2-yl)methyl)-7,8-dihydropteridin-6(5*H*)-one, 6s



Dihydropteridinone **13s** (200 mg, 0.62 mmol) was reacted with methyl iodide (39 μ L, 0.62 mmol) using general method **5** to afford the title compound **6s** as a yellow solid (110 mg, 53%). LCMS purity >95%, ret. time 1.54 mins; HRMS (ESI +ve): found [M+H]⁺ 337.0866, [C₁₅H₁₈ClN₄OS]⁺ requires 337.0890; [α]_D^{23.5}: +1.7° (c 1.0, MeOH); δ _H (CDCl₃, 500 MHz): 7.69 (1H, s, H7), 6.85 (1H, d, *J* = 3.5 Hz, H3), 6.61 – 6.59 (1H, m, H2), 5.53 (1H, d, *J* = 15.5 Hz, ArCHH), 4.33 – 4.29 (2H, m, ArCHH & CHCH₂CH₃), 3.32 (3H, s, CONCH₃), 2.45 (3H, s, ArCH₃), 2.04 – 1.95 (1H, m, CHCHHCH₃), 1.91 – 1.83 (1H, m, CHCHHCH₃), 0.82 (3H, t, *J* = 7.4 Hz, CHCH₂CH₃); δ _C (CDCl₃, 126 MHz): 163.6 (CONCH₃), 154.2 (C8), 151.8 (C5), 141.3 (C1), 138.0 (C7), 134.5 (C4), 128.1 (C3), 124.8 (C2), 120.5 (C6), 56.0 (CHCH₂CH₃), 43.1 (ArCH₂), 28.2 (CONCH₃), 24.9 (CHCH₂CH₃), 15.4 (ArCH₃), 8.5 (CHCH₂CH₃)

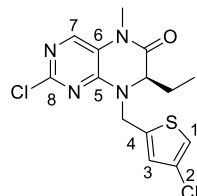
(*R*)-8-((4-Bromothiophen-2-yl)methyl)-2-chloro-7-ethyl-5-methyl-7,8-dihydropteridin-6(5*H*)-one, 6t



Dihydropteridinone **13t** (217 mg, 0.56 mmol) was reacted with methyl iodide (46 μ L, 0.73 mmol) using general method **5** to afford the title compound **6t** as a yellow solid (165 mg, 69%). LCMS purity >95%, ret. time 1.56 mins; HRMS (ESI +ve): found [M+H]⁺ 402.9801, [C₁₄H₁₅BrClN₄OS]⁺ requires 402.9811; [α]_D^{23.7}: -18.7° (c 1.0, MeOH); δ _H (CDCl₃, 500 MHz): 7.72 (1H, s, H7), 7.17 (1H, s, H1), 6.99 (1H, s, H3), 5.47 (1H, d, *J* = 15.8 Hz, ArCHH), 4.41 (1H, d, *J* = 15.8 Hz, ArCHH), 4.31 (1H, dd, *J* = 6.3, 3.5 Hz, CHCH₂CH₃), 3.33 (3H, s, CONCH₃), 2.05 – 1.98 (1H, m, CHCHHCH₃), 1.90 – 1.82 (1H, m, CHCHHCH₃), 0.81 (3H, t, *J* = 7. Hz, CHCH₂CH₃); δ _C (CDCl₃, 126 MHz): 163.3 (CO₂CH₃), 154.0 (C8), 151.7 (C5), 139.0 (C4), 138.3 (C7), 130.3 (C3), 123.8 (C1),

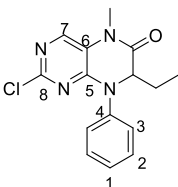
120.5 (C6), 109.4 (C2), 60.8 ($\underline{\text{C}}\text{HCH}_2\text{CH}_3$), 43.0 (ArCH_2), 28.3 (CONCH_3), 25.1 (CHCH_2CH_3), 8.5 (CHCH_2CH_3)

(*R*)-8-((4-Chlorothiophen-2-yl)methyl)-2-chloro-7-ethyl-5-methyl-7,8-dihydropteridin-6(5*H*)-one, 6u



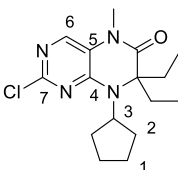
Dihydropteridinone **13u** (120 mg, 0.35 mmol) was reacted with methyl iodide (28 μL , 0.45 mmol) using general method **5** to afford the title compound **6u** as a yellow solid (114 mg, 91%). LCMS purity >95%, ret. time 1.54 mins; HRMS (ESI +ve): found $[\text{M}+\text{H}]^+$ 357.0334, $[\text{C}_{14}\text{H}_{15}\text{Cl}_2\text{N}_4\text{OS}]^+$ requires 357.0338; $[\alpha]_D^{22.8}$: -2.8° (c 1.0, MeOH); δ_{H} (CDCl_3 , 500 MHz): 7.72 (1H, s, H7), 7.06 (1H, d, $J = 1.3$ Hz, H1), 6.95 – 6.94 (1H, m, H3), 5.45 (1H, d, $J = 15.6$ Hz, ArCHH), 4.39 (1H, d, $J = 15.6$ Hz, ArCHH), 4.31 (1H, dd, $J = 6.0, 3.5$ Hz, CHCH_2CH_3), 3.34 (3H, s, CONCH_3), 2.06 – 1.98 (1H, m, CHCHHCH_3), 1.91 – 1.82 (1H, m, CHCHHCH_3), 0.81 (3H, t, $J = 7.4$ Hz, CHCH_2CH_3); δ_{C} (CDCl_3 , 126 MHz): 163.3 (CO_2CH_3), 154.1 (C8), 151.7 (C6), 138.3 (C4 & C7), 128.0 (C3), 124.8 (C2), 120.9 (C1), 120.5 (C6), 60.8 (CHCH_2CH_3), 43.2 (ArCH_2), 28.3 (CONCH_3), 25.1 (CHCH_2CH_3), 8.5 (CHCH_2CH_3)

2-Chloro-7-ethyl-5-methyl-8-phenyl-7,8-dihydropteridin-6(5*H*)-one, 6v



Dihydropteridinone **13v** (190 mg, 0.66 mmol) was reacted with methyl iodide (54 μL , 0.86 mmol) using general method **5** to afford the title compound **6v** as a white solid (135 mg, 69%). LCMS purity >95%, ret. time 1.40 mins; HRMS (ESI +ve): found $[\text{M}+\text{H}]^+$ 303.1013, $[\text{C}_{15}\text{H}_{16}\text{ClN}_4\text{O}]^+$ requires 303.1013; δ_{H} (CDCl_3 , 500 MHz): 7.81 (1H, s, H7), 7.51 – 7.45 (2H, m, H2), 7.40 – 7.33 (3H, m, H1 & H3), 4.66 (1H, dd, $J = 6.3, 3.6$ Hz, CHCH_2CH_3), 3.42 (3H, s, NCH_3), 2.06 – 1.97 (1H, m, CHCHHCH_3), 1.77 – 1.68 (1H, m, CHCHHCH_3), 0.93 (3H, t, $J = 7.9$ Hz, CHCH_2CH_3); δ_{C} (CDCl_3 , 126 MHz): 163.5 (CONCH_3), 154.1 (C8), 151.7 (C5), 139.1 (C7), 139.0 (C4), 129.6 (C2), 127.8 (C1), 126.9 (C3), 120.6 (C6), 64.6 (CHCH_2CH_3), 28.4 (NCH_3), 25.6 (CHCH_2CH_3), 8.5 (CHCH_2CH_3)

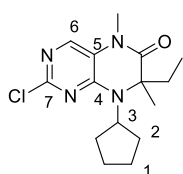
2-Chloro-8-cyclopentyl-7,7-diethyl-5-methyl-7,8-dihydropteridin-6(5*H*)-one, 14a



Under nitrogen conditions, *n*BuLi (1.6 M solution in hexane, 42 μL , 0.46 mmol) was added dropwise to a stirred solution of diisopropyl amine (68 μL , 0.49 mmol) in THF (3.05 mL, 0.1 M) at -78°C . The solution was stirred for 5 mins then warmed to 0°C for a further 20 mins. The resulting solution was added dropwise to dihydropteridinone **6a** (90 mg, 0.30 mmol) in THF (3.05 mL, 0.1 M) at -78°C . After 30 mins, iodoethane (0.47 mL,

0.92 mmol) was added and the solution stirred for 1 hour. Upon completion, water was added, and the aqueous phase extracted with EtOAc (X3). The combined organic phases were washed with water, dried over MgSO₄, filtered and concentrated *in vacuo*. The residue was purified by Biotage column chromatography (cHex:EtOAc 0 – 20%) to afford the title compound **14a** (62 mg, 63%) as a white solid. LCMS purity >95%, ret. time 1.62 mins; HRMS (ESI +ve): found [M+H]⁺ 323.1632, [C₁₆H₂₄ClN₄O]⁺ requires 323.1633; δ_H (CDCl₃, 500 MHz): 7.53 (1H, s, H6), 3.80 (1H, quin, *J* = 8.7 Hz, H3), 3.31 (3H, s, CONCH₃), 2.43 – 2.34 (2H, m, H2), 2.23 – 2.09 (4H, m, H1 & (CH₂CH₃)₂), 1.88 – 1.77 (2H, m, (CH₂CH₃)₂), 1.74 – 1.65 (2H, m, H2), 1.61 – 1.51 (2H, m, H1), 0.82 (1H, tt, *J* = 7.3, 1.3 Hz, (CH₂CH₃)₂); δ_C (CDCl₃, 126 MHz): 166.0 (CONCH₃), 153.2 (C7), 151.0 (C4), 136.6 (C6), 119.8 (C5), 73.0 (C(CH₂CH₃)₂), 56.8 (C3), 31.8 ((CH₂CH₃)₂), 28.7 (C2), 28.1 (NCH₃), 26.1 (C1), 8.7 ((CH₂CH₃)₂)

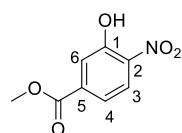
2-Chloro-8-cyclopentyl-7-ethyl-5,7-dimethyl-7,8-dihydropteridin-6(5H)-one, **14b**



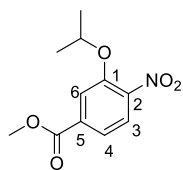
To dihydropteridinone **6a** (53 mg, 0.18 mmol) in THF (1.78 mL, 0.1 M) at –78 °C was added LiHDMS (1 M solution in THF, 37 μ L, 0.20 mmol). The solution stirred at RT for 4 hrs. Upon completion, sat. aq. NH₄Cl was added, and the aqueous phase extracted with CH₂Cl₂ (X3).

The combined organic phases were dried over MgSO₄, filtered and concentrated *in vacuo*. The residue was purified by Biotage column chromatography (cHex:EtOAc 0 – 20%) to afford the title compound **14b** (35 mg, 64%) as a white solid. LCMS purity >95%, ret. time 1.59 mins; HRMS (ESI +ve): found [M+H]⁺ 309.1474, [C₁₅H₂₂ClN₄O]⁺ requires 309.1477; δ_H (CDCl₃, 500 MHz): 7.55 (1H, s, H6), 3.89 - 3.82 (1H, m, H3), 3.31 (3H, s, NCH₃), 2.46 – 2.39 (1H, m, H2), 2.35 – 2.09 (4H, m, cPeH & CH₂CH₃), 1.99 – 1.80 (1H, m, CH₂CH₃), 1.75 – 1.69 (2H, m, H2), 1.67 (3H, s, CH₃), 1.63 – 1.52 (2H, m, H1), 0.84 (3H, t, *J* = 7.4 Hz, CH₂CH₃); δ_C (CDCl₃, 126 MHz): 165.6 (CONCH₃), 153.2 (C7), 150.4 (C4), 136.7 (C6), 112.0 (C5), 67.8 (C(CH₃)(CH₂CH₃)), 57.4 (C3), 32.4 (CH₂CH₃), 29.2 (C2), 28.5 (C2'), 28.4 (NCH₃), 26.3 (C1), 26.1 (C1'), 8.9 (CH₂CH₃)

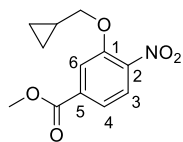
Methyl 3-Hydroxy-4-nitrobenzoate, **16**



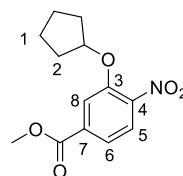
3-Hydroxy-4-nitrobenzoic acid **15** (1 g, 5.46 mmol) was subjected to general method **1** to afford the title compound **16** (HCl salt) as a yellow solid (1.05 g, 82%). LCMS purity >95%, ret. time 1.20 mins, correct mass not observed; δ_H (CDCl₃, 500 MHz): 10.51 (1H, s, OH), 8.18 (1H, d, *J* = 8.5 Hz, H3), 7.84 (1H, d, *J* = 1.6 Hz, H6), 7.62 (1H, dd, *J* = 8.5, 1.6 Hz, H4), 3.97 (3H, s, CO₂CH₃); δ_C (CDCl₃, 126 MHz): 164.8 (CO₂CH₃), 154.7 (C1), 138.0 (C5), 135.8 (C2), 125.3 (C3), 121.7 (C6), 52.9 (CO₂CH₃)

Methyl 3-isopropoxy-4-nitrobenzoate, 17a

Methyl 3-hydroxy-4-nitrobenzoate **16** (200 mg, 0.86 mmol) was reacted with 2-iodopropane (0.12 mL, 1.20 mmol) using general method **6** to afford the title compound **17a** as a yellow oil (180 mg, 88%). LCMS purity >95%, ret. time 1.48 mins, correct mass not observed; δ_{H} (CDCl_3 , 500 MHz): 7.76 (1H, d, $J = 8.5$ Hz, H3), 7.75 (1H, d, $J = 1.6$ Hz, H6), 7.65 (1H, dd, $J = 8.5, 1.6$ Hz, H4), 4.78 (1H, sept, $J = 6.0$ Hz, $\text{CH}(\text{CH}_3)_2$), 3.97 (3H, s, OCH_3), 1.42 (6H, d, $J = 6.0$ Hz, $\text{CH}(\text{CH}_3)_2$); δ_{C} (CDCl_3 , 126 MHz): 165.3 ($\text{C}=\text{O}$), 150.7 (C1), 143.7 (C2), 134.4 (C5), 125.0 (C3), 121.0 (C4), 116.9 (C6), 72.9 ($\text{CH}(\text{CH}_3)_2$), 52.7 (OCH_3), 21.7 ($\text{CH}(\text{CH}_3)_2$).

Methyl 3-(cyclopropylmethoxy)-4-nitrobenzoate, 17b

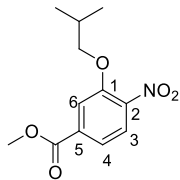
Methyl 3-hydroxy-4-nitrobenzoate **16** (130 mg, 0.56 mmol) was reacted with (bromomethyl)cyclopropane (76 μL , 0.78 mmol) using general method **6** to afford the title compound **17b** as a yellow solid (119 mg, 85%). LCMS purity >95%, ret. time 1.49 mins, correct mass not observed; δ_{H} (CDCl_3 , 500 MHz): 7.81 (1H, d, $J = 8.5$ Hz, H3), 7.72 (1H, d, $J = 1.6$ Hz, H6), 7.69 – 7.66 (1H, m, H4), 4.04 (2H, d, $J = 6.6$ Hz, OCH_2), 3.96 (3H, s, CO_2CH_3), 1.36 – 1.27 (1H, m, $\text{CH}(\text{CH}_2)_2$), 0.71 – 0.64 (2H, m, $\text{CH}(\text{CH}_2)(\text{CH}_2)$), 0.45 – 0.39 (2H, m, $\text{CH}(\text{CH}_2)(\text{CH}_2)$); δ_{C} (CDCl_3 , 126 MHz): 165.3 ($\text{C}=\text{O}$), 151.8 (C1), 142.9 (C2), 134.6 (C5), 125.2 (C3), 121.3 (C4), 116.0 (C6), 74.6 (OCH_2), 52.8 (CO_2CH_3), 9.8 ($\text{CH}(\text{CH}_2)_2$), 3.3 ($\text{CH}(\text{CH}_2)_2$).

Methyl 3-(cyclopentyloxy)-4-nitrobenzoate, 17c

Methyl 3-hydroxy-4-nitrobenzoate **16** (200 mg, 1.01 mmol), cyclopentanol (74 μL , 0.81 mmol) and triphenylphosphine (346 mg, 1.32 mmol) were dissolved in THF (0.1 M). Di-(tert-butyl) azodicarboxylate (234 mg, 1.01 mmol) was added and the reaction stirred at rt for 18 hrs during which time LCMS analysis revealed the progress of the reaction. Upon its completion, the reaction was quenched with water (5 mL) and the aqueous phase extracted with CH_2Cl_2 (X3). The organic phases were combined, dried over MgSO_4 and concentrated *in vacuo*. The reaction was purified by Biotage column chromatography (cHex/EtOH, 4:1) to afford the title compound **17c** as a yellow solid (230 mg, 85%). LCMS purity >95%, ret. time 1.57 mins, correct mass not observed; δ_{H} (CDCl_3 , 500 MHz): 7.77 (1H, d, $J = 8.2$ Hz, H5), 7.74 (1H, d, $J = 1.3$ Hz, H8), 7.64 (1H, dd, $J = 8.2, 1.3$ Hz, H6), 5.02 – 4.98 (1H, m, OCH), 3.97 (3H, s, CO_2CH_3), 2.01 –

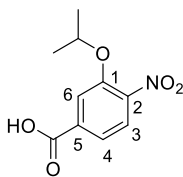
1.90 (4H, m, H₂), 1.89 – 1.80 (2H m, H₁), 1.73 – 1.62 (2H m, H₁); δ_{C} (CDCl₃, 126 MHz): 165.4 (C=O₂CH₃), 151.0 (C₃), 143.3 (C₄), 134.4 (C₇), 125.1 (C₅), 120.8 (C₆), 116.6 (C₈), 81.8 (OCH), 52.8 (CO₂C_H), 32.7 (C₂), 23.8 (C₁)

Methyl 3-isobutoxy-4-nitrobenzoate, 17d



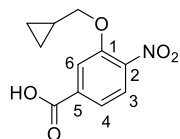
Methyl 3-hydroxy-4-nitrobenzoate **16** (200 mg, 0.86 mmol) was reacted with 1-iodo-2-methylpropane (0.12 mL, 1.20 mmol) using general method **6** to afford the title compound **17d** as a colourless oil (158 mg, 73%). LCMS purity >95%, ret. time 1.60 mins, correct mass not observed; δ_{H} (CDCl₃, 500 MHz): 7.81 (1H, d, J = 8.2 Hz, H₃), 7.71 (1H, d, J = 1.6 Hz, H₆), 7.67 – 7.64 (1H, m, H₄), 3.96 (3H, s, CO₂CH₃), 3.92 (1H, d, J = 6.3 Hz, OCH₂), 2.20 – 2.11 (1H, m, CH(CH₃)₂), 1.05 (6H, d, J = 6.9 Hz, CH(CH₃)₂); δ_{C} (CDCl₃, 126 MHz): 165.3 (C=O₂CH₃), 152.0 (C₁), 142.4 (C₂), 134.7 (C₅), 125.1 (C₃), 121.0 (C₄), 115.3 (C₆), 75.9 (OCH₂), 52.8 (CO₂C_H), 28.2 (CH(CH₃)₂), 19.0 (CH(CH₃)₂)

3-Isopropoxy-4-nitrobenzoic acid, 18a

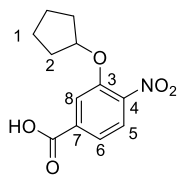


Methyl 3-isopropoxy-4-nitrobenzoate **17a** (180 mg, 0.75 mmol) was subjected general method **7** to afford the title compound **18a** as a yellow solid (153 mg, 90%). LCMS purity >95%, ret. time 1.47 mins, correct mass not observed; δ_{H} (CDCl₃, 500 MHz): 7.81 (1H, d, J = 8.4 Hz, H₃), 7.79 (1H, d, J = 1.6 Hz, H₆), 7.74 (1H, dd, J = 8.4, 1.6 Hz, H₄), 4.80 (1H, sept., J = 6.0 Hz, CH(CH₃)₂), 1.44 (6H, d, J = 6.0 Hz, CH(CH₃)₂); δ_{C} (CDCl₃, 126 MHz): 169.1 (C=O₂H), 150.8 (C₁), 144.3 (C₂), 133.2 (C₅), 125.2 (C₃), 121.7 (C₄), 117.3 (C₆), 73.1 (CH(CH₃)₂), 21.8 (CH(CH₃)₂)

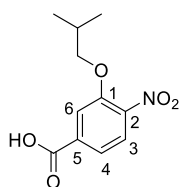
3-(Cyclopropylmethoxy)-4-nitrobenzoic acid, 18b



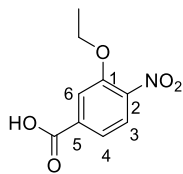
Methyl 3-(cyclopropylmethoxy)-4-nitrobenzoate **17b** (110 mg, 0.44 mmol) was subjected to general method **7** to afford the title compound **18b** as a yellow solid (58 mg, 56%). LCMS purity >95%, ret. time 1.47 mins, correct mass not observed; δ_{H} (CDCl₃, 500 MHz): 7.84 (1H, d, J = 8.5 Hz, H₃), 7.79 (1H, d, J = 1.3 Hz, H₆), 7.78 – 7.75 (1H, m, H₄), 4.07 (2H, d, J = 6.9 Hz, OCH₂), 1.38 – 1.28 (1H, m, CH(CH₂)₂), 0.73 – 0.63 (2H, m, CH(CH₂)₂), 0.47 – 0.39 (2H, m, CH(CH₂)₂); δ_{C} (CDCl₃, 126 MHz): δ 169.3 (CO₂H), 151.8 (C₁), 143.5 (C₂), 133.5 (C₅), 125.2 (C₃), 122.0 (C₄), 116.4 (C₆), 74.7 (OCH₂), 9.8 (CH(CH₂)₂), 3.4 (CH(CH₂)₂)

3-(Cyclopentyloxy)-4-nitrobenzoic acid, 18c

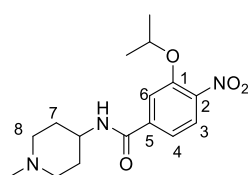
Methyl 3-(cyclopentylmethoxy)-4-nitrobenzoate **17c** (225 mg, 0.81 mmol) was subjected to general method **7** to afford the title compound **18c** as a yellow solid (181 mg, 89%). LCMS purity >95%, ret. time 1.49 mins, correct mass not observed; δ_{H} (CDCl_3 , 500 MHz): 7.81 (1H, d, $J = 8.2$ Hz, H5), 7.80 (1H, d, $J = 1.6$ Hz, H8), 7.73 (1H, dd, $J = 8.2, 1.6$ Hz, H6), 5.03 – 4.99 (1H, m, OCH), 2.03 – 1.88 (4H, m, H2), 1.90 – 1.78 (2H m, H1), 1.73 – 1.59 (2H m, H1); δ_{C} (CDCl_3 , 126 MHz): 168.9 (CO_2H), 151.0 (C5), 144.0 (C4), 133.2 (C7), 125.2 (C5), 121.5 (C6), 117.0 (C8), 82.0 (OCH), 32.7 (C2), 23.1 (C1)

3-Isobutoxy-4-nitrobenzoic acid, 18d

Methyl 3-isobutoxy-4-nitrobenzoate **17d** (150 mg, 0.59 mmol) was subjected to general method **7** to afford the title compound **18d** as a yellow solid (100 mg, 71%). LCMS purity >95%, ret. time 1.47 mins, correct mass not observed; δ_{H} (CDCl_3 , 500 MHz): 7.85 (1H, d, $J = 8.2$ Hz, H3), 7.79 (1H, d, $J = 1.3$ Hz, H6), 7.76 (1H, dd, $J = 8.2, 1.3$ Hz, H4), 3.95 (1H, d, $J = 6.3$ Hz, OCH_2), 2.23 – 2.14 (1H, m, $\text{CH}(\text{CH}_3)_2$), 1.08 (6H, d, $J = 6.9$ Hz, $\text{CH}(\text{CH}_3)_2$); δ_{C} (CDCl_3 , 126 MHz): 169.0 (CO_2H), 152.1 (C1), 143.1 (C2), 133.5 (C5), 125.3 (C3), 121.7 (C4), 115.8 (C6), 76.0 (OCH_2), 28.2 ($\text{CH}(\text{CH}_3)_2$), 19.0 ($\text{CH}(\text{CH}_3)_2$)

3-Ethoxy-4-nitrobenzoic acid, 18e

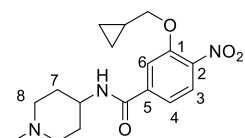
To a solution of 3-fluoro-4-nitrobenzoic acid (500 mg, 2.70 mmol) in EtOH (0.3 M) was added KOH (348 mg, 2.3 equiv.). The mixture was heated under microwave irradiation at 100 °C for 5 mins. The reaction mixture was acidified using 2N HCl and extracted with EtOAc (X3). The combined organic phases were washed with water, dried over MgSO_4 , filtered and concentrated *in vacuo* to afford the title compound **18e** as a brown solid (550 mg, 96%). δ_{H} (CDCl_3 , 500 MHz): 7.83 – 7.80 (2H, m, H3 & H6), 7.70 (1H, dd, $J = 8.2, 1.6$ Hz, H4), 4.27 (2H, q, $J = 6.9$ Hz, OCH_2CH_3), 1.44 (3H, t, $J = 6.9$ Hz, OCH_2CH_3); δ_{C} (CDCl_3 , 126 MHz): 167.3 (COOH), 149.5 (C1), 139.8 (C2), 134.3 (C4), 124.4 (C3), 121.4 (C4), 115.2 (C6), 65.3 (OCH_2CH_3), 13.3 (OCH_2CH_3)

3-Isopropoxy-N-(1-methylpiperidin-4-yl)-4-nitrobenzamide, 19a

Benzoic acid **18a** (50 mg, 0.22 mmol) was reacted with 1-methylpiperidin-4-amine (25.4 mg, 0.22 mmol) using general method **8** to afford the title compound **19a** as a yellow solid (55 mg, 76%). LCMS purity >95%, ret. time 0.97 mins; HRMS (ESI

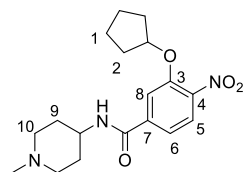
+ve): found $[M+H]^+$ 322.1744, $[C_{16}H_{24}N_3O_4]^+$ requires 322.1767; δ_H ($CDCl_3$, 500 MHz): 7.77 (1H, d, $J = 8.5$ Hz, H3), 7.58 (1H, d, $J = 1.6$ Hz, H6), 7.21 (1H, dd, $J = 8.5, 1.6$ Hz, H4), 6.07 (1H, d, $J = 7.3$ Hz, NH), 4.78 (1H, sept., $J = 6.1$ Hz, $\underline{CH}(\underline{CH_3})_2$), 4.05 – 3.91 (1H, m, \underline{NHCH}), 2.85 (2H, d, $J = 11.4$ Hz, H8), 2.32 (3H, s, $\underline{NCH_3}$), 2.21 – 2.14 (2H, m, H8), 2.09 – 1.99 (2H, m, H7), 1.68 – 1.55 (2H, m, H7), 1.40 (6H, d, $J = 6.3$ Hz, $\underline{CH}(\underline{CH_3})_2$); δ_C ($CDCl_3$, 126 MHz): 165.0 (\underline{CONH}), 151.4 (C1), 142.5 (C2), 139.4 (C5), 125.4 (C3), 117.1 (C4), 115.5 (C6), 73.0 ($\underline{CH}(\underline{CH_3})_2$), 54.5 (C8), 47.1 (\underline{NHCH}), 46.1 ($\underline{NCH_3}$), 32.1 (C7), 21.8 ($\underline{CH}(\underline{CH_3})_2$)

3-(Cyclopropylmethoxy)-*N*-(1-methylpiperidin-4-yl)-4-nitrobenzamide, 19b

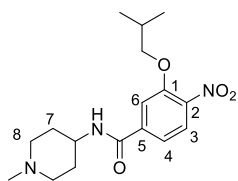


Benzoic acid **18b** (52 mg, 0.22 mmol) was reacted with 1-methylpiperidin-4-amine (25 mg, 0.22 mmol) using general method **8** to afford the title compound **19b** as a white solid (41 mg, 56%). LCMS purity >95%, ret. time 1.02 mins; HRMS (ESI +ve): found $[M+H]^+$ 334.1776 $[C_{17}H_{24}N_3O_4]^+$ requires 334.1767; δ_H ($CDCl_3$, 500 MHz): 7.83 (1H, d, $J = 8.3$ Hz, H3), 7.56 (1H, d, $J = 1.6$ Hz, H6), 7.23 (1H, dd, $J = 8.3, 1.6$ Hz, H4), 5.99 (1H, s, NH), 4.05 (2H, d, $J = 6.9$ Hz, $\underline{OCH_2}$), 4.03 – 3.93 (1H, m, \underline{NHCH}), 2.85 (2H, d, $J = 11.4$ Hz, H8), 2.32 (3H, s, $\underline{NCH_3}$), 2.20 – 2.13 (2H, m, H8), 2.10 – 2.01 (2H, m, H7), 1.65 – 1.54 (2H, m, H7), 1.36 – 1.27 (1H, m, $\underline{CH}(\underline{CH_2})_2$), 0.72 – 0.64 (2H, m, $\underline{CH}(\underline{CH_2})(\underline{C'H_2})$), 0.43 – 0.37 (2H, m, $\underline{CH}(\underline{CH_2})(\underline{C'H_2})$); δ_C ($CDCl_3$, 126 MHz): 164.9 (\underline{CONH}), 152.5 (C1), 141.7 (C2), 139.7 (C5), 125.5 (C3), 117.3 (C4), 114.6 (C6), 74.6 ($\underline{OCH_2}$), 54.4 (C8), 47.2 (\underline{NHCH}), 46.2 ($\underline{NCH_3}$), 32.2 (C7), 9.8 ($\underline{CH}(\underline{CH_2})_2$), 3.3 ($\underline{CH}(\underline{CH_2})_2$)

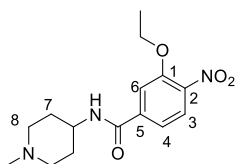
3-(Cyclopentyloxy)-*N*-(1-methylpiperidin-4-yl)-4-nitrobenzamide, 19c



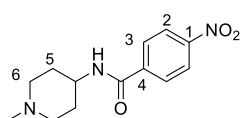
Benzoic acid **18c** (50 mg, 0.20 mmol) was reacted with 1-methylpiperidin-4-amine (23 mg, 0.20 mmol) using general method **8** to afford the title compound **19c** as a yellow solid (42 mg, 61%). LCMS purity >95%, ret. time 1.15 mins; HRMS (ESI +ve): found $[M+H]^+$ 348.1920 $[C_{18}H_{26}N_3O_4]^+$ requires 348.1923; δ_H ($CDCl_3$, 500 MHz): 7.78 (1H, d, $J = 8.2$ Hz, H5), 7.59 (1H, d, $J = 1.6$ Hz, H8), 7.22 (1H, dd, $J = 8.2, 1.6$ Hz, H6), 6.28 (1H, d, $J = 6.9$ Hz, NH), 5.02 – 4.98 (1H, m, \underline{OCH}), 4.07 – 4.00 (1H, m, \underline{NHCH}), 2.99 (2H, d, $J = 11.4$ Hz, H10), 2.40 (3H, s, $\underline{NCH_3}$), 2.33 – 2.26 (2H, m, H10), 2.12 – 2.06 (2H, m, H9), 2.00 – 1.65 (2H, m, cPeH & H9); δ_C ($CDCl_3$, 126 MHz): 165.1 (\underline{CONH}), 151.6 (C3), 142.2 (C4), 139.5 (C5), 125.4 (C5), 117.0 (C6), 115.2 (C8), 81.8 (\underline{OCH}), 54.3 (C10), 46.6 (\underline{NHCH}), 45.6 ($\underline{NCH_3}$), 32.7 (C2), 31.5 (C9), 23.8 (C1)

3-Isobutoxy-*N*-(1-methylpiperidin-4-yl)-4-nitrobenzamide, 19d

Benzoic acid **18d** (50 mg, 0.21 mmol) was reacted with 1-methylpiperidin-4-amine (23.9 mg, 0.21 mmol) using general method **8** to afford the title compound **19d** as a yellow solid (60 mg, 86%). LCMS purity >95%, ret. time 1.02 mins; HRMS (ESI +ve): found $[M+H]^+$ 336.1927, $[C_{17}H_{26}N_3O_4]^+$ requires 336.1923; δ_H (CDCl₃, 500 MHz): 7.81 (1H, d, J = 8.2 Hz, H3), 7.55 (1H, d, J = 1.6 Hz, H6), 7.28 (1H, dd, J = 8.2, 1.6 Hz, H4), 6.44 (1H, d, J = 7.6 Hz, NH), 4.06 – 3.97 (1H, m, NHCH), 3.92 (2H, d, J = 6.3 Hz, OCH₂), 2.94 (2H, d, J = 11.7 Hz, H8), 2.37 (3H, s, NCH₃), 2.31 – 2.23 (2H, m, H8), 2.18 – 2.10 (1H, m, CH(CH₃)₂), 2.09 – 2.03 (2H, m, H7), 1.78 – 1.69 (2H, m, H7), 1.04 (6H, d, J = 6.6 Hz, CH(CH₃)₂); δ_C (CDCl₃, 126 MHz): 165.0 (CONH), 152.6 (C1), 141.2 (C2), 139.6 (C5), 125.4 (C3), 117.4 (C4), 114.0 (C6), 76.0 (OCH₂), 54.4 (C8), 46.7 (NHCH), 45.7 (NCH₃), 31.5 (C7), 28.1 (CH(CH₃)₂), 19.0 (CH(CH₃)₂)

3-Ethoxy-*N*-(1-methylpiperidin-4-yl)-4-nitrobenzamide, 19e

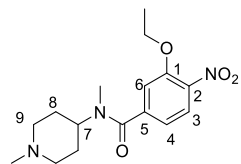
Benzoic acid **18e** (100 mg, 0.47 mmol) was reacted with 1-methylpiperidin-4-amine (54.1 mg, 0.47 mmol) using general method **8** to afford the title compound **19e** as an orange solid (100 mg, 69%). LCMS purity >95%, ret. time 0.88 mins; HRMS (ESI +ve): found $[M+H]^+$ 308.1624 $[C_{15}H_{22}N_3O_4]^+$ requires 308.1610; δ_H (CDCl₃, 500 MHz): 7.82 (1H, d, J = 8.2 Hz, H3), 7.58 (1H, d, J = 1.9 Hz, H6), 7.23 (1H, dd, J = 8.2, 1.9 Hz, H4), 5.99 (1H, d, J = 7.3 Hz, NH), 4.26 (2H, q, J = 7.2 Hz, OCH₂CH₃), 4.05 – 3.94 (1H, m, NHCH), 2.87 (2H, d, J = 11.2 Hz, H8), 2.33 (3H, s, NCH₃), 2.23 – 2.16 (2H, m, H8), 2.10 – 2.03 (2H, m, H7), 1.65 – 1.56 (2H, m, H7), 1.49 (3H, t, J = 6.9 Hz, OCH₂CH₃); δ_C (CDCl₃, 126 MHz): 164.9 (CONH), 152.4 (C1), 140.6 (C2), 139.7 (C5), 125.5 (C3), 117.3 (C4), 114.2 (C6), 65.8 (OCH₂CH₃), 54.5 (NHCH), 53.4 (C8), 46.2 (NCH₃), 32.2 (C7^{a+b}), 14.5 (OCH₂CH₃)

***N*-(1-Methylpiperidin-4-yl)-4-nitrobenzamide, 19f**

4-Nitrobenzoic acid **18f** (400 mg, 2.39 mmol) was reacted with 1-methylpiperidin-4-amine (273 mg, 2.39 mmol) using general method **8** to afford the title compound **19f** as a white solid (350 mg, 55%). LCMS purity >95%, ret. time 0.18 mins; HRMS (ESI +ve): found $[M+H]^+$ 264.1335 $[C_{13}H_{18}N_3O_3]^+$ requires 264.1343; δ_H (CDCl₃, 500 MHz): 8.29 (2H, d, J = 8.2 Hz, H2), 7.93 (2H, d, J = 8.2 Hz, H3), 6.08 (1H, d, J = 6.0 Hz, NH), 4.06 – 3.97 (1H, m, NHCH), 2.87 (2H, d, J = 13.9 Hz, H6), 2.33 (3H, s, NCH₃), 2.29 – 2.22 (2H, m, H6), 2.11 – 2.05 (2H, m, H5), 1.64 (2H, qd, J = 11.9, 3.8 Hz, H5); δ_C (CDCl₃, 126

MHz): 164.9 (CONH), 149.6 (C1), 140.3 (C4), 128.1 (C3), 123.8 (C2), 54.4 (C6), 46.8 (NHCH), 45.8 (NCH₃), 31.7 (C5)

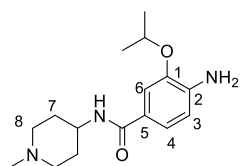
3-Ethoxy-*N*-methyl-*N*-(1-methylpiperidin-4-yl)-4-nitrobenzamide, **19g**



Benzoic acid **18e** (300 mg, 1.42 mmol) was reacted with *N*,1-dimethylpiperidin-4-amine (0.21 mL, 1.42 mmol) using general method **8** to afford the title compound **19g** as an orange solid (255 mg, 55%). LCMS purity >95%, ret. time 0.57 mins; HRMS

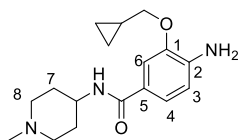
(ESI +ve): found $[M+H]^+$ 322.1756, $[C_{16}H_{23}N_3O_4]^+$ requires 322.1761; *Rotomer A* δ_H (CDCl₃, 500 MHz): 7.77 (1H, d, J = 8.5 Hz, H3), 7.58 (1H, d, J = 1.6 Hz, H6), 7.21 (1H, dd, J = 8.5, 1.6 Hz, H4), 4.59 – 4.50 (1H, m, H7), 4.22 (2H, q, J = 6.9 Hz, OCH₂CH₃), 3.05 – 2.95 (2H, m, H9), 2.82 (3H, s, CONCH₃), 2.36 (3H, s, NCH₃), 2.28 – 2.18 (2H, m, H9), 1.98 – 1.75 (2H, m, H8), 1.48 (3H, d, J = 6.9 Hz, OCH₂CH₃); δ_C (CDCl₃, 126 MHz): 169.3 (CONCH₃), 152.5 (C1), 142.5 (C2), 140.1 (C5), 125.7 (C3), 117.7 (C4), 112.8 (C6), 65.7 (OCH₂CH₃), 54.9 (C9), 50.9 (C7), 45.9 (NCH₃), 32.0 (CONCH₃), 28.3 (C8), 14.5 (CH₂CH₃); *Rotomer B* δ_H (CDCl₃, 500 MHz): 7.77 (1H, d, J = 8.5 Hz, H3), 7.58 (1H, d, J = 1.6 Hz, H6), 7.21 (1H, dd, J = 8.5, 1.6 Hz, H4), 3.41 – 3.33 (1H, m, H7), 4.22 (2H, q, J = 6.9 Hz, OCH₂CH₃), 2.90 – 2.84 (2H, m, H9), 2.82 (3H, s, CONCH₃), 2.23 (3H, s, NCH₃), 2.04 – 1.75 (5H, m, 3 x H8 & 2 x H9), 1.62 – 1.56 (1H, m, H8), 1.48 (3H, d, J = 6.9 Hz, OCH₂CH₃); δ_C (CDCl₃, 126 MHz): 169.3 (CONCH₃), 152.5 (C1), 142.5 (C2), 140.1 (C5), 125.7 (C3), 117.7 (C4), 112.8 (C6), 65.7 (OCH₂CH₃), 56.4 (C7), 54.7 (C9), 45.9 (NCH₃), 29.8 (C8), 27.7 (CONCH₃), 14.5 (OCH₂CH₃)

4-Amino-3-isopropoxy-*N*-(1-methylpiperidin-4-yl)benzamide, **20a**



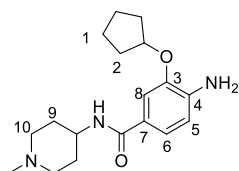
4-Nitrobenzamide **19a** (55 mg, 0.17 mmol) was subjected to general method 9 to afford the title compound **20a** as a yellow solid (34 mg, 68%). LCMS purity >95%, ret. time 0.32 mins;

HRMS (ESI +ve): found $[M+H]^+$ 292.2015, $[C_{16}H_{26}N_3O_2]^+$ requires 292.2025; δ_H (CDCl₃, 500 MHz) 7.36 (1H, d, J = 1.9 Hz, H6), 7.09 (1H, dd, J = 8.2, 1.9 Hz, H4), 6.65 (1H, d, J = 8.2 Hz, H3), 5.87 (1H, d, J = 7.3 Hz, NH), 4.65 (1H, sept., J = 6.3 Hz, CH(CH₃)₂), 4.11 (2H, s, NH₂), 4.02 – 3.93 (1H, m, NHCH), 2.83 (2H, d, J = 11.5 Hz, H8), 2.31 (3H, s, NCH₃), 2.20 – 2.13 (2H, m, H8), 2.06 – 2.00 (2H, m, H7), 1.63 – 1.53 (2H, m, H7), 1.36 (6H, d, J = 6.3 Hz, CH(CH₃)₂); δ_C (CDCl₃, 126 MHz): 166.8 (CONH), 144.8 (C1), 140.7 (C2), 124.2 (C5), 119.3 (C4), 113.4 (C3), 112.7 (C6), 70.8 (CH(CH₃)₂), 54.5 (C8), 46.3 (NHCH), 46.1 (NCH₃), 32.3 (C7), 22.2 (CH(CH₃)₂)

4-Amino-3-(cyclopropylmethoxy)-*N*-(1-methylpiperidin-4-yl)benzamide, 20b

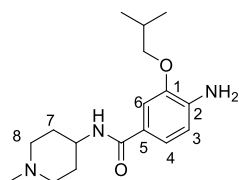
4-nitrobenzamide **19b** (40 mg, 0.12 mmol) was subjected to general method **9** to afford the title compound **20b** as a white solid (20 mg, 55%). LCMS purity >95%, ret. time 0.52 mins;

HRMS (ESI +ve): found $[M+H]^+$ 304.2008 $[C_{17}H_{26}N_3O_2]^+$ requires 304.2020; δ_H (CDCl₃, 500 MHz): 7.29 (1H, d, J = 1.9 Hz, H6), 7.11 (1H, dd, J = 8.2, 1.9 Hz, H4), 6.65 (1H, dd, J = 8.2 Hz, H3), 5.94 (1H, s, NH), 4.18 (2H, s, NH₂), 4.03 – 3.91 (1H, m, NHCH), 3.87 (2H, d, J = 6.9 Hz, OCH₂CH₃), 2.84 (2H, d, J = 11.0 Hz, H8), 2.31 (3H, s, NCH₃), 2.26 – 2.19 (2H, m, H8), 2.05 – 1.99 (2H, m, H7), 1.64 – 1.53 (2H, m, H7), 1.31 – 1.22 (1H, m, CH(CH₂)₂), 0.65 – 0.59 (2H, m, CH(CH₂)(C'H₂)), 0.36 – 0.31 (2H, m, CH(CH₂)(C'H₂)); δ_C (CDCl₃, 126 MHz): 166.8 (CONH), 146.1 (C1), 139.9 (C2), 124.2 (C5), 119.5 (C5), 113.2 (C3), 111.0 (C6), 73.4 (OCH₂), 54.5 (C8), 46.2 (NHCH), 46.0 (NCH₃), 32.1 (C7), 10.3 (CH(CH₂)₂), 3.2 (CH(CH₂)₂)

4-Amino-3-(cyclopentyloxy)-*N*-(1-methylpiperidin-4-yl)benzamide, 20c

4-Nitrobenzamide **19c** (37 mg, 0.11 mmol) was subjected to general method **9** to afford the title compound **20c** as a white solid (25 mg, 74%). LCMS purity >95%, ret. time 0.89 mins;

HRMS (ESI +ve): found $[M+H]^+$ 318.2172 $[C_{17}H_{28}N_3O_2]^+$ requires 318.2176; δ_H (CDCl₃, 500 MHz): 7.34 (1H, d, J = 1.9 Hz, H8), 7.08 (1H, dd, J = 7.9, 1.9 Hz, H6), 6.64 (1H, d, J = 7.9 Hz, H5), 5.93 (1H, d, J = 7.9 Hz, NH), 4.87 (1H, tt, J = 5.7, 2.8 Hz, OCH), 4.03 – 3.93 (1H, m, NHCH), 2.93 – 2.84 (2H, m, H10), 2.33 (3H, s, NCH₃), 2.20 (2H, t, J = 10.9 Hz, H10), 2.06 – 2.00 (2H, m, H9), 1.99 – 1.64 (6H, m, cPeH), 1.68 – 1.57 (4H, m, cPeH & H9); δ_C (CDCl₃, 126 MHz): 166.9 (CONH), 145.0 (C3), 140.3 (C4), 124.1 (C7), 119.1 (C6), 113.2 (C5), 112.0 (C8), 79.9 (OCH), 54.4 (C10), 46.2 (NHCH), 45.9 (NCH₃), 32.9 (C2), 32.1 (C9), 24.0 (C1); *NH₂ peak not observed.*

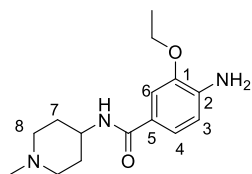
4-Amino-3-isobutoxy-*N*-(1-methylpiperidin-4-yl)benzamide, 20d

4-Nitrobenzamide **19d** (60 mg, 0.18 mmol) was subjected to general method **9** to afford the title compound **20d** as a yellow solid (30 mg, 55%). LCMS purity >95%, ret. time 0.90 mins;

HRMS (ESI +ve): found $[M+H]^+$ 306.22161, $[C_{17}H_{28}N_3O_2]^+$ requires 306.2176; δ_H (CDCl₃, 500 MHz) 7.32 (1H, d, J = 1.9 Hz, H6), 7.10 (1H, d, J = 8.2, 1.9 Hz, H4), 6.66 (1H, d, J = 8.2 Hz, H3), 5.86 (1H, d, J = 6.3 Hz, NH), 4.12 (2H, s, NH₂), 4.02 – 3.92 (1H, m, NHCH), 3.83 (2H, d, J = 6.3 Hz, OCH₂), 2.83 (2H, d, J = 11.0 Hz, H8), 2.31 (3H, s, NCH₃), 2.22 – 2.09 (3H, m, H8 & CH(CH₃)₂), 2.07 – 2.00

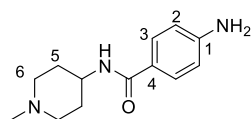
(2H, m, H7), 1.57 (2H, qd, $J = 11.7, 3.6$ Hz, H7), 1.04 (6H, d, $J = 6.9$ Hz, $\text{CH}(\text{CH}_3)_2$); δ_{C} (CDCl_3 , 126 MHz): 166.8 (CONH), 146.2 (C1), 139.7 (C2), 124.3 (C5), 119.3 (C4), 113.1 (C3), 110.7 (C6), 74.7 (OCH_2), 54.5 (C8), 46.3 (NHCH), 46.1 (NCH_3), 32.4 (C7), 28.3 ($\text{CH}(\text{CH}_3)_2$), 19.3 ($\text{CH}(\text{CH}_3)_2$)

4-Amino-3-ethoxy-*N*-(1-methylpiperidin-4-yl)benzamide, 20e



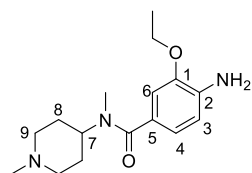
4-Nitrobenzamide **19e** (95 mg, 0.18 mmol) was subjected to general method **9** to afford the title compound **20e** as a yellow solid (28 mg, 32%). LCMS purity >95%, ret. time 0.21 mins; HRMS (ESI +ve): found $[\text{M}+\text{H}]^+$ 278.1874 $[\text{C}_{15}\text{H}_{24}\text{N}_3\text{O}_2]^+$ requires 278.1863; δ_{H} (CDCl_3 , 500 MHz) 7.33 (1H, d, $J = 1.9$ Hz, H6), 7.11 (1H, dd, $J = 8.1, 1.9$ Hz, H4), 6.66 (1H, dd, $J = 8.1$ Hz, H3), 5.86 (1H, d, $J = 7.3$ Hz, NH), 4.18 – 4.09 (4H, m, NH_2 & OCH_2CH_3), 4.05 – 3.94 (1H, m, NHCH), 2.86 (2H, d, $J = 11.0$ Hz, H8), 2.33 (3H, s, NCH_3), 2.24 – 2.17 (2H, m, H8), 2.07 – 2.01 (2H, m, H7), 1.59 (2H, qd, $J = 11.6, 3.6$ Hz, H7), 1.45 (3H, t, $J = 6.9$ Hz, OCH_2CH_3); δ_{C} (CDCl_3 , 126 MHz): 166.8 (CONH), 146.1 (C1), 139.8 (C2), 124.3 (C5), 119.4 (C4), 113.2 (C3), 110.7 (C6), 64.0 (OCH_2CH_3), 53.4 (C8), 46.3 (NHCH), 46.1 (NCH_3), 31.0 (C7), 14.9 (CH_2CH_3)

4-Amino-*N*-(1-methylpiperidin-4-yl)benzamide, 20f



4-Nitrobenzamide **19f** (160 mg, 0.61 mmol) was subjected to general method **9** to afford the title compound **20f** as a colourless gum (80 mg, 56%). LCMS purity >95%, ret. time 0.09 mins; HRMS (ESI +ve): found $[\text{M}+\text{H}]^+$ 234.1619 $[\text{C}_{13}\text{H}_{20}\text{N}_3\text{O}]^+$ requires 234.1601; δ_{H} (CDCl_3 , 500 MHz): 7.61 – 7.58 (2H, m, H3), 6.68 – 6.65 (2H, m, H2), 5.83 (1H, d, $J = 6.6$ Hz, NH), 4.02 – 3.93 (3H, m, NH_2 & NHCH), 2.85 (2H, d, $J = 11.7$ Hz, H6), 2.32 (3H, s, NCH_3), 2.20 – 2.115 (2H, m, H6), 2.07 – 2.01 (2H, m, H5), 1.63 – 1.54 (2H, m, H5); δ_{C} (CDCl_3 , 126 MHz): 166.6 (CONH), 149.5 (C1), 128.6 (C3), 124.3 (C4), 114.2 (C2), 54.6 (C6), 46.3 (NHCH), 46.1 (NCH_3), 32.4 (C5)

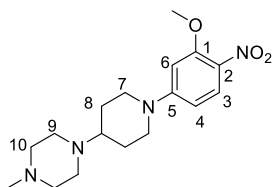
4-Amino-3-ethoxy-*N*-methyl-*N*-(1-methylpiperidin-4-yl)benzamide, 20g



Nitrobenzene **19g** (215 mg, 0.67 mmol) was subjected to general method **9** to afford the title compound **20g** as a colourless oil (180 mg, 92%). LCMS purity >95%, ret. time 0.12 mins; HRMS (ESI +ve): found $[\text{M}+\text{H}]^+$ 292.2025 $[\text{C}_{16}\text{H}_{26}\text{N}_3\text{O}_2]^+$ requires 292.2020; δ_{H} (CDCl_3 , 500 MHz): 6.82 (1H, d, $J = 1.5$ Hz, H6), 6.78 (1H, dd, $J = 8.0, 1.5$ Hz, H4), 6.61 (1H, d, $J = 8.0$ Hz, H3), 4.05 – 3.97 (4H, m, OCH_2CH_3 & H7), 2.90 – 2.83 (5H, m, CONCH_3 & H9), 2.23 (3H, s, NCH_3), 2.05 – 1.81 (4H, m, 2 x H8 +

2 x H9), 1.70 - 1.60 (2H, m, H8), 1.39 (3H, t, $J = 7.1$ Hz, OCH_2CH_3); δ_{C} (CDCl_3 , 126 MHz): 172.2 (CONCH_3), 145.9 (C1), 137.9 (C2), 126.1 (C5), 120.1 (C4), 113.6 (C3), 110.7 (C6), 63.8 (C7 & OCH_2CH_3), 55.0 (CONCH_3 & C9), 45.9 (NCH_3), 29.0 (C8), 14.9 (OCH_2CH_3); NH_2 peak not observed

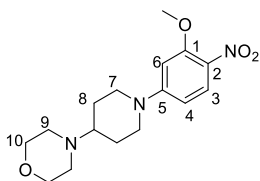
1-(1-(3-Methoxy-4-nitrophenyl)piperidin-4-yl)-4-methylpiperazine, **22a**



1-Methyl-4-(piperidin-4-yl)piperazine (200 mg, 1.09 mmol) was reacted with nitrobenzene **21a** (187 mg, 1.09 mmol) using general method **10** to afford the title compound **22a** as a yellow solid (234 mg, 64%). LCMS purity >95%, ret. time 0.43 mins;

HRMS (ESI +ve): found $[\text{M}+\text{H}]^+$ 335.2078 $[\text{C}_{17}\text{H}_{27}\text{N}_4\text{O}_3]^+$ requires 335.2083; δ_{H} (CDCl_3 , 500 MHz): 8.00 (1H, d, $J = 9.5$ Hz, H3), 6.42 (1H, dd, $J = 9.5$, 2.5 Hz, H4), 6.31 (1H, d, $J = 2.5$ Hz, H6), 3.95 (3H, s OCH_3), 2.98 (2H, td, $J = 12.6$, 2.5 Hz, H7), 2.72 – 2.57 (4H, m, H9), 2.57 – 2.43 (5H, m, NCH & H7), 2.31 (3H, s, NCH_3), 2.01 – 1.95 (2H, m, H8), 1.69 – 1.57 (2H, m, H8); δ_{C} (CDCl_3 , 126 MHz): 156.5 (C5), 155.3 (C1), 129.1 (C2), 129.0 (C3), 105.6 (C4), 97.0 (C1), 61.3 (NCH), 56.2 (OCH_3), 55.4 (C10), 49.0 (C9), 47.0 (C7), 46.0 (NCH_3), 27.8 (C8)

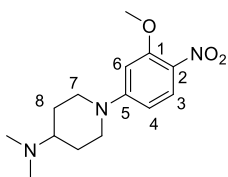
4-(1-(3-Methoxy-4-nitrophenyl)piperidin-4-yl)morpholine, **22b**



4-(Piperidin-4-yl)morpholine (200 mg, 1.18 mmol) was reacted with nitrobenzene **21a** (201 mg, 1.18 mmol) using general method **10** to afford the title compound **22b** as a yellow solid (353 mg, 94%). LCMS purity >95%, ret. time 0.47 mins; HRMS (ESI +ve):

found $[\text{M}+\text{H}]^+$ 322.1781 $[\text{C}_{16}\text{H}_{24}\text{N}_3\text{O}_4]^+$ requires 322.1767; δ_{H} (CDCl_3 , 500 MHz): 8.00 (1H, d, $J = 9.2$ Hz, H3), 6.43 (1H, dd, $J = 9.2$, 2.5 Hz, H4), 6.32 (1H, d, $J = 2.5$ Hz, H6), 3.97 – 3.92 (2H, m, H7), 3.95 (3H, s OCH_3), 3.76 – 3.72 (4H, m, H10), 3.02 – 2.95 (2H, m, H7), 2.60 – 2.57 (4H, m, H9), 2.49 – 2.42 (1H, m, NCH), 2.01 – 1.95 (2H, m, H8), 1.66 – 1.56 (2H, m, H8); δ_{C} (CDCl_3 , 126 MHz): 156.5 (C5), 155.3 (C1), 129.3 (C2), 129.0 (C3), 105.6 (C4), 97.0 (C1), 67.2 (C10), 61.5 (NCH), 56.2 (OCH_3), 49.8 (C9), 46.8 (C7), 27.8 (C8)

1-(3-Methoxy-4-nitrophenyl)-N, N-dimethylpiperidin-4-amine, **22c**

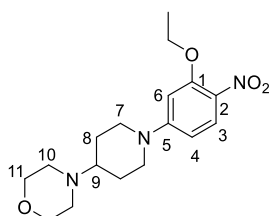


N,N-Dimethylpiperidin-4-amine (200 mg, 1.56 mmol) was reacted with nitrobenzene **21a** (267 mg, 1.56 mmol) using general method **10** to afford the title compound **22c** as a yellow oil (365 mg, 84%).

LCMS purity >95%, ret. time 0.55 mins; HRMS (ESI +ve): found $[\text{M}+\text{H}]^+$ 335.2078 $[\text{C}_{14}\text{H}_{22}\text{N}_3\text{O}_3]^+$ requires 335.2083; δ_{H} (CDCl_3 , 500 MHz): 8.00 (1H, d,

$J = 9.5$ Hz, H3), 6.42 (1H, dd, $J = 9.5, 2.5$ Hz, H4), 6.32 (1H, d, $J = 2.5$ Hz, H6), 3.97 – 3.91 (2H, m, H7), 3.95 (3H, s, OCH₃), 2.98 (2H, td, $J = 12.5, 2.7$ Hz, H7), 2.47 – 2.37 (1H, m, NCH), 2.32 (6H, s, N(CH₃)₂), 2.01 – 1.92 (2H, m, H8), 1.66 – 1.53 (2H, m, H8); δ_c (CDCl₃, 126 MHz): 156.5 (C5), 155.3 (C1), 129.1 (C2), 129.0 (C3), 105.6 (C4), 97.0 (C1), 61.7 (NCH), 56.2 (OCH₃), 46.8 (C7), 41.7 ((NCH₃)₂), 27.9 (C8)

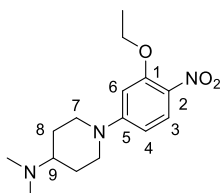
4-(1-(3-Ethoxy-4-nitrophenyl)piperidin-4-yl)morpholine, **22d**



4-Morpholinepiperidine (92 mg, 0.54 mmol) was reacted with nitrobenzene **21b** (100 mg, 1.56 mmol) using general method **10** to afford the title compound **22d** as a yellow oil (142 mg, 78%). LCMS purity >95%, ret. time 0.90 mins; HRMS (ESI +ve): found $[M+H]^+$ 336.1906 $[C_{17}H_{26}N_3O_4]^+$ requires 336.1918;

δ_H (CDCl₃, 500 MHz): 8.00 (1H, d, $J = 9.1$ Hz, H3), 6.42 (1H, dd, $J = 9.1, 2.5$ Hz, H4), 6.32 (1H, d, $J = 2.5$ Hz, H6), 4.15 (2H, q, $J = 7.0$ Hz, OCH₂CH₃), 3.95 – 3.89 (2H, m, H7), 3.75 – 3.72 (4H, m, H11), 2.99 – 2.93 (2H, m, H7), 2.59 – 2.56 (4H, m, H10), 2.44 (1H, tt, $J = 11.0, 3.7$ Hz, H9), 1.99 – 1.94 (2H, m, H8), 1.65 – 1.56 (2H, m, H8), 1.55 (3H, t, $J = 7.0$ Hz, OCH₂CH₃); δ_c (CDCl₃, 126 MHz): 155.8 (C1), 155.2 (C5), 129.0 (C2), 128.8 (C3), 105.7 (C4), 98.5 (C6), 67.2 (C11), 65.3 (OCH₂CH₃), 61.5 (C9), 49.9 (C10), 46.9 (C7), 27.7 (C8), 14.7 (OCH₂CH₃)

1-(3-Ethoxy-4-nitrophenyl)-*N,N*-dimethyl-piperidin-4-amine, **22e**

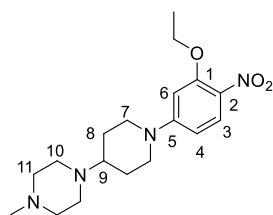


4-(Dimethylamino)piperidine (64 mg, 0.50 mmol) was reacted with nitrobenzene **21b** (100 mg, 0.50 mmol) using general method **10** to afford the title compound **22e** as a yellow oil (86 mg, 59%).

LCMS purity >95%, ret. time 0.94 mins; HRMS (ESI +ve): found $[M+H]^+$ 294.1805 $[C_{15}H_{24}N_3O_3]^+$ requires 294.1812; δ_H (CDCl₃, 500 MHz): 7.98 (1H, d, $J = 9.1$ Hz, H3), 6.43 (1H, dd, $J = 9.1, 2.5$ Hz, H4), 6.33 (1H, d, $J = 2.5$ Hz, H6), 4.16 (2H, q, $J = 6.9$ Hz, OCH₂CH₃), 3.97 – 3.91 (2H, m, H7), 2.96 (2H, td, $J = 13.2, 2.5$ Hz, H7), 2.66 – 2.57 (1H, m, H9), 2.44 (6H, s, N(CH₃)₂), 2.07 – 2.01 (2H, m, H8), 1.66 (2H, qd, $J = 12.0, 4.1$ Hz, H8), 1.51 (3H, t, $J = 6.9$ Hz, OCH₂CH₃); δ_c (CDCl₃, 126 MHz): 155.7 (C1), 155.0 (C5), 129.7 (C2), 128.7 (C3), 105.8 (C4), 98.8 (C6), 65.3 (OCH₂CH₃), 62.1 (C9), 46.8 (N(CH₃)₂), 41.2 (C7), 27.3 (C8), 14.7 (OCH₂CH₃)

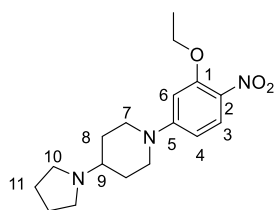
1-(1-(3-Ethoxy-4-nitrophenyl)piperidin-4-yl)-4-methylpiperazine, **22f**

4-Morpholinepiperidine (68 mg, 0.37 mmol) was reacted with nitrobenzene **21b** (69 mg, 0.37 mmol) using general method **10** to afford the title compound **22f** as a yellow oil (92 mg, 71%). LCMS purity >95%, ret. time 0.95 mins; HRMS (ESI +ve): found



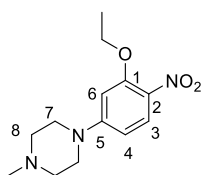
$[M+H]^+$ 349.2229 $[C_{18}H_{29}N_4O_3]^+$ requires 349.2234; δ_H ($CDCl_3$, 500 MHz): 7.97 (1H, d, $J = 9.3$ Hz, H3), 6.41 (1H, dd, $J = 9.3$, 2.5 Hz, H4), 6.31 (1H, d, $J = 2.5$ Hz, H6), 4.15 (2H, q, $J = 7.0$ Hz, OCH_2CH_3), 3.92 (2H d, $J = 12.7$ Hz, H7), 2.95 (2H, td, $J = 12.7$, 2.2 Hz, H7), 2.71 – 2.47 (9H, m, H9, H10 & H11), 2.33 (3H, s, NCH_3), 1.98 – 1.94 (2H, m, H8), 1.65 – 1.57 (2H, m, H8), 1.50 (3H, t, $J = 7.0$ Hz, OCH_2CH_3); δ_C ($CDCl_3$, 126 MHz): 155.8 (C1), 155.2 (C5), 129.0 (C2), 128.8 (C3), 105.7 (C4), 98.5 (C6), 67.2 (C11), 65.3 (OCH_2CH_3), 61.5 (C9), 49.9 (C10), 46.9 (C7), 27.7 (C8), 14.7 (OCH_2CH_3)

1-(3-Ethoxy-4-nitrophenyl)-4-(pyrrolidin-1-yl)piperidine, **22g**

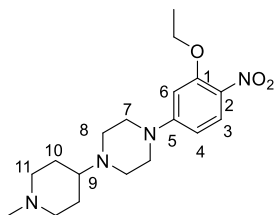


4-(1-Pyrrolidinyl)-piperidine (153 mg, 0.99 mmol) was reacted with nitrobenzene **21b** (200 mg, 0.99 mmol) using general method **10** to afford the title compound **22g** as a yellow oil (207 mg, 65%). LCMS purity >95%, ret. time 0.94 mins; HRMS (ESI +ve): found $[M+H]^+$ 320.1961 $[C_{17}H_{26}N_3O_3]^+$ requires 320.1969; δ_H ($CDCl_3$, 500 MHz): 7.96 (1H, d, $J = 9.1$ Hz, H3), 6.42 (1H, dd, $J = 9.1$, 2.5 Hz, H4), 6.33 (1H, d, $J = 2.5$ Hz, H6), 4.15 (2H, q, $J = 7.0$ Hz, OCH_2CH_3), 3.93 (2H, d, $J = 13.9$ Hz, H7), 3.09 – 3.01 (4H, m, H10), 2.98 – 2.93 (2H, m, H7), 2.85 – 2.77 (1H, m, H9), 2.17 – 2.11 (2H, m, H8), 2.05 – 1.90 (6H, m, 2 x H8 & H11), 1.51 (3H, t, $J = 7.0$ Hz, OCH_2CH_3); δ_C ($CDCl_3$, 126 MHz): 155.6 (C1), 155.0 (C5), 130.4 (C2), 128.6 (C3), 106.0 (C4), 99.2 (C6), 63.4 (OCH_2CH_3), 61.5 (C9), 50.9 (C10), 46.4 (C7), 28.8 (C8), 23.2 (C11), 14.7 (OCH_2CH_3)

1-(3-Ethoxy-4-nitrophenyl)-4-(pyrrolidin-1-yl)piperidine, **22h**



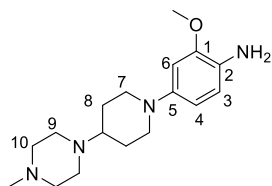
1-Methylpiperazine (61 mg, 0.60 mmol) was reacted with nitrobenzene **21b** (112 mg, 0.60 mmol) using general method **10** to afford the title compound **22h** as a yellow oil (66 mg, 41%). LCMS purity >95%, ret. time 0.56 mins; HRMS (ESI +ve): found $[M+H]^+$ 266.1494 $[C_{13}H_{20}N_3O_3]^+$ requires 266.1499; δ_H ($CDCl_3$, 500 MHz): 7.98 (1H, d, $J = 9.3$ Hz, H3), 6.42 (1H, dd, $J = 9.3$, 2.5 Hz, H4), 6.33 (1H, d, $J = 2.5$ Hz, H6), 4.16 (2H, q, $J = 6.9$ Hz, OCH_2CH_3), 3.41 – 3.37 (4H, m, H7), 2.57 – 2.52 (4H, m, H8), 2.36 (3H, s, NCH_3), 1.50 (3H, t, $J = 6.9$ Hz, OCH_2CH_3); δ_C ($CDCl_3$, 126 MHz): 155.6 (C1 & C5), 130.1 (C2), 128.6 (C3), 105.6 (C4), 98.5 (C6), 65.3 (OCH_2CH_3), 54.6 (C8), 47.1 (C7), 46.1 (NCH_3), 14.7 (OCH_2CH_3)

1-(3-Ethoxy-4-nitrophenyl)-4-(1-methylpiperidin-4-yl)piperazine, 22i

1-(1-Methylpiperidin-4-yl)piperazine (229 mg, 1.25 mmol) was reacted with nitrobenzene **21b** (307 mg, 1.25 mmol) using general method **10** to afford the title compound **22i** as a yellow solid (77 mg, 18%). LCMS purity >95%, ret. time 0.16 mins;

HRMS (ESI +ve): found $[M+H]^+$ 349.2223 $[C_{18}H_{29}N_4O_3]^+$

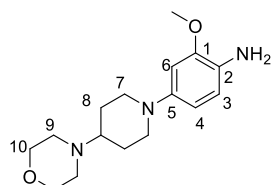
requires 349.2234; δ_H (CDCl₃, 500 MHz): 7.98 (1H, d, J = 9.1 Hz, H3), 6.42 (1H, dd, J = 9.1, 2.5 Hz, H4), 6.32 (1H, d, J = 2.5 Hz, H6), 4.15 (2H, q, J = 7.2 Hz, OCH₂CH₃), 3.40 – 3.36 (4H, m, H7), 2.94 (2H, d, J = 12.0 Hz, H11), 2.72 – 2.68 (4H, m, H8), 2.35 – 2.30 (1H, m, H9), 2.29 (3H, s, NCH₃), 2.00 – 1.94 (2H, m, H11), 1.85 – 1.79 (2H, m, H10), 1.66 – 1.58 (2H, m, H10), 1.50 (3H, t, J = 7.2 Hz, OCH₂CH₃); δ_C (CDCl₃, 126 MHz): 155.5 (C1), 154.0 (C5), 130.1 (C2), 128.6 (C3), 105.2 (C4), 98.4 (C6), 65.3 (OCH₂CH₃), 61.4 (C9), 55.3 (C11), 48.7 (C8), 47.6 (C7), 46.1 (NCH₃), 28.1 (C10), 14.7 (OCH₂CH₃)

2-Methoxy-4-(4-(4-methylpiperazin-1-yl)piperidin-1-yl)aniline, 23a

Nitrobenzene **22a** (230 mg, 0.69 mmol) was subjected to general method **9** to afford the title compound **23a** as a yellow solid (67 mg, 32%). LCMS purity >95%, ret. time 0.13 mins;

HRMS (ESI +ve): found $[M+H]^+$ 305.2339 $[C_{17}H_{29}N_4O]^+$

requires 305.2341; δ_H (CDCl₃, 500 MHz): 6.64 (1H, d, J = 8.2 Hz, H3), 6.53 (1H, d, J = 2.5 Hz, H6), 6.42 (1H, dd, J = 8.2, 2.5 Hz, H4), 3.84 (3H, s OCH₃), 3.52 (2H, d, J = 12.3 Hz, H7), 2.77 – 2.47 (10H, m, 2 x H7, H9 & H10), 2.38 (1H, tt, J = 11.6, 3.6 Hz, NCH), 2.33 (3H, s, NCH₃), 1.97 – 1.90 (2H, m, H8), 1.77 – 1.68 (2H, m, H8); δ_C (CDCl₃, 126 MHz): 148.0 (C1), 145.3 (C5), 130.0 (C2), 115.4 (C3), 109.8 (C4), 102.8 (C6), 61.8 (NCH), 55.5 (OCH₃), 55.3 (C10), 51.5 (C7), 48.8 (C9), 45.8 (NCH₃), 28.4 (C8); *NH₂ peak not observed.*

2-Methoxy-4-(4-morpholinopiperidin-1-yl)aniline, 23b

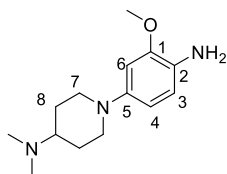
Nitrobenzene **22b** (350 mg, 1.09 mmol) was subjected to general method **9** to afford the title compound **23b** as a yellow solid (283 mg, 89%). LCMS purity >95%, ret. time 0.13 mins;

HRMS (ESI +ve): found $[M+H]^+$ 292.2025 $[C_{16}H_{26}N_3O_2]^+$

requires 292.2025; δ_H (CDCl₃, 500 MHz) 6.64 (1H, d, J = 8.2 Hz, H3), 6.53 (1H, d, J = 2.5 Hz, H6), 6.43 (1H, dd, J = 8.2, 2.5 Hz, H4), 3.84 (3H, s OCH₃), 3.77 – 3.73 (4H, m, H10), 3.56 – 3.50 (2H, m, H7), 2.67 – 2.57 (6H, m, 2 x H7 & H9), 2.30 (1H, tt, J = 11.4, 3.8 Hz, NCH), 1.97 – 1.90 (2H, m, H8), 1.75 – 1.66 (2H, m, H8); δ_C (CDCl₃, 126

MHz): 148.0 (C1), 145.3 (C5), 130.0 (C2), 115.4 (C3), 109.8 (C4), 102.8 (C6), 67.3 (C10), 62.1 (NCH), 55.4 (OCH₃), 51.4 (C7), 49.8 (C9), 28.4 (C8); *NH₂ peak not observed*.

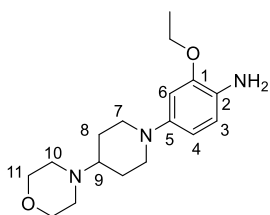
1-(4-Amino-3-methoxyphenyl)-N, N-dimethylpiperidin-4-amine, 23c



Nitrobenzene **22c** (360 mg, 1.29 mmol) was subjected to reacted general method **9** to afford the title compound **23c** as a yellow solid (120 mg, 37%). LCMS purity >95%, ret. time 0.14 mins;

HRMS (ESI +ve): found $[M+H]^+$ 250.1939 $[C_{14}H_{24}N_3O]^+$ requires 250.1919; δ_H (CDCl₃, 500 MHz) 6.64 (1H, d, J = 8.2 Hz, H3), 6.54 (1H, d, J = 2.5 Hz, H6), 6.43 (1H, dd, J = 8.2, 2.5 Hz, H4), 3.84 (3H, s OCH₃), 3.54 – 3.49 (2H, m, H7), 2.62 (2H, td, J = 12.0, 2.4 Hz, H7), 2.34 (6H, s, N(CH₃)₂), 2.32 – 2.24 (1H, m, NCH), 1.96 – 1.90 (2H, m, H8), 1.74 – 1.65 (2H, m, H8); δ_C (CDCl₃, 126 MHz): 147.9 (C1), 145.3 (C5), 130.0 (C2), 115.4 (C3), 109.8 (C4), 102.9 (C6), 62.1 (NCH), 55.4 (OCH₃), 51.5 (C7), 41.6 ((NCH₃)₂), 28.5 (C8); *NH₂ peak not observed*.

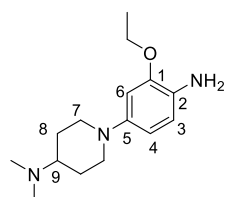
2-Ethoxy-4-(4-morpholinopiperidin-1-yl)aniline, 23d



Nitrobenzene **22d** (142 mg, 0.42 mmol) was subjected to general method **11** to afford the title compound **23d** as a brown oil (40 mg, 31%). LCMS purity >95%, ret. time 0.13 mins; HRMS (ESI +ve): found $[M+H]^+$ 306.2181 $[C_{17}H_{28}N_3O_2]^+$ requires 306.2176; δ_H (CDCl₃, 500 MHz): 6.64 (1H, d, J = 8.5

Hz, H3), 6.54 (1H, d, J = 2.4 Hz, H6), 6.43 (1H, dd, J = 8.5, 2.4 Hz, H4), 4.05 (2H, q, J = 6.9 Hz, OCH₂CH₃), 3.89 – 3.83 (4H, m, H11), 3.53 (2H, d, J = 12.3 Hz, H7), 2.79 – 2.73 (4H, m, H10), 2.70 – 2.62 (2H, m, H7), 2.58 – 2.50 (1H, m, H9), 2.04 (2H, d, J = 12.0 Hz, H8), 1.85 – 1.76 (2H, m, H8), 1.43 (3H, t, J = 6.9 Hz, OCH₂CH₃); δ_C (CDCl₃, 126 MHz): 147.3 (C1), 144.1 (C5), 130.7 (C2), 115.4 (C3), 110.0 (C4), 104.1 (C6), 66.4 (C11), 63.9 (OCH₂CH₃), 62.6 (C9), 51.4 (C7), 49.4 (C10), 27.6 (C8), 15.0 (OCH₂CH₃); *NH₂ peak not observed*.

1-(4-Amino-3-ethoxyphenyl)-N,N-dimethylpiperidin-4-amine, 23e

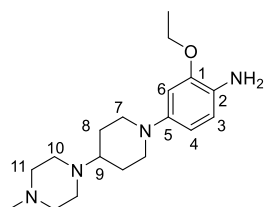


Nitrobenzene **22e** (25 mg, 85 μ mol) was subjected to general method **11** to afford the title compound **23e** as a yellow oil (12 mg, 53%). LCMS purity >95%, ret. time 0.02 mins; HRMS (ESI +ve):

found $[M+H]^+$ 264.2067 $[C_{15}H_{26}N_3O]^+$ requires 264.2070; δ_H (CDCl₃, 500 MHz): 6.64 (1H, d, J = 8.5 Hz, H3), 6.53 (1H, d, J = 2.5 Hz, H6), 6.43 (1H, dd, J = 8.5, 2.5 Hz, H4), 4.05 (2H, q, J = 6.9 Hz, OCH₂CH₃), 3.53 – 3.47 (2H, m,

H7), 2.64 – 2.58 (2H, m, H7), 2.33 (6H, s, N(CH₃)₂), 2.29 – 2.23 (1H, m, H9), 1.95 – 1.89 (2H, m, H8), 1.72 – 1.65 (2H, m, H8), 1.43 (3H, t, *J* = 6.9 Hz, OCH₂CH₃); δ_{C} (CDCl₃, 126 MHz): 147.3 (C1), 145.3 (C5), 130.2 (C2), 115.4 (C3), 109.9 (C4), 104.0 (C6), 63.8 (OCH₂CH₃), 62.1 (C9), 51.5 (C7), 41.6 (N(CH₃)₂), 28.5 (C8), 15.0 (OCH₂CH₃); *NH₂ peak not observed*

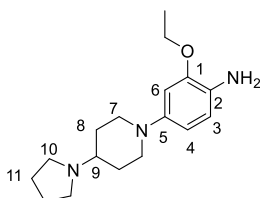
2-Ethoxy-4-(4-(4-methylpiperazin-1-yl)piperidin-1-yl)aniline, 23f



Nitrobenzene **22f** (167 mg, 0.48 mmol) was subjected to general method **9** to afford the title compound **23f** as a brown oil (40 mg, 31%). LCMS purity >95%, ret. time 0.03 mins; HRMS (ESI +ve): found [M+H]⁺ 319.2488 [C₁₈H₃₁N₄O]⁺ requires 319.2492; δ_{H} (CDCl₃, 500 MHz): 6.61 (1H, d, *J* = 8.2 Hz, H3),

6.49 (1H, d, *J* = 2.5 Hz, H6), 6.39 (1H, dd, *J* = 8.2, 2.5 Hz, H4), 4.02 (2H, q, *J* = 6.6 Hz, OCH₂CH₃), 3.67 (2H, s, NH₂), 3.51 – 3.46 (2H, m, H7), 2.71 – 2.55 (6H, m, 2 x H7 & H10), 2.54 – 2.40 (4H, m, H11), 2.36 – 2.20 (1H, m, H9), 2.28 (3H, s, NCH₃), 1.93 – 1.87 (2H, m, H8), 1.69 (2H, qd, *J* = 12.1, 3.8 Hz, H8), 1.40 (3H, t, *J* = 6.6 Hz, OCH₂CH₃); δ_{C} (CDCl₃, 126 MHz): 147.3 (C1), 145.2 (C5), 130.1 (C2), 115.4 (C3), 109.8 (C4), 103.8 (C6), 63.8 (OCH₂CH₃), 61.8 (C9), 55.4 (C11), 51.6 (C7), 48.9 (C10), 46.0 (NCH₃), 28.4 (C8), 15.0 (OCH₂CH₃)

2-Ethoxy-4-(4-pyrrolidin-1-yl)piperidin-1-yl)aniline, 23g

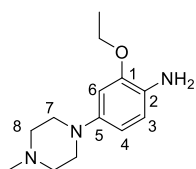


Nitrobenzene **22g** (207 mg, 0.65 mmol) was subjected to general method **11** to afford the title compound **23g** as a brown oil (20 mg, 11%). LCMS purity >95%, ret. time 0.04 mins; HRMS (ESI +ve): found [M+H]⁺ 290.2221 [C₁₇H₂₈N₃O]⁺ requires 290.2227; δ_{H} (CDCl₃, 500 MHz): 6.68 (1H, d, *J* = 8.2 Hz, H3), 6.50 (1H, d, *J* =

2.5 Hz, H6), 6.45 (1H, dd, *J* = 8.2, 2.5 Hz, H4), 4.07 (2H, q, *J* = 6.6 Hz, OCH₂CH₃), 3.86 – 3.70 (2H, m, H7), 3.52 – 3.25 (5H, m, H9 & H11), 3.20 – 2.98 (2H, m, H7), 2.49 – 2.40 (2H, m, H8), 2.36 – 2.27 (2H, m, H8), 2.20 – 2.10 (4H, m, H11), 1.44 (3H, t, *J* = 6.6 Hz, OCH₂CH₃); δ_{C} (CDCl₃, 126 MHz): 147.4 (C1), 142.9 (C5), 121.2 (C2), 115.2 (C3), 108.8 (C4), 102.1 (C6), 64.3 (OCH₂CH₃), 60.0 (C9), 51.3 (C7), 51.1 (C10), 26.7 (C8), 23.5 (C11), 14.9 (OCH₂CH₃); *NH₂ peak not observed*.

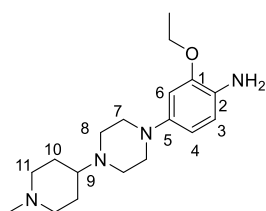
2-Ethoxy-4-(4-methylpiperazin-1-yl)aniline, 23h

Nitrobenzene **22h** (66 mg, 0.25 mmol) was subjected to general method **11** to afford the title compound **23h** as a brown oil (35 mg, 60%). LCMS purity >95%, ret. time 0.02 mins; HRMS (ESI +ve): found [M+H]⁺ 236.1757 [C₁₃H₂₂N₃O]⁺ requires 236.1757;



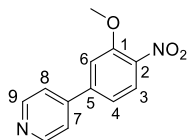
δ_{H} (CDCl_3 , 500 MHz): 6.66 (1H, d, $J = 8.2$ Hz, H3), 6.48 (1H, d, $J = 2.3$ Hz, H5), 6.42 (1H, dd, $J = 8.2, 2.3$ Hz, H4), 4.04 (2H, q, $J = 7.0$ Hz, OCH_2CH_3), 3.27 – 3.23 (4H, m, H7) 3.19 – 3.14 (4H, m, H8), 2.71 (3H, s, NCH_3), 1.43 (3H, t, $J = 7.0$ Hz, OCH_2CH_3); δ_{C} (CDCl_3 , 126 MHz): 147.3 (C1), 143.1 (C5), 131.6 (C2), 115.4 (C3), 110.8 (C4), 103.9 (C6), 63.9 (OCH_2CH_3), 53.6 (C8), 49.3 (C7), 43.5 (NCH_3), 15.0 (OCH_2CH_3); NH_2 peak not observed.

2-Ethoxy-4-(4-(1-methylpiperidin-4-yl)piperazin-1-yl)aniline, **23i**



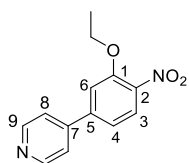
Nitrobenzene **22i** (77 mg, 0.11 mmol) was subjected to general method **9** to afford the title compound **23i** as a brown oil (56 mg, 79%). LCMS purity >95%, ret. time 0.03 mins; HRMS (ESI +ve): found $[\text{M}+\text{H}]^+$ 319.2496 [$\text{C}_{18}\text{H}_{31}\text{N}_4\text{O}$] $^+$ requires 319.2492; δ_{H} (CDCl_3 , 500 MHz): 6.64 (1H, d, $J = 8.2$ Hz, H3), 6.52 (1H, d, $J = 2.5$ Hz, H6), 6.42 (1H, dd, $J = 8.5, 2.5$ Hz, H4), 4.04 (2H, q, $J = 6.9$ Hz, OCH_2CH_3), 3.51 (2H, d, $J = 12.3$ Hz, H8), 2.70 – 2.58 (6H, H7 & 2 x H8), 2.55 – 2.40 (4H, m, H11), 2.38 – 2.32 (1H, m, H9), 2.30 (3H, s, NCH_3), 1.95 – 1.89 (2H, m, H10), 1.71 (2H, qd, $J = 12.1, 3.5$ Hz, H10), 1.43 (3H, t, $J = 6.9$ Hz, OCH_2CH_3); δ_{C} (CDCl_3 , 126 MHz): 147.3 (C1), 145.3 (C5), 130.1 (C2), 115.4 (C3), 109.8 (C4), 103.9 (C6), 63.8 (OCH_2CH_3), 61.8 (H9), 55.5 (C11), 51.6 (C8), 49.0 (C7), 46.1 (NCH_3), 28.4 (C10), 15.0 (OCH_2CH_3); NH_2 peak not observed

4-(3-Methoxy-4-nitrophenyl)pyridine, **25a**



4-Chloro-2-methoxy-1-nitrobenzene **24a** (250 mg, 1.33 mmol), was reacted with pyridine-4-ylboronic acid (164 mg, 1.33 mmol) using general method **12** to afford the title compound **25a** as a yellow solid (200 mg, 65%). LCMS purity >95%, ret. time 0.79 mins; HRMS (ESI +ve): found $[\text{M}+\text{H}]^+$ 231.0803 [$\text{C}_{12}\text{H}_{11}\text{N}_2\text{O}_3$] $^+$ requires 231.0770; δ_{H} (CDCl_3 , 500 MHz): 8.74 – 8.72 (2H, m, H9), 7.99 – 7.96 (1H, m, H3), 7.51 – 7.48 (2H, m, H8), 7.28 – 7.25 (2H, m, H4 & H6), 4.05 (3H, s, OCH_3); δ_{C} (CDCl_3 , 126 MHz): 153.4 (C1), 150.6 (C9), 146.4 (C7), 144.5 (C5), 139.6 (C2), 126.6 (C3), 121.7 (C8), 119.0 (C4), 112.2 (C6) 56.7 (OCH_3)

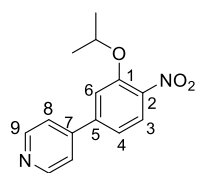
4-(3-Ethoxy-4-nitrophenyl)pyridine, **25b**



4-Bromo-2-ethoxy-1-nitrobenzene **24b** (1.5 g, 6.10 mmol) was reacted with pyridine-4-ylboronic acid (749 mg, 6.10 mmol) using general method **12** to afford the title compound **25b** as a yellow solid (81 mg, 54%). LCMS purity >95%, ret. time 1.09 mins; HRMS (ESI

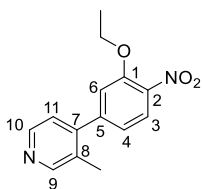
+ve): found $[M+H]^+$ 245.0917 $[C_{13}H_{13}N_2O_3]^+$ requires 245.0921; δ_H (500 MHz, $CDCl_3$): 8.73 (2H, dd, $J = 4.4$, 1.2 Hz, H9), 7.94 (1H, d, $J = 8.2$ Hz, H3), 7.49 (2H, dd, $J = 4.4$, 1.6 Hz, H8), 7.27 – 7.23 (2H, m, H4 & H6), 4.28 (2H, q, $J = 7.2$ Hz, OCH_2CH_3), 1.53 (3H, t, $J = 7.0$ Hz, OCH_2CH_3); δ_C ($CDCl_3$, 126 MHz): 152.8 (C1), 150.6 (C9), 146.5 (C2), 144.2 (C5), 140.0 (C7), 126.4 (C3), 121.8 (C8), 118.9 (C4), 113.2 (C6)

4-(3-Isopropoxy-4-nitrophenyl)pyridine, 25c



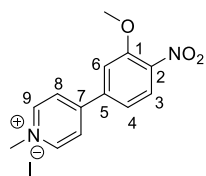
4-Bromo-2-isopropoxy-1-nitrobenzene **24c** (1.20 g, 4.63 mmol) was reacted with pyridine-4-ylboronic acid (570 mg, 4.63 mmol) using general method **12** to afford the title compound **25c** as a yellow solid (770 mg, 64%). LCMS purity >95%, ret. time 1.21 mins; HRMS (ESI +ve): found $[M+H]^+$ 259.1079 $[C_{14}H_{15}N_2O_3]^+$ requires 259.1077; δ_H (500 MHz, $CDCl_3$): 8.74 (2H, dd, $J = 4.4$, 1.9 Hz, H9), 7.91 (1H, d, $J = 8.4$ Hz, H3), 7.49 (2H, dd, $J = 4.4$, 1.9 Hz, H8), 7.28 (1H, d, $J = 1.7$ Hz, H6), 7.24 (1H, dd, $J = 8.4$, 1.7 Hz, H4), 4.79 (1H, sept., $J = 6.0$ Hz, $CH(CH_3)_2$), 1.46 (6H, d, $J = 6.0$ Hz, $CH(CH_3)_2$); δ_C ($CDCl_3$, 126 MHz): 151.8 (C1), 150.5 (C9), 146.6 (C7), 143.9 (C5), 141.1 (C2), 126.3 (C3), 121.7 (C8), 118.8 (C4), 114.8 (C6), 73.1 ($CH(CH_3)_2$), 21.9 ($CH(CH_3)_2$)

4-(3-Ethoxy-4-nitrophenyl)-3-methyl-pyridine, 25d



4-Bromo-2-ethoxy-1-nitrobenzene **24b** (400 mg, 1.63 mmol) was reacted with 3-methylpyridine-4-boronic acid (223 mg, 1.63 mmol) using general method **12** to afford the title compound **25c** as a yellow solid (225 mg, 54%). LCMS purity >95%, ret. time 1.07 mins; HRMS (ESI +ve): found $[M+H]^+$ 259.1080 $[C_{14}H_{15}N_2O_3]^+$ requires 259.1077; δ_H (500 MHz, $CDCl_3$): 8.57 (1H, s, H9), 8.54 (1H, d, $J = 4.7$ Hz, H10), 7.92 (1H, d, $J = 8.2$ Hz, H3), 7.15 (1H, d, $J = 4.7$ Hz, H11), 7.00 (1H, d, $J = 1.6$ Hz, H6), 6.97 (1H, dd, $J = 8.2$, 1.6 Hz, H4), 4.22 (1H, q, $J = 7.0$ Hz, OCH_2CH_3), 2.29 (3H, s, CH_3), 1.51 (3H, t, $J = 7.0$ Hz, OCH_2CH_3); δ_C ($CDCl_3$, 126 MHz): 152.3 (C1), 151.6 (C9), 147.6 (C10), 147.3 (C7), 145.1 (C5), 139.4 (C2), 130.3 (C8), 125.8 (C3), 123.3 (C11), 120.3 (C4), 114.7 (C6), 65.6 (OCH_2CH_3), 17.1 (CH_3), 14.5 (OCH_2CH_3)

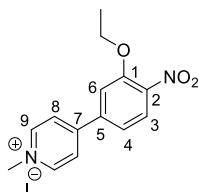
4-(3-Methoxy-4-nitrophenyl)-1-methylpyridinium iodide, 26a



25a (200 mg, 0.87 mmol) was reacted with methyl iodide (0.19 mL, 3.04 mmol) using general method **13** to afford the title compound **26a** as a yellow solid (295 mg, 91%). LCMS purity >95%, ret. time 0.28 mins; HRMS (ESI +ve): found $[M]^+$ 245.0920 $[C_{13}H_{13}N_2O_3]^+$ requires 245.0926; δ_H (CD_3OD , 500 MHz) 8.99 (2H, d, $J = 6.7$ Hz, H9), 8.49 (2H, d, $J = 6.7$ Hz, H8), 8.01 (1H, d, $J = 8.2$ Hz, H3), 7.81 (1H, d, $J = 1.9$ Hz, H6), 7.66 (1H, dd,

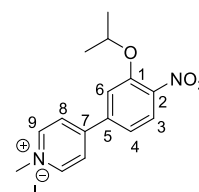
$J = 8.2, 1.9 \text{ Hz}$, H4), 4.45 (3H, s, NCH₃), 4.10 (3H, s OCH₃); δ_{C} (CD₃OD, 126 MHz): 154.5 (C1), 147.2 (C9), 143.6 (C2), 140.8 (C5), 127.3 (C3), 127.1 (C8), 121.4 (C4), 115.0 (C6), 57.8 (OCH₃) 49.4 (NCH₃)

4-(3-Ethoxy-4-nitrophenyl)-1-methylpyridin1-ium iodide, 26b



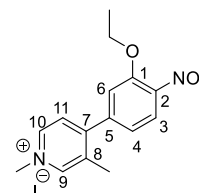
25b (600 mg, 2.47 mmol) was reacted with methyl iodide (0.54 mL, 8.65 mmol) using general method **13** to afford **26b** as a yellow solid (945 mg, 99%). LCMS purity >95%, ret. time 0.83 mins; HRMS (ESI +ve): found $[M]^+$ 259.1076 $[C_{14}H_{15}N_2O_3]^+$ requires 259.1082; δ_{H} (500 MHz, CD₃OD): 8.99 (2H, d, $J = 6.7 \text{ Hz}$, H9), 8.48 (2H, d, $J = 6.7 \text{ Hz}$, H8), 7.98 (1H, d, $J = 8.2 \text{ Hz}$, H3), 7.79 (1H, d, $J = 1.9 \text{ Hz}$, H6), 7.64 (1H, dd, $J = 8.2, 1.9 \text{ Hz}$, H4), 4.46 (3H, s, NCH₃), 4.38 (2H, q, $J = 6.9 \text{ Hz}$, OCH₂CH₃), 1.48 (3H, t, $J = 6.9 \text{ Hz}$, OCH₂CH₃); δ_{C} (CD₃OD, 126 MHz): 154.4 (C7), 152.2 (C1), 145.6 (C9), 142.1 (C2), 139.2 (C5), 125.6 (C3), 125.3 (C8), 119.8 (C4), 114.3 (C6), 65.9 (OCH₂CH₃), 47.1 (NCH₃) 13.4 (OCH₂CH₃)

4-(3-Isopropoxy-4-nitrophenyl)-1-methylpyridin1-ium iodide, 26c



25c (718 mg, 2.78 mmol) was reacted with methyl iodide (0.61 mL, 9.73 mmol) using general method **13** to afford **26c** as a yellow solid (1.03 g, 93%). LCMS purity >95%, ret. time 0.94 mins; HRMS (ESI +ve): found $[M]^+$ 273.1245 $[C_{15}H_{17}N_2O_3]^+$ requires 273.1239; δ_{H} (500 MHz, CD₃OD): 8.98 (2H, d, $J = 6.8 \text{ Hz}$, H9), 8.46 (2H, d, $J = 6.8 \text{ Hz}$, H8), 7.95 (1H, d, $J = 8.5 \text{ Hz}$, H3), 7.81 (1H, d, $J = 1.9 \text{ Hz}$, H6), 7.66 (1H, dd, $J = 8.5, 1.9 \text{ Hz}$, H4), 5.03 (1H, sept., $J = 6.0 \text{ Hz}$, CH(CH₃)₂), 4.45 (3H, s, NCH₃), 1.41 (6H, d, $J = 6.0 \text{ Hz}$, CH(CH₃)₂); δ_{C} (CD₃OD, 126 MHz): 154.5 (C7), 151.1 (C1), 145.6 (C9), 143.2 (C2), 138.9 (C5), 125.6 (C3), 125.5 (C8), 119.9 (C4), 115.6 (C6), 73.0 (CH(CH₃)₂), 47.1 (NCH₃), 20.7 (CH(CH₃)₂)

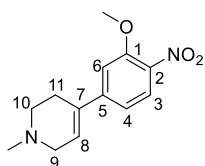
4-(3-Ethoxy-4-nitrophenyl)-1,3-dimethylpyridin1-ium iodide, 26d



25d (225 mg, 0.87 mmol) was reacted with methyl iodide (0.19 mL, 3.05 mmol) using general method **13** to afford **26d** as a brown solid (344 mg, 99%). LCMS purity >95%, ret. time 0.87 mins; HRMS (ESI +ve): found $[M]^+$ 273.1232 $[C_{15}H_{17}N_2O_3]^+$ requires 273.1239; δ_{H} (500 MHz, CD₃OD): 8.94 (1H, s, H9), 8.83 (1H, d, $J = 6.3 \text{ Hz}$, H10), 8.00 (1H, d, $J = 6.3 \text{ Hz}$, H11), 7.97 (1H, d, $J = 8.3 \text{ Hz}$, H3), 7.42 (1H, d, $J = 1.8 \text{ Hz}$, H6), 7.20 (1H, dd, $J = 8.3, 1.8 \text{ Hz}$, H4), 4.44 (3H, s, NCH₃), 4.28 (2H, q, $J = 6.9 \text{ Hz}$, OCH₂CH₃), 2.50 (3H, s, CH₃), 1.46 (3H, t, $J = 6.9 \text{ Hz}$, OCH₂CH₃); δ_{C} (CD₃OD, 126 MHz): 156.0 (C7), 151.8 (C1), 146.0 (C9), 142.6 (C10), 140.9 (C4), 140.8 (C2), 137.0 (C8), 127.7 (C11), 125.2

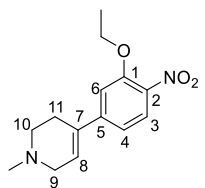
(C3), 120.1 (C4), 114.8 (C6), 65.7 (OCH₂CH₃), 46.9 (NCH₃), 16.5 (CH₃), 13.4 (OCH₂CH₃)

4-(3-Methoxy-4-nitrophenyl)-1-methyl-1,2,3,6-tetrahydropyridine, 27a



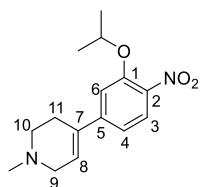
Pyridinium iodide **26a** (212 mg, 0.57 mmol) was subjected to general method **14** to afford the title compound **27a** as a yellow oil (80 mg, 56%). LCMS purity >95%, ret. time 0.33 mins; HRMS (ESI +ve): found [M+H]⁺ 245.1239 [C₁₃H₁₇N₂O₃]⁺ requires 249.1243; δ_{H} (CDCl₃, 500 MHz): 7.85 (1H, d, J = 8.5 Hz, H3), 7.04 (1H, d, J = 1.9 Hz, H6), 7.02 (1H, dd, J = 8.5, 1.9 Hz, H4), 6.21 – 6.19 (1H, m, H8), 3.96 (3H, s, OCH₃), 3.17 – 3.14 (2H, m, H9), 2.71 – 2.67 (2H, m, H10), 2.60 – 2.56 (2H, m, H11), 2.42 (3H, s, NCH₃); δ_{C} (CDCl₃, 126 MHz): 153.3 (C1), 147.6 (C5), 138.0 (C2), 133.7 (C7), 126.1 (C3), 125.7 (C8), 116.9 (C4), 110.0 (C6), 56.4 (OCH₃), 54.9 (C9), 51.9 (C10), 45.6 (NCH₃), 28.1 (C11)

4-(3-Ethoxy-4-nitrophenyl)-1-methyl-1,2,3,6-tetrahydropyridine, 27b

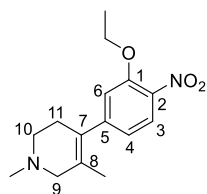


Pyridinium iodide **26b** (945 mg, 2.45 mmol) was subjected to general method **14** to afford **27b** as a yellow oil (609 mg, 95%). LCMS purity >95%, ret. time 0.30 mins; HRMS (ESI +ve): found [M+H]⁺ 263.1387 [C₁₄H₁₉N₂O₃]⁺ requires 263.1390; δ_{H} (500 MHz, CDCl₃): 7.85 (1H, d, J = 8.5 Hz, H3), 7.04 – 7.00 (2H, m, H4 & H6), 6.21 – 6.18 (1H, m, H8), 4.20 (2H, q, J = 6.9 Hz, OCH₂CH₃), 3.17 – 3.14 (2H, m, H9), 2.69 (2H, t, J = 5.7 Hz, H10), 2.60 – 2.56 (2H, m, H11), 2.43 (3H, s, NCH₃), 1.49 (3H, t, J = 6.9 Hz, OCH₂CH₃); δ_{C} (CDCl₃, 126 MHz): 152.7 (C1), 147.3 (C5), 138.4 (C2), 133.7 (C7), 126.0 (C3), 125.9 (C3), 125.6 (C8), 116.8 (C4), 111.1 (C6), 65.4 (OCH₂CH₃), 54.9 (C9), 52.0 (C10), 45.6 (NCH₃), 28.1 (C11), 14.6 (OCH₂CH₃)

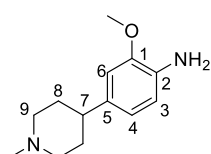
4-(3-Isopropoxy-4-nitrophenyl)-1-methyl-1,2,3,6-tetrahydropyridine, 27c



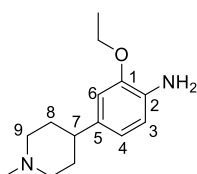
Pyridinium iodide **26c** (315 mg, 0.78 mmol) was subjected to general method **14** to afford **27c** as a brown oil (215 mg, 99%). LCMS purity >95%, ret. time 0.90 mins; HRMS (ESI +ve): found [M+H]⁺ 277.1560 [C₁₅H₂₁N₂O₃]⁺ requires 277.1552; δ_{H} (500 MHz, CDCl₃): 7.76 (1H, d, J = 8.5 Hz, H3), 7.02 (1H, d, J = 1.8 Hz, H6), 6.97 (1H, dd, J = 8.5, 1.8 Hz, H4), 6.17 – 6.13 (1H, m, H8), 4.71 – 4.63 (1H, m, OCH(CH₃)₂), 3.15 – 3.10 (2H, m, H9), 2.66 (2H, t, J = 5.4 Hz, H10), 2.57 – 2.52 (2H, m, H11), 2.39 (3H, s, NCH₃), 1.38 (6H, d, J = 5.7 Hz, OCH(CH₃)₂); δ_{C} (CDCl₃, 126 MHz): 151.5 (C1), 146.9 (C6), 139.3 (C2), 133.6 (C7), 125.9 (C3), 125.4 (C8), 116.8 (C4), 112.8 (C6), 72.6 (OCH(CH₃)₂), 54.8 (C9), 51.9 (C10), 45.5 (NCH₃), 28.0 (C11), 21.8 (OCH(CH₃)₂)

4-(3-Ethoxy-4-nitrophenyl)-1,5-dimethyl-1,2,3,6-tetrahydropyridine, 27d

Pyridinium iodide **26d** (404 mg, 1.00 mmol) was subjected to general method **14** to afford **27d** as a brown oil (202 mg, 72%). LCMS purity >95%, ret. time 0.90 mins; HRMS (ESI +ve): found $[M+H]^+$ 277.1550 $[C_{15}H_{21}N_2O_3]^+$ requires 277.1552; δ_H (500 MHz, $CDCl_3$): 7.81 (1H, d, $J = 8.2$ Hz, H3), 6.86 (1H, d, $J = 1.6$ Hz, H5), 6.80 (1H, dd, $J = 8.2, 1.6$ Hz, H4), 4.15 (2H, q, $J = 6.6$ Hz, OCH_2CH_3), 2.95 (2H, s, H9), 2.63 (2H, t, $J = 5.8$ Hz, H10), 2.44 – 2.40 (5H, m, NCH_3 & H11), 1.58 (3H, s, CH_3), 1.47 (3H, t, $J = 6.6$ Hz, OCH_2CH_3); δ_C ($CDCl_3$, 126 MHz): 152.3 (C1), 149.3 (C5), 138.1 (C2), 129.5 (C8), 129.3 (C7), 125.7 (C3), 120.2 (C4), 114.6 (C6), 65.3 (OCH_2CH_3), 59.6 (C9), 52.4 (C10), 45.6 (NCH_3), 32.0 (C11), 18.0 (CH_3), 14.6 (OCH_2CH_3)

2-Methoxy-4-(1-methylpiperidin-4-yl)aniline, 28a

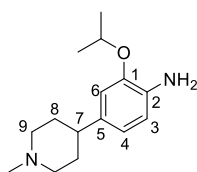
Tetrahydropyridine **27a** (40 mg, 0.16 mmol) was subjected to general method **15** to afford the title compound **28a** as a yellow oil (30 mg, 85%). LCMS purity >95%, ret. time 0.12 mins; HRMS (ESI +ve): found $[M+H]^+$ 245.0920 $[C_{13}H_{13}N_2O_3]^+$ requires 245.0926; δ_H ($CDCl_3$, 500 MHz) 6.65 – 6.61 (3H, m, H3, H4 & H6), 3.84 (3H, s, OCH_3), 3.31 – 3.26 (2H, m, H9), 2.51 – 2.45 (4H, m, H7 & NCH_3), 2.37 (2H, td, $J = 12.1, 2.5$ Hz, H9), 2.01 – 1.94 (2H, m, H8), 1.90 – 1.84 (2H, m, H8); δ_C ($CDCl_3$, 126 MHz): 147.3 (C1), 136.3 (C2), 134.3 (C5), 119.0 (C4), 114.9 (C3), 109.1 (C6), 55.9 (OCH_3), 55.3 (C9), 45.6 (NCH_3), 42.1 (C7), 33.1 (C8); NH_2 peak not observed

2-Ethoxy-4-(1-methylpiperidin-4-yl)aniline, 28b

Tetrahydropyridine **27b** (600 mg, 2.32 mmol) was subjected to general method **15** to afford the title compound **28b** as an orange oil (410 mg, 75%). LCMS purity >95%, ret. time 0.08 mins; HRMS (ESI +ve): found $[M+H]^+$ 235.1819 $[C_{14}H_{23}N_2O]^+$ requires 235.1809; δ_H (500 MHz, $CDCl_3$): 6.68 - 6.60 (3H, m, H3, H4 & H6), 5.52 (2H, s, NH_2), 4.05 (2H, q, $J = 7.0$ Hz, OCH_2CH_3), 3.15 (2H, d, $J = 11.7$ Hz, H9), 2.46 – 2.38 (4H, s, NCH_3 & H7), 2.24 (2H, td, $J = 11.7, 2.5$ Hz, H9), 1.95 – 1.79 (4H, m, H8), 1.42 (3H, t, $J = 7.0$ Hz, OCH_2CH_3); δ_C ($CDCl_3$, 126 MHz): 146.7 (C1), 135.8 (C2), 134.6 (C5), 119.0 (C4), 114.9 (C3), 110.2 (C6), 63.8 (OCH_2CH_3), 55.5 (C9), 45.1 (NCH_3), 40.9 (C7), 32.5 (C8), 15.0 (OCH_2CH_3)

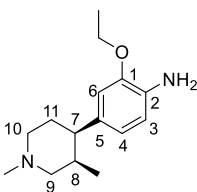
2-Isopropoxy-4-(1-methylpiperidin-4-yl)aniline, 28c

Tetrahydropyridine **27c** (200 mg, 0.72 mmol) was subjected to general method **15** to afford the title compound **28c** as a yellow oil (152 mg, 85%). LCMS purity >70%, ret.



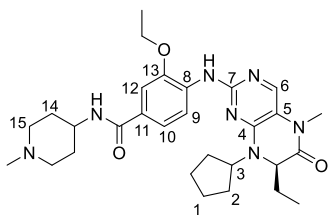
time 0.16 mins; HRMS (ESI +ve): found $[M+H]^+$ 250.2042 $[C_{15}H_{25}N_2O]^+$ requires 250.2045; δ_H (500 MHz, $CDCl_3$): 6.72 – 6.61 (3H, m, H3, H4 & H6), 4.51 (1H, sept., $J = 6.2$ Hz, $OCH(CH_3)_2$), 3.12 (2H, d, $J = 11.3$ Hz, H9), 2.44 – 2.37 (4H, m, H7 & NCH_3), 2.20 (2H, td, $J = 11.3, 4.1$ Hz, H9), 1.92 – 1.80 (4H, m, H8), 1.34 (6H, d, $J = 6.2$ Hz, $OCH(CH_3)_2$); δ_C ($CDCl_3$, 126 MHz): 145.4 (C1), 136.0 (C2), 135.5 (C5), 119.2 (C4), 115.3 (C3), 112.3 (C6), 70.6 (OCH_3), 55.7 (C9), 45.5 (NCH_3), 41.0 (C7), 32.8 (C8), 22.3 ($OCH(CH_3)_2$); NH_2 peak not observed

Cis-4-(1,3-Dimethylpiperidin-4-yl)-2-ethoxyaniline, 28d



Tetrahydropyridine **27d** (200 mg, 0.72 mmol) was subjected to general method **15** to afford the title compound **28d** as an orange oil (142 mg, 79%). LCMS purity >95%, ret. time 0.08 mins; HRMS (ESI +ve): found $[M+H]^+$ 249.1964 $[C_{15}H_{25}N_2O]^+$ requires 249.1961; δ_H (500 MHz, $CDCl_3$): 6.66 (1H, d, $J = 7.9$ Hz, H3), 6.57 – 6.54 (2H, m, H4 & H6), 4.03 (2H, q, $J = 6.6$ Hz, OCH_2CH_3), 2.94 – 2.83 (3H, m, H7 & H9), 2.74 (3H, s, NCH_3), 2.70 – 2.60 (4H, m, H10 & H11), 2.26 – 2.21 (1H, m, H8), 1.42 (3H, t, $J = 6.6$ Hz, OCH_2CH_3), 0.93 (3H, d, $J = 7.3$ Hz, CH_3); δ_C ($CDCl_3$, 126 MHz): 146.7 (C1), 134.7 (C2), 132.0 (C5), 119.6 (C4), 115.0 (C3), 110.8 (C6), 63.9 (OCH_2CH_3), 60.1 (C9), 54.9 (C10), 44.5 (C11 & NCH_3), 42.1 (C7), 34.1 (C8), 15.0 (OCH_2CH_3), 12.2 (CH_3)

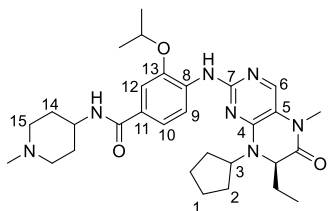
(R)-4-((8-Cyclopentyl-7-ethyl-5-methyl-6-oxo-5,6,7,8-tetrahydropteridin-2-yl)amino)-3-ethoxy-N-(1-methylpiperidin-4-yl)benzamide, 29



Dihydropteridinone **6a** (30.0 mg, 102 μ mol) was reacted with aniline **20e** (28.2 mg, 102 μ mol) using general method **16** to afford the title compound **29** as a white solid (13.0 mg, 24%). LCMS purity >95%, ret. time 1.22 mins; HRMS (ESI +ve): found $[M+H]^+$ 536.3345, $[C_{29}H_{42}N_7O_3]^+$ requires 536.3349; m.p.: 74 – 76 °C; ν_{max} (thin film, cm^{-1}): 3418 (w, N-H), 2966 (w, CON-H), 1659 (C=O), 1592 (C=O); $[\alpha]_D^{21.8}$: -62.3° (c 1.0, MeOH); δ_H ($CDCl_3$, 500 MHz): 8.55 (1H, d, $J = 8.2$ Hz, H9), 7.73 (1H, s, ArNH), 7.68 (1H, s, H6), 7.41 (1H, d, $J = 1.9$ Hz, H12), 7.35 (1H, dd, $J = 8.2, 1.9$ Hz, H10), 6.56 (1H, s, CONH), 4.52 – 4.44 (1H, m, H3), 4.28 – 4.18 (4H, m, OCH_2CH_3 , $NHCH_2$ & $CHCH_2CH_3$), 3.50 (2H, d, $J = 10.4$ Hz, H15), 3.34 (3H, s, $CONCH_3$), 2.72 – 2.64 (2H, m, H15), 2.74 (3H, s, NCH_3), 2.20 – 1.97 (6H, m, 4 x H14 & cPeH), 1.93 – 1.68 (8H, m, cPeH & $CHCH_2CH_3$), 1.51 (6H, t, $J = 6.9$ Hz, OCH_2CH_3), 0.88 (3H, t, $J = 7.4$ Hz, $CHCH_2CH_3$); δ_C ($CDCl_3$, 126 MHz): 166.8 (CONH), 163.7 ($CONCH_3$), 154.9 (C7), 152.2 (C4), 146.4 (C13), 137.6 (C6), 133.5 (C8), 125.4 (C11), 119.4 (C10), 116.3 (C9), 116.0 (C5), 109.8 (C12), 64.5

(OCH₂CH₃), 60.2 (CHCH₂CH₃), 58.7 (C3), 53.9 (C15), 44.4 (NHCH), 43.7 (NCH₃), 29.7 (C14), 29.4 (C2), 29.3 (C2'), 28.2 (CONCH₃), 27.2 (CHCH₂CH₃), 23.7 (C1), 23.3 (C1'), 14.8 (OCH₂CH₃), 9.1 (CHCH₂CH₃)

(R)-4-((8-Cyclopentyl-7-ethyl-5-methyl-6-oxo-5,6,7,8-tetrahydropteridin-2-yl)amino)-3-isopropoxy-N-(1-methylpiperidin-4-yl)benzamide, 30

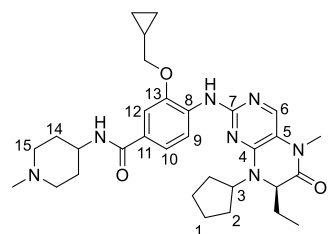


Dihydropteridinone **6a** (18 mg, 61 μmol) was reacted with aniline **20a** (18 mg, 61 μmol) using general method **16** to afford the title compound **30** as a white solid (10 mg, 30%). LCMS purity >95%, ret. time 1.19 mins; HRMS (ESI +ve):

found [M+H]⁺ 550.3493, [C₃₀H₄₄N₇O₃]⁺ requires 550.3506;

m.p.: 175 – 177 °C; ν_{\max} (thin film, cm⁻¹): 3338 (w, N-H), 2931 (w, CON-H), 1674 (C=O), 1624 (C=O); $[\alpha]_D^{22.0}$: -63.7° (c 1.0, MeOH); δ_H (CDCl₃, 500 MHz): 8.55 (1H, d, J = 8.5 Hz, H9), 7.68 (1H, s, H6), 7.65 (1H, s, ArNH), 7.44 (1H, d, J = 1.4 Hz, H12), 7.22 (1H, dd, J = 8.5, 1.4 Hz, H10), 5.93 (1H, d, J = 6.9 Hz, CONH), 4.82 – 4.68 (1H, m, CH(CH₃)₂), 4.49 – 4.42 (1H, m, H3), 4.23 (1H, dd, J = 7.6, 3.5 Hz, CHCH₂CH₃), 4.11 – 3.91 (1H, m, NHCH), 3.33 (3H, s, CONCH₃), 2.87 (2H, d, J = 10.4 Hz, H15), 2.33 (3H, s, NCH₃), 2.24 – 2.16 (2H, m, H15), 2.16 – 1.57 (14H, m, H14, cPeH & CHCH₂CH₃), 1.42 (6H, d, J = 6.0 Hz, CH(CH₃)₂), 0.88 (3H, t, J = 7.6 Hz, CHCH₂CH₃); δ_C (CDCl₃, 126 MHz): 166.7 (CONH), 163.7 (CONCH₃), 155.0 (C7), 152.1 (C4), 145.3 (C13), 137.9 (C6), 134.2 (C8), 126.4 (C11), 118.7 (C10), 116.3 (C9), 116.0 (C5), 11.8 (C12), 71.5 (CH(CH₃)₂), 60.4 (CHCH₂CH₃), 58.8 (C3), 54.6 (C15), 46.5 (NHCH), 46.1 (NCH₃), 32.3 (C14), 29.7 (C2), 29.4 (C2'), 28.2 (CONCH₃), 27.1 (CHCH₂CH₃), 23.9 (C1), 23.5 (C1'), 22.2 (CH(CH₃)₂), 9.2 (CHCH₂CH₃)

(R)-4-((8-Cyclopentyl-7-ethyl-5-methyl-6-oxo-5,6,7,8-tetrahydropteridin-2-yl)amino)-3-(cyclopropylmethoxy)-N-(1-methylpiperidin-4-yl)benzamide, 31



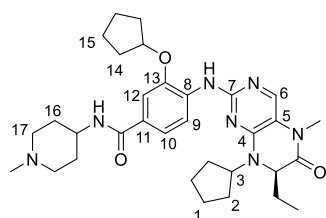
Dihydropteridinone **6a** (15 mg, 49 μmol) was reacted with aniline **20b** (15 mg, 49 μmol) using general method **16** to afford the title compound **31** as a white solid (11 mg, 40%). LCMS purity >95%, ret. time 1.22 mins; HRMS (ESI +ve):

found [M+H]⁺ 562.3495, [C₃₁H₄₄N₇O₃]⁺ requires 562.3506;

m.p.: 118 – 120 °C; ν_{\max} (thin film, cm⁻¹): 3412 (w, N-H), 2818 (w, CON-H), 1646 (C=O), 1612 (C=O); $[\alpha]_D^{21.8}$: -52.6° (c 1.0, MeOH); δ_H (CDCl₃, 500 MHz): 8.51 (1H, d, J = 8.8 Hz, H9), 7.92 (1H, s, ArNH), 7.68 (1H, s, H6), 7.44 – 7.41 (2H, m, H10 & H12), 6.89 (1H, d, J = 7.6 Hz, CONH), 4.48 – 4.40 (1H, m, H3), 4.33 – 4.26 (1H, m, NHCH), 4.25 (1H, dd, J = 7.6, 3.5 Hz, CHCH₂CH₃), 3.97 (2H, d, J = 7.3 Hz, OCH₂), 3.55 (2H,

d, $J = 11.7$ Hz, H15), 3.33 (3H, s, CONCH₃), 2.84 – 2.77 (2H, m, H15), 2.78 (3H, s, NCH₃), 2.27 – 2.11 (5H, m, cPeH & H14), 2.04 – 1.65 (9H, m, cPeH & CHCH₂CH₃), 1.40 – 1.31 (1H, m, CH(CH₂)₂), 0.88 (3H, t, $J = 7.6$ Hz, CHCH₂CH₃), 0.69 – 0.65 (2H, m, CH(CH₂)(C'H₂), 0.41 – 0.36 (2H, m, CH(CH₂)(C'H₂); δ_c (CDCl₃, 126 MHz): 166.8 (CONH), 163.7 (CONCH₃), 154.7 (C7), 152.2 (C4), 146.7 (C13), 137.0 (C6), 133.5 (C8), 125.6 (C11), 119.8 (C10), 116.4 (C9), 116.2 (C5), 110.3 (C12), 74.0 (OCH₂), 60.4 (CHCH₂CH₃), 59.1 (C3), 54.0 (C15), 44.2 (NHCH), 43.6 (NCH₃), 29.6 (C14), 29.2 (C2), 29.0 (C2'), 28.2 (CONCH₃), 27.2 (CHCH₂CH₃), 23.7 (C1), 23.4 (C1'), 10.3 (CH(CH₂)₂), 9.1 (CHCH₂CH₃), 3.3 (CH(CH₂)₂)

(*R*)-4-((8-Cyclopentyl-7-ethyl-5-methyl-6-oxo-5,6,7,8-tetrahydropteridin-2-yl)amino)-3-(cyclopentyloxy)-*N*-(1-methylpiperidin-4-yl)benzamide, 32

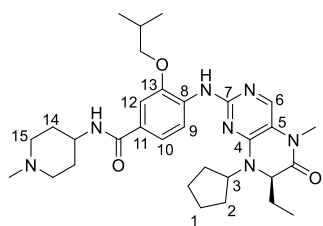


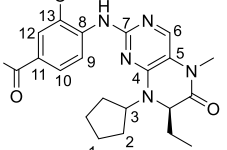
Dihydropteridinone **6a** (20.0 mg, 68 μ mol) was reacted with aniline **20c** (21.5 mg, 68 μ mol) using general method **16** to afford the title compound **32** as a yellow solid (8.6 mg, 22%). LCMS purity >95%, ret. time 1.27 mins; HRMS (ESI +ve): found $[M+H]^+$ 576.3663, $[C_{32}H_{46}N_7O_3]^+$ requires

576.3662; m.p.: 159 – 161 °C; ν_{\max} (thin film, cm⁻¹): 3423 (w, N-H), 2869 (w, CON-H), 1658 (C=O), 1593 (C=O); $[\alpha]_D^{21.7}$: -37.4° (c 1.0, MeOH); δ_H (CDCl₃, 500 MHz): 8.51 (1H, d, $J = 8.5$ Hz, H9), 7.77 (1H, s, ArNH), 7.68 (1H, s, H6), 7.45 (1H, d, $J = 1.9$ Hz, H12), 7.37 (1H, dd, $J = 8.5, 1.9$ Hz, H10), 6.78 (1H, d, $J = 7.6$ Hz, CONH), 5.00 – 4.95 (1H, m, OCH), 4.46 – 4.37 (1H, m, H3), 4.32 – 4.27 (1H, m, NHCH), 4.25 (1H, dd, $J = 7.9, 4.1$ Hz, CHCH₂CH₃), 3.55 (2H, d, $J = 11.7$ Hz, H17), 3.33 (3H, s, CONCH₃), 2.84 – 2.76 (2H, m, H17), 2.78 (3H, s, NCH₃), 2.30 – 2.10 (6H, m, H2 & H16), 2.04 – 1.64 (16H, m, cPeH & CHCH₂CH₃), 0.88 (3H, t, $J = 7.4$ Hz, CHCH₂CH₃); δ_c (CDCl₃, 126 MHz): 166.9 (CONH), 163.7 (CONCH₃), 154.7 (C7), 152.2 (C4), 145.6 (C13), 137.0 (C6), 134.0 (C8), 125.6 (C11), 119.3 (C10), 116.3 (C9), 116.2 (C5), 111.4 (C12), 80.7 (OCH), 60.6 (CHCH₂CH₃), 59.1 (C3), 54.0 (C17), 44.3 (NHCH), 43.6 (NCH₃), 32.9 (C14), 29.6 (C16), 29.3 (C2), 29.0 (C2'), 28.2 (CONCH₃), 27.2 (CHCH₂CH₃), 24.0 (C15), 23.8 (C1), 23.5 (C1'), 9.1 (CHCH₂CH₃)

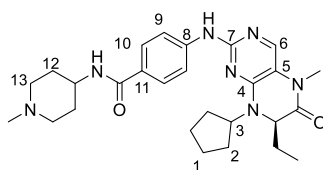
(*R*)-4-((8-Cyclopentyl-7-ethyl-5-methyl-6-oxo-5,6,7,8-tetrahydropteridin-2-yl)amino)-3-isobutoxy-*N*-(1-methylpiperidin-4-yl)benzamide, 33

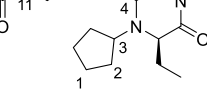
Dihydropteridinone **6a** (13 mg, 44 μ mol) was reacted with aniline **20d** (13 mg, 44 μ mol) using general method **16** to afford the title compound **33** as a white solid (7 mg, 28%). LCMS purity >95%, ret. time 1.26 mins; HRMS (ESI +ve): found $[M+H]^+$ 564.3652, $[C_{31}H_{46}N_7O_3]^+$ requires 564.3657; m.p.: 121 – 123 °C; ν_{\max} (thin film, cm⁻¹):



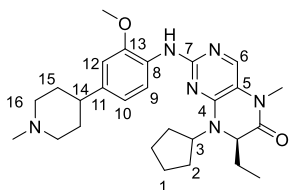

 3418 (w, N-H), 2956 (w, CON-H), 1673 (C=O), 1595 (C=O); $[\alpha]_D^{20.8}$: -31.2° (c 1.0, MeOH); δ_H (CDCl₃, 500 MHz): 8.55 (1H, d, J = 8.3 Hz, H9), 7.68 (1H, s, H6), 7.67 (1H, s, PhNH), 7.40 (1H, d, J = 1.6 Hz, H12), 7.22 (1H, dd, J = 8.3, 1.6 Hz, H10), 6.50 (1H, d, J = 6.9 Hz, CONH), 4.40 – 4.32 (1H, m, H3), 4.23 (1H, dd, J = 7.4, 3.3 Hz, CHCH₂CH₃), 4.22 – 4.17 (1H, m, NHCH), 3.90 (2H, d, J = 6.3 Hz, OCH₂), 3.41 (2H, d, J = 10.4 Hz, H15), 3.33 (3H, s, CONCH₃), 2.72 – 2.63 (5H, m, H15 & NCH₃), 2.26 – 1.65 (15H, m, 4 x H14, cPeH, CH(CH₃)₂ & CHCH₂CH₃), 1.09 (6H, d, J = 6.6 Hz, CH(CH₃)₂), 0.87 (3H, t, J = 7.4 Hz, CHCH₂CH₃); δ_C (CDCl₃, 126 MHz): 166.8 (CONH), 163.8 (CONCH₃), 154.9 (C7), 152.1 (C4), 146.5 (C13), 137.7 (C6), 133.6 (C8), 125.6 (C11), 119.4 (C10), 116.4 (C9), 115.9 (C5), 109.8 (C12), 75.3 (OCH₂), 60.8 (CHCH₂CH₃), 59.3 (C3), 53.8 (C15), 44.7 (NHCH), 43.9 (NCH₃), 29.7 (C14), 29.6 (C2), 29.3 (C2'), 28.3 (CH(CH₃)₂), 28.2 (CONCH₃), 27.2 (CHCH₂CH₃), 23.9 (C1), 23.6 (C1'), 19.4 (CH(CH₃)₂), 9.1 (CHCH₂CH₃)

(R)-4-((8-Cyclopentyl-7-ethyl-5-methyl-6-oxo-5,6,7,8-tetrahydropteridin-2-yl)amino)-N-(1-methyl-piperidin-4-yl)benzamide, 34




 Dihydropteridinone **6a** (25.mg, 90 μ mol) was reacted with aniline **20f** (18 mg, 80 μ mol) using general method **16** to afford the title compound **34** as a white solid (15 mg, 36%). LCMS purity >95%, ret. time 1.06 mins; HRMS (ESI +ve): found $[M+H]^+$ 492.3060, $[C_{27}H_{38}N_7O_2]^+$ requires 492.3087; m.p 210 – 212 $^{\circ}$ C; ν_{\max} (thin film, cm^{-1}): 3295 (w, N-H), 2940 (w, CON-H), 1662 (C=O), 1607 (C=O); $[\alpha]_D^{21.5}$: -31.9° (*c* 1.0, MeOH); δ_H ($CDCl_3$, 500 MHz): 7.73 – 7.69 (2H, m, H10), 7.68 – 7.65 (3H, m, H6 & H9), 7.14 (1H, s, PhNH), 5.95 (1H, d, $J = 7.9$ Hz, CONH), 4.50 – 4.42 (1H, m, H3), 4.22 (1H, dd, $J = 7.9, 3.8$ Hz, $\underline{CH}CH_2CH_3$), 4.03 – 3.95 (1H, m, NHCH), 3.32 (3H, s, $CONCH_3$), 2.83 (2H, d, $J = 11.4$ Hz, H13), 2.30 (3H, s, NCH_3), 2.19 – 2.11 (3H, m, 1 x H2 & 2 x H13), 2.07 – 2.02 (2H, m, H12), 2.00 – 1.96 (1H, m, H2) 1.90 – 1.78 (4H, m, *c*PeH & $\underline{CHCH}HCH_3$), 1.76 – 1.64 (4H, m, *c*PeH & $\underline{CHCH}HCH_3$), 1.63 – 1.54 (2H, m, H12), 0.87 (3H, t, $J = 7.6$ Hz, \underline{CHCH}_2CH_3); δ_C ($CDCl_3$, 126 MHz): 166.4 (CONH), 163.7 (\underline{CONCH}_3), 155.0 (C7), 152.2 (C4), 143.3 (C8), 137.8 (C6), 127.8 (C10), 127.1 (C11), 117.4 (C9), 116.4 (C5), 59.9 (\underline{CHCH}_2CH_3), 58.5 (C3), 54.5 (C13), 46.4 (NHCH), 46.2 (NCH_3), 32.4 (C12), 29.6 (C2), 29.2 (C2'), 28.1 ($CONCH_3$), 27.1 (\underline{CHCH}_2CH_3), 23.5 (C1), 23.1 (C1'), 9.1 (\underline{CHCH}_2CH_3)

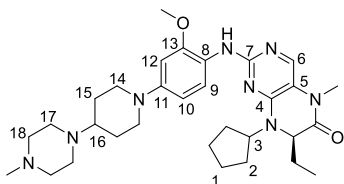
(*R*)-8-Cyclopentyl-7-ethyl-2-((2-methoxy-4-(1-methylpiperidin-4-yl)phenyl)amino)-5-methyl-7,8-dihydropteridin-6(5*H*)-one, 35



Dihydropteridinone **6a** (25 mg, 80 μ mol) was reacted with aniline **28a** (18 mg, 80 μ mol) using general method **16** to afford the title compound **35** as a yellow gum (9 mg, 22%).

LCMS purity >95%, ret. time 1.04 mins; HRMS (ESI +ve): found $[M+H]^+$ 479.3101, $[C_{27}H_{39}N_6O_2]^+$ requires 479.3129; ν_{\max} (thin film, cm^{-1}): 2940 (w, N-H), 1671 (C=O); $[\alpha]_D^{21.8}$: -9.1° (c 1.0, MeOH); δ_H (CDCl_3 , 500 MHz): 8.20 (1H, d, $J=8.2$ Hz, H9), 7.88 (1H, s, NH), 7.61 (1H, s, H6), 6.80 (1H, dd, $J=8.2, 1.9$ Hz, H10), 6.75 (1H, d, $J=1.9$ Hz, H12), 4.42 (1H, quin., $J=8.0$ Hz, H3), 4.21 (1H, dd, $J=7.7, 3.6$ Hz, CHCH_2CH_3), 3.90 (3H, s, OCH_3), 3.59 (2H, d, $J=10.7$ Hz, H16), 3.31 (3H, s, CONCH_3), 2.75 (3H, s, NCH_3), 2.77 – 2.67 (3H, m, H14 & H16), 2.27 (2H, q, $J=12.5$ Hz, H15), 2.14 – 1.92 (4H, m, 2 x H2 & 2 x H15), 1.92 – 1.60 (8H, m, cPeH & CHCH_2CH_3), 0.87 (3H, t, $J=7.6$ Hz, CHCH_2CH_3); δ_C (CDCl_3 , 126 MHz): 163.6 (CONCH_3), 155.0 (C7), 152.4 (C4), 148.8 (C13), 136.1 (C6 & C11), 128.3 (C8), 119.2 (C9), 118.7 (C10), 115.7 (C5), 108.5 (C12), 60.0 (CHCH_2CH_3), 58.6 (C3), 55.8 (OCH_3), 54.8 (C16), 43.5 (NCH_3), 40.1 (C14), 30.6 (C15), 29.5 (C2), 29.2 (C2'), 28.2 (CONCH_3), 27.2 (CHCH_2CH_3), 23.5 (C1), 23.3 (C1'), 9.1 (CHCH_2CH_3)

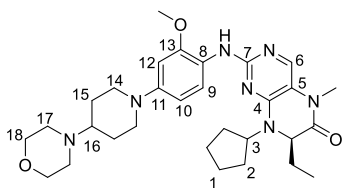
(*R*)-8-Cyclopentyl-7-ethyl-2-((2-methoxy-4-(4-(4-methylpiperazin-1-yl)piperidin-1-yl)phenyl)amino)-5-methyl-7,8-dihydropteridin-6(5*H*)-one, 36



Dihydropteridinone **6a** (25 mg, 85 μ mol) was reacted with aniline **23a** (25 mg, 85 μ mol) using general method **16** to afford the title compound **36** as a brown solid (14 mg, 30%). LCMS purity >95%, ret. time 1.02 mins; HRMS (ESI

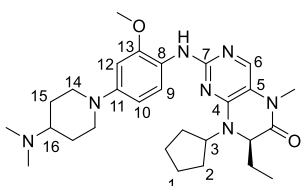
+ve): found $[M+H]^+$ 563.3813, $[C_{31}H_{47}N_8O_2]^+$ requires 563.3822; m.p.: 63 – 65 $^\circ\text{C}$; ν_{\max} (thin film, cm^{-1}): 3421 (w, N-H), 1654 (C=O); $[\alpha]_D^{21.6}$: -36.8° (c 1.0, MeOH); δ_H (CDCl_3 , 500 MHz): 7.88 (1H, d, $J=8.5$ Hz, H9), 7.55 (1H, s, H6), 7.13 (1H, s, NH), 6.53 (1H, d, $J=2.2$ Hz, H12), 6.50 (1H, dd, $J=8.5, 2.2$ Hz, H10), 4.33 – 4.23 (1H, m, H3), 4.21 (1H, dd, $J=8.0, 3.6$ Hz, CHCH_2CH_3), 3.88 (3H, s, OCH_3), 3.66 (2H, d, $J=12.3$ Hz, H14), 3.29 (3H, s, CONCH_3), 3.11 – 2.89 (8H, m, H17 & H18), 2.75 – 2.65 (3H, m, H14 & H16), 2.58 (3H, s, NCH_3), 2.06 – 1.51 (14H, m, cPeH, CHCH_2CH_3 & 4 x H15), 0.88 (3H, t, $J=7.4$ Hz, CHCH_2CH_3); δ_C (CDCl_3 , 126 MHz): 163.5 (CONCH_3), 154.7 (C7), 152.5 (C4), 150.6 (C13), 147.7 (C11), 133.9 (C6), 122.1 (C8), 121.6 (C9), 115.2 (C5), 108.6 (C10), 101.4 (C12), 61.7 (C16), 60.8 (CHCH_2CH_3), 59.5 (C3), 55.7 (OCH_3), 53.2 (C18), 50.2 (C14), 46.7 (C17), 43.9 (NCH_3), 29.2 (C2), 28.9 (C2'), 28.2 (CONCH_3), 27.7 (C15), 27.2 (CHCH_2CH_3), 23.5 (C1), 23.2 (C1'), 8.9 (CHCH_2CH_3)

(*R*)-8-Cyclopentyl-7-ethyl-2-((2-methoxy-4-(4-(4-morpholinopiperidin-1-yl)phenyl)amino)-5-methyl-7,8-dihydropteridin-6(5H)-one, 37



Dihydropteridinone **6a** (25 mg, 85 μ mol) was reacted with aniline **23b** (25 mg, 85 μ mol) using general method **16** to afford the title compound **37** as a yellow solid (22 mg, 47%). LCMS purity >95%, ret. time 1.04 mins; HRMS (ESI +ve): found $[M+H]^+$ 550.3489, $[C_{30}H_{44}N_7O_3]^+$ requires 550.3506; m.p.: 109 – 112 $^{\circ}$ C; ν_{\max} (thin film, cm^{-1}): 3431 (w, N-H), 1667 (C=O); $[\alpha]_D^{21.7}$: -54.7° (c 1.0, MeOH); δ_H (CDCl_3 , 500 MHz): 8.20 (1H, d, J = 8.8 Hz, H9), 7.64 (1H, s, H6), 7.15 (1H, s, NH), 6.57 (1H, d, J = 2.5 Hz, H12), 6.54 (1H, dd, J = 8.8, 2.5 Hz, H10), 4.52 – 4.44 (1H, m, H3), 4.25 (1H, dd, J = 7.8, 3.7 Hz, CHCH_2CH_3), 3.88 (3H, s, OCH_3), 3.77 – 3.73 (4H, m, H18), 3.64 (2H, d, J = 12.6 Hz, H14), 3.31 (3H, s, CONCH_3), 2.73 – 2.66 (2H, m, H14), 2.62 – 2.58 (4H, m, H17), 2.33 (1H, tt, J = 11.4, 3.6 Hz, H16), 2.15 – 2.08 (1H, m, H2), 2.02 – 1.63 (13H, m, cPeH, CHCH_2CH_3 & 4 x H15), 0.88 (3H, t, J = 7.6 Hz, CHCH_2CH_3); δ_C (CDCl_3 , 126 MHz): 163.7 (CONCH_3), 156.0 (C7), 152.3 (C4), 148.8 (C13), 146.8 (C11), 138.3 (C6), 123.2 (C8), 119.1 (C9), 115.4 (C5), 108.6 (C10), 101.3 (C12), 67.3 (C17), 62.0 (C16), 60.0 (CHCH_2CH_3), 58.3 (C3), 55.6 (OCH_3), 50.6 (C14), 49.8 (C17), 29.7 (C2), 29.2 (C2'), 28.2 (CONCH_3), 28.1 (C15), 27.0 (CHCH_2CH_3), 23.5 (C1), 23.1 (C1'), 9.2 (CHCH_2CH_3)

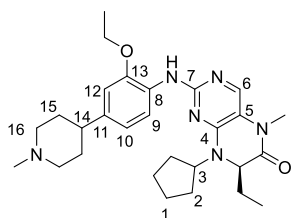
(*R*)-8-Cyclopentyl-2-((4-(4-(dimethylamino)piperdin-1-yl)-2-methoxyphenyl)amino)-7-ethyl-5-methyl-7,8-dihydropteridin-6(5H)-one, 38



Dihydropteridinone **6a** (25 mg, 85 μ mol) was reacted with aniline **23c** (25 mg, 85 μ mol) using general method **16** to afford the title compound **38** as a yellow gum (21 mg, 50%). LCMS purity >95%, ret. time 1.03 mins; HRMS (ESI +ve): found $[M+H]^+$ 508.3358, $[C_{28}H_{42}N_7O_2]^+$ requires 508.3340; ν_{\max} (thin film, cm^{-1}): 3429 (w, N-H), 1664 (C=O); $[\alpha]_D^{21.5}$: -70.0° (c 1.0, MeOH); δ_H (CDCl_3 , 500 MHz): 8.22 (1H, s, NH), 7.93 (1H, d, J = 8.8 Hz, H9), 7.55 (1H, s, H6), 6.54 – 6.47 (2H, m, H10 & H12), 4.33 – 4.24 (1H, m, H3), 4.21 (1H, dd, J = 7.8, 3.8 Hz, CHCH_2CH_3), 3.86 (3H, s, OCH_3), 3.69 (2H, d, J = 12.0 Hz, H14), 3.29 (3H, s, CONCH_3), 3.16 (1H, t, J = 11.5, H16), 2.81 – 2.68 (8H, m, H14 & $\text{N}(\text{CH}_3)_2$), 2.13 (2H, d, J = 10.7 Hz, H15), 2.06 – 1.98 (1H, m, H2), 1.94 – 1.52 (11H, m, cPeH, CHCH_2CH_3 & 2 x H15), 0.85 (3H, t, J = 7.3 Hz, CHCH_2CH_3); δ_C (CDCl_3 , 126 MHz): 163.5 (CONCH_3), 154.7 (C7), 152.5 (C4), 150.5 (C13), 147.1 (C11), 134.2 (C6), 122.7 (C8), 121.5 (C9), 115.3 (C5), 109.0 (C10), 101.7 (C12), 62.5 (NCH), 60.8 (CHCH_2CH_3), 59.5 (C3), 55.7 (OCH_3), 50.0

(C14), 38.9 (N(CH₃)₂), 29.3 (C2), 28.9 (C2'), 28.2 (CONCH₃), 27.2 (CHCH₂CH₃), 26.0 (C15), 23.5 (C1), 23.2 (C1'), 8.9 (CHCH₂CH₃)

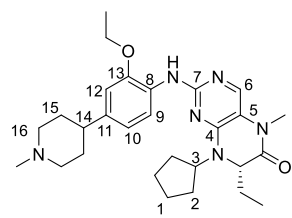
(R)-8-Cyclopentyl-7-ethyl-2-((2-ethoxy-4-(1-methylpiperidin-4-yl)phenyl)amino)-5-methyl-7,8-dihydropteridin-6(5H)-one, 39



Dihydropteridinone **6a** (43.0 mg, 146 μ mol) was reacted with aniline **28b** (32.5 mg, 139 μ mol) using general method **16** to afford the title compound **39** as a brown solid (16.9 mg, 24%). LCMS purity >95%, ret. time 1.05 mins; HRMS (ESI +ve): found [M+H]⁺ 493.3280, [C₂₈H₄₁N₆O₂]⁺ requires

493.3286; m.p.: 97 – 99 °C; ν_{\max} (thin film, cm⁻¹): 3424 (w, N-H), 1669 (C=O); $[\alpha]_D^{23.0}$: -36.0° (c 1.0, MeOH); δ_H (CDCl₃, 500 MHz): 8.26 (1H, d, *J* = 8.3 Hz, H9), 7.77 (1H, s, NH), 7.63 (1H, s, H6), 6.79 (1H, d, *J* = 8.3 Hz, H10), 6.74 (1H, s, H12), 4.42 (1H, quin., *J* = 7.4 Hz, H3), 4.22 (1H, dd, *J* = 7.9, 3.6 Hz, CHCH₂CH₃), 4.12 (2H, q, *J* = 6.9 Hz, OCH₂CH₃), 3.58 (2H, d, *J* = 11.7 Hz, H16), 3.32 (3H, s, CONCH₃), 2.76 – 2.62 (6H, m, NCH₃, H14 & H16), 2.27 – 2.16 (2H, m, H15), 2.13 – 2.07 (1H, m, H2), 2.02 – 1.94 (3H, m, 1 x H2 & 2 x H15), 1.92 – 1.62 (8H, m, cPeH, 2 x H15 & CHCH₂CH₃), 1.48 (3H, t, *J* = 6.9 Hz, OCH₂CH₃), 0.88 (3H, t, *J* = 7.5 Hz, CHCH₂CH₃); δ_C (CDCl₃, 126 MHz): 163.6 (CONCH₃), 155.1 (C7), 152.3 (C4), 147.8 (C13), 136.7 (C8), 136.6 (C6), 128.5 (C11), 118.7 (C9), 118.5 (C10), 115.6 (C5), 109.5 (C12), 64.4 (OCH₂CH₃), 60.4 (CHCH₂CH₃), 59.0 (C3), 54.6 (C16), 43.5 (NCH₃), 40.1 (C14), 30.6 (C15), 29.5 (C2), 29.2 (C2'), 28.2 (CONCH₃), 27.2 (CHCH₂CH₃), 23.6 (C1), 23.3 (C1'), 14.9 (OCH₂CH₃), 9.1 (CHCH₂CH₃)

(S)-8-Cyclopentyl-2-((2-ethoxy-4-(1-methylpiperidin-4-yl)phenyl)amino)-7-ethyl-5-methyl-7,8-dihydropteridin-6(5H)-one, 40

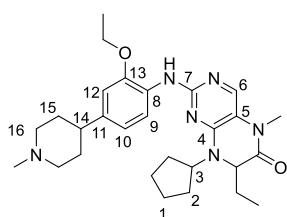


Dihydropteridinone **6b** (30 mg, 102 μ mol) was reacted with aniline **28b** (23 mg, 97 μ mol) using general method **16** to afford the title compound **40** as a brown solid (11 mg, 26%). LCMS purity >95%, ret. time 1.09 mins; HRMS (ESI +ve): found [M+H]⁺ 493.3272, [C₂₈H₄₁N₆O₂]⁺ requires 493.3286;

m.p.: 97 – 99 °C; ν_{\max} (thin film, cm⁻¹): 3421 (w, N-H), 1668 (C=O); $[\alpha]_D^{20.5}$: +9.0° (c 1.0, MeOH); δ_H (CDCl₃, 500 MHz): 8.19 (1H, d, *J* = 8.2 Hz, H9), 7.96 (1H, s, NH), 7.62 (1H, s, H6), 6.78 (1H, dd, *J* = 8.2, 1.6 Hz, H10), 6.74 (1H, d, *J* = 1.6 Hz, H12), 4.39 (1H, quin., *J* = 8.3 Hz, H3), 4.23 (1H, dd, *J* = 7.6, 3.5 Hz, CHCH₂CH₃), 4.11 (2H, q, *J* = 6.9 Hz, OCH₂CH₃), 3.61 (2H, d, *J* = 10.4 Hz, H16), 3.31 (3H, s, CONCH₃), 2.77 – 2.61 (6H, m, NCH₃, H14 & H16), 2.25 – 2.15 (2H, m, H15), 2.03 – 1.83 (5H, m, 2 x H1, 2 x H15 & CHCH₂CH₃), 1.81 – 1.60 (5H, cPeH & CHCH₂CH₃), 1.47 (3H, t, *J* =

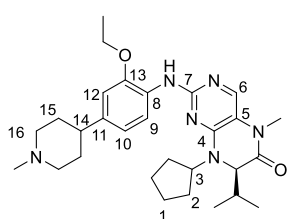
6.9 Hz, OCH_2CH_3), 0.87 (3H, t, $J = 7.64$ Hz, CHCH_2CH_3); δ_{C} (CDCl_3 , 126 MHz): 163.6 (CONCH_3), 154.9 (C7), 152.4 (C4), 137.0 (C11), 136.0 (C6), 128.3 (C8), 119.2 (C9), 118.5 (C10), 115.5 (C5), 109.5 (C12), 64.4 (OCH_2CH_3), 60.5 (CHCH_2CH_3), 59.1 (C3), 54.6 (C16), 43.5 (NCH_3), 40.0 (C14), 30.5 (C15), 29.5 (C2), 29.2 (C2'), 28.2 (CONCH_3), 27.2 (CHCH_2CH_3), 23.6 (C1), 13.3 (C1'), 14.9 (OCH_2CH_3), 9.0 (CHCH_2CH_3)

8-Cyclopentyl-7-ethyl-2-((2-ethoxy-4-(1-methylpiperidin-4-yl)phenyl)amino)-5-methyl-7,8-dihydropteridin-6(5H)-one, 41



Dihydropteridinone **6c** (38 mg, 129 μmol) was reacted with aniline **28b** (29 mg, 123 μmol) using general method **16** to afford the title compound **41** as a brown solid (4 mg, 6%). LCMS purity >95%, ret. time 1.05 mins; HRMS (ESI +ve): found $[\text{M}+\text{H}]^+$ 493.3280, $[\text{C}_{28}\text{H}_{41}\text{N}_6\text{O}_2]^+$ requires 493.3286; m.p.: 98 – 100 $^{\circ}\text{C}$; ν_{max} (thin film, cm^{-1}): 3424 (w, N-H), 1667 (C=O); δ_{H} (CDCl_3 , 500 MHz): 8.26 (1H, d, $J = 8.3$ Hz, H9), 7.77 (1H, s, NH), 7.63 (1H, s, H6), 6.79 (1H, d, $J = 8.3$ Hz, H10), 6.74 (1H, s, H12), 4.42 (1H, quin. $J = 7.4$ Hz, H3), 4.22 (1H, dd, $J = 7.9$, 3.6 Hz, CHCH_2CH_3), 4.12 (2H, q, $J = 6.9$ Hz, OCH_2CH_3), 3.58 (2H, d, $J = 11.7$ Hz, H16), 3.32 (3H, s, CONCH_3), 2.76 – 2.62 (6H, m, NCH_3 , H14 & H16), 2.27 – 2.16 (2H, m, H15), 2.13 – 2.07 (1H, m, H2), 2.02 – 1.94 (3H, m, 1 x H2 & 2 x H15), 1.92 – 1.62 (8H, m, CpH, 2 x H15 & CHCH_2CH_3), 1.48 (3H, t, $J = 6.9$ Hz, OCH_2CH_3), 0.88 (3H, t, $J = 7.5$ Hz, CHCH_2CH_3); δ_{C} (CDCl_3 , 126 MHz): 163.6 (CONCH_3), 155.1 (C7), 152.3 (C4), 147.8 (C13), 136.7 (C8), 136.6 (C6), 128.5 (C11), 118.7 (C9), 118.5 (C10), 115.6 (C5), 109.5 (C12), 64.4 (OCH_2CH_3), 60.4 (CHCH_2CH_3), 59.0 (C3), 54.6 (C16), 43.5 (NCH_3), 40.1 (C14), 30.6 (C15), 29.5 (C2), 29.2 (C2'), 28.2 (CONCH_3), 27.2 (CHCH_2CH_3), 23.6 (C1), 23.3 (C1'), 14.9 (OCH_2CH_3), 9.1 (CHCH_2CH_3)

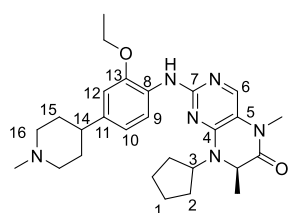
(R)-8-Cyclopentyl-7-isopropyl-2-((2-ethoxy-4-(1-methylpiperidin-4-yl)phenyl)amino)-5-methyl-7,8-dihydropteridin-6(5H)-one, 42



Dihydropteridinone **6d** (50 mg, 162 μmol) was reacted with aniline **28b** (36 mg, 154 μmol) using general method **16** to afford the title compound **42** as a yellow solid (17 mg, 21%). LCMS purity >95%, ret. time 1.14 mins; HRMS (ESI +ve): found $[\text{M}+\text{H}]^+$ 507.3425, $[\text{C}_{29}\text{H}_{43}\text{N}_6\text{O}_2]^+$ requires 507.3442; m.p.: 67 – 70 $^{\circ}\text{C}$; ν_{max} (thin film, cm^{-1}): 3425 (w, N-H), 1666 (C=O); $[\alpha]_D^{23.0}$: - 54.0 $^{\circ}$ (c 1.0, MeOH); δ_{H} (CDCl_3 , 500 MHz): 8.16 (1H, d, $J = 8.4$ Hz, H9), 8.02 (1H, s, NH), 7.58 (1H, s, H6), 6.77 (1H, dd, $J = 8.4$, 1.6 Hz, H10), 6.73 (1H, d, $J = 1.6$ Hz, H12),

4.28 (1H, quin, $J = 8.3$ Hz, H3), 4.12 – 4.08 (3H, m, $\text{CHCH}(\text{CH}_3)_2$ & OCH_2CH_3), 3.59 (2H, d, $J = 9.8$ Hz, H16), 3.30 (3H, s, CONCH_3), 2.77 – 2.62 (6H, m, NCH_3 , H14 & H16), 2.25 – 2.15 (2H, m, H15), 2.11 – 2.03 (1H, m, $\text{CHCH}(\text{CH}_3)_2$), 2.02 – 1.95 (3H, m, 1 x H2 & 2 x H15). 1.91 – 1.67 (4H, m, cPeH), 1.65 – 1.57 (2H, m, H1), 1.46 (3H, t, $J = 6.9$ Hz, OCH_2CH_3), 1.08 (3H, d, $J = 7.3$ Hz, $(\text{CH}_3)(\text{C}'\text{H}_3)$), 0.78 (3H, d, $J = 6.9$ Hz, $(\text{CH}_3)(\text{C}'\text{H}_3)$); δ_{C} (CDCl_3 , 126 MHz): 161.9 (CONCH_3), 154.7 (C7), 152.4 (C4), 148.3 (C13), 137.1 (C11), 135.1 (C6), 128.2 (C8), 119.4 (C9), 118.5 (C10), 116.2 (C5), 109.5 (C12), 65.4 (OCH_2CH_3), 64.3 ($\text{CHCH}(\text{CH}_3)_2$), 60.4 (C3), 54.6 (C16), 43.5 (NCH_3), 40.1 (C14), 34.5 ($\text{CHCH}(\text{CH}_3)_2$), 30.5 (C15), 29.6 (C2), 28.0 (CONCH_3), 23.6 (C1), 23.4 (C1'), 20.3 ($(\text{CH}_3)(\text{C}'\text{H}_3)$), 16.7 ($(\text{CH}_3)(\text{C}'\text{H}_3)$), 14.9 (OCH_2CH_3)

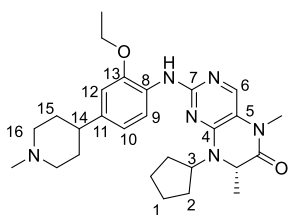
(R)-8-Cyclopentyl-2-((2-ethoxy-4-(1-methylpiperidin-4-yl)phenyl)amino)-5,7-dimethyl-7,8-dihydropteridin-6(5H)-one, 43



Dihydropteridinone **6e** (36.2 mg, 129 μmol) was reacted with aniline **28b** (28.7 mg, 123 μmol) using general method **16** to afford the title compound **43** as a brown oil (13.2 mg, 21%). LCMS purity >95%, ret. time 1.05 mins; HRMS (ESI +ve): found $[\text{M}+\text{H}]^+$ 479.3115, $[\text{C}_{27}\text{H}_{39}\text{N}_6\text{O}_2]^+$ requires 479.3129;

ν_{max} (thin film, cm^{-1}): 3422 (w, N-H), 1666 (C=O); $[\alpha]_D^{22.3}$: -27.7° (c 1.0, MeOH); δ_{H} (CDCl_3 , 500 MHz): 8.23 (1H, d, $J = 8.3$ Hz, H9), 7.86 (1H, s, NH), 7.67 (1H, s, H6), 6.78 (1H, dd, $J = 8.3, 1.3$ Hz, H11), 6.74 (1H, d, $J = 1.3$ Hz, H13), 4.49 (1H, quin, $J = 8.0$ Hz, H3), 4.32 (1H, q, $J = 6.7$ Hz, CHCH_3), 4.12 (2H, q, $J = 6.8$ Hz, OCH_2CH_3), 3.61 (2H, d, $J = 8.5$ Hz, H16), 3.31 (3H, s, CONCH_3), 2.80 – 2.63 (6H, m, NCH_3 , H14 & H16), 2.27 – 2.16 (2H, m, H15), 2.13 – 3.06 (1H, m, H2), 2.04 – 1.96 (3H, m, 1 x H2 & 2 x H15), 1.84 – 1.63 (6H, m, cPeH), 1.47 (3H, t, $J = 6.8$ Hz, OCH_2CH_3), 1.35 (3H, d, $J = 6.7$ Hz, CHCH_3); δ_{C} (CDCl_3 , 126 MHz): 164.9 (CONCH_3), 155.1 (C7), 151.9 (C4), 147.9 (C13), 136.7 (C6 & C11), 128.4 (C8), 118.9 (C9), 118.5 (C10), 115.5 (C5), 109.5 (C12), 64.4 (OCH_2CH_3), 58.2 (C3), 54.9 (CHCH_3), 54.6 (C16), 43.5 (NCH_3), 40.0 (C14), 30.5 (C15), 29.8 (C2), 29.4 (C2'), 28.3 (CONCH_3), 23.7 (C1), 23.3 (C1'), 19.2 (CHCH_3), 14.9 (OCH_2CH_3)

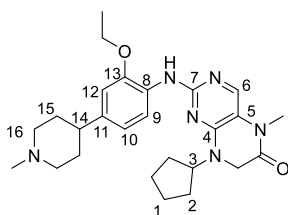
(S)-8-Cyclopentyl-2-((2-ethoxy-4-(1-methylpiperidin-4-yl)phenyl)amino)-5,7-dimethyl-7,8-dihydropteridin-6(5H)-one, 44



Dihydropteridinone **6f** (29 mg, 102 μmol) was reacted with aniline **28b** (23 mg, 96 μmol) using general method **16** to afford the title compound **44** as a brown oil (7 mg, 15%). LCMS purity >95%, ret. time 1.05 mins; HRMS (ESI +ve):

found $[M+H]^+$ 479.3107, $[C_{27}H_{39}N_6O_2]^+$ requires 479.3129; ν_{\max} (thin film, cm^{-1}): 3425 (w, N-H), 1666 (C=O); $[\alpha]_D^{22.3}$: +34.0° (c 1.0, MeOH); δ_H (CDCl_3 , 500 MHz): 8.23 (1H, d, J = 8.3 Hz, H9), 7.86 (1H, s, NH), 7.67 (1H, s, H6), 6.78 (1H, dd, J = 8.3, 1.3 Hz, H11), 6.74 (1H, d, J = 1.3 Hz, H13), 4.49 (1H, quin., J = 8.0 Hz, H3), 4.32 (1H, q, J = 6.7 Hz, CHCH_3), 4.12 (2H, q, J = 6.8 Hz, OCH_2CH_3), 3.61 (2H, d, J = 8.5 Hz, H16), 3.31 (3H, s, CONCH_3), 2.80 – 2.63 (6H, m, NCH_3 , H14 & H16), 2.27 – 2.16 (2H, m, H15), 2.13 – 3.06 (1H, m, H2), 2.04 – 1.96 (3H, m, 1 x H2 & 2 x H15), 1.84 – 1.63 (6H, m, cPeH), 1.47 (3H, t, J = 6.8 Hz, OCH_2CH_3), 1.35 (3H, d, J = 6.7 Hz, CHCH_3); δ_C (CDCl_3 , 126 MHz): 164.9 (CONCH_3), 155.1 (C7), 151.9 (C4), 147.9 (C13), 136.7 (C6 & C11), 128.4 (C8), 118.9 (C9), 118.5 (C10), 115.5 (C5), 109.5 (C12), 64.4 (OCH_2CH_3), 58.2 (C3), 54.9 (CHCH_3), 54.6 (C16), 43.5 (NCH_3), 40.0 (C14), 30.5 (C15), 29.8 (C2), 29.4 (C2'), 28.3 (CONCH_3), 23.7 (C1), 23.3 (C1'), 19.2 (CHCH_3), 14.9 (OCH_2CH_3)

8-Cyclopentyl-2-((2-ethoxy-4-(1-methylpiperidin-4-yl)phenyl)amino)-5-methyl-7,8-dihydropteridin-6(5H)-one, 45

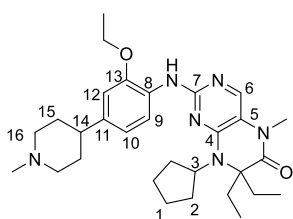


Dihydropteridinone **6g** (30 mg, 113 μmol) was reacted with aniline **28b** (25 mg, 107 μmol) using general method **16** to afford the title compound **45** as a yellow solid (8 mg, 15%). LCMS purity >95%, ret. time 1.05 mins; HRMS (ESI +ve): found $[M+H]^+$ 465.2969, $[C_{26}H_{37}N_6O_2]^+$ requires 465.2973;

m.p.: decomp.; ν_{\max} (thin film, cm^{-1}): 3434 (w, N-H), 1675 (C=O); δ_H (CDCl_3 , 500 MHz): 8.31 (1H, d, J = 8.3 Hz, H9), 7.63 (1H, s, H6), 7.53 (1H, s, NH), 6.79 (1H, dd, J = 8.3, 1.5 Hz, H10), 6.73 (1H, d, J = 1.5 Hz, H12), 5.13 (1H, quin, J = 8.2 Hz, H3), 4.12 (2H, q, J = 6.8 Hz, OCH_2CH_3), 4.06 (2H, s, CH_2), 3.55 (2H, d, J = 11.0 Hz, H16), 3.30 (3H, s, CONCH_3), 2.71 (3H, s, NCH_3), 2.70 – 2.61 (3H, m, H14 & H16), 2.23 – 2.13 (2H, m, H15), 2.01 – 1.92 (4H, 2 x H2 & 2 x H15), 1.84 – 1.59 (6H, m, cPeH), 1.48 (3H, t, J = 6.8 Hz, OCH_2CH_3); δ_C (CDCl_3 , 126 MHz): 161.7 (CONCH_3), 154.5 (C7), 152.0 (C4), 147.3 (C13), 137.7 (C11), 136.4 (C6), 128.7 (C8), 118.6 (C10), 117.9 (C9), 115.2 (C5), 109.5 (C12), 64.4 (OCH_2CH_3), 55.2 (C3), 54.6 (C16), 45.3 (CH_2), 43.6 (NCH_3), 40.2 (C14), 30.7 (C15), 27.8 (CONCH_3), 27.2 (C2), 24.2 (C1), 15.0 (OCH_2CH_3)

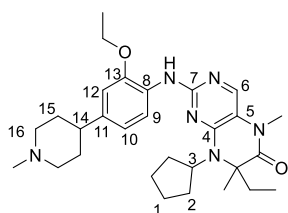
8-Cyclopentyl-2-((2-ethoxy-4-(1-methylpiperidin-4-yl)phenyl)amino)-7,7-diethyl-5-methyl-7,8-dihydropteridin-6(5H)-one, 46

Dihydropteridinone **14a** (30 mg, 93 μmol) was reacted with aniline **28b** (21 mg, 88 μmol) using general method **16** to afford the title compound **46** as a yellow solid (5



mg, 11%). LCMS purity >95%, ret. time 1.13 mins; HRMS (ESI +ve): found $[M+H]^+$ 521.3598, $[C_{30}H_{45}N_6O_2]^+$ requires 521.3599; m.p.: 96 – 98 °C; ν_{\max} (thin film, cm^{-1}): 3424 (w, N-H), 1657 (C=O); δ_{H} (CDCl_3 , 500 MHz): 7.83 (1H, d, J = 8.0 Hz, H10), 7.46 (1H, s, H6), 6.79 (1H, dd, J = 8.0, 1.9 Hz, H11), 6.73 (1H, d, J = 1.9 Hz, H13), 4.07 (2H, q, J = 6.9 Hz, OCH_2CH_3), 3.74 – 3.67 (1H, m, H3), 3.59 (2H, d, J = 10.4 Hz, H16), 3.30 (3H, s, CONCH_3), 2.74 (3H, s, NCH_3), 2.76 – 2.63 (3H, m, H14 & H16), 2.47 – 2.39 (2H, m, H2), 2.26 – 2.15 (4H, m, 2 x H15 & $\text{C}(\text{CH}_2\text{CH}_3)(\text{C}'\text{H}_2\text{CH}_3)$), 1.98 (2H, d, J = 14.5 Hz, H15), 1.83 – 1.76 (2H, m, $\text{C}(\text{CH}_2\text{CH}_3)(\text{C}'\text{H}_2\text{CH}_3)$), 1.63 – 1.53 (4H, m, cPeH), 1.42 (5H, m, H1 & OCH_2CH_3), 0.82 (6H, t, J = 7.3 Hz, $\text{C}(\text{CH}_2\text{CH}_3)_2$); δ_{C} (CDCl_3 , 126 MHz): 165.4 (CONCH_3), 153.6 (C7), 151.4 (C4), 150.0 (C13), 137.8 (C11), 131.2 (C6), 127.5 (C8), 121.9 (C9), 118.9 (C10), 114.4 (C5), 109.7 (C12), 73.0 ($\text{C}(\text{CH}_2\text{CH}_3)_2$), 60.8 (OCH_2CH_3), 57.3 (C3), 54.6 (C16), 43.6 (NCH_3), 40.1 (C14), 31.7 ($\text{C}(\text{CH}_2\text{CH}_3)_2$), 30.5 (C15), 28.1 (CONCH_3), 28.0 (C2), 25.2 (C1), 14.8 (OCH_2CH_3), 8.7 ($\text{C}(\text{CH}_2\text{CH}_3)_2$).

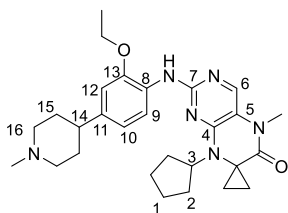
8-Cyclopentyl-2-((2-ethoxy-4-(1-methylpiperidin-4-yl)phenyl)amino)-7-diethyl-5,7-dimethyl-7,8-dihydropteridin-6(5H)-one, 47



Dihydropteridinone **14b** (25.0 mg, 81 μmol) was reacted with aniline **28b** (18.0 mg, 77 μmol) using general method **16** to afford the title compound **47** as a yellow oil (2 mg, 5%). LCMS purity >95%, ret. time 1.12 mins; HRMS (ESI +ve): found $[M+H]^+$ 507.3426, $[C_{29}H_{42}N_6O_2]^+$ requires 507.3442;

ν_{\max} (thin film, cm^{-1}): 3423 (w, N-H), 1653 (C=O); δ_{H} (CDCl_3 , 500 MHz): 8.05 (1H, d, J = 8.2 Hz, H9), 8.01 (1H, s, NH), 7.51 (1H, s, H6), 6.81 (1H, dd, J = 8.2, 1.6 Hz, H10), 6.76 (1H, d, J = 1.6 Hz, H12), 4.09 (2H, q, J = 6.9 Hz, OCH_2CH_3), 3.82 – 3.75 (1H, m, H3), 3.62 – 3.54 (2H, m, H16), 3.30 (3H, s, CONCH_3), 2.77 – 2.62 (3H, m, H14 & H16), 2.56 – 2.50 (1H, m, H2), 2.45 – 2.30 (3H, m, 1 x H2 & 2 x H15), 2.25 – 2.18 (1H, m, CHHCH_3), 2.02 (2H, d, J = 13.2 Hz, H15), 1.86 – 1.75 (3H, m, CHHCH_3 & H2), 1.70 – 1.60 (5H, m, CCH_3 & H1), 1.56 – 1.48 (2H, m, H1), 1.45 (3H, t, J = 6.9 Hz, OCH_2CH_3), 0.84 (3H, t, J = 7.4 Hz, CH_2CH_3); δ_{C} (CDCl_3 , 126 MHz): 166.1 (CONCH_3), 156.2 (C7), 150.5 (C4), 146.8 (C13), 137.4 (C11), 133.6 (C6), 128.3 (C8), 119.1 (C9), 117.0 (C10), 114.7 (C5), 109.4 (C12), 67.6 ($\text{C}(\text{CH}_3)(\text{CH}_2\text{CH}_3)$), 64.3 (OCH_2CH_3), 57.5 (C3), 54.6 (C16), 43.5 (NCH_3), 40.0 (C14), 32.4 (C15), 28.2 (CONCH_3), 28.0 (C2), 26.1 (CCH_3), 25.5 (CH_2CH_3), 25.4 (C1), 14.8 (OCH_2CH_3), 8.8 (CH_2CH_3).

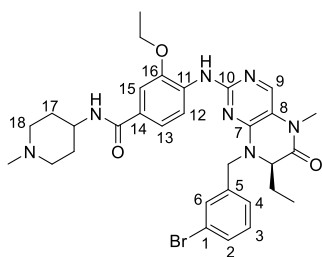
8-Cyclopentyl-2-((2-ethoxy-4-(1-methylpiperidin-4-yl)phenyl)amino)-5-methyl-5,8-dihydro-6H-spiro(cyclopropane-1,7-pteridin)-6-one, 48



Dihydropteridinone **6h** (33 mg, 111 μ mol) was reacted with aniline **28b** (25 mg, 106 μ mol) using general method **16** to afford the title compound **48** as a brown solid (4 mg, 7%). LCMS purity >95%, ret. time 1.10 mins; HRMS (ESI +ve): found $[M+H]^+$ 493.3112, $[C_{28}H_{39}N_6O_2]^+$ requires 491.3129;

m.p.: 120 – 122 °C; ν_{\max} (thin film, cm^{-1}): 3424 (w, N-H), 1667 (C=O); δ_{H} (CDCl_3 , 500 MHz): 8.29 (1H, d, J = 8.2 Hz, H9), 7.73 (1H, s, H6), 7.43 (1H, s, NH), 6.79 (1H, dd, J = 8.2, 1.6 Hz, H10), 6.75 (1H, d, J = 1.6 Hz, H12), 4.11 (2H, q, J = 6.9 Hz, OCH_2CH_3), 3.96 (1H, quin., J = 9.1 Hz, H3), 3.41 (2H, d, J = 11.0 Hz, H16), 3.30 (3H, s, CONCH_3), 2.61 (3H, s, NCH_3), 2.60 – 2.47 (3H, m, H14 & 2 x H16), 2.18 – 2.05 (4H, m, 2 x H2 & 2 x H15), 1.98 – 1.85 (4H, m, 2 x H1 & 2 x H15), 1.80 – 1.72 (2H, m, H2), 1.65 – 1.55 (2H, m, H1), 1.50 – 1.45 (5H, m, $\text{C}(\text{CH}_2)(\text{C}'\text{H}_2)^a$ & OCH_2CH_3), 1.23 – 1.19 (2H, m, $\text{C}(\text{CH}_2)(\text{C}'\text{H}_2)$); δ_{C} (CDCl_3 , 126 MHz): 165.9 (CONCH_3), 155.1 (C7), 154.7 (C4), 147.3 (C13), 138.7 (C6), 137.2 (C8), 128.5 (C11), 118.7 (C10), 118.0 (C9), 117.3 (C5), 109.4 (C12), 64.3 (OCH_2CH_3), 58.4 (C3), 55.0 (C16), 44.2 (NCH_3), 43.4 ($\text{C}(\text{CH}_2)_2$), 31.4 (C15), 28.9 (C2 & CONCH_3), 24.8 (C1), 14.9 (OCH_2CH_3), 12.9 ($\text{C}(\text{CH}_2)_2$)

(R)-4-((8-(3-Bromobenzyl)-7-ethyl-5-methyl-6-oxo-5,6,7,8-tetrahydropteridin-2-yl)amino)-3-ethoxy-N-(1-methylpiperidin-4-yl)benzamide, 49

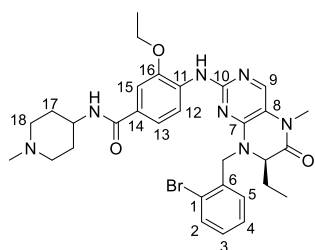


Dihydropteridinone **6i** (65.0 mg, 164 μ mol) was reacted with aniline **20e** (45.6 mg, 164 μ mol) using general method **16** to afford the title compound **49** as a white solid (55.0 mg, 53%). LCMS purity >95%, ret. time 1.08 mins; HRMS (ESI +ve): found $[M+H]^+$ 622.2302, $[C_{31}H_{39}\text{BrN}_7\text{O}_3]^+$ requires 636.2298; m.p.: 212 – 214 °C;

ν_{\max} (thin film, cm^{-1}): 3415 (w, N-H), 3311 (w, CON-H), 1664 (C=O), 1630 (C=O); $[\alpha]_D^{22.1}$: +5.1° (c 1.0, MeOH); δ_{H} (CDCl_3 , 500 MHz): 8.23 (1H, d, J = 8.5 Hz, H12), 7.74 (1H, s, H9), 7.63 (1H, s, ArNH), 7.50 (1H, t, J = 1.6 Hz, H6), 7.44 (1H, dt, J = 7.6, 1.6 Hz, H2), 7.42 (1H, d, J = 1.9 Hz, H15), 7.28 – 7.20 (2H, m, H3 & H4), 7.14 (1H, dd, J = 8.5, 1.9 Hz, H13), 5.96 (1H, d, J = 7.9 Hz, CONH), 5.51 (1H, d, J = 15.8 Hz, ArCHH), 4.23 – 4.16 (4H, m, OCH_2CH_3 , ArCHH & CHCH_2CH_3), 4.04 – 3.94 (1H, m, NHCH), 3.38 (3H, s, CONCH_3), 2.76 – 2.67 (2H, m, H18), 2.31 (3H, s, NCH_3), 2.17 (2H, t, J = 10.9 Hz, H18), 2.09 – 2.01 (2H, m, H17), 2.00 – 1.93 (1H, m, CHCHHCH_3), 1.89 – 1.80 (1H, m, CHCHHCH_3), 1.63 – 1.58 (2H, m, H17), 1.49 (3H, t, J = 7.1 Hz,

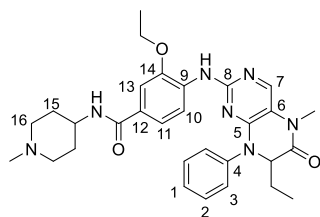
OCH₂CH₃), 0.87 (3H, t, J = 7.4 Hz, CHCH₂CH₃); δ_c (CDCl₃, 126 MHz): 166.5 (CONH), 163.3 (CONCH₃), 155.2 (C10), 151.8 (C7), 146.6 (C16), 138.7 (C5), 138.5 (C9), 132.8 (C11), 131.0 (C2), 130.7 (C6), 130.5 (C3), 126.7 (C14), 126.1 (C4), 122.9 (C1), 118.5 (C13), 116.1 (C12), 115.3 (C8), 110.1 (C15), 64.5 (OCH₂CH₃), 61.4 (CHCH₂CH₃), 54.6 (C18), 47.7 (ArCH₂), 46.3 (NHCH), 46.2 (NCH₃), 32.5 (C17), 28.2 (CONCH₃), 24.9 (CHCH₂CH₃), 14.9 (OCH₂CH₃), 8.7 (CHCH₂CH₃)

(*R*)-4-((8-(2-Bromobenzyl)-7-ethyl-5-methyl-6-oxo-5,6,7,8-tetrahydropteridin-2-yl)amino)-3-ethoxy-*N*-(1-methylpiperidin-4-yl)benzamide, 50



Dihydropteridinone **6j** (31 mg, 80 μ mol) was reacted with aniline **20e** (21 mg, 70 μ mol) using general method **16** to afford the title compound **50** as a white solid (5 mg, 10%). LCMS purity >95%, ret. time 1.27 mins; HRMS (ESI +ve): found $[M+H]^+$ 638.2242, $[C_{31}H_{39}BrN_7O_3]^+$ requires 636.2298; m.p.: 166 – 168 °C; ν_{max} (thin film, cm⁻¹): 3411 (w, N-H), 2964 (w, CON-H), 1663 (C=O), 1589 (C=O); $[\alpha]_D^{21.8}$: -15.9° (c 1.0, MeOH); δ_H (CDCl₃, 500 MHz): 8.34 (1H, d, J = 8.5 Hz, H12), 7.76 (1H, s, PhNH), 7.74 (1H, s, H9), 7.63 (1H, dd, J = 7.6, 1.3 Hz, H2), 7.41 (1H, d, J = 1.9 Hz, H15), 7.33 – 7.26 (3H, m, H4, H5 & H13), 7.21 – 7.16 (1H, m, H3), 6.67 (1H, d, J = 8.2 Hz, CONH), 5.66 (1H, d, J = 15.8 Hz, ArCHH), 4.34 (1H, d, J = 15.8 Hz, ArCHH), 4.30 – 4.22 (1H, m, NHCH), 4.20 (2H, q, J = 7.0 Hz, OCH₂CH₃) 4.16 (1H, dd, J = 6.6, 3.8 Hz, CHCH₂CH₃), 3.52 (2H, d, J = 11.4 Hz, H18), 3.38 (3H, s, CONCH₃), 2.82 – 2.75 (2H, m, H18), 2.76 (3H, s, NCH₃), 2.24 – 2.12 (4H, m, H17), 2.05 – 1.96 (1H, m, CHCHHCH₃), 1.95 – 1.86 (1H, m, CHCHHCH₃), 1.50 (3H, t, J = 7.0 Hz, OCH₂CH₃), 0.91 (3H, t, J = 7.4 Hz, CHCH₂CH₃); δ_c (CDCl₃, 126 MHz): 166.6 (CONH), 163.4 (CONCH₃), 155.0 (C10), 151.9 (C9), 146.5 (C16), 137.8 (C9), 134.9 (C6), 133.3 (C2), 133.1 (C11), 129.5 (C3), 129.4 (C5), 127.9 (C4), 125.7 (C14), 123.7 (C1), 119.7 (C13), 116.4 (C12), 115.4 (C8), 109.7 (C15), 64.5 (OCH₂CH₃), 61.2 (CHCH₂CH₃), 53.9 (C18), 48.1 (ArCH₂), 44.3 (NHCH), 43.6 (NCH₃), 29.1 (C17), 28.2 (CONCH₃), 25.3 (CHCH₂CH₃), 14.9 (OCH₂CH₃), 9.0 (CHCH₂CH₃)

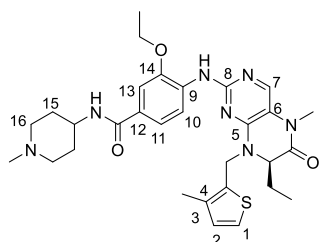
3-Ethoxy-4-((7-ethyl-5-methyl-6-oxo-8-phenyl-5,6,7,8-tetrahydropteridin-2-yl)amino)-*N*-(1-methylpiperidin-4-yl)benzamide, 51



Dihydropteridinone **6v** (30 mg, 99 μ mol) was reacted with aniline **20e** (28 mg, 99 μ mol) using general method **16** to afford the title compound **51** as a white solid (19 mg, 35%). LCMS purity >95%, ret. time 1.22 mins; HRMS (ESI +ve): found $[M+H]^+$ 544.3030, $[C_{30}H_{38}N_7O_3]^+$ requires 544.3036;

m.p.: 136 – 139 °C; ν_{\max} (thin film, cm^{-1}): 3417 (w, N-H), 2971 (w, CON-H), 1667 (C=O), 1587 (C=O); δ_{H} (CDCl_3 , 500 MHz): 7.87 (1H, d, J = 8.5 Hz, H10), 7.78 (1H, s, H7), 7.74 (1H, s, ArNH), 7.57 – 7.52 (2H, m, H2), 7.47 (1H, t, J = 7.3 Hz, H1), 7.42 – 7.38 (2H, m, H3), 7.33 (1H, d, J = 1.3 Hz, H13), 7.01 (1H, dd, J = 8.5, 1.3 Hz, H11), 6.80 (1H, d, J = 7.9 Hz, CONH), 4.66 (1H, dd, J = 6.2, 3.6 Hz, CHCH_2CH_3), 4.28 – 4.18 (1H, m, NHCH), 4.13 (2H, q, J = 6.9 Hz, OCH_2CH_3), 3.51 (2H, d, J = 11.0 Hz, H16), 3.41 (3H, s, CONCH_3), 2.81 – 2.73 (2H, m, H16), 2.74 (3H, s, NCH_3), 2.24 – 2.01 (5H, m, CHCH_2CH_3 & H14), 1.82 – 1.72 (1H, m, CHCH_2CH_3), 1.44 (3H, t, J = 6.9 Hz, OCH_2CH_3), 0.95 (3H, t, J = 7.4 Hz, CHCH_2CH_3); δ_{C} (CDCl_3 , 126 MHz): 166.9 (CONH), 163.3 (CONCH_3), 154.7 (C8), 151.5 (C5), 146.1 (C14), 140.1 (C4), 138.8 (C7), 133.1 (C9), 129.6 (C2), 127.8 (C3), 127.7 (C1), 125.4 (C12), 119.6 (C11), 116.1 (C10), 115.0 (C6), 109.5 (C13), 64.5 (OCH_2), 64.4 (CHCH_2CH_3), 53.9 (C16), 44.3 (NHCH), 43.6 (NCH_3), 29.1 (C15), 28.2 (CONCH_3), 25.5 (CHCH_2CH_3), 14.8 (OCH_2CH_3), 8.5 (CHCH_2CH_3)

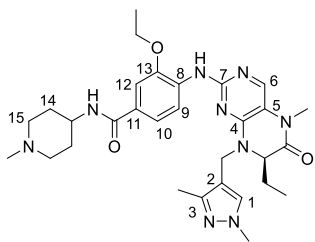
(*R*)-3-Ethoxy-4-((7-ethyl-5-methyl-8-((3-methylthiophen-2-yl)methyl)-6-oxo-5,6,7,8-tetrahydropteridin-2-yl)amino)-*N*-(1-methylpiperidin-4-yl)benzamide, 52



Dihydropteridinone **6k** (37 mg, 110 μmol) was reacted with aniline **20e** (29 mg, 104 μmol) using general method **16** to afford the title compound **52** as a white solid (15 mg, 24%). LCMS purity >95%, ret. time 1.26 mins; HRMS (ESI +ve): found $[\text{M}+\text{H}]^+$ 578.2981, $[\text{C}_{30}\text{H}_{39}\text{N}_7\text{O}_3\text{S}]^+$ requires 578.2908;

m.p.: decomp.; ν_{\max} (thin film, cm^{-1}): 3420 (w, N-H), 2971 (w, CON-H), 1660 (C=O), 1591 (C=O); $[\alpha]_D^{23.7}$: -4.2° (c 1.0, MeOH); δ_{H} (CDCl_3 , 500 MHz): 8.51 (1H, d, J = 8.3 Hz, H10), 7.93 (1H, s, ArNH), 7.71 (1H, s, H7), 7.42 (1H, d, J = 1.2 Hz, H13), 7.37 (1H, dd, J = 8.3, 1.2 Hz, H11), 7.16 (1H, d, J = 5.2 Hz, H1), 6.84 (1H, d, J = 5.2 Hz, H2), 6.77 (1H, d, J = 7.9 Hz, CONH), 5.62 (1H, d, J = 15.5 Hz, ArCHH), 4.39 (1H, d, J = 15.5 Hz, ArCHH), 4.34 – 4.26 (1H, m, NHCH), 4.25 – 4.18 (3H, m, OCH_2CH_3 & CHCH_2CH_3), 3.58 (2H, d, J = 10.1 Hz, H16), 3.34 (3H, s, CONCH_3), 2.95 – 2.85 (2H, m, H16), 2.83 (3H, s, NCH_3), 2.31 – 2.16 (7H, m, ArCH_3 & H15), 2.01 – 1.93 (1H, m, CHCH_2CH_3), 1.91 – 1.81 (1H, m, CHCH_2CH_3), 1.52 (3H, t, J = 7.1 Hz, OCH_2CH_3), 0.86 (3H, t, J = 7.6 Hz, CHCH_2CH_3); δ_{C} (CDCl_3 , 126 MHz): 166.9 (CONH), 163.3 (CONCH_3), 154.8 (C8), 151.6 (C5), 146.7 (C14), 137.2 (C7), 136.2 (C4), 133.2 (C9), 130.1 (C2), 125.7 (C12), 124.4 (C1), 119.8 (C11), 116.7 (C10), 115.5 (C6), 109.8 (C13), 64.6 (OCH_2CH_3), 60.2 (CHCH_2CH_3), 54.2 (C16), 44.2 (NHCH), 43.7 (NCH_3), 40.7 (C5), 29.0 (C15), 28.1 (CONCH_3), 24.9 (CHCH_2CH_3), 14.9 (OCH_2CH_3), 14.0 (CHCH_2CH_3)

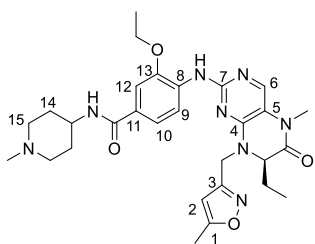
(*R*)-4-((8-(1,3-Dimethyl-1*H*-pyrazol-4-yl)methyl)-7-ethyl-5-methyl-6-oxo-5,6,7,8-tetrahydropteridin-2-yl)amino)-3-ethoxy-*N*-(1-methylpiperidin-4-yl)benzamide, **53**



Dihydropteridinone **6l** (35 mg, 104 μmol) was reacted with aniline **20e** (13 mg, 136 μmol) using general method **16** to afford the title compound **53** as a colourless oil (17 mg, 29%). LCMS purity >95%, ret. time 1.11 mins; HRMS (ESI +ve): found $[\text{M}+\text{H}]^+$ 576.3388, $[\text{C}_{30}\text{H}_{42}\text{N}_9\text{O}_3]^+$ requires

576.3405; ν_{max} (thin film, cm^{-1}): 3418 (w, N-H), 2924 (w, CON-H), 1658 (C=O), 1591 (C=O); $[\alpha]_D^{23.8}$: +18.0° (*c* 1.0, MeOH); δ_{H} (CDCl_3 , 500 MHz): 8.43 (1H, d, J = 8.0 Hz, H9), 7.81 (1H, s, ArNH), 7.67 (1H, s, H7), 7.44 (1H, d, J = 1.3 Hz, H12), 7.37 (1H, dd, J = 8.0, 1.3 Hz, H10), 7.26 (1H, s, H1), 7.05 (1H, s, CONH), 5.32 (1H, d, J = 15.1 Hz, ArHH), 4.31 - 4.24 (1H, m, NHCH), 4.24 - 4.16 (3H, m, OCH_2CH_3 & CHCH_2CH_3), 4.06 (1H, d, J = 15.1 Hz, ArHH), 3.78 (3H, s, ArNCH₃), 3.54 (2H, d, J = 10.4 Hz, H15), 3.32 (3H, s, CONCH₃), 2.90 - 2.75 (5H, m, H15 & NCH₃), 2.30 - 2.12 (7H, m, ArCH₃ & H14), 2.00 - 1.90 (1H, m, CHCH_2CH_3), 1.86 - 1.77 (1H, m, CHCH_2CH_3), 1.49 (3H, t, J = 6.5 Hz, OCH_2CH_3), 0.84 (3H, t, J = 7.4 Hz, CHCH_2CH_3); δ_{C} (CDCl_3 , 126 MHz): 166.9 (CONH), 163.4 (CONCH₃), 154.9 (C7), 151.7 (C4), 147.2 (C3), 146.6 (C13), 137.3 (C6), 133.2 (C10), 130.7 (C1), 125.8 (C11), 119.7 (C10), 116.4 (C9), 115.4 (C5), 113.1 (C2), 109.9 (C12), 64.5 (OCH_2CH_3), 60.0 (CHCH_2CH_3), 54.1 (C16^a), 44.2 (NHCH), 43.6 (NCH₃), 38.7 (ArNCH₃), 38.2 (C4), 29.0 (C14), 28.1 (CONCH₃), 24.8 (CHCH_2CH_3), 14.9 (OCH_2CH_3), 11.9 (ArCH₃), 8.8 (CHCH_2CH_3)

(*R*)-3-Ethoxy-4-((7-ethyl-5-methyl-8-((5-methylisoxazol-3-yl)methyl)-6-oxo-5,6,7,8-tetrahydropteridin-2-yl)amino)-*N*-(1-methylpiperidin-4-yl)benzamide, **54**

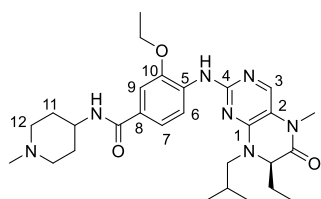


Dihydropteridinone **6m** (30 mg, 93 μmol) was reacted with aniline **20e** (25 mg, 89 μmol) using general method **16** to afford the title compound **54** as a yellow solid (2 mg, 3%). LCMS purity >95%, ret. time 1.12 mins; HRMS (ESI +ve): found $[\text{M}+\text{H}]^+$ 563.3077, $[\text{C}_{29}\text{H}_{39}\text{N}_8\text{O}_4]^+$ requires 563.3089;

m.p.: decomp.; ν_{max} (thin film, cm^{-1}): 3387 (w, N-H), 2963 (w, CON-H), 1660 (C=O), 1585 (C=O); $[\alpha]_D^{23.6}$: +38.8° (*c* 1.0, MeOH); δ_{H} (CDCl_3 , 500 MHz): 8.41 (1H, d, J = 8.6 Hz, H9), 8.17 (1H, s, ArNH), 7.71 (1H, s, H6), 7.40 (1H, d, J = 1.7 Hz, H12), 7.36 (1H, d, J = 8.6, 1.7 Hz, H10), 6.74 (1H, d, J = 7.3 Hz, CONH), 5.99 (1H, s, H2), 5.40 (1H, d, J = 15.8 Hz, ArCHH), 4.40 (1H, d, J = 15.8 Hz, ArCHH), 4.35 - 4.27 (1H, m, NHCH), 4.26 (1H, dd, J = 6.3, 3.5 Hz, CHCH_2CH_3), 4.20 (2H, q, J = 7.0 Hz, OCH_2CH_3), 3.61 (2H, d, J = 9.5 Hz, H15), 3.34 (3H, s, CONCH₃), 2.97 - 2.89 (2H, m, H15), 2.86 (3H, s, NCH₃), 2.40 (3H, s, ArCH₃), 2.31 - 2.19 (4H, m, H14), 2.05 - 1.96

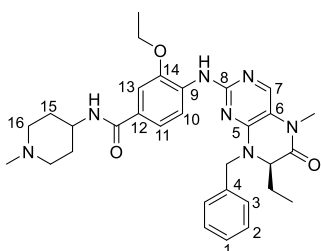
(1H, m, CHCH₂HCH₃), 1.93 – 1.85 (1H, m, CHCH₂HCH₃), 1.50 (3H, t, *J* = 7.0 Hz, OCH₂CH₃), 0.83 (3H, t, *J* = 7.6 Hz, CHCH₂CH₃); δ_c (CDCl₃, 126 MHz): 170.6 (C1), 166.9 (CONH), 163.1 (CONCH₃), 159.6 (C3), 154.7 (C10), 151.6 (C7), 146.7 (C14), 135.6 (C6), 133.0 (C4), 125.8 (C11), 119.7 (C10), 116.7 (C9), 115.5 (C5), 109.8 (C12), 101.2 (C2), 64.6 (OCH₂CH₃), 61.4 (CHCH₂CH₃), 54.5 (C15), 44.2 (NHCH), 43.8 (NCH₃), 40.2 (ArCH₂), 29.1 (C14), 28.2 (CONCH₃), 24.8 (CHCH₂CH₃), 14.8 (OCH₂CH₃), 12.4 (ArCH₃), 8.8 (CHCH₂CH₃)

(*R*)-3-Ethoxy-4-((7-ethyl-8-isobutyl-5-methyl-6-oxo-5,6,7,8-tetrahydropteridin-2-yl)amino)-*N*-(1-methylpiperidin-4-yl)benzamide, 55



Dihydropteridinone **6n** (25 mg, 88 μ mol) was reacted with aniline **20e** (23 mg, 84 μ mol) using general method **16** to afford the title compound **55** as a yellow solid (7 mg, 16%). LCMS purity >95%, ret. time 1.16 mins; HRMS (ESI +ve): found $[M+H]^+$ 524.3362, $[C_{28}H_{42}N_7O_3]^+$ requires 524.3344; m.p.: decomp.; ν_{max} (thin film, cm⁻¹): 3412 (w, N-H), 2958 (w, CON-H), 1660 (C=O), 1584 (C=O); $[\alpha]_D^{23.3}$: -22.9° (c 1.0, MeOH); δ_H (CDCl₃, 500 MHz): 8.44 (1H, d, *J* = 8.2 Hz, H6), 8.11 (1H, s, ArNH), 7.64 (1H, s, H3), 7.46 – 7.40 (2H, m, H7 & H9), 7.01 (1H, d, *J* = 6.9 Hz, CONH), 4.36 – 4.25 (1H, m, NHCH), 4.25 – 4.15 (4H, m, OCH₂CH₃, NCH₂H & CHCH₂CH₃), 3.58 (2H, d, *J* = 6.9 Hz, H12), 3.34 (3H, s, CONCH₃), 2.97 – 2.85 (2H, m, H12), 2.83 (3H, s, NCH₃), 2.71 – 2.64 (1H, m, NCH₂H), 2.34 – 2.14 (5H, m, CH(CH₃)₂ & H11), 1.97 – 1.88 (1H, m, CHCH₂HCH₃), 1.87 – 1.78 (1H, m, CHCH₂HCH₃), 1.49 (3H, t, *J* = 6.6 Hz, OCH₂CH₃), 0.99 (6H, t, *J* = 6.3 Hz, CH(CH₃)₂), 0.86 (3H, t, *J* = 7.3 Hz, CHCH₂CH₃); δ_c (CDCl₃, 126 MHz): 165.8 (CONH), 163.3 (CONCH₃), 154.3 (C4), 152.2 (C1), 146.9 (C10), 135.6 (C3), 133.0 (C5), 126.0 (C8), 119.6 (C7), 116.8 (C6), 115.4 (C2), 110.0 (C9), 64.6 (OCH₂CH₃), 63.1 (CHCH₂CH₃), 54.3 (C12), 53.3 (CH₂CH(CH₃)₂), 44.2 (C11), 43.7 (NCH₃), 28.9 (C11), 28.2 (CONCH₃), 26.6 (CH(CH₃)₂), 25.5 (CHCH₂CH₃), 20.3 (CH(CH₃)₂), 14.8 (OCH₂CH₃), 9.1 (CHCH₂CH₃)

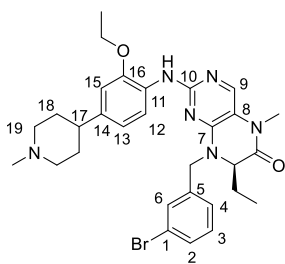
(*R*)-4-((8-Benzyl-7-ethyl-5-methyl-6-oxo-5,6,7,8-tetrahydropteridin-2-yl)amino)-3-ethoxy-*N*-(1-methylpiperidin-4-yl)benzamide, 56



Compound **49** (10 mg, 16 μ mol) was subjected to general method **17** to afford the title compound **56** as a pale yellow solid (4 mg, 46%). LCMS purity >95%, ret. time 1.20 mins; HRMS (ESI +ve): found $[M+H]^+$ 558.3161, $[C_{31}H_{40}N_7O_3]^+$ requires 558.3193; m.p.: 158 – 160 °C; ν_{max} (thin film, cm⁻¹

¹): 3416 (w, CON-H), 2932 (w, N-H), 1668 (C=O), 1592 (C=O); $[\alpha]_D^{21.9}$: -9.7° (c 1.0, MeOH); δ_H (CDCl₃, 500 MHz): 8.45 (1H, d, J = 8.5 Hz, H10), 7.75 (1H, s, PhNH), 7.73 (1H, s, H7), 7.42 (1H, d, J = 1.6 Hz, H13), 7.40 – 7.29 (6H, m, H1, H2, H3 & H11), 6.61 (1H, d, J = 8.2 Hz, CONH), 5.66 (1H, d, J = 15.1 Hz, ArCHH), 4.28 – 4.19 (4H, m, OCH₂CH₃, ArCHH & NHCH), 4.18 (1H, dd, J = 6.3, 3.5 Hz, CHCH₂CH₃), 3.48 (2H, d, J = 11.7 Hz, H16), 3.37 (3H, s, CONCH₃), 2.80 – 2.72 (2H, m, H16), 2.73 (3H, s, NCH₃), 2.20 – 2.12 (4H, m, H15), 2.01 – 1.92 (1H, m, CHCHHCH₃), 1.91 – 1.82 (1H, m, CHCHHCH₃), 1.51 (3H, t, J = 6.9 Hz, OCH₂CH₃), 0.87 (3H, t, J = 7.9 Hz, CHCH₂CH₃); δ_C (CDCl₃, 126 MHz): 166.8 (CONH), 163.4 (CONCH₃), 155.1 (C8), 152.0 (C5), 146.5 (C14), 137.8 (C7), 135.9 (C4), 133.3 (C9), 129.0 (C2), 128.0 (C1 & C3), 125.7 (C12), 119.6 (C11), 116.4 (C10), 115.4 (C6), 109.8 (C13), 64.5 (OCH₂CH₃), 60.6 (CHCH₂CH₃), 53.8 (C16), 47.8 (ArCH₂), 44.4 (NHCH), 43.7 (NCH₃), 29.3 (C15), 28.1 (CONCH₃), 24.7 (CHCH₂CH₃), 14.9 (OCH₂CH₃), 8.8 (CHCH₂CH₃)

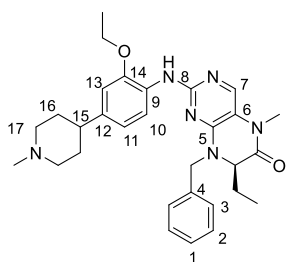
(*R*)-8-(3-Bromobenzyl)-2-((2-ethoxy-4-(1-methylpiperidin-4-yl)phenyl)amino)-7-ethyl-5-methyl-7,8-dihydropteridin-6(5*H*)-one, 57



Dihydropteridinone **6i** (100 mg, 252 μ mol) was reacted with aniline **28b** (56.3 mg, 240 μ mol) using general method **16** to afford the title compound **57** as a white solid (28.0 mg, 19%). LCMS purity >95%, ret. time 1.21 mins; HRMS (ESI +ve): found $[M+H]^+$ 593.2209, $[C_{30}H_{38}BrN_6O_2]^+$ requires 593.2234; m.p.: 94 – 97°C; ν_{max} (thin film, cm⁻¹): 3415 (w, N-H), 1664

(C=O); $[\alpha]_D^{24.1}$: +1.7° (c 1.0, MeOH); δ_H (CDCl₃, 500 MHz): 8.13 (1H, s, PhNH), 7.96 (1H, d, J = 8.2 Hz, H12), 7.68 (1H, s, H9), 7.46 – 7.42 (2H, m, H2 & H6), 7.23 – 7.20 (2H, m, H3 & H4), 6.74 – 6.70 (2H, m, H13 & H15), 5.51 (1H, d, J = 15.5 Hz, ArCHH), 4.19 – 4.13 (2H, m, ArCHU & CHCH₂CH₃), 4.11 (2H, q, J = 6.9 Hz, OCH₂CH₃), 3.70 – 3.61 (2H, m, H19), 3.35 (3H, s, CONCH₃), 2.85 – 2.75 (5H, m, H19 & NCH₃), 2.70 – 2.61 (1H, m, H17), 2.28 (2H, q, J = 12.3 Hz, H18), 2.05 – 1.94 (3H, m, H18 & CHCHHCH₃), 1.90 – 1.80 (1H, m, CHCHHCH₃), 1.47 (3H, t, J = 6.9 Hz, OCH₂CH₃), 0.85 (3H, t, J = 7.6 Hz, CHCH₂CH₃); δ_C (CDCl₃, 126 MHz): 163.1 (CONCH₃), 154.6 (C10), 152.1 (C7), 148.3 (C16), 138.2 (C6), 137.0 (C14), 135.5 (C9), 131.2 (C2), 130.9 (C6), 130.5 (C3), 127.8 (C12), 126.4 (C4), 123.0 (C1), 119.5 (C12), 118.5 (C13), 114.7 (C8), 109.7 (C15), 64.5 (OCH₂CH₃), 61.1 (CHCH₂CH₃), 55.1 (C19), 47.7 (ArCH₂), 43.8 (NCH₃), 39.9 (C17), 30.5 (C18), 28.2 (CONCH₃), 25.0 (CHCH₂CH₃), 14.9 (OCH₂CH₃), 8.7 (CHCH₂CH₃)

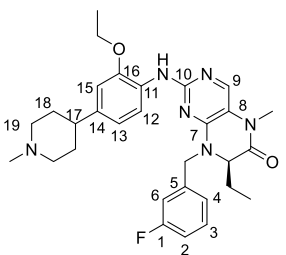
(*R*)-8-Benzyl-2-((2-ethoxy-4-(1-methylpiperidin-4-yl)phenyl)amino)-7-ethyl-5-methyl-7,8-dihydropteridin-6(5*H*)-one, 58



Compound **57** (14 mg, 24 μ mol) was subjected to general method **17** to afford the title compound **58** as a yellow solid (5 mg, 41%). LCMS purity >95%, ret. time 1.12 mins; HRMS (ESI +ve): found $[M+H]^+$ 515.3114, $[C_{30}H_{39}N_6O_2]^+$ requires 515.3129; m.p.: 65 – 68 $^{\circ}$ C; ν_{\max} (thin film, cm^{-1}): 3420 (w, CON-H), 1666 (C=O), $[\alpha]_D^{21.9}$: +24.2 $^{\circ}$ (c 1.0, MeOH); δ_H

(CDCl_3 , 500 MHz): 8.22 (1H, d, J = 8.6 Hz, H10), 7.68 (1H, s, H7), 7.58 (1H, s, PhNH), 7.37 – 7.29 (5H, m, H1, H2 & H3), 6.72 (1H, d, J = 1.6 Hz, H13), 6.70 (1H, dd, J = 8.6, 1.6 Hz, H11), 5.62 (1H, d, J = 15.1 Hz, PhCHH), 4.18 – 4.15 (3H, m, PhCHH & CHCH₂CH₃), 4.11 (2H, q, J = 7.2 Hz, OCH₂CH₃), 3.64 (2H, d, J = 10.4 Hz, H17), 3.34 (3H, s, CONCH₃), 2.73 (3H, s, NCH₃), 2.73 – 2.58 (3H, m, H15 & H17), 2.25 – 2.15 (2H, m, H16), 2.02 – 1.92 (3H, m, H16 & CHCH₂CH₃), 1.90 – 1.81 (1H, m, CHCH₂CH₃), 1.48 (3H, t, J = 6.9 Hz, OCH₂CH₃), 0.85 (3H, t, J = 7.4 Hz, CHCH₂CH₃); δ_C (CDCl_3 , 126 MHz): 163.4 (CONCH₃), 155.6 (C8), 152.1 (C5), 147.4 (C14), 137.8 (C7), 136.0 (C4), 131.6 (C9), 128.9 (C2), 128.5 (C12), 128.1 (C3), 127.9 (C1), 118.7 (C11), 118.2 (C10), 114.7 (C6), 109.3 (C13), 64.4 (OCH₂CH₃), 60.5 (CHCH₂CH₃), 53.4 (C17), 47.8 (PhCH₂), 43.6 (NCH₃), 39.5 (C15), 30.6 (C16), 28.1 (CONCH₃), 24.7 (CHCH₂CH₃), 15.0 (OCH₂CH₃), 8.8 (CHCH₂CH₃)

(*R*)-2-((2-Ethoxy-4-(1-methylpiperidin-4-yl)phenyl)amino)-7-ethyl-8-(3-fluorobenzyl)-5-methyl-7,8-dihydropteridin-6(5*H*)-one, 59

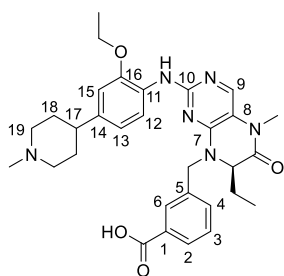


Dihydropteridinone **6o** (40 mg, 120 μ mol) was reacted with aniline **28b** (27 mg, 114 μ mol) using general method **16** to afford the title compound **59** as a yellow solid (18 mg, 28%). LCMS purity >95%, ret. time 1.11 mins; HRMS (ESI +ve): found $[M+H]^+$ 533.3013, $[C_{30}H_{38}FN_6O_2]^+$ requires 533.3035; m.p.: 60 – 63 $^{\circ}$ C; ν_{\max} (thin film, cm^{-1}): 3421 (w, N-H), 1665

(C=O); $[\alpha]_D^{23.5}$: +20.8 $^{\circ}$ (c 1.0, MeOH); δ_H (CDCl_3 , 500 MHz): 8.14 (1H, d, J = 8.2 Hz, H12), 7.70 (1H, s, H9), 7.61 (1H, s, NH), 7.33 (1H, td, J = 7.9, 6.0 Hz, H3), 7.11 (1H, d, J = 7.9 Hz, H4), 7.05 – 6.98 (2H, m, H2 & H6), 6.73 – 6.70 (2H, m, H13 & H15), 5.58 (1H, d, J = 15.5 Hz, ArCHH), 4.18 (1H, d, J = 15.5 Hz, ArCHH), 4.15 (1H, dd, J = 6.3, 3.8 Hz, CHCH₂CH₃), 4.12 (2H, q, J = 6.9 Hz, OCH₂CH₃), 3.59 (2H, d, J = 9.5 Hz, H19), 3.36 (3H, s, CONCH₃), 2.74 (3H, s, NCH₃), 2.75 – 2.60 (3H, m, H17 & H19), 2.20 (2H, m, H18), 2.02 – 1.92 (3H, m, 2 x H18 & CHCH₂CH₃), 1.88 – 1.79 (1H, m, CHCH₂CH₃), 1.48 (3H, t, J = 6.9 Hz, OCH₂CH₃), 0.87 (3H, t, J = 7.6 Hz,

CHCH₂CH₃); δ_C (CDCl₃, 126 MHz): 163.2 (CONCH₃), 163.1 (d, J_{C-F} = 246 Hz, C1), 155.5 (C10), 152.0 (C7), 147.5 (C16), 138.8 (d, J_{C-F} = 6 Hz, C5), 137.8 (C9), 136.5 (C14), 130.4 (d, J_{C-F} = 8 Hz, C3), 128.4 (C11), 123.4 (d, J_{C-F} = 3 Hz, C4), 118.6 (C13), 118.4 (C12), 114.9 (d, J_{C-F} = 24 Hz, C2/C6), 114.8 (C8), 114.7 (d, J_{C-F} = 24 Hz, C2/C6), 109.4 (C15), 64.4 (OCH₂CH₃), 61.0 (CHCH₂CH₃), 54.6 (C19), 47.6 (ArCH₂), 43.6 (NCH₃), 40.1 (C17), 30.5 (C18), 28.1 (CONCH₃), 24.8 (CHCH₂CH₃), 14.9 (OCH₂CH₃), 8.8 (CHCH₂CH₃); $\delta_{F\{H\}}$ (CDCl₃, 471 MHz): -112.3

(R)-3-((2-((2-Ethoxy-4-(1-methylpiperidin-4-yl)phenyl)amino)-7-ethyl-5-methyl-6-oxo-6,7-dihydropteridin-8(5H)-yl)methyl)benzoic acid, 60

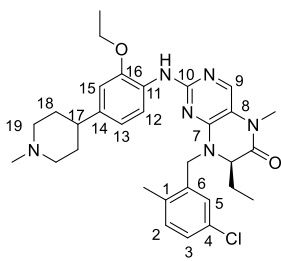


Dihydropteridinone **6p** (40 mg, 107 μ mol) was reacted with aniline **28b** (14 mg, 139 μ mol) using general method **16** to afford the title compound **60** as a brown solid (7 mg, 12%). LCMS purity >95%, ret. time 1.08 mins; HRMS (ESI +ve): found $[M+H]^+$ 559.3020, $[C_{31}H_{39}N_6O_4]^+$ requires 559.3027; m.p.: 186 – 189 °C; ν_{max} (thin film, cm⁻¹): 3425 (w, N-H), 1676

(C=O); $[\alpha]_D^{23.3}$: -42.9° (c 1.0, MeOH); δ_H (CDCl₃, 500 MHz): 8.50 (1H, s, COOH), 8.18 (1H, s, H6), 8.00 (1H, d, J = 6.6 Hz, H2), 7.89 (1H, s, NH), 7.65 (1H, s, H9), 7.50 (1H, d, J = 8.2 Hz, H12), 7.42 – 7.36 (2H, m, H3 & H4), 6.84 (1H, d, J = 8.2 Hz, H13), 6.59 (1H, s, H15), 5.25 (1H, d, J = 16.1 Hz, ArCHH), 4.46 (1H, dd, J = 6.2, 4.3 Hz, CHCH₂CH₃), 4.38 (1H, d, J = 16.1 Hz, ArCHH), 4.07 – 3.99 (2H, m, OCH₂CH₃), 3.73 – 3.64 (2H, m, H19), 3.40 (3H, s, CONCH₃), 2.92 (3H, s, NCH₃), 2.77 (2H, q, J = 12.3 Hz, H19), 2.58 – 2.50 (1H, m, H17), 2.38 (1H, q, J = 12.6 Hz, H18), 2.19 – 2.08 (1H, m, H18) 2.08 – 1.99 (2H, m, H18 & CHCH₂CH₃), 1.95 – 1.86 (2H, m, H18 & CHCH₂CH₃), 1.43 (3H, t, J = 6.9 Hz, OCH₂CH₃), 0.93 (3H, t, J = 7.6 Hz, CHCH₂CH₃); δ_C (CDCl₃, 126 MHz): 166.9 (COOH), 163.3 (CONCH₃), 154.7 (C10), 151.8 (C7), 147.0 (C16), 136.8 (C5), 136.4 (C9 & C14), 135.5 (C1), 129.1 (C2), 128.9 (C4), 128.5 (C3 & C6), 127.6 (C11), 119.2 (C12), 117.4 (C13), 114.7 (C8), 110.9 (C15), 64.8 (CHCH₂CH₃), 64.3 (OCH₂CH₃), 55.2 (C19), 50.1 (ArCH₂), 44.2 (NCH₃), 40.5 (C17), 30.3 (C18), 28.3 (CONCH₃), 26.0 (CHCH₂CH₃), 14.9 (OCH₂CH₃), 9.2 (CHCH₂CH₃)

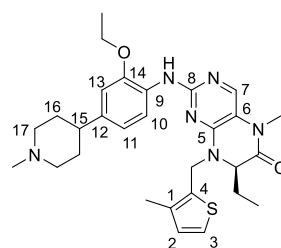
(R)-8-(5-Chloro-2-methylbenzyl)-2-((2-ethoxy-4-(1-methylpiperidin-4-yl)phenyl)amino)-7-ethyl-5-methyl-7,8-dihydropteridin-6(5H)-one, 61

Dihydropteridinone **6q** (40 mg, 110 μ mol) was reacted with aniline **28b** (24 mg, 104 μ mol) using general method **16** to afford the title compound **61** as a brown solid (20 mg, 32%). LCMS purity >95%, ret. time 1.23 mins; HRMS (ESI +ve): found $[M+H]^+$ 563.2876, $[C_{31}H_{40}ClN_6O_2]^+$ requires 563.2896; m.p.: 72 – 75 °C; ν_{max} (thin film, cm⁻¹):



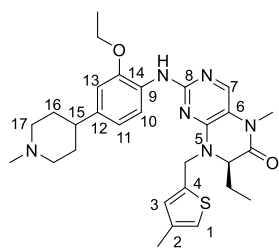
3415 (w, N-H), 1669 (C=O); $[\alpha]_D^{22.2}$: +3.5° (c 1.0, MeOH); δ_H (CDCl₃, 500 MHz): 8.06 (1H, d, J = 8.2 Hz, H12), 7.69 (1H, s, H9), 7.61 (1H, s, NH), 7.21 – 7.14 (3H, m, H2, H3 & H5), 6.72 (1H, s, H15), 6.67 (1H, d, J = 8.2 Hz, H13), 5.59 (1H, d, J = 15.5 Hz, ArCHH), 4.10 (1H, d, J = 15.5 Hz, ArCHH), 4.06 – 4.01 (2H, m, CHCH₂CH₃ & OCH₂CH₃), 3.58 (2H, d, J = 10.1 Hz, H19), 3.35 (3H, s, CONCH₃), 2.76 – 2.66 (5H, m, NCH₃ & 2 x H19), 2.65 – 2.58 (1H, m, H17), 2.26 (3H, s, ArCH₃), 2.24 – 2.13 (2H, m, H18), 2.00 – 1.93 (3H, m, 2 x H18 & CHCH₂CH₃), 1.89 – 1.81 (1H, m, CHCH₂CH₃), 1.46 (3H, t, J = 6.9 Hz, OCH₂CH₃), 0.87 (3H, t, J = 7.4 Hz, CHCH₂CH₃); δ_C (CDCl₃, 126 MHz): 163.3 (COOCH₃), 155.4 (C10), 151.9 (C7), 147.5 (C16), 137.7 (C9), 136.5 (C14), 135.4 (C1/6), 135.0 (C1/6), 132.1 (C2), 131.9 (C4), 128.3 (C11), 128.3 (C3/5), 128.0 (C3/5), 118.5 (C13), 118.3 (C12), 114.8 (C8), 109.4 (C15), 64.3 (OCH₂CH₃), 60.4 (CHCH₂CH₃), 54.6 (C19), 45.7 (ArCH₂), 43.5 (NCH₃), 40.0 (C17), 30.5 (C18), 28.1 (CONCH₃), 24.7 (CHCH₂CH₃), 18.9 (CH₃), 14.9 (OCH₂CH₃), 8.9 (CHCH₂CH₃)

(R)-2-((2-Ethoxy-4-(1-methylpiperidin-4-yl)phenyl)amino)-7-ethyl-5-methyl-8-((3-methylthiophen-2-yl)methyl)-7,8-dihydropteridin-6(5H)-one, 62



Dihydropteridinone **6k** (50 mg, 148 μmol) was reacted with aniline **28b** (19 mg, 141 μmol) using general method **16** to afford the title compound **62** as a yellow solid (9 mg, 11%). LCMS purity >95%, ret. time 1.10 mins; HRMS (ESI +ve): found $[M+H]^+$ 535.2828, $[C_{29}H_{39}N_6O_2S]^+$ requires 535.2850; m.p.: 117 – 119 °C; ν_{max} (thin film, cm⁻¹): 3419 (w, N-H), 1665 (C=O); $[\alpha]_D^{24.0}$: +7.6° (c 1.0, MeOH); δ_H (CDCl₃, 500 MHz): 8.31 (1H, d, J = 8.2 Hz, H10), 7.67 (1H, s, H7), 7.64 (1H, s, NH), 7.15 (1H, d, J = 5.0 Hz, H3), 6.83 (1H, d, J = 5.0 Hz, H2), 6.78 (1H, dd, J = 8.2, 1.6 Hz, H11), 6.73 (1H, d, J = 1.6 Hz, H13), 5.63 (1H, d, J = 15.3 Hz, ArCHH), 4.33 (1H, d, J = 15.3 Hz, ArCHH), 4.19 (1H, dd, J = 6.5, 3.6 Hz, CHCH₂CH₃), 4.13 (2H, q, J = 6.9 Hz, OCH₂CH₃), 3.57 (2H, d, J = 9.1 Hz, H17), 3.32 (3H, s, CONCH₃), 2.76 – 2.60 (6H, m, H15, 2 x H17 & NCH₃), 2.25 (3H, s, ArCH₃), 2.24 – 2.15 (2H, m, H16), 2.02 – 1.91 (3H, m, 2 x H16 & CHCH₂CH₃), 1.88 – 1.79 (1H, m, CHCH₂CH₃), 1.49 (3H, t, J = 6.9 Hz, OCH₂CH₃), 0.85 (3H, t, J = 7.4 Hz, CHCH₂CH₃); δ_C (CDCl₃, 126 MHz): 163.4 (CONCH₃), 155.4 (C8), 151.6 (C5), 147.4 (C14), 137.6 (C7), 136.5 (C12), 136.1 (C4), 131.5 (C1), 130.1 (C2), 128.5 (C9), 124.2 (C3), 118.8 (C11), 118.4 (C10), 114.9 (C6), 109.4 (C14), 64.4 (OCH₂CH₃), 60.1 (CHCH₂CH₃), 54.7 (C17), 45.5 (NCH₃), 40.6 (ArCH₂), 40.1 (C15), 30.5 (C16), 28.1 (CONCH₃), 24.8 (CHCH₂CH₃), 15.0 (OCH₂CH₃), 14.0 (ArCH₃), 8.9 (CHCH₂CH₃)

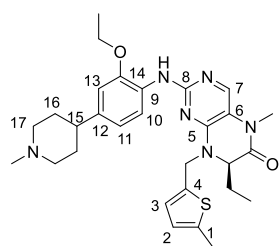
(*R*)-2-((2-Ethoxy-4-(1-methylpiperidin-4-yl)phenyl)amino)-7-ethyl-5-methyl-8-((5-methylthiophen-2-yl)methyl)-7,8-dihydropteridin-6(5*H*)-one, 63



Dihydropteridinone **6r** (55 mg, 163 μmol) was reacted with aniline **28b** (36 mg, 155 μmol) using general method **16** to afford the title compound **63** as a yellow solid (20 mg, 23%). LCMS purity >95%, ret. time 1.17 mins; HRMS (ESI +ve): found $[\text{M}+\text{H}]^+$ 535.2835, $[\text{C}_{29}\text{H}_{39}\text{N}_6\text{O}_2\text{S}]^+$ requires 535.2850;

m.p.: 83 – 86 $^{\circ}\text{C}$; ν_{max} (thin film, cm^{-1}): 3420 (w, N-H), 1665 (C=O); $[\alpha]_D^{23.1}$: +7.6 $^{\circ}$ (c 1.0, MeOH); δ_{H} (CDCl_3 , 500 MHz): 8.33 (1H, d, J = 8.2 Hz, H11), 7.67 (1H, s, H7), 7.57 (1H, s, NH), 6.85 (1H, s, H3), 6.81 (1H, s, H1), 6.78 (1H, dd, J = 8.2, 1.6 Hz, H11), 6.74 (1H, d, J = 1.6 Hz, H13), 5.61 (1H, d, J = 15.3 Hz, ArCHH), 4.34 (1H, d, J = 15.3 Hz, ArCHH), 4.36 (1H, dd, J = 6.0, 3.5 Hz, CHCH₂CH₃) 4.13 (2H, q, J = 6.9 Hz, OCH₂CH₃), 3.54 (2H, d, J = 10.7 Hz, H17), 3.32 (3H, s, CONCH₃), 2.67 (3H, s, NCH₃), 2.73 – 2.59 (3H, m, H15 & 2 x H17), 2.22 (3H, s, ArCH₃), 2.24 – 2.16 (2H, m, H16), 2.01 – 1.92 (3H, m, 2 x H16 & CHCHHCH₃), 1.89 – 1.81 (1H, m, CHCHHCH₃), 1.48 (3H, t, J = 6.9 Hz, OCH₂CH₃), 0.84 (3H, t, J = 7.4 Hz, CHCH₂CH₃); δ_{C} (CDCl_3 , 126 MHz): δ 163.34 (CONCH₃), 155.5 (C8), 151.4 (C5), 147.4 (C14), 138.2 (C4), 137.9 (C7), 137.4 (C2), 136.5 (C14), 129.7 (C3), 128.5 (C9), 121.2 (C1), 118.8 (C11), 118.3 (C9), 114.8 (C6), 109.4 (C13), 64.4 (OCH₂CH₃), 60.3 (CHCH₂CH₃), 54.7 (C17), 43.6 (NCH₃), 42.9 (ArCH₂), 40.2 (C14), 30.8 (C16), 28.1 (CONCH₃), 24.7 (CHCH₂CH₃), 15.7 (ArCH₃), 15.0 (OCH₂CH₃), 8.7 (CHCH₂CH₃)

(*R*)-2-((2-Ethoxy-4-(1-methylpiperidin-4-yl)phenyl)amino)-7-ethyl-5-methyl-8-((5-methylthiophen-2-yl)methyl)-7,8-dihydropteridin-6(5*H*)-one, 64

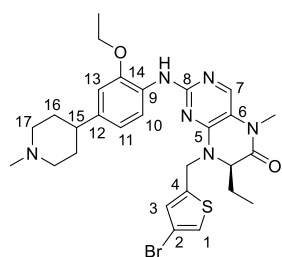


Dihydropteridinone **6s** (45 mg, 134 μmol) was reacted with aniline **28b** (30 mg, 127 μmol) using general method **16** to afford the title compound **64** as a yellow oil (18 mg, 25%). LCMS purity >95%, ret. time 1.16 mins; HRMS (ESI +ve): found $[\text{M}+\text{H}]^+$ 535.2833, $[\text{C}_{29}\text{H}_{39}\text{N}_6\text{O}_2\text{S}]^+$ requires 535.2850;

ν_{max} (thin film, cm^{-1}): 3420 (w, N-H), 1666 (C=O); $[\alpha]_D^{23.1}$: +11.1 $^{\circ}$ (c 1.0, MeOH); δ_{H} (CDCl_3 , 500 MHz): 8.34 (1H, d, J = 8.3 Hz, H10), 7.67 (1H, s, H7), 7.63 (1H, s, NH), 6.83 (1H, d, J = 3.2 Hz, H3), 6.79 (1H, dd, J = 8.3, 1.8 Hz, H11), 6.75 (1H, d, J = 1.8 Hz, H13), 6.6 (1H, d, J = 3.2 Hz, H2), 5.57 (1H, d, J = 15.5 Hz, ArCHH), 4.43 (1H, d, J = 15.5 Hz, ArCHH), 4.26 (1H, dd, J = 6.2, 3.6 Hz, CHCH₂CH₃), 4.14 (2H, q, J = 6.9 Hz, OCH₂CH₃), 3.57 (2H, d, J = 10.1 Hz, H17), 3.32 (3H, s, CONCH₃), 2.73 (3H, s, NCH₃), 2.75 – 2.61 (3H, m, H15 & 2 x H17), 2.44 (3H, s, ArCH₃), 2.20 (2H, qd, J = 12.3, 3.2 Hz, H16), 2.02 – 1.92 (3H, m, 2 x H16 & CHCHHCH₃), 1.89 – 1.80 (1H, m,

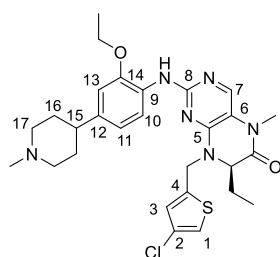
CHCH \underline{H} CH $\underline{3}$), 1.60 (3H, t, J = 7.1 Hz, OCH $\underline{2}$ CH $\underline{3}$), 0.84 (3H, t, J = 7.4 Hz, CHCH $\underline{2}$ CH $\underline{3}$); δ_{C} (CDCl $\underline{3}$, 126 MHz): 163.4 (C=O), 155.4 (C8), 151.5 (C5), 147.4 (C14), 140.9 (C1), 137.6 (C7), 136.5 (C12), 135.8 (C4), 128.5 (C9), 127.5 (C3), 124.7 (C2), 118.8 (C11), 118.4 (C10), 114.8 (C6), 109.4 (C13), 64.4 (OCH $\underline{2}$ CH $\underline{3}$), 60.2 (CHCH $\underline{2}$ CH $\underline{3}$), 54.6 (C17), 43.5 (NCH $\underline{3}$), 43.1 (ArCH $\underline{2}$), 40.1 (C15), 30.6 (C16), 28.1 (CONCH $\underline{3}$), 24.7 (CHCH $\underline{2}$ CH $\underline{3}$), 15.4 (ArCH $\underline{3}$), 15.0 (OCH $\underline{2}$ CH $\underline{3}$), 8.7 (CHCH $\underline{2}$ CH $\underline{3}$)

(*R*)-8-((4-Bromothiophen-2-yl)methyl)-2-((2-ethoxy-4-(1-methylpiperidin-4-yl)phenyl)amino)-7-ethyl-5-methyl-7,8-dihydropteridin-6(5*H*)-one, 65



Dihydropteridinone **6t** (55 mg, 137 μ mol) was reacted with aniline **28b** (31 mg, 130 μ mol) using general method **16** to afford the title compound **65** as a yellow solid (13 mg, 16%). LCMS purity >95%, ret. time 1.20 mins; HRMS (ESI +ve): found $[M+H]^+$ 601.1776, $[C_{28}H_{36}BrN_6O_2S]^+$ requires 601.1781; m.p.: 59 – 61 $^{\circ}\text{C}$; ν_{max} (thin film, cm^{-1}): 3417 (w, N-H), 1665 (C=O); $[\alpha]_D^{22.5}$: +21.5 $^{\circ}$ (c 1.0, MeOH); δ_{H} (CDCl $\underline{3}$, 500 MHz): 8.25 (1H, d, J = 8.2 Hz, H10), 7.69 (1H, s, H7), 7.57 (1H, s, NH), 7.14 (1H, d, J = 1.6 Hz, H1), 6.96 (1H, s, H3), 6.78 (1H, dd, J = 8.2, 1.7 Hz, H11), 6.74 (1H, d, J = 1.7 Hz, H13), 5.50 (1H, d, J = 15.5 Hz, ArCH \underline{H}), 4.42 (1H, d, J = 15.5 Hz, ArCH \underline{H}), 4.25 (1H, dd, J = 6.3, 3.5 Hz, CHCH $\underline{2}$ CH $\underline{3}$), 4.13 (2H, q, J = 6.9 Hz, OCH $\underline{2}$ CH $\underline{3}$), 3.58 (2H, d, J = 10.7 Hz, H17), 3.33 (3H, s, CONCH $\underline{3}$), 2.75 – 2.65 (5H, m, NCH $\underline{3}$ & 2 x H17), 2.65 – 2.60 (1H, m, H15), 2.27 – 2.16 (2H, m, H16), 2.02 – 1.93 (3H, m, 2 x H16 & CHCH \underline{H} CH $\underline{3}$), 1.88 – 1.79 (1H, m, CHCH \underline{H} CH $\underline{3}$), 1.48 (3H, t, J = 6.9 Hz, OCH $\underline{2}$ CH $\underline{3}$), 0.83 (3H, t, J = 7.6 Hz, CHCH $\underline{2}$ CH $\underline{3}$); δ_{C} (CDCl $\underline{3}$, 126 MHz): 163.1 (C=O), 155.5 (C8), 151.3 (C5), 147.5 (C14), 140.4 (C4), 138.2 (C7), 136.6 (C12), 129.5 (C3), 128.4 (C9), 123.2 (C1), 118.8 (C11), 118.4 (C10), 114.8 (C6), 109.4 (C13), 109.2 (C2), 64.4 (OCH $\underline{2}$ CH $\underline{3}$), 61.1 (CHCH $\underline{2}$ CH $\underline{3}$), 54.6 (C17), 43.5 (NCH $\underline{3}$), 43.3 (ArCH $\underline{2}$), 40.6 (C15), 30.5 (C16), 28.1 (CONCH $\underline{3}$), 25.0 (CHCH $\underline{2}$ CH $\underline{3}$), 15.0 (OCH $\underline{2}$ CH $\underline{3}$), 8.7 (CHCH $\underline{2}$ CH $\underline{3}$)

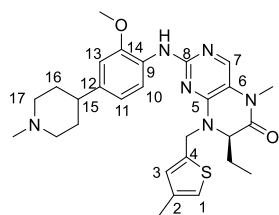
(*R*)-8-((4-Chlorothiophen-2-yl)methyl)-2-((2-ethoxy-4-(1-methylpiperidin-4-yl)phenyl)amino)-7-ethyl-5-methyl-7,8-dihydropteridin-6(5*H*)-one, 66



Dihydropteridinone **6u** (39 mg, 109 μ mol) was reacted with aniline **28b** (24 mg, 104 μ mol) using general method **16** to afford the title compound **66** as a yellow solid (11 mg, 18%). LCMS purity >95%, ret. time 1.19 mins; HRMS (ESI +ve): found $[M+H]^+$ 555.2298, $[C_{28}H_{36}ClN_6O_2S]^+$ requires 555.2303; m.p.: 82 – 85 $^{\circ}\text{C}$; ν_{max} (thin film, cm^{-1}): 3420 (w, N-H), 1665

(C=O); $[\alpha]_D^{22.2}$: -17.3° (c 1.0, MeOH); δ_H (CDCl₃, 500 MHz): 8.24 (1H, d, J = 8.3 Hz, H10), 7.69 (1H, s, H7), 7.62 (1H, s, NH), 7.01 (1H, d, J = 1.6 Hz, H1), 6.92 (1H, s, H3), 6.78 (1H, dd, J = 8.3, 1.6 Hz, H11), 6.75 (1H, d, J = 1.6 Hz, H13), 5.48 (1H, d, J = 15.5 Hz, ArCHH), 4.41 (1H, d, J = 15.5 Hz, ArCHH), 4.26 (1H, dd, J = 6.3, 3.8 Hz, CHCH₂CH₃), 4.13 (2H, q, J = 6.9 Hz, OCH₂CH₃), 3.60 (2H, d, J = 11.4 Hz, H17), 3.33 (3H, s, CONCH₃), 2.78 – 2.60 (6H, m, NCH₃, H15 & 2 x H17), 2.26 – 2.15 (2H, m, H16), 2.03 – 1.94 (3H, m, 2 x H16 & CHCHHCH₃), 1.88 – 1.70 (1H, m, CHCHHCH₃), 1.49 (3H, t, J = 6.9 Hz, OCH₂CH₃), 0.84 (3H, t, J = 7.4 Hz, CHCH₂CH₃); δ_C (CDCl₃, 126 MHz): 163.1 (CONCH₃), 155.4 (C8), 151.3 (C5), 147.5 (C14), 139.7 (C4), 138.0 (C7), 136.6 (C12), 128.4 (C9), 127.3 (C3), 124.6 (C2), 120.4 (C1), 118.7 (C11), 118.6 (C10), 114.8 (C6), 109.4 (C13), 64.4 (OCH₂CH₃), 61.1 (CHCH₂CH₃), 54.6 (C17), 43.3 (ArCH₂ & NCH₃), 40.0 (C15), 30.5 (C16), 28.1 (CONCH₃), 25.0 (CHCH₂CH₃), 15.0 (OCH₂CH₃), 8.7 (CHCH₂CH₃)

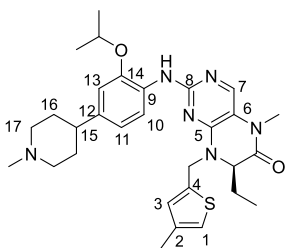
(*R*)-7-Ethyl-2-((2-methoxy-4-(1-methylpiperidin-4-yl)phenyl)amino-5-methyl-8-((4-methylthiophen-2-yl)methyl)-7,8-dihydropteridin-6(5*H*)-one, 67



Dihydropteridinone **6r** (60 mg, 178 μ mol) was reacted with aniline **28a** (37 mg, 169 μ mol) using general method **16** to afford the title compound **67** as a yellow oil (20 mg, 22%). LCMS purity >95%, ret. time 1.14 mins; HRMS (ESI +ve): found $[M+H]^+$ 521.2674, $[C_{28}H_{37}N_6O_2S]^+$ requires 521.2693;

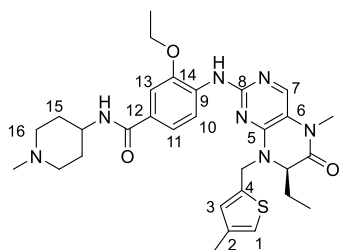
ν_{\max} (thin film, cm⁻¹): 3423 (w, N-H), 1665 (C=O); $[\alpha]_D^{22.8}$: $+9.7^\circ$ (c 1.0, MeOH); δ_H (CDCl₃, 500 MHz): 8.24 (1H, d, J = 8.3 Hz, H10), 7.78 (1H, s, NH), 7.63 (1H, s, H7), 6.85 – 6.69 (4H, m, H1, H3, H11 & H13), 5.57 (1H, d, J = 15.4 Hz, ArCHH), 4.30 (1H, d, J = 15.4 Hz, ArCHH), 4.26 – 4.23 (1H, m, CHCH₂CH₃), 3.89 (3H, s, OCH₃), 3.61 – 3.51 (2H, m, H17), 3.29 (3H, s, CONCH₃), 2.74 – 2.60 (6H, m, NCH₃, 2 x H15 & H17), 2.22 – 2.15 (5H, m, ArCH₃ & 2 x H16), 2.01 – 1.90 (3H, m, 2 x H16 & CHCHHCH₃), 1.88 – 1.77 (1H, m, CHCHHCH₃), 0.81 (3H, t, J = 7.4 Hz, CHCH₂CH₃); δ_C (CDCl₃, 126 MHz): 163.3 (CONCH₃), 155.1 (C8), 151.5 (C5), 148.4 (C14), 137.9 (C4), 137.4 (C2), 136.8 (C7), 136.7 (C12), 129.7 (C3), 128.2 (C9), 121.2 (C1), 118.9 (C10), 118.8 (C11), 114.8 (C6), 108.5 (C13), 60.2 (CHCH₂CH₃), 55.8 (OCH₃), 54.6 (C17), 43.4 (NCH₃), 42.8 (ArCH₂), 40.0 (C15), 30.5 (C16), 28.1 (CONCH₃), 24.8 (CHCH₂CH₃), 15.7 (ArCH₃), 8.7 (CHCH₂CH₃)

(*R*)-7-Ethyl-2-((2-isopropoxy-4-(1-methylpiperidin-4-yl)phenyl)amino-5-methyl-8-((4-methylthiophen-2-yl)methyl)-7,8-dihydropteridin-6(5*H*)-one, 68



Dihydropteridinone **6r** (70 mg, 208 μ mol) was reacted with aniline **28c** (49 mg, 197 μ mol) using general method **16** to afford the title compound **68** as a yellow solid (13 mg, 12%). LCMS purity >95%, ret. time 1.25 mins; HRMS (ESI +ve): found $[M+H]^+$ 549.2991, $[C_{30}H_{41}N_6O_2S]^+$ requires 549.3006; m.p.: 76 – 78 $^{\circ}$ C; ν_{\max} (thin film, cm^{-1}): 3416 (w, N-H), 1668 (C=O); $[\alpha]_D^{23.3}$: +11.1 $^{\circ}$ (c 1.0, MeOH); δ_H (CDCl_3 , 500 MHz): 8.33 (1H, d, J = 7.9 Hz, H10), 7.68 (1H, s, H7), 7.44 (1H, s, NH), 6.86 (1H, s, H3), 6.82 – 6.78 (3H, m, H1, H11 & H13), 5.61 (1H, d, J = 15.3 Hz, ArCHH), 4.59 (1H, sept., J = 6.0 Hz, OCH(CH₃)₂), 4.35 (1H, d, J = 15.3 Hz, ArCHH), 4.26 (1H, dd, J = 6.3, 3.5 Hz, CHCH₂CH₃), 3.32 (3H, s, CONCH₃), 3.01 – 2.96 (2H, m, H17), 2.47 – 2.40 (1H, m, H15), 2.34 (3H, s, NCH₃), 2.23 (3H, s, ArCH₃), 2.06 (2H, td, J = 11.4, 3.2 Hz, H17), 1.99 – 1.92 (1H, m, CHCHHCH₃), 1.89 – 1.77 (5H, m, 4 x H16 & CHCHHCH₃), 1.40 (3H, t, J = 6.6 Hz, OCH(CH₃)₂), 0.84 (3H, t, J = 7.6 Hz, CHCH₂CH₃); δ_C (CDCl_3 , 126 MHz): 163.4 (CONCH₃), 155.8 (C8), 151.4 (C5), 145.8 (C14), 139.3 (C12), 138.4 (C4 & C7), 137.6 (C2), 129.5 (C3), 128.8 (C9), 121.1 (C1), 118.9 (C11), 118.1 (C10), 114.7 (C6), 111.3 (C13), 71.1 (OCH(CH₃)₂), 60.4 (CHCH₂CH₃), 56.4 (C17), 46.5 (NCH₃), 42.9 (ArCH₂), 41.8 (C15), 33.7 (C16), 28.1 (CONCH₃), 24.8 (CHCH₂CH₃), 22.3 (OCH(CH₃)₂), 15.7 (ArCH₃), 8.8 (CHCH₂CH₃)

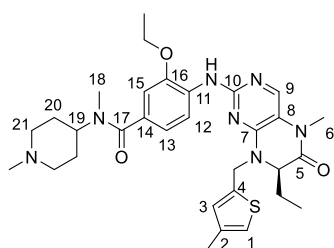
(*R*)-3-Ethoxy-4-((7-ethyl-5-methyl-8-((4-methylthiophen-2-yl)methyl)-6-oxo-5,6,7,8-tetrahydropteridin-2-yl)amino)-*N*-1-methylpiperidin-4-yl)benzamide, 69



Dihydropteridinone **6r** (47 mg, 140 μ mol) was reacted with aniline **20e** (37 mg, 133 μ mol) using general method **16** to afford the title compound **69** as a yellow solid (20 mg, 24%). LCMS purity >95%, ret. time 1.27 mins; HRMS (ESI +ve): found $[M+H]^+$ 578.2882, $[C_{30}H_{40}N_7O_3S]^+$ requires 578.2908; m.p.: 126 – 129 $^{\circ}$ C; ν_{\max} (thin film, cm^{-1}): 3413 (w, N-H), 2933, (w, N-H), 1667 (s, C=O), 1591 (s, C=O); $[\alpha]_D^{23.7}$: +2.8 $^{\circ}$ (c 1.0, MeOH); δ_H (CDCl_3 , 500 MHz): 8.46 (1H, d, J = 8.5 Hz, H10), 8.04 (1H, s, ArNH), 7.69 (1H, s, H8), 7.46 (1H, d, J = 1.6 Hz, H13), 7.42 (1H, dd, J = 8.5, 1.6 Hz, H11), 7.00 (1H, d, J = 7.3 Hz, CONH), 6.85 (1H, s, H3), 6.81 (1H, s, H1), 5.57 (1H, d, J = 15.5 Hz, ArCHH), 4.38 (1H, d, J = 15.5 Hz, ArCHH), 4.32 – 4.25 (2H, m, CHCH₂CH₃ & NHCH), 4.21 (2H, q, J = 6.9 Hz, OCH₂CH₃), 3.57 (2H, d, J = 11.0 Hz, H16), 3.33 (3H, s, CONCH₃), 2.87 – 2.79 (5H, m, NCH₃ & 2 x H16), 2.25 – 2.19 (5H, m, ArCH₃ & 2 x H15), 2.16 – 2.10 (2H, m, H15), 2.03 – 1.94 (1H, m, CHCHHCH₃), 1.91 – 1.82 (1H, m, CHCHHCH₃), 1.50 (3H, t,

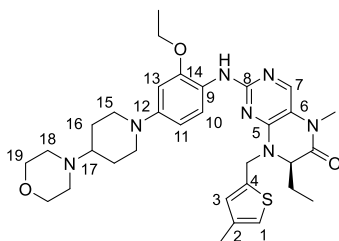
$J = 6.9$ Hz, OCH_2CH_3), 0.83 (3H, t, $J = 7.4$ Hz, CHCH_2CH_3); δ_{C} (CDCl_3 , 126 MHz): 166.9 (CONH), 163.3 (CONCH_3), 154.6 (C8), 151.5 (C5), 146.9 (C14), 137.7 (C4), 137.5 (C2), 136.7 (C7), 132.9 (C9), 129.7 (C3), 126.0 (C12), 121.3 (C1), 119.8 (C11), 117.1 (C10), 115.3 (C6), 109.9 (C13), 64.5 (OCH_2CH_3), 60.4 (CHCH_2CH_3), 54.1 (C16), 44.1 (NHCH), 43.6 (NCH_3), 43.1 (ArCH_2), 28.8 (C15), 28.1 (CONCH_3), 15.6 (CHCH_2CH_3), 14.8 (OCH_2CH_3), 8.6 (CHCH_2CH_3)

(R)-3-Ethoxy-4-((7-ethyl-5-methyl-8-((4-methylthiophen-2-yl)methyl)-6-oxo-5,6,7,8-tetrahydropteridin-2-yl)amino)-N-methyl-N-(1-methylpiperidin-4-yl)benzamide, 70



Dihydropteridinone **6r** (47 mg, 140 μmol) was reacted with aniline **20g** (39 mg, 133 μmol) using general method **16** to afford the title compound **70** as a yellow oil (7 mg, 8%). LCMS purity >95%, ret. time 1.19 mins; HRMS (ESI +ve): found $[\text{M}+\text{H}]^+$ 592.3048, $[\text{C}_{31}\text{H}_{41}\text{N}_7\text{O}_3\text{S}]^+$ requires 592.3064; ν_{max} (thin film, cm^{-1}): 3415 (w, N-H), 3311 (w, CON-H), 1664 (C=O), 1630 (C=O); $[\alpha]_D^{22.3}$: + 8.3° (c 1.0, MeOH); δ_{H} (CDCl_3 , 500 MHz): 8.51 (1H, d, $J = 8.1$ Hz, H12), 7.72 (1H, s, H9), 7.64 (1H, s, NH), 7.00 – 6.96 (2H, m, H13 & H15), 6.87 (1H, s, H3), 6.83 (1H, s, H1), 5.60 (1H, d, $J = 15.4$ Hz, ArCHH), 4.39 (1H, d, $J = 15.5$ Hz, ArCHH), 4.29 (1H, dd, $J = 6.4, 3.6$ Hz, CHCH_2CH_3), 4.17 (2H, q, $J = 6.8$ Hz, OCH_2CH_3), 3.35 (3H, s, CONCH_3), 1.52 (3H, t, $J = 6.8$ Hz, OCH_2CH_3), 0.86 (3H, d, $J = 7.4$ Hz, CHCH_2CH_3); δ_{C} (CDCl_3 , 126 MHz): 168.7 (C17), 163.4 (C5), 155.3 (C10), 151.4 (C7), 146.5 (C16), 138.2 (C4), 138.1 (C9), 137.4 (C2), 131.3 (C11), 129.6 (C3), 128.7 (C14), 121.2 (C1), 116.4 (C12), 115.3 (C7), 64.4 (OCH_2CH_3), 60.4 (CHCH_2CH_3), 54.8 (C16), 43.0 (ArCH_2), 28.1 (CONCH_3), 24.8 (CHCH_2CH_3), 15.7 (ArCH_3), 14.9 (OCH_2CH_3), 8.7 (CHCH_2CH_3); peaks for piperidine and connected amide can't be seen due to rotomers

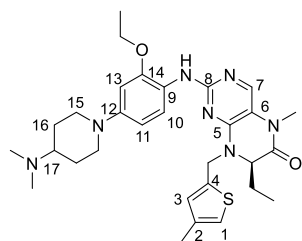
(R)-2-((2-Ethoxy-4-(4-morpholinopiperidin-1-yl)phenyl)amino)-7-ethyl-5-methyl-8-((4-methylthiophen-2-yl)methyl)-7,8-dihydropteridin-6(5H)-one, 71



Dihydropteridinone **6r** (35 mg, 104 μmol) was reacted with aniline **23d** (30 mg, 99 μmol) using general method **16** to afford the title compound **71** as a brown solid (11 mg, 18%). LCMS purity >95%, ret. time 1.11 mins; HRMS (ESI +ve): found $[\text{M}+\text{H}]^+$ 606.3189, $[\text{C}_{32}\text{H}_{44}\text{N}_7\text{O}_3\text{S}]^+$ requires 606.3221; m.p.: 72 – 74 °C; ν_{max} (thin film, cm^{-1}): 3418 (w, N-H), 1666 (C=O); $[\alpha]_D^{22.9}$: +9.7° (c 1.0, MeOH); δ_{H} (CDCl_3 , 500 MHz): 8.14 (1H, d, $J = 8.8$ Hz, H10), 7.62

(1H, s, H7), 7.54 (1H, s, NH), 6.81 (1H, s, H3), 6.79 (1H, s, H1), 6.54 (1H, d, $J = 2.5$ Hz, H13), 6.50 (1H, dd, $J = 8.8, 2.5$ Hz, H11), 5.58 (1H, d, $J = 15.4$ Hz, ArCH_H), 4.28 (1H, d, $J = 15.4$ Hz, ArCH_H), 4.23 (1H, dd, $J = 6.3, 3.5$ Hz, CHCH₂CH₃), 4.08 (2H, q, $J = 7.0$ Hz, OCH₂CH₃), 3.81 – 3.78 (4H, m, H19), 3.64 – 3.60 (2H, m, H15), 3.29 (3H, s, CONCH₃), 2.74 – 2.71 (4H, m, H18), 2.71 – 2.64 (2H, m, H15), 2.55 – 2.49 (1H, m, H17), 2.20 (3H, s, ArCH₃), 2.00 – 1.92 (3H, m, 2 x H16 & CHCH₂CH₃), 1.86 – 1.79 (1H, m, CHCH₂CH₃), 1.78 – 1.70 (2H, m, H16), 1.45 (3H, t, $J = 7.0$ Hz, OCH₂CH₃), 0.81 (3H, t, $J = 7.5$ Hz, CHCH₂CH₃); δ_c (CDCl₃, 126 MHz): 163.3 (CONCH₃), 155.5 (C8), 151.5 (C5), 148.4 (C14), 146.7 (C12), 138.2 (C4), 137.4 (C2), 137.3 (C7), 129.7 (C3), 123.1 (C9), 121.2 (C1), 119.7 (C10), 114.4 (C6), 108.8 (C11), 102.4 (C13), 66.4 (C19), 64.3 (OCH₂CH₃), 62.3 (C17), 60.2 (CHCH₂CH₃), 50.4 (C15), 49.2 (C18), 42.7 (ArCH₂), 28.1 (CONCH₃), 27.5 (C16), 24.7 (CHCH₂CH₃), 15.7 (ArCH₃), 15.0 (OCH₂CH₃), 8.7 (CHCH₂CH₃)

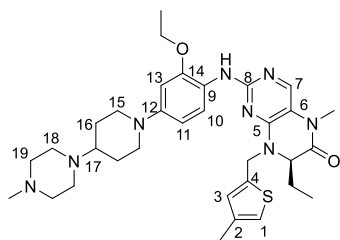
(*R*)-2-((4-(4-dimethylamino)piperidin-1-yl)-2-ethoxyphenyl)amino)-7-ethyl-5-methyl-8-((4-methylthiophen-2-yl)methyl)-7,8-dihydropteridin-6(5*H*)-one, 72



Dihydropteridinone **6r** (30 mg, 89 μ mol) was reacted with aniline **23e** (22 mg, 85 μ mol) using general method **16** to afford the title compound **72** as a brown solid (5 mg, 11%). LCMS purity >95%, ret. time 1.12 mins; HRMS (ESI +ve): found $[M+H]^+$ 564.3106, $[C_{30}H_{42}N_7O_2S]^+$ requires 564.3121;

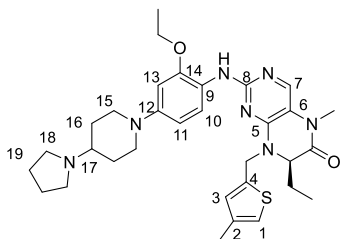
m.p.: 64 – 66 °C; ν_{\max} (thin film, cm⁻¹): 3422 (w, N-H), 1666 (C=O); $[\alpha]_D^{23.1}$: +23.5° (c 1.0, MeOH); δ_H (CDCl₃, 500 MHz): 8.19 (1H, d, $J = 8.7$ Hz, H10), 7.63 (1H, s, H7), 7.49 (1H, s, NH), 6.82 (1H, s, H3), 6.80 (1H, s, H1), 6.54 – 6.44 (2H, m, H11 & H13), 5.59 (1H, d, $J = 15.4$ Hz, ArCH_H), 4.31 (1H, d, $J = 15.4$ Hz, ArCH_H), 4.24 (1H, dd, $J = 6.3, 3.5$ Hz, CHCH₂CH₃), 4.09 (2H, q, $J = 7.0$ Hz, OCH₂CH₃), 3.66 (2H, d, $J = 12.6$ Hz, H15), 3.30 (3H, s, CONCH₃), 3.08 (1H, tt, $J = 12.3, 3.8$ Hz, H17), 2.76 – 2.69 (2H, m, H15), 2.67 (6H, s, N(CH₃)₂), 2.21 (3H, s, ArCH₃), 2.13 – 2.08 (2H, m, H16), 1.99 – 1.92 (1H, m, CHCH₂CH₃), 1.90 – 1.79 (3H, 2 x H16 & CHCH₂CH₃), 1.47 (3H, t, $J = 7.0$ Hz, OCH₂CH₃), 0.82 (3H, t, $J = 7.4$ Hz, CHCH₂CH₃); δ_c (CDCl₃, 126 MHz): 163.3 (CONCH₃), 155.6 (C8), 151.5 (C5), 148.3 (C14), 145.9 (C12), 138.2 (C4), 137.6 (C7), 137.4 (C2), 129.6 (C3), 123.8 (C9), 121.2 (C1), 119.4 (C10), 114.5 (C6), 109.2 (C11), 102.7 (C13), 64.3 (OCH₂CH₃), 62.3 (C17), 60.2 (CHCH₂CH₃), 50.1 (C15), 42.8 (ArCH₂), 41.0 (N(CH₃)₂), 28.1 (CONCH₃), 26.0 (C16), 24.7 (CHCH₂CH₃), 15.7 (ArCH₃), 15.0 (OCH₂CH₃), 8.7 (CHCH₂CH₃)

(*R*)-2-((2-Ethoxy-4-(4-methylpiperazin-1-yl)piperidin-1-yl)phenyl)amino-7-ethyl-5-methyl-8-((4-methylthiophen-2-yl)methyl)-7,8-dihydropteridin-6(5*H*)-one, 73



Dihydropteridinone **6r** (35 mg, 104 μ mol) was reacted with aniline **23f** (31 mg, 99 μ mol) using general method **16** to afford the title compound **73** as a brown solid (10 mg, 16%). LCMS purity >95%, ret. time 0.93 mins; HRMS (ESI +ve): found $[M+H]^+$ 619.3549, $[C_{33}H_{47}N_8O_2S]^+$ requires 619.3542; m.p.: 65 – 67 $^{\circ}$ C; ν_{\max} (thin film, cm^{-1}): 3426 (w, N-H), 1665 (C=O); $[\alpha]_D^{22.9}$: +6.2 $^{\circ}$ (c 1.0, MeOH); δ_H (CDCl₃, 500 MHz): 8.06 (1H, s, NH), 8.03 (1H, d, J = 8.8 Hz, H10), 7.61 (1H, s, H7), 6.82 – 6.78 (2H, m, H1 & H3), 6.53 (1H, d, J = 2.5 Hz, H13), 6.48 (1H, dd, J = 8.8, 2.5 Hz, H11), 5.57 (1H, d, J = 15.4 Hz, ArCH_H), 4.30 – 4.24 (2H, m, ArCH_H & CHCH₂CH₃), 4.08 (2H, q, J = 7.0 Hz, OCH₂CH₃), 3.62 (2H, d, J = 12.0 Hz, H15), 3.29 (3H, s, CONCH₃), 3.08 – 2.92 (8H, m, H18 & H19), 2.72 – 2.63 (3H, m, 2 x H15 & H17), 2.59 (3H, s, CONCH₃), 2.20 (3H, s, NCH₃), 2.00 – 1.93 (3H, m, 2 x H16 & CHCH₂CH₃), 1.89 – 1.81 (1H, m, CHCH₂CH₃), 1.78 – 1.69 (2H, m, H16), 1.45 (3H, t, J = 7.0 Hz, OCH₂CH₃), 0.82 (3H, t, J = 7.4 Hz, CHCH₂CH₃); δ_C (CDCl₃, 126 MHz): 163.1 (CONCH₃), 154.8 (C8), 151.7 (C5), 149.2 (C14), 147.0 (C12), 137.7 (C4), 137.5 (C1), 135.2 (C7), 129.8 (C3), 122.4 (C9), 121.3 (C1), 120.7 (C10), 114.3 (C6), 108.7 (C11), 102.4 (C13), 64.3 (OCH₂CH₃), 61.8 (C17), 60.2 (CHCH₂CH₃), 53.0 (C19), 50.2 (C15), 4.66 (C18), 43.8 (NCH₃), 42.8 (ArCH₂), 28.1 (CONCH₃), 27.5 (C16), 24.8 (CHCH₂CH₃), 15.7 (ArCH₃), 15.0 (OCH₂CH₃), 8.6 (CHCH₂CH₃)

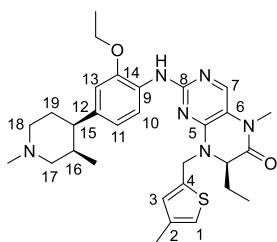
(*R*)-2-((2-Ethoxy-4-(4-(pyrrolidin-1-yl)piperidin-1-yl)phenyl)amino-7-ethyl-5-methyl-8-((4-methylthiophen-2-yl)methyl)-7,8-dihydropteridin-6(5*H*)-one, 74



Dihydropteridinone **6r** (25 mg, 74 μ mol) was reacted with aniline **23g** (20 mg, 71 μ mol) using general method **16** to afford the title compound **74** as a brown solid (5 mg, 10%). LCMS purity >95%, ret. time 0.95 mins; HRMS (ESI +ve): found $[M+H]^+$ 590.3290, $[C_{32}H_{44}N_7O_2S]^+$ requires 590.3277; ν_{\max} (thin film, cm^{-1}): 3425 (w, N-H), 1668 (C=O); $[\alpha]_D^{22.3}$: +12.2 $^{\circ}$ (c 1.0, MeOH); δ_H (CDCl₃, 500 MHz): 8.15 (1H, d, J = 8.7 Hz, H10), 7.62 (2H, m, NH & H7), 6.82 (1H, s, H3), 6.80 (1H, s, H1), 6.52 (1H, d, J = 2.5 Hz, H13), 6.48 (1H, dd, J = 8.7, 2.5 Hz, H11), 5.59 (1H, d, J = 15.4 Hz, ArCH_H), 4.31 (1H, d, J = 15.4 Hz, ArCH_H), 4.25 (1H, dd, J = 6.3, 3.5 Hz, CHCH₂CH₃), 4.09 (2H, q, J = 7.0 Hz, OCH₂CH₃), 3.67 – 3.60 (2H, m, H15), 3.35 – 3.20 (7H, m, 4 x H18 & CONCH₃), 3.00 (1H, tt, J = 12.1, 4.3 Hz, H17), 3.71 – 2.64 (2H, m, H15), 2.21 (3H, s, ArCH₃), 2.11 (2H, d, J = 11.2 Hz, H16), 2.09 –

2.00 (6H, m, 2 x H16 & H19), 1.98 – 1.92 (1H, m, CHCH₂HCH₃), 1.88 – 1.80 (1H, m, CHCH₂HCH₃), 1.47 (3H, t, *J* = 7.0 Hz, OCH₂CH₃), 0.82 (3H, t, *J* = 7.4 Hz, CHCH₂CH₃); δ_c (CDCl₃, 126 MHz): 163.3 (CONCH₃), 155.4 (C8), 151.5 (C5), 148.5 (C14), 146.2 (C12), 138.1 (C4), 137.4 (C1), 137.1 (C7), 129.7 (C3), 123.6 (C9), 121.1 (C10), 119.7 (C11), 114.5 (C6), 109.0 (C13), 64.3 (OCH₂CH₃), 61.6 (C17), 60.2 (CHCH₂CH₃), 50.0 (C18), 49.9 (C15), 42.8 (ArCH₂), 28.1 (CONCH₃), 28.0 (C16), 24.8 (CHCH₂CH₃), 23.4 (C19), 15.7 (ArCH₃), 15.0 (OCH₂CH₃), 8.7 (CHCH₂CH₃)

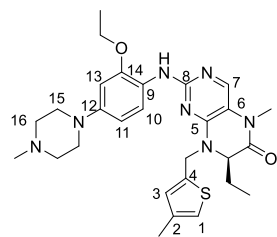
(7*R*)-2-((-4-(1,3-dimethylpiperidin-4-yl)-2-ethoxyphenyl)amino)-7-ethyl-5-methyl-8-((4-methylthiophen-2-yl)methyl)-7,8-dihydropteridin-6(5*H*)-one, 75



Dihydropteridinone **6r** (45 mg, 134 μ mol) was reacted with aniline **28d** (32 mg, 127 μ mol) using general method **16** to afford the title compound **75** as a yellow oil (4 mg, 5%). LCMS purity >95%, ret. time 1.19 mins; HRMS (ESI +ve): found $[M+H]^+$ 549,2986, $[C_{30}H_{41}N_6O_2S]^+$ requires 549.3006; ν_{max}

(thin film, cm⁻¹): 3417 (w, N-H), 1667 (C=O); δ_H (CDCl₃, 500 MHz): 8.34 (1H, d, *J* = 8.2 Hz, H10), 7.67 (1H, s, H7), 7.63 (1H, s, NH), 7.14 (1H, s, H1), 6.85 (1H, s, H3), 6.73 (1H, dd, *J* = 8.2, 1.6 Hz, H11), 6.66 (1H, d, *J* = 1.6 Hz, H13), 5.60 (1H, d, *J* = 15.5 Hz, ArCH₂H), 4.35 (1H, dd, *J* = 15.5, 5.4 Hz, ArCH₂H), 4.27 (1H, dd, *J* = 5.5, 3.0 Hz, CHCH₂CH₃), 4.12 (2H, q, *J* = 6.9 Hz, OCH₂CH₃), 3.80 – 3.65 (1H, m, H18), 3.43 – 3.35 (1H, m, H17), 3.32 (3H, m, CONCH₃), 2.96 – 2.86 (2H, m, H17 & H19), 2.80 – 2.58 (6H, m, NCH₃, H17, H18 & H19), 2.33 – 2.26 (1H, m, H16), 2.22 (3H, s, ArCH₃), 2.01 – 1.92 (2H, m, CHCH₂CH₃), 1.49 (3H, t, *J* = 6.9 Hz, OCH₂CH₃), 0.95 (3H, d, *J* = 7.6 Hz, CHCH₃), 0.83 (3H, t, *J* = 7.6 Hz, CHCH₂CH₃); δ_c (CDCl₃, 126 MHz): 163.3 (CONCH₃), 155.4 (C8), 151.4 (C5), 142.7 (C14), 138.1 (C4), 137.6 (C2), 137.4 (C7), 134.7 (C12), 129.7 (C3), 128.4 (C9), 121.2 (C1), 119.3 (C11), 118.1 (C10), 114.8 (C6), 110.0 (C13), 64.4 (OCH₂CH₃), 60.3 (CHCH₂CH₃ & C17), 54.8 (C18), 44.5 (NCH₃), 42.9 (ArCH₂), 42.3 (C15 & C19), 34.1 (C16), 28.1 (CONCH₃), 24.8 (CHCH₂CH₃), 15.7 (ArCH₃), 14.9 (OCH₂CH₃), 12.0 (CHCH₃), 8.7 (CHCH₂CH₃)

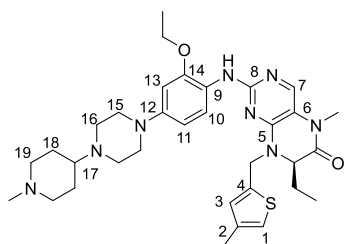
(*R*)-2-((2-Ethoxy-4-(4-methylpiperazin-1-yl)phenyl)amino)-7-ethyl-5-methyl-8-((4-methylthiophen-2-yl)methyl)-7,8-dihydropteridin-6(5*H*)-one, 76



Dihydropteridinone **6r** (35 mg, 104 μ mol) was reacted with aniline **23h** (23 mg, 99 μ mol) using general method **16** to afford the title compound **76** as a brown oil (3 mg, 5%). LCMS purity >95%, ret. time 0.90 mins; HRMS (ESI +ve): found $[M+H]^+$ 536.2814, $[C_{28}H_{38}N_7O_2S]^+$ requires 536.2807; ν_{max}

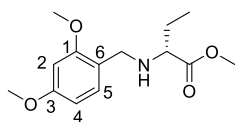
(thin film, cm^{-1}): 3427 (w, N-H), 1663 (C=O); $[\alpha]_D^{23.0}$: +18.0° (c 1.0, MeOH); δ_{H} (CDCl_3 , 500 MHz): 8.10 (1H, d, J = 8.5 Hz, H10), 8.00 (1H, s, NH), 7.62 (1H, s, H7), 6.92 – 6.79 (2H, m, H1 & H3), 6.52 – 6.48 (2H, m, H11 & H13), 5.57 (1H, d, J = 15.4 Hz, ArCHH), 4.33 – 4.25 (2H, m, ArCHH & CHCH₂CH₃), 4.08 (2H, q, J = 7.0 Hz, OCH₂CH₃), 3.35 – 3.28 (7H, m, 4 x H15 & CONCH₃), 3.16 – 3.08 (4H, m, H16), 2.67 (3H, s, NCH₃), 2.21 (3H, s, ArCH₃), 2.01 – 1.93 (1H, m, CHCHHCH₃), 1.89 – 1.81 (1H, m, CHCHHCH₃), 1.47 (3H, t, J = 7.0 Hz, OCH₂CH₃), 0.82 (3H, t, J = 7.4 Hz, CHCH₂CH₃); δ_{C} (CDCl_3 , 126 MHz): 163.3 (CONCH₃), 155.0 (C8), 151.8 (C5), 149.2 (C14), 145.9 (C12), 137.8 (C4), 137.6 (C1), 135.7 (C7), 129.9 (C3), 123.7 (C9), 121.5 (C1), 120.7 (C10), 114.6 (C6), 109.4 (C11), 102.5 (C13), 64.5 (OCH₂CH₃), 60.4 (CHCH₂CH₃), 53.7 (C16), 48.7 (C15), 43.8 (NCH₃), 43.0 (ArCH₂), 28.3 (CONCH₃), 25.0 (CHCH₂CH₃), 15.8 (ArCH₃), 15.0 (OCH₂CH₃), 8.8 (CHCH₂CH₃)

(*R*)-2-((2-Ethoxy-4-(1-methylpiperidin-4-yl)piperazin-1-yl)phenyl)amino)-7-ethyl-5-methyl-8-((4-methylthiophen-2-yl)methyl)-7,8-dihydropteridin-6(5*H*)-one, 77

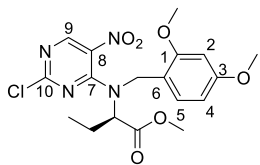


Dihydropteridinone **6r** (50 mg, 148 μmol) was reacted with aniline **23i** (45 mg, 141 μmol) using general method **16** to afford the title compound **77** as a yellow solid (7 mg, 8%). LCMS purity >95%, ret. time 1.21 mins; HRMS (ESI +ve): found $[\text{M}+\text{H}]^+$ 619.3525, $[\text{C}_{33}\text{H}_{47}\text{N}_8\text{O}_2\text{S}]^+$

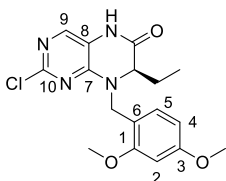
requires 619.3537; m.p.: 83 – 86 °C; ν_{max} (thin film, cm^{-1}): 3424 (w, N-H), 1667 (C=O); $[\alpha]_D^{23.0}$: +16.6° (c 1.0, MeOH); δ_{H} (CDCl_3 , 500 MHz): 8.10 – 8.00 (2H, m, H10 & NH), 7.63 (1H, s, H7), 6.84 – 6.81 (2H, m, H1 & H3), 6.55 (1H, d, J = 2.5 Hz, H13), 6.51 (1H, dd, J = 8.9, 2.5 Hz, H11), 5.50 (1H, d, J = 15.4 Hz, ArCHH), 4.32 – 4.25 (2H, m, ArCHH & CHCH₂CH₃), 4.10 (2H, q, J = 7.0 Hz, OCH₂CH₃), 3.65 (2H, d, J = 12.8 Hz, H19), 3.31 (3H, s, CONCH₃), 3.12 – 2.94 (8H, m, H15 & H16), 2.74 – 2.63 (3H, m, H17 & 2 x H19), 2.61 (3H, s, NCH₃), 2.23 (3H, s, ArCH₃), 2.02 – 1.95 (3H, m, CHCHHCH₃ & 2 x H18), 1.90 – 1.84 (1H, m, CHCHHCH₃), 1.80 – 1.71 (2H, m, H18), 1.48 (3H, t, J = 7.0 Hz, OCH₂CH₃), 0.84 (3H, t, J = 7.4 Hz, CHCH₂CH₃); δ_{C} (CDCl_3 , 126 MHz): 163.3 (CONCH₃), 155.0 (C8), 151.8 (C5), 149.2 (C14), 147.1 (C12), 137.8 (C4), 137.6 (C2), 135.5 (C7), 130.0 (C3), 122.6 (C9), 121.4 (C1), 120.8 (C10), 114.5 (C6), 108.9 (C11), 102.5 (C13), 64.4 (OCH₂CH₃), 61.9 (C17), 60.3 (CHCH₂CH₃), 53.2 (C16), 50.3 (C19), 46.7 (C15), 43.9 (NCH₃), 43.0 (ArCH₂), 28.2 (CONCH₃), 27.7 (C18), 25.0 (CHCH₂CH₃), 15.8 (ArCH₃), 15.0 (OCH₂CH₃), 8.7 (CHCH₂CH₃)

Methyl (*R*)-2-((2,4-dimethoxybenzyl)amino)butanoate, 87

(*R*)-Methyl 2-aminobutanoate **8a** (HCl salt, 5.0 g, 32.0 mmol), was reacted with 2,4-dimethoxybenzaldehyde (4.65 g, 28.0 mmol) using general method **2** to afford the title compound **87** as a colourless oil (8.50 g, 98%). LCMS purity >95%, ret. time 0.88 mins; HRMS (ESI +ve): found $[M+H]^+$ 268.1541, $[C_{14}H_{21}NO_4]^+$ requires 268.1543; $[\alpha]_D^{23.9}$: +11.8° (*c* 1.0, MeOH); δ_H (CDCl₃, 500 MHz): 7.14 (1H, d, *J* = 8.2 Hz, H5), 6.45 – 6.41 (2H, m, H2 & H4), 3.81 (3H, s, C¹OCH₃), 3.81 (3H, s, C³OCH₃), 3.71 (1H, d, *J* = 12.9 Hz, ArCHH), 3.67 (4H, m, CO₂CH₃ & ArCHH), 3.23 (1H, t, *J* = 6.6 Hz, CHCH₂CH₃), 1.94 (1H, s, NH), 1.72 – 1.63 (2H, m, CHCH₂CH₃), 0.91 (3H, t, *J* = 7.4 Hz, CHCH₂CH₃); δ_C (CDCl₃, 126 MHz): 175.8 (CO₂CH₃), 160.1 (C3), 158.7 (C1), 130.4 (C5), 120.5 (C6), 103.7 (C4), 98.5 (C2), 62.1 (CHCH₂CH₃), 55.3 (C¹OCH₃ & C³OCH₃), 51.5 (CO₂CH₃), 47.1 (ArCH₂), 26.6 (CHCH₂CH₃), 10.1 (CHCH₂CH₃)

Methyl (*R*)-2-((2-chloro-5-nitropyrimidin-4-yl)(2,4-dimethoxybenzyl)amino)butanoate, 88

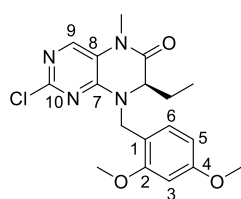
Aminobutanoate **87** (9.70 g, 36.3 mmol) was reacted with pyrimidine **11** (7.74 g, 39.9 mmol) using general method **3** to afford the title compound **88** as a yellow gum (13.0 g, 84%). LCMS purity >95%, ret. time 1.58 mins; HRMS (ESI +ve): found $[M+H]^+$ 425.1211, $[C_{18}H_{22}ClN_4O_6]^+$ requires 425.1222; $[\alpha]_D^{23.7}$: -6.9° (*c* 1.0, MeOH); δ_H (CDCl₃, 500 MHz): 8.64 (1H, s, H9), 7.04 (1H, d, *J* = 8.8 Hz, H5), 6.40 – 6.37 (2H, m, H2 & H4), 4.46 – 4.43 (2H, m, CHCH₂CH₃ & ArCHH), 4.40 (1H, d, *J* = 14.8 Hz, ArCHH), 3.79 (3H, s, C³OCH₃), 3.71 (3H, s, C¹OCH₃), 3.62 (3H, s, CO₂CH₃), 2.28 – 2.19 (1H, m, CHCHHCH₃), 2.06 – 1.97 (1H, m, CHCHHCH₃), 1.05 (3H, t, *J* = 7.4 Hz, CHCH₂CH₃); δ_C (CDCl₃, 126 MHz): 170.5 (CO₂CH₃), 161.4 (C3), 159.7 (C10), 159.0 (C1), 156.0 (C9), 154.6 (C7), 131.7 (C8), 131.0 (C5), 113.3 (C6), 104.2 (C4), 98.4 (C2), 63.4 (CHCH₂CH₃), 55.4 (C³OCH₃), 55.2 (C¹OCH₃), 52.2 (CO₂CH₃), 49.8 (ArCH₂), 22.9 (CHCH₂CH₃), 11.1 (CHCH₂CH₃)

(*R*)-2-Chloro-8-(2,4-dimethoxybenzyl)-7-ethyl-7,8-dihydropteridin-6(5*H*)-one, 89

Aminobutanoate **88**, (13.0 g, 30.6 mmol) was subjected to general method **18** to afford the title compound **89** as a brown solid (11.0 g, 98%). LCMS purity >95%, ret. time 1.48 mins; HRMS (ESI +ve): found $[M+H]^+$ 363.1198, $[C_{17}H_{20}ClN_4O_3]^+$ requires 363.1218; $[\alpha]_D^{23.4}$: +15.2° (*c* 1.0, MeOH); δ_H (CDCl₃, 500 MHz): 9.72 (1H, s, NH), 7.65 (1H, s, H9), 7.30 (1H, d, *J* = 9.1 Hz, H5), 6.47 – 6.45 (2H, m, H2 & H4), 5.35 (1H, d, *J* = 14.7

Hz, ArCHH), 4.28 (1H, dd, $J = 5.4, 4.4$ Hz, CHCH₂CH₃), 4.20 (1H, d, $J = 14.7$ Hz, ArCHH), 3.80 (6H, s, C¹OCH₃ & C³OCH₃), 2.03 – 1.94 (2H, m, CHCH₂CH₃), 0.94 (3H, d, $J = 7.3$ Hz, CHCH₂CH₃); δ_c (CDCl₃, 126 MHz): 166.2 (CONH), 161.0 (C3), 159.0 (C1), 154.3 (C10), 151.9 (C7), 138.7 (C9), 132.0 (C5), 117.5 (C8), 115.6 (C6), 104.4 (C4), 98.6 (C2), 60.7 (CHCH₂CH₃), 55.4 (C¹OCH₃ & C³OCH₃), 47.7 (ArCH₂), 25.0 (CHCH₂CH₃), 8.7 (CHCH₂CH₃)

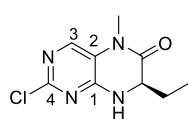
(R)-2-Chloro-8-(2,4-dimethoxybenzyl)-7-ethyl-5-methyl-7,8-dihydropteridin-6(5H)-one, 86



Dihydropteridinone **89** (10.8 g, 29.8 mmol) was reacted with methyl iodide (2.42 mL, 38.7 mmol) using general method **5** to afford the title compound **86** as a white solid (9.67 g, 86%).

LCMS purity >95%, ret. time 1.54 mins; HRMS (ESI +ve): found $[M+H]^+$ 377.1366, $[C_{18}H_{22}ClN_4O_3]^+$ requires 377.1375; $[\alpha]_D^{23.7}$: +35.3° (c 1.0, MeOH); δ_H (CDCl₃, 500 MHz): 7.62 (1H, s, H9), 7.32 (1H, d, $J = 8.8$ Hz, H5), 6.47 – 6.45 (2H, m, H2 & H4), 5.34 (1H, d, $J = 14.5$ Hz, ArCHH), 4.34 (1H, dd, $J = 6.3, 3.8$ Hz, CHCH₂CH₃), 4.20 (1H, d, $J = 14.5$ Hz, ArCHH), 3.81 (C¹OCH₃ & C³OCH₃), 3.30 (3H, s, NCH₃), 1.99 – 1.85 (1H, m, CHCH₂CH₃), 0.85 (3H, t, $J = 7.9$ Hz, CHCH₂CH₃); δ_c (CDCl₃, 126 MHz): 164.0 (CONCH₃), 161.0 (C3), 159.0 (C1), 154.2 (C10), 152.3 (C7), 137.6 (C9), 132.1 (C5), 120.6 (C8), 115.7 (C6), 104.3 (C4), 98.6 (C2), 60.8 (CHCH₂CH₃), 55.5 (C¹OCH₃ & C³OCH₃), 43.0 (ArCH₂), 28.1 (CONCH₃), 25.4 (CHCH₂CH₃), 8.9 (CHCH₂CH₃)

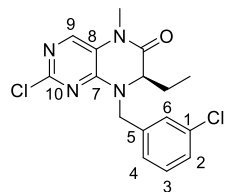
(R)-2-Chloro-7-ethyl-5-methyl-7,8-dihydropteridin-6(5H)-one, 79



A solution of dihydropteridinone **86** (5.09 g, 13.5 mmol) in TFA (1.3 M) was stirred at 80 °C for 4 hrs. Upon completion, the reaction was concentrated *in vacuo* to remove the majority of the TFA. The remaining TFA was quenched with sat. aq. NaHCO₃ until pH 7 – 8 was reached and extracted with DCM (X3). The organic layers were washed with brine, dried over MgSO₄, filtered and concentrated *in vacuo*. The residue was purified by Biotage column chromatography (DCM/MeOH, 0 – 15%) to afford the title compound **79** as a brown solid (2.02 g, 66%). LCMS purity >95%, ret. time 0.88 mins; HRMS (ESI +ve): found $[M+H]^+$ 227.0695, $[C_9H_{12}ClN_4O]^+$ requires 227.0694; $[\alpha]_D^{23.7}$: +35.3° (c 1.0, MeOH); δ_H (CDCl₃, 500 MHz): 7.73 (1H, s, H3), 6.23 (1H, s, NH), 4.36 – 4.32 (1H, m, CHCH₂CH₃), 3.35 (CONCH₃), 2.01 – 1.88 (2H, m, CHCH₂CH₃), 0.99 (3H, t, $J = 7.4$ Hz, CHCH₂CH₃); δ_c (CDCl₃, 126 MHz): 164.1 (CONCH₃), 154.2 (C4), 152.6 (C1),

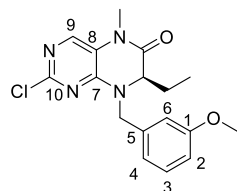
138.3 (C3), 120.1 (C2), 56.9 ($\underline{\text{CHCH}_2\text{CH}_3}$), 28.3 ($\text{CON}\underline{\text{CH}_3}$), 28.2 ($\text{CH}\underline{\text{CH}_2\text{CH}_3}$), 8.9 ($\text{CHCH}_2\underline{\text{CH}_3}$)

(*R*)-2-Chloro-8-(3-chlorobenzyl)-7-ethyl-5-methyl-7,8-dihydropteridin-6(5*H*)-one, 90a



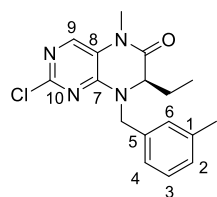
Dihydropteridinone **79** (50 mg, 0.22 mmol) was reacted with 3-chlorobenzyl bromide (57 mg, 0.28 mmol) using general method **19** to afford the title compound **90a** as a yellow solid (51 mg, 66%). LCMS purity >95%, ret. time 1.56 mins; HRMS (ESI +ve): found $[\text{M}+\text{H}]^+$ 351.0770, $[\text{C}_{16}\text{H}_{17}\text{Cl}_2\text{N}_4\text{O}]^+$ requires 351.0774; $[\alpha]_D^{23.0}$: -15.2° (c 1.0, MeOH); δ_{H} (CDCl_3 , 500 MHz): 7.72 (1H, s, H9), 7.31 – 7.28 (3H, m, H2, H3 & H6), 7.20 – 7.17 (1H, m, H4), 5.62 (1H, d, $J = 15.3$ Hz, $\text{ArCH}\underline{\text{H}}$), 4.16 (1H, dd, $J = 6.3, 3.5$ Hz, $\text{CH}\underline{\text{CH}_2\text{CH}_3}$), 4.08 (1H, d, $J = 15.3$ Hz, $\text{ArCH}\underline{\text{H}}$), 3.35 (3H, s, CONCH_3), 2.01 – 1.92 (1H, m, $\text{CHCH}\underline{\text{HCH}_3}$), 1.90 – 1.80 (1H, m, $\text{CHCH}\underline{\text{HCH}_3}$), 0.83 (3H, t, $J = 7.6$ Hz, $\text{CHCH}_2\underline{\text{CH}_3}$); δ_{C} (CDCl_3 , 126 MHz): 163.4 ($\underline{\text{CONCH}_3}$), 154.2 (C10), 152.3 (C7), 138.3 (C9), 137.2 (C5), 134.9 (C1), 130.3 (C3), 128.5 (C2/C6), 128.4 (C2/C6), 126.5 (C4), 120.5 (C8), 60.3 ($\underline{\text{CHCH}_2\text{CH}_3}$), 47.2 (ArCH_2), 28.3 ($\text{CON}\underline{\text{CH}_3}$), 24.8 ($\text{CH}\underline{\text{CH}_2\text{CH}_3}$), 8.6 ($\text{CHCH}_2\underline{\text{CH}_3}$)

(*R*)-2-Chloro-7-ethyl-8-(3-methoxybenzyl)-5-methyl-7,8-dihydropteridin-6(5*H*)-one, 90b



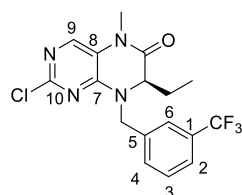
Dihydropteridinone **79** (50 mg, 0.22 mmol) was reacted with 3-methoxybenzyl bromide (56 μL , 0.28 mmol) using general method **19** to afford the title compound **90b** as a yellow solid (50 mg, 65%). LCMS purity >95%, ret. time 1.49 mins; HRMS (ESI +ve): found $[\text{M}+\text{H}]^+$ 347.1262, $[\text{C}_{17}\text{H}_{20}\text{ClN}_4\text{O}_2]^+$ requires 347.1269; $[\alpha]_D^{23.6}$: -9.7° (c 1.0, MeOH); δ_{H} (CDCl_3 , 500 MHz): 7.73 (1H, s, H9), 7.31 – 7.27 (1H, m, H3), 6.91 – 6.86 (3H, m, H2, H4 & H6), 5.63 (1H, d, $J = 15.5$ Hz, $\text{ArCH}\underline{\text{H}}$), 4.21 (1H, dd, $J = 6.3, 3.5$ Hz, $\text{CH}\underline{\text{CH}_2\text{CH}_3}$), 4.10 (1H, d, $J = 15.5$ Hz, $\text{ArCH}\underline{\text{H}}$), 3.82 (3H, s, OCH_3), 3.36 (3H, s, CONCH_3), 2.04 – 1.83 (2H, m, $\text{CHCH}_2\underline{\text{CH}_3}$), 0.85 (3H, t, $J = 7.4$ Hz, $\text{CHCH}_2\underline{\text{CH}_3}$); δ_{C} (CDCl_3 , 126 MHz): 163.6 ($\underline{\text{CONCH}_3}$), 160.0 (C1), 15.2 (C10), 152.5 (C7), 132.1 (C9), 136.5 (C5), 130.0 (C3), 120.7 (C4), 120.5 (C8), 114.4 (C6), 113.4 (C2), 60.0 ($\underline{\text{CHCH}_2\text{CH}_3}$), 55.3 (OCH_3), 47.7 (ArCH_2), 28.2 ($\text{CON}\underline{\text{CH}_3}$), 24.8 ($\text{CH}\underline{\text{CH}_2\text{CH}_3}$), 8.6 ($\text{CHCH}_2\underline{\text{CH}_3}$)

(*R*)-2-Chloro-7-ethyl-5-methyl-8-(3-methylbenzyl)-7,8-dihydropteridin-6(5*H*)-one, 90c



Dihydropteridinone **79** (70.0 mg, 0.31 mmol) was reacted with 1-(bromomethyl)-3-methyl-benzene (68.5 μ L, 0.37 mmol) using general method **19** to afford the title compound **90c** as a yellow solid (56.0 mg, 55%). LCMS purity >95%, ret. time 1.57 mins; HRMS (ESI +ve): found $[M+H]^+$ 331.1326, $[C_{17}H_{20}ClN_4O]^+$ requires 331.1320; $[\alpha]_D^{23.7}$: + 4.9° (*c* 1.0, MeOH); δ_H (CDCl₃, 500 MHz): 7.70 (1H, s, H₉), 7.26 – 7.22 (1H, m, H₃), 7.13 (1H, d, *J* = 7.6 Hz, H_{2/6}), 7.10 – 7.08 (2H, m, H₅ & H_{2/6}), 5.66 (1H, d, *J* = 14.8 Hz, ArCH_H), 4.18 (1H, dd, *J* = 6.3, 3.5 Hz, CHCH₂CH₃), 4.03 (1H, d, *J* = 14.8 Hz, ArCH_H), 3.34 (3H, s, CONCH₃), 2.35 (ArCH₃), 1.99 – 1.92 (CHCH₂CH₃), 1.91 – 1.84 (1H, m, CHCH₂CH₃), 0.83 (3H, t, *J* = 7.6 Hz, CHCH₂CH₃); δ_C (CDCl₃, 126 MHz): 163.7 (CONCH₃), 154.3 (C₁₀), 152.4 (C₇), 138.8 (C₁), 138.0 (C₉), 134.7 (C₅), 129.2 (C_{2/6}), 129.1 (C_{2/6}), 128.9 (C₃), 125.6 (C₄), 120.4 (C₈), 59.8 (CHCH₂CH₃), 47.5 (ArCH₂), 26.9 (CONCH₃), 24.7 (CHCH₂CH₃), 21.4 (ArCH₃), 8.6 (CHCH₂CH₃)

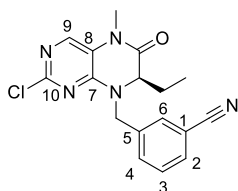
(*R*)-2-Chloro-7-ethyl-5-methyl-8-(3-(trifluoromethyl)benzyl)-7,8-dihydropteridin-6(5*H*)-one, 90d



Dihydropteridinone **79** (55 mg, 0.24 mmol) was reacted with 1-(chloromethyl)-3-(trifluoromethyl)benzene (60 mg, 0.31 mmol) using general method **19** to afford the title compound **90d** as a colourless oil (64 mg, 69%). LCMS purity >95%, ret. time 1.56 mins; HRMS (ESI +ve): found $[M+H]^+$ 385.1040, $[C_{17}H_{17}F_3ClN_4O]^+$ requires 385.1043; $[\alpha]_D^{23.7}$: -6.2° (*c* 1.0, MeOH); δ_H (CDCl₃, 500 MHz): 7.74 (1H, s, H₇), 7.61 – 7.58 (2H, m, H₂ & H₆), 7.52 – 7.47 (2H, m, H₃ & H₄), 5.63 (1H, d, *J* = 15.1 Hz, ArCH_H), 4.21 (1H, d, *J* = 15.1 Hz, ArCH_H), 4.17 (1H, dd, *J* = 6.3, 3.5 Hz, CHCH₂CH₃), 3.35 (3H, s, CONCH₃), 2.03 – 1.94 (1H, m, CHCH₂CH₃), 1.89 – 1.80 (1H, m, CHCH₂CH₃), 0.84 (3H, t, *J* = 7.6 Hz, CHCH₂CH₃); δ_C (CDCl₃, 126 MHz): 163.3 (CONCH₃), 154.2 (C₈), 152.3 (C₅), 138.4 (C₇), 136.3 (C₅), 131.7 (C₄), 131.3 (q, *J*_{C-F} = 32 Hz, C₁), 129.5 (C₃), 125.3 – 125.1 (m, C₂ & C₆), 123.8 (q, *J*_{C-F} = 272 Hz, CF₃), 120.5 (C₆), 60.6 (CHCH₂CH₃), 47.5 (ArCH₂), 28.3 (CONCH₃), 24.9 (CHCH₂CH₃), 8.6 (CHCH₂CH₃); $\delta_{F(H)}$ (CDCl₃, 471 MHz): -62.7

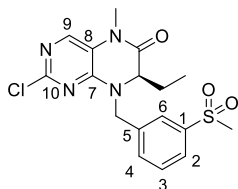
(*R*)-3-((2-Chloro-7-ethyl-5-methyl-6-oxo-6,7-dihydropteridin-8(5*H*)-yl)methyl)benzonitrile, 90e

Dihydropteridinone **79** (50 mg, 0.22 mmol) was reacted with 3-(bromomethyl)benzonitrile (35 μ L, 0.28 mmol) using general method **19** to afford the



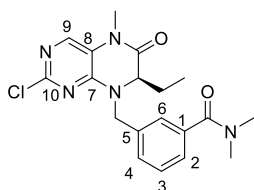
title compound **90e** as a white solid (28 mg, 37%). LCMS purity >95%, ret. time 1.39 mins; HRMS (ESI +ve): found $[M+H]^+$ 342.1112, $[C_{17}H_{17}ClN_5O]^+$ requires 342.1116; $[\alpha]_D^{22.9}$: -4.9° (c 1.0, MeOH); δ_H (CDCl₃, 500 MHz): 7.74 (1H, s, H₉), 7.63 – 7.59 (2H, m, H₂ & H₆), 7.56 (1H, d, J = 7.7 Hz, H₄), 7.47 (1H, t, J = 7.7 Hz, H₃), 5.58 (1H, d, J = 15.5 Hz, ArCH_H), 4.18 (1H, d, J = 15.5 Hz, ArCH_H), 4.15 (1H, dd, J = 6.5, 3.6 Hz, CHCH₂CH₃), 3.35 (3H, s, CONCH₃), 2.01 – 1.94 (1H, m, CHCH₂CH₃), 1.87 – 1.78 (1H, m, CHCH₂CH₃), 0.83 (3H, t, J = 7.6 Hz, CHCH₂CH₃); δ_C (CDCl₃, 126 MHz): 163.1 (CONCH₃), 154.1 (C₁₀), 152.1 (C₇), 138.4 (C₉), 137.0 (C₅), 132.6 (C₄), 131.8 (C₆), 131.6 (C₂), 129.8 (C₃), 120.4 (C₈), 118.2 (CN), 113.1 (C₁), 60.8 (CHCH₂CH₃), 47.2 (ArCH₂), 28.3 (CONCH₃), 24.9 (CHCH₂CH₃), 8.5 (CHCH₂CH₃)

(R)-2-Chloro-7-ethyl-5-methyl-8-(3-(methylsulfonyl)benzyl)-7,8-dihydropteridin-6(5H)-one, 90f



Dihydropteridinone **79** (70.0 mg, 0.31 mmol) was reacted with 1-(bromomethyl)-3-(methylsulfonyl)benzene (92.3 mg, 0.37 mmol) using general method **19** to afford the title compound **90f** as a white solid (42.0 mg, 34%). LCMS purity >95%, ret. time 1.29 mins; HRMS (ESI +ve): found $[M+H]^+$ 359.0943, $[C_{17}H_{20}ClN_4O_3S]^+$ requires 359.0939; $[\alpha]_D^{22.5}$: -13.9° (c 1.0, MeOH); δ_H (CDCl₃, 500 MHz): 7.92 – 7.88 (2H, m, H₂ & H₆), 7.74 (1H, s, H₉), 7.61 (1H, d, J = 7.6 Hz, H₄), 7.59 – 7.54 (1H, m, H₃), 5.59 (1H, d, J = 15.3 Hz, ArCH_H), 4.25 (1H, d, J = 15.3 Hz, ArCH_H), 4.19 (1H, dd, J = 6.6, 3.5 Hz, CHCH₂CH₃), 3.35 (3H, s, CONCH₃), 3.07 (3H, s, SO₂CH₃), 2.03 – 1.95 (1H, m, CHCH₂CH₃), 1.89 – 1.80 (CHCH₂CH₃), 0.80 (3H, t, J = 7.6 Hz, CHCH₂CH₃); δ_C (CDCl₃, 126 MHz): 163.2 (CONCH₃), 154.1 (C₁₀), 152.2 (C₇), 141.3 (C₁), 138.5 (C₉), 137.4 (C₅), 133.4 (C₄), 130.1 (C₃), 127.3 (C₂/6), 127.2 (C₂/6), 120.6 (C₈), 61.1 (CHCH₂CH₃), 47.7 (ArCH₂), 44.6 (SO₂CH₃), 28.3 (CONCH₃), 25.0 (CHCH₂CH₃), 8.6 (CHCH₂CH₃)

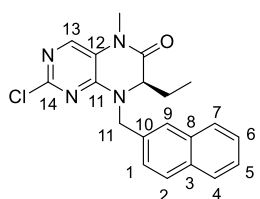
(R)-3-((2-Chloro-7-ethyl-5-methyl-6-oxo-6,7-dihydropteridin-8(5H)-yl)methyl)-N,N-dimethylbenzamide, 90g



Dihydropteridinone **79** (80 mg, 0.35 mmol) was reacted with 3-(chloromethyl)-N,N-dimethylbenzamide (88 mg, 0.45 mmol) using general method **19** to afford the title compound **90g** as a white solid (42 mg, 34%). LCMS purity >95%, ret. time 1.35 mins; HRMS (ESI +ve): found $[M+H]^+$ 388.1532, $[C_{19}H_{23}ClN_5O_2]^+$ requires 388.1540; $[\alpha]_D^{23.9}$: $+4.2^\circ$ (c 1.0, MeOH); δ_H (CDCl₃, 500 MHz): 7.72 (1H, s, H₉), 7.41 – 7.34 (4H,

m, H1, H3, H4, H6), 5.63 (1H, d, $J = 15.2$ Hz, ArCHH), 4.20 (1H, dd, $J = 6.3, 3.4$ Hz, CHCH₂CH₃), 4.16 (1H, d, $J = 15$ Hz, ArCHH), 3.35 (3H, s, CONCH₃), 3.11 (3H, s, N(CH₃)(C'H₃)), 2.97 (3H, s, N(CH₃)(C'H₃)), 2.01 – 1.95 (1H, m, CHCH₂HCH₃), 1.89 – 1.84 (1H, m, CHCH₂HCH₃), 0.84 (3H, t, $J = 7.5$ Hz, CHCH₂CH₃); δ_c (CDCl₃, 126 MHz): 171.0 (CON(CH₃)₂), 163.4 (CONCH₃), 154.2 (C10), 152.3 (C7), 138.2 (C9), 137.1 (C2), 135.6 (C6), 129.3 (C1/C5), 129.0 (C3/C4), 127.1 (C1/C5), 126.9 (C3/C4), 120.5 (C8), 60.5 (CHCH₂CH₃), 47.8 (ArCH₂), 39.6 (N(CH₃)(C'H₃)), 35.4 (N(CH₃)(C'H₃)), 28.3 (CONCH₃), 24.8 (CHCH₂CH₃), 8.6 (CHCH₂CH₃)

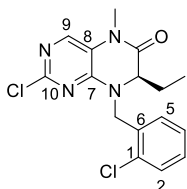
(R)-2-Chloro-7-ethyl-5-methyl-8-(naphthalen-2-ylmethyl)-7,8-dihydropteridin-6(5H)-one, 90h



Dihydropteridinone **79** (50 mg, 0.22 mmol) was reacted with 2-(bromomethyl)naphthalene (34 μ L, 0.26 mmol) using general method **19** to afford the title compound **90h** as a white solid (35 mg, 43%). LCMS purity >95%, ret. time 1.61 mins; HRMS (ESI +ve): found $[M+H]^+$ 367.1322, $[C_{20}H_{20}ClN_4O]^+$ requires

367.1320; $[\alpha]_D^{23.5}$: +6.2° (c 1.0, MeOH); δ_H (CDCl₃, 500 MHz): 7.86 – 7.81 (3H, m, H2, H4, & H7), 7.76 (1H, s, H9), 7.72 (1H, s, H14), 7.53 – 7.50 (2H, m, H5 & H6), 7.40 (1H, dd, $J = 8.4, 1.7$ Hz, H1), 5.82 (1H, d, $J = 15.1$ Hz, H11^a), 5.82 (1H, d, $J = 15.1$ Hz, H11^b), 4.21 (1H, dd, $J = 6.3, 3.5$ Hz, CHCH₂CH₃), 3.34 (3H, s, NCH₃), 2.01 – 1.86 (CHCH₂CH₃), 0.85 (3H, t, $J = 7.4$ Hz, CHCH₂CH₃); δ_c (CDCl₃, 126 MHz): 163.6 (CONCH₃), 154.3 (C13), 152.5 (C12), 138.2 (C14), 133.3 (C8), 133.1 (C3), 132.3 (C10), 129.1 (C4), 127.8 (C2/7/9 & C2/7/9), 127.7 (C2/7/9), 126.6 (C6), 126.4 (C5), 125.9 (C1), 120.5 (C13), 60.0 (CHCH₂CH₃), 47.9 (C11), 28.2 (NCH₃), 24.8 (CHCH₂CH₃), 8.6 (CHCH₂CH₃)

(R)-2-Chloro-8-(2-chlorobenzyl)-7-ethyl-5-methyl-7,8-dihydropteridin-6(5H)-one, 90i

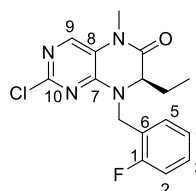


Dihydropteridinone **79** (95 mg, 0.42 mmol) was reacted with 1-(bromomethyl)-2-chloro-benzene (103 mg, 0.50 mmol) using general method **19** to afford the title compound **90i** as a white solid (100 mg, 68%). LCMS purity >95%, ret. time 1.56 mins; HRMS (ESI

+ve): found $[M+H]^+$ 351.0789, $[C_{16}H_{17}Cl_2N_4O]^+$ requires 351.0774; $[\alpha]_D^{22.7}$: -19.4° (c 1.0, MeOH); δ_H (CDCl₃, 500 MHz): 7.72 (1H, s, H9), 7.42 – 7.38 (2H, m, H2/4 & H5), 7.40 – 7.25 (2H, m, H2/4 & H3), 5.64 (1H, d, $J = 15.3$ Hz, ArCHH), 4.35 (1H, d, $J = 15.3$ Hz, ArCHH), 4.21 (1H, dd, $J = 6.6, 3.8$ Hz, CHCH₂CH₃), 3.35 (3H, s, CONCH₃), 2.02 – 1.93 (CHCH₂HCH₃), 1.92 – 1.85 (CHCH₂HCH₃), 0.89 (3H, t, $J = 7.6$ Hz,

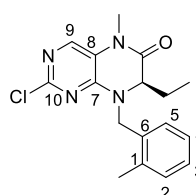
CHCH₂CH₃); δ_{C} (CDCl₃, 126 MHz): 163.6 (CONCH₃), 154.2 (C10), 152.4 (C7), 138.2 (C9), 134.2 (C6), 132.6 (C1), 130.8 (C5), 130.0 (C2/4), 129.6 (C2/4), 127.2 (C3), 120.6 (C8), 60.7 (CHCH₂CH₃), 45.6 (ArCH₂), 28.2 (CONCH₃), 25.2 (CHCH₂CH₃), 8.8 (CHCH₂CH₃)

(R)-2-Chloro-7-ethyl-8-(2-fluorobenzyl)-5-methyl-7,8-dihydropteridin-6(5H)-one, 90j



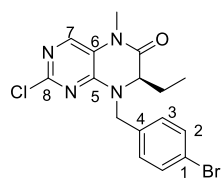
Dihydropteridinone **79** (55 mg, 0.24 mmol) was reacted with 1-(bromomethyl)-2-fluoro-benzene (55 mg, 0.29 mmol) using general method **19** to afford the title compound **90j** as a white solid (64 mg, 69%). LCMS purity >95%, ret. time 1.52 mins; HRMS (ESI +ve): found $[M+H]^+$ 335.1074, $[C_{16}H_{17}ClFN_4O]^+$ requires 335.1069; $[\alpha]_D^{22.5}$: - 8.2° (c 1.0, MeOH); δ_{H} (CDCl₃, 500 MHz): 7.69 (1H, s, H9), 7.41 (1H, td, $J = 7.5, 1.7$ Hz, H5), 7.34 – 7.29 (1H, m, H3), 7.14 (1H, td, $J = 7.5, 1.1$ Hz, H4), 7.10 – 7.06 (1H, m, H2), 5.56 (1H, d, $J = 14.8$ Hz, ArCHH), 4.30 – 4.24 (2H, m, ArCHH & CHCH₂CH₃), 3.33 (3H, s, CONCH₃), 2.04 – 1.86 (CHCH₂CH₃), 1.94 – 1.85 (CHCH₂CH₃), 0.86 (3H, t, $J = 7.4$ Hz, CHCH₂CH₃); δ_{C} (CDCl₃, 126 MHz): 163.6 (CONCH₃), 162.4 (d, $J_{\text{C-F}} = 247$ Hz, C1), 154.2 (C10), 152.3 (C7), 138.1 (C9), 131.2 (d, $J_{\text{C-F}} = 3.7$ Hz, C5), 130.1 (d, $J_{\text{C-F}} = 8.3$ Hz, C3), 124.6 (d, $J_{\text{C-F}} = 3.7$ Hz, C4), 122.1 (d, $J_{\text{C-F}} = 14.7$ Hz, C6), 120.6 (d, $J_{\text{C-F}} = 21.1$ Hz, C2), 60.6 (CHCH₂CH₃), 41.6 (ArCH₂), 28.2 (CONCH₃), 25.1 (CHCH₂CH₃), 8.7 (CHCH₂CH₃); $\delta_{\text{F}\{\text{H}\}}$ (CDCl₃, 471 MHz): - 117.7

(R)-2-Chloro-7-ethyl-5-methyl-8-(2-methylbenzyl)- 7,8-dihydropteridin-6(5H)-one, 90k



Dihydropteridinone **79** (95 mg, 0.42 mmol) was reacted with 1-(bromomethyl)-2-methyl-benzene (93 mg, 0.50 mmol) using general method **19** to afford the title compound **90k** as a yellow solid (98 mg, 71%). LCMS purity >95%, ret. time 1.54 mins; HRMS (ESI +ve): found $[M+H]^+$ 331.1319, $[C_{17}H_{20}ClN_4O]^+$ requires 331.1320; $[\alpha]_D^{22.4}$: +24.9° (c 1.0, MeOH); δ_{H} (CDCl₃, 500 MHz): 7.71 (1H, s, H9), 7.26 – 7.22 (1H, m, H3), 7.20 – 7.17 (3H, m, H2, H4 & H5), 5.70 (1H, d, $J = 15.1$ Hz, ArCHH), 4.07 (1H, d, $J = 15.1$ Hz, ArCHH), 4.04 (1H, dd, $J = 6.5, 3.6$ Hz, CHCH₂CH₃), 3.34 (3H, s, CONCH₃), 2.26 (3H, s, ArCH₃), 1.97 – 1.82 (2H, m, CHCH₂CH₃), 0.80 (3H, t, $J = 7.6$ Hz, CHCH₂CH₃); δ_{C} (CDCl₃, 126 MHz): 163.7 (CONCH₃), 154.3 (C10), 153.4 (C7), 138.1 (C9), 137.1 (C1), 132.3 (C6), 131.0 (C2), 129.3 (C5), 128.5 (C3), 126.3 (C4), 120.6 (C8), 59.3 (CHCH₂CH₃), 45.8 (ArCH₂), 28.2 (CONCH₃), 24.8 (CH₃), 19.3 (CHCH₂CH₃), 8.7 (CHCH₂CH₃)

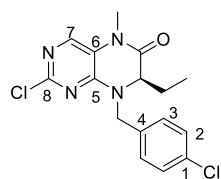
(R)-2-Chloro-8-(4-bromobenzyl)-7-ethyl-5-methyl-7,8-dihydropteridin-6(5H)-one, 90l



Dihydropteridinone **79** (44 mg, 0.19 mmol) was reacted with 4-bromobenzyl bromide (61 mg, 0.25 mmol) using general method **19** to afford the title compound **90l** as a white solid (29 mg, 37%).

LCMS purity >95%, ret. time 1.53 mins; HRMS (ESI +ve): found $[M+H]^+$ 397.0249, $[C_{16}H_{17}BrClN_4O]^+$ requires 397.0247; $[\alpha]_D^{22.3}$: -47.1° (c 1.0, MeOH); δ_H (CDCl₃, 500 MHz): 7.71 (1H, s, H7), 7.47 (1H, d, J = 8.5 Hz, H2), 7.18 (2H, d, J = 8.5 Hz, H3), 5.52 (1H, d, J = 15.1 Hz, ArCHH), 4.14 (1H, dd, J = 6.3, 3.5 Hz, CHCH₂CH₃), 4.10 (1H, d, J = 15.1 Hz, ArCHH), 3.33 (3H, s, CONCH₃), 1.98 – 1.90 (CHCH₂CH₃), 1.86 – 1.77 (CHCH₂CH₃), 0.81 (3H, t, J = 7.6 Hz, CHCH₂CH₃); δ_C (CDCl₃, 126 MHz): 163.4 (CONCH₃), 154.2 (C8), 152.3 (C5), 138.2 (C6), 134.2 (C4), 132.1 (C2), 130.1 (C3), 122.3 (C1), 120.5 (C6), 60.4 (CHCH₂CH₃), 47.3 (ArCH₂), 28.3 (CONCH₃), 24.9 (CHCH₂CH₃), 8.6 (CHCH₂CH₃)

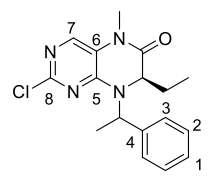
(R)-2-Chloro-8-(4-chlorobenzyl)-7-ethyl-5-methyl-7,8-dihydropteridin-6(5H)-one, 90m



Dihydropteridinone **79** (70 mg, 0.31 mmol) was reacted with 1-(bromomethyl)-4-chloro-benzene (41 mg, 0.20 mmol) using general method **19** to afford the title compound **90m** as a white solid (44 mg, 40%). LCMS purity >95%, ret. time 1.56 mins; HRMS

(ESI +ve): found $[M+H]^+$ 351.0780, $[C_{16}H_{17}Cl_2N_4O]^+$ requires 351.0774; $[\alpha]_D^{24.1}$: $+2.8^\circ$ (c 1.0, MeOH); δ_H (CDCl₃, 500 MHz): 7.71 (1H, s, H7), 7.33 (2H, d, J = 8.3 Hz, H2), 7.25 (2H, d, J = 8.3 Hz, H3), 5.55 (1H, d, J = 15.1 Hz, ArCHH), 4.15 (1H, dd, J = 6.3, 3.5 Hz, CHCH₂CH₃), 4.12 (1H, d, J = 15.1 Hz, ArCHH), 3.34 (3H, s, CONCH₃), 2.00 – 1.92 (CHCH₂CH₃), 1.87 – 1.78 (CHCH₂CH₃), 0.83 (3H, t, J = 7.6 Hz, CHCH₂CH₃); δ_C (CDCl₃, 126 MHz): 163.4 (CONCH₃), 154.2 (C8), 152.3 (C5), 138.3 (C7), 134.2 (C1), 133.6 (C4), 129.8 (C3), 129.2 (C2), 120.5 (C6), 60.3 (CHCH₂CH₃), 47.3 (ArCH₂), 28.3 (CONCH₃), 24.9 (CHCH₂CH₃), 8.8 (CHCH₂CH₃)

(7R)-2-Chloro-7-ethyl-5-methyl-8-(1-phenylethyl)-7,8-dihydropteridin-6(5H)-one, 90n

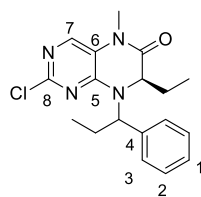


Dihydropteridinone **79** (80 mg, 0.35 mmol) was reacted with (1-bromoethyl)benzene (58 μ L, 0.42 mmol) using general method **19** to afford the title compound **90n** as a white solid (43 mg, 37% d.r. 2:1).

LCMS purity >95%, ret. time 1.54 mins; HRMS (ESI +ve): found $[M+H]^+$ 331.1317, $[C_{17}H_{20}ClN_4O]^+$ requires 331.1320; *Major Isomer* δ_H (CDCl₃, 500

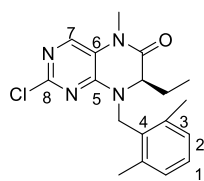
MHz): 7.73 (1H, s, H7), 7.40 – 7.36 (2H, m, H2), 7.35 – 7.30 (3H, m, H1 & H3), 5.95 (1H, q, $J = 7.2$ Hz, CHCH_3), 3.93 (1H, dd, $J = 7.6, 3.2$ Hz, CHCH_2CH_3), 3.32 (3H, s, CONCH_3), 1.91 – 1.83 (1H, m, CHCHHCH_3), 1.78 (3H, d, $J = 7.3$ Hz, CHCH_3), 1.75 – 1.69 (1H, m, CHCHHCH_3), 0.83 (3H, t, $J = 7.6$ Hz, CHCH_2CH_3); δ_{C} (CDCl_3 , 126 MHz): 163.5 (CONCH_3), 154.2 (C8), 152.5 (C5), 138.3 (C4 & C7), 129.0 (C2), 128.3 (C1), 127.6 (C3), 120.9 (C6), 58.1 (CHCH_2CH_3), 54.6 (CHCH_3), 28.3 (CONCH_3), 28.1 (CHCH_2CH_3), 17.4 (CHCH_3), 8.8 (CHCH_2CH_3); *Minor Isomer* δ_{H} (CDCl_3 , 500 MHz): 7.72 (1H, s, H7), 7.57 – 7.54 (2H, m, H2), 7.40 – 7.36 (1H, m, H1), 7.35 – 7.30 (2H, m, H3), 6.15 (1H, d, $J = 7.3$ Hz, CHCH_3), 4.22 (1H, dd, $J = 8.2, 3.5$ Hz, CHCH_2CH_3), 3.32 (3H, s, NCH_3), 1.68 (3H, d, $J = 6.9$ Hz, CHCH_3), 1.11 – 1.03 (CHCHHCH_3), 1.02 – 0.93 (CHCHHCH_3), 0.54 (3H, t, $J = 7.4$ Hz, CHCH_2CH_3); δ_{C} (CDCl_3 , 126 MHz): 163.4 (CONCH_3), 154.1 (C8), 152.4 (C5), 139.6 (C4), 138.6 (C7), 128.7 (C2), 128.4 (C1), 128.1 (C3), 121.2 (C6), 58.1 (CHCH_2CH_3), 53.1 (CHCH_3), 28.4 (CONCH_3), 17.4 (CHCH_3), 16.6 (CHCH_2CH_3), 9.0 (CHCH_2CH_3)

(7*R*)-2-Chloro-7-ethyl-5-methyl-8-(1-phenylpropyl)-7,8-dihydropteridin-6(5*H*)-one, **90o**



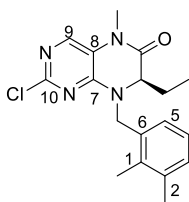
Dihydropteridinone **79** (80 mg, 0.35 mmol) was reacted with (1-bromopropyl)benzene 64 μL , 0.42 mmol) using general method **19** to afford the title compound **90o** as a white solid (43 mg, 35% d.r. 2:1). LCMS purity >95%, ret. time 1.59 mins; HRMS (ESI +ve): found $[\text{M}+\text{H}]^+$ 345.1477, $[\text{C}_{18}\text{H}_{22}\text{ClN}_4\text{O}]^+$ requires 345.1477; *Major Isomer* δ_{H} (CDCl_3 , 500 MHz): 7.70 (1H, s, H7), 7.38 – 7.30 (5H, m, H1, H2 & H3), 5.58 (1H, d, $J = 7.6$ Hz, $\text{ArCHCH}_2\text{CH}_3$), 3.93 (1H, dd, $J = 7.7, 3.3$ Hz, CHCH_2CH_3), 3.27 (3H, s, CONCH_3), 2.20 (2H, *app. quin.*, $J = 7.3$ Hz, $\text{ArCHCH}_2\text{CH}_3$), 1.90 – 1.82 (1H m, CHCHHCH_3), 1.74 – 1.66 (1H, m, CHCHHCH_3), 1.03 (3H, t, $J = 7.3$ Hz, $\text{ArCHCH}_2\text{CH}_3$), 0.81 (3H, t, $J = 7.4$ Hz, $\text{ArCHCH}_2\text{CH}_3$); δ_{C} (CDCl_3 , 126 MHz): 163.4 (CONCH_3), 154.1 (C8), 152.5 (C4), 138.3 (C7), 136.9 (C4), 129.0 (C2/3), 128.5 (C2/3), 128.4 (C1), 120.8 (C6), 61.8 ($\text{ArCHCH}_2\text{CH}_3$), 58.4 (CHCH_2CH_3), 28.3 (CONCH_3), 28.1 (CHCH_2CH_3), 24.4 ($\text{ArCHCH}_2\text{CH}_3$), 11.6 ($\text{ArCHCH}_2\text{CH}_3$), 8.9 (CHCH_2CH_3); *Minor Isomer* δ_{H} (CDCl_3 , 500 MHz): 7.72 (1H, s, H7), 7.38 – 7.30 (5H, m, H1, H2 & H3), 5.94 (1H, d, $J = 8.0$ Hz, $\text{ArCHCH}_2\text{CH}_3$), 4.14 – 4.10 (1H, m, CHCH_2CH_3), 3.32 (3H, s, CONCH_3), 2.11 (2H, *app. quin.*, $J = 7.2$ Hz, $\text{ArCHCH}_2\text{CH}_3$), 0.92 – 0.86 (5H, m, CHCH_2CH_3 & $\text{ArCHCH}_2\text{CH}_3$), 0.51 (3H, t, $J = 7.4$ Hz, CHCH_2CH_3); δ_{C} (CDCl_3 , 126 MHz): 163.3 (CONCH_3), 154.1 (C8), 153.1 (C4), 138.9 (C4), 138.8 (C7), 128.8 (C1/2/3), 128.5 (C1/2/3), 128.4 (C1/2/3), 59.0 ($\text{ArCHCH}_2\text{CH}_3$), 57.6 (CHCH_2CH_3), 28.5 (CONCH_3), 26.4 (CHCH_2CH_3), 23.1 ($\text{ArCHCH}_2\text{CH}_3$), 11.1 ($\text{ArCHCH}_2\text{CH}_3$), 9.2 (CHCH_2CH_3)

(*R*)-2-Chloro-8-(2,6-dimethylbenzyl)-7-ethyl-5-methyl-7,8-dihydropteridin-6(5*H*)-one, 90p



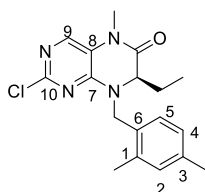
Dihydropteridinone **79** (58 mg, 0.26 mmol) was reacted with 2-(chloromethyl)-1,3-dimethyl-benzene (65 μ L, 0.30 mmol) using general method **19** to afford the title compound **90p** as a white solid (30 mg, 34%). LCMS purity >95%, ret. time 1.59 mins; HRMS (ESI +ve): found $[M+H]^+$ 345.1474, $[C_{18}H_{22}ClN_4O]^+$ requires 345.1477; $[\alpha]_D^{22.5}$: +4.2° (c 1.0, MeOH); δ_H (CDCl₃, 500 MHz): 7.72 (1H, s, H7), 7.13 (1H, t, J = 7.6 Hz, H1), 7.04 (2H, d, J = 7.6 Hz, H2), 5.53 (1H, d, J = 15.0 Hz, ArCHH), 4.34 (1H, d, J = 15.0 Hz, ArCHH), 3.81 (1H, dd, J = 7.6, 3.5 Hz, CHCH₂CH₃), 3.32 (3H, s, CONCH₃), 2.28 (6H, s, 2 x ArCH₃), 1.94 – 1.86 (CHCH₂CH₃), 1.78 – 1.69 (CHCH₂CH₃), 0.85 (3H, t, J = 7.6 Hz, CHCH₂CH₃); δ_C (CDCl₃, 126 MHz): 163.8 (CONCH₃), 154.3 (C8), 152.5 (C5), 138.0 (C3 & C7), 130.5 (C4), 129.0 (C2), 128.3 (C1), 120.8 (C6), 58.7 (CHCH₂CH₃), 42.6 (ArCH₂), 28.2 (CONCH₃), 25.4 (CHCH₂CH₃), 20.2 (2 x ArCH₃), 9.2 (CHCH₂CH₃)

(*R*)-2-Chloro-8-(2,3-dimethylbenzyl)-7-ethyl-5-methyl-7,8-dihydropteridin-6(5*H*)-one, 90q



Dihydropteridinone **79** (59 mg, 0.26 mmol) was reacted with 1-(chloromethyl)-2,3-dimethyl-benzene (65 μ L, 0.31 mmol) using general method **19** to afford the title compound **90q** as a white solid (60 mg, 69%). LCMS purity >95%, ret. time 1.60 mins; HRMS (ESI +ve): found $[M+H]^+$ 345.1475, $[C_{18}H_{22}ClN_4O]^+$ requires 345.1477; $[\alpha]_D^{22.4}$: +33.9° (c 1.0, MeOH); δ_H (CDCl₃, 500 MHz): 7.70 (1H, s, H9), 7.14 (1H, d, J = 7.4 Hz, H3), 7.10 – 7.06 (1H, m, H4), 7.05 (1H, d, J = 6.5 Hz, H5), 5.73 (1H, d, J = 15.1 Hz, ArCHH), 4.04 (1H, d, J = 15.1 Hz, ArCHH), 3.99 (1H, dd, J = 6.5, 3.6 Hz, CHCH₂CH₃), 3.33 (3H, s, CONCH₃), 2.29 (3H, s, C¹CH₃), 2.12 (C²CH₃), 1.95 – 1.80 (CHCH₂CH₃), 0.83 (3H, t, J = 7.5 Hz, CHCH₂CH₃); δ_C (CDCl₃, 126 MHz): 163.8 (CONCH₃), 154.3 (C10), 152.3 (C7), 138.0 (C9), 137.9 (C1), 131.9 (C6), 130.3 (C3), 127.6 (C5), 125.8 (C4), 120.6 (C8), 58.9 (CHCH₂CH₃), 46.4 (ArCH₂), 28.2 (CONCH₃), 24.7 (CHCH₂CH₃), 20.5 (C²CH₃), 15.2 (C¹CH₃), 8.7 (CHCH₂CH₃)

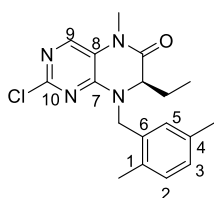
(*R*)-2-Chloro-8-(2,4-dimethylbenzyl)-7-ethyl-5-methyl-7,8-dihydropteridin-6(5*H*)-one, 90r



Dihydropteridinone **79** (57 mg, 0.25 mmol) was reacted with 1-(bromomethyl)-2,4-dimethyl-benzene (48 μ L, 0.32 mmol) using general method **19** to afford the title compound **90r** as a white solid (68 mg, 79%). LCMS purity >95%, ret. time 1.60 mins; HRMS (ESI

(+ve): found $[M+H]^+$ 345.1472, $[C_{18}H_{22}ClN_4O]^+$ requires 345.1477; $[\alpha]_D^{22.3}$: +24.9° (*c* 1.0, MeOH); δ_H (CDCl₃, 500 MHz): 7.70 (1H, s, H₉), 7.08 (1H, d, *J* = 7.8 Hz, H₅), 7.02 (1H, s, H₂), 6.99 (1H, d, *J* = 7.8 Hz, H₄), 5.66 (1H, d, *J* = 15.1 Hz, ArCHH), 4.05 – 4.01 (2H, m, ArCHH & CHCH₂CH₃), 3.33 (3H, s, CONCH₃), 2.32 (3H, s, C³CH₃), 2.21 (3H, s, C¹CH₃), 1.96 – 1.79 (2H, m, CHCH₂CH₃), 0.84 (3H, t, *J* = 7.4 Hz, CHCH₂CH₃); δ_C (CDCl₃, 126 MHz): 163.8 (CONCH₃), 154.3 (C₁₀), 152.4 (C₇), 138.3 (C₃), 138.0 (C₉), 136.9 (C₁), 131.9 (C₂), 129.6 (C₅), 129.0 (C₆), 126.9 (C₄), 120.5 (C₈), 59.1 (CHCH₂CH₃), 45.7 (ArCH₂), 28.2 (CONCH₃), 24.7 (CHCH₂CH₃), 21.0 (C³CH₃), 19.3 (C¹CH₃), 8.7 (CHCH₂CH₃)

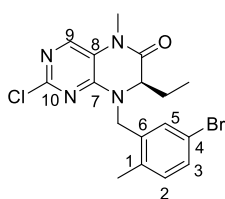
(*R*)-2-Chloro-8-(2,5-dimethylbenzyl)-7-ethyl-5-methyl-7,8-dihydropteridin-6(5*H*)-one, 90s



Dihydropteridinone **79** (65 mg, 0.29 mmol) was reacted with 2-(bromomethyl)-1,4-dimethyl-benzene (65 μ L, 0.34 mmol) using general method **19** to afford the title compound **90s** as a white solid (35 mg, 35%). LCMS purity >95%, ret. time 1.60 mins; HRMS

(ESI +ve): found $[M+H]^+$ 345.1474, $[C_{18}H_{22}ClN_4O]^+$ requires 345.1477; $[\alpha]_D^{22.0}$: +22.9° (*c* 1.0, MeOH); δ_H (CDCl₃, 500 MHz): 7.70 (1H, s, H₉), 7.09 – 7.03 (1H, m, H₂ & H₃), 6.99 (1H, s, H₅), 5.68 (1H, d, *J* = 15.0 Hz, ArCHH), 4.05 (1H, dd, *J* = 6.5, 3.6 Hz, CHCH₂CH₃), 4.01 (1H, d, *J* = 15.0 Hz, ArCHH), 3.34 (3H, s, CONCH₃), 2.31 (3H, s, C⁴CH₃), 2.20 (C¹CH₃), 1.98 – 1.81 (2H, m, CHCH₂CH₃), 0.84 (3H, t, *J* = 7.6 Hz, CHCH₂CH₃); δ_C (CDCl₃, 126 MHz): 163.8 (CONCH₃), 154.3 (C₁₀), 153.4 (C₇), 138.0 (C₉), 135.8 (C₄), 134.0 (C₁), 131.9 (C₆), 131.0 (C₂), 130.2 (C₅), 129.2 (C₃), 120.5 (C₈), 59.1 (CHCH₂CH₃), 45.8 (ArCH₂), 28.2 (CONCH₃), 24.7 (CHCH₂CH₃), 21.0 (C⁴CH₃), 19.0 (C¹CH₃), 8.7 (CHCH₂CH₃)

(*R*)-8-(5-bromo-2-methylbenzyl)-2-chloro-7-ethyl-5-methyl-7,8-dihydropteridin-6(5*H*)-one, 90t

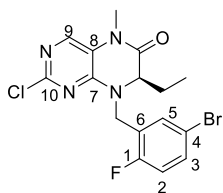


Dihydropteridinone **79** (50 mg, 0.22 mmol) was reacted with 4-bromo-2-(bromomethyl)-1-methyl-benzene (91 μ L, 0.26 mmol) using general method **19** to afford the title compound **90t** as a white solid (44 mg, 49%). LCMS purity >95%, ret. time 1.59 mins;

HRMS (ESI +ve): found $[M+H]^+$ 411.0401, $[C_{17}H_{19}BrClN_4O]^+$ requires 411.0404; $[\alpha]_D^{23.5}$: -10.4° (*c* 1.0, MeOH); δ_H (CDCl₃, 500 MHz): 7.74 (1H, s, H₉), 7.37 (1H, dd, *J* = 8.2, 2.2 Hz, H₃), 7.32 (1H, d, *J* = 2.2 Hz, H₅), 7.08 (1H, d, *J* = 8.2 Hz, H₂), 5.65 (1H, d, *J* = 15.3 Hz, ArCHH), 4.06 (1H, dd, *J* = 6.6, 3.5 Hz, CHCH₂CH₃), 4.02 (1H, d, *J* = 15.3 Hz, ArCHH), 3.36 (3H, s, CONCH₃), 2.23 (3H, s, CH₃), 2.01 – 1.93

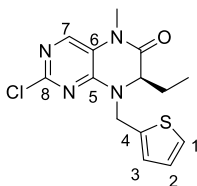
(CHCH₂CH₃), 1.90 – 1.81 (CHCH₂CH₃), 0.86 (3H, t, J = 7.6 Hz, CHCH₂CH₃); δ_C (CDCl₃, 126 MHz): 163.5 (CONCH₃), 154.3 (C10), 152.3 (C7), 138.3 (C9), 136.0 (C1), 134.8 (C6), 132.6 (C2), 131.9 (C5), 131.4 (C3), 120.6 (C8), 119.9 (C4), 59.7 (CHCH₂CH₃), 45.3 (ArCH₂), 28.3 (CONCH₃), 24.8 (CHCH₂CH₃), 19.0 (CH₃), 8.7 (CHCH₂CH₃)

(*R*)-8-(5-bromo-2-fluorobenzyl)-2-chloro-7-ethyl-5-methyl-7,8-dihydropteridin-6(5*H*)-one, 90u



Dihydropteridinone **79** (100 mg, 0.44 mmol) was reacted with 4-bromo-2-(bromomethyl)-1-fluoro-benzene (141 mg, 0.53 mmol) using general method **19** to afford the title compound **90u** as a white solid (50 mg, 27%). LCMS purity >95%, ret. time 1.59 mins; HRMS (ESI +ve): found $[M+H]^+$ 415.0150, $[C_{16}H_{16}BrClFN_4O]^+$ requires 415.0153; $[\alpha]_D^{24.2}$: -13.9° (c 1.0, MeOH); δ_H (CDCl₃, 500 MHz): 7.71 (1H, s, H9), 7.55 (1H, dd, J = 6.5, 2.4 Hz, H5), 7.43 – 7.40 (1H, m, H3), 6.98 (1H, t, J = 9.1 Hz, H2), 5.48 (1H, d, J = 14.8 Hz, ArCH₂), 4.25 – 4.21 (2H, m, ArCH₂ & CHCH₂CH₃), 3.34 (3H, s, CONCH₃), 2.06 – 1.99 (CHCH₂CH₃), 1.98 – 1.85 (CHCH₂CH₃), 0.86 (3H, t, J = 7.6 Hz, CHCH₂CH₃); δ_C (CDCl₃, 126 MHz): 163.4 (CONCH₃), 160.4 (d, J_{C-F} = 247 Hz, C1), 154.1 (C10), 152.1 (C7), 138.3 (C9), 134.0 (d, J_{C-F} = 3.7 Hz, C5), 133.0 (d, J_{C-F} = 8.3 Hz, C3), 124.5 (d, J_{C-F} = 16.5 Hz, C6), 120.6 (C8), 117.5 (d, J_{C-F} = 23.8 Hz, C2), 117.0 (d, J_{C-F} = 3.7 Hz, C4), 61.0 (CHCH₂CH₃), 41.3 (d, J_{C-F} = 3.7 Hz, ArCH₂), 28.3 (CONCH₃), 25.1 (CHCH₂CH₃), 8.7 (CHCH₂CH₃); $\delta_{F(H)}$ (CDCl₃, 471 MHz): - 117.7

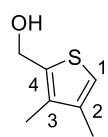
(*R*)-2-Chloro-7-ethyl-5-methyl-8-(thiophen-2-ylmethyl)-7,8-dihydropteridin-6(5*H*)-one, 90v



Dihydropteridinone **79** (70 mg, 0.31 mmol) was reacted with 2-(chloromethyl)thiophene (33% in toluene, 149 mg, 0.37 mmol,) using general method **19** to afford the title compound **90v** as a white solid (60 mg, 60%). LCMS purity >95%, ret. time 1.47 mins; HRMS (ESI +ve): found $[M+H]^+$ 323.0727, $[C_{14}H_{16}ClN_4OS]^+$ requires 323.0728; $[\alpha]_D^{22.6}$: -15.9° (c 1.0, MeOH); δ_H (CDCl₃, 500 MHz): 7.70 (1H, s, H7), 7.28 (1H, dd, J = 5.0, 1.3 Hz, H1), 7.09 – 7.07 (1H, m, H3), 6.98 (1H, dd, J = 5.0, 3.5 Hz, H2), 5.59 (1H, dd, J = 15.5, 1.3 Hz, ArCH₂), 4.43 (1H, d, J = 15.5 Hz, ArCH₂), 4.32 (1H, dd, J = 6.3, 3.2 Hz, CHCH₂CH₃), 3.33 (3H, s, CONCH₃), 2.05 – 1.97 (1H, m, CHCH₂CH₃), 1.93 – 1.84 (1H, m, CHCH₂CH₃), 0.82 (3H, t, J = 7.6 Hz, CHCH₂CH₃); δ_C (CDCl₃, 126 MHz): 163.5 (CONCH₃), 155.8 (C8), 153.7 (C5), 138.1 (C7), 137.1 (C4), 128.0 (C3), 129.9

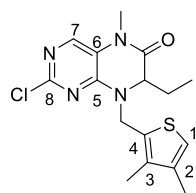
(C2), 126.6 (C1), 120.5 (C6), 60.3 ($\underline{\text{CHCH}_2\text{CH}_3}$), 42.9 (ArCH₂), 28.2 (CON $\underline{\text{CH}_3}$), 25.0 ($\text{CH}\underline{\text{CH}_2\text{CH}_3}$), 8.5 ($\text{CHCH}_2\underline{\text{CH}_3}$)

(3,4-Dimethylthiophen-2-yl)methanol, **132**



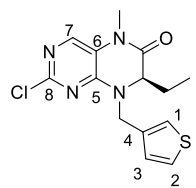
To a solution of 3,4-dimethylthiophene-2-carboxylic acid **131** (70 mg, 0.49 mmol) in THF (0.06 M), at 0 °C was added borane tetrahydrofuran complex (1.0 M in THF, 1.79 mL, 1.79 mmol). Upon completion, MeOH was added and concentrated *in vacuo*. Sat. aq. NaHCO₃ was added and the aqueous phase extracted with EtOAc (X3). The organic phases were combined, dried over MgSO₄ and concentrated *in vacuo* to afford the title compound **132** as a white solid (60 mg, 94%). δ_{H} (CDCl₃, 500 MHz): 6.84 (1H, d, J = 0.8 Hz, H1), 4.72 (2H, s, $\underline{\text{CH}_2\text{OH}}$), 2.16 (1H, d, J = 0.8 Hz, C²CH₃), 2.13 (3H, s, C³CH₃); δ_{C} (CDCl₃, 126 MHz): 138.2 (C2), 136.6 (C4), 134.7 (C3), 119.2 (C1), 58.1 (CH_2OH), 15.0 (C² $\underline{\text{CH}_3}$), 12.1 (C³ $\underline{\text{CH}_3}$)

(*R*)-2-Chloro-8-(3,4-dimethylthiophen-2-yl)methyl-7-ethyl-5-methyl-7,8-dihydropteridin-6(5*H*)-one, **90w**



Dihydropteridinone **79** (50 mg, 0.22 mmol) was reacted with **132** (50 mg, 0.35 mmol) using general method **19** to afford the title compound **90w** as a yellow oil (45 mg, 58%). LCMS purity >95%, ret. time 1.57 mins; HRMS (ESI +ve): found $[\text{M}+\text{H}]^+$ 351.1041, $[\text{C}_{16}\text{H}_{20}\text{ClN}_4\text{OS}]^+$ requires 351.1046; δ_{H} (CDCl₃, 500 MHz): 7.69 (1H, s, H7), 6.84 (1H, d, J = 0.8 Hz, H1), 5.66 (1H, d, J = 15.5 Hz, ArCH $\underline{\text{H}}$), 4.27 – 4.22 (2H, m, ArCH $\underline{\text{H}}$ & $\underline{\text{CHCH}_2\text{CH}_3}$), 3.32 (3H, s, CONCH₃), 2.14 (3H, d, J = 0.8 Hz, C²CH₃), 2.12 (3H, s, C³CH₃), 2.03 – 1.94 (1H, m, CHCH $\underline{\text{H}}$ CH₃), 1.90 – 1.80 (1H, m, CHCH $\underline{\text{H}}$ CH₃), 0.84 (3H, t, J = 7.4 Hz, $\text{CHCH}_2\underline{\text{CH}_3}$); δ_{C} (CDCl₃, 126 MHz): 166.6 ($\underline{\text{CONCH}_3}$), 154.2 (C8), 151.9 (C5), 138.1 (C2), 138.0 (C7), 136.6 (C3), 130.1 (C4), 120.5 (C6), 120.0 (C1), 59.6 ($\underline{\text{CHCH}_2\text{CH}_3}$), 41.0 (ArCH₂), 28.2 (CON $\underline{\text{CH}_3}$), 25.0 ($\text{CH}\underline{\text{CH}_2\text{CH}_3}$), 15.2 (C² $\underline{\text{CH}_3}$), 12.6 (C³CH₃), 8.7 ($\text{CHCH}_2\underline{\text{CH}_3}$)

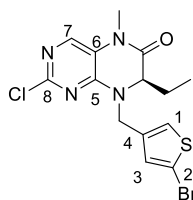
(*R*)-2-Chloro-7-ethyl-5-methyl-8-(thiophen-3-ylmethyl)-7,8-dihydropteridin-6(5*H*)-one, **90x**



Dihydropteridinone **79** (62 mg, 0.27 mmol) was reacted with 2-(bromomethyl)thiophene (38 μL , 0.35 mmol) using general method **19** to afford the title compound **90x** as a white solid (62 mg, 70%). LCMS purity >95%, ret. time 1.47 mins; HRMS (ESI +ve): found $[\text{M}+\text{H}]^+$ 323.0723, $[\text{C}_{14}\text{H}_{16}\text{ClN}_4\text{OS}]^+$ requires 323.0728; $[\alpha]_{\text{D}}^{23.2}$: -20.1° (c 1.0, MeOH); δ_{H} (CDCl₃, 500 MHz): 7.69 (1H, s, H7), 7.34 – 7.32 (1H, d, J = 4.7, H2), 7.27 – 7.26 (1H, s, H1), 7.05 (1H, d, J = 4.7 Hz, H3), 5.47 (1H, d, J = 15.1 Hz, ArCH $\underline{\text{H}}$), 4.26 –

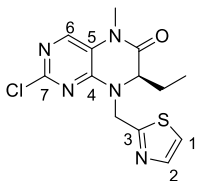
4.21 (2H, m, ArCH₂ & CHCH₂CH₃), 3.33 (3H, s, CONCH₃), 2.01 – 1.93 (1H, m, CHCH₂CH₃), 1.90 – 1.81 (1H, m, CHCH₂CH₃), 0.81 (3H, t, $J = 7.4$ Hz, CHCH₂CH₃); δ_c (CDCl₃, 126 MHz): 163.6 (CONCH₃), 154.2 (C8), 152.1 (C5), 128.0 (C7), 135.6 (C4), 127.6 (C3), 127.0 (C2), 124.4 (C1), 120.5 (C6), 60.2 (CHCH₂CH₃), 43.1 (ArCH₂), 28.2 (NCH₃), 24.9 (CHCH₂CH₃) 8.5 (CHCH₂CH₃)

(*R*)-8-((5-Bromothiophen-3-yl)methyl)-2-chloro-7-ethyl-5-methyl-7,8-dihydropteridin-6(5*H*)-one, 90y



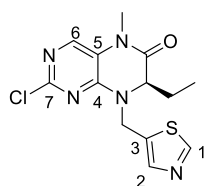
Dihydropteridinone **79** (55 mg, 0.24 mmol) was reacted with 4-bromo-2-(chloromethyl)thiophene (65 mg, 0.31 mmol,) using general method **19** to afford the title compound **90y** as a white solid (45 mg, 46%). LCMS purity >95%, ret. time 1.58 mins; HRMS (ESI +ve): found $[M+H]^+$ 402.9802, $[C_{14}H_{15}BrClN_4OS]^+$ requires 402.9811; $[\alpha]_D^{23.0}$: -11.1° (c 1.0, MeOH); δ_H (CDCl₃, 500 MHz): 7.69 (1H, s, H7), 7.16 – 7.15 (1H, m, H1), 6.99 (1H, d, $J = 1.6$ Hz, H3), 5.39 (1H, d, $J = 15.1$ Hz, ArCH₂), 4.21 (1H, dd, $J = 6.3, 3.5$ Hz, CHCH₂CH₃), 4.13 (1H, d, $J = 15.1$ Hz, ArCH₂), 3.32 (3H, s, CONCH₃), 2.02 – 1.93 (1H, m, CHCH₂CH₃), 1.87 – 1.80 (1H, m, CHCH₂CH₃), 0.80 (3H, t, $J = 7.4$ Hz, CHCH₂CH₃); δ_c (CDCl₃, 126 MHz): 163.4 (CONCH₃), 154.2 (C8), 151.9 (C5), 138.2 (C7), 136.4 (C4), 130.1 (C3), 125.7 (C1), 120.5 (C6), 113.7 (C2), 60.4 (CHCH₂CH₃), 43.1 (ArCH₂), 28.3 (CONCH₃), 24.9 (CHCH₂CH₃) 8.5 (CHCH₂CH₃)

(*R*)-2-Chloro-7-ethyl-5-methyl-8-(thiazol-2-ylmethyl)-7,8-dihydropteridin-6(5*H*)-one, 90z



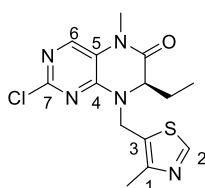
Dihydropteridinone **79** (60 mg, 0.26 mmol) was reacted with 2-(chloromethyl)thiazole (42 mg, 0.32 mmol) using general method **19** to afford the title compound **90z** as a white solid (37 mg, 43%). LCMS purity >95%, ret. time 1.30 mins; HRMS (ESI +ve): found $[M+H]^+$ 324.0674, $[C_{13}H_{15}ClN_5OS]^+$ requires 324.0680; $[\alpha]_D^{22.4}$: -11.1° (c 1.0, MeOH); δ_H (CDCl₃, 500 MHz): 7.74 (1H, d, $J = 3.5$ Hz, H2), 7.72 (1H, s, H6), 7.35 (1H, d, $J = 3.5$ Hz, H1), 5.49 (1H, d, $J = 15.5$ Hz, ArCH₂), 4.78 (1H, d, $J = 15.5$ Hz, ArCH₂), 4.45 (1H, dd, $J = 6.0, 3.5$ Hz, CHCH₂CH₃), 3.34 (3H, s, CONCH₃), 2.06 – 1.91 (2H, m, CHCH₂CH₃), 0.75 (3H, t, $J = 7.6$ Hz, CHCH₂CH₃); δ_c (CDCl₃, 126 MHz): 164.0 (C3), 163.3 (CONCH₃), 154.0 (C7), 151.6 (C4), 142.4 (C2), 138.2 (C6), 121.0 (C1), 120.6 (C5), 61.8 (CHCH₂CH₃), 46.1 (ArCH₂), 28.2 (CONCH₃), 25.2 (CHCH₂CH₃), 8.3 (CHCH₂CH₃)

(*R*)-2-Chloro-7-ethyl-5-methyl-8-(thiazol-5-ylmethyl)-7,8-dihydropteridin-6(5*H*)-one, 90aa



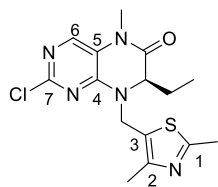
Dihydropteridinone **79** (75 mg, 0.33 mmol) was reacted with 5-(chloromethyl)thiazole (53 mg, 0.40 mmol) using general method **19** to afford the title compound **90aa** as a white solid (13 mg, 12%). LCMS purity >95%, ret. time 1.30 mins; HRMS (ESI +ve): found $[M+H]^+$ 324.0674, $[C_{13}H_{15}ClN_5OS]^+$ requires 324.0680; $[\alpha]_D^{22.5}$: -13.9° (c 1.0, MeOH); δ_H (CDCl₃, 500 MHz): 8.79 (1H, s, H1), 7.89 (1H, s, H3), 7.72 (1H, s, H6), 5.39 (1H, d, $J = 15.5$ Hz, ArCHH), 4.62 (1H, d, $J = 15.8$ Hz, ArCHH), 4.32 (1H, dd, $J = 6.2, 3.3$ Hz, CHCH₂CH₃), 3.33 (3H, s, CONCH₃), 2.08 – 2.00 (CHCH₂CH₃), 1.92 – 1.83 (CHCH₂CH₃), 0.78 (3H, t, $J = 7.4$ Hz, CHCH₂CH₃); δ_C (CDCl₃, 126 MHz): 163.1 (CONCH₃), 154.9 (C1), 154.0 (C7), 151.5 (C4), 143.5 (C3), 138.2 (C6), 132.2 (C2), 120.5 (C5), 61.3 (CHCH₂CH₃), 41.2 (ArCH₂), 28.3 (CONCH₃), 25.4 (CHCH₂CH₃), 8.4 (CHCH₂CH₃)

(*R*)-2-Chloro-7-ethyl-5-methyl-8-((4-methylthiazol-5-yl)methyl)-7,8-dihydropteridin-6(5*H*)-one, 90ab



Dihydropteridinone **79** (70.0 mg, 0.31 mmol) was reacted with 5-(chloromethyl)-4-methyl-1,3-thiazole hydrochloride (68.2 mg, 0.37 mmol) using general method **19** to afford the title compound **90ab** as a white solid (41.0 mg, 39%). LCMS purity >95%, ret. time 1.32 mins; HRMS (ESI +ve): found $[M+H]^+$ 338.0813, $[C_{14}H_{17}ClN_5OS]^+$ requires 338.0837; $[\alpha]_D^{22.7}$: -14.5° (c 1.0, MeOH); δ_H (CDCl₃, 500 MHz): 8.68 (1H, s, H2), 7.71 (1H, s, H6), 5.46 (1H, d, $J = 15.6$ Hz, ArCHH), 4.46 (1H, d, $J = 15.6$ Hz, ArCHH), 4.27 (1H, dd, $J = 6.3, 3.5$ Hz, CHCH₂CH₃), 3.33 (3H, s, CONCH₃), 2.53 (3H, s, ArCH₃), 2.04 – 1.98 (1H, m, CHCH₂CH₃), 1.88 – 1.70 (1H, m, CHCH₂CH₃), 0.83 (3H, t, $J = 7.4$ Hz, CHCH₂CH₃); δ_C (CDCl₃, 126 MHz): 163.2 (CONCH₃), 154.1 (C7), 152.2 (C2), 151.6 (C4), 149.9 (C1), 138.3 (C6), 125.0 (C3), 120.6 (C5), 61.1 (CHCH₂CH₃), 40.4 (ArCH₂), 28.3 (CONCH₃), 25.3 (CHCH₂CH₃), 15.4 (ArCH₃), 8.6 (CHCH₂CH₃)

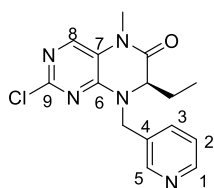
(*R*)-2-Chloro-8-((2,4-dimethylthiazol-5-yl)methyl)-7-ethyl-5-methyl-7,8-dihydropteridin-6(5*H*)-one, 90ac



Dihydropteridinone **79** (60 mg, 0.26 mmol) was reacted with 5-(chloromethyl)-2,4-dimethyl-1,3-thiazole (51 mg, 0.32 mmol) using general method **19** to afford the title compound **90ac** as a white solid (26 mg, 28%). LCMS purity >95%, ret. time 1.36 mins; HRMS (ESI +ve): found $[M+H]^+$ 352.0997, $[C_{15}H_{19}ClN_5OS]^+$ requires 352.0993; $[\alpha]_D^{22.2}$: -4.8°

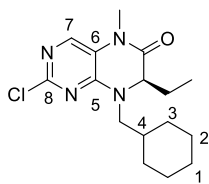
(*c* 1.0, MeOH); δ_{H} (CDCl₃, 500 MHz): 7.69 (1H, s, H₆), 5.40 (1H, d, *J* = 15.5 Hz, ArCHH), 4.34 (1H, d, *J* = 15.5 Hz, ArCHH), 4.25 (1H, dd, *J* = 6.6, 3.5 Hz, CHCH₂CH₃), 3.32 (3H, s, CONCH₃), 2.62 (C¹CH₃), 2.42 (C²CH₃), 2.04 – 1.97 (CHCHHCH₃), 1.86 – 1.77 (CHCHHCH₃), 0.82 (3H, t, *J* = 7.4 Hz, CHCH₂CH₃); δ_{C} (CDCl₃, 126 MHz): 165.3 (C1), 163.3 (CONCH₃), 154.1 (C7), 151.6 (C4), 150.8 (C2), 138.2 (C6), 124.3 (C3), 120.5 (C5), 60.7 (CHCH₂CH₃), 40.3 (ArCH₂), 28.2 (CONCH₃), 25.3 (CHCH₂CH₃), 19.2 (C¹CH₃), 15.2 (C²CH₃), 8.7 (CHCH₂CH₃)

(*R*)-2-Chloro-7-ethyl-5-methyl-8-(pyridine-3-ylmethyl)-7,8-dihydropteridin-6(5*H*)-one, 90ad



Dihydropteridinone **79** (80 mg, 0.35 mmol) was reacted with 3-picolylchloride (HCl salt, 75 mg, 0.46 mmol) using general method **19** to afford the title compound **90ad** as a yellow solid (56 mg, 50%). LCMS purity >95%, ret. time 0.93 mins; HRMS (ESI +ve): found [M+H]⁺ 318.1115, [C₁₅H₁₇ClN₅O]⁺ requires 318.1116; $[\alpha]_D^{22.9}$: -9.7° (*c* 1.0, MeOH); δ_{H} (CDCl₃, 500 MHz): 8.64 – 8.58 (2H, m, H1 & H2), 7.74 (1H, s, H8), 7.70 (1H, d, *J* = 7.9 Hz, H4), 7.32 (1H, dd, *J* = 7.9, 4.9 Hz, H3), 5.56 (1H, d, *J* = 15.2 Hz, ArCHH), 4.24 – 4.18 (2H, m, ArCHH & CHCH₂CH₃), 3.36 (3H, s, CONCH₃), 2.04 – 1.98 (1H, m, CHCHHCH₃), 1.91 – 1.83 (1H, m, CHCHHCH₃), 0.86 (3H, t, *J* = 7.4 Hz, CHCH₂CH₃); δ_{C} (CDCl₃, 126 MHz): 163.2 (CONCH₃), 154.2 (C9), 152.2 (C6), 149.7 (C1 & C2), 138.6 (C8), 136.1 (C4), 131.2 (C5), 123.8 (C3), 120.5 (C7), 60.8 (CHCH₂CH₃), 46.7 (ArCH₂), 28.3 (CONCH₃), 25.0 (CHCH₂CH₃), 8.6 (CHCH₂CH₃)

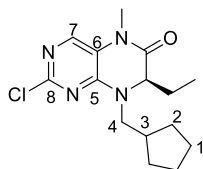
(*R*)-2-Chloro-8-(cyclohexylmethyl)-7-ethyl-5-methyl-7,8-dihydropteridin-6(5*H*)-one, 90ae



Dihydropteridinone **79** (80 mg, 0.35 mmol) was reacted with (bromomethyl)cyclohexane (54 μ L, 0.46 mmol) using general method **19** to afford the title compound **90ae** as a colourless oil (53 mg, 46%). LCMS purity >95%, ret. time 1.62 mins; HRMS (ESI +ve): found [M+H]⁺ 323.1654, [C₁₆H₂₄ClN₄O]⁺ requires 323.1633; $[\alpha]_D^{22.9}$: -11.1° (*c* 1.0, MeOH); δ_{H} (CDCl₃, 500 MHz): 7.65 (1H, s, H7), 4.24 (1H, dd, *J* = 13.8, 7.8 Hz, NCHH), 4.20 (1H, dd, *J* = 6.6, 4.0 Hz, CHCH₂CH₃), 3.35 (3H, s, CONCH₃), 2.71 (1H, dd, *J* = 13.8, 6.8 Hz, NCHH), 1.96 – 1.89 (1H, m, CHCHHCH₃), 1.84 – 1.63 (7H, m, 1 x H1, 2 x H2, 2 x H3, H4 & CHCHHCH₃), 1.27 – 1.14 (3H, m, 1 x H1 & 2 x H2), 1.08 – 1.00 (1H, m, H3), 0.98 – 0.90 (1H, m, H3), 0.85 (3H, t, *J* = 7.5 Hz, CHCH₂CH₃); δ_{C} (CDCl₃, 126 MHz): 163.6 (CONCH₃), 154.3 (C8), 152.7 (C5), 137.8 (C7), 120.5 (C6),

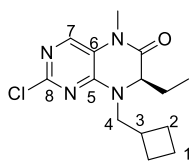
62.0 (CHCH₂CH₃), 50.8 (NCH₂), 35.5 (C4), 31.0 (C3), 30.5 (C3'), 28.2 (CONCH₃), 26.2 (C1), 25.8 (C2), 25.6 (C2'), 25.3 (CHCH₂CH₃), 9.0 (CHCH₂CH₃)

(*R*)-2-Chloro-8-(cyclopentylmethyl)-7-ethyl-5-methyl-7,8-dihydropteridin-6(5*H*)-one, 90af



Dihydropteridinone **79** (55.0 mg, 0.24 mmol) was reacted with (bromomethyl)cyclopentane (39 μ L, 0.31 mmol,) using general method **19** to afford the title compound **90af** as a white solid (26.0 mg, 35%). LCMS purity >95%, ret. time 1.56 mins; HRMS (ESI +ve): found $[M+H]^+$ 309.1478, $[C_{15}H_{22}ClN_4O]^+$ requires 309.1477; $[\alpha]_D^{23.0}$: -20.2° (*c* 1.0, MeOH); δ_H (CDCl₃, 500 MHz): 7.64 (1H, s, H7), 4.31 – 4.25 (2H, m, H4^a & CHCH₂CH₃), 3.34 (3H, s, CONCH₃), 2.86 (1H, dd, *J* = 13.7, 7.1 Hz, H4^b), 2.31 (1H, sept, *J* = 7.6 Hz, H3), 1.98 – 1.89 (1H, m, CHCH₂CH₃), 1.85 – 1.62 (5H, m, cPeH & CHCH₂CH₃), 1.61 – 1.51 (2H, m, H1), 1.31 – 1.16 (2H, m, H2), 0.84 (3H, t, *J* = 7.4 Hz, CHCH₂CH₃); δ_C (CDCl₃, 126 MHz): 163.7 (CONCH₃), 154.3 (C8), 152.6 (C5), 137.8 (C7), 120.5 (C6), 61.5 (CHCH₂CH₃), 49.3 (C4), 37.4 (C3), 30.5 (C2), 30.1 (C2'), 28.2 (CONCH₃), 25.3 (CHCH₂CH₃), 25.0 (C1), 24.8 (C1'), 8.9 (CHCH₂CH₃)

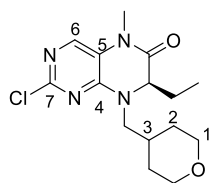
(*R*)-2-Chloro-8-(cyclobutylmethyl)-7-ethyl-5-methyl-7,8-dihydropteridin-6(5*H*)-one, 90ag



Dihydropteridinone **79** (65.0 mg, 0.29 mmol) was reacted with (bromomethyl)cyclobutane (54.0 mg, 0.36 mmol,) using general method **19** to afford the title compound **90ag** as a white solid (32.0 mg, 38%). LCMS purity >95%, ret. time 1.59 mins; HRMS (ESI +ve): found $[M+H]^+$ 295.1314, $[C_{14}H_{20}ClN_4O]^+$ requires 295.1320; $[\alpha]_D^{22.5}$: -18.7° (*c* 1.0, MeOH); δ_H (CDCl₃, 500 MHz): 7.63 (1H, s, H7), 4.30 (1H, dd, *J* = 14.0, 7.7 Hz, H4^a), 4.21 (1H, dd, *J* = 6.6, 3.8 Hz, CHCH₂CH₃), 3.33 (3H, s, NCH₃), 3.04 (1H, dd, *J* = 14.0, 7.7 Hz, H4^b), 2.69 (1H, sept., *J* = 7.7 Hz, H3), 2.15 – 2.02 (2H, m, H2), 2.01 – 1.87 (3H, m, H1 & CHCH₂CH₃), 1.85 – 1.72 (3H, m, H2 & CHCH₂CH₃), 0.83 (3H, t, *J* = 7.6 Hz, CHCH₂CH₃); δ_C (CDCl₃, 126 MHz): 163.6 (CONCH₃), 154.3 (C8), 152.5 (C5), 137.7 (C7), 120.5 (C6), 61.5 (CHCH₂CH₃), 50.0 (C4), 33.1 (C3), 28.2 (NCH₃), 26.7 (C2), 26.3 (C2'), 25.4 (CHCH₂CH₃), 18.5 (C1), 8.8 (CHCH₂CH₃)

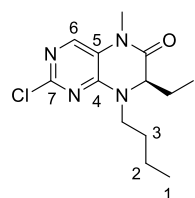
(*R*)-2-Chloro-7-ethyl-5-methyl-8-((tetrahydro-2*H*-pyran-4-yl)methyl)-7,8-dihydropteridin-6(5*H*)-one, 90ah

Dihydropteridinone **79** (80 mg, 0.35 mmol) was reacted with 4-(bromomethyl)tetrahydropyran (61 μ L, 0.46 mmol) using general method **19** to afford the title compound **90ah** as a white solid (41 mg, 36%). LCMS purity >95%, ret. time



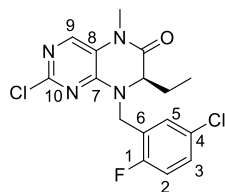
1.33 mins; HRMS (ESI +ve): found $[M+H]^+$ 325.1422, $[C_{15}H_{22}ClN_4O_2]^+$ requires 325.1426; $[\alpha]_D^{22.6}$: -13.2° (c 1.0, MeOH); δ_H (CDCl₃, 500 MHz): 7.67 (1H, s, H6), 4.27 (1H, dd, J = 13.9, 7.2 Hz, NCHH), 4.17 (1H, dd, J = 6.7, 4.1 Hz, CHCH₂CH₃), 3.99 – 3.93 (2H, m, H1), 3.39 – 3.31 (5H, m, H1 & CONCH₃), 2.75 (1H, dd, J = 13.9, 7.4 Hz, NCHH), 2.06 – 1.98 (1H, m, H3), 1.95 – 1.88 (1H, m, CHCH₂CH₃), 1.84 – 1.77 (1H, m, CHCH₂CH₃), 1.64 – 1.54 (2H, m, H2), 1.43 – 1.30 (2H, m, H2), 0.85 (3H, t, J = 7.5 Hz, CHCH₂CH₃); δ_C (CDCl₃, 126 MHz): 163.5 (CONCH₃), 154.3 (C7), 152.6 (C4), 137.9 (C6), 120.6 (C5), 67.4 (C1), 62.6 (CHCH₂CH₃), 50.6 (NCH₂), 33.1 (C3), 30.8 (C2), 30.3 (C2), 28.3 (CONCH₃), 25.4 (CHCH₂CH₃), 9.0 (CHCH₂CH₃)

(R)-8-Butyl-2-chloro-7-ethyl-5-methyl-7,8-dihydropteridin-6(5H)-one, 90ai



Dihydropteridinone **79** (80 mg, 0.35 mmol) was reacted with 1-bromobutane (50 μ L, 0.46 mmol) using general method **19** to afford the title compound **90ai** as a yellow solid (51 mg, 51%). LCMS purity >95%, ret. time 1.50 mins; HRMS (ESI +ve): found $[M+H]^+$ 283.1321, $[C_{13}H_{20}ClN_4O]^+$ requires 283.1320; $[\alpha]_D^{22.9}$: -14.5° (c 1.0, MeOH); δ_H (CDCl₃, 500 MHz): 7.63 (1H, s, H6), 4.25 (1H, dd, J = 6.3, 3.8 Hz, CHCH₂CH₃), 4.19 (1H, ddd, J = 14.0, 8.7, 6.5 Hz, NCHH), 3.33 (3H, s, CONCH₃), 3.01 (1H, ddd, J = 14.0, 8.6, 5.8 Hz, NCHH), 2.00 – 1.94 (1H, m, CHCH₂CH₃), 1.86 – 1.78 (1H, m, CHCH₂CH₃), 1.68 – 1.56 (2H, m, H3), 1.39 – 1.33 (2H, m, H2), 0.95 (3H, t, J = 7.4 Hz, H1), 0.83 (3H, t, J = 7.6 Hz, CHCH₂CH₃); δ_C (CDCl₃, 126 MHz): 163.6 (CONCH₃), 154.4 (C7), 152.2 (C4), 137.6 (C6), 120.4 (C5), 61.4 (CHCH₂CH₃), 44.9 (NCH₂), 28.8 (C3), 28.2 (CONCH₃), 25.5 (CHCH₂CH₃), 20.0 (C2), 13.8 (C1), 8.7 (CHCH₂CH₃)

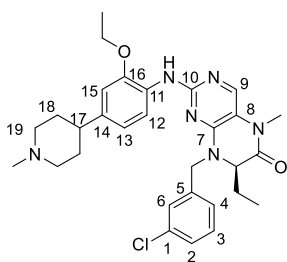
(R)-2-Chloro-8-(5-chloro-2-fluorobenzyl)-7-ethyl-5-methyl-7,8-dihydropteridin-6(5H)-one, 90aj



Dihydropteridinone **79** (205 mg, 0.58 mmol) was reacted with 4-chloro-2-(bromomethyl)-1-fluoro-benzene (155 mg, 0.70 mmol) using general method **19** to afford the title compound **90aj** as a white solid (83 mg, 39%). LCMS purity >95%, ret. time 1.57 mins; HRMS (ESI +ve): found $[M+H]^+$ 369.0675, $[C_{16}H_{16}Cl_2FN_4O]^+$ requires 369.0680; $[\alpha]_D^{23.0}$: -4.2° (c 1.0, MeOH); δ_H (CDCl₃, 500 MHz): 7.72 (1H, s, H9), 7.40 (1H, dd, J = 6.3, 2.5 Hz, H5), 7.29 – 7.26 (1H, m, H3), 7.0 (1H, t, J = 9.1 Hz, H2), 5.49 (1H, dd, J = 15.1, 1.3 Hz, ArCHH), 4.26 – 4.21 (2H, m, ArCHH & CHCH₂CH₃), 3.34 (3H, s, CONCH₃), 2.05 – 1.97 (1H, m, CHCH₂CH₃), 1.94 – 1.85 (1H, m, CHCH₂CH₃), 0.87 (3H, t, J = 7.4 Hz, CHCH₂CH₃); δ_C (CDCl₃, 126 MHz): 163.4 (CO₂CH₃), 159.8 (d, J_{C-F}

= 247.4 Hz, C1), 154.2 (C10), 152.1 (C7), 138.3 (C9), 130.9 (d, J_{C-F} = 4.6 Hz, C5), 130.0 (d, J_{C-F} = 8.3 Hz, C3), 129.7 (C4), 124.0 (d, J_{C-F} = 16.5 Hz, C6), 120.6 (C8), 61.0 ($\underline{C}HCH_2CH_3$), 41.3 ($Ar\overline{C}H_2$), 28.3 ($CON\overline{C}H_3$), 25.1 ($CHCH_2\overline{C}H_3$), 8.7 ($CHCH_2\overline{C}H_3$); $\delta_{F\{H\}}$ ($CDCl_3$, 471 MHz): - 120.4

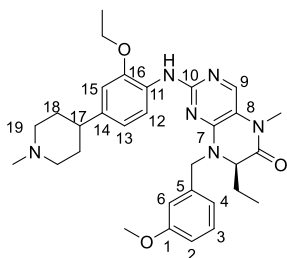
(*R*)-2-((2-Ethoxy-4-(1-methylpiperidin-4-yl)phenyl)amino)-7-ethyl-8-(3-chlorobenzyl)-5-methyl-7,8-dihydropteridin-6(5*H*)-one, **91**



Dihydropteridinone **90a** (40 mg, 114 μ mol) was reacted with aniline **28b** (25 mg, 108 μ mol) using general method **16** to afford the title compound **91** as a yellow solid (8 mg, 13%). LCMS purity >95%, ret. time 1.16 mins; HRMS (ESI +ve): found $[M+H]^+$ 549.2727, $[C_{30}H_{38}ClN_6O_2]^+$ requires 549.2739; m.p.: 108 – 111 $^{\circ}C$; ν_{max} (thin film, cm^{-1}): 3422 (w, N-H), 1666

(C=O); $[\alpha]_D^{23.7}$: +15.2 $^{\circ}$ (c 1.0, MeOH); δ_H ($CDCl_3$, 500 MHz): 8.16 (1H, d, J = 8.2 Hz, H12), 7.71 (1H, s, H9), 7.46 (1H, s, ArNH), 7.30 – 7.27 (2H, m, H2 & H3), 7.23 – 7.20 (1H, m, H4), 6.76 – 6.70 (2H, m, H13 & H15), 5.58 (1H, d, J = 15.5 Hz, $Ar\overline{C}H\overline{H}$), 4.18 – 4.09 (4H, m, $ArCH\overline{H}$, $\overline{C}HCH_2CH_3$ & OCH_2CH_3), 3.50 (2H, m, H19), 3.36 (3H, s, $CONCH_3$), 2.69 (3H, s, NCH_3), 2.69 – 2.59 (3H, m, H17 & 2 x H19), 2.17 (2H, q, J = 12.3 Hz, H18), 2.00 – 1.91 (3H, m, 2 x H18 & $CHCH\overline{H}CH_3$), 1.88 – 1.80 (1H, m, $CHCH\overline{H}CH_3$), 1.47 (3H, t, J = 7.6 Hz, OCH_2CH_3), 0.87 (3H, t, J = 7.0 Hz, $CHCH_2\overline{C}H_3$); δ_C ($CDCl_3$, 126 MHz): 163.3 ($\overline{C}ONCH_3$), 155.7 (C10), 151.9 (C7), 147.3 (C16), 138.4 (C5 & C9), 136.7 (C14), 134.7 (C1), 130.1 (C3), 128.4 (C11), 128.1 (C2/C6), 128.0 (C2/C6), 126.0 (C4), 118.7 (C13), 118.1 (C12), 114.7 (C8), 109.4 (C15), 64.3 (OCH_2CH_3), 61.0 ($\overline{C}HCH_2CH_3$), 54.7 (C19), 47.4 ($ArCH_2$), 43.7 (NCH_3), 40.3 (C17), 30.9 (C18), 28.1 ($CONCH_3$), 24.7 ($CHCH_2CH_3$), 15.0 (OCH_2CH_3), 8.8 ($CHCH_2\overline{C}H_3$)

(*R*)-2-((2-Ethoxy-4-(1-methylpiperidin-4-yl)phenyl)amino)-7-ethyl-8-(3-methoxybenzyl)-5-methyl-7,8-dihydropteridin-6(5*H*)-one, **92**

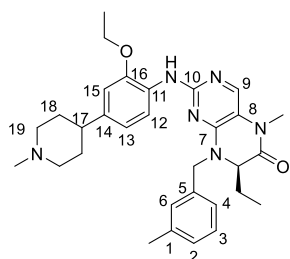


Dihydropteridinone **90b** (40 mg, 115 μ mol) was reacted with aniline **28b** (26 mg, 110 μ mol) using general method **16** to afford the title compound **92** as a yellow solid (20 mg, 32%). LCMS purity >95%, ret. time 1.16 mins; HRMS (ESI +ve): found $[M+H]^+$ 545.3221, $[C_{31}H_{41}N_6O_3]^+$ requires 545.3235; m.p.: 64 – 66 $^{\circ}C$; ν_{max} (thin film, cm^{-1}): 3425 (w, N-H), 1666

(C=O); $[\alpha]_D^{24.0}$: +13.2 $^{\circ}$ (c 1.0, MeOH); δ_H ($CDCl_3$, 500 MHz): 8.19 (1H, d, J = 8.8 Hz, H12), 7.71 (1H, s, ArNH), 7.67 (1H, s, H9), 7.29 – 7.26 (1H, m, H3), 6.91 (1H, d, J = 7.6 Hz, H4), 6.88 – 6.84 (2H, m, H2 & H6), 6.75 – 6.72 (2H, m, H13 & H15), 5.61 (1H,

d, $J = 15.1$ Hz, ArCHH), 4.18 – 4.09 (4H, m, OCH₂CH₃, ArCHH & CHCH₂CH₃), 3.77 (OCH₃), 3.61 (2H, m, H19), 3.34 (3H, s, CONCH₃), 2.80 – 2.69 (2H, m, H19), 2.75 (3H, s, NCH₃), 2.67 – 2.60 (1H, m, H17), 2.19 (2H, q, $J = 12.4$ Hz, H18), 2.02 – 1.90 (3H, m, 2 x H18 & CHCH₂CH₃), 1.89 – 1.80 (1H, m, CHCH₂CH₃), 1.48 (3H, t, $J = 6.9$ Hz, OCH₂CH₃), 0.85 (3H, t, $J = 7.6$ Hz, CHCH₂CH₃); δ_c (CDCl₃, 126 MHz): 163.4 (CONCH₃), 160.0 (C1), 155.3 (C10), 152.1 (C7), 147.5 (C16), 137.5 (C9), 137.2 (C5), 136.5 (C14), 130.0 (C3), 128.4 (C11), 120.4 (C4), 118.7 (C13), 118.5 (C12), 114.7 (C8), 114.0 (C6), 113.0 (C2), 109.3 (C15), 64.4 (OCH₂CH₃), 60.5 (CHCH₂CH₃), 55.3 (OCH₃), 54.6 (C19), 47.8 (ArCH₂), 43.5 (NCH₃), 40.0 (C17), 30.5 (C18), 28.1 (CONCH₃), 24.7 (CHCH₂CH₃), 14.9 (OCH₂CH₃), 8.8 (CHCH₂CH₃)

(*R*)-2-((2-Ethoxy-4-(1-methylpiperidin-4-yl)phenyl)amino)-7-ethyl-8-(3-methylbenzyl)-5-methyl-7,8-dihydropteridin-6(5*H*)-one, 93

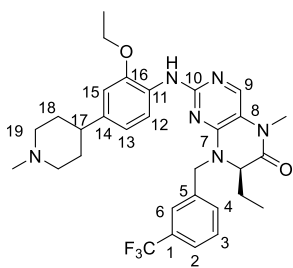


Dihydropteridinone **90c** (42 mg, 127 μ mol) was reacted with aniline **28b** (28 mg, 121 μ mol) using general method **16** to afford the title compound **93** as a yellow solid (15 mg, 22%). LCMS purity >95%, ret. time 1.18 mins; HRMS (ESI +ve): found $[M+H]^+$ 529.3307, $[C_{31}H_{41}N_6O_2]^+$ requires 529.3286; m.p.: 80 – 83 °C; ν_{\max} (thin film, cm⁻¹): 3424 (w, N-H), 1666

(C=O); $[\alpha]_D^{23.6}$: +5.9° (c 1.0, MeOH); δ_H (CDCl₃, 500 MHz): 8.26 (1H, d, $J = 7.9$ Hz, H12), 7.68 (1H, s, H9), 7.49 (1H, s, NH), 7.22 (1H, t, $J = 7.4$ Hz, H3), 7.13 – 7.09 (3H, m, H2 H4 & H6), 7.23 – 7.20 (1H, m, H4), 6.75 – 6.71 (2H, m, H13 & H15), 5.64 (1H, d, $J = 15.1$ Hz, ArCHH), 4.14 – 4.06 (4H, m, ArCHH, CHCH₂CH₃ & OCH₂CH₃), 3.48 (2H, d, $J = 11.0$ Hz, H19), 3.33 (3H, s, CONCH₃), 2.66 (3H, s, NCH₃), 2.65 – 2.56 (3H, m, H17 & 2 x H19), 2.33 (3H, s, ArCH₃), 2.17 (2H, q, $J = 12.9$ Hz, H18), 2.00 – 1.89 (3H, m, 2 x H18 & CHCH₂CH₃), 1.86 – 1.80 (1H, m, CHCH₂CH₃), 1.47 (3H, t, $J = 6.8$ Hz, OCH₂CH₃), 0.87 (3H, t, $J = 7.3$ Hz, CHCH₂CH₃); δ_c (CDCl₃, 126 MHz): 163.5 (CONCH₃), 155.7 (C10), 152.1 (C7), 147.2 (C16), 138.6 (C1), 138.0 (C9), 136.6 (C14), 135.9 (C1), 128.8 (C3 & C2/C6), 128.7 (C2/C6), 125.2 (C4), 118.6 (C13), 118.1 (C12), 114.7 (C8), 109.4 (C15), 64.3 (OCH₂CH₃), 60.3 (CHCH₂CH₃), 54.7 (C19), 47.6 (ArCH₂), 43.8 (NCH₃), 40.3 (C17), 30.9 (C18), 28.1 (CONCH₃), 24.6 (CHCH₂CH₃), 21.4 (ArCH₃), 15.0 (OCH₂CH₃), 8.8 (CHCH₂CH₃)

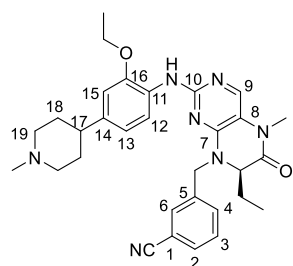
(*R*)-2-((2-Ethoxy-4-(1-methylpiperidin-4-yl)phenyl)amino)-7-ethyl-5-methyl-8-(3-(trifluoromethyl)benzyl)-7,8-dihydropteridin-6(5*H*)-one, 94

Dihydropteridinone **90d** (40 mg, 104 μ mol) was reacted with aniline **28b** (23 mg, 99 μ mol) using general method **16** to afford the title compound **94** as a yellow solid (10



mg, 17%). LCMS purity >95%, ret. time 1.24 mins; HRMS (ESI +ve): found $[M+H]^+$ 583.2981, $[C_{31}H_{38}F_3N_6O_2]^+$ requires 583.3003; m.p.: 83 – 85 °C; ν_{\max} (thin film, cm^{-1}): 3424 (w, N-H), 1668 (s, C=O); $[\alpha]_D^{23.2}$: - 7.6° (c 1.0, MeOH); δ_H (CDCl_3 , 500 MHz): 8.14 (1H, d, J = 8.2 Hz, H13), 7.71 (1H, s, H8), 7.60 – 7.55 (2H, m, H2 & H6), 7.52 – 7.45 (3H, m, H3, H4 & ArNH), 6.72 – 6.78 (2H, m, H3 & H15), 5.59 (1H, d, J = 15.5 Hz, ArCHH), 4.27 (1H, d, J = 15.5 Hz, ArCHH), 4.13 – 4.08 (2H, m, CHCH₂CH₃ & OCH₂CH₃), 3.53 (2H, d, J = 11.0 Hz, H19), 3.35 (3H, s, CONCH₃), 2.70 – 2.57 (6H, m, NCH₃, H17 & 2 x H19), 2.20 – 2.11 (2H, m, H18), 1.98 – 1.91 (3H, 2 x H18 & CHCHHCH₃), 1.86 – 1.78 (1H, m, CHCHHCH₃), 1.46 (3H, t, J = 6.9 Hz, OCH₂CH₃), 0.86 (3H, t, J = 7.6 Hz, CHCH₂CH₃); δ_C (CDCl_3 , 126 MHz): 163.2 (CONCH₃), 155.6 (C10), 151.9 (C7), 147.3 (C16), 138.3 (C9), 134.5 (C5), 136.6 (C14), 131.1 (q, J_{C-F} = 32 Hz, C1), 11.1 (C4), 129.4 (C3), 128.3 (C11), 124.8 (q, J_{C-F} = 4 Hz, C2/6), 124.7 (q, J_{C-F} = 4 Hz, C2/6), 123.9 (q, J_{C-F} = 272 Hz, CF₃), 118.6 (C13), 118.1 (C12), 114.8 (C8), 109.3 (C15), 64.3 (OCH₂CH₃), 61.3 (CHCH₂CH₃), 54.6 (C19), 47.7 (ArCH₂), 43.6 (NCH₃), 40.1 (C17), 30.7 (C18), 28.1 (CONCH₃), 24.8 (CHCH₂CH₃), 14.9 (OCH₂CH₃), 8.8 (CHCH₂CH₃); $\delta_{F\{H\}}$ (CDCl_3 , 471 MHz): - 62.5

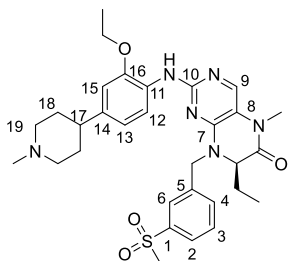
(R)-3-((2-((2-Ethoxy-4-(1-methylpiperidin-4-yl)phenyl)amino)-7-ethyl-5-methyl-6-methyl-6-oxo-6,7-dihydropteridin-8(5H-yl)methyl)benzonitrile, 95



Dihydropteridinone **90e** (40 mg, 117 μmol) was reacted with aniline **28b** (26 mg, 111 μmol) using general method **16** to afford the title compound **95** as a yellow solid (7 mg, 10%). LCMS purity >95%, ret. time 1.08 mins; HRMS (ESI +ve): found $[M+H]^+$ 540.3071, $[C_{31}H_{38}N_7O_2]^+$ requires 540.3081; m.p.: 137 – 139 °C; ν_{\max} (thin film, cm^{-1}): 3424 (w, N-H), 2228 (s, C \equiv N), 1661 (C=O); $[\alpha]_D^{23.5}$: -2.1° (c 1.0, MeOH); δ_H (CDCl_3 , 500 MHz): 8.08 (1H, d, J = 8.2 Hz, H12), 7.73 (1H, s, H9), 7.62 – 7.55 (3H, m, H2, H4 & H6), 7.47 (1H, t, J = 7.9 Hz, H3), 7.41 (1H, s, NH), 6.73 – 6.69 (2H, m, H13 & H15), 5.55 (1H, d, J = 15.5 Hz, ArCHH), 4.23 (1H, d, J = 15.5 Hz, ArCHH), 4.14 – 4.07 (3H, m, CHCH₂CH₃ & OCH₂CH₃), 3.44 (2H, d, J = 11.7 Hz, H19), 3.37 (3H, s, CONCH₃), 2.64 (3H, s, NCH₃), 2.63 – 2.52 (3H, m, H17 & 2 x H19), 2.12 (2H, q, J = 13.2 Hz, H18), 2.00 – 1.91 (3H, m, H18 & CHCHHCH₃), 1.86 – 1.77 (1H, m, CHCHHCH₃), 1.46 (3H, t, J = 6.9 Hz, OCH₂CH₃), 0.87 (3H, t, J = 7.4 Hz, CHCH₂CH₃); δ_C (CDCl_3 , 126 MHz): 163.1 (CONCH₃), 155.7 (C10), 151.7 (C7), 147.3 (C16), 138.8 (C9), 138.3 (C5), 137.2 (C14), 132.1 (C6), 131.5 (C4), 131. (C2), 129.7 (C3), 128.2 (C11), 118.6 (CN & C13),

118.1 (C12), 114.8 (C8), 112.9 (C1), 109.5 (C15), 64.3 (OCH₂CH₃), 61.7 (CHCH₂CH₃), 54.9 (C19), 47.6 (ArCH₂), 40.4 (C17), 31.3 (C18), 28.2 (CONCH₃), 24.9 (CHCH₂CH₃), 15.0 (OCH₂CH₃), 8.9 (CHCH₂CH₃)

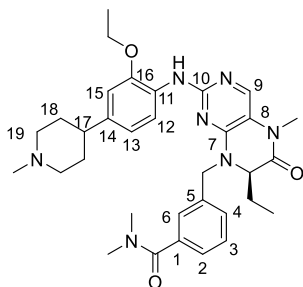
(R)-2-((2-Ethoxy-4-(1-methylpiperidin-4-yl)phenyl)amino)-7-ethyl-5-methyl-8-(3-(methylsulfonyl)benzyl)-7,8-dihydropteridin-6(5H)-one, 96



Dihydropteridinone **90f** (35 mg, 89 μmol) was reacted with aniline **28b** (20 mg, 84 μmol) using general method **16** to afford the title compound **96** as a brown solid (25 mg, 48%). LCMS purity >95%, ret. time 1.05 mins; HRMS (ESI +ve): found [M+H]⁺ 593.2897, [C₃₁H₄₁N₆O₄S]⁺ requires 593.2905; m.p.: 68 – 71 °C; ν_{\max} (thin film, cm⁻¹): 3414 (w, N-H), 1664

(C=O), 1140 (s, S=O); $[\alpha]_D^{22.8}$: -4.2° (c 1.0, MeOH); δ_H (CDCl₃, 500 MHz): 8.01 (1H, d, J = 7.9 Hz, H12), 7.91 (1H, s, H6), 7.87 (1H, d, J = 7.3 Hz, H2), 7.76 (1H, s, NH), 7.71 (1H, s, H9), 7.62 – 7.54 (2H, m, H3 & H4), 6.73 – 6.68 (2H, m, H13 & H15), 5.58 (1H, d, J = 15.8 Hz, ArCHH), 4.32 (1H, d, J = 15.8 Hz, ArCHH), 4.17 (1H, dd, J = 6.2, 3.6 Hz, CHCH₂CH₃), 4.10 (2H, q, J = 6.9 Hz, OCH₂CH₃), 3.68 – 2.56 (2H, m, H19), 3.37 (3H, s, CONCH₃), 3.01 (3H, s, SO₂CH₃), 2.85 – 2.70 (5H, m, NCH₃ & 2 x H19), 2.70 – 2.61 (1H, m, H17), 2.25 – 2.15 (2H, m, H18), 2.04 – 1.95 (3H, m, 2 x H18 & CHCHHCH₃), 1.89 – 1.80 (1H, m, CHCHHCH₃), 1.47 (3H, t, J = 6.9 Hz, OCH₂CH₃), 0.88 (3H, t, J = 7.4 Hz, CHCH₂CH₃); δ_C (CDCl₃, 126 MHz): 163.0 (CONCH₃), 155.2 (C10), 151.9 (C7), 14.7. (C16), 141.2 (C1), 138.4 (C5), 137.5 (C9), 136.7 (C14), 132.7 (C4), 130.1 (C3), 128.0 (C11), 126.8 (C2), 126.6 (C6), 118.6 (C13), 118.5 (C12), 114.7 (C8), 109.5 (C15), 64.4 (OCH₂CH₃), 61.8 (CHCH₂CH₃), 54.7 (C19), 48.0 (ArCH₂), 44.5 (SO₂CH₃), 43.5 (NCH₃), 39.8 (C17), 30.4 (C18), 28.2 (CONCH₃), 25.0 (CHCH₂CH₃), 14.9 (OCH₂CH₃), 8.9 (CHCH₂CH₃)

(R)-2-((2-Ethoxy-4-(1-methylpiperidin-4-yl)phenyl)amino)-7-ethyl-5-methyl-6-oxo-6,7-dihydropteridin-8(5H-yl)methyl)-N,N-dimethylbenzamide, 97

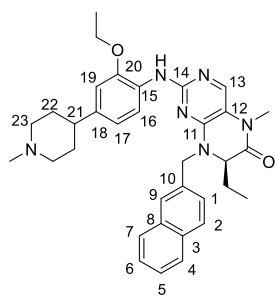


Dihydropteridinone **90g** (33 mg, 85 μmol) was reacted with aniline **28b** (19 mg, 81 μmol) using general method **16** to afford the title compound **97** as a brown oil (25 mg, 48%). LCMS purity >95%, ret. time 1.09 mins; HRMS (ESI +ve): found [M+H]⁺ 586.3474, [C₃₃H₄₄N₇O₃]⁺ requires 586.3500; ν_{\max} (thin film, cm⁻¹): 3420 (w, N-H), 1673 (s, C=O), 1592

(C=O); $[\alpha]_D^{22.8}$: -4.8° (c 1.0, MeOH); δ_H (CDCl₃, 500 MHz): 8.06 (1H, d, J = 8.1 Hz, H12), 7.80 (1H, s, NH), 7.66 (1H, s, H9), 7.38 – 3.30 (4H, m, H2, H3, H4 & H6), 6.70

– 6.66 (2H, m, H13 & H15), 5.58 (1H, d, $J = 15.4$ Hz, ArCHH), 4.18 (1H, d, $J = 15.4$ Hz, ArCHH), 4.13 (1H, dd, $J = 6.4, 3.6$ Hz, CHCH₂CH₃), 4.09 (2H, q, $J = 6.9$ Hz, OCH₂CH₃), 3.64 – 3.54 (2H, m, H19), 3.32 (3H, s, CONCH₃), 3.06 (3H, s, N(CH₃)(C'H₃)), 2.89 (3H, s, N(CH₃)(C'H₃)), 2.78 – 2.70 (5H, m, NCH₃, & 2 x H19), 2.67 – 2.63 (1H, m, H17), 2.22 – 2.13 (2H, m, H18), 1.99 – 1.90 (3H, 2 x H18 & CHCHHCH₃), 1.85 – 1.78 (1H, m, CHCHHCH₃), 1.44 (3H, t, $J = 6.9$ Hz, OCH₂CH₃), 0.83 (3H, t, $J = 7.4$ Hz, CHCH₂CH₃); δ_c (CDCl₃, 126 MHz): 171.2 (CON(CH₃)₂), 163.1 (CONCH₃), 155.1 (C10), 152.1 (C7), 147.8 (C16), 136.8 (C1), 136.7 (C9 & C14), 136.5 (C5), 129.0 (C4), 128.9 (C3), 128.1 (C11), 126.6 (C6), 126.5 (C2), 118.8 (C12), 118.6 (C13), 114.7 (C8), 109.4 (C15), 64.4 (OCH₂CH₃), 60.9 (CHCH₂CH₃), 54.6 (C19), 47.7 (ArCH₂), 43.5 (NCH₃), 39.8 (C17), 35.4 (N(CH₃)₂), 30.4 (C18), 28.1 (CONCH₃), 24.8 (CHCH₂CH₃), 14.9 (OCH₂CH₃), 8.8 (CHCH₂CH₃)

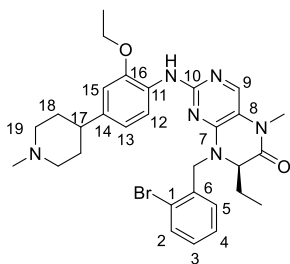
(*R*)-2-((2-Ethoxy-4-(1-methylpiperidin-4-yl)phenyl)amino)-7-ethyl-5-methyl-8-(naphthalene-2-ylmethyl)-7,8-dihydropteridin-6(5*H*)-one, **98**



Dihydropteridinone **90h** (35 mg, 95 μ mol) was reacted with aniline **28b** (21 mg, 91 μ mol) using general method **16** to afford the title compound **98** as a white solid (10 mg, 19%). LCMS purity >95%, ret. time 1.23 mins; HRMS (ESI +ve): found $[M+H]^+$ 565.3273, $[C_{34}H_{41}N_6O_2]^+$ requires 565.3286; m.p.: 80 – 83 °C; ν_{max} (thin film, cm⁻¹): 3419 (w, N-H), 1665

(C=O); $[\alpha]_D^{23.6}$: +55.4° (c 1.0, MeOH); δ_H (CDCl₃, 500 MHz): 8.18 (1H, d, $J = 8.2$ Hz, H16), 7.86 – 7.79 (4H, m, NH & H2/4/5/6/7), 7.76 (1H, s, H9), 7.70 (1H, s, H9), 7.52 – 7.48 (2H, m, H2/4/5/6/7), 7.42 (1H, d, $J = 8.2$ Hz, H1), 6.72 (1H, s, H19), 6.68 (1H, d, $J = 8.2$ Hz, H17), 5.78 (1H, d, $J = 15.1$ Hz, ArCHH), 4.35 (1H d, $J = 15.1$ Hz, ArCHH), 4.19 (1H, dd, $J = 5.8, 3.6$ Hz, CHCH₂CH₃), 4.12 (2H, q, $J = 6.9$ Hz, OCH₂CH₃), 3.65 – 3.55 (2H, m, H23), 3.35 (3H, s, CONCH₃), 2.75 (3H, s, NCH₃), 2.76 – 2.58 (3H, m, H21 & 2 x H23), 2.18 (2H, q, $J = 12.1$ Hz, H22), 2.02 – 1.93 (3H, m, 2 x H22 & CHCHHCH₃), 1.93 – 1.86 (1H, m, CHCHHCH₃), 1.48 (3H, t, $J = 6.9$ Hz, OCH₂CH₃), 0.87 (3H, t, $J = 6.3$ Hz, CHCH₂CH₃); δ_c (CDCl₃, 126 MHz): 163.3 (CONCH₃), 155.3 (C14), 152.2 (C11), 147.7 (C20), 136.9 (C13), 136.6 (C19), 133.3 (C8 & C10), 133.0 (C3), 128.9 (C2/4/5/6/7), 128.3 (C15), 127.8 (C2/4/5/6/7), 127.7 (C2/4/5/6/7), 127.1 (C9), 126.5 (C2/4/5/6/7), 126.2 (C2/4/5/6/7), 125.7 (C18), 118.7 (C17), 118.6 (C16), 114.5 (C12), 109.4 (C19), 64.4 (OCH₂CH₃), 60.6 (CHCH₂CH₃), 54.7 (C23), 48.2 (ArCH₂), 43.4 (NCH₃), 39.9 (C21), 30.3 (C22), 28.1 (CONCH₃), 24.8 (CHCH₂CH₃), 14.9 (OCH₂CH₃), 8.8 (CHCH₂CH₃)

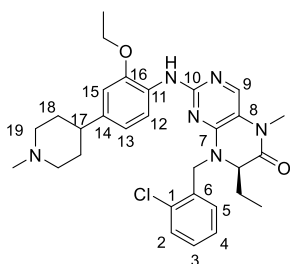
(*R*)-2-((2-Ethoxy-4-(1-methylpiperidin-4-yl)phenyl)amino)-7-ethyl-5-methyl-8-(2-bromobenzyl)-7,8-dihydropteridin-6(5*H*)-one, 99



Dihydropteridinone **6j** (33 mg, 83 μ mol) was reacted with aniline **28b** (19 mg, 79 μ mol) using general method **16** to afford the title compound **99** as a brown solid (9 mg, 18%). LCMS purity >95%, ret. time 1.23 mins; HRMS (ESI +ve): found $[M+H]^+$ 593.2210, $[C_{30}H_{38}BrN_6O_2]^+$ requires 593.2234; m.p.: 77 – 79 $^{\circ}$ C; ν_{\max} (thin film, cm^{-1}): 3416 (w, N-H), 1666

(C=O), 751 (C-Br); $[\alpha]_D^{22.0}$: -19.4° (c 1.0, MeOH); δ_H (CDCl₃, 500 MHz): 8.06 (1H, d, J = 8.8 Hz, H12), 7.70 (1H, s, H9), 7.57 (1H, d, J = 7.6 Hz, H2), 7.52 (1H, s, ArNH), 7.29 – 7.26 (2H, m, H4 & H3/5), 7.19 – 7.16 (1H, m, H3/5), 6.72 – 6.70 (2H, m, H13 & H15), 5.41 (1H, d, J = 16.1 Hz, ArCHH), 4.30 (1H, d, J = 16.1 Hz, ArCHH), 4.15 (1H, dd, J = 6.6, 3.8 Hz, CHHCH₂CH₃), 4.10 (2H, q, J = 6.9 Hz, OCH2CH₃), 3.54 (2H, d, J = 10.7 Hz, H19), 3.37 (3H, s, CONCH₃), 2.74 – 2.60 (6H, m, NCH₃, H17 & 2 x H19), 2.21 – 2.14 (2H, m, H18), 2.02 – 1.86 (4H, m, 2 x H18 & CHCH2CH₃), 1.47 (3H, t, J = 6.9 Hz, OCH₂CH3), 0.90 (3H, t, J = 7.6 Hz, CHCH₂CH3); δ_C (CDCl₃, 126 MHz): 163.3 (CONCH₃), 155.5 (C10), 151.9 (C7), 147.3 (C16), 138.1 (C9), 136.5 (C14), 135.1 (C6), 133.2 (C2), 129.3 (C3 & C5), 128.3 (C11), 127.8 (C4), 123.6 (C1), 118.8 (C13), 118.1 (C12), 114.8 (C8), 109.2 (C15), 64.3 (OCH2CH₃), 61.3 (CHCH2CH₃), 54.6 (C19), 48.2 (ArCH₂), 43.6 (NCH₃), 40.1 (C17), 30.7 (C18), 28.1 (CONCH₃), 25.1 (CHCH₂CH3), 15.0 (OCH₂CH3), 9.0 (CHCH₂CH3)

(*R*)-2-((2-Ethoxy-4-(1-methylpiperidin-4-yl)phenyl)amino)-7-ethyl-5-methyl-8-(2-chlorobenzyl)-7,8-dihydropteridin-6(5*H*)-one, 100

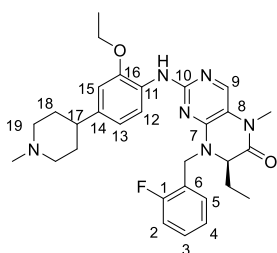


Dihydropteridinone **89i** (30 mg, 85 μ mol) was reacted with aniline **28b** (19 mg, 81 μ mol) using general method **16** to afford the title compound **100** as a yellow solid (6 mg, 13%). LCMS purity >95%, ret. time 1.19 mins; HRMS (ESI +ve): found $[M+H]^+$ 549.2729, $[C_{30}H_{38}ClN_6O_2]^+$ requires 549.2739; m.p.: 88 – 91 $^{\circ}$ C; ν_{\max} (thin film, cm^{-1}): 3420 (w, N-H), 1667

(s, C=O); $[\alpha]_D^{22.9}$: -5.5° (c 1.0, MeOH); δ_H (CDCl₃, 500 MHz): 8.09 (1H, d, J = 8.2 Hz, H12), 7.69 (1H, s, H9), 7.51 (1H, s, ArNH), 7.43 (1H, dd, J = 7.7, 1.4 Hz, H2), 7.30 (1H, dd, J = 7.6, 2.2 Hz, H5), 7.25 – 7.20 (2H, m, H3 & H4), 6.72 – 6.69 (2H, m, H13 & H15), 5.65 (1H, d, J = 16.1 Hz, ArCHHH), 4.31 (1H, d, J = 16.1 Hz, ArCHHH), 4.15 (1H, dd, J = 6.6, 3.8 Hz, CHHCH₂CH₃), 4.10 (2H, q, J = 6.9 Hz, OCH₂CH₃), 3.52 (2H, d, J = 10.7 Hz, H19), 3.36 (3H, s, CONCH₃), 2.70 (3H, s, NCH₃), 2.69 – 2.57 (3H, m, H17 & 2 x H19), 2.22 – 2.16 (2H, m, H18), 2.02 – 1.93 (3H, m, 2 x H18 &

CHCH₂HCH₃), 1.90 – 1.84 (1H, m, CHCH₂HCH₃), 1.47 (3H, t, J = 6.9 Hz, OCH₂CH₃), 0.89 (3H, t, J = 7.6 Hz, CHCH₂CH₃); δ_{C} (CDCl₃, 126 MHz): 163.4 (CONCH₃), 155.6 (C10), 151.9 (C7), 147.3 (C16), 138.1 (C9), 136.5 (C14), 133.7 (C1), 133.6 (C6), 129.9 (C2), 129.4 (C5), 129.1 (C3), 127.2 (C4), 118.9 (C13), 118.1 (C12), 114.8 (C8), 109.2 (C15), 64.3 (OCH₂CH₃), 61.3 (CHCH₂CH₃), 54.7 (C19), 46.7 (ArCH₂), 43.6 (NCH₃), 40.2 (C17), 30.7 (C18), 28.1 (CONCH₃), 25.1 (CHCH₂CH₃), 15.0 (OCH₂CH₃), 9.0 (CHCH₂CH₃)

(*R*)-2-((2-Ethoxy-4-(1-methylpiperidin-4-yl)phenyl)amino)-7-ethyl-5-methyl-8-(2-fluorobenzyl)-7,8-dihydropteridin-6(5*H*)-one, 101

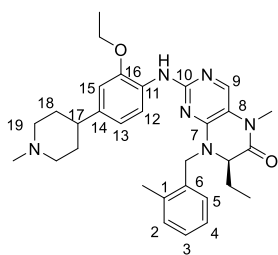


Dihydropteridinone **90j** (36 mg, 108 μ mol) was reacted with aniline **28b** (24 mg, 102 μ mol) using general method **16** to afford the title compound **101** as a colourless oil (11 mg, 19%). LCMS purity >95%, ret. time 1.15 mins; HRMS (ESI +ve): found $[M+H]^+$ 533.3027, $[C_{30}H_{38}FN_6O_2]^+$ requires 533.3040; ν_{max} (thin film, cm⁻¹): 3320 (w, N-H), 1638 (C=O);

$[\alpha]_D^{23.6}$: +29.8° (c 1.0, MeOH); δ_{H} (CDCl₃, 500 MHz): 8.23 (1H, d, J = 8.2 Hz, H12), 7.68 (1H, s, H9), 7.43 (1H, s, NH), 7.33 (1H, t, J = 7.6 Hz, H5), 7.31 – 7.26 (1H, m, H3), 7.12 – 7.07 (2H, m, H2 & H4), 6.76 – 6.72 (2H, m, H13 & H15), 5.61 (1H, d, J = 15.3 Hz, ArCH₂H), 4.29 (1H, d, J = 15.3 Hz, ArCH₂H), 4.16 (1H, dd, J = 6.3, 3.5 Hz, CHCH₂CH₃), 4.11 (2H, q, J = 6.9 Hz, OCH₂CH₃), 3.41 (2H, d, J = 10.7 Hz, H19), 3.33 (3H, s, CONCH₃), 2.62 (3H, s, NCH₃), 2.62 – 2.49 (3H, m, H17 & 2 x H19), 2.11 (2H, q, J = 11.8 Hz, H18), 2.00 – 1.83 (3H, m, 2 x H18 & CHCH₂CH₃), 1.88 – 1.80 (1H, m, CHCH₂CH₃), 1.47 (3H, t, J = 6.9 Hz, OCH₂CH₃), 0.87 (3H, t, J = 6.9 Hz, CHCH₂CH₃); δ_{C} (CDCl₃, 126 MHz): 163.4 (CONCH₃), 161.2 (d, $J_{\text{C-F}}$ = 247 Hz, C1), 155.7 (C10), 151.9 (C7), 147.2 (C16), 138.3 (C9), 137.1 (C14), 130.2 (d, $J_{\text{C-F}}$ = 5 Hz, C5), 129.6 (d, $J_{\text{C-F}}$ = 8 Hz, C3), 128.4 (C11), 124.5 (d, $J_{\text{C-F}}$ = 4 Hz, C4), 123.2 (d, $J_{\text{C-F}}$ = 14 Hz, C6), 118.8 (C13), 118.1 (C12), 115.6 (d, $J_{\text{C-F}}$ = 22 Hz, C2), 114.8 (C8), 109.4 (C15), 64.3 (OCH₂CH₃), 61.0 (CHCH₂CH₃), 54.9 (C19), 44.2 (NCH₃), 41.3 (ArCH₂), 40.5 (C17), 31.3 (C18), 28.1 (CONCH₃), 24.8 (CHCH₂CH₃), 15.0 (OCH₂CH₃), 8.9 (CHCH₂CH₃); $\delta_{\text{F}\{\text{H}\}}$ (CDCl₃, 471 MHz): -118.3

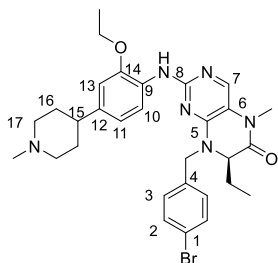
(*R*)-2-((2-Ethoxy-4-(1-methylpiperidin-4-yl)phenyl)amino)-7-ethyl-5-methyl-8-(2-methylbenzyl)-7,8-dihydropteridin-6(5*H*)-one, 102

Dihydropteridinone **89k** (45 mg, 136 μ mol) was reacted with aniline **28b** (17 mg, 177 μ mol) using general method **16** to afford the title compound **102** as a brown oil (10 mg, 14%). LCMS purity >95%, ret. time 1.17 mins; HRMS (ESI +ve): found $[M+H]^+$



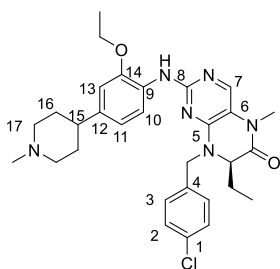
529.3283, $[\text{C}_{31}\text{H}_{41}\text{N}_6\text{O}_2]^+$ requires 529.3286; ν_{max} (thin film, cm^{-1}): 3421 (w, N-H), 1666 (C=O); $[\alpha]_D^{23.4}$: +13.2° (c 1.0, MeOH); δ_{H} (CDCl_3 , 500 MHz): 8.10 (1H, d, J = 8.2 Hz, H12), 7.74 (1H, s, NH), 7.67 (1H, s, H9), 7.26 – 7.15 (4H, m, H12, H3, H4 & H5), 6.71 (1H, s, H15), 6.68 (1H, d, J = 8.5 Hz, H13), 5.67 (1H, d, J = 15.1 Hz, ArCHH), 4.12 – 4.08 (3H, m, ArCHH & OCH_2CH_3), 4.03 (1H, dd, J = 6.3, 3.8 Hz, CHCH_2CH_3), 3.59 (2H, d, J = 7.3 Hz, H19), 3.34 (3H, s, CONCH_3), 2.74 (3H, s, NCH_3), 2.78 – 2.68 (2H, m, H19), 2.66 – 2.59 (1H, m, H17), 2.28 (3H, s, ArCH₃), 2.23 – 2.17 (2H, m, H18), 2.01 – 1.91 (3H, m, 2 x H18 & CHCH_2CH_3), 1.90 – 1.81 (1H, m, CHCH_2CH_3), 1.47 (3H, t, J = 6.9 Hz, OCH_2CH_3), 0.86 (3H, t, J = 7.4 Hz, CHCH_2CH_3); δ_{C} (CDCl_3 , 126 MHz): 163.5 (CONCH_3), 155.3 (C10), 152.0 (C7), 147.6 (C16), 137.0 (C9), 136.8 (C14), 136.5 (C6), 133.1 (C1), 130.9 (C2), 128.7 (C5), 128.1 (C3/4), 126.3 (C3/4), 118.6 (C12), 118.5 (C13), 114.8 (C8), 109.4 (C15), 64.4 (OCH_2CH_3), 59.9 (CHCH_2CH_3), 54.6 (C19), 46.0 (ArCH₂), 43.5 (NCH_3), 40.0 (C17), 30.5 (C18), 28.1 (CONCH_3), 24.7 (CHCH_2CH_3), 19.4 (ArCH₃), 14.9 (OCH_2CH_3), 8.9 (CHCH_2CH_3)

(R)-2-((2-Ethoxy-4-(1-methylpiperidin-4-yl)phenyl)amino)-7-ethyl-5-methyl-8-(4-bromobenzyl)-7,8-dihydropteridin-6(5H)-one, 103



Dihydropteridinone **89I** (35 mg, 89 μmol) was reacted with aniline **28b** (20 mg, 84 μmol) using general method **16** to afford the title compound **103** as a white solid (3 mg, 6%). LCMS purity >95%, ret. time 1.24 mins; HRMS (ESI +ve): found $[\text{M}+\text{H}]^+$ 593.2242, $[\text{C}_{30}\text{H}_{38}\text{BrN}_6\text{O}_2]^+$ requires 593.2234; m.p.: 118 – 120 °C; ν_{max} (thin film, cm^{-1}): 3419 (w, N-H), 1668 (C=O), 767 (C-Br); $[\alpha]_D^{23.4}$: +6.2° (c 1.0, MeOH); δ_{H} (CDCl_3 , 500 MHz): 8.16 (1H, d, J = 7.9 Hz, H10), 7.69 (1H, s, H7), 7.59 (1H, s, NH), 7.47 (2H, d, J = 8.2 Hz, H2), 7.20 (2H, d, J = 8.2 Hz, H3), 6.74 – 6.69 (2H, m, H11 & H13), 5.51 (1H, d, J = 15.5 Hz, ArCHH), 4.19 – 4.09 (4H, m, ArCHH, CHCH_2CH_3 & OCH_2CH_3), 3.58 (2H, d, J = 9.1 Hz, H17), 3.34 (3H, s, CONCH_3), 2.74 (3H, s, NCH_3), 2.75 – 2.59 (3H, m, H15 & 2 x H17), 2.22 – 2.16 (2H, m, H16), 2.02 – 1.90 (3H, m, 2 x H16 & CHCH_2CH_3), 1.85 – 1.76 (1H, m, CHCH_2CH_3), 1.47 (3H, t, J = 6.9 Hz, OCH_2CH_3), 0.85 (3H, t, J = 7.4 Hz, CHCH_2CH_3); δ_{C} (CDCl_3 , 126 MHz): 163.2 (CONCH_3), 155.5 (C8), 151.9 (C5), 147.4 (C14), 137.9 (C7), 136.5 (C12), 135.2 (C4), 132.0 (C2), 129.7 (C3), 128.4 (C9), 121.8 (C1), 118.6 (C11), 118.3 (C10), 114.7 (C6), 109.4 (C13), 64.4 (OCH_2CH_3), 60.9 (CHCH_2CH_3), 54.7 (C17), 47.5 (ArCH₂), 44.0 (NCH_3), 40.1 (C15), 30.7 (C16), 28.1 (CONCH_3), 24.8 (CHCH_2CH_3), 14.9 (OCH_2CH_3), 8.8 (CHCH_2CH_3)

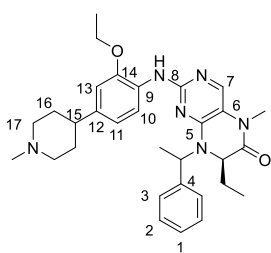
(*R*)-2-((2-Ethoxy-4-(1-methylpiperidin-4-yl)phenyl)amino)-7-ethyl-5-methyl-8-(4-chlorobenzyl)-7,8-dihydropteridin-6(5*H*)-one, 104



Dihydropteridinone **90m** (43 mg, 122 μ mol) was reacted with aniline **28b** (27 mg, 116 μ mol) using general method **16** to afford the title compound **104** as a white solid (6 mg, 9%). LCMS purity >95%, ret. time 1.20 mins; HRMS (ESI +ve): found $[M+H]^+$ 549.2761, $[C_{30}H_{38}ClN_6O_2]^+$ requires 549.2739; m.p.: 94 – 97 $^{\circ}C$; ν_{max} (thin film, cm^{-1}): 3420 (w, N-H), 1666

(C=O); $[\alpha]_D^{23.4}$: +31.4 $^{\circ}$ (c 1.0, MeOH); δ_H ($CDCl_3$, 500 MHz): 8.16 (1H, d, J = 6.6 Hz, H12), 7.68 (1H, s, H9), 7.63 (1H, s, NH), 7.32 (2H, d, J = 8.2 Hz, H2), 7.27 – 7.24 (2H, m, H3), 6.73 – 6.70 (2H, m, H13 & H15), 5.53 (1H, d, J = 15.1 Hz, ArCHH), 4.18 (2H, d, J = 15.1 Hz, ArCHH) 4.14 – 4.09 (3H, m, CHCH₂CH₃ & OCH₂CH₃), 3.80 (2H, d, J = 10.0 Hz, H19), 3.34 (3H, s, CONCH₃), 2.74 (3H, s, NCH₃), 2.76 – 2.66 (2H, m, H19), 2.65 – 2.59 (1H, m, H17), 2.24 – 2.17 (2H, m, H18), 2.02 – 1.89 (3H, m, 2 x H18 & CHCH₂CH₃), 1.85 – 1.78 (1H, m, CHCH₂CH₃), 1.47 (3H, t, J = 6.9 Hz, OCH₂CH₃), 0.85 (3H, t, J = 7.6 Hz, CHCH₂CH₃); δ_C ($CDCl_3$, 126 MHz): 163.2 (CONCH₃), 155.5 (C10), 152.0 (C7), 147.5 (C16), 137.8 (C9), 136.5 (C14), 134.7 (C4), 133.7 (C1), 129.3 (C2), 129.0 (C3), 128.4 (C11), 118.6 (C13), 118.3 (C12), 114.7 (C8), 109.4 (C15), 64.4 (OCH₂CH₃), 60.9 (CHCH₂CH₃), 54.7 (C19), 47.4 (ArCH₂), 43.6 (NCH₃), 40.0 (C17), 30.6 (C18), 28.2 (CONCH₃), 24.8 (CHCH₂CH₃), 14.9 (OCH₂CH₃), 8.8 (CHCH₂CH₃)

(\pm)-7*R*-2-((2-Ethoxy-4-(1-methylpiperidin-4-yl)phenyl)amino)-7-ethyl-5-methyl-8-(1-phenylethyl)-7,8-dihydropteridin-6(5*H*)-one, 105

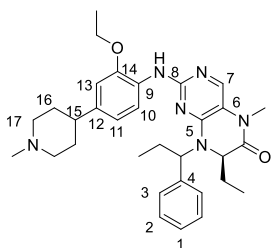


Dihydropteridinone **90n** (43 mg, 130 μ mol) was reacted with aniline **28b** (29 mg, 124 μ mol) using general method **16** to afford the title compound **105** as a white solid (8 mg, 12%, *d.r* 2:1). LCMS purity >95%, ret. time 1.16 mins; HRMS (ESI +ve): found $[M+H]^+$ 529.3288, $[C_{31}H_{41}N_6O_2]^+$ requires 529.3286;

Major diastereomer δ_H and δ_C see compound **135** experimental. Minor diastereomer δ_H and δ_C see compound **134** experimental.

(7*R*)-2-((2-Ethoxy-4-(1-methylpiperidin-4-yl)phenyl)amino)-7-ethyl-5-methyl-8-(1-phenylpropyl)-7,8-dihydropteridin-6(5*H*)-one, 106

Dihydropteridinone **90o** (40 mg, 116 μ mol) was reacted with aniline **28b** (26 mg, 110 μ mol) using general method **16** to afford the title compound **106** as a white solid (2 mg, 2%, *d.r* 1.5:1). LCMS purity >95%, ret. time 1.21 mins; HRMS (ESI +ve): found

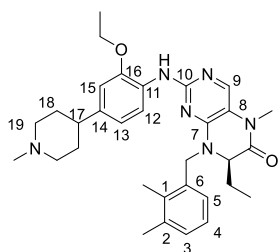


$[M+H]^+$ 543.3442, $[C_{32}H_{43}N_6O_2]^+$ requires 543.3442; *Major diastereomer* δ_H and δ_C see compound **146** experimental.

Minor Isomer δ_H (CDCl₃, 500 MHz): 8.44 (1H, d, J = 7.9 Hz, H10), 7.72 (1H, s, H7), 7.65 (1H, s, NH), 7.38 – 7.30 (5H, m, H1, H2 & H3), 6.81 – 6.74 (2H, m, H11 & H13), 5.66 (1H,

dd, J = 9.3, 5.5 Hz, ArCH₂CH₂CH₃), 4.16 (2H, q, J = 7.1 Hz, OCH₂CH₃), 3.86 (1H, dd, J = 7.4, 3.3 Hz, CHCH₂CH₃), 3.61 – 3.53 (2H, m, H17), 3.28 (3H, s, CONCH₃), 2.80 – 2.62 (6H, m, NCH₃, H15 & 2 x H17), 2.27 – 2.08 (2H, m, 2 x H16 & ArCHCH₂CH₃), 2.04 – 1.82 (3H, m, 3 x H16 & CHCH₂CH₃), 1.74 – 1.66 (1H, m, CHCH₂CH₃), 1.49 (3H, t, J = 7.1 Hz, OCH₂CH₃), 1.90 – 1.82 (1H, m, CHCH₂CH₃), 1.74 – 1.66 (1H, m, CHCH₂CH₃), 1.07 (3H, t, J = 7.3 Hz, ArCHCH₂CH₃), 0.84 (3H, t, J = 7.6 Hz, CHCH₂CH₃); δ_C (CDCl₃, 126 MHz): 163.3 (CONCH₃), 155.5 (C8), 152.5 (C5), 147.8 (C14), 138.3 (C7), 136.9 (C4), 136.6 (C12), 129.0 (C2/3), 128.6 (C9), 128.5 (C2/3), 128.4 (C1), 118.7 (C10 & C11), 114.3 (C6), 109.2 (C13), 64.4 (OCH₂CH₃), 61.8 (ArCHCH₂CH₃), 58.4 (CHCH₂CH₃), 54.8 (C17), 43.8 (NCH₃), 40.1 (C15), 30.7 (C16), 28.3 (CONCH₃), 28.1 (CHCH₂CH₃), 24.4 (ArCHCH₂CH₃), 15.0 (OCH₂CH₃), 11.6 (ArCHCH₂CH₃), 8.9 (CHCH₂CH₃)

(R)-8-(2,3-Dimethylbenzyl)-2-((2-ethoxy-4-(1-methylpiperidin-4-yl)phenyl)amino)-7-ethyl-5-methyl-7,8-dihydropteridin-6(5H)-one, 107

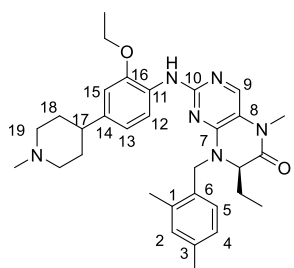


Dihydropteridinone **90p** (30 mg, 87 μ mol) was reacted with aniline **28b** (19 mg, 83 μ mol) using general method **16** to afford the title compound **107** as an orange oil (2 mg, 4%). LCMS purity >95%, ret. time 1.03 mins; HRMS (ESI +ve): found $[M+H]^+$ 543.3425, $[C_{32}H_{43}N_6O_2]^+$ requires 543.3442;

ν_{\max} (thin film, cm⁻¹): 3434 (w, N-H), 1665 (C=O); $[\alpha]_D^{22.6}$: +5.5° (c 1.0, MeOH); δ_H (CDCl₃, 500 MHz): 8.24 (1H, d, J = 8.2 Hz, H12), 7.68 (1H, s, H9), 7.43 (1H, s, NH), 7.14 – 7.11 (1H, m, H3), 7.09 – 7.06 (2H, m, H4 & H5), 6.75 – 6.70 (2H, m, H13 & H15), 5.74 (1H, d, J = 15.0 Hz, ArCH₂H), 4.11 (2H, q, J = 7.0 Hz, OCH₂CH₃), 4.06 (1H, d, J = 15.0 Hz, ArCH₂H), 3.96 (1H, dd, J = 6.6, 3.6 Hz, CHCH₂CH₃), 3.36 – 3.30 (5H, m, CONCH₃ & 2 x H19), 2.62 – 2.43 (7H, m, NCH₃, H17 & 2 x H19), 2.30 (3H, s, C²CH₃), 2.16 (3H, s, C¹CH₃), 2.16 – 2.07 (2H, m, H18), 1.95 – 1.80 (4H, m, 2 x H18 & CHCH₂CH₃), 1.46 (3H, t, J = 7.0 Hz, OCH₂CH₃), 0.85 (3H, t, J = 7.6 Hz, CHCH₂CH₃); δ_C (CDCl₃, 126 MHz): 163.6 (CONCH₃), 155.8 (C10), 151.9 (C7), 138.2 (C9), 137.7 (C2 & C14), 135.6 (C1), 133.0 (C6), 129.9 (C3), 128.5 (C11), 127.2 (C5), 125.7 (C4), 118.7 (C13), 117.8 (C12), 114.8 (C8), 109.3 (C15), 64.3 (OCH₂CH₃), 59.3 (CHCH₂CH₃), 55.4 (C19), 46.4 (ArCH₂), 44.5 (NCH₃), 40.7 (C17), 31.6 (C18), 28.0

(CONCH₃), 24.5 (CHCH₂CH₃), 20.5 (C²CH₃), 15.1 (C¹CH₃), 15.0 (OCH₂CH₃), 8.9 (CHCH₂CH₃)

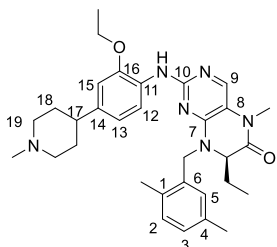
(*R*)-8-(2,4-Dimethylbenzyl)-2-((2-ethoxy-4-(1-methylpiperidin-4-yl)phenyl)amino)-7-ethyl-5-methyl-7,8-dihydropteridin-6(5*H*)-one, 108



Dihydropteridinone **90q** (40 mg, 116 μmol) was reacted with aniline **28b** (26 mg, 110 μmol) using general method **16** to afford the title compound **108** as a yellow solid (6 mg, 9%). LCMS purity >95%, ret. time 1.24 mins; HRMS (ESI +ve): found [M+H]⁺ 543.3423, [C₃₂H₄₃N₆O₂]⁺ requires 543.3442; m.p.: 83 – 85 °C; ν_{max} (thin film, cm⁻¹): 3425 (w, N-H), 1668

(s, C=O); [α]_D^{23.2}: +20.1° (c 1.0, MeOH); δ_H (CDCl₃, 500 MHz): 8.13 (1H, d, *J* = 7.9 Hz, H12), 7.84 (1H, s, NH), 7.66 (1H, s, H9), 7.09 (1H, d, *J* = 7.6 Hz, H5), 7.03 (1H, s, H2), 6.98 (1H, d, *J* = 7.6 Hz, H4), 6.73 – 6.68 (2H, m, H13 & H15), 5.65 (1H, d, *J* = 15.1 Hz, ArCHH), 4.11 (2H, q, *J* = 6.9 Hz, OCH₂CH₃), 4.05 (1H, d, *J* = 15.1 Hz, ArCHH), 4.01 (1H, dd, *J* = 6.5, 3.6 Hz, CHCH₂CH₃), 3.60 (2H, d, *J* = 8.2 Hz, H19), 3.33 (3H, s, CONCH₃), 2.78 – 2.69 (5H, m, NCH₃ & 2 x H19), 2.67 – 2.60 (1H, m, H17), 2.31 (3H, s, C³CH₃), 2.24 – 2.14 (5H, m, C¹CH₃ & 2 x H18), 2.02 – 1.82 (4H, m, 2 x H18 & CHCH₂CH₃), 1.47 (3H, t, *J* = 6.9 Hz, OCH₂CH₃), 0.85 (3H, t, *J* = 7.4 Hz, CHCH₂CH₃); δ_C (CDCl₃, 126 MHz): 163.4 (CONCH₃), 155.1 (C10), 152.0 (C7), 147.7 (C16), 137.9 (C3), 136.7 (C1), 136.5 (C11), 136.4 (C9), 131.7 (C2), 129.8 (C6), 129.0 (C5), 128.2 (C14), 126.8 (C4), 118.6 (C12), 118.5 (C13), 114.7 (C8), 109.4 (C15), 64.3 (OCH₂CH₃), 59.5 (CHCH₂CH₃), 54.6 (C19), 45.7 (ArCH₂), 43.4 (NCH₃), 39.9 (C17), 30.5 (C18), 28.0 (CONCH₃), 24.6 (CHCH₂CH₃), 21.0 (C³CH₃), 19.2 (C¹CH₃), 14.9 (OCH₂CH₃), 8.8 (CHCH₂CH₃)

(*R*)-8-(2,5-Dimethylbenzyl)-2-((2-ethoxy-4-(1-methylpiperidin-4-yl)phenyl)amino)-7-ethyl-5-methyl-7,8-dihydropteridin-6(5*H*)-one, 109

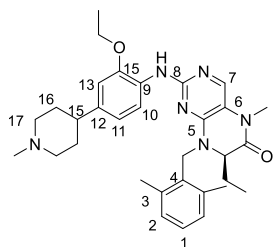


Dihydropteridinone **90r** (35 mg, 102 μmol) was reacted with aniline **28b** (23 mg, 96 μmol) using general method **16** to afford the title compound **109** as a brown solid (7 mg, 12%). LCMS purity >95%, ret. time 1.23 mins; HRMS (ESI +ve): found [M+H]⁺ 543.3434, [C₃₂H₄₃N₆O₂]⁺ requires 543.3442;

m.p.: 70 – 73 °C; ν_{max} (thin film, cm⁻¹): 3424 (w, N-H), 1667 (C=O); [α]_D^{22.4}: +7.6° (c 1.0, MeOH); δ_H (CDCl₃, 500 MHz): 8.12 (1H, d, *J* = 8.2 Hz, H12), 7.88 (1H, s, NH), 7.67 (1H, s, H9), 7.10 (1H, d, *J* = 7.5 Hz, H2), 7.5 (1H, d, *J* = 7.5 Hz, H3), 7.01 (1H, s, H5), 6.75 – 6.78 (2H, m, H13 & H15), 5.67 (1H, d, *J* = 15.1 Hz, ArCHH), 4.12 (1H,

dd, $J = 6.9$ Hz, OCH_2CH_3), 4.07 – 4.03 (2H, m, ArCHH & CHCH_2CH_3), 3.67 – 3.57 (2H, m, H19), 3.35 (3H, s, CONCH_3), 2.80 – 2.70 (5H, m, NCH_3 & 2 x H19), 2.68 – 2.60 (1H, m, H17), 2.31 (3H, s, C^4CH_3), 2.26 – 2.15 (5H, m, C^1CH_3 & 2 x H18), 2.03 – 1.85 (4H, m, 2 x H18 & CHCH_2CH_3), 1.48 (3H, t, $J = 6.9$ Hz, OCH_2CH_3), 0.87 (3H, t, $J = 7.4$ Hz, CHCH_2CH_3); δ_{C} (CDCl_3 , 126 MHz): 163.5 (CONCH_3), 155.1 (C10), 152.1 (C7), 147.8 (C16), 136.6 (14), 136.4 (C9), 135.8 (C4), 133.7 (C1), 132.7 (C6), 130.9 (C2), 129.6 (C5), 128.9 (C3), 128.2 (C11), 118.712, 118.6 (C13), 114.7 (C8), 109.4 (C15), 64.4 (OCH_2CH_3), 59.6 (CHCH_2CH_3), 54.7 (C19), 46.0 (ArCH_2), 43.5 (NCH_3), 39.9 (C17), 30.4 (C18), 28.1 (CONCH_3), 24.7 (CHCH_2CH_3), 21.0 (C^4CH_3), 18.9 (C^1CH_3), 14.9 (OCH_2CH_3), 8.8 (CHCH_2CH_3)

(*R*)-8-(2,6-Dimethylbenzyl)-2-((2-ethoxy-4-(1-methylpiperidin-4-yl)phenyl)amino)-7-ethyl-5-methyl-7,8-dihydropteridin-6(5*H*)-one, 110

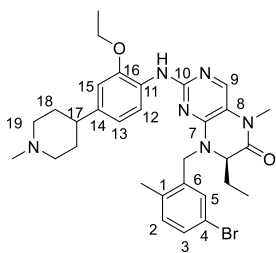


Dihydropteridinone **90s** (25 mg, 73 μmol) was reacted with aniline **28b** (16 mg, 69 μmol) using general method **16** to afford the title compound **110** as a brown solid (9 mg, 24%). LCMS purity >95%, ret. time 1.25 mins; HRMS (ESI +ve): found $[\text{M}+\text{H}]^+$ 543.3419, $[\text{C}_{32}\text{H}_{43}\text{N}_6\text{O}_2]^+$ requires 543.3442;

m.p.: 93 – 96 $^{\circ}\text{C}$; ν_{max} (thin film, cm^{-1}): 3424 (w, N-H), 1669 (C=O); $[\alpha]_D^{22.4}$: +17.1 $^{\circ}$ (c 1.0, MeOH); δ_{H} (CDCl_3 , 500 MHz): 8.39 (1H, d, $J = 8.5$ Hz, H10), 7.69 (1H, s, H7), 7.59 (1H, s, NH), 7.13 (1H, t, $J = 7.6$ Hz, H1), 7.04 (2H, d, $J = 7.6$ Hz, H2), 6.80 (1H, d, $J = 8.5$ Hz, H11), 6.75 (1H, s, H13), 5.61 (1H, d, $J = 14.6$ Hz, ArCHH), 4.35 (1H, d, $J = 14.6$ Hz, ArCHH), 4.13 (2H, d, $J = 6.9$ Hz, OCH_2CH_3), 3.75 (1H, dd, $J = 7.7, 3.3$ Hz, CHCH_2CH_3), 3.54 (2H, d, $J = 10.7$ Hz, H17), 3.31 (3H, s, CONCH_3), 2.72 – 2.60 (7H, m, NCH_3 , H15 & 2 x H17), 2.31 (6H, s, 2 x ArCH_3), 2.24 – 2.15 (2H, m, H16), 2.00 – 1.94 (2H, m, H16) 1.92 – 1.87 (1H, m, CHCHHCH_3), 1.78 – 1.71 (1H, m, CHCHHCH_3), 1.49 (3H, t, $J = 6.9$ Hz, OCH_2CH_3), 0.87 (3H, t, $J = 7.6$ Hz, CHCH_2CH_3); δ_{C} (CDCl_3 , 126 MHz): 163.5 (CONCH_3), 155.6 (C8), 152.2 (C5), 147.3 (C14), 138.1 (C7), 137.9 (C3), 136.4 (C12), 131.5 (C4), 128.9 (C2), 128.6 (C9), 128.1 (C1), 118.8 (C11), 118.0 (C10), 115.1 (C6), 109.3 (C13), 64.3 (OCH_2CH_3), 58.7 (CHCH_2CH_3), 54.6 (C17), 43.6 (NCH_3), 41.8 (ArCH_2), 40.1 (C15), 30.6 (C16), 28.1 (CONCH_3), 24.8 (CHCH_2CH_3), 20.3 (2 x ArCH_3), 15.0 (OCH_2CH_3), 9.3 (CHCH_2CH_3)

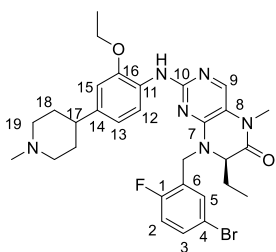
(*R*)-8-(5-Bromo-2-methylbenzyl)-2-((2-ethoxy-4-(1-methylpiperidin-4-yl)phenyl)amino)-7-ethyl-5-methyl-7,8-dihydropteridin-6(5*H*)-one, 111

Dihydropteridinone **90t** (44 mg, 107 μmol) was reacted with aniline **28b** (24 mg, 102 μmol) using general method **16** to afford the title compound **111** as a white solid (10



mg, 15%). LCMS purity >95%, ret. time 1.24 mins; HRMS (ESI +ve): found $[M+H]^+$ 608.2378, $[C_{31}H_{40}BrN_6O_2]^+$ requires 608.2421; m.p.: 86 – 89 °C; ν_{\max} (thin film, cm^{-1}): 3417 (w, N-H), 1666 (C=O), 757 (C-Br); $[\alpha]_D^{23.6}$: +7.6° (c 1.0, MeOH); δ_H (CDCl_3 , 500 MHz): 8.11 (1H, d, J = 8.3 Hz, H12), 7.70 (1H, s, H9), 7.55 (1H, s, NH), 7.37 – 7.33 (2H, m, H3 & H5), 7.10 (1H, d, J = 7.9 Hz, H2), 6.72 (1H, d, J = 1.3 Hz, H15), 6.69 (1H, dd, J = 8.3, 1.3 Hz, H13), 5.60 (1H, d, J = 15.5 Hz, ArCHH), 4.11 (2H, q, J = 6.9 Hz, OCH_2CH_3), 4.06 – 4.02 (2H, m, ArCHH & CHCH₂CH₃), 3.57 (2H, d, J = 9.1 Hz, H19), 3.36 (3H, s, CONCH₃), 2.72 (3H, s, NCH₃), 2.74 – 2.58 (3H, m, H17 & 2 x H19), 2.25 (3H, s, ArCH₃), 2.25 – 2.15 (2H, m, H18), 2.00 – 1.92 (3H, m, 2 x H18 & CHCH₂CH₃), 1.89 – 1.81 (1H, m, CHCH₂CH₃), 1.47 (3H, t, J = 6.9 Hz, OCH_2CH_3), 0.88 (3H, t, J = 7.4 Hz, CHCH₂CH₃); δ_C (CDCl_3 , 126 MHz): 163.4 (CONCH₃), 155.5 (C10), 151.9 (C7), 147.4 (C16), 138.1 (C9), 136.5 (C14), 135.8 (C1/6), 135.7 (C1/6), 132.5 (C2), 131.3 (C5), 131.0 (C3), 128.4 (C11), 119.9 (C4), 118.6 (C13), 118.1 (C12), 114.8 (C8), 109.4 (C15), 64.3 (OCH_2CH_3), 60.3 (CHCH₂CH₃), 54.7 (C19), 45.6 (ArCH₂), 43.6 (NCH₃), 40.2 (C17), 30.6 (C18), 28.1 (CONCH₃), 24.7 (CHCH₂CH₃), 19.0 (CH₃), 15.0 (OCH_2CH_3), 8.9 (CHCH₂CH₃)

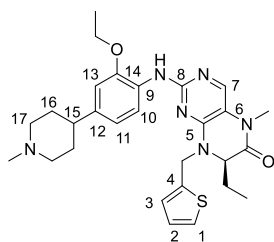
(R)-8-(5-Bromo-2-fluorobenzyl)-2-((2-ethoxy-4-(1-methylpiperidin-4-yl)phenyl)amino)-7-ethyl-5-methyl-7,8-dihydropteridin-6(5H)-one, 112



Dihydropteridinone **90u** (43 mg, 104 μmol) was reacted with aniline **28b** (23 mg, 99 μmol) using general method **16** to afford the title compound **112** as a white solid (2 mg, 3%). LCMS purity >95%, ret. time 1.22 mins; HRMS (ESI +ve): found $[M+H]^+$ 613.2131, $[C_{30}H_{37}BrFN_6O_2]^+$ requires 613.2124; ν_{\max} (thin film, cm^{-1}): 3421 (w, N-H), 1666 (s, C=O); $[\alpha]_D^{23.1}$: +13.9° (c 1.0, MeOH); δ_H (CDCl_3 , 500 MHz): 8.20 (1H, d, J = 8.2 Hz, H12), 7.70 (1H, s, H9), 7.46 – 7.44 (2H, m, H5 & NH), 7.39 (1H, ddd, J = 8.7, 4.6, 2.5 Hz, H3), 7.0 (1H, t, J = 8.8 Hz, H2), 6.77 (1H, dd, J = 8.4, 1.7 Hz, H13), 6.7 (1H, d, J = 1.7 Hz, H15), 5.52 (1H, d, J = 15.5 Hz, ArCHH), 4.24 (1H, d, J = 15.5 Hz, ArCHH), 4.17 (1H, dd, J = 6.5, 3.6 Hz, CHCH₂CH₃), 4.12 (1H, q, J = 7.2 Hz, OCH_2CH_3), 3.51 (2H, d, J = 12.0 Hz, H19), 3.35 (3H, s, CONCH₃), 2.72 (3H, s, NCH₃), 2.72 – 2.61 (3H, m, H17 & 2 x H19), 2.20 – 2.14 (2H, m, H18), 2.01 – 1.95 (3H, m, 2 x H18 & CHCH₂CH₃), 1.91 – 1.84 (1H, m, CHCH₂CH₃), 1.48 (3H, t, J = 6.9 Hz, OCH_2CH_3), 0.88 (3H, t, J = 7.6 Hz, CHCH₂CH₃); δ_C (CDCl_3 , 126 MHz): 163.3 (CONCH₃), 158.3 (d, $J_{\text{C-F}}$ = 246 Hz, C1), 155.6 (C10), 151.7 (C7), 147.4 (C16), 138.4 (C9), 136.5 (C14), 133.0 (d, $J_{\text{C-F}}$ = 6 Hz, C5), 132.5 (d, $J_{\text{C-F}}$ = 8 Hz, C3), 128.6 (C11), 125.6 (d, J = 24 Hz, C6), 118.7 (C13),

118.3 (C12), 117.5 (d, J_{C-F} = 22 Hz, C2), 117.3 (d, J_{C-F} = 4 Hz, C4), 114.5 (C8), 109.4 (C15), 64.4 (OCH₂CH₃), 61.4 (CHCH₂CH₃), 54.9 (C19), 43.9 (NCH₃), 41.0 (C17 & ArCH₂), 30.0 (C18), 28.1 (CONCH₃), 24.9 (CHCH₂CH₃), 15.0 (OCH₂CH₃), 8.9 (CHCH₂CH₃); $\delta_{F\{H\}}$ (CDCl₃, 471 MHz): -120.1

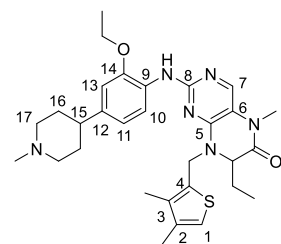
(*R*)-2-((2-Ethoxy-4-(1-methylpiperidin-4-yl)phenyl)amino)-7-ethyl-5-methyl-8-(thiophen-2-ylmethyl)-7,8-dihydropteridin-6(5*H*)-one, 113



Dihydropteridinone **90v** (35 mg, 108 μ mol) was reacted with aniline **28b** (24 mg, 103 μ mol) using general method **16** to afford the title compound **113** as a yellow oil (12 mg, 21%). LCMS purity >95%, ret. time 1.11 mins; HRMS (ESI +ve): found $[M+H]^+$ 521.2679, $[C_{28}H_{37}N_6O_2S]^+$ requires 521.2693;

ν_{max} (thin film, cm⁻¹): 3418 (w, N-H), 1665 (C=O); $[\alpha]_D^{22.7}$: -2.8° (c 1.0, MeOH); δ_H (CDCl₃, 500 MHz): 8.35 (1H, d, J = 8.2 Hz, H10), 7.68 (1H, s, H7), 7.50 (1H, s, NH), 7.26 (1H, d, J = 5.0 Hz, H1), 7.06 (1H, d, J = 3.5 Hz, H3), 6.97 (1H, dd, J = 5.0, 3.5 Hz, H2), 6.79 (1H, dd, J = 8.2, 1.4 Hz, H11), 6.74 (1H, d, J = 1.4 Hz, H13), 5.62 (1H, d, J = 15.5 Hz, ArCHH), 4.46 (1H, d, J = 15.5 Hz, ArCHH), 4.25 (1H, dd, J = 6.2, 3.6 Hz, CHCH₂CH₃), 4.13 (2H, q, J = 6.9 Hz, OCH₂CH₃), 3.47 (2H, d, J = 11.7 Hz, H17), 3.32 (3H, s, CONCH₃), 2.65 (3H, s, NCH₃), 2.64 – 2.56 (3H, m, H15 & 2 x H17), 2.19 – 2.10 (2H, m, H16), 1.99 – 1.92 (3H, m, 2 x H16 & CHCH₂CH₃), 1.89 – 1.80 (1H, m, CHCH₂CH₃), 1.49 (3H, t, J = 6.9 Hz, OCH₂CH₃), 0.83 (3H, t, J = 7.6 Hz, CHCH₂CH₃); δ_C (CDCl₃, 126 MHz): 163.3 (CONCH₃), 155.6 (C7), 151.4 (C5), 147.2 (C14), 138.6 (C4), 138.2 (C7), 136.8 (C12), 128.5 (C9), 127.3 (C3), 126.7 (C2), 126.1 (C1), 118.8 (C11), 118.1 (C10), 114.8 (C6), 109.4 (C13), 64.3 (OCH₂CH₃), 60.5 (CHCH₂CH₃), 54.8 (C17), 43.9 (NCH₃), 42.9 (ArCH₂), 40.4 (C15), 31.1 (C16), 28.1 (CONCH₃), 24.8 (CHCH₂CH₃), 15.0 (OCH₂CH₃), 8.7 (CHCH₂CH₃)

8-((3,4-Dimethylthiophen-2-yl)methyl)-2-((2-ethoxy-4-(1-methylpiperidin-4-yl)phenyl)amino)-7-ethyl-5-methyl-7,8-dihydropteridin-6(5*H*)-one, 114

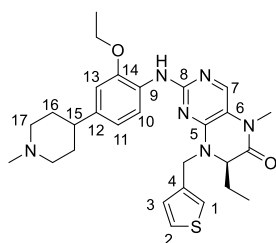


Dihydropteridinone **90w** (26 mg, 74 μ mol) was reacted with aniline **28b** (16 mg, 70 μ mol) using general method **16** to afford the title compound **114** as a yellow solid (3 mg, 8%). LCMS purity >95%, ret. time 1.26 mins; HRMS (ESI +ve): found $[M+H]^+$ 549.2983, $[C_{30}H_{41}N_6O_2S]^+$ requires 549.3006;

m.p.: 82 – 85 °C; ν_{max} (thin film, cm⁻¹): 3425 (w, N-H), 1669 (s, C=O); δ_H (CDCl₃, 500 MHz): 8.35 (1H, d, J = 8.2 Hz, H10), 7.68 (1H, s, H7), 7.51 (1H, s, NH), 6.83 (1H, s, H1), 6.79 (1H, d, J = 8.2 Hz, H11), 6.75 (1H, s, H13), 5.71 (1H, d, J = 15.5 Hz,

ArCH₂H), 4.28 (1H, d, $J = 15.5$ Hz, ArCH₂H), 4.20 – 4.17 (1H, m, CHCH₂CH₃), 4.13 (2H, q, $J = 6.8$ Hz, OCH₂CH₃), 3.52 – 3.46 (2H, m, H17), 3.32 (CONCH₃), 2.67 (3H, s, NCH₃), 2.65 – 2.57 (3H, m, H15 & 2 x H17), 2.22 – 2.11 (8H, m, C²CH₃, C³CH₃ & 2 x H16), 2.01 – 1.91 (3H, m, 2 x H16 & CHCH₂CH₃), 1.88 – 1.77 (1H, m, CHCH₂CH₃), 1.49 (3H, t, $J = 6.8$ Hz, OCH₂CH₃), 0.86 (3H, t, $J = 7.6$ Hz, CHCH₂CH₃); δ_c (CDCl₃, 126 MHz): 163.3 (CONCH₃), 155.6 (C8), 151.6 (C5), 147.2 (C14), 138.1 (C7), 138.0 (C2), 136.6 (C12), 136.0 (C3), 131.4 (C4), 128.5 (C9), 119.8 (C1), 118.8 (C11), 118.1 (C10), 114.9 (C6), 109.3 (C13), 64.3 (OCH₂CH₃), 59.7 (CHCH₂CH₃), 54.8 (C17), 43.9 (NCH₃), 41.0 (ArCH₂), 40.3 (C15), 31.0 (C16), 28.0 (CONCH₃), 24.7 (CHCH₂CH₃), 15.2 (C²CH₃), 15.0 (OCH₂CH₃), 12.6 (C³CH₃), 8.9 (CHCH₂CH₃)

(*R*)-2-((2-Ethoxy-4-(1-methylpiperidin-4-yl)phenyl)amino)-7-ethyl-5-methyl-8-(thiophen-3-ylmethyl)-7,8-dihydropteridin-6(5*H*)-one, 115

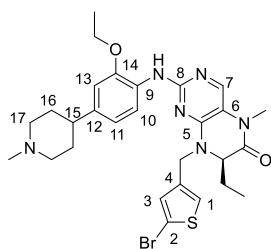


Dihydropteridinone **90x** (45 mg, 139 μ mol) was reacted with aniline **28b** (24 mg, 103 μ mol) using general method **16** to afford the title compound **115** as a yellow oil (4 mg, 6%). LCMS purity >95%, ret. time 1.12 mins; HRMS (ESI +ve): found $[M+H]^+$ 521.2676, $[C_{28}H_{37}N_6O_2S]^+$ requires 521.2693;

ν_{\max} (thin film, cm⁻¹): 3426 (w, N-H), 1665 (s, C=O); $[\alpha]_D^{23.2}$: +11.1° (c 1.0, MeOH); δ_H (CDCl₃, 500 MHz): 8.26 (1H, d, $J = 8.2$ Hz, H10), 7.66 (1H, s, H7), 7.60 (1H, s, NH), 7.32 (1H, dd, $J = 5.0, 2.6$ Hz, H3), 7.23 (1H, d, $J = 2.6$ Hz, H1), 7.06 (1H, d, $J = 5.0$ Hz, H2), 6.76 – 6.73 (2H, m, H11 & H13), 5.50 (1H, d, $J = 15.1$ Hz, ArCH₂H), 4.28 (1H, d, $J = 15.1$ Hz, ArCH₂H), 4.17 (1H, dd, $J = 6.3, 3.5$ Hz, CHCH₂CH₃), 4.12 (2H, q, $J = 6.6$ Hz, OCH₂CH₃), 3.56 (2H, m, H17), 3.33 (3H, s, CONCH₃), 2.72 (3H, s, NCH₃), 2.72 – 2.60 (3H, m, H15 & 2 x H17), 2.24 – 2.15 (2H, m, H16), 2.00 – 1.91 (3H, m, 2 x H16 & CHCH₂CH₃), 1.86 – 1.78 (1H, m, CHCH₂CH₃), 1.48 (3H, t, $J = 6.9$ Hz, OCH₂CH₃), 0.83 (3H, t, $J = 7.4$ Hz, CHCH₂CH₃); δ_c (CDCl₃, 126 MHz): 163.4 (CONCH₃), 155.5 (C8), 151.8 (C4), 147.4 (C14), 137.7 (C7), 136.7 (C4), 136.4 (C12), 128.5 (C9), 127.5 (C2), 126.8 (C3), 123.6 (C1), 118.7 (C11), 118.2 (C10), 114.8 (C5), 109.3 (C13), 64.4 (OCH₂CH₃), 60.5 (CHCH₂CH₃), 54.6 (C17), 43.5 (NCH₃), 43.3 (ArCH₂), 40.1 (C15), 30.6 (C16), 28.1 (CONCH₃), 24.8 (CHCH₂CH₃), 15.0 (OCH₂CH₃), 8.7 (CHCH₂CH₃)

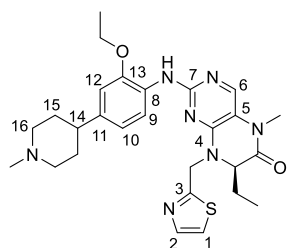
(*R*)-8-((5-Bromothiophen-3-yl)methyl)-2-((2-ethoxy-4-(1-methylpiperidin-4-yl)phenyl)amino)-7-ethyl-5-methyl-7,8-dihydropteridin-6(5*H*)-one, 116

Dihydropteridinone **90y** (50 mg, 125 μ mol) was reacted with aniline **28b** (28 mg, 118 μ mol) using general method **16** to afford the title compound **116** as a yellow oil (4 mg,



5%). LCMS purity >95%, ret. time 1.20 mins; HRMS (ESI +ve): found $[M+H]^+$ 601.1770, $[C_{28}H_{36}BrN_6O_2S]^+$ requires 601.1781; ν_{\max} (thin film, cm^{-1}): 3427 (w, N-H), 1666 (s, C=O); $[\alpha]_D^{23.2}$: -2.1° (c 1.0, MeOH); δ_H (CDCl_3 , 500 MHz): 8.19 (1H, d, $J = 8.2$ Hz, H10), 7.68 (1H, s, H7), 7.58 (1H, s, NH), 7.11 (1H, s, H1), 7.00 (1H, s, H3), 6.76 (1H, dd, $J = 8.2, 1.6$ Hz, H11), 6.74 (1H, d, $J = 1.6$ Hz, H13), 5.41 (1H, d, $J = 15.1$ Hz, ArCHH), 4.19 – 4.15 (2H, m, ArCHH & CHCH_2CH_3), 4.12 (2H, q, $J = 6.9$ Hz, OCH_2CH_3), 3.57 (2H, d, $J = 9.6$ Hz, H17), 3.34 (3H, s, CONCH_3), 2.74 – 2.60 (6H, m, NCH_3 , H15 & 2 x H17), 2.26 – 2.17 (2H, m, H16), 2.01 – 1.91 (3H, m, 2 x H16 & CHCHHCH_3), 1.88 – 1.77 (1H, m, CHCHHCH_3), 1.48 (3H, t, $J = 6.9$ Hz, OCH_2CH_3), 0.84 (3H, t, $J = 7.6$ Hz, CHCH_2CH_3); δ_C (CDCl_3 , 126 MHz): 163.2 (CONCH_3), 155.5 (C8), 151.6 (C5), 147.5 (C14), 137.9 (C7), 137.5 (C4), 136.6 (C12), 130.0 (C3), 128.4 (C9), 124.8 (C1), 118.7 (C11), 118.3 (C10), 114.7 (C6), 113.4 (C2), 109.4 (C13), 64.4 (OCH_2CH_3), 60.8 (CHCH_2CH_3), 54.6 (C17), 43.4 (ArCH_2 & NCH_3), 40.1 (C15), 30.6 (C16), 28.1 (CONCH_3), 24.8 (CHCH_2CH_3), 15.0 (OCH_2CH_3), 8.7 (CHCH_2CH_3)

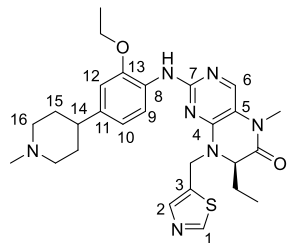
(R)-2-((2-Ethoxy-4-(1-methylpiperidin-4-yl)phenyl)amino)-7-ethyl-5-methyl-8-(thiazol-2-ylmethyl)-7,8-dihydropteridin-6(5H)-one, 117



Dihydropteridinone **90z** (33 mg, 110 μmol) was reacted with aniline **28b** (23 mg, 97 μmol) using general method **16** to afford the title compound **117** as an orange solid (9 mg, 16%). LCMS purity >95%, ret. time 1.03 mins; HRMS (ESI +ve): found $[M+H]^+$ 522.2651, $[C_{27}H_{36}N_7O_2S]^+$ requires 522.2646; m.p.: 97 – 99 $^\circ\text{C}$; ν_{\max} (thin film, cm^{-1}): 3418 (w, N-H), 1665 (C=O); $[\alpha]_D^{22.7}$: $+13.9^\circ$ (c 1.0, MeOH); δ_H (CDCl_3 , 500 MHz): 8.22 (1H, d, $J = 8.3$ Hz, H9), 7.75 (1H, d, $J = 3.5$ Hz, H2), 7.70 (1H, s, H6), 7.62 (1H, s, NH), 7.31 (1H, d, $J = 3.5$ Hz, H1), 6.75 (1H, dd, $J = 8.3, 1.6$ Hz, H10), 6.73 (1H, d, $J = 1.6$ Hz, H12), 5.57 (1H, d, $J = 15.8$ Hz, ArCHH), 4.76 (1H, d, $J = 15.8$ Hz, ArCHH), 4.36 (1H, dd, $J = 6.0, 3.5$ Hz, CHCH_2CH_3), 4.12 (2H, q, $J = 6.9$ Hz, OCH_2CH_3), 3.59 (2H, d, $J = 10.0$ Hz, H16), 3.34 (3H, s, CONCH_3), 2.75 (3H, s, NCH_3), 2.75 – 2.60 (3H, m, H14 & 2 x H16), 2.15 – 2.09 (2H, m, H15), 2.02 – 1.95 (3H, m, 2 x H15 & CHCHHCH_3), 1.93 – 1.85 (1H, m, CHCHHCH_3), 1.48 (3H, t, $J = 7.1$ Hz, OCH_2CH_3), 0.80 (3H, t, $J = 7.4$ Hz, CHCH_2CH_3); δ_C (CDCl_3 , 126 MHz): 163.3 (CONCH_3), 163.1 (C3), 155.3 (C8), 151.2 (C4), 147.5 (C13), 142.3 (C2), 138.0 (C7), 136.6 (C11), 128.3 (C9), 120.5 (C1), 118.8 (C11), 118.5 (C10), 114.9 (C5), 109.3 (C12), 64.4 (OCH_2CH_3), 62.1 (CHCH_2CH_3), 54.6

(C16), 46.3 (ArCH₂), 43.5 (NCH₃), 40.0 (C14), 30.5 (C15), 28.1 (CONCH₃), 25.1 (CHCH₂CH₃), 15.0 (OCH₂CH₃), 8.6 (CHCH₂CH₃)

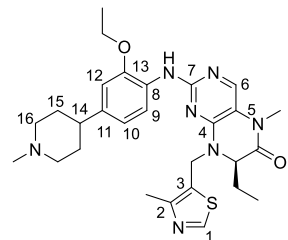
(*R*)-2-((2-Ethoxy-4-(1-methylpiperidin-4-yl)phenyl)amino)-7-ethyl-5-methyl-8-(thiazol-5-ylmethyl)-7,8-dihydropteridin-6(5*H*)-one, 118



Dihydropteridinone **90aa** (20 mg, 62 μmol) was reacted with aniline **28b** (14 mg, 14 μmol) using general method **16** to afford the title compound **118** as a yellow oil (2 mg, 6%). LCMS purity >95%, ret. time 1.00 mins; HRMS (ESI +ve): found [M+H]⁺ 522.2651, [C₂₇H₃₆N₇O₂S]⁺ requires 522.2646;

ν_{\max} (thin film, cm⁻¹): 3362 (w, N-H), 1661 (C=O); [α]_D^{22.4}: +3.5° (c 1.0, MeOH); δ_{H} (CDCl₃, 500 MHz): 8.75 (1H, s, H1), 8.29 (1H, d, *J* = 8.4 Hz, H9), 7.87 (1H, s, H2), 7.70 (1H, s, H6), 7.51 (1H, s, NH), 6.79 (1H, dd, *J* = 8.4, 1.8 Hz, H10), 6.77 (1H, d, *J* = 1.8 Hz, H12), 5.57 (1H, d, *J* = 15.6 Hz, ArCHH), 4.62 (1H, d, *J* = 15.6 Hz, ArCHH), 4.24 (1H, dd, *J* = 6.3, 3.5 Hz, CHCH₂CH₃), 4.14 (2H, q, *J* = 6.9 Hz, OCH₂CH₃), 3.42 (2H, d, *J* = 11.0 Hz, H16), 3.32 (3H, s, CONCH₃), 2.67 (3H, s, NCH₃), 2.65 – 2.57 (3H, m, H14 & 2 x H16), 2.31 – 2.20 (2H, m, H15), 2.02 – 1.94 (3H, m, 2 x H15 & CHCH₂CH₃), 1.89 – 1.79 (1H, m, CHCH₂CH₃), 1.49 (3H, t, *J* = 6.9 Hz, OCH₂CH₃), 0.82 (3H, t, *J* = 7.6 Hz, CHCH₂CH₃); δ_{C} (CDCl₃, 126 MHz): 163.0 (CONCH₃), 155.5 (C7), 154.4 (C1), 151.1 (C4), 147.4 (C13), 142.9 (C2), 138.5 (C6), 137.2 (C11), 133.5 (C3), 128.4 (C8), 118.9 (C10), 118.2 (C9), 114.8 (C5), 109.4 (C12), 64.4 (OCH₂CH₃), 61.4 (CHCH₂CH₃), 55.3 (C16), 44.3 (NCH₃), 41.1 (ArCH₂), 40.4 (C14), 31.2 (C15), 28.1 (CONCH₃), 25.1 (CHCH₂CH₃), 15.0 (OCH₂CH₃), 8.6 (CHCH₂CH₃)

(*R*)-2-((2-Ethoxy-4-(1-methylpiperidin-4-yl)phenyl)amino)-7-ethyl-5-methyl-8-(4-methylthiazol-5-ylmethyl)-7,8-dihydropteridin-6(5*H*)-one, 119

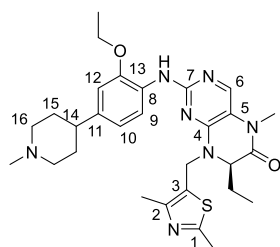


Dihydropteridinone **90ab** (35 mg, 104 μmol) was reacted with aniline **28b** (23 mg, 98 μmol) using general method **16** to afford the title compound **119** as an orange solid (17 mg, 31%). LCMS purity >95%, ret. time 1.05 mins; HRMS (ESI +ve): found [M+H]⁺ 536.2787, [C₂₈H₃₈N₇O₂S]⁺ requires

536.2802; m.p.: 84 – 86 °C; ν_{\max} (thin film, cm⁻¹): 3422 (w, N-H), 1664 (C=O); [α]_D^{22.5}: -8.3° (c 1.0, MeOH); δ_{H} (CDCl₃, 500 MHz): 8.65 (1H, s, H1), 8.24 (1H, d, *J* = 8.3 Hz, H9), 7.69 (1H, s, H6), 7.64 (1H, s, NH), 6.77 (1H, dd, *J* = 8.3, 1.8 Hz, H10), 6.74 (1H, d, *J* = 1.8 Hz, H12), 5.47 (1H, d, *J* = 15.8 Hz, ArCHH), 4.48 (1H, d, *J* = 15.8 Hz, ArCHH), 4.17 (1H, dd, *J* = 6.5, 3.6 Hz, CHCH₂CH₃), 4.13 (2H, q, *J* = 6.9 Hz,

OCH₂CH₃), 3.61 (2H, d, J = 10.4 Hz, H16), 3.32 (3H, s, CONCH₃), 2.75 (3H, s, NCH₃), 2.75 – 2.70 (2H, m, H16), 2.66 – 2.63 (1H, m, H14), 2.52 (ArCH₃), 2.26 – 2.15 (2H, m, H15), 2.03 – 1.94 (3H, m, 2 x H15 & CHCH₂HCH₃), 1.86 – 1.76 (1H, m, CHCH₂HCH₃), 1.49 (3H, t, J = 7.1 Hz, OCH₂CH₃), 0.84 (3H, t, J = 7.6 Hz, CHCH₂CH₃); δ_c (CDCl₃, 126 MHz): 163.0 (CONCH₃), 155.3 (C7), 152.0 (C1), 151.3 (C2/4), 151.2 (C2/4), 147.5 (C13), 137.8 (C6), 136.6 (C11), 128.3 (C8), 126.4 (C3), 118.7 (C10), 118.4 (C9), 114.9 (C4), 109.4 (C5), 64.4 (OCH₂CH₃), 61.2 (CHCH₂CH₃), 54.7 (C16), 43.6 (NCH₃), 40.3 (ArCH₂), 40.0 (C14), 30.4 (C15), 28.1 (CONCH₃), 25.1 (CHCH₂CH₃), 15.3 (ArCH₃), 15.0 (OCH₂CH₃), 8.8 (CHCH₂CH₃)

(*R*)-8-((2,4-dimethylthiazol-5-yl)methyl)-2-((2-ethoxy-4-(1-methylpiperidin-4-yl)phenyl)amino)-7-ethyl-5-methyl-7,8-dihydropteridin-6(5*H*)-one, 120

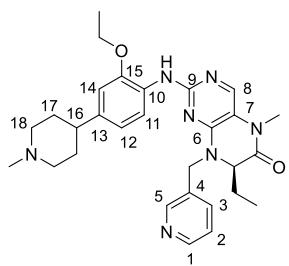


Dihydropteridinone **90ac** (30 mg, 85 μ mol) was reacted with aniline **28b** (19 mg, 81 μ mol) using general method **16** to afford the title compound **120** as an orange solid (5 mg, 11%). LCMS purity >95%, ret. time 1.05 mins; HRMS (ESI +ve): found $[M+H]^+$ 550.2935, $[C_{29}H_{40}N_7O_2S]^+$ requires 550.2959;

m.p.: 68 – 71 °C; ν_{max} (thin film, cm⁻¹): 3419 (w, N-H), 1667 (C=O); $[\alpha]_D^{22.6}$: +13.2° (c 1.0, MeOH); δ_H (CDCl₃, 500 MHz): 8.26 (1H, d, J = 8.2 Hz, H9), 7.67 (1H, s, H6), 7.65 (1H, s, NH), 6.78 (1H, dd, J = 8.2, 1.6 Hz, H10), 6.74 (1H, d, J = 1.6 Hz, H12), 5.43 (1H, d, J = 15.8 Hz, ArCH₂H), 4.76 (1H, d, J = 15.8 Hz, ArCH₂H), 4.18 (1H, dd, J = 6.2, 3.5 Hz, CHCH₂CH₃), 4.13 (2H, q, J = 6.9 Hz, OCH₂CH₃), 3.60 (2H, d, J = 10.7 Hz, H16), 3.31 (3H, s, CONCH₃), 2.75 (3H, s, NCH₃), 2.75 – 2.70 (2H, m, H16), 2.66 – 2.63 (1H, m, H14), 2.60 (3H, s, C¹CH₃), 2.41 (C²CH₃), 2.20 (2H, qd, J = 14.5, 3.8 Hz, H15), 2.02 – 1.92 (3H, m, 2 x H15 & CHCH₂HCH₃), 1.84 – 1.76 (1H, m, CHCH₂HCH₃), 1.49 (3H, t, J = 6.9 Hz, OCH₂CH₃), 0.84 (3H, t, J = 7.6 Hz, CHCH₂CH₃); δ_c (CDCl₃, 126 MHz): 165.1 (C1), 163.1 (CONCH₃), 155.3 (C7), 151.3 (C4), 150.0 (C2), 147.5 (C13), 137.7 (C6), 136.7 (C11), 128.4 (C8), 125.5 (C3), 118.7 (C10), 118.4 (C9), 114.9 (C5), 109.4 (C12), 64.4 (OCH₂CH₃), 60.8 (CHCH₂CH₃), 54.6 (C16), 43.4 (NCH₃), 40.1 (ArCH₂), 40.0 (C14), 30.5 (C15), 28.1 (CONCH₃), 25.0 (CHCH₂CH₃), 19.1 (C¹CH₃), 15.2 (C²CH₃), 15.0 (OCH₂CH₃), 8.8 (CHCH₂CH₃)

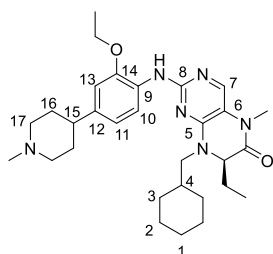
(*R*)-2-((2-Ethoxy-4-(1-methylpiperidin-4-yl)phenyl)amino)-7-ethyl-5-methyl-8-(pyridine-3-ylmethyl)-7,8-dihydropteridin-6(5*H*)-one, 121

Dihydropteridinone **90ad** (30 mg, 94 μ mol) was reacted with aniline **28b** (21 mg, 90 μ mol) using general method **16** to afford the title compound **121** as a yellow solid (10 mg, 21%). LCMS purity >95%, ret. time 0.91 mins; HRMS (ESI +ve): found $[M+H]^+$



516.3073, $[\text{C}_{29}\text{H}_{37}\text{N}_7\text{O}_2]^+$ requires 516.3081; m.p.: 61 – 64 °C; ν_{max} (thin film, cm^{-1}): 3427 (w, N-H), 1666 (s, C=O); $[\alpha]_D^{22.8}$: +2.8° (c 1.0, MeOH); δ_{H} (CDCl_3 , 500 MHz): 8.62 (1H, m, H5), 8.58 (1H, d, $J = 4.8$ Hz, H1), 8.10 (1H, d, $J = 8.2$ Hz, H11), 7.71 (1H, s, H8), 7.70 – 7.67 (1H, m, H3), 7.61 (1H, s, NH), 7.33 – 7.30 (1H, dd, $J = 7.9, 4.8$ Hz, H2), 6.74 – 6.71 (2H, m, H12 & H14), 5.56 (1H, d, $J = 15.5$ Hz, ArCHH), 4.26 (1H, d, $J = 15.5$ Hz, ArCHH), 4.16 – 4.10 (3H, m, OCH_2CH_3 & CHCH_2CH_3), 3.60 (2H, d, $J = 11.1$ Hz, H18), 3.36 (3H, s, CONCH_3), 2.77 – 2.68 (5H, m, 2 x H18 & NCH_3), 2.67 – 2.61 (1H, m, H16), 2.25 – 2.16 (2H, m, H17), 2.02 – 1.95 (3H, m, 2 x H17 & CHCH_2CH_3), 1.88 – 1.81 (1H, m, CHCH_2CH_3), 1.48 (3H, t, $J = 6.9$ Hz, OCH_2CH_3), 0.88 (3H, t, $J = 7.5$ Hz, CHCH_2CH_3); δ_{C} (CDCl_3 , 126 MHz): 163.0 (CONCH_3), 155.4 (C9), 151.9 (C6), 148.9 (C1 & C5), 147.5 (C15), 137.9 (C8), 136.6 (C13), 135.8 (C3), 132.3 (C4), 128.3 (C10), 123.9 (C2), 118.6 (C12), 118.4 (C11), 114.8 (C7), 109.3 (C14), 64.4 (OCH_2CH_3), 61.4 (CHCH_2CH_3), 54.7 (C18), 45.8 (ArCH₂), 43.5 (NCH_3), 40.0 (C16), 30.6 (C17), 28.2 (CONCH_3), 24.9 (CHCH_2CH_3), 14.9 (OCH_2CH_3), 8.8 (CHCH_2CH_3).

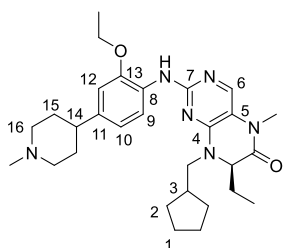
(R)-8-(Cyclohexylmethyl)-2-((2-ethoxy-4-(1-methylpiperidin-4-yl)phenyl)amino)-7-ethyl-5-methyl-7,8-dihydropteridin-6(5H)-one, 122



Dihydropteridinone **90ae** (30 mg, 93 μmol) was reacted with aniline **28b** (27 mg, 88 μmol) using general method **16** to afford the title compound **122** as a yellow solid (14 mg, 28%). LCMS purity >95%, ret. time 1.20 mins; HRMS (ESI +ve): found $[\text{M}+\text{H}]^+$ 521.3595, $[\text{C}_{30}\text{H}_{45}\text{N}_6\text{O}_2]^+$ requires 521.3599; m.p.: 70 – 73 °C; ν_{max} (thin film, cm^{-1}): 3427 (w, N-H), 1668

(C=O); $[\alpha]_D^{23.3}$: -10.4° (c 1.0, MeOH); δ_{H} (CDCl_3 , 500 MHz): 8.32 (1H, d, $J = 8.2$ Hz, H10), 7.62 (1H, s, H7), 7.60 (1H, s, NH), 6.79 – 6.73 (2H, m, H11 & H13), 4.23 (1H, dd, $J = 13.7, 6.2$ Hz, NCHH), 5.17 – 4.10 (3H, m, CHCH_2CH_3 & OCH_2CH_3), 3.54 (2H, d, $J = 11.7$ Hz, H17), 3.34 (3H, s, CONCH_3), 2.71 – 2.61 (6H, m, H15, 2 x H17 & NCH_3), 2.23 – 2.14 (2H, m, H16), 2.01 – 1.96 (2H, m, H16), 1.92 – 1.63 (8H, m, 2 x H1, 1 x H2, 2 x H3, H4 & CHCH_2CH_3), 1.49 (3H, t, $J = 7.0$ Hz, OCH_2CH_3), 1.27 – 1.16 (3H, m, H2), 1.05 – 0.96 (2H, m, H3), 0.86 (3H, t, $J = 7.5$ Hz, CHCH_2CH_3); δ_{C} (CDCl_3 , 126 MHz): 163.4 (CONCH_3), 155.5 (C8), 152.1 (C5), 147.3 (C14), 137.3 (C7), 136.6 (C12), 128.6 (C9), 118.5 (C11), 118.1 (C10), 114.8 (C6), 109.4 (C13), 54.5 (OCH_2CH_3), 62.1 (CHCH_2CH_3), 54.6 (C17), 51.7 (NCH_2), 43.7 (NCH_3), 40.2 (C15), 35.9 (C4), 31.2 (C3), 30.8 (C16), 28.1 (CONCH_3), 26.4 (C1), 25.7 (C2), 25.3 (CHCH_2CH_3), 14.9 (OCH_2CH_3), 9.2 (CHCH_2CH_3).

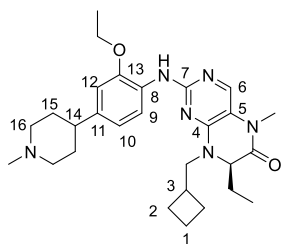
(*R*)-8-(Cyclopentylmethyl)-2-((2-ethoxy-4-(1-methylpiperidin-4-yl)phenyl)amino)-7-ethyl-5-methyl-7,8-dihydropteridin-6(5*H*)-one, 123



Dihydropteridinone **90af** (30 mg, 97 μmol) was reacted with aniline **28b** (22 mg, 92 μmol) using general method **16** to afford the title compound **123** as a yellow oil (4 mg, 8%). LCMS purity >95%, ret. time 1.16 mins; HRMS (ESI +ve): found $[\text{M}+\text{H}]^+$ 507.3426, $[\text{C}_{29}\text{H}_{43}\text{N}_6\text{O}_2]^+$ requires 507.3442;

ν_{max} (thin film, cm^{-1}): 3423 (w, N-H), 1667 (s, C=O); $[\alpha]_D^{23.1}$: -6.2° (c 1.0, MeOH); δ_{H} (CDCl_3 , 500 MHz): 8.26 (1H, d, J = 8.2 Hz, H9), 7.79 (1H, s, NH), 7.58 (1H, s, H6), 6.76 (1H, dd, J = 8.3, 1.9 Hz, H10), 6.72 (1H, d, J = 1.9 Hz, H12), 4.30 (1H, dd, J = 13.7, 7.2 Hz, NCHH), 4.21 (1H, dd, J = 6.3, 3.5 Hz, CHCH₂CH₃), 4.10 (2H, q, J = 7.0 Hz, OCH₂CH₃), 3.58 (2H, d, J = 11.7 Hz, H16), 3.31 (3H, s, CONCH₃), 2.80 (1H, dd, J = 13.7, 7.9 Hz, NCHH), 2.74 – 2.61 (5H, m, NCH₃, H14 & 2 x H16), 2.39 (1H, quin, J = 7.5 Hz, H3), 2.24 – 2.15 (2H, m, H15), 2.01 – 1.96 (2H, m, H15), 1.93 – 1.87 (1H, m, CHCH₂CH₃), 1.82 – 1.70 (3H, m, H2 & CHCH₂CH₃), 1.68 – 1.61 (2H, m, H1), 1.58 – 1.50 (2H, m, H1), 1.46 (3H, t, J = 7.0 Hz, OCH₂CH₃), 1.30 – 1.21 (2H, m, H2), 0.83 (3H, t, J = 7.5 Hz, CHCH₂CH₃); δ_{C} (CDCl_3 , 126 MHz): 163.4 (CONCH₃), 155.1 (C7), 152.2 (C4), 147.7 (C13), 136.6 (C11), 136.6 (C7), 128.5 (C8), 118.5 (C9 & C10), 114.7 (C6), 109.4 (C12), 64.6 (OCH₂CH₃), 62.3 (CHCH₂CH₃), 54.6 (C16), 50.0 (NCH₂), 43.5 (NCH₃), 40.0 (C14), 37.8 (C3), 30.6 (C2), 30.5 (C15), 30.1 (C2'), 28.1 (CONCH₃), 25.3 (CHCH₂CH₃), 25.2 (C1), 24.8 (C1'), 14.9 (OCH₂CH₃), 9.1 (CHCH₂CH₃)

(*R*)-8-(Cyclobutylmethyl)-2-((2-ethoxy-4-(1-methylpiperidin-4-yl)phenyl)amino)-7-ethyl-5-methyl-7,8-dihydropteridin-6(5*H*)-one, 124

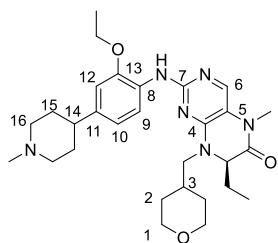


Dihydropteridinone **90ag** (30 mg, 102 μmol) was reacted with aniline **28b** (23 mg, 97 μmol) using general method **16** to afford the title compound **124** as a yellow oil (21 mg, 42%). LCMS purity >95%, ret. time 1.12 mins; HRMS (ESI +ve): found $[\text{M}+\text{H}]^+$ 493.3271, $[\text{C}_{28}\text{H}_{41}\text{N}_6\text{O}_2]^+$ requires 493.3286; ν_{max}

(thin film, cm^{-1}): 3423 (w, N-H), 1665 (C=O); $[\alpha]_D^{23.0}$: -3.5° (c 1.0, MeOH); δ_{H} (CDCl_3 , 500 MHz): 8.33 (1H, d, J = 8.5 Hz, H9), 7.59 (1H, s, H6), 7.56 (1H, s, NH), 6.78 (1H, d, J = 8.2 Hz, H10), 6.73 (1H, s, H12), 4.29 (1H, dd, J = 13.9, 6.9 Hz, NCHH), 4.16 (1H, dd, J = 6.5, 3.9 Hz, CHCH₂CH₃), 4.11 (2H, q, J = 6.9 Hz, OCH₂CH₃), 3.52 (2H, d, J = 11.4 Hz, H16), 3.31 (3H, s, CONCH₃), 3.06 (1H, dd, J = 13.9, 7.6 Hz, NCHH), 2.77 (1H, quin, J = 7.3 Hz, H3), 2.70 – 2.60 (7H, m, NCH₃, H14 & 2 x H16), 2.22 – 2.03 (4H, m, 2 x H2 & 2 x H15), 2.00 – 1.85 (5H, m, 2 x H1, 2 x H15 & CHCH₂CH₃),

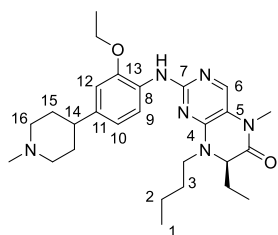
1.83 – 1.74 (3H, m, 2 x H₂ & CHCH₂CH₃), 1.47 (3H, t, *J* = 6.9 Hz, OCH₂CH₃), 0.83 (3H, t, *J* = 7.4 Hz, CHCH₂CH₃); δ_c (CDCl₃, 126 MHz): 163.5 (CONCH₃), 155.5 (C7), 152.1 (C4), 147.3 (C13), 137.4 (C6), 136.5 (C11), 128.7 (C8), 118.6 (C10), 118.1 (C9), 114.7 (C5), 109.4 (C12), 64.3 (OCH₂CH₃), 62.1 (CHCH₂CH₃), 54.6 (C16), 50.4 (NCH₂), 43.6 (NCH₃), 40.2 (C14), 33.4 (C3), 30.8 (C15), 28.0 (CONCH₃), 26.9 (C2), 26.2 (C2'), 25.3 (CHCH₂CH₃), 18.5 (C1), 14.5 (OCH₂CH₃), 9.0 (CHCH₂CH₃)

(*R*)-2-((2-Ethoxy-4-(1-methylpiperidin-4-yl)phenyl)amino)-7-ethyl-5-methyl-8-((tetrahydro-2*H*-pyran-4-yl)methyl)-7,8-dihydropteridin-6(5*H*)-one, 125



Dihydropteridinone **90ah** (25 mg, 77 μ mol) was reacted with aniline **28b** (17 mg, 73 μ mol) using general method **16** to afford the title compound **125** as a pale orange solid (14 mg, 34%). LCMS purity >95%, ret. time 1.02 mins; HRMS (ESI +ve): found $[M+H]^+$ 523.3380, $[C_{29}H_{43}N_6O_3]^+$ requires 523.3391; m.p.: 82 – 85 °C; ν_{max} (thin film, cm⁻¹): 3424 (w, N-H), 1667 (s, C=O); $[\alpha]_D^{23.2}$: -9.0° (c 1.0, MeOH); δ_H (CDCl₃, 500 MHz): 8.26 (1H, d, *J* = 8.7 Hz, H10), 7.76 (1H, s, NH), 7.64 (1H, s, H6), 7.15 (1H, d, *J* = 5.0 Hz, H3), 6.77 – 6.74 (2H, m, H10 & H12), 4.30 (1H, dd, *J* = 13.8, 6.4 Hz, NCHH), 4.16 – 4.11 (3H, m, CHCH₂CH₃ & OCH₂CH₃), 4.00 – 3.96 (2H, m, H1), 3.61 (2H, d, *J* = 10.5 Hz, H16), 3.38 – 3.32 (5H, m, H1 & CONCH₃), 2.77 – 2.63 (7H, m, NCHH, H14, 2 x H16 & NCH₃), 2.26 – 2.17 (2H, m, H16), 2.15 – 2.08 (1H, m, H3), 2.03 – 1.98 (2H, m, H15), 1.94 – 1.87 (1H, m, CHCH₂CH₃), 1.84 – 1.78 (1H, m, CHCH₂CH₃), 1.72 – 1.68 (1H, m, H2), 1.63 – 1.58 (1H, m, H2), 1.49 (3H, t, *J* = 7.0 Hz, OCH₂CH₃), 1.44 – 1.34 (2H, m, H2), 0.87 (3H, t, *J* = 7.5 Hz, CHCH₂CH₃); δ_c (CDCl₃, 126 MHz): 163.2 (CONCH₃), 155.3 (C7), 152.2 (C4), 147.7 (C13), 136.9 (C6), 136.7 (C11), 128.4 (C8), 118.4 (C9 & C10), 114.8 (C5), 109.4 (C11), 67.5 (C1), 64.4 (OCH₂CH₃), 63.3 (CHCH₂CH₃), 54.6 (C16), 51.2 (C4), 43.5 (NCH₃), 40.0 (ArCH₂), 33.5 (C3), 31.1 (C2), 30.8 (C2' & C15), 28.1 (CONCH₃), 25.3 (CHCH₂CH₃), 14.9 (OCH₂CH₃), 9.2 (CHCH₂CH₃)

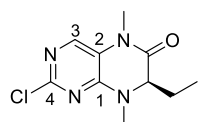
(*R*)-8-Butyl-2-((2-ethoxy-4-(1-methylpiperidin-4-yl)phenyl)amino)-7-ethyl-5-methyl-7,8-dihydropteridin-6(5*H*)-one, 126



Dihydropteridinone **90ai** (30 mg, 106 μ mol) was reacted with aniline **28b** (24 mg, 101 μ mol) using general method **16** to afford the title compound **126** as a brown oil (9 mg, 17%). LCMS purity >95%, ret. time 1.12 mins; HRMS (ESI +ve): found $[M+H]^+$ 481.3276, $[C_{27}H_{41}N_6O_2]^+$ requires 481.3286; ν_{max} (thin film, cm⁻¹): 3428 (w, N-H), 1665 (s, C=O); $[\alpha]_D^{23.3}$: -12.5° (c 1.0, MeOH); δ_H (CDCl₃, 500 MHz): 8.38 (1H, s, NH), 8.15 (1H, d, *J* = 8.2 Hz, H9), 7.60 (1H, s, H6),

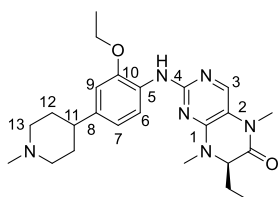
6.79 – 6.74 (2H, m, H10 & H12), 4.25 (1H, dd, $J = 6.2, 3.6$ Hz, CHCH_2CH_3), 4.15 – 4.07 (3H, m, NCHH & OCH_2CH_3), 3.70 – 3.62 (2H, m, H16), 3.33 (3H, s, CONCH_3), 3.12 – 3.06 (1H, m, NCHH), 2.82 – 2.64 (6H, m, H14, 2 x H16 & NCH_3), 2.27 – 2.18 (2H, m, H15), 2.06 – 1.97 (3H, m, 2 x H15 & CHCHHCH_3), 1.89 – 1.81 (1H, m, CHCHHCH_3), 1.77 – 1.61 (2H, m, H3), 1.49 (3H, t, $J = 7.0$ Hz, OCH_2CH_3), 1.42 – 1.35 (2H, m, H2), 0.96 (3H, t, $J = 7.4$ Hz, H1), 0.85 (3H, t, $J = 7.6$ Hz, CHCH_2CH_3); δ_{C} (CDCl_3 , 126 MHz): 163.1 (CONCH_3), 154.2 (C7), 152.0 (C4), 148.4 (C13), 137.3 (C11), 133.5 (C6), 122.8 (C8), 119.6 (C9), 118.2 (C10), 114.6 (C5), 109.7 (C12), 66.4 (OCH_2CH_3), 62.1 (CHCH_2CH_3), 54.7 (C16), 45.9 (NCH_2), 43.4 (NCH_3), 39.9 (C14), 30.5 (C15), 29.1 (C3), 28.1 (CONCH_3), 25.7 (CHCH_2CH_3), 20.3 (C2), 14.8 (OCH_2CH_3), 13.8 (C1), 8.7 (CHCH_2CH_3)

(R)-2-Chloro-7-ethyl-5,8-dimethyl-7,8-dihydropteridin-6(5H)-one, 133



Dihydropteridinone **81** (125 mg, 0.59 mmol) was reacted with methyl iodide (80.9 μL , 1.29 mmol) using general method **5** to afford the title compound **133** as a colourless oil (55.0 mg, 39%). LCMS purity >95%, ret. time 1.15 mins; HRMS (ESI +ve): found $[\text{M}+\text{H}]^+$ 241.0858, $[\text{C}_{10}\text{H}_{14}\text{ClN}_4\text{O}]^+$ requires 241.0851; $[\alpha]_D^{23.5}$: -8.3° (c 1.0, MeOH); δ_{H} (CDCl_3 , 500 MHz): 7.61 (1H, s, H3), 4.22 (1H, dd, $J = 6.0, 3.5$ Hz, CHCH_2CH_3), 3.31 (3H, s, CONCH_3), 3.11 (3H, s, CONCH_3), 2.05 – 1.99 (1H, m, CHCHHCH_3), 1.90 – 1.81 (1H, m, CHCHHCH_3), 0.79 (3H, t, $J = 7.9$ Hz, CHCH_2CH_3); δ_{C} (CDCl_3 , 126 MHz): 163.4 (CONCH_3), 154.3 (C4), 152.4 (C1), 137.2 (C3), 120.4 (C2), 63.7 (CHCH_2CH_3), 33.4 (NCH_3), 28.2 (CONCH_3), 25.1 (CHCH_2CH_3), 8.4 (CHCH_2CH_3)

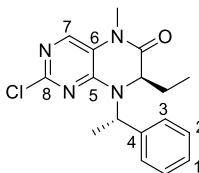
(R)-2-((2-Ethoxy-4-(1-methylpiperidin-4-yl)phenyl)amino)-7-ethyl-5,8-dimethyl-7,8-dihydropteridin-6(5H)-one, 127



Dihydropteridinone **133** (40 mg, 166 μmol) was reacted with aniline **28b** (37 mg, 158 μmol) using general method **16** to afford the title compound **127** as a brown solid (11 mg, 15%). LCMS purity >95%, ret. time 1.24 mins; HRMS (ESI +ve): found $[\text{M}+\text{H}]^+$ 439.2802, $[\text{C}_{24}\text{H}_{35}\text{N}_6\text{O}_2]^+$ requires 439.2816; m.p.: 65 – 68 $^\circ\text{C}$; ν_{max} (thin film, cm^{-1}): 3422 (w, N-H), 1663 (C=O); $[\alpha]_D^{22.6}$: -18.0° (c 1.0, MeOH); δ_{H} (CDCl_3 , 500 MHz): 8.35 (1H, d, $J = 8.2$ Hz, H6), 7.74 (1H, s, ArNH), 7.59 (1H, s, H3), 6.81 (1H, d, $J = 8.2$ Hz, H7), 6.73 (1H, s, H9), 4.12 (1H, dd, $J = 5.5, 3.6$ Hz), 4.12 (2H, q, $J = 6.5$ Hz, OCH_2CH_3), 3.59 (2H, d, $J = 9.8$ Hz, H13), 3.32 (3H, s, CONCH_3), 3.16 (3H, s, CHNCH_3), 2.74 (NCH_3), 2.75 – 2.64 (3H, m, H11 & 2 x H13), 2.25 – 2.19 (2H, m, H12), 2.05 – 1.96 (3H, m, 2 x H12 & CHCHHCH_3), 1.91 – 1.83 (1H, m, CHCHHCH_3),

1.48 (3H, t, $J = 6.5$ Hz, OCH_2CH_3), 0.83 (3H, t, $J = 7.4$ Hz, CHCH_2CH_3); δ_{C} (CDCl_3 , 126 MHz): 163.2 (CONCH_3), 155.3 (C4), 152.2 (C1), 147.5 (C10), 136.4 (C8), 136.2 (C3), 128.5 (C5), 118.5 (C7), 118.4 (C6), 114.7 (C2), 109.5 (C9), 64.4 (OCH_2CH_3), 63.9 (CHCH_2CH_3), 54.7 (C13), 43.6 (NCH_3), 40.0 (C11), 33.5 (CHNCH_3), 30.9 (C12), 28.0 (CONCH_3), 24.9 (CHCH_2CH_3), 14.9 (OCH_2CH_3), 8.6 (CHCH_2CH_3)

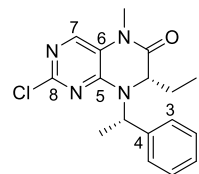
(R)-2-Chloro-7-ethyl-5-methyl-8-((S)-1-phenylethyl)-7,8-dihydropteridin-6(5H)-one, 137



Dihydropteridinone **79** (300 mg, 1.32 mmol) was reacted with (*R*)-1-phenylethan-1-ol (260 μL , 2.18 mmol) using general method **20** to afford the title compound **137** as a white solid (94 mg, d.r 20:1, 21%). *separated from diastereomer 138*. LCMS purity >95%, ret.

time 1.54 mins; HRMS (ESI +ve): found $[\text{M}+\text{H}]^+$ 331.1321, $[\text{C}_{17}\text{H}_{20}\text{ClN}_4\text{O}]^+$ requires 331.1325; $[\alpha]_{\text{D}}^{22.4}$: -209.8° (c 1.0, MeOH); δ_{H} (CDCl_3 , 500 MHz): 7.72 (1H, s, H7), 7.57 – 7.54 (2H, m, H2), 7.40 – 7.31 (3H, m, H1 & H3), 6.15 (1H, d, $J = 7.2$ Hz, CHCH_3), 4.23 (1H, dd, $J = 8.2, 3.5$ Hz, CHCH_2CH_3), 3.33 (3H, s, NCH_3), 1.68 (3H, d, $J = 7.2$ Hz, CHCH_3), 1.11 – 0.93 (2H, m, CHCH_2CH_3), 0.54 (3H, t, $J = 7.6$ Hz, CHCH_2CH_3); δ_{C} (CDCl_3 , 126 MHz): 163.4 (CONCH_3), 154.0 (C8), 152.4 (C5), 139.6 (C4), 138.5 (C7), 128.7 (C2), 128.4 (C1), 128.1 (C3), 121.2 (C6), 58.1 (CHCH_2CH_3), 53.1 (CHCH_3), 28.4 (NCH_3), 26.7 (CHCH_2CH_3), 16.6 (CHCH_3), 9.0 (CHCH_2CH_3)

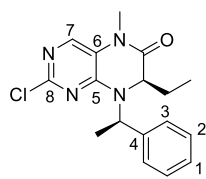
(S)-2-Chloro-7-ethyl-5-methyl-8-((S)-1-phenylethyl)-7,8-dihydropteridin-6(5H)-one, 138



Dihydropteridinone **79** (300 mg, 1.32 mmol) was reacted with (*R*)-1-phenylethan-1-ol (260 μL , 2.18 mmol) using general method **20** to afford the title compound **138** as a white solid (27 mg, d.r 18:1, 6%). *separated from diastereomer 137*. LCMS purity >95%, ret. time

1.56 mins; HRMS (ESI +ve): found $[\text{M}+\text{H}]^+$ 331.1322, $[\text{C}_{17}\text{H}_{20}\text{ClN}_4\text{O}]^+$ requires 331.1325; δ_{H} (CDCl_3 , 500 MHz): 7.73 (1H, s, H7), 7.41 – 7.37 (2H, m, H2), 7.36 – 7.31 (3H, m, H1 & H3), 5.96 (1H, q, $J = 7.2$ Hz, CHCH_3), 3.95 (1H, dd, $J = 7.6, 3.2$ Hz, CHCH_2CH_3), 3.33 (3H, s, NCH_3), 1.92 – 1.85 (1H, m, CHCH_2CH_3), 1.79 (3H, d, $J = 7.2$ Hz, CHCH_3), 1.77 – 1.70 (1H, m, CHCH_2CH_3), 0.84 (3H, t, $J = 7.6$ Hz, CHCH_2CH_3); δ_{C} (CDCl_3 , 126 MHz): 163.5 (CONCH_3), 154.2 (C8), 152.5 (C5), 138.3 (C4 & C7), 129.0 (C2), 128.3 (C1), 127.6 (C3), 120.9 (C6), 58.1 (CHCH_2CH_3), 54.6 (CHCH_3), 28.3 (NCH_3), 28.1 (CHCH_2CH_3), 17.4 (CHCH_3), 8.8 (CHCH_2CH_3)

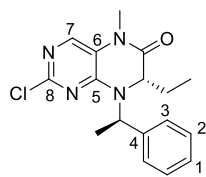
(R)-2-Chloro-7-ethyl-5-methyl-8-((R)-1-phenylethyl)-7,8-dihydropteridin-6(5H)-one, 139



Dihydropteridinone **79** (115 mg, 0.51 mmol) was reacted with (S)-1-phenylethan-1-ol (100 μ L, 0.82 mmol) using general method **20** to afford the title compound **139** as a white solid (21 mg, d.r 9:1, 13%).

separated from diastereomer 140. LCMS purity >95%, ret. time 1.56 mins; HRMS (ESI +ve): found $[M+H]^+$ 331.1321, $[C_{17}H_{20}ClN_4O]^+$ requires 331.1325; δ_H (CDCl₃, 500 MHz): 7.73 (1H, s, H7), 7.41 – 7.37 (2H, m, H2), 7.36 – 7.31 (3H, m, H1 & H3), 5.96 (1H, q, $J = 7.2$ Hz, $\underline{CHCH_3}$), 3.95 (1H, dd, $J = 7.6, 3.2$ Hz, $\underline{CHCH_2CH_3}$), 3.33 (3H, s, NCH₃), 1.92 – 1.85 (1H, m, $\underline{CHCH_2CH_3}$), 1.79 (3H, d, $J = 7.2$ Hz, $\underline{CHCH_3}$), 1.77 – 1.70 (1H, m, $\underline{CHCH_2CH_3}$), 0.84 (3H, t, $J = 7.6$ Hz, $\underline{CHCH_2CH_3}$); δ_C (CDCl₃, 126 MHz): 163.5 ($\underline{CONCH_3}$), 154.2 (C8), 152.5 (C5), 138.3 (C4 & C7), 129.0 (C2), 128.3 (C1), 127.6 (C3), 120.9 (C6), 58.1 ($\underline{CHCH_2CH_3}$), 54.6 ($\underline{CHCH_3}$), 28.3 (NCH₃), 28.1 ($\underline{CHCH_2CH_3}$), 17.4 ($\underline{CHCH_3}$), 8.8 ($\underline{CHCH_2CH_3}$)

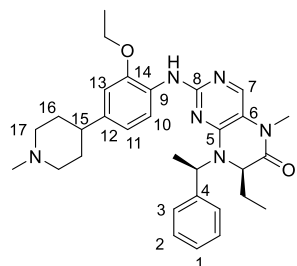
(S)-2-Chloro-7-ethyl-5-methyl-8-((R)-1-phenylethyl)-7,8-dihydropteridin-6(5H)-one, 140



Dihydropteridinone **79** (115 mg, 0.51 mmol) was reacted with (S)-1-phenylethan-1-ol (100 μ L, 0.82 mmol) using general method **20** to afford the title compound **140** as a white solid (21 mg, d.r 14:1, 12%). *separated from diastereomer 139.* LCMS purity >95%, ret.

time 1.54 mins; HRMS (ESI +ve): found $[M+H]^+$ 331.1322, $[C_{17}H_{20}ClN_4O]^+$ requires 331.1325; δ_H (CDCl₃, 500 MHz): 7.72 (1H, s, H7), 7.57 – 7.54 (2H, m, H2), 7.40 – 7.31 (3H, m, H1 & H3), 6.15 (1H, d, $J = 7.2$ Hz, $\underline{CHCH_3}$), 4.23 (1H, dd, $J = 8.2, 3.5$ Hz, $\underline{CHCH_2CH_3}$), 3.33 (3H, s, NCH₃), 1.68 (3H, d, $J = 7.2$ Hz, $\underline{CHCH_3}$), 1.11 – 0.93 (2H, m, $\underline{CHCH_2CH_3}$), 0.54 (3H, t, $J = 7.6$ Hz, $\underline{CHCH_2CH_3}$); δ_C (CDCl₃, 126 MHz): 163.4 ($\underline{CONCH_3}$), 154.0 (C8), 152.4 (C5), 139.6 (C4), 138.5 (C7), 128.7 (C2), 128.4 (C1), 128.1 (C3), 121.2 (C6), 58.1 ($\underline{CHCH_2CH_3}$), 53.1 ($\underline{CHCH_3}$), 28.4 (NCH₃), 26.7 ($\underline{CHCH_2CH_3}$), 16.6 ($\underline{CHCH_3}$), 9.0 ($\underline{CHCH_2CH_3}$)

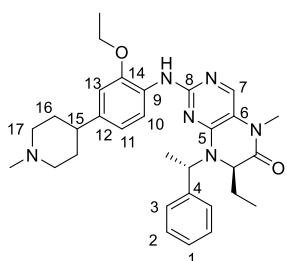
(R)-2-((2-Ethoxy-4-(1-methylpiperidin-4-yl)phenyl)amino)-7-ethyl-5-methyl-8-((R)-1-phenylethyl)-7,8-dihydropteridin-6(5H)-one, 134



Dihydropteridinone **139** (16 mg, 47 μ mol) was reacted with aniline **28b** (10 mg, 45 μ mol) using general method **16** to afford the title compound **134** as a yellow solid (3 mg, d.r 9:1, 12%). LCMS purity >95%, ret. time 1.12 mins; HRMS (ESI +ve): found $[M+H]^+$ 529.3261, $[C_{31}H_{41}N_6O_2]^+$ requires

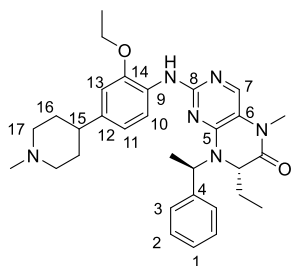
529.3286; δ_{H} (CDCl_3 , 500 MHz): 8.33 (1H, d, $J = 8.7$ Hz, H10), 7.70 (1H, s, H7), 7.49 (1H, s, NH), 7.40 – 7.30 (5H, m, H1, H2 & H3), 6.79 – 6.74 (2H, m, H11 & H13), 5.99 (1H, q, $J = 7.1$ Hz, CHCH_3), 4.14 (2H, q, $J = 7.0$ Hz, OCH_2CH_3), 3.92 (1H, dd, $J = 7.8$, 3.3 Hz, CHCH_2CH_3), 3.59 (2H, d, $J = 11.7$ Hz, H17), 3.33 (3H, s, CONCH_3), 2.77 – 2.67 (6H, m, NCH_3 , H15 & 2 x H17), 2.28 – 2.15 (2H, m, H16), 2.00 (2H, d, $J = 14.3$ Hz, H16), 1.89 – 1.81 (4H, m, CHCH_3 & CHCHHCH_3), 1.78 – 1.71 (1H, m, CHCHHCH_3), 1.50 (3H, t, $J = 7.0$ Hz, OCH_2CH_3), 0.86 (3H, t, $J = 7.5$ Hz, CHCH_2CH_3); δ_{C} (CDCl_3 , 126 MHz): 163.4 (CONCH_3), 155.4 (C8), 152.2 (C5), 147.4 (C14), 139.3 (C4), 137.7 (C7), 136.4 (C13), 128.9 (C2), 128.5 (C9), 128.0 (C1), 127.5 (C3), 118.6 (C11), 118.2 (C10), 115.2 (C6), 109.4 (C13), 64.4 (OCH_2CH_3), 58.3 (CHCH_2CH_3), 54.7 (C17), 54.2 (CHCH_3), 43.5 (NCH_3), 40.1 (C15), 30.6 (C16), 28.2 (CONCH_3), 27.9 (CHCH_2CH_3), 17.6 (CHCH_3), 15.0 (OCH_2CH_3), 9.0 (CHCH_2CH_3)

(*R*)-2-((2-Ethoxy-4-(1-methylpiperidin-4-yl)phenyl)amino)-7-ethyl-5-methyl-8-((*S*)-1-phenylethyl)-7,8-dihydropteridin-6(5*H*)-one, 135



Dihydropteridinone **137** (17 mg, 51 μmol) was reacted with aniline **28b** (11 mg, 49 μmol) using general method **16** to afford the title compound **135** as a yellow solid (7 mg, d.r. >20:1, 26%). LCMS purity >95%, ret. time 1.10 mins; HRMS (ESI +ve): found $[\text{M}+\text{H}]^+$ 529.3269, $[\text{C}_{31}\text{H}_{41}\text{N}_6\text{O}_2]^+$ requires 529.3286; m.p.: 72 – 76 $^\circ\text{C}$; ν_{max} (thin film, cm^{-1}): 3420 (w, N-H), 1667 (C=O); $[\alpha]_D^{23.4}$: -147.5 $^\circ$ (c 1.0, MeOH); δ_{H} (CDCl_3 , 500 MHz): 8.33 (1H, d, $J = 8.7$ Hz, H10), 7.70 (1H, s, H7), 7.62 (1H, s, NH), 7.59 – 7.55 (2H, m, H3), 7.40 – 7.30 (3H, m, H1 & H2), 6.77 – 6.74 (2H, m, H11 & H13), 6.20 (1H, q, $J = 7.1$ Hz, CHCH_3), 4.19 – 4.13 (3H, m, CHCH_2CH_3 & OCH_2CH_3), 3.55 (2H, d, $J = 11.7$ Hz, H17), 3.33 (3H, s, CONCH_3), 2.74 – 2.60 (6H, m, NCH_3 , H15 & 2 x H17), 2.24 – 2.15 (2H, m, H16), 2.01 – 1.96 (2H, m, H16), 1.70 (3H, d, $J = 7.1$ Hz, CHCH_3), 1.51 (3H, t, $J = 7.0$ Hz, OCH_2CH_3), 1.10 – 0.99 (2H, m, CHCH_2CH_3), 0.57 (3H, t, $J = 7.5$ Hz, CHCH_2CH_3); δ_{C} (CDCl_3 , 126 MHz): 163.3 (CONCH_3), 155.5 (C8), 152.1 (C5), 147.4 (C14), 140.7 (C4), 138.4 (C7), 136.5 (C13), 128.6 (C2 & C9), 128.0 (C1), 127.8 (C3), 118.8 (C11), 118.3 (C10), 115.5 (C6), 109.3 (C13), 64.4 (OCH_2CH_3), 58.2 (CHCH_2CH_3), 54.7 (C17), 52.5 (CHCH_3), 43.5 (NCH_3), 41.0 (C15), 30.7 (C16), 28.3 (CONCH_3), 26.4 (CHCH_2CH_3), 16.8 (CHCH_3), 15.0 (OCH_2CH_3), 9.1 (CHCH_2CH_3)

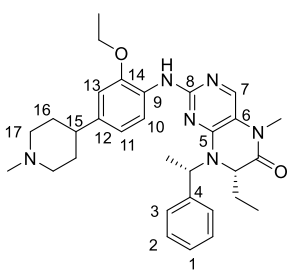
(S)-2-((2-Ethoxy-4-(1-methylpiperidin-4-yl)phenyl)amino)-7-ethyl-5-methyl-8-((R)-1-phenylethyl)-7,8-dihydropteridin-6(5H)-one, 141



Dihydropteridinone **140** (16 mg, 48 μ mol) was reacted with aniline **28b** (11 mg, 46 μ mol) using general method **16** to afford the title compound **141** as a yellow solid (5 mg, d.r 20:1, 20%). LCMS purity >95%, ret. time 1.10 mins; HRMS (ESI +ve): found $[M+H]^+$ 529.3267, $[C_{31}H_{41}N_6O_2]^+$ requires 529.3286; δ_H (CDCl₃, 500 MHz): 8.33 (1H, d, J = 8.7 Hz,

H10), 7.70 (1H, s, H7), 7.62 (1H, s, NH), 7.59 – 7.55 (2H, m, H3), 7.40 – 7.30 (3H, m, H1 & H2), 6.77 – 6.74 (2H, m, H11 & H13), 6.20 (1H, q, J = 7.1 Hz, CHCH₃), 4.19 – 4.13 (3H, m, CHCH₂CH₃ & OCH₂CH₃), 3.55 (2H, d, J = 11.7 Hz, H17), 3.33 (3H, s, CONCH₃), 2.74 – 2.60 (6H, m, NCH₃, H15 & 2 x H17), 2.24 – 2.15 (2H, m, H16), 2.01 – 1.96 (2H, m, H16), 1.70 (3H, d, J = 7.1 Hz, CHCH₃), 1.51 (3H, t, J = 7.0 Hz, OCH₂CH₃), 1.10 – 0.99 (2H, m, CHCH₂CH₃), 0.57 (3H, t, J = 7.5 Hz, CHCH₂CH₃); δ_C (CDCl₃, 126 MHz): 163.3 (CONCH₃), 155.5 (C8), 152.1 (C5), 147.4 (C14), 140.7 (C4), 138.4 (C7), 136.5 (C13), 128.6 (C2 & C9), 128.0 (C1), 127.8 (C3), 118.8 (C11), 118.3 (C10), 115.5 (C6), 109.3 (C13), 64.4 (OCH₂CH₃), 58.2 (CHCH₂CH₃), 54.7 (C17), 52.5 (CHCH₃), 43.5 (NCH₃), 41.0 (C15), 30.7 (C16), 28.3 (CONCH₃), 26.4 (CHCH₂CH₃), 16.8 (CHCH₃), 15.0 (OCH₂CH₃), 9.1 (CHCH₂CH₃)

(S)-2-((2-Ethoxy-4-(1-methylpiperidin-4-yl)phenyl)amino)-7-ethyl-5-methyl-8-((S)-1-phenylethyl)-7,8-dihydropteridin-6(5H)-one, 142

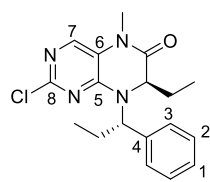


Dihydropteridinone **138** (23 mg, 70 μ mol) was reacted with aniline **28b** (16 mg, 66 μ mol) using general method **16** to afford the title compound **142** as a yellow solid (5 mg, d.r 20:1, 14%). LCMS purity >95%, ret. time 1.12 mins; HRMS (ESI +ve): found $[M+H]^+$ 529.3261, $[C_{31}H_{41}N_6O_2]^+$ requires 529.3286; δ_H (CDCl₃, 500 MHz): 8.33 (1H, d, J = 8.7 Hz,

H10), 7.70 (1H, s, H7), 7.68 (1H, s, NH), 7.40 – 7.30 (5H, m, H1, H2 & H3), 6.79 – 6.74 (2H, m, H11 & H13), 5.99 (1H, q, J = 7.1 Hz, CHCH₃), 4.14 (2H, q, J = 7.0 Hz, OCH₂CH₃), 3.92 (1H, dd, J = 7.8, 3.3 Hz, CHCH₂CH₃), 3.59 (2H, d, J = 11.7 Hz, H17), 3.33 (3H, s, CONCH₃), 2.77 – 2.67 (6H, m, NCH₃, H15 & 2 x H17), 2.28 – 2.15 (2H, m, H16), 2.00 (2H, d, J = 14.3 Hz, H16), 1.89 – 1.81 (4H, m, CHCH₃ & CHCH₂CH₃), 1.78 – 1.71 (1H, m, CHCH₂CH₃), 1.50 (3H, t, J = 7.0 Hz, OCH₂CH₃), 0.86 (3H, t, J = 7.5 Hz, CHCH₂CH₃); δ_C (CDCl₃, 126 MHz): 163.4 (CONCH₃), 155.4 (C8), 152.2 (C5), 147.4 (C14), 139.3 (C4), 137.7 (C7), 136.4 (C13), 128.9 (C2), 128.5 (C9), 128.0 (C1), 127.5 (C3), 118.6 (C11), 118.2 (C10), 115.2 (C6), 109.4 (C13), 64.4 (OCH₂CH₃), 58.3

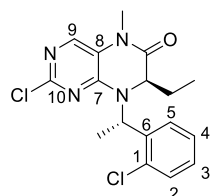
(CHCH₂CH₃), 54.7 (C17), 54.2 (CHCH₃) 43.5 (NCH₃), 40.1 (C15), 30.6 (C16), 28.2 (CONCH₃), 27.9 (CHCH₂CH₃), 17.6 (CHCH₃), 15.0 (OCH₂CH₃), 9.0 (CHCH₂CH₃)

(*R*)-2-Chloro-7-ethyl-5-methyl-8-((*S*)-1-phenylpropyl)-7,8-dihydropteridin-6(5*H*)-one, 145a



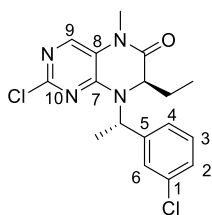
Dihydropteridinone **79** (100 mg, 0.44 mmol) was reacted with (*R*)-1-phenylpropan-1-ol **144a** (96 mg, 0.71 mmol) using general method **20** to afford the title compound **145a** as a white solid (33 mg, d.r 24:1, 22%). LCMS purity >95%, ret. time 1.54 mins; HRMS (ESI +ve): found [M+H]⁺ 345.1483, [C₁₈H₂₂ClN₄O]⁺ requires 345.1477; δ_H (CDCl₃, 500 MHz): 7.73 (1H, s, H7), 7.57 (2H, m, H3), 7.40 – 7.33 (3H, m, H1 & H2), 5.96 (1H, t, *J* = 8.0 Hz, ArCHCH₂CH₃), 4.13 (1H, dd, *J* = 7.3, 5.0 Hz, CHCH₂CH₃), 3.34 (3H, s, NCH₃), 2.16 – 2.10 (2H, m, ArCHCH₂CH₃), 0.94 – 0.88 (5H, m, ArCHCH₂CH₃ & CHCH₂CH₃), 0.52 (3H, t, *J* = 7.4 Hz, CHCH₂CH₃); δ_C (CDCl₃, 126 MHz): 163.3 (CONCH₃), 154.1 (C10), 153.1 (C7), 138.9 (C4), 138.8 (C9), 128.8 (C2), 128.4 (C1 & C3), 121.1 (C8), 59.0 (ArCHCH₂CH₃), 57.5 (CHCH₂CH₃), 28.5 (NCH₃), 26.3 (CHCH₂CH₃), 23.0 (ArCHCH₂CH₃), 11.0 (ArCHCH₂CH₃), 9.1 (CHCH₂CH₃)

(*R*)-2-Chloro-8-((*S*)-1-(2-chlorophenyl)ethyl)-7-ethyl-5-methyl-7,8-dihydropteridin-6(5*H*)-one, 145b



Dihydropteridinone **79** (80 mg, 0.35 mmol) was reacted with (*R*)-1-(2-chlorophenyl)ethan-1-ol **144b** (88 mg, 0.56 mmol) using general method **20** to afford the title compound **145b** as a white solid (22 mg, d.r >20:1, 17%). LCMS purity >95%, ret. time 1.52 mins; HRMS (ESI +ve): found [M+H]⁺ 365.0922, [C₁₇H₁₉Cl₂N₄O]⁺ requires 365.0930; δ_H (CDCl₃, 500 MHz): 7.78 (1H, dd, *J* = 7.7, 1.4 Hz, H5), 7.65 (1H, s, H9), 7.39 – 7.33 (1H, m, H2 & H4), 7.29 – 7.26 (1H, m, H3), 5.63 (1H, q, *J* = 7.0 Hz, CHCH₃), 4.44 (1H, dd, *J* = 7.3, 3.5 Hz, CHCH₂CH₃), 3.30 (3H, s, NCH₃), 1.84 (3H, d, *J* = 7.0 Hz, CHCH₃), 1.68 – 1.61 (1H, m, CHCH₂CH₃), 1.47 – 1.38 (1H, m, CHCH₂CH₃), 0.72 3H, t, *J* = 7.4 Hz, CHCH₂CH₃); δ_C (CDCl₃, 126 MHz): 163.4 (CONCH₃), 153.6 (C10), 151.5 (C7), 138.2 (C9), 135.9 (C6), 135.1 (C1), 130.8 (C5), 129.7 (C2), 129.5 (C3), 126.5 (C4), 121.0 (C8), 61.9 (CHCH₂CH₃), 54.4 (CHCH₃), 28.3 (NCH₃), 27.1 (CHCH₂CH₃), 17.3 (CHCH₃), 8.7 (CHCH₂CH₃)

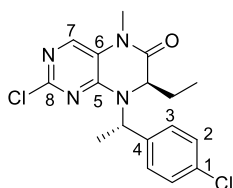
(*R*)-2-Chloro-8-((*S*)-1-(3-chlorophenyl)ethyl)-7-ethyl-5-methyl-7,8-dihydropteridin-6(5*H*)-one, 145c



Dihydropteridinone **79** (145 mg, 0.64 mmol) was reacted with (*R*)-1-(3-chlorophenyl)ethan-1-ol **144c** (127 mg, 0.81 mmol) using general method **20** to afford the title compound **145c** as a white solid (45 mg, d.r >20:1, 19%). LCMS purity >95%, ret. time 1.55 mins; HRMS (ESI +ve): found $[M+H]^+$ 365.0922, $[C_{17}H_{19}Cl_2N_4O]^+$

requires 365.0930; δ_H (CDCl₃, 500 MHz): 7.73 (1H, s, H₉), 7.54 (1H, s, H₆), 7.48 – 7.44 (1H, m, H₄), 7.32 – 7.30 (2H, m, H₂ & H₃), 6.05 (1H, q, $J = 7.2$ Hz, CHCH₃), 4.24 (1H, dd, $J = 8.2, 3.5$ Hz, CHCH₂CH₃), 3.33 (3H, s, NCH₃), 1.68 (3H, d, $J = 7.2$ Hz, CHCH₃), 1.22 – 1.14 (1H, m, CHCH₂CH₃), 1.12 – 1.03 (1H, m, CHCH₂CH₃), 0.59 (3H, t, $J = 7.6$ Hz, CHCH₂CH₃); δ_C (CDCl₃, 126 MHz): 163.2 (CONCH₃), 154.0 (C₁₀), 152.2 (C₇), 141.9 (C₅), 138.8 (C₉), 134.6 (C₁), 130.0 (C₃), 128.6 (C₂), 128.1 (C₆), 126.3 (C₄), 121.1 (C₈), 58.4 (CHCH₂CH₃), 52.9 (CHCH₃), 28.4 (NCH₃), 26.7 (CHCH₂CH₃), 16.4 (CHCH₃), 8.9 (CHCH₂CH₃)

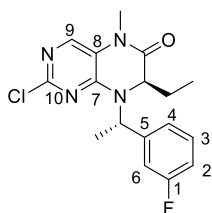
(*R*)-2-Chloro-8-((*S*)-1-(4-chlorophenyl)ethyl)-7-ethyl-5-methyl-7,8-dihydropteridin-6(5*H*)-one, 145d



Dihydropteridinone **79** (145 mg, 0.64 mmol) was reacted with (*R*)-1-(4-chlorophenyl)ethan-1-ol **144d** (160 mg, 1.02 mmol) using general method **20** to afford the title compound **145d** as a white solid (63 mg, d.r >20:1, 27%). LCMS purity >95%, ret. time 1.56

mins; HRMS (ESI +ve): found $[M+H]^+$ 365.0936, $[C_{17}H_{19}Cl_2N_4O]^+$ requires 365.0930; δ_H (CDCl₃, 500 MHz): 7.72 (1H, s, H₇), 7.50 (2H, d, $J = 8.2$ Hz, H₃), 7.35 (2H, d, $J = 8.2$ Hz, H₂), 6.05 (1H, q, $J = 7.2$ Hz, CHCH₃), 4.23 (1H, dd, $J = 8.0, 3.6$ Hz, CHCH₂CH₃), 3.32 (3H, s, NCH₃), 1.67 (3H, d, $J = 7.2$ Hz, CHCH₃), 1.21 – 1.13 (1H, m, CHCH₂CH₃), 1.10 – 1.01 (1H, m, CHCH₂CH₃), 0.58 (3H, t, $J = 7.6$ Hz, CHCH₂CH₃); δ_C (CDCl₃, 126 MHz): 163.2 (CONCH₃), 154.0 (C₈), 152.3 (C₄), 138.8 (C₇), 138.3 (C₄), 134.2 (C₁), 129.4 (C₃), 128.9 (C₂), 121.1 (C₆), 58.3 (CHCH₂CH₃), 52.7 (CHCH₃), 28.4 (NCH₃), 26.7 (CHCH₂CH₃), 16.5 (CHCH₃), 8.9 (CHCH₂CH₃)

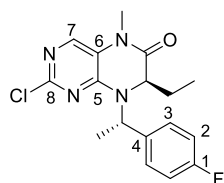
(*R*)-2-Chloro-8-((*S*)-1-(3-fluorophenyl)ethyl)-7-ethyl-5-methyl-7,8-dihydropteridin-6(5*H*)-one, 145e



Dihydropteridinone **79** (110 mg, 0.49 mmol) was reacted with (*R*)-1-(3-fluorophenyl)ethan-1-ol **144e** (109 mg, 0.78 mmol) using general method **20** to afford the title compound **145e** as a white solid (42 mg, d.r 10:1, 25%). LCMS purity >95%, ret. time 1.50

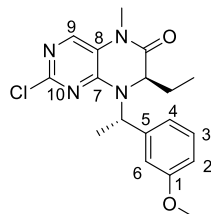
mins; HRMS (ESI +ve): found $[M+H]^+$ 349.1214, $[C_{17}H_{19}ClFN_4O]^+$ requires 349.1226; δ_H ($CDCl_3$, 500 MHz): 7.74 (1H, s, H9), 7.37 – 7.32 (2H, m, H3 & H4), 7.30 – 7.26 (1H, m, H6), 7.06 – 7.02 (1H, m, H2), 6.09 (1H, q, $J = 7.0$ Hz, $CHCH_3$), 4.24 (1H, dd, $J = 8.2, 3.5$ Hz, $CHCH_2CH_3$), 3.33 (3H, s, NCH_3), 1.69 (3H, d, $J = 7.0$ Hz, $CHCH_3$), 1.20 – 1.12 (1H, m, $CHCHHCH_3$), 1.10 – 1.02 (1H, m, $CHCHHCH_3$), 0.58 (3H, t, $J = 7.6$ Hz, $CHCH_2CH_3$); δ_C ($CDCl_3$, 126 MHz): 163.2 ($CONCH_3$), 162.9 (d, $J_{C-F} = 247$ Hz, C1), 154.0 (C10), 142.5 (d, $J_{C-F} = 7$ Hz, C5), 138.8 (C9), 130.2 (d, $J_{C-F} = 7$ Hz, C3), 123.6 (d, $J_{C-F} = 3$ Hz, C4), 121.1 (C8), 115.3 (d, $J_{C-F} = 20$ Hz, C2), 58.3 ($CHCH_2CH_3$), 52.7 ($CHCH_3$), 28.4 (NCH_3), 26.6 ($CHCH_2CH_3$), 16.4 ($CHCH_3$), 8.9 ($CHCH_2CH_3$); $\delta_{F\{H\}}$ ($CDCl_3$, 471 MHz): -112.0

(*R*)-2-Chloro-8-((*S*)-1-(4-fluorophenyl)ethyl)-7-ethyl-5-methyl-7,8-dihydropteridin-6(5*H*)-one, 145f



Dihydropteridinone **79** (120 mg, 0.53 mmol) was reacted with (*R*)-1-(4-fluorophenyl)ethan-1-ol **144f** (119 mg, 0.85 mmol) using general method **20** to afford the title compound **145f** as a white solid (63 mg, d.r 14:1, 11%). LCMS purity >95%, ret. time 1.51 mins; HRMS (ESI +ve): found $[M+H]^+$ 349.1227, $[C_{17}H_{19}ClFN_4O]^+$ requires 349.1226; δ_H ($CDCl_3$, 500 MHz): 7.72 (1H, s, H7), 7.56 – 7.52 (2H, m, H3), 7.09 – 7.04 (2H, m, H2), 6.10 (1H, q, $J = 7.3$ Hz, $CHCH_3$), 4.21 (1H, dd, $J = 8.2, 3.5$ Hz, $CHCH_2CH_3$), 3.32 (3H, s, NCH_3), 1.67 (3H, d, $J = 7.3$ Hz, $CHCH_3$), 1.15 – 1.08 (1H, m, $CHCHHCH_3$), 1.05 – 0.98 (1H, m, $CHCHHCH_3$), 0.56 (3H, t, $J = 7.6$ Hz, $CHCH_2CH_3$); δ_C ($CDCl_3$, 126 MHz): 163.2 ($CONCH_3$), 162.6 (d, $J_{C-F} = 247$ Hz, C1), 154.0 (C8), 152.3 (C5), 138.7 (C7), 135.6 (d, $J_{C-F} = 4$ Hz, C4), 129.7 (d, $J_{C-F} = 8$ Hz, C3), 121.1 (C6), 115.6 (d, $J_{C-F} = 21$ Hz, C2), 58.1 ($CHCH_2CH_3$), 52.5 ($CHCH_3$), 28.4 (NCH_3), 26.6 ($CHCH_2CH_3$), 16.7 ($CHCH_3$), 8.9 ($CHCH_2CH_3$); $\delta_{F\{H\}}$ ($CDCl_3$, 471 MHz): -113.3

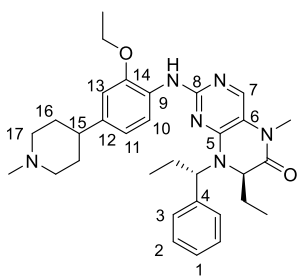
(*R*)-2-Chloro-8-((*S*)-1-(3-methoxyphenyl)ethyl)-7-ethyl-5-methyl-7,8-dihydropteridin-6(5*H*)-one, 145g



Dihydropteridinone **79** (120 mg, 0.53 mmol) was reacted with (*R*)-1-(3-methoxyphenyl)ethan-1-ol **144g** (129 mg, 0.85 mmol) using general method **20** to afford the title compound **145g** as an orange oil (87 mg, d.r 11:1, 46%). LCMS purity >95%, ret. time 1.50 mins; HRMS (ESI +ve): found $[M+H]^+$ 361.1424, $[C_{18}H_{22}ClN_4O_2]^+$ requires 361.1431; δ_H ($CDCl_3$, 500 MHz): 7.72 (1H, s, H9), 7.32 – 7.27 (1H, m, H3), 7.18 – 7.16 (1H, m, H6), 7.15 – 7.12 (1H, m, H4), 6.91 – 6.85 (1H, m, H2), 6.10 (1H, q, $J = 7.1$ Hz, $CHCH_3$), 4.25 (1H, dd, $J = 8.3, 3.5$ Hz, $CHCH_2CH_3$), 3.83 (3H, s, OCH_3), 3.33 (3H, s, NCH_3), 1.67 (3H, d, $J = 7.1$ Hz, $CHCH_3$), 1.17 – 1.10 (1H, m, $CHCHHCH_3$),

1.08 – 0.99 (1H, m, CHCH₂CH₃), 0.58 (3H, t, J = 7.5 Hz, CHCH₂CH₃); δ_c (CDCl₃, 126 MHz): 163.4 (CONCH₃), 159.8 (C1), 154.0 (C10), 152.4 (C7), 141.3 (C5), 138.6 (C9), 129.7 (C3), 121.2 (C8), 120.1 (C4), 114.0 (C6), 113.7 (C2), 58.2 (CHCH₂CH₃), 55.3 (OCH₃), 53.1 (CHCH₃), 28.4 (NCH₃), 26.6 (CHCH₂CH₃), 17.0 (CHCH₃), 9.0 (CHCH₂CH₃)

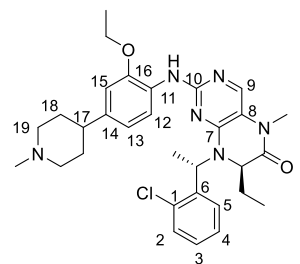
(*R*)-2-((2-Ethoxy-4-(1-methylpiperidin-4-yl)phenyl)amino)-7-ethyl-5-methyl-8-((*S*)-1-phenylpropyl)-7,8-dihydropteridin-6(5*H*)-one, 146



Dihydropteridinone **145a** (16 mg, 46 μ mol) was reacted with aniline **28b** (10 mg, 44 μ mol) using general method **16** to afford the title compound **146** as a brown solid (7 mg, d.r. 19:1, 29%). LCMS purity >95%, ret. time 1.20 mins; HRMS (ESI +ve): found $[M+H]^+$ 543.3442, $[C_{32}H_{43}N_6O_2]^+$ requires 543.3442; δ_H (CDCl₃, 500 MHz): 8.33 (1H, d, J = 7.9 Hz,

H10), 7.88 (1H, s, NH), 7.70 (1H, s, H7), 7.55 (2H, d, J = 6.9 Hz, H3), 7.38 – 7.30 (3H, m, H1 & H2), 6.81 – 6.74 (2H, m, H11 & H13), 6.02 (1H, dd, J = 9.0, 6.8 Hz, ArCHCH₂CH₃), 4.16 (2H, q, J = 7.1 Hz, OCH₂CH₃), 4.07 (1H, dd, J = 8.4, 3.9 Hz, CHCH₂CH₃), 3.61 (2H, d, J = 8.8 Hz, H17), 3.33 (3H, s, CONCH₃), 2.80 – 2.62 (6H, m, NCH₃, H15 & 2 x H17), 2.27 – 2.08 (4H, m, ArCHCH₂CH₃ & 2 x H16), 2.04 – 1.98 (2H, m, H16), 1.49 (3H, t, J = 7.1 Hz, OCH₂CH₃), 0.95 – 0.81 (5H, m, ArCHCH₂CH₃ & CHCH₂CH₃), 0.52 (3H, t, J = 7.6 Hz, CHCH₂CH₃); δ_c (CDCl₃, 126 MHz): 163.2 (CONCH₃), 155.2 (C8), 153.0 (C5), 147.8 (C14), 139.7 (C4), 137.6 (C7), 136.6 (C12), 128.8 (C2), 128.5 (C9), 128.4 (C3), 128.2 (C1), 118.7 (C10 & C11), 115.4 (C6), 109.4 (C13), 64.6 (OCH₂CH₃), 58.7 (ArCHCH₂CH₃), 57.8 (CHCH₂CH₃), 54.7 (C17), 43.4 (NCH₃), 40.0 (C15), 30.5 (C16), 28.4 (CONCH₃), 26.2 (CHCH₂CH₃), 23.3 (ArCHCH₂CH₃), 14.9 (OCH₂CH₃), 11.2 (ArCHCH₂CH₃), 9.2 (CHCH₂CH₃)

(*R*)-8-((*S*)-1-(2-chlorophenyl)ethyl)-2-((2-ethoxy-4-(1-methylpiperidin-4-yl)phenyl)amino)-7-ethyl-5-methyl-7,8-dihydropteridin-6(5*H*)-one, 147

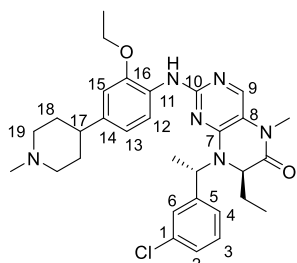


Dihydropteridinone **145b** (23 mg, 63 μ mol) was reacted with aniline **28b** (14 mg, 60 μ mol) using general method **16** to afford the title compound **147** as a white solid (12 mg, d.r. 14:1, 34%). LCMS purity >95%, ret. time 1.13 mins; HRMS (ESI +ve): found $[M+H]^+$ 563.2887, $[C_{31}H_{40}ClN_6O_2]^+$ requires 563.2896; δ_H (CDCl₃, 500 MHz): 8.39 (1H, d, J = 8.2 Hz,

H12), 7.72 (1H, s, NH), 7.65 (1H, s, H9), 7.59 – 7.54 (1H, m, H5), 7.44 – 7.39 (1H, m, H2), 7.32 – 7.27 (2H, m, H3 & H4), 6.81 (1H, dd, J = 8.2, 1.3 Hz, H13), 6.75 (1H, d, J = 1.3 Hz, H15), 6.12 (1H, q, J = 6.9 Hz, CHCH₃), 4.19 (1H, dd, J = 7.6, 3.5 Hz,

CHCH₂CH₃), 4.13 (2H, q, J = 6.9 Hz, OCH₂CH₃), 3.58 (2H, d, J = 9.8 Hz, H19), 3.31 (3H, s, CONCH₃), 2.76 – 2.62 (6H, m, NCH₃, H17 & 2 x H19), 2.27 – 2.15 (2H, m, H18), 2.04 – 1.97 (2H, m, H18), 1.69 (3H, d, J = 6.9 Hz, CHCH₃), 1.50 (3H, t, J = 6.9 Hz, OCH₂CH₃), 1.42 – 1.33 (1H, m, CHCH₂CH₃), 1.22 – 1.14 (1H, m, CHCH₂CH₃), 0.66 (3H, t, J = 7.4 Hz, CHCH₂CH₃); δ_c (CDCl₃, 126 MHz): 163.1 (CONCH₃), 155.3 (C10), 151.4 (C7), 147.7 (C16), 137.5 (C9), 136.7 (C6), 136.6 (C14), 135.7 (C1), 129.9 (C5), 129.8 (C2), 129.5 (C3), 128.5 (C11), 126.7 (C4), 118.9 (C12/13), 118.8 (C12/13), 115.5 (C8), 109.4 (C15), 64.4 (OCH₂CH₃), 59.9 (CHCH₂CH₃), 54.6 (C19), 52.4 (CHCH₃), 45.5 (NCH₃), 40.2 (C17), 30.6 (C18), 28.2 (CONCH₃), 27.1 (CHCH₂CH₃), 17.7 (CHCH₃), 15.0 (OCH₂CH₃), 8.9 (CHCH₂CH₃)

(*R*)-8-((*S*)-1-(3-chlorophenyl)ethyl)-2-((2-ethoxy-4-(1-methylpiperidin-4-yl)phenyl)amino)-7-ethyl-5-methyl-7,8-dihydropteridin-6(5*H*)-one, 148

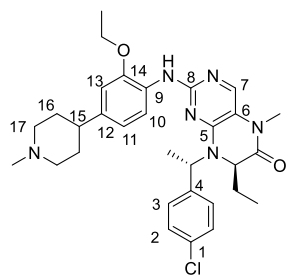


Dihydropteridinone **145c** (35 mg, 96 μ mol) was reacted with aniline **28b** (21 mg, 91 μ mol) using general method **16** to afford the title compound **148** as a pink solid (10 mg, d.r. >20:1, 18%). LCMS purity >95%, ret. time 1.14 mins; HRMS (ESI +ve): found $[M+H]^+$ 563.2895, $[C_{31}H_{40}ClN_6O_2]^+$ requires 563.2896; $[\alpha]_D^{23.2}$: -120.5° (c 1.0, MeOH); δ_H (CDCl₃, 500

MHz): 8.08 (1H, d, J = 7.9 Hz, H12), 7.95 (1H, s, NH), 7.69 (1H, s, H9), 7.51 (1H, s, H6), 7.42 – 7.37 (1H, m, H4), 7.31 – 7.26 (2H, m, H2 & H3), 6.77 – 6.72 (2H, m, H13 & H15), 5.98 (1H, q, J = 7.1 Hz, CHCH₃), 4.21 (1H, dd, J = 7.9, 3.8 Hz, CHCH₂CH₃), 4.13 (2H, q, J = 6.9 Hz, OCH₂CH₃), 3.68 – 3.58 (2H, m, H19), 3.33 (3H, s, CONCH₃), 2.80 – 2.60 (6H, m, NCH₃, H17 & 2 x H19), 2.26 – 2.16 (2H, m, H18), 2.03 – 1.97 (2H, m, H18), 1.69 (3H, d, J = 7.1 Hz, CHCH₃), 1.48 (3H, t, J = 6.9 Hz, OCH₂CH₃), 1.26 – 1.10 (2H, m, CHCH₂CH₃), 0.63 (3H, t, J = 7.6 Hz, CHCH₂CH₃); δ_c (CDCl₃, 126 MHz): 163.0 (CONCH₃), 154.9 (C10), 152.1 (C7), 148.2 (C16), 142.7 (C5), 137.0 (C9 & C14), 134.6 (C1), 129.9 (C3), 128.2 (C2), 128.1 (C11), 127.9 (C6), 125.7 (C4), 119.4 (C12), 118.6 (C13), 115.3 (C8), 109.5 (C15), 64.4 (OCH₂CH₃), 58.7 (CHCH₂CH₃), 54.7 (C19), 52.8 (CHCH₃), 43.4 (NCH₃), 39.9 (C17), 30.5 (C18), 28.9 (CONCH₃), 26.6 (CHCH₂CH₃), 16.7 (CHCH₃), 14.9 (OCH₂CH₃), 8.9 (CHCH₂CH₃)

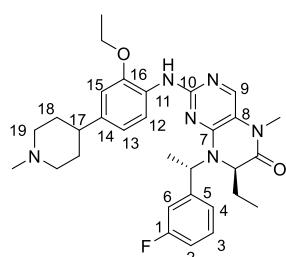
(*R*)-8-((*S*)-1-(4-chlorophenyl)ethyl)-((2-ethoxy-4-(1-methylpiperidin-4-yl)phenyl)amino)-7-ethyl-5-methyl-7,8-dihydropteridin-6(5*H*)-one, 149

Dihydropteridinone **145d** (30 mg, 82 μ mol) was reacted with aniline **28b** (18 mg, 78 μ mol) using general method **16** to afford the title compound **149** as a brown solid (12 mg, d.r. >20:1, 12%). LCMS purity >95%, ret. time 1.14 mins; HRMS (ESI +ve): found



[M+H]⁺ 563.2889, [C₃₁H₄₀ClN₆O₂]⁺ requires 563.2896; m.p.: 80 – 82 °C; ν_{max} (thin film, cm⁻¹): 3425 (w, N-H), 1667 (C=O); $[\alpha]_D^{23.2}$: -204.3° (c 1.0, MeOH); δ_{H} (CDCl₃, 500 MHz): 8.22 (1H, d, J = 8.2 Hz, H10), 7.71 (1H, s, NH), 7.69 (1H, s, H7), 7.48 (2H, d, J = 8.3 Hz, H3), 7.31 (2H, d, J = 8.3 Hz, H2), 6.08 (1H, q, J = 6.9 Hz, CHCH₃), 4.18 – 4.11 (3H, m, CHCH₂CH₃ & OCH₂CH₃), 3.60 (2H, d, J = 9.8 Hz, H17), 3.32 (3H, s, CONCH₃), 2.77 – 2.60 (6H, m, NCH₃, H15 & 2 x H17), 2.25 – 2.15 (2H, m, H16), 2.02 – 1.96 (2H, m, H16), 1.68 (3H, d, J = 6.9 Hz, CHCH₃), 1.49 (3H, t, J = 6.9 Hz, OCH₂CH₃), 1.18 – 1.03 (2H, m, CHCH₂CH₃), 0.59 (3H, t, J = 7.4 Hz, CHCH₂CH₃); δ_{C} (CDCl₃, 126 MHz): 163.1 (CONCH₃), 155.3 (C8), 152.1 (C5), 14.7.7 (C14), 139.4 (C4), 138.0 (C7), 136.7 (C12), 133.8 (C1), 129.1 (C3), 128.7 (C2), 128.4 (C9), 118.7 (C11), 118.6 (C10), 155.4 (C6), 109.4 (C13), 64.6 (OCH₂CH₃), 58.3 (CHCH₂CH₃), 54.6 (C17), 52.1 (CHCH₃), 43.5 (NCH₃), 40.0 (C15), 30.5 (C16), 28.3 (CONCH₃), 26.5 (CHCH₂CH₃), 16.7 (CHCH₃), 14.9 (OCH₂CH₃), 9.0 (CHCH₂CH₃)

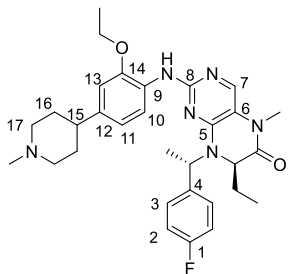
(R)-8-((S)-1-(3-fluorophenyl)ethyl)-2-((2-ethoxy-4-(1-methylpiperidin-4-yl)phenyl)amino)-7-ethyl-5-methyl-7,8-dihydropteridin-6(5H)-one, 150



Dihydropteridinone **145e** (35 mg, 101 μ mol) was reacted with aniline **28b** (23 mg, 96 μ mol) using general method **16** to afford the title compound **150** as a yellow solid (12 mg, d.r. >20:1, 22%). LCMS purity >95%, ret. time 1.16 mins; m.p.: 78 – 80 °C; ν_{max} (thin film, cm⁻¹): 3423 (w, N-H), 1667 (C=O), 1041 (C-F); $[\alpha]_D^{23.7}$: -126.7° (c 1.0, MeOH); HRMS (ESI +ve): found [M+H]⁺ 547.3176, [C₃₁H₄₀FN₆O₂]⁺ requires 547.3196; δ_{H} (CDCl₃, 500 MHz): 8.24 (1H, d, J = 8.5 Hz, H12), 7.70 (1H, s, H9), 7.53 (1H, s, NH), 7.36 – 7.26 (3H, m, H3, H4 & H2/6), 7.03 – 6.98 (1H, m, H2/6), 6.76 – 6.72 (2H, m, H13 & H15), 6.08 (1H, q, J = 6.9 Hz, CHCH₃), 4.18 (1H, dd, J = 7.9, 3.8 Hz, CHCH₂CH₃), 4.13 (2H, q, J = 6.9 Hz, OCH₂CH₃), 3.53 (2H, d, J = 10.7 Hz, H19), 3.32 (3H, s, CONCH₃), 2.71 – 2.58 (6H, m, NCH₃, H17 & 2 x H19), 2.20 – 2.15 (2H, m, H18), 1.99 – 1.94 (2H, m, H18), 1.69 (3H, d, J = 6.9 Hz, CHCH₃), 1.48 (3H, t, J = 6.9 Hz, OCH₂CH₃), 1.19 – 1.07 (2H, m, CHCH₂CH₃), 0.60 (3H, t, J = 7.6 Hz, CHCH₂CH₃); δ_{C} (CDCl₃, 126 MHz): 163.1 (CONCH₃), 162.9 (d, $J_{\text{C-F}}$ = 246 Hz, C1), 155.5 (C10), 151.9 (C7), 147.4 (C16), 143.6 (d, $J_{\text{C-F}}$ = 6 Hz, C5), 138.7 (C9), 136.7 (C14), 130.1 (d, $J_{\text{C-F}}$ = 8 Hz, C3), 128.5 (C11), 123.3 (d, $J_{\text{C-F}}$ = 3 Hz, C4), 118.7 (C13), 118.0 (C12), 115.4 (C8), 114.9 (d, $J_{\text{C-F}}$ = 22 Hz, C2 & C6), 109.4 (C15), 64.4 (OCH₂CH₃), 58.9 (CHCH₂CH₃), 54.6 (C19), 52.2

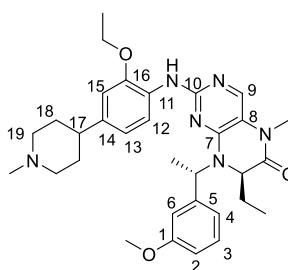
(CHCH₃), 43.6 (C17), 40.2 (C17), 30.7 (C18), 28.3 (CONCH₃), 26.4 (CHCH₂CH₃), 16.7 (CHCH₃), 15.0 (OCHCH₃), 9.0 (CHCH₂CH₃); $\delta_{F\{H\}}$ (CDCl₃, 471 MHz): -112.3

(*R*)-8-((*S*)-1-(4-fluorophenyl)ethyl)-((2-ethoxy-4-(1-methylpiperidin-4-yl)phenyl)amino)-7-ethyl-5-methyl-7,8-dihydropteridin-6(5*H*)-one, 151



Dihydropteridinone **145f** (24 mg, 69 μ mol) was reacted with aniline **28b** (15 mg, 65 μ mol) using general method **16** to afford the title compound **151** as a yellow solid (10 mg, d.r >20:1, 28%). LCMS purity >95%, ret. time 1.15 mins; HRMS (ESI +ve): found $[M+H]^+$ 547.3183, $[C_{31}H_{40}FN_6O_2]^+$ requires 547.3196; m.p.: 77 – 79 °C; ν_{max} (thin film, cm⁻¹): 3420 (w, N-H), 1667 (C=O), 1042 (C-F); $[\alpha]_D^{23.4}$: -149.6° (c 1.0, MeOH); δ_H (CDCl₃, 500 MHz): 8.30 (1H, d, J = 8.5 Hz, H10), 7.70 (1H, s, H7), 7.58 (1H, s, NH), 7.54 (2H, dd, J = 7.9, 5.7 Hz, H3), 7.04 (2H, t, J = 8.5 Hz, H2), 6.76 – 6.73 (2H, m, H11 & H13), 6.16 (1H, q, J = 6.9 Hz, CHCH₃), 4.16 – 4.11 (3H, m, CHCH₂CH₃ & OCH₂CH₃), 3.55 (2H, d, J = 10.1 Hz, H17), 3.32 (3H, s, CONCH₃), 2.72 – 2.59 (6H, m, NCH₃, H15 & 2 x H17), 2.21 – 2.16 (2H, m, H16), 2.00 – 1.96 (2H, m, H16), 1.68 (3H, d, J = 6.9 Hz, CHCH₃), 1.49 (3H, t, J = 6.9 Hz, OCH₂CH₃), 1.12 – 0.98 (2H, m, CHCH₂CH₃), 0.57 (3H, t, J = 7.4 Hz, CHCH₂CH₃); δ_C (CDCl₃, 126 MHz): 163.1 (CONCH₃), 162.4 (d, J_{C-F} = 247 Hz, C1), 155.5 (C8), 152.0 (C5), 147.4 (C14), 138.6 (C7), 136.7 (d, J_{C-F} = 3 Hz, C4), 136.6 (C12), 129.5 (d, J_{C-F} = 8 Hz, C3), 128.5 (C9), 118.7 (C11), 118.2 (C9), 115.5 (d, J_{C-F} = 21 Hz, C2), 115.4 (C7), 109.4 (C13), 64.4 (OCH₂CH₃), 58.0 (CHCH₂CH₃), 54.6 (C17), 51.8 (CHCH₃), 45.5 (NCH₃), 40.1 (C15), 30.7 (C16), 28.3 (CONCH₃), 26.4 (CHCH₂CH₃), 16.9 (CHCH₃), 15.0 (OCH₂CH₃), 9.1 (CHCH₂CH₃); $\delta_{F\{H\}}$ (CDCl₃, 471 MHz): -114.0

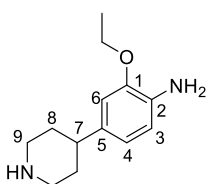
(*R*)-8-((*S*)-1-(3-methoxyphenyl)ethyl)-2-((2-ethoxy-4-(1-methylpiperidin-4-yl)phenyl)amino)-7-ethyl-5-methyl-7,8-dihydropteridin-6(5*H*)-one, 152



Dihydropteridinone **145g** (36 mg, 99 μ mol) was reacted with aniline **28b** (22 mg, 95 μ mol) using general method **16** to afford the title compound **152** as a pale orange solid (20 mg, d.r 18:1, 36%). LCMS purity >95%, ret. time 1.15 mins; HRMS (ESI +ve): found $[M+H]^+$ 559.3382, $[C_{32}H_{42}N_6O_3]^+$ requires 559.3391; δ_H (CDCl₃, 500 MHz): 8.27 (1H, d, J = 8.8 Hz, H12), 7.86 (1H, s, NH), 7.69 (1H, s, H9), 7.28 – 7.25 (1H, m, H3), 7.15 – 7.11 (2H, m, H4 & H6), 6.85 (1H, dd, J = 8.2, 2.6 Hz, H2), 6.77 – 6.74 (2H, m, H13 & H15), 6.13 (1H, q, J = 7.1 Hz, CHCH₃), 4.20 (1H, dd, J = 8.1, 3.7 Hz, CHCH₂CH₃), 4.14 (2H,

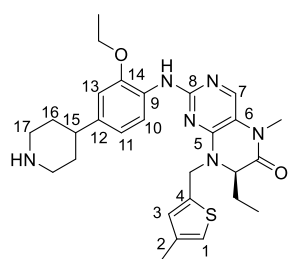
q, $J = 6.7$ Hz, OCH_2CH_3), 3.73 (3H, s, OCH_3), 3.64 – 3.57 (2H, m, H19), 3.32 (3H, s, CONCH_3), 2.77 – 2.70 (5H, m, 2 x H19 & NCH_3), 2.67 – 2.61 (1H, m, H17), 2.24 – 2.16 (2H, m, H18), 2.02 – 1.97 (2H, m, H18), 1.68 (3H, d, $J = 7.1$ Hz, CHCH_3), 1.50 (3H, t, $J = 7.0$ Hz, OCH_2CH_3), 1.15 – 1.02 (2H, m, CHCH_2CH_3), 0.58 (3H, t, $J = 7.5$ Hz, CHCH_2CH_3); δ_{C} (CDCl_3 , 126 MHz): 163.2 (CONCH_3), 159.8 (C1), 155.1 (C10), 152.2 (C7), 147.8 (C16), 137.3 (C9), 136.7 (C14), 129.6 (C3), 128.3 (C11), 119.8 (C4), 118.9 (C12), 1118.7 (C13), 115.4 (C8), 113.7 (C6), 113.4 (C2), 109.4 (C15), 64.6 (OCH_2CH_3), 58.2 (CHCH_2CH_3), 55.2 (OCH_3), 54.7 (C19), 52.6 (CHCH_3), 43.5 (NCH_3), 40.0 (C17), 30.5 (C18), 28.3 (CONCH_3), 26.4 (CHCH_2CH_3), 16.7 (CHCH_3), 14.9 (OCH_2CH_3), 9.1 (CHCH_2CH_3)

2-Ethoxy-4-(piperidin-4-yl)aniline, 163



Pyridine **25b** (400 mg, 1.63 mmol) was subjected to general method **15** to afford the title compound **163** as a brown oil (355 mg, 98%). LCMS purity >95%, ret. time 0.02 mins; HRMS (ESI +ve): found $[\text{M}+\text{H}]^+$ 221.1651 $[\text{C}_{13}\text{H}_{21}\text{N}_2\text{O}]^+$ requires 221.1654; δ_{H} (500 MHz, CDCl_3): 6.68 – 6.63 (3H, m, H3, H4 & H6), 4.06 (2H, q, $J = 6.9$ Hz, OCH_2CH_3), 3.23 – 3.17 (2H, m, H9), 2.74 (2H, td, $J = 12.3, 2.5$ Hz, H9), 2.52 (1H, tt, $J = 12.1, 3.7$ Hz, H7), 1.83 (2H, d, $J = 13.9$ Hz, H8), 1.60 – 1.61 (2H, m, H8), 1.43 (3H, t, $J = 7.1$ Hz, OCH_2CH_3); δ_{C} (CDCl_3 , 126 MHz): 146.7 (C1), 137.1 (C5), 134.4 (C2), 118.8 (C4), 115.0 (C3), 110.2 (C6), 63.7 (OCH_2CH_3), 46.8 (C9), 42.4 (C7), 34.3 (C8), 15.1 (OCH_2CH_3); NH_2 peak not observed.

(R)-2-((2-Ethoxy-4-(piperidin-4-yl)phenyl)amino)-7-ethyl-5-methyl-8-((4-methylthiophen-2-yl)methyl)-7,8-dihydropteridin-6(5H)-one, 158

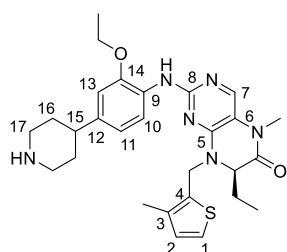


Dihydropteridinone **6r** (100 mg, 297 μmol) was reacted with aniline **163** (62 mg, 282 μmol) using general method **16** to afford the title compound **158** as a yellow solid (67 mg, 43%). LCMS purity >95%, ret. time 1.17 mins; HRMS (ESI +ve): found $[\text{M}+\text{H}]^+$ 521.2693, $[\text{C}_{28}\text{H}_{37}\text{N}_6\text{O}_2\text{S}]^+$ requires 521.2695; m.p.: 102 – 105 $^{\circ}\text{C}$; ν_{max} (thin film, cm^{-1}): 3419 (w, N-H), 2928

(w, N-H), 1676 (C=O); $[\alpha]_{\text{D}}^{23.0}$: +17.3 $^{\circ}$ (c 1.0, MeOH); δ_{H} (CDCl_3 , 500 MHz): 8.31 (1H, d, $J = 8.4$ Hz, H10), 7.67 – 7.64 (2H, m, H7 & ArNH), 6.84 (1H, s, H3), 6.81 (1H, s, H1), 6.78 (1H, dd, $J = 8.4, 1.5$ Hz, H11), 6.74 (1H, d, $J = 1.5$ Hz, H13), 5.59 (1H, d, $J = 15.5$ Hz, ArCHH), 4.34 (1H, d, $J = 15.5$ Hz, ArCHH), 4.26 (1H, dd, $J = 6.3, 3.5$ Hz, CHCH_2CH_3), 4.13 (2H, q, $J = 6.9$ Hz, OCH_2CH_3), 3.50 (2H, d, $J = 11.7$ Hz, H17), 3.31 (3H, s, CONCH_3), 3.02 – 2.93 (2H, m, H17), 2.74 – 2.66 (1H, m, H15), 2.22 (3H, s,

ArCH₃), 2.10 – 1.93 (5H, m, H16 & CHCH₂HCH₃), 1.89 – 1.80 (1H, m, CHCH₂HCH₃), 1.48 (3H, t, *J* = 6.9 Hz, OCH₂CH₃), 0.83 (3H, t, *J* = 7.6 Hz, CHCH₂CH₃); δ_C (CDCl₃, 126 MHz): 163.3 (CONCH₃), 155.3 (C8), 151.5 (C5), 147.5 (C14), 138.1 (C2), 137.5 (C4), 137.4 (C7), 137.0 (C12), 129.7 (C3), 128.4 (C9), 121.2 (C1), 118.5 (C10 & C11), 114.8 (C6), 109.5 (C13), 64.4 (OCH₂CH₃), 60.3 (CHCH₂CH₃), 44.2 (C17), 42.9 (ArCH₂), 40.5 (C15), 30.2 (C16), 28.1 (CONCH₃), 24.8 (CHCH₂CH₃), 15.7 (ArCH₃), 15.0 (OCH₂CH₃), 8.7 (CHCH₂CH₃); *Piperidine NH* not observed in NMR.

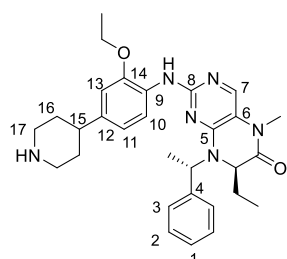
(*R*)-2-((2-Ethoxy-4-(piperidin-4-yl)phenyl)amino)-7-ethyl-5-methyl-8-((3-methylthiophen-2-yl)methyl)-7,8-dihydropteridin-6(5*H*)-one, 164



Dihydropteridinone **6k** (40 mg, 119 μmol) was reacted with aniline **163** (25 mg, 113 μmol) using general method **16** to afford the title compound **164** as a yellow solid (7 mg, 11%). LCMS purity >95%, ret. time 1.15 mins; HRMS (ESI +ve): found [M+H]⁺ 521.2679, [C₂₈H₃₇N₆O₂S]⁺ requires 521.2695; m.p.: 103 – 106 °C; ν_{max} (thin film, cm⁻¹): 3420 (w, N-H), 1665

(C=O); [α]_D^{23.2}: -18.0° (c 1.0, MeOH); δ_H (CDCl₃, 500 MHz): 8.37 (1H, d, *J* = 8.2 Hz, H10), 7.70 (1H, s, H7), 7.48 (1H, s, ArNH), 7.16 (1H, d, *J* = 5.1 Hz, H1), 6.90 – 6.79 (2H, m, H2 & H11), 6.75 (1H, s, H13), 5.65 (1H, d, *J* = 15.6 Hz, ArCH₂H), 4.36 (1H, d, *J* = 15.6 Hz, ArCH₂H), 4.20 (1H, dd, *J* = 6.6, 3.6 Hz, CHCH₂CH₃), 4.15 (2H, q, *J* = 6.9 Hz, OCH₂CH₃), 3.50 (2H, d, *J* = 12.4 Hz, H17), 3.34 (3H, s, CONCH₃), 3.05 – 2.87 (2H, m, H17), 2.73 – 2.67 (1H, m, H15), 2.27 (3H, s, ArCH₃), 2.11 – 1.90 (5H, m, H16 & CHCH₂HCH₃), 1.89 – 1.81 (1H, m, CHCH₂HCH₃), 1.50 (3H, t, *J* = 6.9 Hz, OCH₂CH₃), 0.86 (3H, t, *J* = 7.8 Hz, CHCH₂CH₃); δ_C (CDCl₃, 126 MHz): 163.4 (CONCH₃), 155.6 (C8), 151.5 (C5), 147.1 (C14), 138.3 (C7), 136.7 (C12), 136.1 (C3), 131.6 (C4), 130.1 (C2), 128.6 (C9), 124.2 (C1), 118.7 (C11), 118.0 (C10), 114.8 (C6), 109.4 (C13), 64.3 (OCH₂CH₃), 60.1 (CHCH₂CH₃), 44.3 (C17), 40.7 (C15), 40.5 (ArCH₂), 30.6 (C16), 28.1 (CONCH₃), 24.8 (CHCH₂CH₃), 15.0 (CH₃), 14.0 (OCH₂CH₃), 8.9 (CHCH₂CH₃); ; *Piperidine NH* not observed in NMR.

(*R*)-2-((2-Ethoxy-4-(piperidin-4-yl)phenyl)amino)-7-ethyl-5-methyl-8-((*S*)-1-phenylethyl)-7,8-dihydropteridin-6(5*H*)-one, 165



Dihydropteridinone **137** (60 mg, 181 μmol) was reacted with aniline **163** (38 mg, 172 μmol) using general method **16** to afford the title compound **165** as a yellow solid (17 mg, d.r. >20:1, 18%). LCMS purity >95%, ret. time 1.13 mins; HRMS (ESI +ve): found [M+H]⁺ 515.3128, [C₃₀H₃₉N₆O₂]⁺ requires

515.3129; m.p.: 92 – 95 °C; ν_{max} (thin film, cm^{-1}): 3424 (w, N-H), 2972 (w, N-H), 1676 (C=O); $[\alpha]_D^{23.0}$: -171.8° (c 1.0, MeOH); δ_{H} (CDCl_3 , 500 MHz): 8.22 (1H, d, $J = 8.8$ Hz, H10), 7.71 (1H, s, ArNH), 7.70 (1H, s, H7), 7.56 (2H, d, $J = 7.4$ Hz, H3), 7.39 – 7.31 (3H, m, H1 & H2), 6.78 – 6.74 (2H, m, H11 & H13) 6.18 (1H, q, $J = 7.2$ Hz, CHCH_3), 4.21 – 4.13 (3H, m, CHCH_2CH_3 & OCH_2CH_3), 3.53 (2H, d, $J = 12.5$ Hz, H17), 3.33 (3H, s, CONCH_3), 3.04 – 2.96 (2H, m, H17), 2.75 – 2.68 (1H, m, H15), 2.10 – 2.00 (4H, m, H16), 1.70 (3H, d, $J = 7.2$ Hz, CHCH_3), 1.51 (3H, t, $J = 7.0$ Hz, OCH_2CH_3), 1.13 – 0.99 (2H, m, CHCH_2CH_3), 0.58 (3H, t, $J = 7.5$ Hz, CHCH_2CH_3); δ_{C} (CDCl_3 , 126 MHz): 163.4 (CONCH_3), 155.4 (C8), 152.3 (C5), 14.7.7 (C14), 140.7 (C4), 137.9 (C7), 137.1 (C12), 128.8 (C2), 128.6 (C9), 128.2 (C1), 128.0 (C3), 118.8 (C10), 118.7 (C11), 115.6 (C6), 109.6 (C13), 64.5 (OCH_2CH_3), 58.4 (CHCH_2CH_3), 52.8 (CHCH_3), 44.4 (C17), 40.6 (C15), 30.4 (C16), 28.5 (CONCH_3), 26.5 (CHCH_2CH_3), 16.9 (CHCH_3), 15.1 (OCH_2CH_3), 9.2 (CHCH_2CH_3); *Piperidine NH not observed in NMR.*

Chapter 8 Appendices

8.1 Appendix A: Kinome Screen Data for 63

| Kinase | % Control (1 μ M) | Kinase | % Control (1 μ M) |
|----------------------------|--------------------------|--------------------------------|--------------------------|
| ABL1(E255K)-phosphorylated | 100 | ERK1 | 100 |
| ABL1(T315I)-phosphorylated | 71 | FAK | 60 |
| ABL1-nonphosphorylated | 84 | FGFR2 | 100 |
| ABL1-phosphorylated | 100 | FGFR3 | 98 |
| ACVR1B | 85 | FLT3 | 100 |
| ADCK3 | 100 | GSK3B | 82 |
| AKT1 | 96 | IGF1R | 77 |
| AKT2 | 100 | IKK-alpha | 97 |
| ALK | 7.1 | IKK-beta | 100 |
| AURKA | 99 | INSR | 25 |
| AURKAB | 86 | JAK2 (JH1 domain- catalytic | 83 |
| AXL | 98 | JAK3 (JH1 domain catalytic | 100 |
| BMPR2 | 100 | JNK1 | 64 |
| BRAF | 100 | JNK2 | 44 |
| BRAF(V600E) | 98 | JNK3 | 39 |
| BTK | 100 | KIT | 100 |
| CDK11 | 93 | KIT (D816V) | 100 |
| CDK2 | 100 | KIT (V559D, T670I) | 100 |
| CDK3 | 89 | LKB1 | 82 |
| CDK7 | 88 | MAP3K4 | 92 |
| CDK9 | 100 | MAPKAPK2 | 100 |
| CHEK1 | 100 | MARK3 | 100 |
| CSF1R | 100 | MEK1 | 100 |
| CSNK1D | 90 | MEK2 | 100 |
| CSNK1G2 | 100 | MET | 94 |
| DCAMKL1 | 100 | MKNK1 | 100 |
| DYRK1B | 63 | MKNK2 | 60 |

| | | | |
|-------------|-----|-----------------------------|-----|
| EGFR | 86 | MLK1 | 100 |
| EGFR(L858R) | 69 | p38-alpha | 92 |
| EPHA2 | 100 | p38-beta | 89 |
| ERBB2 | 100 | PAK1 | 100 |
| ERBB4 | 93 | PAK2 | 100 |
| PAK4 | 100 | RET | 99 |
| PCTK1 | 95 | RIOK2 | 74 |
| PDGFRA | 96 | ROCK2 | 100 |
| PDGFRB | 100 | RSK2 (Kin.Dom.1-N-terminal) | 59 |
| PDPK1 | 98 | SNARK | 100 |
| PIK3C2B | 88 | SRC | 100 |
| PIK3CA | 96 | SRPK3 | 100 |
| PIK3CG | 98 | TGFBR1 | 94 |
| PIM1 | 97 | TIE2 | 99 |
| PIM2 | 86 | TRKA | 91 |
| PIM3 | 100 | TSSK1B | 91 |
| PKAC-alpha | 100 | TYK2 (JH1 domain-catalytic) | 100 |
| PLK1 | 1 | ULK2 | 64 |
| PLK3 | 25 | VEGFR2 | 87 |
| PLK4 | 100 | YANK3 | 100 |
| PRKCE | 100 | ZAP70 | 94 |
| RAF1 | 100 | | |

Chapter 9 References

- (1) “Neuroblastoma UK & Childrens Cancer and Leukaemia Group, *Neuroblastoma - Information and Support for Parents*,” 2015.
- (2) Cohn, S. L.; Pearson, A. D. J.; London, W. B.; Monclair, T.; Ambros, P. F.; Brodeur, G. M.; Faldum, A.; Hero, B.; Iehara, T.; Machin, D.; Mosseri, V.; Simon, T.; Garaventa, A.; Castel, V.; Matthay, K. K.; Force, I. T., *Journal of Clinical Oncology*, **2009**, 27, 289.
- (3) Mossé, Y. P.; Laudenslager, M.; Longo, L.; Cole, K. A.; Wood, A.; Attiyeh, E. F.; Laquaglia, M. J.; Sennett, R.; Lynch, J. E.; Perri, P.; Laureys, G.; Speleman, F.; Kim, C.; Hou, C.; Hakonarson, H.; Torkamani, A.; Schork, N. J.; Brodeur, G. M.; Tonini, G. P.; Rappaport, E., *Nature*, **2008**, 455, 930.
- (4) University of California San Francisco, Department of Surgery, Accessed June 2019, <https://surgery.ucsf.edu/conditions--procedures/pediatric-cancer.aspx>
- (5) Monclair, T.; Brodeur, G. M.; Ambros, P. F.; Brisse, H. J.; Cecchetto, G.; Holmes, K.; Kaneko, M.; London, W. B.; Matthay, K. K.; Nuchtern, J. G.; Schweinitz, D. v.; Simon, T.; Cohn, S. L.; Pearson, A. D. J., *Journal of Clinical Oncology*, **2009**, 27, 298.
- (6) London, W. B.; Castleberry, R. P.; Matthay, K. K.; Look, A. T.; Seeger, R. C.; Shimada, H.; Thorner, P.; Brodeur, G.; Maris, J. M.; Reynolds, C. P.; Cohn, S. L., *Journal of Clinical Oncology*, **2005**, 23, 6459.
- (7) Shimada, H.; Chatten, J.; Newton, W. A.; Sachs, N.; Hamoudi, A. B.; Chiba, T.; Marsden, H. B.; Misugi, K., *Journal of the National Cancer Institute*, **1984**, 73, 405.
- (8) Bell, E.; Chen, L.; Liu, T.; Marshall, G. M.; Lunec, J.; Tweddle, D. A., *Cancer Letters*, **2010**, 293, 144.
- (9) Look, A. T.; Hayes, F. A.; Shuster, J. J.; Douglass, E. C.; Castleberry, R. P.; Bowman, L. C.; Smith, E. I.; Brodeur, G. M., *Journal of Clinical Oncology*, **1991**, 9, 581.
- (10) Maris, J. M., *New England Journal of Medicine*, **2010**, 362, 2202.
- (11) Brodeur, G.; Seeger, R.; Schwab, M.; Varmus, H.; Bishop, J., *Science*, **1984**, 224, 1121.
- (12) Barone, G.; Anderson, J.; Pearson, A. D. J.; Petrie, K.; Chesler, L., *Clinical Cancer Research*, **2013**, 19, 5814.
- (13) Soucek, L.; Whitfield, J.; Martins, C. P.; Finch, A. J.; Murphy, D. J.; Sodir, N. M.; Karnezis, A. N.; Swigart, L. B.; Nasi, S.; Evan, G. I., *Nature*, **2008**, 455, 679.
- (14) Amati, B.; Littlewood, T. D.; Evan, G. I.; Land, H., *The EMBO Journal*, **1993**, 12, 5083.
- (15) Müller, I.; Larsson, K.; Frenzel, A.; Oliynyk, G.; Zirath, H.; Prochownik, E. V.; Westwood, N. J.; Henriksson, M. A., *PLOS ONE*, **2014**, 9, 97285.
- (16) Johnsen, J. I.; Dyberg, C.; Fransson, S.; Wickström, M., *Pharmacological Research*, **2018**, 131, 164.
- (17) Chen, H.; Liu, H.; Qing, G., *Signal Transduction and Targeted Therapy*, **2018**, 3, 5.
- (18) Chipumuro, E.; Marco, E.; Christensen, C. L.; Kwiatkowski, N.; Zhang, T.; Hatheway, C. M.; Abraham, B. J.; Sharma, B.; Yeung, C.; Altabef,

- A.; Perez-Atayde, A.; Wong, K.; Yuan, G.; Gray, N. S.; Young, R. A.; George, R. E., *Cell*, **2014**, 159, 1126.
- (19) Chesler, L.; Schlieve, C.; Goldenberg, D. D.; Kenney, A.; Kim, G.; McMillan, A.; Matthay, K. K.; Rowitch, D.; Weiss, W. A., *Cancer Research*, **2006**, 66, 8139.
 - (20) Opel, D.; Poremba, C.; Simon, T.; Debatin, K.-M.; Fulda, S., *Cancer Research*, **2007**, 67, 735.
 - (21) Vaughan, L.; Clarke, P. A.; Barker, K.; Chanthery, Y.; Gustafson, C. W.; Tucker, E.; Renshaw, J.; Raynaud, F.; Li, X.; Burke, R.; Jamin, Y.; Robinson, S. P.; Pearson, A.; Maira, M.; Weiss, W. A.; Workman, P.; Chesler, L., *Oncotarget*, **2016**, 7, 57525.
 - (22) SF1126 for Patients With Relapsed or Refractory Neuroblastoma, Accessed June 2019, <https://clinicaltrials.gov/ct2/show/NCT02337309>
 - (23) European Proof-of-Concept Therapeutic Stratification Trial of Molecular Anomalies in Relapsed or Refractory Tumors, Accessed June 2019, <https://clinicaltrials.gov/ct2/show/NCT02813135>
 - (24) Richards, M. W.; Burgess, S. G.; Poon, E.; Carstensen, A.; Eilers, M.; Chesler, L.; Bayliss, R., *Proceedings of the National Academy of Sciences*, **2016**, 113, 13726.
 - (25) Brockmann, M.; Poon, E.; Berry, T.; Carstensen, A.; Deubzer, Hedwig E.; Rycak, L.; Jamin, Y.; Thway, K.; Robinson, Simon P.; Roels, F.; Witt, O.; Fischer, M.; Chesler, L.; Eilers, M., *Cancer Cell*, **2013**, 24, 75.
 - (26) MLN8237, to Treat Children With Relapsed/Refractory Solid Tumors, Accessed June 2015, <https://clinicaltrials.gov/ct2/show/NCT02444884>
 - (27) Xiao, D.; Yue, M.; Su, H.; Ren, P.; Jiang, J.; Li, F.; Hu, Y.; Du, H.; Liu, H.; Qing, G., *Molecular Cell*, **2016**, 64, 493.
 - (28) Kaelin, W. G., *Nature Reviews Cancer*, **2005**, 5, 689.
 - (29) Cole, K. A.; Huggins, J.; Laquaglia, M.; Hulderman, C. E.; Russell, M. R.; Bosse, K.; Diskin, S. J.; Attiyeh, E. F.; Sennett, R.; Norris, G.; Laudenslager, M.; Wood, A. C.; Mayes, P. A.; Jagannathan, J.; Winter, C.; Mosse, Y. P.; Maris, J. M., *Proceedings of the National Academy of Sciences*, **2011**, 108, 3336.
 - (30) Goga, A.; Yang, D.; Tward, A. D.; Morgan, D. O.; Bishop, J. M., *Nature Medicine*, **2007**, 13, 820.
 - (31) Walton, M. I.; Eve, P. D.; Hayes, A.; Valenti, M. R.; De Haven Brandon, A. K.; Box, G.; Hallsworth, A.; Smith, E. L.; Boxall, K. J.; Lainchbury, M.; Matthews, T. P.; Jamin, Y.; Robinson, S. P.; Aherne, G. W.; Reader, J. C.; Chesler, L.; Raynaud, F. I.; Eccles, S. A.; Collins, I.; Garrett, M. D., *Clinical Cancer Research*, **2012**, 18, 5650.
 - (32) Puissant, A.; Frumm, S. M.; Alexe, G.; Bassil, C. F.; Qi, J.; Chanthery, Y. H.; Nekritz, E. A.; Zeid, R.; Gustafson, W. C.; Greninger, P.; Garnett, M. J.; McDermott, U.; Benes, C. H.; Kung, A. L.; Weiss, W. A.; Bradner, J. E.; Stegmaier, K., *Cancer Discovery*, **2013**, 3, 308.
 - (33) Stathis, A.; Bertoni, F., *Cancer Discovery*, **2017**.
 - (34) Schnepf, R. W.; Maris, J. M., *Cancer Discovery*, **2013**, 3, 255.
 - (35) Yang, Z.; Yik, J. H. N.; Chen, R.; He, N.; Jang, M. K.; Ozato, K.; Zhou, Q., *Molecular Cell*, **2005**, 19, 535.
 - (36) Henssen, A.; Althoff, K.; Odersky, A.; Beckers, A.; Koche, R.; Speleman, F.; Schäfers, S.; Bell, E.; Nortmeyer, M.; Westermann, F.; De Preter, K.; Florin, A.; Heukamp, L.; Spruessel, A.; Astrahanseff, K.

- Lindner, S.; Sadowski, N.; Schramm, A.; Astorgues-Xerri, L.; Riveiro, M. E.; Eggert, A.; Cvitkovic, E.; Schulte, J. H., *Clinical Cancer Research*, **2016**, 22, 2470.
- (37) Study of the Bromodomain (BRD) and Extra-Terminal Domain (BET) Inhibitor BMS-986158 in Pediatric Cancer, Accessed June 2019, <https://clinicaltrials.gov/ct2/show/NCT03936465>
- (38) Bresler, S. C.; Wood, A. C.; Haglund, E. A.; Courtright, J.; Belcastro, L. T.; Plegaria, J. S.; Cole, K.; Toporovskaya, Y.; Zhao, H.; Carpenter, E. L.; Christensen, J. G.; Maris, J. M.; Lemmon, M. A.; Mossé, Y. P., *Science Translational Medicine*, **2011**, 3, 108.
- (39) Chen, Y.; Takita, J.; Choi, Y. L.; Kato, M.; Ohira, M.; Sanada, M.; Wang, L.; Soda, M.; Kikuchi, A.; Igarashi, T.; Nakagawara, A.; Hayashi, Y.; Mano, H.; Ogawa, S., *Nature*, **2008**, 455, 971.
- (40) Berry, T.; Luther, W.; Bhatnagar, N.; Jamin, Y.; Poon, E.; Sanda, T.; Pei, D.; Sharma, B.; Vetharoy, W. R.; Hallsworth, A.; Ahmad, Z.; Barker, K.; Moreau, L.; Webber, H.; Wang, W.; Liu, Q.; Perez-Atayde, A.; Rodig, S.; Cheung, N.; Raynaud, F.; Hallberg, B.; Robinson, S. P.; Gray, N. S.; Pearson, A. D. J.; Eccles, S. A.; Chesler, L.; George, R. E., *Cancer Cell*, **2012**, 22, 117.
- (41) Tucker, E. R.; Danielson, L. S.; Innocenti, P.; Chesler, L., *Cancer Research*, **2015**.
- (42) Schönherr, C.; Ruuth, K.; Kamaraj, S.; Wang, C. L.; Yang, H. L.; Combaret, V.; Djos, A.; Martinsson, T.; Christensen, J. G.; Palmer, R. H.; Hallberg, B., *Oncogene*, **2012**, 31, 5193.
- (43) Gustafson, W. C.; Weiss, W. A., *Oncogene*, **2010**, 29, 1249.
- (44) Tucker, E.; Poon, E.; Chesler, L., *Cancer Drug Resistance*, **2019**, 2.
- (45) Cui, J. J.; Tran-Dubé, M.; Shen, H.; Nambu, M.; Kung, P.-P.; Pairish, M.; Jia, L.; Meng, J.; Funk, L.; Botrous, I.; McTigue, M.; Grodsky, N.; Ryan, K.; Padrique, E.; Alton, G.; Timofeevski, S.; Yamazaki, S.; Li, Q.; Zou, H.; Christensen, J.; Mroczkowski, B.; Bender, S.; Kania, R. S.; Edwards, M. P., *Journal of Medicinal Chemistry*, **2011**, 54, 6342.
- (46) Marsilje, T. H.; Pei, W.; Chen, B.; Lu, W.; Uno, T.; Jin, Y.; Jiang, T.; Kim, S.; Li, N.; Warmuth, M.; Sarkisova, Y.; Sun, F.; Steffy, A.; Pferdekamper, A. C.; Li, A. G.; Joseph, S. B.; Kim, Y.; Liu, B.; Tuntland, T.; Cui, X.; Gray, N. S.; Steensma, R.; Wan, Y.; Jiang, J.; Chopiuk, G.; Li, J.; Gordon, W. P.; Richmond, W.; Johnson, K.; Chang, J.; Groessl, T.; He, Y.-Q.; Phimister, A.; Aycinena, A.; Lee, C. C.; Bursulaya, B.; Karanewsky, D. S.; Seidel, H. M.; Harris, J. L.; Michellys, P.-Y., *Journal of Medicinal Chemistry*, **2013**, 56, 5675.
- (47) Johnson, T. W.; Richardson, P. F.; Bailey, S.; Brooun, A.; Burke, B. J.; Collins, M. R.; Cui, J. J.; Deal, J. G.; Deng, Y.-L.; Dinh, D.; Engstrom, L. D.; He, M.; Hoffman, J.; Hoffman, R. L.; Huang, Q.; Kania, R. S.; Kath, J. C.; Lam, H.; Lam, J. L.; Le, P. T.; Lingardo, L.; Liu, W.; McTigue, M.; Palmer, C. L.; Sach, N. W.; Smeal, T.; Smith, G. L.; Stewart, A. E.; Timofeevski, S.; Zhu, H.; Zhu, J.; Zou, H. Y.; Edwards, M. P., *Journal of Medicinal Chemistry*, **2014**, 57, 4720.
- (48) Menichincheri, M.; Ardini, E.; Magnaghi, P.; Avanzi, N.; Banfi, P.; Bossi, R.; Buffa, L.; Canevari, G.; Ceriani, L.; Colombo, M.; Corti, L.; Donati, D.; Fasolini, M.; Felder, E.; Fiorelli, C.; Fiorentini, F.; Galvani, A.; Isacchi, A.; Borgia, A. L.; Marchionni, C.; Nesi, M.; Orrenius, C.;

- Panzeri, A.; Pesenti, E.; Rusconi, L.; Saccardo, M. B.; Vanotti, E.; Perrone, E.; Orsini, P., *Journal of Medicinal Chemistry*, **2016**, 59, 3392.
- (49) Mossé, Y. P.; Lim, M. S.; Voss, S. D.; Wilner, K.; Ruffner, K.; Laliberte, J.; Rolland, D.; Balis, F. M.; Maris, J. M.; Weigel, B. J.; Ingle, A. M.; Ahern, C.; Adamson, P. C.; Blaney, S. M., *Lancet Oncol*, **2013**, 14, 472.
- (50) Friboulet, L.; Li, N.; Katayama, R.; Lee, C. C.; Gainor, J. F.; Crystal, A. S.; Michellys, P.-Y.; Awad, M. M.; Yanagitani, N.; Kim, S.; Pferdekamper, A. C.; Li, J.; Kasibhatla, S.; Sun, F.; Sun, X.; Hua, S.; McNamara, P.; Mahmood, S.; Lockerman, E. L.; Fujita, N.; Nishio, M.; Harris, J. L.; Shaw, A. T.; Engelman, J. A., *Cancer Discovery*, **2014**, 4, 662.
- (51) Trigg, R. M.; Turner, S. D., *Cancers (Basel)*, **2018**, 10, 113.
- (52) Wood, A. C.; Krytska, K.; Ryles, H. T.; Infarinato, N. R.; Sano, R.; Hansel, T. D.; Hart, L. S.; King, F. J.; Smith, T. R.; Ainscow, E.; Grandinetti, K. B.; Tuntland, T.; Kim, S.; Caponigro, G.; He, Y. Q.; Krupa, S.; Li, N.; Harris, J. L.; Mossé, Y. P., *Clinical Cancer Research*, **2017**, 23, 2856.
- (53) Infarinato, N. R.; Park, J. H.; Krytska, K.; Ryles, H. T.; Sano, R.; Szigety, K. M.; Li, Y.; Zou, H. Y.; Lee, N. V.; Smeal, T.; Lemmon, M. A.; Mossé, Y. P., *Cancer Discovery*, **2016**, 6, 96.
- (54) Guan, J.; Tucker, E. R.; Wan, H.; Chand, D.; Danielson, L. S.; Ruuth, K.; El Wakil, A.; Witek, B.; Jamin, Y.; Umapathy, G.; Robinson, S. P.; Johnson, T. W.; Smeal, T.; Martinsson, T.; Chesler, L.; Palmer, R. H.; Hallberg, B., *Disease Models & Mechanisms*, **2016**, 9, 941.
- (55) Study Of Lorlatinib, P.-. Accessed June 2019, <https://ClinicalTrials.gov/show/NCT03107988>
- (56) Morris, S.; Kirstein, M.; Valentine, M.; Dittmer, K.; Shapiro, D.; Saltman, D.; Look, A., *Science*, **1994**, 263, 1281.
- (57) Hallberg, B.; Palmer, R. H., *Nature Review Cancer*, **2013**, 13, 685.
- (58) Salido, M.; Pijuan, L.; Martínez-Avilés, L.; Galván, A. B.; Cañadas, I.; Rovira, A.; Zanui, M.; Martínez, A.; Longarón, R.; Sole, F.; Serrano, S.; Bellosillo, B.; Wynes, M. W.; Albanell, J.; Hirsch, F. R.; Arriola, E., *Journal of Thoracic Oncology*, **2011**, 6, 21.
- (59) Wang, Y.-W.; Tu, P.-H.; Lin, K.-T.; Lin, S.-C.; Ko, J.-Y.; Jou, Y.-S., *Neoplasia*, **2011**, 13, 704.
- (60) Murugan, A. K.; Xing, M., *Cancer Research*, **2011**, 71, 4403.
- (61) Bossi, R. T.; Saccardo, M. B.; Ardini, E.; Menichincheri, M.; Rusconi, L.; Magnaghi, P.; Orsini, P.; Avanzi, N.; Borgia, A. L.; Nesi, M.; Bandiera, T.; Fogliatto, G.; Bertrand, J. A., *Biochemistry*, **2010**, 49, 6813.
- (62) Bresler, S. C.; Weiser, D. A.; Huwe, P. J.; Park, J. H.; Krytska, K.; Ryles, H.; Laudenslager, M.; Rappaport, E. F.; Wood, A. C.; McGrady, P. W.; Hogarty, M. D.; London, W. B.; Radhakrishnan, R.; Lemmon, M. A.; Mossé, Y. P., *Cancer Cell*, **2014**, 26, 682.
- (63) Epstein, L. F.; Chen, H.; Emkey, R.; Whittington, D. A., *Journal of Biological Chemistry*, **2012**, 287, 37447.
- (64) Donella-Deana, A.; Marin, O.; Cesaro, L.; Gunby, R. H.; Ferrarese, A.; Coluccia, A. M. L.; Tartari, C. J.; Mologni, L.; Scapozza, L.; Gambacorti-Passerini, C.; Pinna, L. A., *Biochemistry*, **2005**, 44, 8533.
- (65) Wang, W.-C.; Shiao, H.-Y.; Lee, C.-C.; Fung, K.-S.; Hsieh, H.-P., *MedChemComm*, **2014**, 5, 1266.

- (66) Iragavarapu, C.; Mustafa, M.; Akinleye, A.; Furqan, M.; Mittal, V.; Cang, S.; Liu, D., *Journal of Hematology & Oncology*, **2015**, 8, 17.
- (67) Katayama, R.; Shaw, A. T.; Khan, T. M.; Mino-Kenudson, M.; Solomon, B. J.; Halmos, B.; Jessop, N. A.; Wain, J. C.; Yeo, A. T.; Benes, C.; Drew, L.; Saeh, J. C.; Crosby, K.; Sequist, L. V.; Iafrate, A. J.; Engelman, J. A., *Science Translational Medicine*, **2012**, 4, 120ra17.
- (68) Doebele, R. C.; Pilling, A. B.; Aisner, D. L.; Kutateladze, T. G.; Le, A. T.; Weickhardt, A. J.; Kondo, K. L.; Linderman, D. J.; Heasley, L. E.; Franklin, W. A.; Varella-Garcia, M.; Camidge, D. R., *Clinical Cancer Research*, **2012**, 18, 1472.
- (69) Choi, Y. L.; Soda, M.; Yamashita, Y.; Ueno, T.; Takashima, J.; Nakajima, T.; Yatabe, Y.; Takeuchi, K.; Hamada, T.; Haruta, H.; Ishikawa, Y.; Kimura, H.; Mitsudomi, T.; Tanio, Y.; Mano, H., *New England Journal of Medicine*, **2010**, 363, 1734.
- (70) McKeage, K., *Drugs*, **2015**, 75, 75.
- (71) Kinoshita, K.; Asoh, K.; Furuichi, N.; Ito, T.; Kawada, H.; Hara, S.; Ohwada, J.; Miyagi, T.; Kobayashi, T.; Takanashi, K.; Tsukaguchi, T.; Sakamoto, H.; Tsukuda, T.; Oikawa, N., *Bioorganic & Medicinal Chemistry*, **2012**, 20, 1271.
- (72) Sakamoto, H.; Tsukaguchi, T.; Hiroshima, S.; Kodama, T.; Kobayashi, T.; Fukami, Takaaki A.; Oikawa, N.; Tsukuda, T.; Ishii, N.; Aoki, Y., *Cancer Cell*, **2011**, 19, 679.
- (73) Gainor, J. F.; Dardaei, L.; Yoda, S.; Friboulet, L.; Leshchiner, I.; Katayama, R.; Dagogo-Jack, I.; Gadgeel, S.; Schultz, K.; Singh, M.; Chin, E.; Parks, M.; Lee, D.; DiCecca, R. H.; Lockerman, E.; Huynh, T.; Logan, J.; Ritterhouse, L. L.; Le, L. P.; Muniappan, A.; Digumarthy, S.; Channick, C.; Keyes, C.; Getz, G.; Dias-Santagata, D.; Heist, R. S.; Lennerz, J.; Sequist, L. V.; Benes, C. H.; Iafrate, A. J.; Mino-Kenudson, M.; Engelman, J. A.; Shaw, A. T., *Cancer Discovery*, **2016**, 6, 1118.
- (74) Huang, W.-S.; Liu, S.; Zou, D.; Thomas, M.; Wang, Y.; Zhou, T.; Romero, J.; Kohlmann, A.; Li, F.; Qi, J.; Cai, L.; Dwight, T. A.; Xu, Y.; Xu, R.; Dodd, R.; Toms, A.; Parillon, L.; Lu, X.; Anjum, R.; Zhang, S.; Wang, F.; Keats, J.; Wardwell, S. D.; Ning, Y.; Xu, Q.; Moran, L. E.; Mohemmad, Q. K.; Jang, H. G.; Clackson, T.; Narasimhan, N. I.; Rivera, V. M.; Zhu, X.; Dalgarno, D.; Shakespeare, W. C., *Journal of Medicinal Chemistry*, **2016**, 59, 4948.
- (75) Markham, A., *Drugs*, **2017**, 77, 1131.
- (76) Basit, S.; Ashraf, Z.; Lee, K.; Latif, M., *European Journal of Medicinal Chemistry*, **2017**, 134, 348.
- (77) Kouzarides, T., *Cell*, **2007**, 128, 693.
- (78) Marushige, K., *Proceedings of the National Academy of Sciences*, **1976**, 73, 3937.
- (79) Choudhary, C.; Kumar, C.; Gnad, F.; Nielsen, M. L.; Rehman, M.; Walther, T. C.; Olsen, J. V.; Mann, M., *Science*, **2009**, 325, 834.
- (80) Filippakopoulos, P.; Knapp, S., *Nature Reviews Drug Discovery*, **2014**, 13, 337.
- (81) Rodriguez-Paredes, M.; Esteller, M., *Nature Medicine*, **2011**, 330.
- (82) Muller, S.; Filippakopoulos, P.; Knapp, S., *Expert Reviews in Molecular Medicine*, **2011**, 13.
- (83) Moustakim, M.; Clark, P. G. K.; Hay, D. A.; Dixon, D. J.; Brennan, P. E., *MedChemComm*, **2016**, 7, 2246.

- (84) Romero, F. A.; Taylor, A. M.; Crawford, T. D.; Tsui, V.; Côté, A.; Magnuson, S., *Journal of Medicinal Chemistry*, **2016**, 59, 1271.
- (85) Vidler, L. R.; Brown, N.; Knapp, S.; Hoelder, S., *Journal of Medicinal Chemistry*, **2012**, 55, 7346.
- (86) Zhang, G.; Smith, S. G.; Zhou, M.-M., *Chemical Reviews*, **2015**, 115, 11625.
- (87) Gong, F.; Chiu, L.-Y.; Miller, K. M., *PLOS Genetics*, **2016**, 12, e1006272.
- (88) Filippakopoulos, P.; Picaud, S.; Mangos, M.; Keates, T.; Lambert, J.-P.; Barsyte-Lovejoy, D.; Felletar, I.; Volkmer, R.; Müller, S.; Pawson, T.; Gingras, A.-C.; Arrowsmith, Cheryl H.; Knapp, S., *Cell*, **2012**, 149, 214.
- (89) Belkina, A. C.; Denis, G. V., *Nature Reviews Cancer*, **2012**, 12, 465.
- (90) Stathis, A.; Bertoni, F., *Cancer Discovery*, **2018**, 8, 24.
- (91) Drouin, L.; McGrath, S.; Vidler, L. R.; Chaikuad, A.; Monteiro, O.; Tallant, C.; Philpott, M.; Rogers, C.; Fedorov, O.; Liu, M.; Akhtar, W.; Hayes, A.; Raynaud, F.; Müller, S.; Knapp, S.; Hoelder, S., *Journal of Medicinal Chemistry*, **2015**, 58, 2553.
- (92) Martin, L. J.; Koegl, M.; Bader, G.; Cockcroft, X.-L.; Fedorov, O.; Fiegen, D.; Gerstberger, T.; Hofmann, M. H.; Hohmann, A. F.; Kessler, D.; Knapp, S.; Knesl, P.; Kornigg, S.; Müller, S.; Nar, H.; Rogers, C.; Rumpel, K.; Schaaf, O.; Steurer, S.; Tallant, C.; Vakoc, C. R.; Zeeb, M.; Zoephel, A.; Pearson, M.; Boehmelt, G.; McConnell, D., *Journal of Medicinal Chemistry*, **2016**, 59, 4462.
- (93) Moustakim, M.; Clark, P. G. K.; Trulli, L.; Fuentes de Arriba, A. L.; Ehebauer, M. T.; Chaikuad, A.; Murphy, E. J.; Mendez-Johnson, J.; Daniels, D.; Hou, C.-F. D.; Lin, Y.-H.; Walker, J. R.; Hui, R.; Yang, H.; Dorrell, L.; Rogers, C. M.; Monteiro, O. P.; Fedorov, O.; Huber, K. V. M.; Knapp, S.; Heer, J.; Dixon, D. J.; Brennan, P. E., *Angewandte Chemie International Edition*, **2017**, 56, 827.
- (94) Filippakopoulos, P.; Qi, J.; Picaud, S.; Shen, Y.; Smith, W. B.; Fedorov, O.; Morse, E. M.; Keates, T.; Hickman, T. T.; Felletar, I.; Philpott, M.; Munro, S.; McKeown, M. R.; Wang, Y.; Christie, A. L.; West, N.; Cameron, M. J.; Schwartz, B.; Heightman, T. D.; La Thangue, N.; French, C. A.; Wiest, O.; Kung, A. L.; Knapp, S.; Bradner, J. E., *Nature*, **2010**, 468, 1067.
- (95) Nicodeme, E.; Jeffrey, K. L.; Schaefer, U.; Beinke, S.; Dwell, S.; Chung, C.-w.; Chandwani, R.; Marazzi, I.; Wilson, P.; Coste, H.; White, J.; Kirilovsky, J.; Rice, C. M.; Lora, J. M.; Prinjha, R. K.; Lee, K.; Tarakhovsky, A., *Nature*, **2010**, 468, 1119.
- (96) Dawson, M. A.; Prinjha, R. K.; Dittmann, A.; Giotopoulos, G.; Bantscheff, M.; Chan, W.-I.; Robson, S. C.; Chung, C.-w.; Hopf, C.; Savitski, M. M.; Huthmacher, C.; Gudgin, E.; Lugo, D.; Beinke, S.; Chapman, T. D.; Roberts, E. J.; Soden, P. E.; Auger, K. R.; Mirguet, O.; Doehner, K.; Delwel, R.; Burnett, A. K.; Jeffrey, P.; Drewes, G.; Lee, K.; Huntly, B. J. P.; Kouzarides, T., *Nature*, **2011**, 478, 529.
- (97) Fish, P. V.; Filippakopoulos, P.; Bish, G.; Brennan, P. E.; Bunnage, M. E.; Cook, A. S.; Fedorov, O.; Gerstenberger, B. S.; Jones, H.; Knapp, S.; Marsden, B.; Nocka, K.; Owen, D. R.; Philpott, M.; Picaud, S.; Primiano, M. J.; Ralph, M. J.; Sciammetta, N.; Trzupek, J. D., *Journal of Medicinal Chemistry*, **2012**, 55, 9831.

- (98) Waring, M. J.; Chen, H.; Rabow, A. A.; Walker, G.; Bobby, R.; Boiko, S.; Bradbury, R. H.; Callis, R.; Clark, E.; Dale, I.; Daniels, D. L.; Dulak, A.; Flavell, L.; Holdgate, G.; Jowitt, T. A.; Kikhney, A.; McAlister, M.; Méndez, J.; Ogg, D.; Patel, J.; Petteruti, P.; Robb, G. R.; Robers, M. B.; Saif, S.; Stratton, N.; Svergun, D. I.; Wang, W.; Whittaker, D.; Wilson, D. M.; Yao, Y., *Nature Chemical Biology*, **2016**, *12*, 1097.
- (99) Ottis, P.; Crews, C. M., *ACS Chemical Biology*, **2017**, *12*, 892.
- (100) Lu, J.; Qian, Y.; Altieri, M.; Dong, H.; Wang, J.; Raina, K.; Hines, J.; Winkler, James D.; Crew, Andrew P.; Coleman, K.; Crews, Craig M., *Chemistry & Biology*, **2015**, *22*, 755.
- (101) Delmore, Jake E.; Issa, Ghayas C.; Lemieux, Madeleine E.; Rahl, Peter B.; Shi, J.; Jacobs, Hannah M.; Kastiris, E.; Gilpatrick, T.; Paranal, Ronald M.; Qi, J.; Chesi, M.; Schinzel, Anna C.; McKeown, Michael R.; Heffernan, Timothy P.; Vakoc, Christopher R.; Bergsagel, P. L.; Ghobrial, Irene M.; Richardson, Paul G.; Young, Richard A.; Hahn, William C.; Anderson, Kenneth C.; Kung, Andrew L.; Bradner, James E.; Mitsiades, Constantine S., *Cell*, **2011**, *146*, 904.
- (102) Zengerle, M.; Chan, K.-H.; Ciulli, A., *ACS Chemical Biology*, **2015**, *10*, 1770.
- (103) Gadd, M. S.; Testa, A.; Lucas, X.; Chan, K.-H.; Chen, W.; Lamont, D. J.; Zengerle, M.; Ciulli, A., *Nature Chemical Biology*, **2017**, *13*, 514.
- (104) Galdeano, C.; Ciulli, A., *Future medicinal chemistry*, **2016**, *8*, 1655.
- (105) Raux, B.; Voitovich, Y.; Derviaux, C.; Lugari, A.; Rebuffet, E.; Milhas, S.; Priet, S.; Roux, T.; Trinquet, E.; Guillemot, J.-C.; Knapp, S.; Brunel, J.-M.; Fedorov, A. Y.; Collette, Y.; Roche, P.; Betzi, S.; Combes, S.; Morelli, X., *Journal of Medicinal Chemistry*, **2016**, *59*, 1634.
- (106) Lejeune, P.; Sugawara, T.; Gelato, K. A.; Ellinger-Ziegelbauer, H.; Fernandez-Montalvan, A. E.; Schmees, N.; Siegel, S.; Weinmann, H.; Gekeler, V.; Walter, A. O.; Ocker, M.; Ince, S.; Haendler, B., *Cancer Research*, **2015**, *75*, 3524.
- (107) Gacias, M.; Gerona-Navarro, G.; Plotnikov, Alexander N.; Zhang, G.; Zeng, L.; Kaur, J.; Moy, G.; Rusinova, E.; Rodriguez, Y.; Matikainen, B.; Vincek, A.; Joshua, J.; Casaccia, P.; Zhou, M.-M., *Chemistry & Biology*, **2014**, *21*, 841.
- (108) Zhang, G.; Plotnikov, A. N.; Rusinova, E.; Shen, T.; Morohashi, K.; Joshua, J.; Zeng, L.; Mujtaba, S.; Ohlmeyer, M.; Zhou, M.-M., *Journal of Medicinal Chemistry*, **2013**, *56*, 9251.
- (109) Picaud, S.; Wells, C.; Felletar, I.; Brotherton, D.; Martin, S.; Savitsky, P.; Diez-Dacal, B.; Philpott, M.; Bountra, C.; Lingard, H.; Fedorov, O.; Müller, S.; Brennan, P. E.; Knapp, S.; Filippakopoulos, P., *Proceedings of the National Academy of Sciences*, **2013**, *110*, 19754.
- (110) Watts, E.; Heidenreich, D.; Tucker, E.; Raab, M.; Strebhardt, K.; Chesler, L.; Knapp, S.; Bellenie, B.; Hoelder, S., *Journal of Medicinal Chemistry*, **2019**, *62*, 2618.
- (111) Peters, J.-U., *Journal of Medicinal Chemistry*, **2013**, *56*, 8955.
- (112) Anighoro, A.; Bajorath, J.; Rastelli, G., *Journal of Medicinal Chemistry*, **2014**, *57*, 7874.
- (113) Wu, M.; Sirota, M.; Butte, A. J.; Chen, B., *Pacific Symposium on Biocomputing*, **2015**, 68.
- (114) Proschak, E.; Stark, H.; Merk, D., *Journal of Medicinal Chemistry*, **2019**, *62*, 420.

- (115) Ciceri, P.; Muller, S.; O'Mahony, A.; Fedorov, O.; Filippakopoulos, P.; Hunt, J. P.; Lasater, E. A.; Pallares, G.; Picaud, S.; Wells, C.; Martin, S.; Wodicka, L. M.; Shah, N. P.; Treiber, D. K.; Knapp, S., *Nature Chemical Biology*, **2014**, 10, 305.
- (116) Patyar, S., Prakash, A. and Medhi, B., *Journal of Pharmacy and Pharmacology*, **2011**, 63, 459.
- (117) Cheng, H.; Li, C.; Bailey, S.; Baxi, S. M.; Goulet, L.; Guo, L.; Hoffman, J.; Jiang, Y.; Johnson, T. O.; Johnson, T. W.; Knighton, D. R.; Li, J.; Liu, K. K. C.; Liu, Z.; Marx, M. A.; Walls, M.; Wells, P. A.; Yin, M.-J.; Zhu, J.; Zientek, M., *ACS Medicinal Chemistry Letters*, **2013**, 4, 91.
- (118) Apsel, B.; Blair, J. A.; Gonzalez, B.; Nazif, T. M.; Feldman, M. E.; Aizenstein, B.; Hoffman, R.; Williams, R. L.; Shokat, K. M.; Knight, Z. A., *Nat Chem Biol*, **2008**, 4, 691.
- (119) Wu, H.; Hu, C.; Wang, A.; Weisberg, E. L.; Chen, Y.; Yun, C. H.; Wang, W.; Liu, Y.; Liu, X.; Tian, B.; Wang, J.; Zhao, Z.; Liang, Y.; Li, B.; Wang, L.; Wang, B.; Chen, C.; Buhrlage, S. J.; Qi, Z.; Zou, F.; Nonami, A.; Li, Y.; Fernandes, S. M.; Adamia, S.; Stone, R. M.; Galinsky, I. A.; Wang, X.; Yang, G.; Griffin, J. D.; Brown, J. R.; Eck, M. J.; Liu, J.; Gray, N. S.; Liu, Q., *Leukemia*, **2016**, 30, 173.
- (120) Carlino, L.; Rastelli, G., *Journal of Medicinal Chemistry*, **2016**.
- (121) Li, J.; Favata, M.; Kelley, J. A.; Caulder, E.; Thomas, B.; Wen, X.; Sparks, R. B.; Arvanitis, A.; Rogers, J. D.; Combs, A. P.; Vaddi, K.; Solomon, K. A.; Scherle, P. A.; Newton, R.; Fridman, J. S., *Neoplasia*, **2010**, 12, 28.
- (122) Smith, C. C.; Wang, Q.; Chin, C.-S.; Salerno, S.; Damon, L. E.; Levis, M. J.; Perl, A. E.; Travers, K. J.; Wang, S.; Hunt, J. P.; Zarrinkar, P. P.; Schadt, E. E.; Kasarskis, A.; Kuriyan, J.; Shah, N. P., *Nature*, **2012**, 485, 260.
- (123) Fiskus, W.; Sharma, S.; Qi, J.; Shah, B.; Devaraj, S. G. T.; Leveque, C.; Portier, B. P.; Iyer, S.; Bradner, J. E.; Bhalla, K. N., *Molecular Cancer Therapeutics*, **2014**, 13, 2315.
- (124) Sun, B.; Shah, B.; Fiskus, W.; Qi, J.; Rajapakshe, K.; Coarfa, C.; Li, L.; Devaraj, S. G. T.; Sharma, S.; Zhang, L.; Wang, M. L.; Saenz, D. T.; Krieger, S.; Bradner, J. E.; Bhalla, K. N., *Blood*, **2015**, 126, 1565.
- (125) Stratikopoulos, Elias E.; Dendy, M.; Szabolcs, M.; Khaykin, Alan J.; Lefebvre, C.; Zhou, M.-M.; Parsons, R., *Cancer Cell*, **2015**, 27, 837.
- (126) Tinsley, S.; Meja, K.; Shepherd, C.; Khwaja, A., *British Journal of Haematology*, **2015**, 170, 275.
- (127) Ember, S. W. J.; Zhu, J.-Y.; Olesen, S. H.; Martin, M. P.; Becker, A.; Berndt, N.; Georg, G. I.; Schönbrunn, E., *ACS Chemical Biology*, **2014**, 9, 1160.
- (128) Davis, M. I.; Hunt, J. P.; Herrgard, S.; Ciceri, P.; Wodicka, L. M.; Pallares, G.; Hocker, M.; Treiber, D. K.; Zarrinkar, P. P., *Nature Biotechnology*, **2011**, 29, 1046.
- (129) Gohda, J.; Suzuki, K.; Liu, K.; Xie, X.; Takeuchi, H.; Inoue, J.-i.; Kawaguchi, Y.; Ishida, T., *Scientific Reports*, **2018**, 8, 3521.
- (130) Hu, J.; Wang, Y.; Li, Y.; Xu, L.; Cao, D.; Song, S.; Damaneh, M. S.; Wang, X.; Meng, T.; Chen, Y.-L.; Shen, J.; Miao, Z.; Xiong, B., *European Journal of Medicinal Chemistry*, **2017**, 137, 176.

- (131) Chen, L.; Yap, J. L.; Yoshioka, M.; Lanning, M. E.; Fountain, R. N.; Rajé, M.; Scheenstra, J. A.; Strovel, J. W.; Fletcher, S., *ACS Medicinal Chemistry Letters*, **2015**, 6, 764.
- (132) Liu, S.; Yosief, H. O.; Dai, L.; Huang, H.; Dhawan, G.; Zhang, X.; Muthengi, A. M.; Roberts, J.; Buckley, D. L.; Perry, J. A.; Wu, L.; Bradner, J. E.; Qi, J.; Zhang, W., *Journal of Medicinal Chemistry*, **2018**.
- (133) Ember, S. W.; Lambert, Q. T.; Berndt, N.; Gunawan, S.; Ayaz, M.; Tauro, M.; Zhu, J.-Y.; Cranfill, P. J.; Greninger, P.; Lynch, C. C.; Benes, C. H.; Lawrence, H. R.; Reuther, G. W.; Lawrence, N. J.; Schönbrunn, E., *Molecular Cancer Therapeutics*, **2017**, 16, 1054.
- (134) Divakaran, A.; Talluri, S. K.; Ayoub, A. M.; Mishra, N. K.; Cui, H.; Widen, J. C.; Berndt, N.; Zhu, J.-Y.; Carlson, A. S.; Topczewski, J. J.; Schonbrunn, E. K.; Harki, D. A.; Pomerantz, W. C. K., *Journal of Medicinal Chemistry*, **2018**, 61, 9316.
- (135) Andrews, F. H.; Singh, A. R.; Joshi, S.; Smith, C. A.; Morales, G. A.; Garlich, J. R.; Durden, D. L.; Kutateladze, T. G., *Proceedings of the National Academy of Sciences*, **2017**, 114, E1072.
- (136) Wang, J.; Erazo, T.; Ferguson, F. M.; Buckley, D. L.; Gomez, N.; Muñoz-Guardiola, P.; Diéguez-Martínez, N.; Deng, X.; Hao, M.; Masefski, W.; Fedorov, O.; Offei-Addo, N. K.; Park, P. M.; Dai, L.; DiBona, A.; Becht, K.; Kim, N. D.; McKeown, M. R.; Roberts, J. M.; Zhang, J.; Sim, T.; Alessi, D. R.; Bradner, J. E.; Lizcano, J. M.; Blacklow, S. C.; Qi, J.; Xu, X.; Gray, N. S., *ACS Chemical Biology*, **2018**.
- (137) Amirouchene-Angelozzi, N.; Swanton, C.; Bardelli, A., *Cancer Discovery*, **2017**, 7, 805.
- (138) Chou, T.-C., *Cancer Research*, **2010**, 70, 440.
- (139) Steegmaier, M.; Hoffmann, M.; Baum, A.; Lénárt, P.; Petronczki, M.; Krššák, M.; Gürtler, U.; Garin-Chesa, P.; Lieb, S.; Quant, J.; Grauert, M.; Adolf, G. R.; Kraut, N.; Peters, J.-M.; Rettig, W. J., *Current Biology*, **2007**, 17, 316.
- (140) Kothe, M.; Kohls, D.; Low, S.; Coli, R.; Rennie, G. R.; Feru, F.; Kuhn, C.; Ding, Y.-H., *Chemical Biology & Drug Design*, **2007**, 70, 540.
- (141) Galkin, A. V.; Melnick, J. S.; Kim, S.; Hood, T. L.; Li, N.; Li, L.; Xia, G.; Steensma, R.; Chopiuk, G.; Jiang, J.; Wan, Y.; Ding, P.; Liu, Y.; Sun, F.; Schultz, P. G.; Gray, N. S.; Warmuth, M., *Proceedings of the National Academy of Sciences*, **2007**, 104, 270.
- (142) Reinhardt, H. C.; Yaffe, M. B., *Nature Reviews Molecular Cell Biology*, **2013**, 14, 563.
- (143) Barr, F. A.; Silljé, H. H. W.; Nigg, E. A., *Nature Reviews Molecular Cell Biology*, **2004**, 5, 429.
- (144) Liu, X., *Translational Oncology*, **2015**, 8, 185.
- (145) Cholewa, B. D.; Liu, X.; Ahmad, N., *Cancer Research*, **2013**, 73, 6848.
- (146) Strebhardt, K.; Ullrich, A., *Nature Reviews Cancer*, **2006**, 6, 321.
- (147) Rudolph, D.; Steegmaier, M.; Hoffmann, M.; Grauert, M.; Baum, A.; Quant, J.; Haslinger, C.; Garin-Chesa, P.; Adolf, G. R., *Clinical Cancer Research*, **2009**, 15, 3094.
- (148) Berg, A.; Berg, T., *ChemBioChem*, **2016**, 17, 650.
- (149) Degenhardt, Y.; Lampkin, T., *Clinical Cancer Research*, **2010**, 16, 384.

- (150) Zhan, M.-M.; Yang, Y.; Luo, J.; Zhang, X.-X.; Xiao, X.; Li, S.; Cheng, K.; Xie, Z.; Tu, Z.; Liao, C., *European Journal of Medicinal Chemistry*, **2018**, *143*, 724.
- (151) Madhavi Sastry, G.; Adzhigirey, M.; Day, T.; Annabhimoju, R.; Sherman, W., *Journal of Computer-Aided Molecular Design*, **2013**, *27*, 221.
- (152) Budin, G.; Yang, K. S.; Reiner, T.; Weissleder, R., *Angewandte Chemie International Edition*, **2011**, *50*, 9378.
- (153) Abdel-Magid, A. F.; Carson, K. G.; Harris, B. D.; Maryanoff, C. A.; Shah, R. D., *The Journal of Organic Chemistry*, **1996**, *61*, 3849.
- (154) Tang, P. C.; Zhang, N.; Dong, Z.; Zeng, X.; Shu, S.; Liu, L. WO2011113293, 2011.
- (155) Sythana, S. K.; Naramreddy, S. R.; Kavitate, S.; Ch, V. K.; Bhagat, P. R., *Organic Process Research & Development*, **2014**, *18*, 912.
- (156) ThermoFisher; Scientific, Accessed June 2019, http://assets.thermofisher.com/TFS-Assets/BID/Methods-&-Protocols/20180123_SSBK_Customer_Protocol_and_Assay_Conditions.pdf
- (157) Achary, R.; Mathi, G. R.; Lee, D. H.; Yun, C. S.; Lee, C. O.; Kim, H. R.; Park, C. H.; Kim, P.; Hwang, J. Y., *Bioorganic & Medicinal Chemistry Letters*, **2017**, *27*, 2185.
- (158) Mathi, G. R.; Kang, C. H.; Lee, H. K.; Achary, R.; Lee, H.-Y.; Lee, J.-Y.; Ha, J. D.; Ahn, S.; Park, C. H.; Lee, C. O.; Hwang, J. Y.; Yun, C.-S.; Jung, H. J.; Cho, S. Y.; Kim, H. R.; Kim, P., *European Journal of Medicinal Chemistry*, **2017**, *126*, 536.
- (159) Wuts, P. G. M.; Greene, T. W. *Protective Groups in Organic Synthesis*; John Wiley & Sons, 1991.
- (160) Horita, K.; Yoshioka, T.; Tanaka, T.; Oikawa, Y.; Yonemitsu, O., *Tetrahedron*, **1986**, *42*, 3021.
- (161) Linz, G.; Sieger, P.; Schmid, R.; Goepper, S. WO2009019205, 2009.
- (162) Baumeister, P.; Blaser, H.-U.; Studer, M., *Catalysis Letters*, **1997**, *49*, 219.
- (163) Sastri, V. S.; Bünzli, J.-C.; Rao, V. R.; Rayudu, G. V. S.; Perumareddi, J. R. In *Modern Aspects of Rare Earths and Their Complexes*; Elsevier: Amsterdam, 2003, p 779.
- (164) McCreary, M. D.; Lewis, D. W.; Wernick, D. L.; Whitesides, G. M., *Journal of the American Chemical Society*, **1974**, *96*, 1038.
- (165) Craig, P. N., *Journal of Medicinal Chemistry*, **1971**, *14*, 680.
- (166) Gramec, D.; Peterlin Mašič, L.; Sollner Dolenc, M., *Chemical Research in Toxicology*, **2014**, *27*, 1344.
- (167) Tucker, E. R.; Tall, J. R.; Danielson, L. S.; Gowan, S.; Jamin, Y.; Robinson, S. P.; Banerji, U.; Chesler, L., *Molecular Oncology*, **2017**, *11*, 996.
- (168) Chung, C.-W.; Coste, H.; White, J. H.; Mirguet, O.; Wilde, J.; Gosmini, R. L.; Delves, C.; Magny, S. M.; Woodward, R.; Hughes, S. A.; Boursier, E. V.; Flynn, H.; Bouillot, A. M.; Bamborough, P.; Brusq, J.-M. G.; Gellibert, F. J.; Jones, E. J.; Riou, A. M.; Homes, P.; Martin, S. L.; Uings, I. J.; Toum, J.; Clément, C. A.; Boullay, A.-B.; Grimley, R. L.; Blandel, F. M.; Prinjha, R. K.; Lee, K.; Kirilovsky, J.; Nicodeme, E., *Journal of Medicinal Chemistry*, **2011**, *54*, 3827.

- (169) Law, R. P.; Atkinson, S. J.; Bamborough, P.; Chung, C.-w.; Demont, E. H.; Gordon, L. J.; Lindon, M.; Prinjha, R. K.; Watson, A. J. B.; Hirst, D. J., *Journal of Medicinal Chemistry*, **2018**, 61, 4317.
- (170) Ceccon, M.; Mologni, L.; Bisson, W.; Scapozza, L.; Gambacorti-Passerini, C., *Molecular Cancer Research*, **2013**, 11, 122.
- (171) Kinoshita, K.; Kobayashi, T.; Asoh, K.; Furuichi, N.; Ito, T.; Kawada, H.; Hara, S.; Ohwada, J.; Hattori, K.; Miyagi, T.; Hong, W.-S.; Park, M.-J.; Takanashi, K.; Tsukaguchi, T.; Sakamoto, H.; Tsukuda, T.; Oikawa, N., *Journal of Medicinal Chemistry*, **2011**, 54, 6286.
- (172) Kooistra, A. J.; Kanev, G. K.; de Esch, I. J. P.; van Linden, O. P. J.; Leurs, R.; de Graaf, C., *Nucleic Acids Research*, **2015**, 44, D365.
- (173) Raab, M.; Krämer, A.; Hehlhans, S.; Sanhaji, M.; Kurunci-Csacsco, E.; Dötsch, C.; Bug, G.; Ottmann, O.; Becker, S.; Pachl, F.; Kuster, B.; Strebhardt, K., *Molecular Oncology*, **2015**, 9, 140.
- (174) Swamy, K. C. K.; Kumar, N. N. B.; Balaraman, E.; Kumar, K. V. P. P., *Chemical Reviews*, **2009**, 109, 2551.
- (175) Fletcher, S., *Organic Chemistry Frontiers*, **2015**, 2, 739.
- (176) Tsunoda, T.; Nagino, C.; Oguri, M.; Itô, S., *Tetrahedron Letters*, **1996**, 37, 2459.
- (177) Tsunoda, T.; Ozaki, F.; Itô, S., *Tetrahedron Letters*, **1994**, 35, 5081.
- (178) Tsunoda, T.; Kaku, H.; Ito, S., June 2019, <https://www.tcichemicals.com/en/in/support-download/tcicemail/backnumber/article/123drE.pdf>
- (179) Hawkins, P. C. D.; Skillman, A. G.; Nicholls, A., *Journal of Medicinal Chemistry*, **2007**, 50, 74.
- (180) Patel, R. Y.; Doerksen, R. J., *Journal of Proteome Research*, **2010**, 9, 4433.
- (181) Corey, E. J.; Helal, C. J., *Angewandte Chemie International Edition*, **1998**, 37, 1986.
- (182) Kerns, E. H.; Li, D., *Drug-like Properties: Concepts, Structure Design and Methods*; Elsevier, 2008.
- (183) Lin, M.; Tesconi, M.; Tischler, M., *International Journal of Pharmaceutics*, **2009**, 369, 47.
- (184) Kansy, M.; Senner, F.; Gubernator, K., *Journal of Medicinal Chemistry*, **1998**, 41, 1007.
- (185) Wang, Z.; Hop, C. E. C. A.; Leung, K. H.; Pang, J., *Journal of Mass Spectrometry*, **2000**, 35, 71.
- (186) McGinnity, D. F.; Soars, M. G.; Urbanowicz, R. A.; Riley, R. J., *Drug Metabolism and Disposition*, **2004**, 32, 1247.
- (187) Arnott, J. A.; Planey, S. L., *Expert Opinion on Drug Discovery*, **2012**, 7, 863.
- (188) Waring, M. J., *Expert Opinion on Drug Discovery*, **2010**, 5, 235.
- (189) Milletti, F.; Storchi, L.; Sforza, G.; Cruciani, G., *Journal of Chemical Information and Modeling*, **2007**, 47, 2172.
- (190) Ma, M. F. P.; Li, K.; Zhou, Z.; Tang, C.; Chan, A. S. C., *Tetrahedron: Asymmetry*, **1999**, 10, 3259.
- (191) Kubota, H.; Kubo, A.; Takahashi, M.; Shimizu, R.; Da-te, T.; et al., *Journal of Organic Chemistry*, **1995**, 60, 6776.
- (192) Dale, J. A.; Dull, D. L.; Mosher, H. S., *The Journal of Organic Chemistry*, **1969**, 34, 2543.
- (193) Parker, D., *Chemical Reviews*, **1991**, 91, 1441.

- (194) Phenomenex, *Accessed June 2019*,
<https://www.phenomenex.com/Products/HPLCDetail/lux>